HYDROGEOLOGY OF THE TABLE MOUNTAIN SANDSTONE AQUIFER - KLEIN KAROO

Deur Johanita Christelle Kotze

HYDROGEOLOGY OF THE TABLE MOUNTAIN SANDSTONE AQUIFER - KLEIN KAROO

by

Johanita Christelle KOTZE

THESIS

Submitted in the fulfilment of the requirements for the degree of Doctor of Philosophy in the Faculty of Natural Science and Agriculture, Department of Geohydrology, University of the Free State, Bloemfontein

Promoter: Prof. GJ van Tonder
Co-Promoter: Prof. BTH Verhagen

ACKNOWLEDGEMENTS

This research emanated from a project funded by the Water Research Commission and the Department of Water Affairs entitled:

" TOWARDS A MANAGEMENT TOOL FOR GROUNDWATER EXPLOITATION IN THE TABLE MOUNTAIN FRACTURED SANDSTONE AQUIFER"

The financing of the project by the Water Research Commission and the contribution of the members of the Steering Committee is gratefully acknowledged.

This project was only made possible with the co-operation of many individuals and institutions. The author therefore wishes to record her sincere thanks to the following:

- The Water Research Commission and Department of Water Affairs and Forestry for funding the project.

- SRK Consulting for financial assistance and generous time allocations for research and development as well as the sponsorship for a PhD study.

- Prof. Balt Th Verhagen for all his assistance, training and useful advice with the hydrochemistry and environmental isotope sampling as well as analysis of all the samples.

- Institute for Groundwater Studies in Bloemfontein, in particular Prof. Gerrit van Tonder for his useful discussions and suggestions.

- Overberg Water, in particular Deon Haasbroek and Johan Uys, for all their assistance during the sampling programs, steering committee meetings and for providing data sets and information on request.

- Groundwater Consulting services for providing test pumping data and information on the iron-bacteria clogging of production boreholes.

- DECAS, in particular Gail Cleaver for providing information in connection with springs and partaking in the preliminary spring sampling program.
- Werner Stadler of Earthdata for producing selected GIS maps.

- Council for Geoscience for preparing a report on structural lineament analysis, cross-sections and maps of the geology of the Klein Karoo area.

- Last, but not least Prof. Arie Issar (Institute for Desert Research, Ben Gurion University, Israel – consultant to DWAF) is gratefully acknowledged for the role he played in the Table Mountain Group (TMG) sandstone, fractured rock research. During Prof. Issar's visits to South Africa in 1994 and 1995 he formulated the methodology for this research. Without his ideas, support and useful discussions and suggestions, this research would not have been possible.

TABLE OF CONTENTS

Section **Page**

ACKNOWLEDGEMENTS ..... **II**

APPENDICES ..... **XII**

GLOSSARY ..... **XIII**

CHAPTER 1: INTRODUCTION **1**

1.1 BACKGROUND 1
1.2 OBJECTIVES AND AIMS OF THE RESEARCH 2
1.3 SITE SELECTION 5
1.4 THE KLEIN KAROO RURAL WATER SUPPLY SCHEME 5

CHAPTER 2: INVESTIGATION APPROACH AND RESEARCH METHODOLOGY **8**

2.1 DESK STUDY 8
2.2 FIELDWORK 13
2.2.1 Aquifer testing *13*
2.2.2 Hydrocensus and hydrochemical sampling *15*
2.2.3 Detailed structural analysis of the Kammanassie Mountains *19*
2.2.4 Drilling of additional monitoring boreholes – Eastern Sector of KKRWSS *21*
2.3 SATELLITE LINEAMENT MAPPING AND REMOTE SENSING 21
2.3.1 Remote Sensing *22*
2.3.2 Satellite lineament mapping *23*
2.4 DATA COLLATION 23
2.5 DATA INTERPRETATION 24
2.5.1 Environmental isotopes *25*
2.5.1.1 General applications of environmental isotopes in hydrogeology 25
2.5.1.2 Definitions 26
2.5.1.3 Environmental radioactive isotopes: ^{3}H and ^{14}C 27
2.5.1.4 Approaches to interpretation of ^{14}C and ^{3}H 29
2.5.1.5 Chlorofluorocarbon 33
2.5.1.6 Application of stable isotopes ^{13}C 34
2.5.1.7 Application of stable isotopes ^{18}O and ^{2}H 35
2.5.1.8 Application of environmental isotope and hydrochemistry in this study 37
2.5.2 Aquifer parameters and yield *39*
2.5.2.1 Hydrogeological characteristics of fractured aquifers 40
2.5.2.2 Theoretical models for analysis of test pumping data 41
2.5.2.3 Flow Characteristic method 43
2.5.3 Groundwater recharge *46*
2.5.3.1 Mean Residence Time (MRT) 47

2.5.3.2 Cumulative rainfall departure (CRD) method 48
2.5.3.3 Area related recharge method 51
2.5.3.4 Chloride mass balance method 52
2.5.3.5 Baseflow – experimental catchments at Jonkershoek / Franshoek 53
2.5.3.6 Saturated volume fluctuation method (SVF-method) 53
2.5.3.7 GIS Raster approach 54
2.5.4 Determine radius of influence of abstraction *54*
2.6 CONCEPTUAL HYDROGEOLOGICAL MODEL 54
2.7 DETERMINE GROUNDWATER WATER BALANCE 54
2.8 PROPOSED AQUIFER MANAGEMENT 55

CHAPTER 3: STUDY AREA OVERVIEW 57

3.1 LOCATION AND PHYSIOGRAPHY 57
3.2 KLEIN KAROO RURAL WATER SUPPLY SCHEME 58
3.2.1 The Eastern Sector of the Scheme *58*
3.2.2 The Western Sector of the Scheme *59*
3.2.3 Wellfield capacities *59*
3.3 CLIMATE AND EVAPOTRANSPIRATION 63
3.4 RAINFALL 64
3.5 GEOLOGY AND STRUCTURE 67
3.5.1 Regional geology and structure *68*
3.5.1.1 Stratigraphy and geological history 68
3.5.1.2 Regional Structure 73
3.5.1.3 Regional fracture pattern analysis 74
3.5.2 Hydrodynamics of fractured aquifer *77*
3.5.2.1 Fracturing styles and orientations 78
3.5.2.2 Fracture connectivity 79
3.5.3 Local geology and structure of the Kammanassie Mountains *82*
3.5.3.1 Lithology of the Table Mountain Group sandstones 82
3.5.3.2 Local fracture pattern analysis – Kammanassie Mountains 86
3.5.3.3 Folding and faulting from field mapping 87
3.6 GEOLOGICAL ORIGIN OF HOT SPRINGS 94
3.7 BOREHOLE INFORMATION 94
3.7.1 Additional Monitoring Boreholes – Eastern Section KKRWSS *95*
3.7.2 KKRWSS production borehole data *96*
3.7.3 Original Scheme monitoring boreholes *98*
3.7.4 Existing boreholes – privately owned land Kammanassie Mountains *99*

CHAPTER 4: HYDROCHEMICAL CHARACTERISATION 101

4.1 DATA ANALYSIS TECHNIQUES 101
4.2 MACRO ELEMENT DATA ANALYSIS 104
4.3 TRACE ELEMENT DATA ANALYSIS 111
4.4 HYDROCHEMISTRY AND ENVIRONMENTAL ISOTOPES 113
4.4.1 Stable isotope data *113*
4.4.2 Radioactive environmental isotope data analysis *116*
4.4.3 Major ion chemistry and environmental isotopes *119*
4.4.4 Multi-component cluster analysis *125*

4.4.5 Variation in chemistry and environmental isotope composition with depth *128*
4.5 TEST FOR THE WORKING HYPOTHESIS 129
4.6 SUMMARY 133

CHAPTER 5: CONCEPTUAL HYDROGEOLOGICAL MODEL – TMG SUPER AQUIFER KLEIN KAROO SECTION 135

5.1 AQUIFER DELINEATION 135
5.2 HYDROGEOLOGICAL CHARACTERISTICS OF THE TMG SUPER AQUIFER 138
5.2.1 Definition of hydrostratigraphic units *138*
5.2.2 Aquizones *140*
5.2.3 Groundwater flow regime and water level distribution *141*
5.2.4 Groundwater storage *145*
5.3 SPRINGS OCCURING IN THE TMG SUPER AQUIFER 146
5.4 BOREHOLE YIELDS 149
5.5 HYDROGEOLOGICAL CONCEPTUAL MODEL FOR KAMMANASSIE MOUNTAINS 150

CHAPTER 6: HYDRAULIC PROPERTIES OF AQUIFERS 154

6.1 PENINSULA AQUIFER 156
6.1.1 VR7 ..... *156*
6.1.2 VR6 ..... *159*
6.1.3 VR11 ..... *160*
6.2 NARDOUW AQUIFER 161
6.2.1 DP28 ..... *161*
6.2.2 DP15 ..... *162*
6.2.3 VG3 ..... *163*
6.3 ALLUVIAL BOREHOLE– DP18 164
6.4 SUMMARY 165
6.5 BOREHOLE EFFICIENCY CALCULATED FROM STEP DRAWDOWN TEST RESULTS 167

CHAPTER 7: WATER BALANCE 172

7.1 DISCHARGE FROM THE SYSTEM 175
7.1.1 Groundwater abstraction from the LKRWSS *175*
7.1.2 Other groundwater abstraction in the Kammanassie Mountains *178*
7.1.3 Springflow *179*
7.1.4 Total Discharge from the Kammanassie Mountains *182*
7.2 RECHARGE 183
7.2.1 Baseflow *183*
7.2.2 CRD Method *186*
7.2.3 Area related method *192*
7.2.4 Storage assessment with ^{14}C data *195*
7.2.5 Chloride mass balance method *197*
7.2.6 SVF Method *198*

7.2.7 EQUAL VOLUME Method *200*
7.2.8 RECHARGE Spreadsheet *202*
7.2.9 GIS Raster based approach *205*
7.2.10 Total inflows - Recharge *206*
7.3 WATER BALANCE CALCULATION 206

CHAPTER 8: AQUIFER MANAGEMENT 213

8.1 AQUIFER TESTING 213
8.2 WELLMAN 217
8.2.1 Determining the sustainable yield of a borehole with WELLMAN *219*
8.2.2 Recommended pumping rate for Eastern Sector KKRWSS Production boreholes *222*
8.2.2.1 Recommended yield: Vermaaks River Wellfield 224
8.2.2.2 Recommended yields : other TMG wellfields of Eastern Sector of KKRWSS 227
8.2.2.3 Recommended yield: Voorzorg Wellfield 228
8.2.2.4 Recommended yield: Olifants River Wellfield 228
8.2.2.5 Capacity of the Eastern Sector KKRWSS 229
8.3 RADIUS OF INFLUENCE OF BOREHOLES 230
8.4 TMG MANAGEMENT PLAN 233

CHAPTER 9: CONCLUSIONS 236

CHAPTER 11: REFERENCES 247

LIST OF FIGURES

FIGURES **PAGE**

1-1: LOCALITY MAP 3
2-1: FLOW DIAGRAM – RESEARCH APPROACH 9
2-2 : SPATIAL DISTRIBUTION OF BOREHOLE DATA 10
2-3: HOT SPRINGS AND SEEPAGE SAMPLING POSITIONS 16
2-4: ^{14}C SAMPLING TECHNIQUE 17
2-5: LOCALITY MAP SHOWING SAMPLING / HYDROCENSUS BOREHOLE POSITIONS RELATIVE TO GEOLOGY 20
2-6: GROUNDWATER PROFILE IN PHREATIC AQUIFER 30
2-7: CHANGES IN ATMOSPHERIC ^{3}H FOR SOUTHERN AFRICA 32
2-8: VARIATION IN ATMOSPHERIC ^{14}C 32
2-9: EXPONENTIAL MODEL FOR ^{14}C AND ^{3}H SHOWING MRT 33

2-10: CFC DISTRIBUTION IN GROUNDWATER AND AIR....34
2-11: METEORIC WATER LINES....36
2-12: INFORMATION FROM A DERIVATIVE PLOT....44
3-1: EASTERN SECTOR WELLFIELDS....60
3-2: WESTERN SECTOR WELLFIELDS....61
3-3: COMPARISSON - MONTHLY RAINFALL AND EVAPORATION FIGURES FOR THE KLEIN KAROO....63
3-4: VARIATIONS ANNUAL RAINFALL - VALLEY AREAS....65
3-5: VARIATION ANNUAL RAINFALL - SWARTBERG MOUNTAINS....66
3-6: VARIATION ANNUAL RAINFALL - KAMMANASSIE MOUNTAINS....66
3-7: RAINFALL VARIATION WITH ALTITUDE....67
3-8: GEOLOGICAL MAP....70
3-9: CROSS-SECTION 1....71
3-10: CROSS-SECTION 2....72
3-11 SATELLITE LINEAMENTS - KLEIN KAROO....76
3-12: E-W STRIKING LINEAMENTS - KLEIN KAROO....76
3-13: N-S STRIKING LINEAMENTS - KLEIN KAROO....76
3-14: HYDRODYNAMIC PARAMETERS – KAMMANASSIE MOUNTAINS....81
3-15: SCHEMATIC BLOCK DIAGRAM SHOWING THE 3D GEOLOGY OF THE KAMMANASSIE MOUNTAINS....82
3-16: DETAILED GEOLOGICAL MAPPING OF KAMMANASSIE MOUNTAINS..83
3-17: STRUCTURAL PROFILE – KAMMANASSIE ANTICLINE....85
3-18: FRACTURE STYLES/GEOMETRIES....88
3-19: BLOCK DIAGRAM INDICATING THE KINEMATICS OF KEYSTONE BLOCK FAULTING....92
4-1: BOREHOLES VERSUS STRUCTURES....102
4-2: PIPER DIAGRAM OF ALL HYDROCHEMICAL DATA....106
4-3: DUROV DIAGRAM OF ALL HYDROCHEMICAL DATA....107
4-4: EXPANDED DUROV DIAGRAM OF ALL HYDROCHEMICAL DATA....108
4-5: SAR DIAGRAM OF ALL HYDROCHEMICAL DATA....109
4-6: $\delta^{18}O$ VERSUS $\delta^{2}H$ - TMG AND ALLUVIAL AQUIFERS....114
4-7: $\delta^{18}O$ VERSUS $\delta^{2}H$ - KLEIN KAROO TMG AQUIFERS....114
4-8: SCHEMATIC PRESENTATION SHOWING ^{14}C DISTRIBUTION IN GROUNDWATER, VERMAAKS RIVER VALLEY....117
4-9: EXPONENTIAL MODEL FOR ^{14}C AND ^{3}H SHOWING MRT FOR KKRWSS BOREHOLES....118
4-10: SCATTER PLOT OF $\delta^{18}O$ VERSUS TDS....121

4-11: SCATTER PLOT OF $\delta^{18}O$ VERSUS TDS (ZOOM IN) 122
4-12: SCATTER PLOT OF HCO_3^- VERSUS ^{14}C 123
4-13: SCATTER PLOT OF $\delta^{18}O$ VERSUS ^{14}C 124
4-14: CLUSTER ANALYSIS SHOWING GROUNDWATER TYPES – KLEIN KAROO TMG AQUIFERS 127
4-15: ENVIRONMENTAL ISOTOPE FINGERPRINTING – TOPOGRAPHIC SECTIONS WITH $\delta^{18}O$ VALUES 131
4-16: COMPOSITE DIAGRAM SHOWING FINGERPRINT OF HOT SPRINGS 132
4-17: COMPOSITE DIAGRAM SHOWING FINGERPRINT OF DEEP BOREHOLES IN THE TMG 132
5-1: REGIONAL EXTENT OF TMG SUPER-AQUIFER 137
5-2: PIEZOMETRIC CONTOUR MAP – KAMMANASSIE MOUNTAINS 143
5-3: SCHEMATIC PRESENTATION OF CONCEPTUAL HYDROGEOLOGICAL MODEL 142
5-4: SCHEMATIC CROSS-SECTION THROUGH A MOUNTAIN VALLEY TO SHOW TYPE 2 SPRING AND WATER LEVEL RELATIONSHIPS 148
5-5: CONCEPTUAL MODEL – TMG TYPE 2.1 SPRINGS 149
5-6: LOCAL AND INTERMEDIATE SCALE FLOW SYSTEM BOUNDARIES 151
6-1: BOREHOLE VR7 - WATERLEVEL AND SW/Q VARIATIONS DURING CONSTANT DISCHARGE TESTS 161
6-2: BOREHOLE VR11 –WATER LEVEL AND SW/Q VARIATIONS DURING STEP-DRAWDOWN TESTS CONDUCTED IN 1991 AND 1997 168
6-3: EXAMPLES OF IRON-BACTERIOLOGICAL CLOGGING OF BOREHOLE EQUIPMENT 171
7-1: KAMMANASSIE MOUNTAINS CATCHMENT AREA 173
7-2: THE VERMAAKS RIVER LOCAL CATCHMENT AREA 174
7-3: ANNUAL ABSTRACTION FROM WELLFIELDS OF THE KKRWSS 176
7-4: TOTAL ABSTRACTION VARKIESKLOOF 177
7-5: TOTAL ABSTRACTION DROËKLOOF & OLIFANTS RIVIER 177
7-6: TOTAL ABSTRACTION VERMAAKS 177
7-7: TOTAL ABSTRACTION BOKKRAAL 177
7-8: MONTHLY SPRING FLOW VERSUS RAINFALL 181
7-9: RAINFALL VERSUS STREAM FLOW – VERMAAKS RIVER V-NOTCH 182
7-10: RELATIONSHIP BETWEEN STREAMFLOW AND RAINFALL – MARNEWICKS V-NOTCH 185
7-11: MEASURED VERSUS SIMULATED WATER LEVEL FLUCTUATIONS FOR VG3 (CRD METHOD) 188

7-12: MEASURED VERSUS SIMULATED WATER LEVEL FLUCTUATIONS FOR VR6 (CRD METHOD) 188
7-13: MEASURED VERSUS SIMULATED WATER LEVEL FLUCTUATIONS FOR VR7 (CRD METHOD) 189
7-14: MEASURED VERSUS SIMULATED WATER LEVEL FLUCTUATIONS FOR VR8 (CRD METHOD) 189
7-15: MEASURED VERSUS SIMULATED WATER LEVEL FLUCTUATIONS FOR VR11 (CRD METHOD) 190
7-16: CRD SIMULATION FOR THE PENINSULA AQUIFER 190
7-17: CRD SIMULATION FOR NARDOUW AQUIFER 192
7-18: EVAPOTRANSPIRATION (ET) AND GRAIN SIZE RELATIONSHIP SHOWN BY LYSIMETER RESULTS 192
7-19: TRANSPARENT OVERLAY WITH A/A_U CHARACTERISTIC LINES 193
7-20: DIAGRAM FOR DETERMINATION OF RECHARGE STAGES 194
7-21: RECHARGE CALCULATION USING CHLORIDE MASS BALANCE METHOD 197
7-22: SVF RECHARGE SIMULATION FOR THE NARDOUW AQUIFER 199
7-23: SVF RECHARGE SIMULATION FOR THE PENINSULA AQUIFER 200
7-24: RECHARGE AND STORATIVITY FOR THE NARDOUW AQUIFER USING THE EQUAL VOLUME METHOD. 201
7-25: RECHARGE AND STORATIVITY FOR THE PENINSULA AQUIFER USING THE EQUAL VOLUME METHOD. 202
7-26: RECHARGE SUMMARY FOR NARDOUW AQUIFER 204
7-27: RECHARGE SUMMARY FOR PENINSULA AQUIFER 204
7-28: VERMAAKS RIVER WELLFIELD AND RAINFALL RECHARGE TO VERMAAKS RIVER CATCHMENT 206
7-29: WATER BALANCE CALCULATION FOR THE NARDOUW AQUIFER USING THE RESERVE APPROACH 207
7-30: WATER BALANCE CALCULATION FOR THE PENINSULA AQUIFER USING THE RESERVE APPROACH 208
7-31: PROPOSED WATER BALANCE FOR THE VERMAAKS WINDOW 210
8-1: WELLMAN TITLE PAGE 217
8-2: MAIN MENU - WELLMAN SPREADSHEET 218
8-3: EXAMPLE OF THE GO TO BH1 SUBMENU 220

LIST OF TABLES

TABLES **PAGE**

3-1: GEOLOGICAL SUCCESSION IN THE GREATER OUDTSHOORN AREA.....69
3-2: SUMMARY OF DRILLING RESULTS: ADDITIONAL MONITORING BOREHOLES, EASTERN SECTION 95
3-3: SUMMARY PRODUCTION BOREHOLE DATA: 97
3-4: SUMMARY BOREHOLE INFORMATION: UNSUCCESSFUL PRODUCTION BOREHOLES, KKRWSS.....98
3-5: HYDROCENSUS DATA SOUTHERN KAMMANASSIE MOUNTAINS.....100
4-1: CFC DATING RESULTS – KAMMANASSIE MOUNTAINS, KLEIN KAROO118
6-1: RESULTS OF FC METHOD ANALYSIS OF VR7.....159
6-2: RESULTS OF FC METHOD ANALYSIS OF VR11.....160
6-3: RESULTS FC METHOD ANALYSIS OF DP28.....162
6-4: HYDRAULIC PROPERTIES OF THE TMG AQUIFERS IN THE KLEIN KAROO AREA 165
6-5: SUMMARY – SUSTAINABLE YIELD AND AQUIFER PARAMETERS, USING BEST AVAILABLE DRAWDOWN ESTIMATE 167
6-6: BOREHOLE EFFICIENCIES FROM STEP DRAWDOWN TEST DATA.....170
7-1: TOTAL GROUNDWATER ABSTRACTION, KKRWSS EASTERN SECTOR.176
7-2: SUMMARY OF ABSTRACTION FIGURES FROM THE KAMMANASSIE MOUNTAINS CATCHMENT FOR 1998.....179
7-3: SUMMARY OF AVERAGE ANNUAL SPRING FLOW FROM THE VERMAAKS AND MARNEWICKS SPRINGS.....180
7-4: RECHARGE IN MM/A FOR THE KAMMANASSIE – BASED ON HYDROGRAPH SEPARATION METHOD (JONKERSHOEK) 184
7-5: SUMMARY HYDROGEOLOGICAL INFORMATION FOR BOREHOLES VG3, VR6, 7, 8 AND 11 187
7-6: SUMMARY – CRITERIA USED FOR AREA RELATED RECHARGE CALCULATION 195
7-7: MRT VALUES FOR VERMAAKS WELLFIELD BOREHOLES 197
7-8: ESTIMATED MEAN, MAXIMUM AND MINIMUM RAINFALL RECHARGE TO THE VERMAAKS RIVER GROUNDWATER UNIT 205
8-1: SUMMARY RECOMMENDED PUMPING RATES OF PRODUCTION BOREHOLES, EASTERN SECTOR KKRWSS FROM PUMP TEST ANALYSIS 214

8-2: SUMMARY OF RECOMMENDED SUSTAINABLE BOREHOLE YIELDS: EASTERN SECTOR PRODUCTION BOREHOLES 223
8-3: SUMMARY – RADIUS OF INFLUENCE, VERMAAKS AND VOORZORG PRODUCTION BOREHOLES 232

LIST OF APPENDICES*

APPENDIX A: RAINFALL DATA

APPENDIX B: BACKGROUND INFORMATION

APPENDIX C: HYDROCHEMISTRY DATA

APPENDIX D: WELLFIELD CAPACITIES

APPENDIX E: WATER LEVEL DATA

APPENDIX F: SPATIAL VARIATION IN CHEMISTRY

APPENDIX G: COMPOSITE DIAGRAMS

APPENDIX H: X-Y SCATTER PLOTS

APPENDIX I: CLUSTER ANALYSIS DATA

APPENDIX J: FC METHOD ANALYSIS DATA

APPENDIX K: WELLMAN

APPENIDIX L: RECOMMENDATIONS

*** Appendices are available on the included CD**

GLOSSARY

Altitude effect: Progressive depletion of rainfall in **Oxygen-18** as clouds ascend a mountain range. Groundwater samples become progressively 'lighter', or enriched in **Oxygen-16**, with increase in altitude, see later in Hydrochemical finger-printing for more detail (CHAPTER 5).

Aquifer: Defined as a saturated geological unit that is permeable enough to yield economic quantities of water to wells (Kruseman and de Ridder, 1990).

Aquitard: A geological unit that is permeable enough to transmit water in significant quantities when viewed over large areas and long periods, but its permeability is not sufficient to justify production wells being placed in it (Kruseman and de Ridder, 1990).

Aquiclude: An impermeable geological unit that does not transmit water (Kruseman and de Ridder, 1990).

Balanced cross-sections: Structural profiles along measured sections (taking stratigraphic thickness into account).

Bilinear flow: In a finite conductive fracture, flow is linear from the matrix to the fracture as well as linear (i.e. parallel) inside the fracture towards the borehole (characterised by a slope of 0.25 on log-log paper at early time), *Van Tonder and Xu*, 1999.

Capillary rise: The flow / movement of soil moisture in an upward direction (De Laat, *et al.*, 1996).

Catchment (also drainage or river basin): The area contributing to the discharge at a particular river cross-section

CFB: abbreviation for Cape Fold Belt, a predominant tectonic domain in the Western and Eastern Cape.

Channelling: flow along pathways or channels (obstructions limiting flow).

Conceptual hydrogeological model A pictorial representation of a groundwater flow system, indicating the various water-bearing units, their inter-relationships and individual properties, boundary conditions and groundwater flow directions.

Continental precipitation: rainfall occurring above continents, i.e. land surface.

Detention storage: Water temporarily stored in pools or depressions on the surface (De Laat, *et al.*, 1996).

Durov Diagram: Based on percentage major ion milliequivalent values, the cations and anions together total 100%. The cation and anion values are plotted in the appropriate triangle and projected into the square main field.

Effective recharge: The total recharge minus the losses that occur subsequent to infiltration of groundwater (Bredenkamp *et al.*, 1995).

Environmental isotopes: Isotopes present in the environment: stable isotopes, Hydrogen (^{1}H), Deuterium (^{2}H), Oxygen-16 (^{16}O), Oxygen-18 (^{18}O), Carbon-12 (^{12}C) and Carbon-13 (^{13}C) and the radioactive isotopes, Tritium (^{3}H) and Carbon-14 (^{14}C).

Evapotranspiration: The combined effect of water losses induced by vegetation through the process of transpiration and evaporation losses from soil. In practice it is very difficult to distinguish between transpiration and evaporation losses.

Expanded Durov Diagram: In this diagram the cation and anion triangles are recognised and are separated along the 25 percent axes (represented by each small triangle) so that the main field is conveniently divided.

Fractures: Cracks, fissures, joints and faults, which are caused by (i) geological and environmental processes, e.g. tectonic movement, secondary stresses, release fractures, shrinkage cracks, weathering, chemical action, thermal action and (ii) petrological factors such as mineral composition, internal pressure, grain size, etc.

Fracture aperture: the distance between the fracture walls.

Fracture asperity: irregularities on the fracture surface.

Fracture connectivity: the degree of interconnection between fractures.

Fracture density: number of fractures in a known rock volume.

Fracture orientation: indicated by strike and dip measurements.
Fracture skin: thin zone at the fracture surface.

Governing Equation: Mathematical equations that describe groundwater flow and / or transport processes, developed from the fundamental principle of mass conservation of a fluid or solute.

^{2}H: Abbreviation for deuterium, a stable isotope of hydrogen, with a mass number of 2.

^{3}H: Abbreviation for tritium, a radioactive isotope of hydrogen, with a mass number of 3.

Hydrology: The science dealing with terrestrial waters, their occurrence, circulation and distribution, their physical and chemical properties and their interaction with the physical and biological environment, including man's effect on them (De Laat, *et al.,* 1996).

Infinite acting radial flow: During pumping, once the wellbore storage effects have declined, the wellbore progressive pressure transient reflects the pressure transmission into the aquifer. As time proceeds, the response is characteristic of conditions at increasing distance from the borehole with no influence of external boundaries. During this time the flow is radial (i.e. Theis model) and it is known as the infinite acting radial flow period (after v*an Tonder and Xu*, 1999).

Isotopes: Atoms of an element with the same atomic number but different atomic mass.

Interception storage: Precipitation intercepted by vegetation before it evaporates (De Laat, *et al.,* 1996).

Karoo Aquifers: Secondary aquifers, constituting alternating layers of fractured sandstone, siltstone and mudstone formations, intruded by dolerite sills and dykes. The highest yields are commonly associated with fractured sandstone layers, bounded by a dolerite sill/dyke.

KKRWSS - abbreviation for Klein Karoo Rural Water Supply Scheme.

Long-term sustainable yield of a borehole: This is the amount of water that can be abstracted from a borehole over a long period of time (usually longer than 1 or 2 years), without the water level reaching the position of the pump or main water strike (*Van Tonder and Xu*, 1999).

Matrix: Fractured formations usually consist of at least two sub-systems, namely fractures and matrix. The term matrix refers to the more porous part of a formation, consisting of primary porosity and/or secondary micro-fractures (*Van Tonder and Xu*, 1999).

Multi-component cluster analysis: Statistical data analysis tool, which matches the similarity of differences between variables, based on more than one parameter, e.g. the variables are boreholes and the parameters are hydrochemistry and environmental isotopes.

MWL: meteoric water line, see Appendix M.

Neotectonics: recent tectonic movements, reflecting the expansion of the East African rift system.

NGDB: abbreviation for National Groundwater Database.

^{18}O: Abbreviation for oxygen-18 a heavy isotope of oxygen.

Oblique keystone faulting: A type of faulting mechanism that produces a wedge shaped block (outlier), bounded by parallel, but oblique faults. Movement along bedding planes in the outlier is accomplished by rotation of the outlier beds.

Parshalls: Small flow measuring gauges that were built at the origin of the Vermaaks Spring to monitor springflow, while the v-notch was constructed onto the basement rocks and includes baseflow and surface water. The Parshalls were destroyed in the 1996 flood and will not be replaced, due to inaccurate measurements (comment G van Zyl, DWAF).

Percolation: Flow of soil moisture in a downward direction (De Laat, *et al.,* 1996).

Piper Diagram: A trilinear diagram where major ions are plotted in the two triangles of the diagram as cation and anion percentages of milli-equivalents per litre and the sums are each considered as 100 percent (Hem, 1989). The respective cation and anion locations for an analysis are projected into the diamond shaped field, which represents the total ion relationships.

pMC: per cent Modern Carbon, measure of ^{14}C concentration (see Appendix M).

Recharge: The portion of rainfall which reaches an aquifer irrespective of whether it follows a preferential flow path via fractures, or drains through a soil column, infiltration of standing water in river channels or local surface depressions (Bredenkamp *et al.*, 1995).

Secondary aquifer: Contains porosity that was introduced after deposition of the rock mass, i.e. fractures, dissolution features or weathering.

TMG: abbreviation for Table Mountain Group (hydrogeological unit).

Water balance: A special case of a mass-balance equation, which is the basis of the continuity, momentum, and energy equations for various hydrologic processes. According to the theory, outflows are always negative and inflows positive (De Laat, *et al.*, 1996).

CHAPTER 1: INTRODUCTION

1.1 BACKGROUND

Groundwater is a valuable resource and is especially important as a supply of drinking water, providing 75% of drinking water supplies in Europe, more than 50% in the USA and 15% of the bulk water supply in South Africa (Braune *et al.*, 1998). In South Africa, more than 300 towns are either fully or partially dependent on groundwater.

For many years in South Africa groundwater has been regarded as a cheap source of water supply requiring little or no treatment. A lack of understanding of the occurrence, movement and recharge of groundwater, and its 'private water' legal status, however, frequently led to the unsustainable use of this resource. The consequent failure of boreholes in many instances has unfortunately promoted the view that groundwater is an unreliable water supply which should be replaced as soon as possible by more reliable surface water supplies (Braune *et al.*, 1998).

Fortunately the priority of groundwater as a national water resource has changed considerably through the present government's commitment to providing adequate drinking water to all South Africans, especially those residing in the rural areas. Moreover, South Africa faces a severe problem of rapid urbanisation. This is leading to an increase in demand for an adequate supply of sustainable drinking water and irrigation water. Consequently, the development of the groundwater resources of South Africa will increase in the future, especially in semi-arid areas with no reliable perennial rivers and where surface water is thus insufficient to provide the water requirements. The semi-arid Klein Karoo region in the Southern Cape, approximately 60 km inland from the coast, is one of these regions where groundwater with its widespread, albeit mostly low yielding occurrence, has become a national asset of strategic importance.

The growing importance of groundwater is also strongly reflected in the new National Water Act as well as the new Water Services Act. Water resources, including groundwater, are now seen as an indivisible asset with the National Government as its custodian to ensure that development, apportionment, management and use of the resources are carried out, using criteria of public interest, sustainability, equity and efficiency of use (adapted from Braune *et al., 1998).* This contrasts strongly with groundwater's past 'private water' legal status. Current and future groundwater research in South Africa will continue to focus on the exploration, development and management of our vital groundwater resources, with the

added emphasis on integrated management and stakeholder participation, to ensure the sustainability of this resource (adapted from Braune *et al., 1998)*. Groundwater management no longer focuses on the management of individual boreholes, but integrated management of the entire regional aquifer system.

Ninety percent of all South African aquifer systems are fractured secondary aquifers, of which the Table Mountain Group (TMG) sandstone aquifer in the Western Cape is the second largest aquifer system (next to dolomite aquifers, in the Northwestern and Northern and Gauteng Provinces) in South-Africa (Vegter, 1995). In secondary aquifers, such as the TMG Aquifer, groundwater occurs in discrete fractures, in which the yield and distribution varies according to the fracture geometries and characteristics which are highly variable and difficult to quantify in most cases. On the other hand, groundwater in porous aquifers is much easier to quantify as groundwater is contained in pore spaces between grains, with a generally uniform distribution. For the above reasons secondary aquifers present special problems in terms of groundwater balance and long-term yield calculations, because it is very difficult to accurately define their geometry and hydraulic properties. Management of fractured aquifers by means of conventional methods often leads to over-utilisation, with serious implication for water balance calculations.

1.2 OBJECTIVES AND AIMS OF THE RESEARCH

The TMG sandstones form a major lithological unit in the Western and Eastern Cape Provinces, forming an arc of mountain ranges stretching from the Cedarberg Mountains near Clanwilliam in the north-west to the Baviaanskloof Mountains near Port Elizabeth in the east. The Klein Karoo study area is situated in a wide basin surrounded by TMG Mountain ranges in the north and south (Figure 1-1). The Klein Karoo area is semi-arid with little reliable perennial surface water and relies greatly on the development of groundwater resources for economic growth; understanding of the groundwater flow system is therefore essential in order to optimally manage the TMG Aquifers, associated springs and the impacts of irrigation.

Diagenesis and regional scale tectonic movements during the Cape Fold Belt (CFB) orogeny compacted and deformed the sediments of the TMG to such an extent that most of the primary porosity was lost. It was therefore assumed that groundwater can be found only in locally recharged, shallow fracture systems. These facts, together with the semi-arid nature of the Klein Karoo region, with rainfall varying between 200 and 400 mm/a, gave rise to the development of a conceptual hydrogeological model where relatively small quantities of recharge and storage were postulated. Consequently, very limited resources of available groundwater for abstraction were suggested for the TMG Aquifer of the Klein Karoo.

FIGURE 1-1: LOCALITY MAP

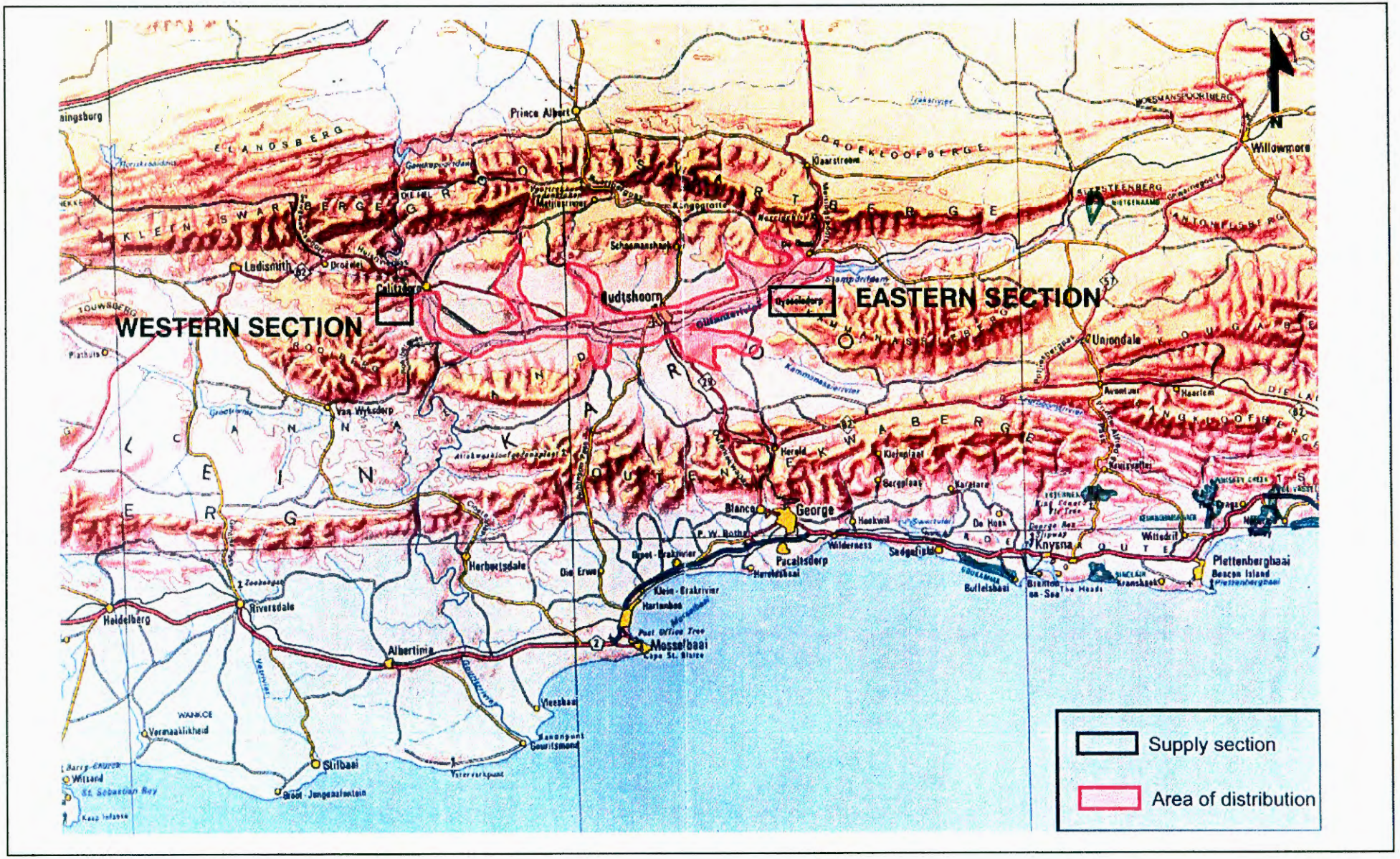

The scientific assumption of this research rejects the conventional conceptual model of a shallow, localised groundwater flow system. Further, the research documented in this report postulates that, in addition to the local shallow system, there also exists a regional flow system, producing regional flow lines, which are interconnected with secondary faults, which may be interconnected with the local shallow fracture system.

These main hypotheses lead to the following secondary hypotheses:

- If there is an interconnection between the regional, secondary and local fracture systems, then there may be a regional groundwater flow system on which large-scale development of groundwater resources could be based.
- The shallow fracture systems would then be regarded as local recharge systems.
- The higher precipitation and snowmelt, occurring at higher altitudes would percolate into the local system, in turn feeding the regional system.
- *Thus the mean regional recharge potential may be much higher than presently assumed and needs to be quantified.*

In conclusion, since the TMG Aquifer is one of the most important aquifers in the Klein Karoo and one of the most significant in the Western Cape, understanding this aquifer system will guide future groundwater exploration programs. In addition, improved management of existing groundwater supply schemes, supplying water for agricultural and domestic use, eg. the Klein Karoo Rural Water Supply Scheme (KKRWSS, see Figure 1-1), will result.

The aims and objectives of this research are to investigate and develop a **conceptual model** for groundwater flow in the TMG fractured aquifer of the Klein Karoo in order to **quantify the inter-regional and local water-balance** in order to **forecast** the **response** of this aquifer system to different scenarios of extraction and recharge.

<u>The specific objectives are:</u>

1. To understand the hydrogeology of the Table Mountain Group sandstone fractured aquifers.
2. To understand and calculate the groundwater balance of the Klein Karoo Region.
3. To develop an effective tool by which the water development plans for the Table Mountain Group sandstone aquifers can be promoted.

It is intended to prove that the TMG Aquifer is a regional aquifer by hydrochemical and environmental isotope fingerprinting of groundwater types and flow systems. Thereafter, the

conceptual hydrogeological model developed for the Kammanassie Mountain Range would be applied to calculate the balance for this aquifers, in order to optimise management of the production boreholes of the Eastern Section of the KKRWSS.

Various management tools are used and developed during the course of this research in the format of a series of Microsoft EXCEL spreadsheets for aquifer management.

1.3 SITE SELECTION

The study area centres on the catchment basin of the Olifants River from Calitzdorp in the west to Dysselsdorp in the east (see Figure 1-1). The area exhibits a variety of fault systems controlling the occurrence of hot springs, e.g. Toorwater, Warmwaterberg and Calitzdorp Spa, near Uniondale, Barrydale and Calitzdorp, respectively. Numerous previous studies in the region provide a good source of background information. The existence of deep boreholes and several hot and cold springs, provide good opportunities for environmental isotope and hydrochemical finger-printing of different groundwater types and flow paths within the TMG Aquifers.

TMG areas in the Klein Karoo generally occur in mountainous terrain, which is commonly incorporated into conservation areas, mostly managed by the Department of Culture and Environment (DECAS). The existence of numerous small magnitude cold springs originating at the prominent Cedarberg Shale (C/S) marker layer, separating the Nardouw Subgroup and Peninsula Formation of the TMG, gives cause for concern that lowering of the water table due to abstraction may reduce springflow, which in turn impacts on existing irrigation practices and vegetation. The inter-relationships between different groundwater flow paths therefore needs to be understood in order to determine the impact, if any, of deep abstraction on vegetation and stream baseflow.

In addition to the promising hydrogeological conditions, another major advantage in terms of available data for this study is the existence of a Government Groundwater Supply Scheme, the Klein Karoo Rural Water Supply Scheme (KKRWSS), within the study area. The KKRWSS supplies purified domestic water at subsidised rates to the town of Dysselsdorp, farms in the Olifants River Valley, tributary valleys downstream of the Stompdrift and Kammanassie Dams and the Gamka River Valley downstream of Calitzdorp.

1.4 THE KLEIN KAROO RURAL WATER SUPPLY SCHEME

Construction on the KKRWSS first started in 1984 and it was commissioned in 1987. The Department of Water Affairs and Forestry (DWAF) funded the KKRWSS and is also

responsible for its management. The KKRWSS is designed to supply up to 4.7 x 10^6 m^3/a of purified water and comprises an Eastern (Dysselsdorp) and Western (Calitzdorp) Sector, with groundwater being abstracted from 18 production boreholes in seven wellfields.

A re-evaluation of existing pumping test results, aquifer water levels, volumes abstracted and rainfall for three years prior to June 1995 indicated that the sustainable yield of the KKRWSS was actually closer to **1.1 x 10^6 m^3/a (3050 m^3/d)** (Kotze, 1995). This is considerably less than the originally estimated **4.7 x 10^6 m^3/a (12 900 m^3/d)** (Mulder, 1995), which forms the design criteria for the KKRWSS. Water demand from the KKRWSS has also differed substantially from initial projections. The considerable difference in sustainable yield calculations can be attributed to the following (Kotze *et al.*, 1999):

- Differences in management scenarios between the Nardouw and Peninsula Aquifers (it was assumed that the TMG Aquifer was one uniform aquifer).
- Interconnectivity between boreholes and wellfields.
- Clogging of borehole screens by iron-oxidizing bacteria.
- Concerns over impact of abstraction on springflow.
- Inefficient borehole construction and drilling.
- Lack of a water balance. The inputs versus the outflows to the groundwater system were therefore unknown.
- Poor understanding of the regional groundwater flow regime and conceptual hydrogeological model for TMG Aquifers.

The eighteen production boreholes and six observation boreholes are monitored by means of telemetry. The following parameters can be observed at any time, for any of the boreholes connected to the system:

- Groundwater level (pumping and rest). The measured groundwater levels obtained from telemetry are calibrated with manual water level measurements on a monthly basis.
- Pumping rate.
- Volume abstracted.
- Time of abstraction - time pumps on/off.

Over the nine years of abstraction from the KKRWSS, several management problems have occurred, e.g. over-abstraction, decline in borehole efficiency, iron-oxidizing bacteriological clogging of some borehole screens, the boreholes themselves and concerns that nearby springs originating on the C/S band in the Kammanassie Mountains will dry up. Therefore, for effective management of groundwater abstraction from the KKRWSS, it is required that

the conceptual hydrogeological model and water balance are more fully understood in order to estimate most or more of the following questions:

- How much groundwater is available for abstraction?
- How many boreholes are required to satisfy the demand and at what spacing?
- What is the annual recharge?
- How does groundwater flow and what is the radius of influence of an abstraction borehole?
- What is the impact of abstraction on springflow and baseflow in streams?
- What are the risks associated with abstraction?
- At what rates must boreholes be pumped to minimise negative effects on the aquifer system and environment?

In order to manage an aquifer, the groundwater flow system needs to be fully understood, i.e. the conceptual hydrogeological model of the aquifer under investigation needs to be defined. A conceptual hydrogeological model normally includes the following:

- Hydrostratigraphic units, i.e. the different geologic formations and their water bearing characteristics.
- Aquifer parameters.
- Groundwater flow boundaries.
- Recharge areas and quantity.
- Water balance.
- Piezometric contour map indicating groundwater flow directions.

The developed hydrogeological conceptual model and management tools are critical for the management of the DWAF wellfields in the Kammanassie Mountains and the KKRWSS and any future development thereof. Further, development of a conceptual hydrogeological model will also point out future research areas. Finally, the results of this research will contribute significantly to the management of TMG Aquifers in general in the Western Cape, and for similar hydrogeological units worldwide.

CHAPTER 2: INVESTIGATION APPROACH AND RESEARCH METHODOLOGY

The flow diagram presented in Figure 2-1 (over page) summarises the research approach followed. The study incorporated the following main steps in the research approach (see Figure 2-1):

- Desk study
- Fieldwork
- Satellite lineament mapping and interpretation
- Data collation
- Interpretation of hydrogeological and hydrochemical data
- Definition of the conceptual hydrogeological model
- Design of an aquifer management strategy.

The different components of the research approach are discussed below.

2.1 DESK STUDY

The desk study involved a review of all relevant available information, including DWAF's National Groundwater database (NGDB), previous sampling surveys, hydrocensus and remote sensing data and a literature survey.

Initially it was assumed that the NGDB would deliver a considerable amount of significant data. This assumption, however, was proven wrong for various reasons. All information captured on the NGDB for the area covering 33°18' to 34°04' E and 21°13' to 23°15' S was obtained. The NGDB data included a total of 1482 boreholes and the information provided dates back to 1960. Very little of the above information, however, contained data on boreholes drilled in the TMG, other than the private boreholes around the Kammanassie Mountains and production boreholes of the KKRWSS. Further, the NGDB data sets contain a considerable amount of duplications and incorrect data.

Consequently, various hydrocensus, environmental isotope surveys and hydrochemical surveys were carried out in the study area to supplement the database for this study.

FIGURE 2-1: FLOW DIAGRAM – RESEARCH APPROACH

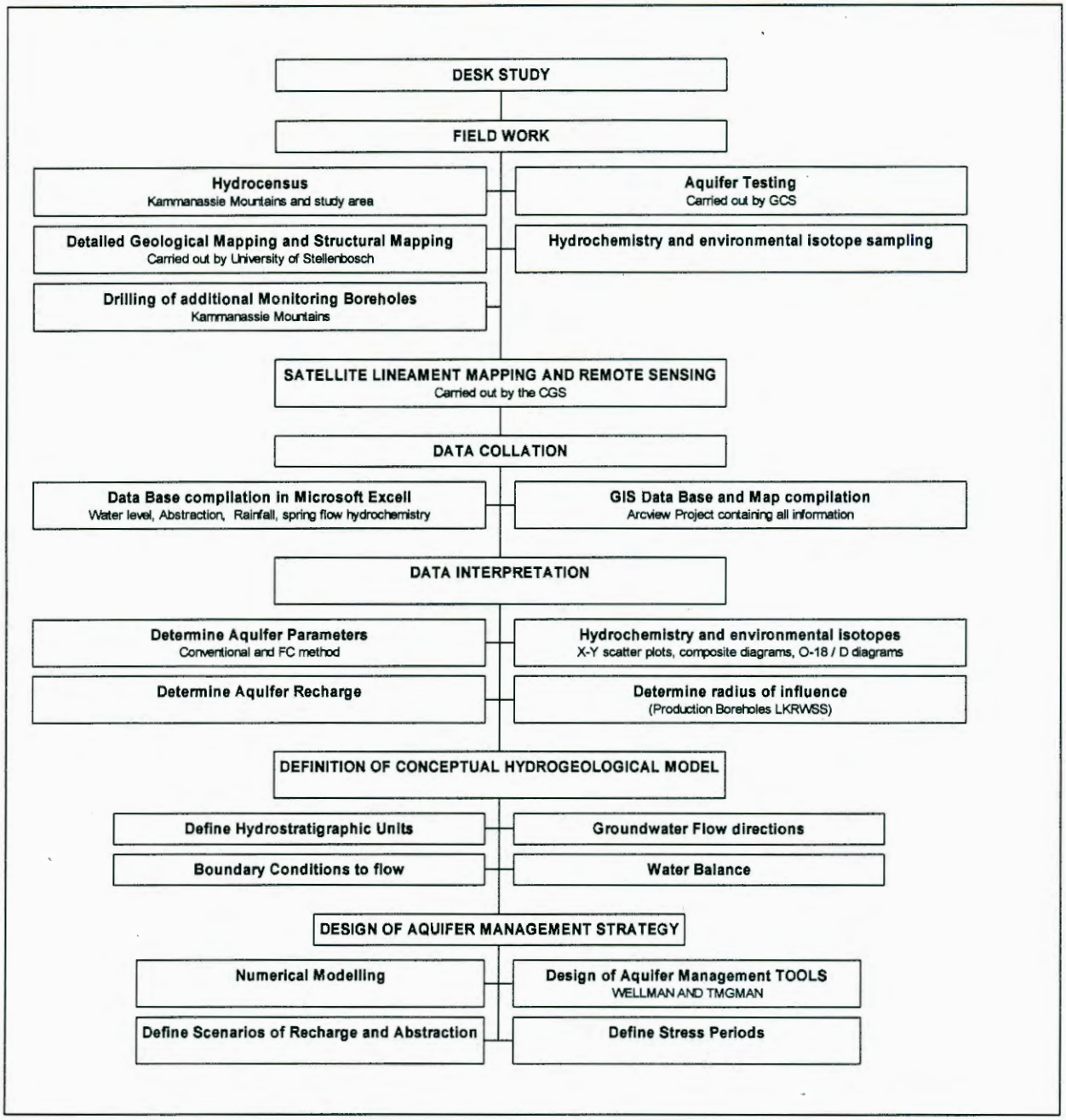

In order to aid screening of the NGDB data sets, planning of the hydrocensus and data analysis, all NGDB data points were plotted onto a series of GIS maps. To facilitate better interpretation and data handling, the study area was divided into four sub-areas, each covering four 1: 50 000 topographic sheets. Figure 2-2 shows all the topographic maps included in the regional study area, together with the subdivision into the four sub-areas. The local study area is composed of those topographic sheets covering the Kammanassie Mountains (see Figure 5-6, later).

FIGURE 2-2 : SPATIAL DISTRIBUTION OF BOREHOLE DATA

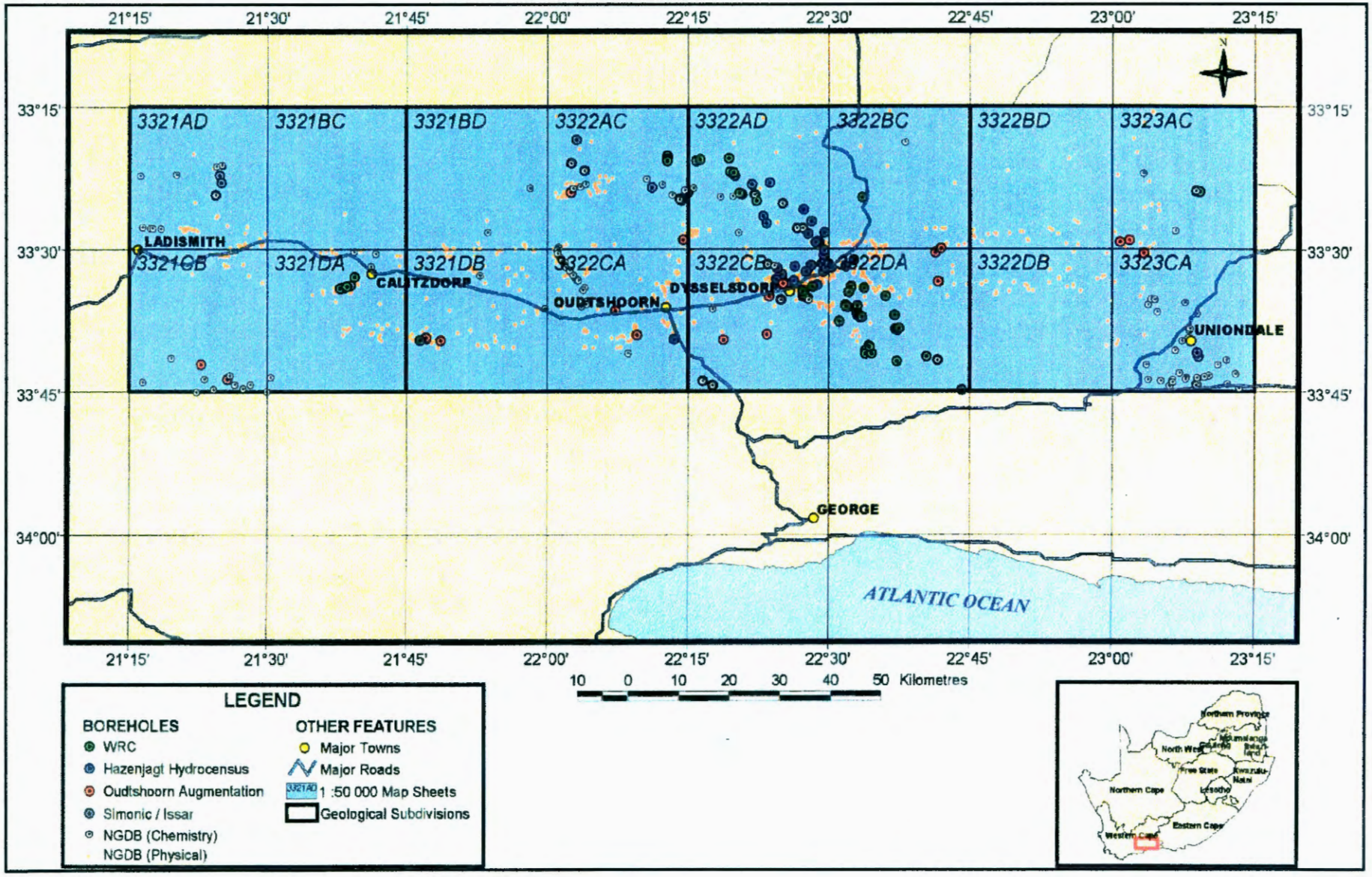

Figure 2-2 indicates the spread of existing TMG data points obtained from various sampling surveys over the study area. Hydrocensus and sampling survey data from a number of previous studies were screened to select relevant data whereafter it was captured in a suitable database. These studies included:

- DWAF hydrocensus, Calitzdorp (Meyer *et al.*, 1989).
- A hydrocensus carried out by SRK Consulting during October 1998 as part of the greater Oudtshoorn augmentation study (Kotze *et al.*, 1999).
- Hazenjagt hydrosensus carried out by DWAF, Mike Smart.
- Hydrocensus carried out by B Dyasan (DWAF, hydrocensus sheets – Appendix D, SRK Report No 230827/2), around the southern flanks of the Kammanassie Mountains.
- Field trip during November 1998, visiting the Rooiberg Nature Conservation area with Tom Barry (DECAS).
- Sampling survey by Issar and Simonic during January 1994 (data obtained from DWAF).
- Sampling survey of hot springs in the Western Cape by Prof. Issar and Simonic (Issar, 1994).
- Sampling survey of hot springs and groundwater seepage along the major mountain passes in the Klein Karoo to establish the altitude effect.

A comprehensive literature search was carried out on the following:

- The application of environmental isotopes and hydrochemistry in hydrogeological aquifer conceptualisation.
- The application of numerical groundwater flow modelling for regional aquifers.
- Numerical modelling techniques in general.
- Methodologies available for the management of regional fractured aquifers.
- Estimation of recharge for regional fractured aquifers.
- Management of fractured aquifers.
- Parameter estimation for fractured aquifers.

The major findings of the literature study are incorporated in the text where appropriate throughout this report.

A considerable amount of research work was carried out on the TMG in the Klein Karoo during the development of the KKRWSS. Initially, the Institute of Groundwater Studies (IGS) at the University of the Orange Free State was involved with geohydrological investigations in order to determine the groundwater potential of the TMG Aquifers of the Kammanassie Mountains and to design the drilling program (Kirchner *et al.*, 1984). In 1985 DWAF

commenced with an exploration drilling program at Dysselsdorp and Calitzdorp in order to determine the groundwater supply potential of this area for possible municipal supply.

Other important contributions related to the KKRWSS include the following:

- Meyer and Dyason (1989) conducted a hydrosensus in the vicinity of the Eastern Sector of the KKRWSS (Kammanassie Mountains) and designed a groundwater monitoring program for the KKRWSS.
- Meyer (1990) sited boreholes for the KKRWSS.
- Mulder (1991) carried out water-balance calculations for the Vermaaks River, Kammanassie Mountains (Eastern Sector of the KKRWSS).
- Bredenkamp (1995) derived an estimate of the groundwater recharge of the Vermaaks River catchment.
- Mulder (1995) summarised the recommended borehole yields for the production boreholes and proposed a management plan for the KKRWSS.
- Kotze (1995) carried out a comprehensive overview of the KKRWSS and recommended reduced pumping rates for the KKRWSS production boreholes.
- Kotze and Rosewarne (1996 and 1997) gave a hydrogeological overview of the KKRWSS and its aquifers.
- Jolly (1996, 1998) investigated existing management and monitoring systems of the KKRWSS.
- Kotze and Rosewarne (1999) provided a summary of potential groundwater augmentation schemes to the existing KKRWSS.

Projects contributing to the understanding of the hydrogeology of TMG Aquifers in general and in the Klein Karoo area include the following:

- The DWAF initiated a project to characterise the groundwater resources of the TMG Aquifers, under the leadership of Mr. S. Meyer during 1990.
- Weaver *et al.* (1996) investigated the application of geochemistry and isotopes in resource evaluation in the TMG.
- Issar (1994, 1995, 1996) initiated investigations on the TMG being considered a regional aquifer.
- Verhagen (1997) investigated the application of environmental isotopes in conceptualising flow in the TMG (Klein Karoo).
- Drilling of additional monitoring boreholes (1998) in the Kammanassie Mountains for groundwater monitoring purposes during pump testing carried out by Groundwater Consulting Services.

- Several SRK Consulting projects by Kotze and Rosewarne (1997, 1999) with respect to groundwater development in TMG in the Western Cape, i.e. Hermanus and Hex River Valley.
- A joint venture between SRK Consulting and Umvoto investigated the exploitation potential of the TMG Aquifers in the vicinity of Citrusdal, in the CAGE study.
- Current WRC project on a TMG Aquifer Handbook.

2.2 FIELDWORK

A large amount of fieldwork, including the following:

- Aquifer testing
- Hydrocensus and hydrochemical sampling surveys of existing boreholes
- Detailed structural analysis of the western part of the Kammanassie Mountains
- Drilling of additional monitoring boreholes by DWAF in the Kammanassie Mountains

were carried out during the course of this project in order to achieve the research objectives and in particular to assist with definition of the conceptual hydrogeological model for the TMG Aquifer of the Kammanassie Mountains.

2.2.1 Aquifer testing

Pump testing carried out at the production boreholes of the Eastern Section of the KKRWSS, is used to determine the following for the aquifers and production boreholes of the Eastern Section of the KKRWSS:

- The hydraulic properties, i.e. storativity (S) and transmissivity (T).
- The sustainable yield of the production boreholes, based on the analysis of pump test data only (later contrasted with sustainable yield calculated for each borehole from other methods).
- The borehole efficiency.

Pump testing data for the production boreholes of the KKRWSS were obtained from Mulder (1995) and recent aquifer tests performed by Groundwater Consulting Services (GCS) documented in Jolly (1998). All the production boreholes, except one, are drilled in the TMG. All the available pump testing data, i.e. constant yield, recovery and step drawdown data for the production boreholes of the Eastern Sector of the KKRWSS are summarised in Appendix I.

The aquifer testing includes the following types of tests:

- Step drawdown tests: Short duration multi-rate tests that provide information on the hydraulic conditions in the immediate vicinity of the well. The borehole is pumped at a constant rate for a period of time (normally 60 to 100 minutes). Thereafter pumping rate is increased for an equal time followed by a third, fourth; etc. step of equal duration with the pumping rate stepped up each time. During this test the water level over time are measured. From these tests the following are determined:

  - The well loss coefficients for an estimate of the efficiency of the borehole at the operational pumping rate. This coefficient also supplies information on whether the borehole needs (further) development and/or whether its yield has deteriorated with time (Kirchner *et al.*, 1995).
  - The maximum potential of the borehole, its optimum operating conditions and the specification of permanent pump installation based on the yield drawdown characteristics (Kirchner *et al.*, 1995).
  - This test is used mainly as a 'calibration' test to determine the optimum pumping rate for the ensuing constant discharge test (Woodford, 2001).

- Constant discharge test: During this test the borehole is pumped at a constant rate, determined from the results of the step drawdown test analysis for a predetermined period of time. The pumping rate for the main test is chosen so that the pumping water level will not drop below the pump intake. The decision of how long a borehole should be pumped during the constant rate test depends on the degree of certainty that is required regarding the sustainable yield of a borehole or a pumping scheme. Most of the pumping tests in South Africa are conducted for short durations of less than 48 hours, often because of the expenses associated with longer duration tests. Considering the total cost of the KKRWS and the high risk of failure, test duration of 72 hours and longer applies in all cases. During each test the water level, groundwater electrical conductivity (EC) and borehole yield is measured according to a predetermined time schedule. From this test the long-term aquifer characteristics and sustainable yield of the borehole is determined.

- Recovery test: Measurement of water level recovery according to a predetermined time schedule directly after the pump is switched off at the end of the constant rate test. The recovery of the water level should be measured for a period equal to the duration of the main test or until the water level has fully recovered, whichever occurs first. From this test it is possible to confirm the aquifer parameters determined during the constant discharge

test and to determine the relationship between the length of pumping time versus time allowed for recovery, i.e. the pumping schedule.

2.2.2 Hydrocensus and hydrochemical sampling

Hydrocensus and hydrochemical sampling surveys were carried out to collect data in order to assist with the definition of the conceptual hydrogeological model and to prove the following working hypothesis:

Boreholes intercepting groundwater along regional flow lines, which serve as preferential flow paths, will deliver sustainable high groundwater yields, recharged over a long period of time over a large area and may travel to the surface from great depths below the surface. On the other hand, local faults and fractures obtain their recharge within local catchments and will yield much less water in the long-term.

The existence of a groundwater flow at depth along regional primary and secondary systems is assumed on the basis of a reconnaissance survey carried out under the supervision of Prof. Issar. This survey included the sampling for isotopic as well as chemical analysis of hot springs emerging in the Western Cape TMG region (including the Klein Karoo study area), along fault systems. Figure 2-3 over page shows the positions of the three hot springs in the Klein Karoo sampled during this survey, e.g. Warmwaterberg (WBG), Calitzdorp Spa (C/S) and Toorwater (T/W), situated at Barrydale, Caltizdorp and Uniondale respectively. Figure 2-3 also shows the location of mountain passes, where seepage samples were collected along a profile cross-cutting the pass, to determine the altitude effect.

A selection of springs, boreholes and seepages in the mountain passes during the winter was sampled in order to give an adequate coverage for regional interpretation. The spring samples are referred to as the Simonic - TMG samples (see Table A-17, Appendix A) and represent recently recharged groundwater.

All the springs, as well as deep (depths varying between 250 and 300 m) and shallow boreholes occurring in the TMG Aquifer of the Klein Karoo (mainly the production boreholes of the KKRWSS) are sampled on more than one occasion, in order to fingerprint the groundwater flow system.

FIGURE 2-3: HOT SPRINGS AND SEEPAGE SAMPLING POSITIONS

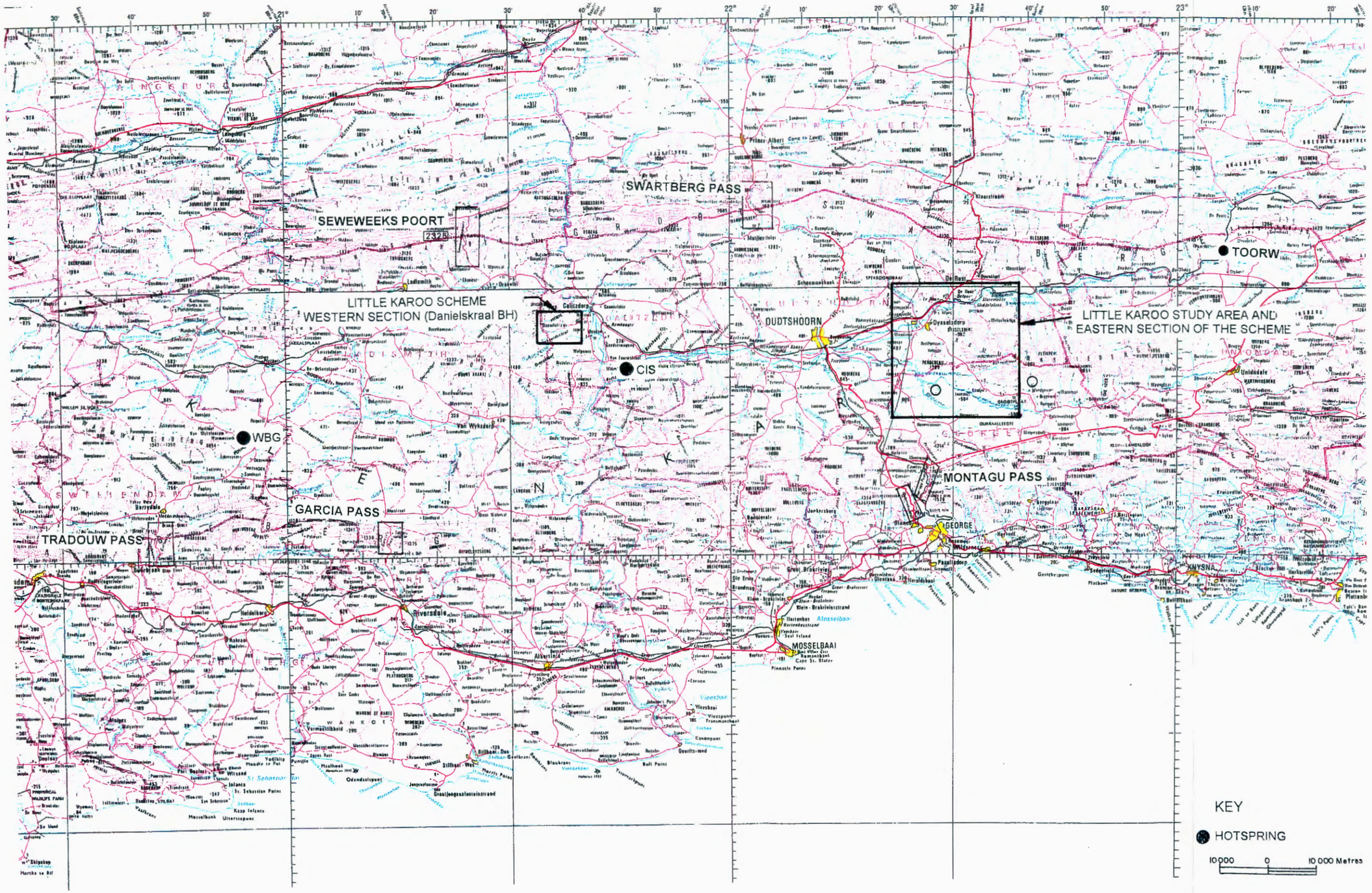

- **Sampling protocol**

The same sampling protocol was applied during each sampling survey. Macro and trace element and stable isotope samples oxygen-18 (^{18}O) and deuterium (^{2}H) were taken in 250 ml plastic bottles, filled to the top.

Tritium (^{3}H) samples were taken in new 1000 ml, amber glass bottles to avoid contamination. The bottle is rinsed with the sample water, completely filled and tightly stoppered. The water is not treated in any way before sampling.

To obtain samples adequate for conventional radiocarbon analysis, it was necessary to extract carbonate in the field from 300 litres or more of this low TDIC water. This was made possible by using the polyethylene bag method of precipitation, which allows up to 150 litre of water to be treated in each bag at the pump outlet (Verhagen *et al.* in preparation). Saturated (carbonate free) sodium hydroxide is added to the samples, to ensure an alkaline solution (indicated by pink colour by using phenolphthalein indicator) whereafter Barium chloride is added to allow Barium carbonate to precipitate (see Figure 2-4). The samples are then left to allow the precipitate to settle whereafter the excess water is drained and the precipitate transferred to polyethylene bottles and submitted for analysis.

For hydrogeological purposes, $\delta^{13}C$ usually is measured on the same precipitate sample taken for radiocarbon and requires no separate sampling.

FIGURE 2-4: ^{14}C SAMPLING TECHNIQUE

$HgCl_2$ was added, as stipulated by the Institute for Water Quality Studies (IWQS), to preserve macro-element samples. Field measurements taken included temperature, electrical conductivity (EC), and pH, alkalinity (Alk) and dissolved oxygen (DO) as well as water level and borehole / spring yield measurements where possible.

Additional information, i.e. volume of abstraction, irrigation practice, depth of borehole, etc, was obtained during the hydrocensus (personal communication with farmers).

- **Sample analysis**

Macro and trace element analyses were carried out by the IWQS and included the following constituents:

Macro element analysis: pH, EC, Total Alkalinity (TAL), Total Dissolved Solids (TDS), Calcium (Ca), Magnesium (Mg), Sodium (Na), Potassium (K), Silicon (Si), Fluoride (F), Chloride (Cl), Sulphate (SO_4), Nitrate (NO_3), Phosphate (PO_4) and Ammonium (NH_4^+).

Trace element analysis: Iron (Fe), Manganese (Mn), Beryllium (Be), Cadmium (Cd), Cobalt (Co), Chrome (Cr), Copper (Cu), Arsenic (As), Mercury (Hg), Boron (B), Molybdenum (Mo), Nickel (Ni), Lead (Pb), Barium (Ba), Strontium (Sr), Aluminium (Al), Vanadium (V), Zinc (Zn) and Titanium (Ti).

The only drawback encountered with sampling analysis conducted by the IWQS was that the trace and macro element analysis of the July 1997 sampling survey was spoilt since some samples were analysed twice for macro elements, while the others were analysed twice for trace elements. The DWAF resampled the boreholes sampled during the July sampling survey in March 1998 for trace and macro elements, but not for environmental isotopes. The July 1997 data set is therefore incomplete for macro and trace elements samples and the March 1998 data set for environmental isotopes. Further the January 1996 trace element sample set was lost. The trace element data are therefore very limited.

Environmental isotope analysis was carried out at the Schonland Research Institute, Wits under the supervision of Prof. Verhagen. These included: carbon-14 (^{14}C), carbon-13 (^{13}C), oxygen-18 (^{18}O), deuterium (^{2}H) and tritium (^{3}H).

Results of the field measurements, environmental isotope and hydrochemistry analyses data, together with the hydrocensus data are summarised in Appendix A.

- **Sampling surveys carried out during investigation**

Figure 2-5 shows the spatial distribution of the various data points obtained from the following sampling surveys carried out during this investigation:

- January 1996: Sampling of the hot springs in the Klein Karoo (Figure 2-3), selected production boreholes of the KKRWSS, cold springs in the Kammanassie Mountains and private boreholes on the southern flanks of the Kammanassie Mountains (chemical analyses in Tables A-1 to A-4, Appendix A).
- July 1997: Resampling of selected production boreholes of the KKRWSS (see Figure 2-5) and hot springs and seepages (Figure 2-3 and chemical analyses in Tables A-5 to A-7, Appendix A).
- Resampling of production and selected boreholes on privately owned land for trace element analysis, March 1998 (chemical analyses in Tables A-8 and A-9, Appendix A).
- June 1998: Extensive hydrocensus and hydrochemical and environmental isotope groundwater sampling program, carried out to investigate the flow relationships between the Nardouw and Peninsula Aquifers, and to estimate the extent of abstraction on farms surrounding the Kammanassie Mountains. During this survey a hydrocensus and sampling program along the Swart and Outeniqua Mountain Ranges were also carried out in order to define the regional water table of the TMG Aquifer in the Klein Karoo (chemical analyses in Tables A-13 to A-15, Appendix A). Relevant data obtained from hydrocensus are summarised in Table 3-5.
- November 1998: sampling of additional monitoring boreholes drilled by DWAF at the Eastern Sector of the KKRWSS (chemical analyses in Tables A-10 to A-12, Appendix A).
- August 1998: Collection of rain samples after a rainfall event. These samplings were analysed for environmental isotopes of ^{18}O and ^{2}H as well as chloride (chemical analyses in Table A-16, Appendix A).

2.2.3 Detailed structural analysis of the Kammanassie Mountains

The Geology Department of the University of Stellenbosch has carried out a detailed structural analysis of the Kammanassie Anticline (western portion of the Kammanassie Mountains (Hälbich *et al.*, 1995). The following summarises the main aspects of this investigation:

- A fold, fault and joint analysis of the TMG formations to determine porosity.
- A study of the kinematic relationships between folding and faulting in the different formations of the TMG and the hydrogeological implications thereof.

FIGURE 2-5: LOCALITY MAP SHOWING SAMPLING / HYDROCENSUS BOREHOLE POSITIONS RELATIVE TO GEOLOGY

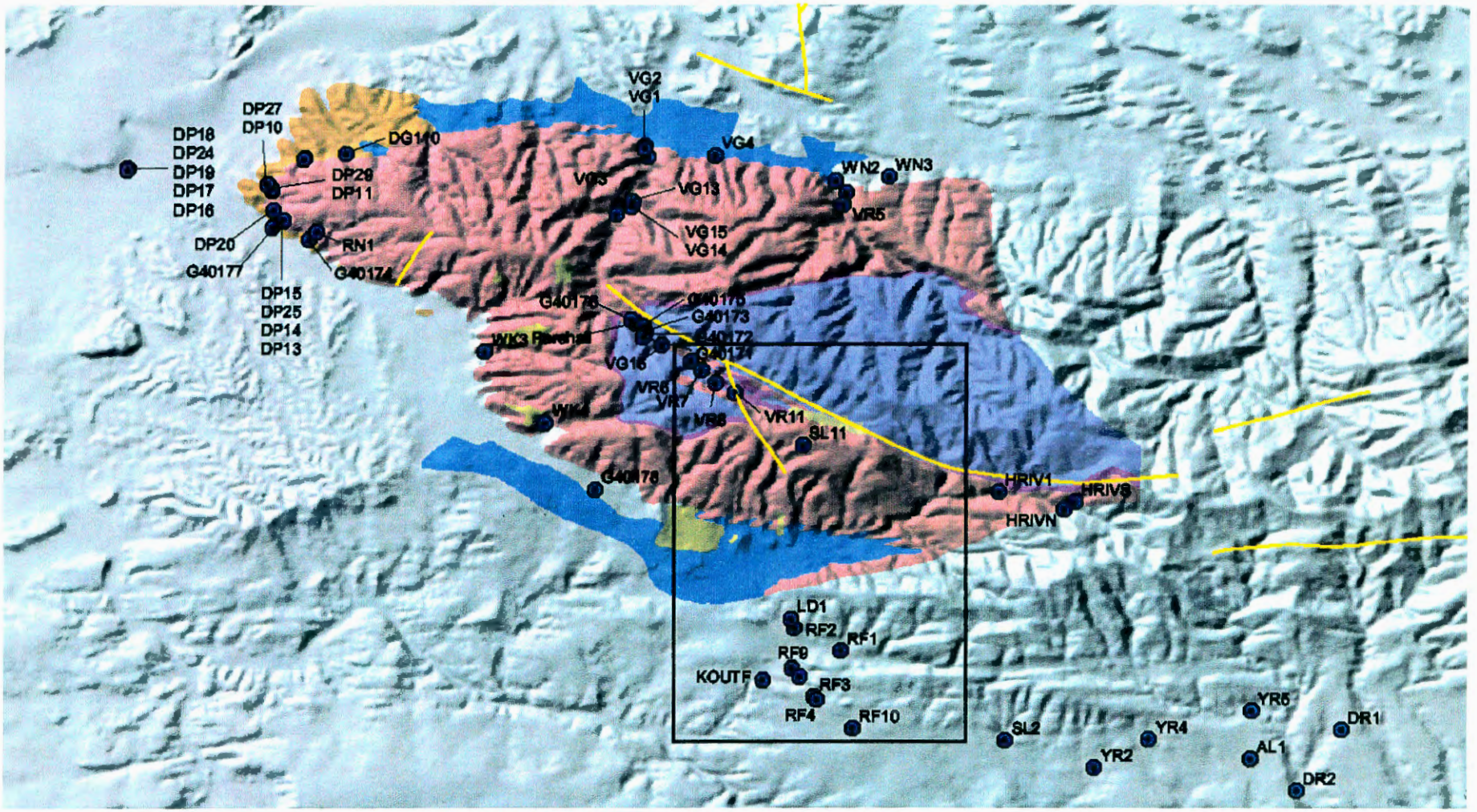

Geology, represents Hälbich (1995), geological mapping of the Kammanassie Mountains, for more detail, refer to Figure 3-10.

- The kinematics of faulting that produced the observed structures.

2.2.4 Drilling of additional monitoring boreholes – Eastern Sector of KKRWSS

During 1997, DWAF initially planned to drill an additional monitoring borehole approximately 1.7 km south of VR11 (see Figure 2-5) to obtain the depth to watertable on the watershed of the Vermaaks River catchment. However, access to this particular site was not possible due to poor road conditions. Accordingly the opportunity of having a drill rig on site was used to upgrade the monitoring system by drilling additional monitoring boreholes (positions are shown on Figure 2-5). In total nine additional monitoring boreholes were completed, i.e. G40171 to G40178, of which G40175 was abandoned and redrilled as G40175A. During drilling of these monitoring boreholes, groundwater samples were collected with depth as drilling progressed and analysed for major and trace elements as well as environmental isotopes (November 1998 sampling survey). The drilling results are summarised in Table 3-2.

2.3 SATELLITE LINEAMENT MAPPING AND REMOTE SENSING

To improve the understanding of TMG hydrogeology in the Kammanassie Mountains, the fractured rock structure within the regional aquifer boundaries was investigated with satellite lineament mapping.

Experience with lineament mapping from satellite imagery has shown that many satellite lineaments often do not correspond with known geological structures on 1: 250 000 geological maps. In order to obtain a more 'complete' geological lineament map for meaningful structural interpretation, the Council for Geoscience considered the following (Chevallier et al., 1999):

- An overview of the regional geology and structures (published information) in the study area.
- Regional structural interpretation for the regional study area, including satellite lineament mapping of available 1 : 250 000 geological sheets (i.e. Ladismith and Oudtshoorn sheets), structural analysis and tectonic interpretation.
- Satellite image processing, enhancement methods and lineament mapping.
- Structural interpretation of lineament information. This included consideration of the strike, geometry and extent of the major faults or lineaments, definition of tectonic domains, structural classification of satellite lineaments in terms of groundwater potential, etc.

- Interpretation of geological information using unpublished 1 : 50 000 geological maps, cross-sections at the same scale and tectonic interpretation.
- Discussion of the different structural features that are likely to play a role in the hydrology of the Klein Karoo area.
- Geological cross-sections at longitude 22° 31', latitude 33-34° and at longitude 22° 43', latitude 33-34°.
- Investigation of the origin of hot springs, i.e. Toorwater, Warmwaterberg and Calitzdorp Spa.

The results of the above are incorporated, where relevant in Chapters 3 to 7 of this report, i.e. the study area overview, hydrochemical characterisation, aquifer parameters, conceptual hydrogeological model and water balance, chapters respectively.

2.3.1 Remote Sensing

The study area extends across two Landsat TM images, i.e. scenes 173-83 and 172-83, respectively. These images were fully rectified and georeferenced to the UTM coordinate system, whereafter imported into ER Mapper and ArcView software packages. The images were georeferenced with the aid of the existing 1 : 250 000 digital geological maps of CGS.

Digital image processing and lineament mapping included the following:

- Geo-referencing and rectification of raster imagery.
- Clipping, contrast matching and production of a satellite mosaic of the study area.
- Satellite image processing, including spatial filtering and spectral enhancements aimed at highlighting the geological lineaments.
- Mapping of satellite lineaments from various derivative false-colour-composite images.
- Digitising and coding of geological lineaments from published geological maps (1 : 250 000 geological maps and other relevant maps).

Mosaicing of the two Landsat images was not straightforward, as the images were taken at different times and dates of the year. In order to produce the best mosaic of the study area, each of the seven Landsat TM bands were checked on an individual basis. The most satisfactory results were obtained with Bands 2, 4 and 5.

Various enhancement techniques and filters were also tested. Contrast stretching and edge enhancement gave the clearest and the sharpest image for the structural and lineament analysis.

Derivative images using statistical manipulation (band ratio, vegetation indices, etc.) were used to complete the lineament mapping but did not contribute significantly to the discovery of any additional or a more clear distinction between existing geological structures.

MAP1 in the folder in the back of the report represents a copy of the processed image. The satellite image is also available in digital format on the CD accompanying the final report.

2.3.2 Satellite lineament mapping

Lineaments were digitised onscreen with the vector module of the ER-Mapper software, at two different scales, i.e. a regional study featuring structural analysis of the entire study area and a smaller local study, focussing on the Kammanassie Mountains. A scale of 1 : 50 000 was used for the regional study (MAP 2 in the folder in the back of this report). However larger lineaments versus tectonically controlled major valleys, required a reduction in the digitising scale to 1 : 100 000. The scale was increased to 1 : 25 000 for the local study (MAP 3 in the folder in the back of this report).

Several types of linear tectonic features were identified, i.e. faults, fractures, master joints and lineaments. After identification, lineaments were compared with known faults, mapped on the digital versions of the 1 : 250 000 and 1 : 50 000 geological maps of the CGS. In general, a good agreement was found between lineament mapping from the LANDSAT images and the above-mentioned maps. Small variations between the position of fault traces between the geological and lineament maps respectively, are attributed to the multiple fractured nature of large faults. However, an interesting observation was made, i.e. that some of the faults shown on the geological map are not indicated on the satellite lineament map and *vice versa*.

2.4 DATA COLLATION

Since the start of the project, all hydrogeological and hydrochemical data are captured and collated in EXCEL spreadsheets, which are continuously improved and updated during the course of this project. To benefit data manipulation and analysis and to develop management tools to manage the TMG Aquifers of the Kammanassie Mountains, the following spreadsheets are produced:

- All the hydrochemistry data used are summarised in an EXCEL spreadsheet titled CHEMDATABANK. Data sets are screened to eliminate meaningless data (mostly from the NGDB). Selected data records are later transferred to a GIS database for spatial analysis of parameters, e.g. the variation of a particular chemical constituent in

groundwater over the area. The remote sensing image, lineaments, topographic and geological maps are incorporated into the same GIS database.

- Additional spreadsheets, specifically designed to improve hydrochemical interpretation are the CHEMDIAGNOSTIC and COMPOSIT spreadsheets. These spreadsheets are designed to generate X-Y scatter-plots and composite (type of Schoeller diagram) diagrams, respectively.
- WELLMAN (borehole and wellfield management spreadsheet). All the information available on boreholes sampled, i.e. borehole depth, construction, water level measured, yield, annual abstraction and field measurements are organised and arranged in a user-friendly way to improve data analysis.
- RECHARGE (recharge estimation tools for TMG Aquifers, after van Tonder and Xu, 2000).
- FC (Flow characteristic method, pump testing analysis spreadsheet, after van Tonder and Xu, 1999).

All the above-mentioned spreadsheets are available on the data CD accompanying this report. The remote sensing image, lineaments, topographic and geological maps are incorporated into the same GIS database.

2.5 DATA INTERPRETATION

The interpretation of hydrochemistry and environmental isotope data of various existing boreholes and springs (hot and cold) in the Klein Karoo, sampled during several sampling surveys, together with the following:

- Interpretation of hydrogeological data
- Remote sensing analysis of satellite images
- Structural interpretation of geological features

are all fundamental in the formulation of the conceptual hydrogeological model for the TMG Aquifers in the Klein Karoo and Kammanassie Mountains.

All the information obtained during the desk study, fieldwork and satellite lineament analysis are **interpreted** and integrated holistically to formulate the **conceptual hydrogeological model** for TMG Aquifers in the Klein Karoo. Based on the conceptual hydrogeological model, an aquifer management strategy and plan is proposed for the TMG Aquifers in the Klein Karoo and Eastern Sector Wellfields of the KKRWSS. This involves the development of aquifer management tools, e.g. WELLMAN.

2.5.1 Environmental isotopes

Analysis of hydrogeological and environmental isotope data in conjunction with hydrogeological and remote sensing data provided an indispensible insight to TMG hydrogeology. A brief summary on the interpretation environmental isotope hydrogeology is given in this section.

2.5.1.1 General applications of environmental isotopes in hydrogeology

A detailed discussion on the application of environmental isotopes in hydrogeology is available in Verhagen (1991, 2000), Gat (1996), Clark and Fritz (1997), Kendall and McDonell (1995) and IAEA (1994).

The radioactive isotopes of hydrogen and carbon, i.e. ^{3}H and ^{14}C respectively, and the stable (i.e. non-radioactive) isotopes of oxygen (^{16}O and ^{18}O), hydrogen (^{1}H and ^{2}H) and carbon (^{12}C and ^{13}C), serve as valuable tools in the assessment of a wide variety of hydrogeological problems. Isotope techniques can be applied at various levels in a groundwater investigation. In cases where very little information is known on the local hydrogeology, the results are efficient in suggesting a hydrogeological conceptual model. In cases where *a priori* conceptual model exists, isotope data can set boundary conditions to these concepts. When isotope data has been interpreted quantitatively in terms of known aquifer parameters, isotope data can be used to calibrate, or at least set limits to conclusions from, numerical groundwater management models (Verhagen, 2000).

Environmental radioactive isotopes ^{3}H and ^{14}C and stable isotopes ^{2}H and ^{18}O are unique for the investigation of hydrogeological processes occurring over much larger and longer spatial and time spans, respectively. Isotopes act as natural occurring tracers in groundwater (commonly referred to as environmental tracers) which can provide valuable information of aquifer characteristics and groundwater flow paths to the hydrogeologist, that would otherwise be difficult, if not impossible, to establish (Verhagen et al, 1991).

The radioactive isotope ^{3}H and stable isotopes ^{2}H and ^{18}O label the water molecule, whilst radioactive ^{14}C and the stable isotope ^{13}C the label the total inorganic carbon (TDIC) (Verhagen, 2000).

2.5.1.2 Definitions

The following definitions are adapted from Verhagen (2000):

Radioactivity is the process during which unstable atoms (nuclides) spontaneously emit one or more particles or quanta to reach stability. This is a random process and the emission rate is proportional to the number of radioactive atoms:

$$dN/dt = -\lambda N \quad \text{.....Equation 1}$$

where N is the number of radioactive atoms; t is the time and λ is the decay constant or probability. The activity of a radionuclide is therefore proportional to the number of atoms. Integrated over a time period t, this equation becomes:

$$N = N_0 e^{-\lambda t} \quad \text{.....Equation 2}$$

where N_0 is the number of radioactive atoms at time t = 0.

When $N / N_0 = ½$, the time elapsed is called the half-life $t_{½}$.

The half-life and the decay constant are related by:

$$t_{½} = 0.693 / \lambda \quad \text{.....Equation 3}$$

Equation 2 governs the concept of radioactive dating. When the initial and final number, or concentration, of radioactive atoms is known, the time t since the initial condition can be determined. The strict concept "dated", cannot be applied to a fluid, as it undergoes processes such as mixing, hydrodynamic dispersion and diffusion.

Fractionation: Molecules differ in mass, as the isotopes of the elements making up molecules differ in mass. These mass differences influence factors such as vapour pressure, diffusivity etc. During phase processes, such as evaporation, condensation and exchange reactions the abundance ratios of the isotopes of individual elements change, or undergo fractionation. Such processes usually take place at the interface of different phases or compounds containing the same

elements, such as vapour in contact with a liquid, a liquid in contact with a solid, etc. These changes in abundance can be traced through natural and other systems.

The unit fractionation factor α is defined as: $\alpha = R_A / R_B$, where R_A and R_B are the abundance ratios of the rare (heavier) isotope to the more abundant (light) isotope in phases A and B respectively; α is temperature dependent.

As isotopic abundances, and changes in these abundances are generally small, it is customary to express these changes as fractional differences δ in per mille with reference to the value of a reference standard:

$$\delta = [(R_S / R_T) - 1] \times 1000 \text{ (‰)} \quad \text{..... Equation 4}$$

where the measured ratios for the heavy to the light isotope are R_S for the sample and R_T for the reference standard, respectively.

2.5.1.3 Environmental radioactive isotopes: ^3H and ^{14}C

Both tritium (^3H) and radiocarbon (^{14}C) occur in the environment as a result of natural (cosmic radiation) and man-made (thermonuclear devices) processes. Tritium concentrations are expressed as an atomic ratio of the abundances of tritium (^3H) and hydrogen (^1H), where:

$^3H / {}^1H = 10^{-18}$ is defined as 1 tritium unit (1 TU).

The half-life of tritium is 12.23 years. When rainwater is isolated from the atmospheric source, i.e. during groundwater recharge, no new tritium is added and the tritium concentration will decrease with this characteristic half-life.

The useful range of measurement of environmental tritium in hydrogeological applications spans four to five half-lives. It is therefore measurable in, and can act as an indicator of, only recently recharged groundwater.

The changes in atmospheric ^3H are monitored by the IAEA through a global monitoring network (IAEA). In Southern Africa, tritium levels in rainfall rose from initial (natural) values of about 5 TU to 60 – 80 TU as a result of fall-out of

nuclear weapon testing in the early 1960's. At present, pre-bomb values of around 5 TU have been reached in non-industrialised areas (Verhagen, 2000). Therefore ^{3}H can be informative on short-term residence times of groundwater.

Tritium levels in groundwater with mean residence times (MRT) in excess of about 200 years, lie at or below the limit of detectability (routinely 0.2 ± 0.2 TU). A value greater than 1 TU at present unequivocally indicates that groundwater has received significant recharge during the thermonuclear era (the past 35 years).

Radiocarbon (^{14}C) is formed in the upper atmosphere by processes similar to tritium, whereafter it is oxidised to $^{14}CO_2$ and becomes part of atmospheric carbon dioxide, in which the natural isotopic ratio ^{14}C / $^{12}C \sim 10^{-12}$, is called 100 pMC (100 per cent modern carbon).

Radiocarbon has a half-life of 8270 years, making it a useful tool for "dating" groundwater up to an age of 50 000 years. As with tritium, thermonuclear tests increased the atmospheric level of radiocarbon to peak in the early 1960's. Plants assimilate atmospheric carbon dioxide through photosynthesis. Humus and roots liberate CO_2 labelled with environmental ^{14}C, which dissolves in infiltrating groundwater, rendering the water chemically aggressive, which leads to the various species of ^{14}C – labelled total dissolved inorganic carbon (TDIC). Thus, radiocarbon:

- Becomes a time dependent radioactive tracer of groundwater and
- Allows for the estimation of groundwater residence times.

In contrast to ^{3}H, ^{14}C is not strictly a conservative tracer of water, as numerous chemical processes can alter the ^{14}C / ^{12}C ratio. Attempts have been made by several authors (Verhagen *et al.,* 1991) to develop correction models, based on the hydrochemistry and $\delta^{13}C$ values (see next section). These models all assume that the hydrochemical processes occur principally during the initial development phases of carbon, and therefore affect the initial isotopic ratio established in the TDIC of groundwater, e.g. during recharge. Once the hydrochemistry has been stabilised, the ^{14}C / ^{12}C ratio is taken to effectively alter only through radioactive decay. Vogel (1970) suggested a rule of thumb initial recharge value of about 85% of atmospheric CO_2 for many aquifers. In principle however, this initial value may be as low as 50% in carbonate aquifers, approach 100% in purely crystalline

terrain and has to be assessed for each area. Subsequent water / rock interactions in the saturated zone of established aquifers are usually regarded as negligible.

In spite of its potentially complex hydrochemistry, radiocarbon is the principal radioactive environmental tracer of deeper-seated groundwater, its useful range of measurement in hydrogeological applications spanning five to six half-lives.

During the early sixties, atmospheric ^{14}C concentrations rose due to thermonuclear fallout and declined since. In qualitative terms therefore, groundwater radiocarbon values of > 100 pMC can be interpreted as falling in the thermonuclear era, i.e. recharged over the past three and a half decades. In this time-span, interpretations can be constrained further by tritium.

2.5.1.4 Approaches to interpretation of ^{14}C and ^{3}H

Radiocarbon and tritium are used in the following ways (Verhagen, 2000):

- As long and short-lived radioactive tracers, respectively, in infiltrating rainwater. In this way, their isotopic ratio is used as a qualitative, or semi-quantitative, indicator of actively turned-over, or dynamic, groundwater, used to delineate recharge areas, and to understand hydrochemical processes. The isotopic ratio of radiocarbon defines the concentration in the TDIC. When the ratio is multiplied by the TDIC concentration (usually closely approximated by alkalinity) a factor is obtained which is proportional to the radiocarbon concentration in the water. It then becomes a tracer similar to tritium (Verhagen *et al.,* 1996) and can be used to assess mass balance in groundwater mixing.
- To interpret groundwater residence times with the use of suitable models, which can provide information on groundwater dynamics and estimates of recharge rates.

As opposed to archaeological dating where the age of an artefact can be given very accurately, in the case of groundwater a sample represents a mixture of water with different transit times (see Figure 2-6 over page). Such a mixture occurs in spring as well as in boreholes in phreatic aquifers, which penetrate different levels of water, generally with increasing transit time from the surface. This links to the concept of mean residence time.

Figure 2-6 (adapted from Gieske, 1995) over page shows the different 'layers' of groundwater in a uniformly recharged isotropic phreatic aquifer, representing mixtures of groundwater with different transit times, responding to different recharge events.

FIGURE 2-6: GROUNDWATER PROFILE IN PHREATIC AQUIFER (ADAPTED FROM GIESKE, 1995)

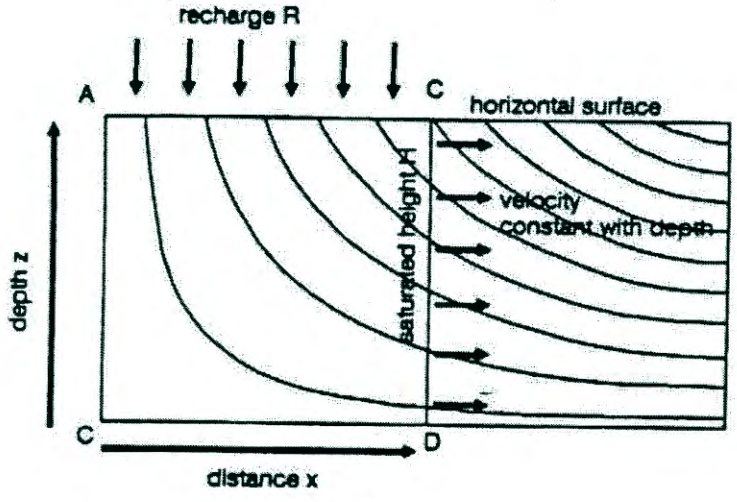

Radiocarbon is a very useful tool to determine the MRT of groundwater in an aquifer (Gieske, 1995). It can be used to determine recharge rates and storage. In a non-carbonate aquifer, such as the TMG, chances for dissolution of organic matter or carbonate within the aquifer are small and it is not necessary to correct for erroneously 'old water', due to the dissolution.

Where the input of the environmental tracer has remained constant over time, the MRT (τ_m) of water pumped from a borehole in a phreatic aquifer is given by the expression (Gieske, 1995):

$$\tau_m = \tau_{avg} [(A_0/A) - 1] \quad \text{..... Equation 5}$$

where,

τ_{avg} = the mean life of the radioisotope (8270 years for ^{14}C and 18.3 years for ^{3}H)

A_O = the constant input concentration and

A = the measured concentration in the pumped sample.

As pointed out earlier, the input concentrations of both ^{14}C and ^{3}H have undergone considerable changes over the past 40 years due to bomb fall-out and are therefore functions of time. These values can be inserted into a convolution integral representing the concentration of the tracer, i.e. the exponential model given by the following expression (Verhagen *et al.,* 1991 quoted in Gieske, 1995):

$$A(t) = \int_0^\infty A_0(t-\tau)e^{-\lambda t}\, f(\tau)dt \qquad \text{..... Equation 6}$$

Where A(t) and A_0 are the tracer concentrations at time t and at recharge, respectively, τ the individual transit time of an individual recharge volume; $A_0(t-\tau)$ is the time-dependent input function; $e^{-\lambda\tau}$ the decay function and $f(\tau)$ the transit time function, or 'model' of the movement of groundwater through the aquifer.

Mean residence times can then be estimated by using a computer routine, into which the input function (i.e. the annual concentrations of ^{3}H and / or ^{14}C, over say the past 50 years) is fed. The programme will then produce curves of tracer concentration against mean residence time for the aquifer, on the assumption of the exponential model weighting function (Gieske, 1995):

$$f(\tau) = e^{-\tau}/T \qquad \text{..... Equation 7}$$

Where **T** is the mean residence time (MRT).

Typical results for Southern Africa (1998) are shown in Figures 2-7 and 2-8 (over page). These curves can be used to estimate MRT values for either the observed ^{3}H or ^{14}C concentrations. With the bomb peak still measurable in the environment, ambiguous MRT values in the range 10 – 60 are produced at values > 2 TU and > 100 pMC. This can often be overcome by considering both ^{3}H and ^{14}C in evaluating the most likely value for MRT, as well as the hydrogeological situation (Verhagen, 2000). Figure 2-9 shows a graphical display of ^{14}C against ^{3}H for different MRT values calculated by the exponential mixing model. When observed values plot close to this line, it implies that conditions conform reasonably to the assumption of an isotropic, diffusely recharged, aquifer.

FIGURE 2-7: CHANGES IN ATMOSPHERIC ^{3}H FOR SOUTHERN AFRICA AFTER VERHAGEN (2000)

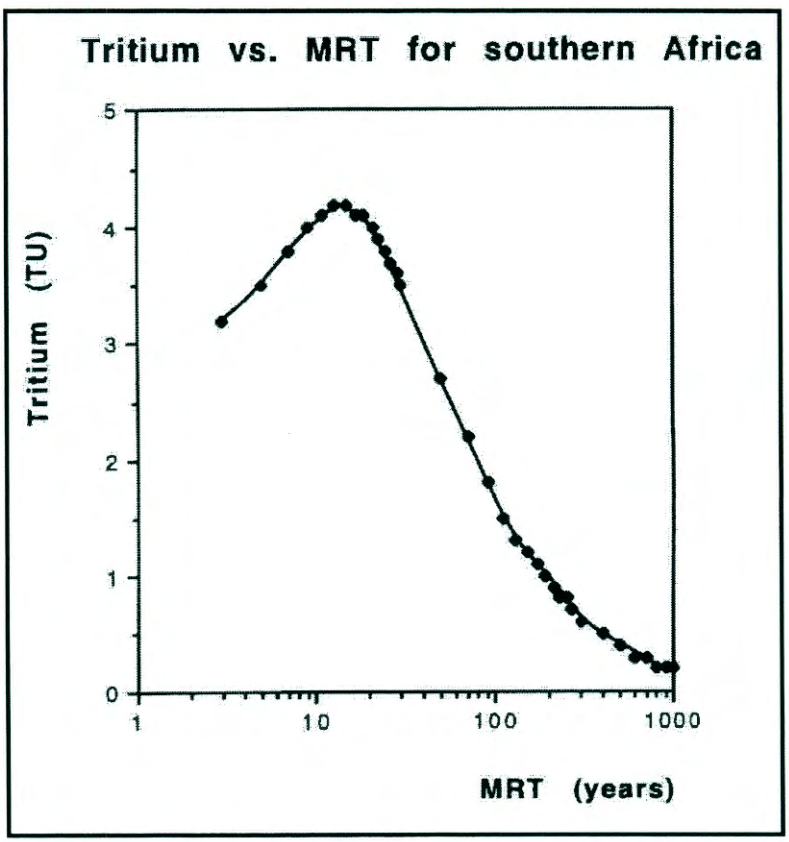

FIGURE 2-8: VARIATION IN ATMOSPHERIC ^{14}C AFTER VERHAGEN (2000)

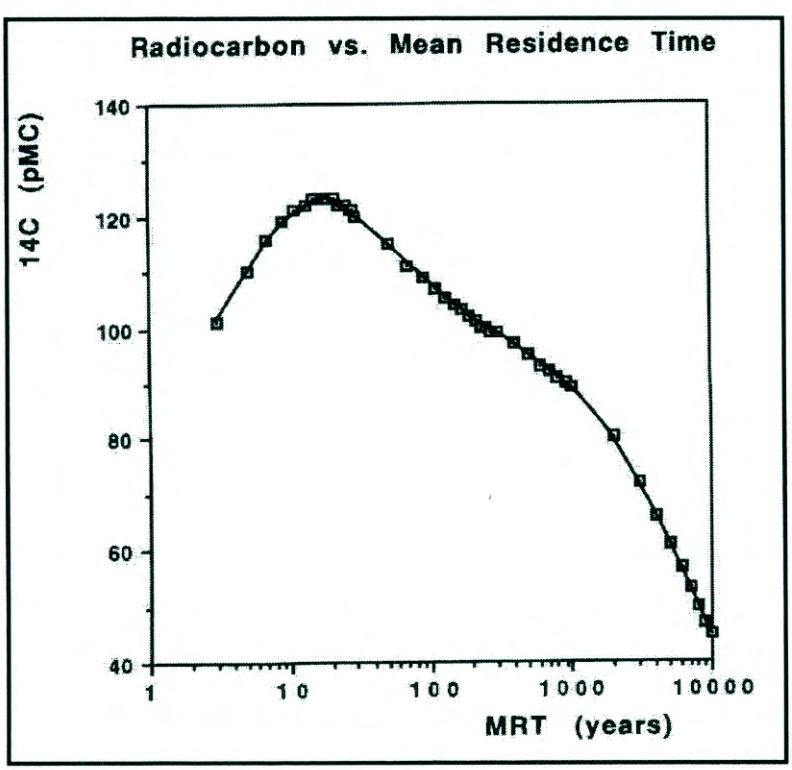

FIGURE 2-9: EXPONENTIAL MODEL FOR ^{14}C AND ^{3}H SHOWING MRT AFTER VERHAGEN (2000)

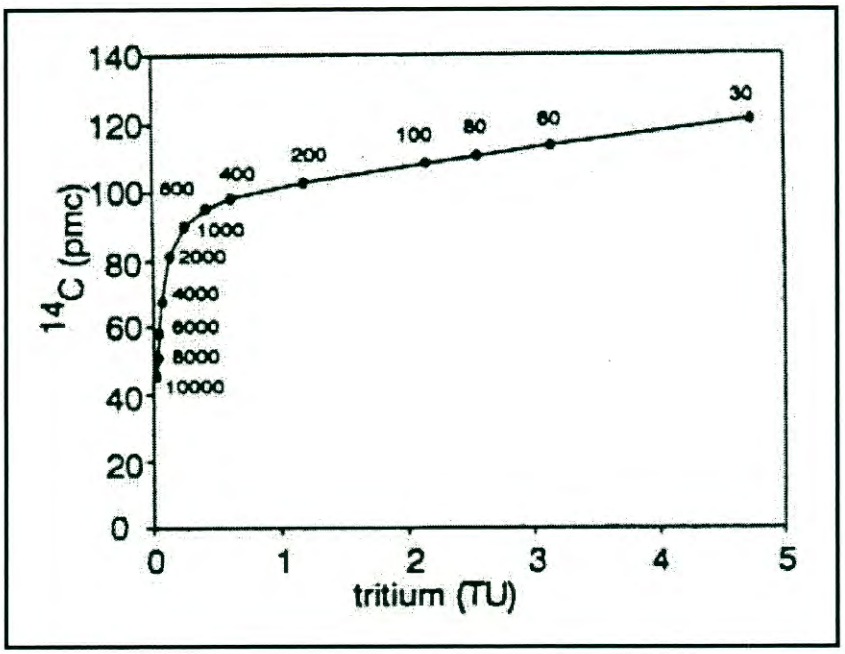

2.5.1.5 Chlorofluorocarbon

In addition to radioactive isotopes, chlorofluorocarbon (CFC) measurements potentially can assist to remove ambiguity in this MRT range, as the atmospheric concentration of these dissolved gas tracers have not undergone a transient, but are monotonously increasing or have levelled off (Verhagen, 2000).

CFC's are gases that have been released into the atmosphere since the 1950's, which concentrations are steadily increasing, with new compounds being added over the past few decades (Figure 2-10, over page). When carefully sampled and measured the concentrations of the different CFC's give a measure of the time since infiltration of groundwater (Verhagen, 2000). The water can therefore be 'dated' in principle over a span of approximately four decades, a very useful range covered also by thermonuclear tritium. The latter exhibits a peak in its input concentration, rendering its interpretation in terms of short residence times ambiguous. Measurements of e.g. radiocarbon values can assist in removing this ambiguity.

The sampling procedure for CFC's, is complicated and requires special sampling equipment to avoid atmospheric contact. During a special sampling survey, the

CSIR (Weaver, 1996) has taken CFC samples in the Vermaaks River Valley production boreholes of the KKRWSS.

FIGURE 2-10: CFC DISTRIBUTION IN GROUNDWATER AND AIR AFTER DUNKLE *ET AL.* (1993)

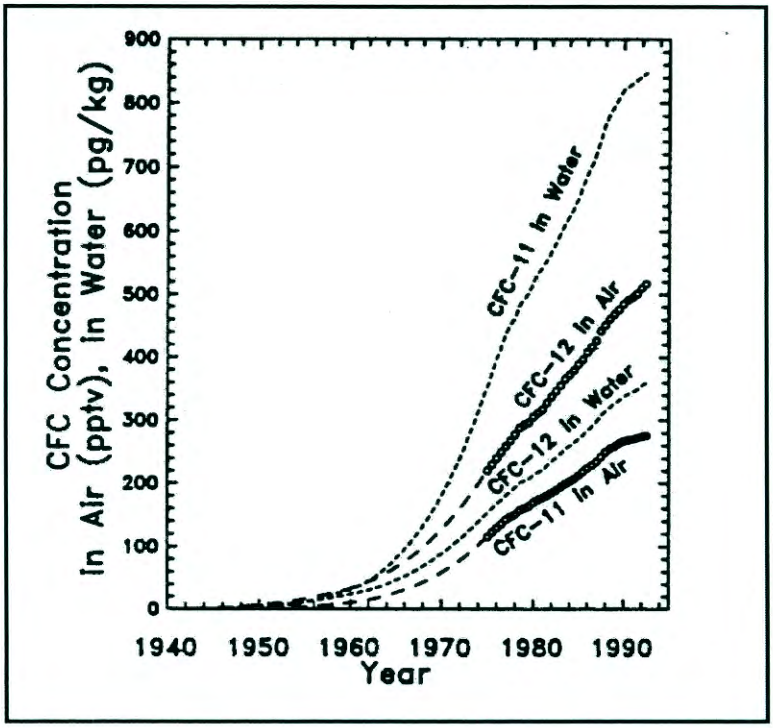

2.5.1.6 Application of stable isotopes ^{13}C

The isotopic abundance ^{13}C / ^{12}C of atmospheric carbon dioxide, when expressed as in Equation 4, is approximately $\delta^{13}C$ = -7 ‰ with reference to a marine limestone isotopic standard PDB (PeeDee Belemnite). During photosynthesis, this abundance is modified through biological isotope fractionation, which establishes organic values of about $\delta^{13}C$ = -25 ‰ in C3 plants (e.g. trees) and -12‰ in C4 plants (e.g. grasses). The soil CO_2 produced by such plants will have similar isotopic ratios. These ratios can be modified through isotopic exchange and dilution processes, such as the dissolution of soil or rock carbonate of differing carbon isotopic abundance, resulting in isotopic ratios in the different DIC species in groundwater, governed by appropriate fractionation factors. The $\delta^{13}C$ is therefore diagnostic of some of the chemical processes which groundwater has undergone, and can provide information of the provenance of the TDIC, and thus

of the water itself. The ^{14}C / ^{12}C ratio is also useful, as it is likewise modified by the above processes, and forms the basis of ^{14}C correction models.

2.5.1.7 Application of stable isotopes ^{18}O and ^{2}H

The changes of ^{18}O and ^{2}H concentrations along groundwater flowpaths is an effective tool to determine the altitude of groundwater recharge, estimation of mixing proportions of different sources or component flows and the relationships between ground and surface water (Gat, 1996).

^{18}O and ^{2}H are present in water in isotopic abundances (or ratios, R) of about $^{18}O/^{16}O$ = 0.2 % and $^{2}H/^{1}H$ = 0.015 %. In various combinations, these isotopes make up water molecules, principally of masses 18, 19 and 20.

Stable isotope abundance is normally expressed in terms of a ratio to the abundant isotope of the same element or as positive or negative deviations of these isotope ratios from a standard, similar to that of the radioactive isotopes (see Equation 4).

The most important physical process resulting in variations in isotopic compositions of natural water is vapour-liquid fractionation process during evaporation and condensation (Weaver *et al.*, 1996). The basic principle is that enrichment of the lighter isotope (^{16}O) occurs in the vapour during evaporation, as opposed to loss of the heavy isotope (^{18}O) from the vapour first during condensation. Phase processes taking place in the atmosphere, during infiltration and in groundwater, leading to enrichment or depletion of the lighter isotope, are discussed in Appendix B (B-1). These small changes can be expressed as a fractional deviation δ form a standard called SMOW (standard mean ocean water).

Values of δ can be diagnostic of water from different recharge altitudes. Water vapour rising from the ocean is depleted in the heavy isotopes. Vapour masses moving inland are subject to equilibrium isotopic exchange processes, with the continued depletion in heavy isotopes in vapour travelling inland as a result of rainout. Consequently, the stable isotopic content of meteoric water lies on a regression line:

$$\delta^{2}H = s\,\delta^{18}O + d \quad \text{..... Equation 8}$$

where s is the slope, and the intercept d on the $\delta^{2}H$ axis the deuterium excess.

The line with s = 8 and d = +10 is called the global meteoric water line (GMWL, Figure 2-11). The ^{2}H - excess is controlled by the deuterium in the vapour source region and the slope by evaporation during rainfall and seasonal variations in precipitation. The position of any pair of $\delta^{2}H$ and $\delta^{18}O$ values on this line for rainwater worldwide will depend on local climatological conditions (temperature, latitude, altitude, and rainfall amount effects).

FIGURE 2-11: METEORIC WATER LINES AFTER GAT (1996)

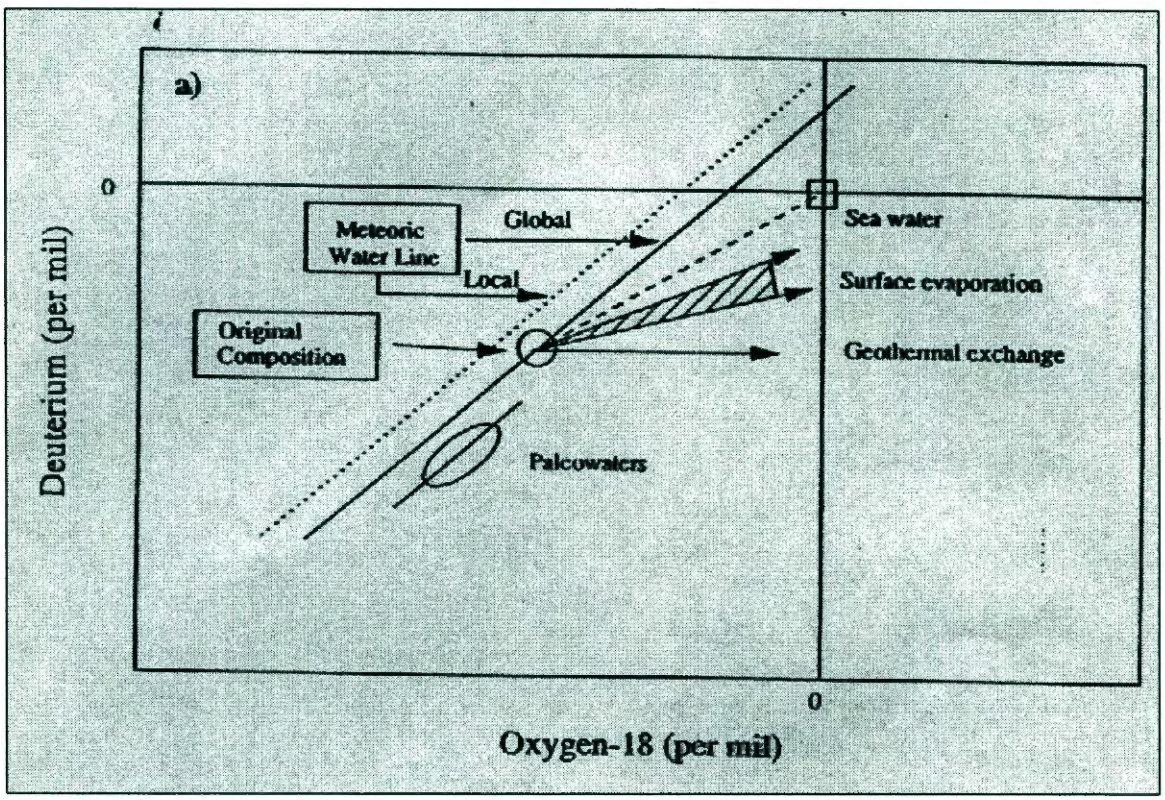

Surface water bodies, such as dams, lakes and pans are enrichment in the heavy isotope content during evaporation. Light isotopes are preferentially transferred to the vapour phase. The resulting surficial layer enriched in the heavy isotope is then readily mixed into the bulk of the water body through convective processes. This evolutionary enrichment produces $\delta^{2}H$ and $\delta^{18}O$ values which lie to the right of the meteoric water line, and plot on an evaporation line of lesser slope s (usually 4 to 5) and lower d than the GMWL (Figure 2-11). ***Groundwater derived through infiltration from such water bodies will carry this distinctive evaporative isotopic signal.***

Evapotranspiration losses from soil and groundwater generally occur under isotopic equilibrium, i.e. without fractionation. In semi-arid environments such as the Klein Karoo, isotopic values of groundwater derived directly from rain will therefore lie on or close to the GMWL. However, it will tend to be displaced to more negative (or "ligther") δ values than the weighted mean in rain, due to the process of rainfall selectivity (Verhagen, 1984). Major rainfall events, which produce isotopically lighter precipitation i.e. with more negative δ values, may contribute proportionately more to recharge. It is possible to distinguished different processes of rainfall recharge by different stable isotope ranges on the GMWL.

2.5.1.8 Application of environmental isotope and hydrochemistry in this study

Environmental isotopes and hydrochemistry data analysis methodologies were applied in this study to establish the different groundwater types in hydraulic interconnection and / or flow systems.

Specific applications of environmental stable isotopes $\delta^{18}O$ and $\delta^{2}H$ in this study are:

- To define groundwater flow paths in the TMG fractured aquifer, where groundwater is confined to specific flow paths, of which the fracture geometry is difficult to determine.
- To assist structural geological and hydrogeological data with the conceptualisation of the TMG Aquifer system in the Klein Karoo by delineating the recharge areas with use of the altitude effect.
- Prove the existence of a regional flow system (working hypothesis) by comparing the $\delta^{18}O$ and $\delta^{2}H$ signatures of groundwater emanating from the hot springs, groundwater and recharge areas.
- Determine groundwater recharge areas.
- Estimate groundwater recharge.

And radioactive isotopes of ^{14}C and ^{3}H are used to determine:

- The mean residence times of groundwater types in the TMG Aquifer.
- The aquifer storage and recharge from MRT.

In order to test the applicability to interpretation of hydrochemical and environmental isotope data analyses methodologies for TMG Aquifers, the data are interpreted with the following:

- Standard groundwater chemistry diagrams: Piper, Durov, Expanded Durov and Wilcox diagrams are used to define the general TMG groundwater chemistry characteristics relative to other groundwater types.

- Diagnostic chemistry diagrams: In the format of X-Y scatter plots or composition diagrams of selected pairs of measured parameters. In general, positive correlations are indicated as straight lines, representing mixing of end-members in different proportions. Clusters of data indicate similar groundwater types or groundwater fed by the same aquifer or fracture set. Several clusters of data isolated from each other represent distinct different water types. Once the end-members are defined, it is possible to calculate the mixing ratios of different groundwater types.

- $\delta^{18}O$ versus $\delta^{2}H$ diagram: The MWL for the Klein Karoo is determined, and recharge area identified.

- Composite or 'fingerprint' diagrams: Historically, the first fingerprint diagram was introduced by Schoeller in 1954 on which the dissolved ion concentration is plotted on a semi-logarithmic scale in milli-equivalents per litre (meq/l). The traditional Schoeller diagram was modified in this study to include $\delta^{18}O$ data for each sample (Issar, unpublished work). This modified fingerprint diagram is referred to as a composite diagram. This multi-parameter diagram shows cumulative major ion concentrations in milli equivalents per litre and $\delta^{18}O$ isotopic composition. It is possible to differentiate between groundwater recharged at different altitudes and following different flowpaths in an aquifer on this diagram. The $\delta^{18}O$-signature of a groundwater type is indicative of the altitude of groundwater recharge, whereas the groundwater major ion chemistry provides information on the dissolution processes occurring along flow paths. Similar groundwater types have similar 'finger-prints' (the same shape curve and similar concentrations) as indicated by the cumulative concentrations of dissolved ions and $\delta^{18}O$ content on the composite diagram.

- Multi-component cluster analysis: Is carried out on hydrochemical and environmental isotope data set to define clusters of groundwater of similar

origin and flow paths. The connection of different clusters can provide information on the groundwater flow system, directions, magnitude and hydraulic interconnection. Adar *et al.* (1992) have proven that the application of multi-component cluster analysis of hydrochemical data sets, incorporating known hydrogeological data, is a valuable tool to assess the groundwater flow system in deep aquifers with scarce data, e.g. the Arava Valley in Israel.

2.5.2 Aquifer parameters and yield

Woodford (2001) compiled a summary on the interpretation and applicability of pumping tests in TMG Aquifers. He states that although the term aquifer- or pumping-test is used interchangeably by many hydrogeologists the two terms can be differentiated quite distinctly:

- A **pumping-test** refers to a more rudimentary form of testing, where the objective is to obtain information on the performance and efficiency of the production borehole itself. Results provide information on the productive capacity of the borehole, efficiency of the screens and for the design of the pump equipment (i.e. pump type and capacity, depth of intake etc.).

- The **hydraulic- or aquifer-test** is more a rigorous testing technique aimed at providing information on the water-bearing formation rather than the individual borehole being tested, although it is also capable of supplying information on the borehole capacity. Proper aquifer testing and data interpretation can yield information on the hydraulic character of the aquifer (transmissivity, storativity etc.), aquitard (leakage factor, hydraulic resistance etc.) and boundary conditions, screen efficiency, optimum pumping rates and the 'safe-yield' of the borehole. Intuitive analysis of aquifer test data can be used to determine unknown hydrogeological information (i.e. depth of major water-bearing fractures) and the effect of borehole rehabilitation procedures.

Kruseman and de Ridder (1991) stated that '*the analysis and evaluation of pumping test data is as much an art as a science*'. It is a science because it is based upon theoretical models that the hydrogeologist must understand and on thorough field investigations. It is also an art in the sense that the intuition and interpretational skills of the practitioner are imperative in obtaining meaningful results (Woodford, 2001). He concludes that conventional step-drawdown and constant discharge aquifer-tests are widely used in Table Mountain Group aquifers to determine the 'safe yield' of potential production boreholes. The hydraulic properties of the aquifer are often incorrectly determined using conventional analytical methods for analysing flow in porous aquifers, but this information is rarely 'tested' or used for further quantitative analysis (i.e. numerical flow modelling).

2.5.2.1 Hydrogeological characteristics of fractured aquifers

The hydrogeological characteristics of fractured aquifers are significantly different from those of primary or porous aquifers, where groundwater occurs in a continuum of pores (interstitial openings between grains). Porous aquifers are generally much more uniform in composition and hydrogeologic properties.

Fractured aquifers, on the contrary, can be considered a multi-porous medium, conceptually consisting of two major components: matrix rock blocks and fractures.

Fractures serve as higher conductivity conduits for flow when the apertures are large enough, whereas the matrix blocks can be permeable or impermeable, with most of the storage usually contained within the matrix. In real terms, a rock mass may contain various fractures of different scales and origin, varying from small-scale micro fractures to regional scale fault systems.

Fractured aquifers are therefore not homogeneous, uniform aquifers with a constant thickness as in the case of conventional or primary aquifers. On the contrary fractured aquifers are heterogeneous, have irregular geometries and thickness depending on fracture characteristics and fracture inter-connectivity. All these fracture properties need to be measured and vary greatly with increasing *in situ* stress below surface, which complicates their estimation even further.

The contribution of fractures (faults and joints) to the permeability and consequently groundwater flow in fractured aquifers, such as the TMG Aquifers depends on:

- The nature of the fractures themselves, i.e., aperture, roughness, presence/absence of mineralisation or fault gouge and preferred flow channels.
- The nature of the fracture system as a whole, i.e., orientation and length distributions, geometry and connectivity (Odling, 1997a).

The above-mentioned fracture characteristics are often very difficult and costly to obtain and are mostly based on laboratory experiments, which applies to a scale several orders of magnitude smaller than 'the real world'.

Another important difference between fractured and primary aquifers is that fractured aquifers contain several internal boundary conditions associated with different scales of fracturing as opposed to the infinite boundary conditions of primary aquifers (e.g. finite extent of fractures / fracture sets, versus Theis conditions in primary aquifers).

The effective management of an aquifer is primarily dependent on how well the aquifer parameters, i.e. storativity and permeability are known. Most interpretation methods use analytical solutions of the groundwater flow equation, based on assumptions, valid for porous aquifers, i.e. homogeneity of the rock mass. On the contrary, in the case of a fractured medium, this assumption is violated. The mixture of horizontal movement in the fractures and vertical leakage in the surrounding matrix cannot be accounted for in the analytical solutions. Incorrect and unrealistic values, especially for the storativity of the aquifer, are therefore calculated (van Tonder, 1999).

2.5.2.2 Theoretical models for analysis of test pumping data

The interpretation of aquifer test data using *conventional* analytical techniques requires the selection and fitting of a suitable theoretical aquifer model to the observed response of the waterlevels, using graphical or computer-aided curve-matching techniques. From a historic perspective these techniques originated from the work of Theis (1935). For a detailed description of the more conventional procedures for aquifer testing and methods of data analysis the reader is referred to Kruseman and de Ridder (1991).

Conventionally, the water level versus time responses from the constant discharge test is commonly evaluated using the Theis or Cooper-Jacob Method (Kruseman & de Ridder, 1991) for confined porous aquifers. From these methods deviations from the type-curve are noted and data extrapolation carried out to determine a 'safe' abstraction rate (Murray, 1996). The water level recovery information is also typically used to determine pumping schedules.

The various theoretical models and type curve methods mentioned in Appendix B (B-2), have complex data requirements and are difficult to apply. The conventional Theis method for porous aquifers gives an over-estimation of the safe borehole yield and hydraulic parameters. Over-estimation occurs due to improper extrapolation of drawdown curves, which ignores boundary conditions and neglects parameter uncertainties arising from imperfect knowledge of the aquifer

parameters. Therefore Van Tonder *et al.* (1998) developed the Flow Characteristics – method (FC-method), specifically for the analysis of test pumping data of fractured aquifers. A user-friendly spreadsheet in an EXCEL format enables fast analysis of data sets.

An investigation of aquifer testing in the Karoo Aquifer (also fractured aquifer) has shown that water level responses vary significantly with test duration (Van der Voort, 1996). After longer pumping times, the true behaviour of the aquifer matrix and the transition between the fracture and matrix dominant flow periods can be distinguished. In some of the fractured aquifers, borehole yields are controlled by intermediate scale fractures (neither matrix, nor regional scale) and the yield might drop suddenly once the fracture is dewatered. The sudden drop in yield occurs when the cone of depression reaches a boundary and the yield becomes dependent on the flow from the matrix. This condition is not accounted for by conventional pump test analysis methods, i.e. Theis and Cooper-Jacob, which assumes a uniform, infinite aquifer.

Kirchner *et al.* (1991) addressed the unrealistic aquifer parameter values obtained by interpretation of aquifer test data of boreholes drilled into the Karoo Aquifer (fractured aquifer). A particular problem was that the estimated values for the storativity were extremely low.

Bredenkamp (1992) and Bredenkamp *et al.* (1994) were the first to observe the distance-dependency of S, which decreases with conventional aquifer test interpretation, as distance between the pumping and observation boreholes increases. This observation is more related to interpretation of test pumping data interpretation than to characteristics of the aquifer itself.

TMG Aquifers consists of a multi-porous medium of interconnected fractures. In a fractured aquifer, such as the TMG, fractures strongly influence the movement of fluid through a rock formation. Conventional well-flow equations, developed primarily for homogeneous aquifers, therefore do not adequately describe the flow in fractured rocks. In recent years, many theoretical fracture-flow models have been developed (Kotze, 1993). These models are often complex due to the complex mechanisms of fluid flow in fractured rocks. Woodford (2001) concludes that the choice of the correct theoretical model is a crucial step in the correct interpretation of aquifer-tests. If the model chosen is incorrect, then the hydraulic parameters calculated will not be correct. A troublesome fact is that some models,

developed for different aquifer systems, respond similarly to a given pumping regime.

2.5.2.3 Flow Characteristic method

Van Tonder and Xu (1999) have developed the so-called Flow Characteristic (FC) Method to provide a first-order estimate of the long-term sustainable yield of a borehole, as well as the hydraulic parameters for both primary and secondary aquifers. The method attempts to ensure that the total abstraction from the aquifer does not exceed the sustainable yield of the aquifer by ensuring that the waterlevel does not drop to the depth of the main water strike. The method is available on an EXCEL spreadsheet.

The FC Method by van Tonder and Xu (1999) allows simultaneous estimation of sustainable borehole yield and aquifer parameters for both primary and secondary aquifers, by incorporating various boundary conditions based on the conceptual hydrogeological model. Based on the developed conceptual hydrogeological model for the TMG Aquifer, the FC Method is used to determine the hydraulic properties of the various aquifers. The aquifer parameters obtained from data analysis with the FC Method is compared with that obtained with conventional pump testing methods. Thereafter the safe-yield of the production boreholes and wellfields are calculated based on aquifer parameters and the water balance for the aquifers.

All the available test pumping data of the KKRWSS production boreholes are inserted into the standard FC spreadsheet designed by van Tonder and Xu (1999). By simply inserting the KKRWSS production borehole data sets into the above-mentioned spreadsheet, a series of macros was used generate the following information for each of the production boreholes:

- Derivative of drawdown with respect to the logarithm of time.
- Variation of aquifer storativity and transmissivity with time.
- A series of diagnostic plots of drawdown versus time, on a logarithmic, semi-logarithmic, square root of time and fourth root of time scales.
- Data sheets allowing sustainable yield calculation, by inserting the required criteria and variables, i.e. extrapolation time, recharge value, boundary conditions, derivative value.
- Risk analysis sheet, to determine the risk of a particular abstraction scenario.

The FC method uses the first, second and third derivatives of drawdown versus time (on a logarithmic scale) to determine the safe yield of a borehole as well as early and late transmissivity values, as well as effective transmissivity (T) and storativity (S) values. A typical derivative graph is shown in Figure 2-12 below, from which the following characteristics are determined (after van Tonder *et. al.*, 1999):

- A line with slope = 1 during early time, indicates well-bore storage.
- A horizontal straight line approximately 1 to 1.5 log cycles after well bore storage, indicates infinite radial flow (Theis-model).
- A characteristic kink after well bore storage, indicates a double porosity aquifer.
- Two- and three fold increase of the derivative, indicates a single or two no-flow boundaries, respectively.
- A straight line with slope=1 during late time, indicates a closed no-flow boundary.
- A recharge boundary (river or dam) is indicated by a drastic decrease in the derivative.
- Fracture positions are interpreted as typical sine wave forms on the derivative plot, i.e. a decrease and increase of the derivative at the fracture position and after dewatering of the fracture, respectively.

FIGURE 2-12: INFORMATION FROM A DERIVATIVE PLOT (AFTER VAN TONDER ET AL., 1999)

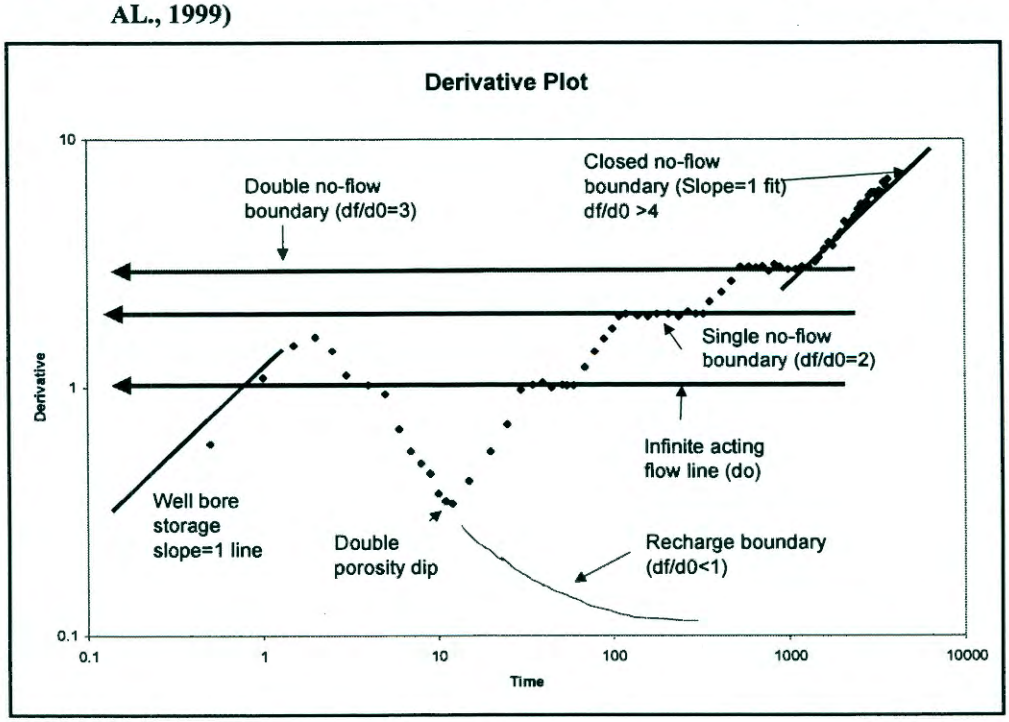

From the ***log derivative graph***, it is possible to obtain the following information, for any particular set of test pumping data:

- A log derivative value = 0.5 indicates a limited fracture (linear flow dominates during early time).
- A log derivative value = 0.25 indicates a good fracture network (bi-linear flow dominates during early time.

A log derivative value < 0.1 indicates a very good developed and inter-connected fracture network (radial flow dominates).

From the second derivative (d") graph of drawdown, it is possible to obtain the following fracture characteristics:

- The value of d" is equal to 1 for closed no-flow boundary conditions.
- The value of d" is equal to 0 for homogeneous, infinite boundary conditions (Theis model).

The aquifer parameters and safe-yield for the production boreholes of the Eastern Sector of the KKRWSS are estimated by using the FC-method (van Tonder *et al.*, 1999), conventional methods, i.e. Theis and Cooper-Jacob methods, from analyses of test pumping data.

The derivative and diagnostic plots of drawdown versus time for each borehole tested is compiled, whereafter the FC Method was applied to determine the following (results in Appendix J):

- The safe yield of each production borehole, for a basic and several advance solutions (incorporating other pumping boreholes and boundary conditions).
- The transmissivity and storativity.

The results of pumping test analyses, hydrochemistry and remote sensing data are combined to define aquifer zones of similar hydrogeological characteristics. A comparison is made between the results obtained from conventional and fractured rock pump testing analyses methods, and other methods, i.e. Equal Volume and Saturated Volume Fluctuation Methods to establish the difference in yield as well as aquifer parameter estimations.

Storativity is estimated by using the FC, SVF (saturated volume fluctuation) and Cooper-Jacob methods together with environmental isotope and hydrodynamic data (including fracture density data, from remote sensing).

2.5.3 Groundwater recharge

In the South African context the most outstanding contribution to the study on recharge of South African aquifers was completed by Bredenkamp *et al.* (1995) in the report called 'Manual on quantitative estimation of groundwater recharge and aquifer storativity'. The manual collates information on groundwater recharge that has been acquired over many years' experience and presents a pragmatic approach to the process of reliable recharge estimation. In the above-mentioned recharge summary, not much information exists on recharge estimations for TMG Aquifers, other than those, based on baseflow calculations for mountainous catchments in the Western Cape.

In the view of the complexity of hydrogeological processes and the high interdependence between the different variables influencing recharge i.e.,

- Complexity of hydrogeological water balance
- Non-linear recharge response with time
- Highly variable aerial distribution of groundwater
- Spatial variation in vegetation cover (Scott, *et al.*, 1998)
- Scarcity of hydrogeological data

it is not surprising that groundwater recharge is still difficult to determine despite all of the various methods available. This is especially so in the case of fractured aquifers, such as the TMG where the dimension of the aquifer and catchment is often unknown and crosscutting fracture-sets connect various hydrostratigraphic units. A further complication in semi-arid areas such as the Klein Karoo is that large amounts of water evaporate before arriving at the water table. Kirchner, *et al.* (1991) showed that groundwater recharge in semi-arid areas, e.g. the Karoo, follows preferred pathways, which have a highly irregular distribution.

Bredenkamp, *et al.* (1995) very effectively summarise the various elements of recharge and their interrelationships mathematically, in terms of the main elements and their governing equations, i.e. recharge is a function of rainfall, the unsaturated zone and evapotranspiration and the constraints affecting each of these as follows:

RE = f (rainfall), f (unsaturated zone), f(Evapotranspiration)

- Volume
- Intensity
- Frequency
- Arial distribution

- Soil type
- Thickness
- Slope
- Soil moisture
- Geology
- Fracturing
- Tectonics

- Temperature
- Humidity
- Soil moisture status
- Soil type
- Vegetation type and density

In order to overcome the difficult interrelationships above, Bredenkamp, *et al.* (1995) introduced the concept of effective recharge, which controls the natural water level fluctuations in an aquifer and therefore already incorporates the effects of evapotranspiration and other losses.

Bredenkamp, *et al.* (1995) have shown that the most reliable estimate for groundwater recharge is obtained by combining the output of recharge calculations of various methods and thereby selecting the most suitable estimate for recharge. Therefore, recharge for the TMG Aquifers of the Klein Karoo is estimated with as many as possible different recharge methodologies. All the recharge estimates calculated for each TMG Aquifer, including known expert guesses are summarised in the RECHARGE spreadsheet. A description of all the methodologies applied follows.

2.5.3.1 Mean Residence Time (MRT)

Recharge is one of the most difficult hydrogeological parameters to assess and usually requires long periods of observation. Recharge rates R (also MRT) can be estimated from the isotope-derived mean residence times by assuming that a pumped borehole produces a well-mixed sample of all the water flowing into it (Verhagen, 2000):

$$R = \frac{\sum_i H_i * p_i}{T} \qquad \text{..... Equation 9}$$

where H_i is the thickness of individual aquifer zones intersected by the borehole and p_i their porosity.

For radiocarbon values less than 80 pMC and tritium at less than 0.5 TU it can be assumed to a good approximation that there is no bomb-produced input. A_0 for modern carbon is therefore essentially constant and (after Gieske, 1995)

$$R = \frac{\sum_i p_i * H_i}{8270[(A_0 / A) - 1]} \quad \text{..... Equation 10}$$

Aquifer porosity is a critical parameter in these calculations. Values may be measured directly, e.g. drill cores but in many cases, such information is not available. The best that can then be done is that porosity is estimated which requires at least a good knowledge of the borehole log and the nature of the local rock formations. In addition, borehole depth and rest water level should be known.

2.5.3.2 Cumulative rainfall departure (CRD) method

This method was improved on by Bredenkamp, *et al.* (1995) and conforms to the concept that equilibrium conditions develop in an aquifer over time until the average rate of losses equals the average recharge of the system. In simple terms, the CRD method calculates the sum of the monthly departures of rainfall from the long-term average monthly rainfall.

The CRD method implies that as the average rainfall changes, the total water balance is adjusted accordingly. In general, groundwater levels will rise if the rainfall exceeds average rainfall and decline if rainfall is less than the average rainfall, while losses from the system vary in proportion to the average precipitation.

Van Tonder and Xu (2001) revisited this method and improved the algorithm so that a user-friendly tool could be developed for groundwater practitioners. The derivation of both formulae follows below.

Assuming an aquifer of area (A) receiving recharge from rainfall (Q_R) is tapped by production boreholes (Q_p) and natural outflow (Q_{out}), a simple water balance equation for a given time interval i can be written as follows:

$$Q_{Ri} = Q_{pi} + Q_{outi} + \Delta h_i AS \quad (i = 1, 2, 3...N)$$

Where Δh_i is water level change and S aquifer storativity. If all the averaged Q_{Ri} are taken as a constant value, then the system is treated at equilibrium when Δh_i approaches zero. This is seldom the case in reality.

If Q_{pi} is a constant rate, Q_{outi} may depend on random rainfall events, while aquifer storage ($\Delta h_i AS$) would adjust itself to accommodate net balance between Q_{Ri} and Q_{outi}. This adjustment of the storage would be reflected in piezometric surface or water level change in boreholes. This cause-effect relationship between rainfall oscillation and water level fluctuation is effectively revealed by the correlation between the CRD and water level fluctuation.

Bredenkamp formula

Bredenkamp *et al.* (1995) defined a CRD as follows

$$ {}^{1}_{av}CRD_i = \sum_{n=1}^{i} R_n - \kappa \sum_{n=1}^{i} R_{av} \quad (i = 0, 1, 2, 3, \ldots N) \qquad \text{..... Equation 12} $$

Where R is rainfall values with subscript "$_i$" indicating i-th month and "$_{av}$" the average. $\kappa = 1+((Q_p+Q_{out})/(AR_{av}))$. $\kappa = 1$ indicates that natural conditions apply and $\kappa > 1$ if pumping takes place.

It is assumed that a CRD has a linear regression with a monthly water level change. Bredenkamp et al. (1995) derived, i.e. **Bredenkamp Formula**:

$$ \Delta h_i = (r/S) \cdot \left({}^{1}_{av}CRD_i \right) \quad (i = 0, 1, 2, 3, \ldots N) \qquad \text{..... Equation 13} $$

Where r is recharge percentage of rainfall. (Others are parameters defined previously.)

The Equation 13 may be used to estimate the ratio of recharge to aquifer storativity through the simple regression between CRD_i and Δh_i.

From Equation 11, the correspondence between the water levels response and the rainfall departure is obtained, i.e.:

- The groundwater level will rise if $Rf > Rf_{av}$.

- The losses from the system vary in proportion to the average precipitation.

The final equilibrium water level of an aquifer results therefore from the incremental water level changes resulting from the outcome of the above equation over the long-term. Experience has further shown that k>1 indicates that the system is being over-exploited. Bredenkamp, *et al.*, (1995) also derived a regression approach, which can be applied to obtain the CRD relationship for different time intervals. Therefore depending on the selected time interval, the variable response of CRD could be determined relative to the rainfall over 1, 3, or 6 months, or even the preceding 12 months. The regression approach is further modified to incorporate the carry-over of recharge from preceding years.

The CRD method is therefore a powerful tool to simulate water level fluctuations by incorporating short and long-term recharge events over time. Deviations from the CRD curve are indicative of changes in the water balance, e.g. abstraction, or changes in the physical catchment, e.g. changes in the vegetation of the catchment. The CRD method is used in this study to simulate recharge, as well as the impact of abstraction in the Vermaaks River Valley.

Deriving of new formula (Xu, 2000)

It is often the case that an appropriate value for the parameter κ in Equation 12 needs to be selected to adequately mimic the water level fluctuation in boreholes. However, its physical meaning is still unclear. Rainfall series in general are composed of random and deterministic components, the latter in the form of trends and periodicities. Especially a short series of data available for analysis often displays a trend to a certain degree, which can not be reflected in Equation 12. Thus a new CRD is defined as

$$ {}_t^1CRD_i = \sum_{n=1}^{i} R_n - \left(2 - \frac{1}{R_{av} i} \sum_{n=1}^{i} R_n\right) \sum_{n=1}^{i} R_t \qquad \text{..... Equation 14} $$

$$ (i = 1, 2, 3, \ldots N) $$

Where R_t, is a threshold value, representing the aquifer boundary conditions, which is determined during the simulation process. It often ranges from 0 to R_{av} with 0 and R_{av} indicating a closed and open aquifer system, respectively, or perhaps regulated by spring flow. It is noted that Equation 14 reduces to Equation 12 if rainfall events R_i do not show a trend ($R_t = \kappa R_{av}$). In this case cumulative rainfall average would conform to R_{av}.

It is assumed that a CRD is the driving force behind a monthly water level change if the other stress is relatively constant. The groundwater level will rise if the cumulative departure is positive and decline if it is negative.

Since CRD $\propto$ ($\Delta h + (Q_p + Q_{out})/(AS)$), thus rCRD = $S(\Delta h + (Q_p + Q_{out})/(AS))$. After rearrangement, Equation 15 is obtained:

$$\Delta h_i = (r/S)\cdot\left({}^{1}_{t}CRD_i\right) - (Q_{pi} + Q_{outi})/(AS) \qquad \text{..... Equation 15}$$
$$(i = 0, 1, 2, 3, \ldots N)$$

The term $(Q_{pi} + Q_{outi})/(AS)$ in Equation 15 is only necessary if a pumping borehole has an influence on the study area where water levels are measured.

It is possible to use Equation 15 to estimate the ratio of recharge to aquifer storativity through minimising difference between calculated and measured Δh_i series.

Comparison of the analysis of Equations 12 and 15, shows the following:

- If rainfall event R_i is constant over time, it is the same as its average R_{av} and groundwater levels would not fluctuate naturally, thus steady state conditions prevails.
- The Term $(Q_{pi} + Q_{outi})/(AS)$ of Equation 15 is only necessary if the influence is evident. This may be true in cases of highly fractured dolomitic aquifers where high values of transmissivity are encountered.
- Only ratio r/S can be determined through water level simulation.
- Since Equation 12 is used in Equation 13, it cannot accommodate dynamic pumping conditions. Equation 14 could account for such dynamic process through incorporation of changing pumping and outflow rates $(Q_{pi} + Q_{outi})$.
- Equation 13 implicitly assumes that oscillation of random rainfall is stationary without any particular trend. This is only valid data over a long period.

Further, water balance based methods are a lumped parameter approach. They do not address spatial parameter variation and should therefore be applied with caution.

Both the Bredenkamp (Equation 12) and new formula (Equation 14) are applied to determine recharge.

2.5.3.3 Area related recharge method

This method was developed by Dörhöfer *et al.* (1981), to determine groundwater recharge for regional aquifers, where the groundwater recharge for various parts of the regional aquifer are different. It takes into account the vegetation type, gradient of the catchment (thus run-off), soil type and evapotranspiration and involves the overlay of a series of graphs depicting these catchments.

This method requires that the regional TMG Aquifer be subdivided into zones of similar topography, rainfall, vegetation and soil type, whereafter the recharge rate is estimated by means of overlaying a series of graphs. The recharge for each zone is calculated by multiplying the surface area of each zone with the estimated recharge rate. The total recharge for the regional aquifer is calculated by the sum of recharge estimates for each zone.

This method seems to be very applicable to the Klein Karoo area with its highly variable rainfall, topography, soil and vegetation, but have limitations.

2.5.3.4 Chloride mass balance method

This is an effective method for determining recharge in the unsaturated zone, as a first approximation. The method is based on the relationship between chloride concentrations in rainfall and groundwater. Chloride is a conservative tracer and enters the soil or rock as part of infiltrating rainfall, whereafter it is concentrated in the soil by transpiration from plants and by direct evaporation from the soil. The method allows recharge to be calculated from the following relationship:

$$\mathbf{RE = (Cl_{input} / Cl_{output}) Rf} \quad \text{..... Equation 16}$$

Where,

RE	=	Recharge (mm)
Cl_{input}	=	Input Chloride concentration measured in rainfall (mg/l)
Cl_{output}	=	Ouput Chloride concentration measured in groundwater (mg/l)
Rf	=	Rainfall (mm).

The Cl-method is not applicable to the valley areas of the Klein Karoo as an underground source of Cl exists in the Bokkeveld Formations and high evaporation rates apply. When groundwater flow rates are very low, evaporative moisture losses renders the Cl-method to be less successful. However, in narrow valleys, with steep flow gradients, such as the Vermaaks River Valley, high groundwater flow rates minimise evaporation losses and improve the accuracy of the Cl-method, although surface runoff reduces the effective value of rainfall.

2.5.3.5 Baseflow – experimental catchments at Jonkershoek / Franshoek

The flows have been accurately monitored in mountainous, experimental catchments in the Jonkershoek and Franshoek catchments for many years.

Scott *et al.* (1992) estimated the empirical relationships between baseflow, annual rainfall and streamflow. From this relationship Bredenkamp, *et al.* (1995) estimated the recharge for mountainous catchments similar to that of the Kammanassie Mountains (geology, topography and vegetation cover), e.g. the TMG catchment areas of Jonkershoek and Zachariashoek. These catchments are still in their natural states, providing a unique opportunity to derive rainfall/run-off relationships that would be characteristic of mountainous areas. Such catchments contain excellent aquifers, sustained by baseflow of the streams, which in turn is derived from groundwater.

The view adopted herein, is that the ratio between base flow and the total run-off is a means of estimating the groundwater recharge in mountainous terrains, i.e. TMG catchments of the Kammanassie Mountains. If base flow and flood flow are separated in a reliable way, average base flow should be proportional to the annual rainfall (Bredenkamp *et al.*, 1995).

The rainfall / recharge relationships obtained in the above-mentioned experimental catchments will be applied to the Klein Karoo area to derive a representative recharge figure for this area.

2.5.3.6 Saturated volume fluctuation method (SVF-method)

In this method the water of an aquifer is analysed by means of lumping the abstraction and integrating the resultant response in the saturated volume of the aquifer over a period of time. Van Tonder (1989) developed the method, while

Bredenkamp et al. (1987) modified the method to enable the estimation of storativity.

The SVF method was applied to all the KKRWSS production boreholes to estimate recharge and storativity.

All the recharge estimations, including expert guesses are summarised in a RECHARGE spreadsheet, developed by van Tonder and Xu (2000).

2.5.3.7 GIS Raster approach

In this method (after Woodford, 2001) the annual volume of recharge to any part of an aquifer is determined from 25 x 25 m cells of mean annual precipitation and it's statistical coefficient of variation (Schultze, 1997), as well as terrain slope. This GIS approach makes the spatial variation of recharge, based on changes in topography and rainfall possible.

2.5.4 Determine radius of influence of abstraction

The radius of influence of abstraction are determined, as a first approximation, by using a conventional method, i.e. the Dupuit analytical equation for steady state flow conditions.

2.6 CONCEPTUAL HYDROGEOLOGICAL MODEL

Definition of the conceptual hydrogeological model is the single most important step in managing an aquifer. This part of the research is seen as the data analysis phase and the largest proportion of time has been devoted to this section.

Accordingly, a conceptual hydrogeological model for the TMG Aquifer in the Klein Karoo, more specifically the Kammanassie Mountains, is formulated and management tools developed to enable management of the KKRWSS. All the hydrogeological, hydrochemical, environmental isotope and remote sensing information obtained during fieldwork and desk study were interpreted and collated into the conceptual hydrogeological model. The aquifer parameters obtained from pump test data analysis methods, remote sensing and hydrochemical data processing assisted in the definition of the hydrogeological boundaries and general groundwater flow regime.

2.7 DETERMINE GROUNDWATER WATER BALANCE

From first principles it can be shown that:

$I(t) - O(t) = \Delta S / \Delta t$ ..... Equation 17

Where,

I = inflow (L^3/t)

O = outflow (L^3/t)

$\Delta S / \Delta t$ = rate of change in storage over a finite time step (L^3/t).

The above equation holds for a specific period of time and may be applied to any given system provided that the boundaries are well defined. A water balance calculation was carried out for the local (Kammanassie Mountain) study area. This water balance incorporated the following elements:

ΔS = Effective Recharge - (Springflow + Abstraction) ..... Equation 18

Groundwater abstraction data obtained from the KKRWSS and the hydrosensus, together with recharge estimates were used to calculate the water balance for the Kammanassie Mountains.

2.8 PROPOSED AQUIFER MANAGEMENT

After formulation the conceptual hydrogeological model and calculation of the water balance for the Kammanassie Mountains, a wellfield management plan for the Eastern Sector of the KKRWSS was developed. Initially numerical modelling was considered to optimise wellfield and aquifer management, however, too many unknowns in the conceptual model rendered alternative methods more favourable.

All the hydrogeological and borehole information for the wellfields of the Eastern Sector of the KKRWSS was captured in a specially designed data base, i.e. WELLMAN. This spreadsheet enables management of a production borehole based on its past and present performance, with respect to water level variations over time for given abstraction and rainfall scenarios. A basic spreadsheet for recharge calculation, i.e. RECHARGE was put together on a template designed by van Tonder and Xu (2000) for the TMG Aquifers of the KKRWSS. The aquifer yield of the local study area (Kammanassie Mountain) was determined by using the latest developed FC-method (Van Tonder, *et. al.,* 1999), for various scenarios of

associated risks and recharge in association with recharge estimates for the TMG Aquifers of the KKRWSS.

The FC-method, together with the newly developed wellfield management database, i.e. WELLMAN was used to determine the best management scenario for TMG Aquifers for different scenarios of abstraction and recharge.

CHAPTER 3: STUDY AREA OVERVIEW

An overview of the local and regional study area and the Klein Karoo Rural Water Supply Scheme follows. Also included in this chapter is all the relevant hydrogeological information of boreholes, sampled during this investigation.

3.1 LOCATION AND PHYSIOGRAPHY

The study area is situated between latitude 33°15' and 33°45' east and longitude 21°15' and 23°15' south, referred to as the regional study area. Uniondale and Ladismith are the main towns in the east and west, respectively, and Oudtshoorn, Calitzdorp, Dysselsdorp and De Rust are the other main towns in the central area (Figure 1-1).

TMG fracture systems do not only control the hydraulic properties of the aquifers but also determine the geomorphology of the landscape. The quartzitic TMG sandstones are highly resistant to chemical weathering and erosion and therefore form the high mountain ranges. This is in contrast to the overlying clay, mica and feldspar-bearing shales or underlying granitic and phyllitic rock types, which form the valleys.

The study area comprises a broad valley, with an elevation of approximately 500 metres above mean sea level (mamsl), surrounded by the following mountain ranges:

- The *Outeniqua and Swartberg* Mountain Ranges form the southern and northern boundaries. These ranges reach a maximum altitude of 1800 m and 2300 mamsl respectively.
- The *Kammanassie* Mountains with a maximum altitude of 1950 mamsl on the eastern side.
- The *Rooiberg and Sandberg* Mountains west of Calitzdorp form the western boundary with maximum altitudes of 1400 and 1223 mamsl, respectively (see Figure 1-1).

The valley has an average slope from east to west of 1 : 345. The mountain ranges rise very steeply above the valley floor, which are approximately 365 mamsl at Dysselsdorp in the east and 190 mamsl at Calitzdorp Spa in the west. The valley is drained primarily in an east to west direction by the following rivers (Figure 1-1):

In the east: The *Olifants River* and its tributaries originating in the Kouga Mountains east of Uniondale and the central Karoo.

In the north-west: The *Dwyka, Leeugamka and Gamka Rivers*, drain the northern slopes of the Swartberg and tributaries of the Gamka River, originating in the Hell (Gamka's Kloof), drain to the north.

From here onwards, the local study area refers to the Kammanassie Mountains study area, marked on Figure 1-1. The local study area includes the Eastern Sector of the KKRWSS and the private boreholes on the southern side of the Kammanasie area. Figure 2-5 is a locality map of the local study area with all the important data points.

3.2 KLEIN KAROO RURAL WATER SUPPLY SCHEME

The study area incorporates the Western and Eastern supply sectors of the KKRWSS (Figure 1-1). The Scheme is composed of an Eastern Sector (Dysselsdorp: 13 boreholes, see Figure 3-1), and a Western Sector (Calitzdorp: 5 boreholes, see Figure 3-2). The abstracted water is then conveyed via a 27 km pipeline to two purification plants, one at Dysselsdorp and the other at Calitzdorp. After purification, the water is conveyed via a total of 365 km of pipeline to end users i.e. the town of Dysselsdorp and irrigation users in the Olifants River Valley (Figure 1-1).

The DWAF monitors rainfall in several rain gauges distributed over the area, water levels in all production and several observation boreholes and abstraction from production boreholes. The flow of springs originating at the C/S layer is also measured at two v-notches in the Marnewicks and Vermaaks River Valleys. A monitoring report is produced on a monthly basis to enable timeous decisions to be made regarding abstraction volumes, distribution and wellfield management.

3.2.1 The Eastern Sector of the Scheme

The Eastern Sector has a design capacity (estimated from test pumping carried out in 1994 by DWAF [Mulder, 1995]) of 9000 m^3/d (3.3 x 10^6 m^3/a) based on peak demand. This section abstracts water from five separate wellfields (see Figure 3-1) which are listed below, with the production boreholes from which water is abstracted shown in bold:

1. Varkieskloof: situated east of Dysselsdorp; water is abstracted from: **DP10**, **DP12** and **DP29**. DP27 is a standby production hole.

2. Bokkraal: situated east of Dysselsdorp; water is abstracted from: **DP15**, **DP25** and **DP28**. Standby boreholes are DP13 and DP14.

3. Olifants River: situated on the banks of the Olifants River; water is abstracted from only one borehole: **DP18**.

4. Droëkloof: situated in Dysselsberg; water is abstracted from only one borehole: **DG110**.

5. Voorzorg: **VG3**, situated in the Vemaarks River Valley on the farm Voorzorg;

6. Vermaaks River: situated in the Vermaaks River Valley, on land owned by DECAS; water is abstracted from: **VR6**, **VR7**, **VR8** and **VR11**.

N.B. standby boreholes can be used in place of but not in conjunction with other boreholes.

3.2.2 The Western Sector of the Scheme

The Western Sector has a design capacity capacity (estimated from test pumping carried out in 1994 by DWAF [Mulder, 1995]) of 3765 m^3/d (1.374 x 10^6 m^3/a) and a peak capacity of 5650 m^3/d. Water is abstracted from 5 boreholes on two farms (see Figure 3-2):

1. Daniëlskraal : water is abstracted from the following boreholes: **DL12 DL13**, **DL15**, **DL16** and **DL17**.

2. Kleinberg : water is abstracted from one borehole: **KG1**.

The Western Sector falls outside the boundaries of the local study area and is not discussed further in any detail.

3.2.3 Wellfield capacities

Since the beginning of groundwater abstraction in 1989 / 1990, estimated wellfield output from the KKRWSS has decreased four times up until 1995 as water levels continued to drop. Based on a re-evaluation of the 1989 pumping tests, Kotze (1995) scaled down the total potential of the Scheme by 60% (DWAF, Technical Report GH3858) and summarised the wellfield potentials, pumping scenarios and aquifer status up to June 1995. The capacity was reduced due to the following possible concerns:

- That the Vermaaks River Spring will dry up.
- Several boreholes are within each other's radius of influence.
- That the large drop in water levels, is due to over-abstraction.

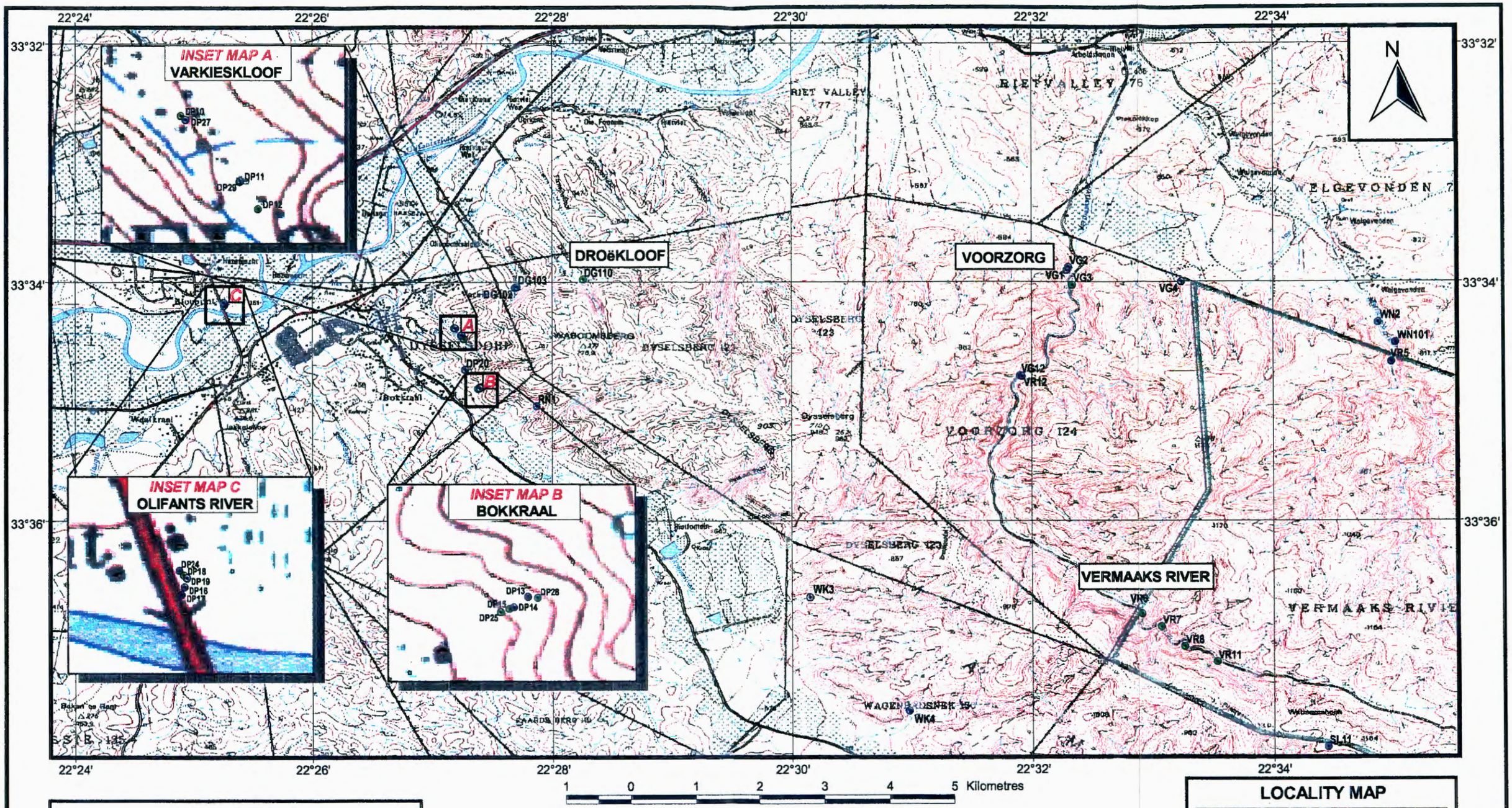

WRC Proj. K5/729	KKRWSS - EASTERN SECTOR WELLFIELDS AND PRODUCTION BOREHOLES	FIGURE 3-1

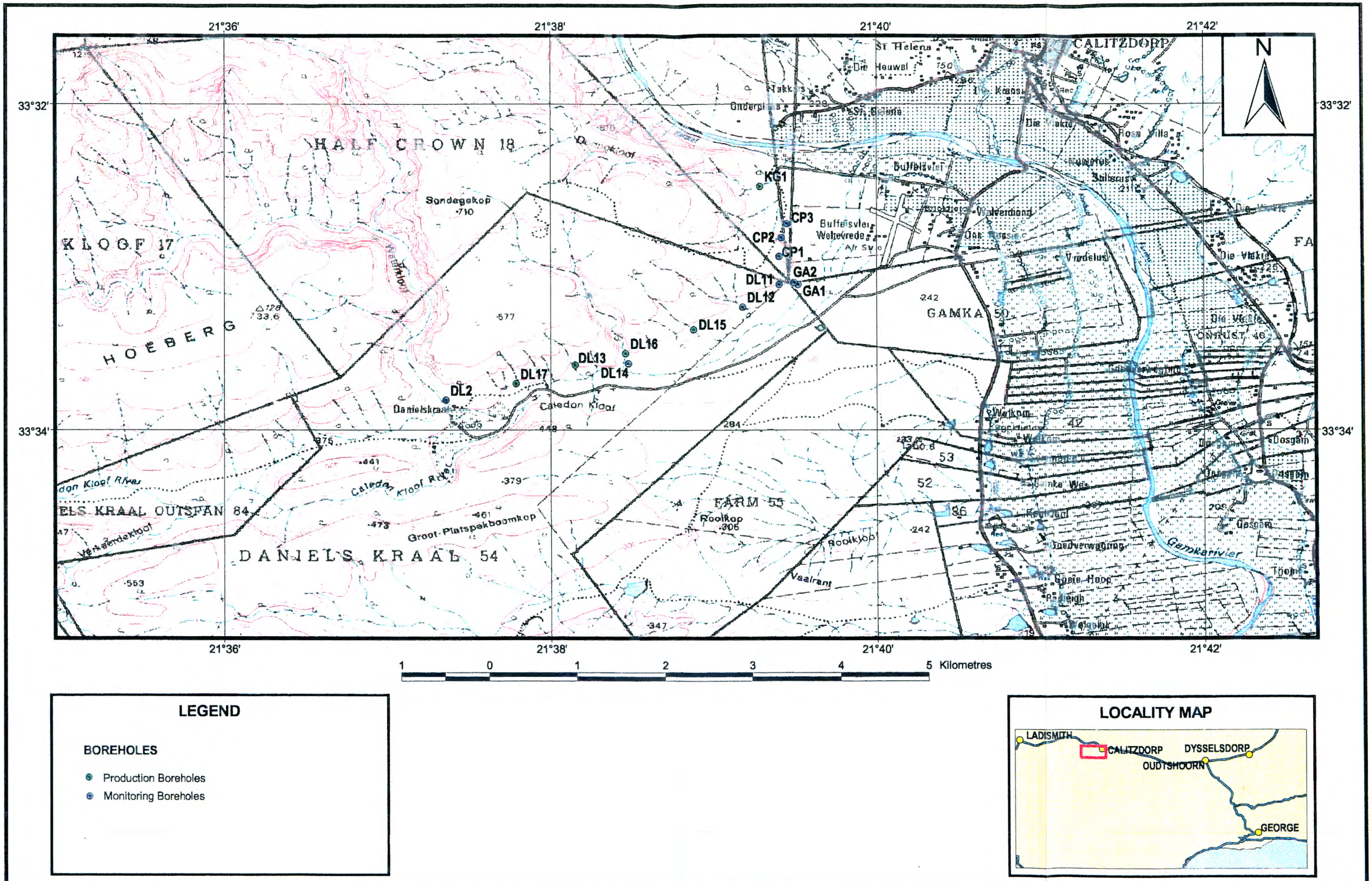

WRC Proj. K5/729

K KRWSS - WESTERN SECTOR WELLFIELDS AND PRODUCTION BOREHOLES

Figure 3-2

Table D-1 (Appendix D) provides a summary of all the changes in individual borehole capacities as well as individual wellfield and total Scheme capacity over the period 1993 to 1995. The current total daily recommended abstraction is 3050 m^3 for the entire Scheme and 5450 m^3/d during peak times (DWAF, Technical Report GH3858). Take note that initial pumping recommendations by Mulder (1995) made provision for peak and normal supply yields, by varying individual borehole yields, while Kotze (1995) replaced peak capacity by pumping more boreholes at the same time, to establish increased yield. The total abstraction and abstraction rates over time for each production borehole are summarised in Appendix K (K-7).

Changes in the operation and management of the KKRWSS have recently been proposed by Groundwater Consulting Services (GCS), who were appointed by DWAF in 1998 to evaluate the operation of the KKRWSS and wellfield performance and monitoring systems. In order to achieve the above-mentioned objectives, GCS carried out rehabilitation, reconstruction and re-testing of a number of boreholes. Re-testing of boreholes was carried out for the following reasons:

- To test the effectiveness of the rehabilitation and construction work.
- To evaluate yields and efficiencies of boreholes not adequately tested in the past.
- To evaluate the interconnectivity between boreholes and aquifers (for providing data and information to this research).
- Evaluation of historical hydrogeological data.

Serious shortcomings of all the wellfield capacity estimations so far are the following:

- Poor understanding of the conceptual hydrogeological model.
- Lack of a water balance for each sector of the KKRWSS.
- Simplistic analytical methods and conventional methods were used to analyse pump testing data, mainly aimed at providing estimates of the 'safe-yield' of the production borehole and information required for the design of pumping equipment.

One of the objectives of this research is to provide a wellfield management plan for the Eastern Sector of the KKRWSS, based on the conceptual hydrogeological model and water balance of the aquifer system hosting the Eastern Sector of the KKRWSS.

3.3 CLIMATE AND EVAPOTRANSPIRATION

One of the characteristic features of the Klein Karoo area is the very large diurnal and seasonal fluctuation in temperature. In addition, the climate is highly variable, thunder storms in the hot summer months, contrasting with snow on the highest mountain peaks in winter until late spring. The area is located at some distance inland from the moderating influence of the ocean and thus temperature extremes between the seasons are common. During the hot summers temperatures commonly reach 38 °C. On the other hand, during cold winter nights, temperatures can drop below freezing. Daily average minimum and maximum temperatures for summer and winter vary between 15 to 42 °C and -3 to 18.5 °C, respectively. Although rain falls throughout the year, the highest rainfall often occurs in autumn or spring. Snowfalls on the mountain peaks in the winter are common and mist occurs throughout the year.

Figure 3-3 compares the evaporation figures measured at Rooiheuwel (Oudtshoorn) and at the Kammanassie Dam with average monthly rainfall measurements for Oudtshoorn (calculated for the period 1878 to 1998). Average annual evaporation varies between 1760 and 2050 mm/a from west to east, and is 50% less (compared to summer figures) in the months of April to September each year (Figure 3-3). Evapotranspiration losses are therefore at a maximum from October to March, reflected in a drop in groundwater levels and concurrent decline in spring flow.

FIGURE 3-3: COMPARISON - MONTHLY RAINFALL AND EVAPORATION FIGURES FOR THE KLEIN KAROO

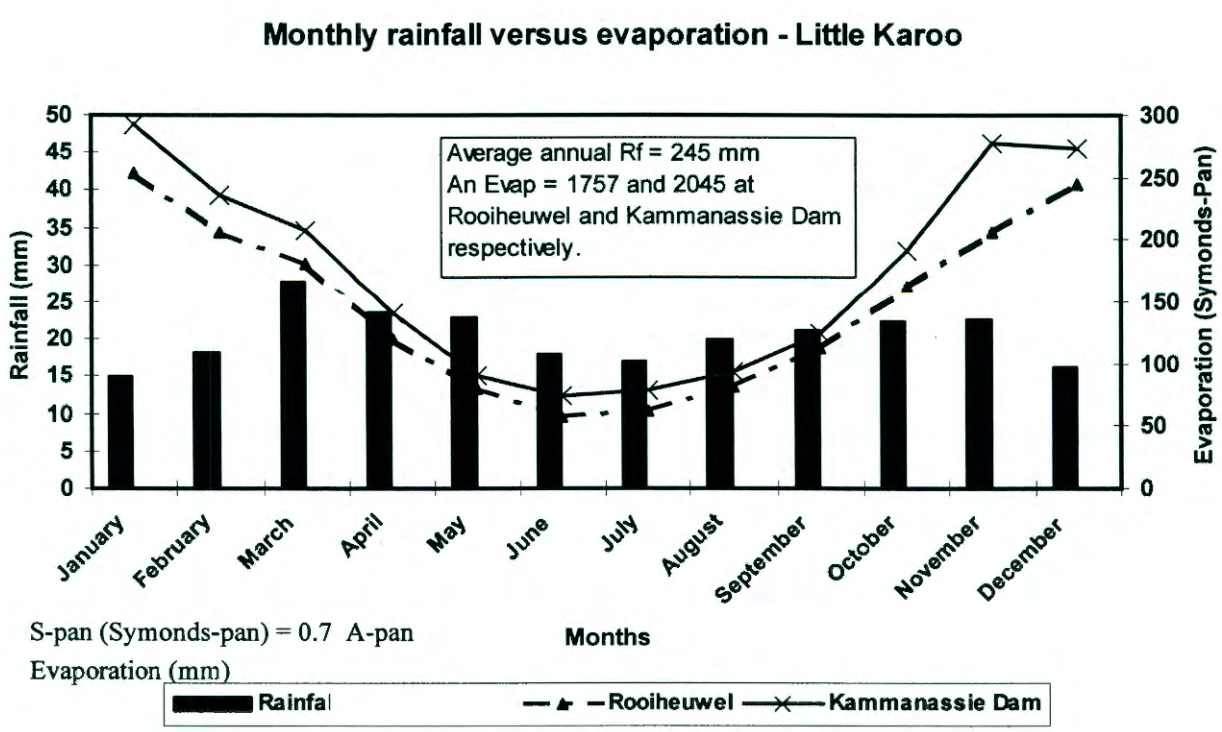

3.4 RAINFALL

One of the most significant characteristics of the Klein Karoo area is its semi-arid broad valley, surrounded by high mountain ranges with rainfall up to ten times that of the dry valley areas. Rainfall in the broad valley area is variable both spatially and temporally, with rainfall being low and variable seasonally and annually (see Figures 3-4 A to D). On the otherhand, rainfall in the mountain areas is higher (see Figures 3-5 and 3-6) and significant snowfalls occur on peaks in winter, mist throughout year. Annual rainfall figures for the entire study area are summarised in Tables C-1 to C-3 (Appendix C). It is postulated that the significant variation in rainfall, snow and mist occurrence between valley and mountain areas may contribute to storage of considerable amounts of groundwater in the TMG Aquifers below the valley areas. The above postulation will be true if an interconnection between the recharge areas in the high mountain ranges and the aquifers in the dry valley exists.

The following are characteristic average annual rainfall figures in the valley areas:

- 245 mm at Oudtshoorn
- 199 mm at Calitzdorp
- 313 mm at Ladismith
- 329 mm at De Rust and
- 315 mm at Uniondale (More detailed rainfall information can be found in Appendix C).

Average annual rainfall on the mountain ranges is generally directly proportional to altitude (see Figure 3-7) and reduces with distance from the coast (Figure C-1, Appendix C) as follows:

- 1800 mm in the Outeniqua Mountains
- 1500 mm in the Swartberg Mountains
- 550 mm in the Kammanassie Mountains and
- 450 mm in the Rooiberg Mountains.

Rainfall increases with altitude in mountain ranges, thereby enhancing recharge. In addition to rainfall, significant contribution to recharge and surface water flow is derived from snowmelt during spring, emanating from snow accumulation on the highest peaks of the mountain ranges.

FIGURE 3-4: VARIATIONS ANNUAL RAINFALL – VALLEY AREAS

(A) ANNUAL RAINFALL VARIATIONS CALITZDORP

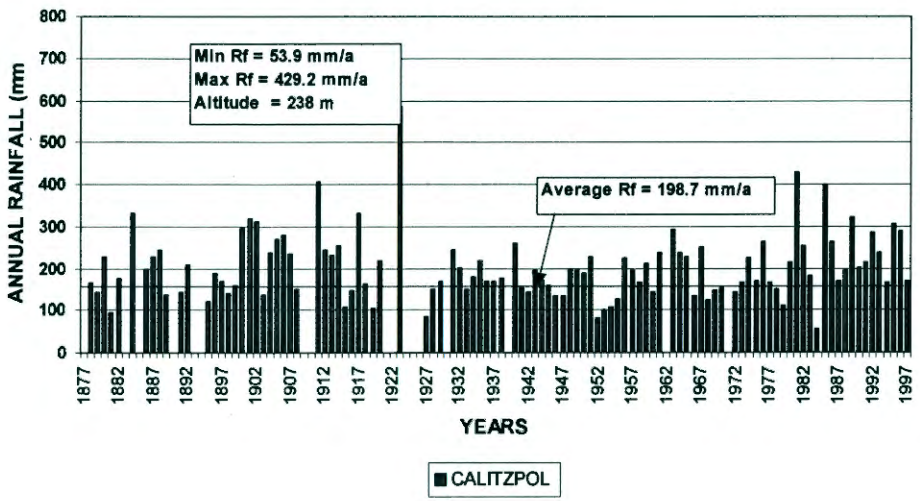

(B) ANNUAL RAINFALL VARIATIONS OUDTSHOORN

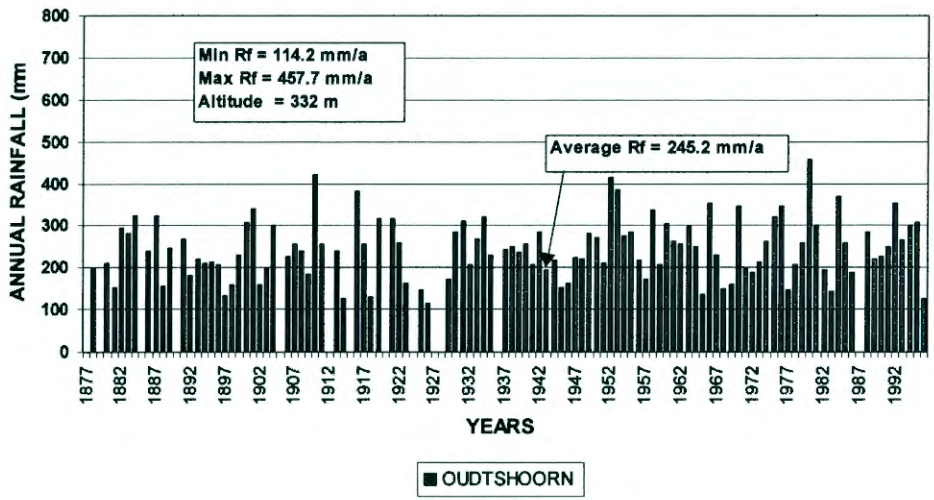

(C) ANNUAL RAINFALL VARIATIONS PRINS ALBERT

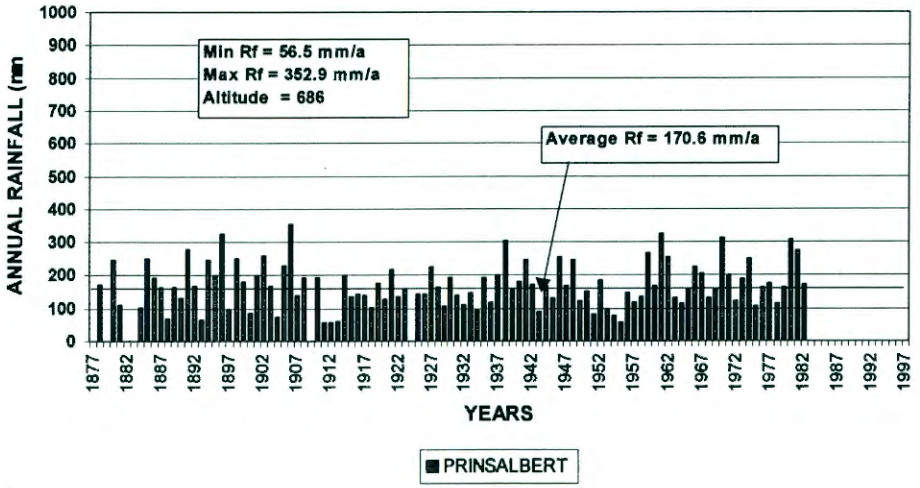

(D) ANNUAL RAINFALL VARIATIONS LADISMITH

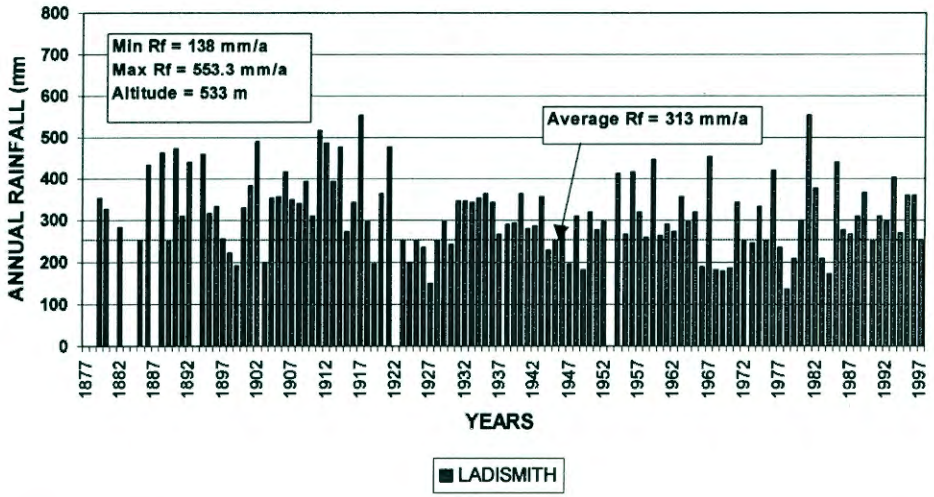

FIGURE 3-5 : RAINFALL – SWARTBERG MOUNTAINS

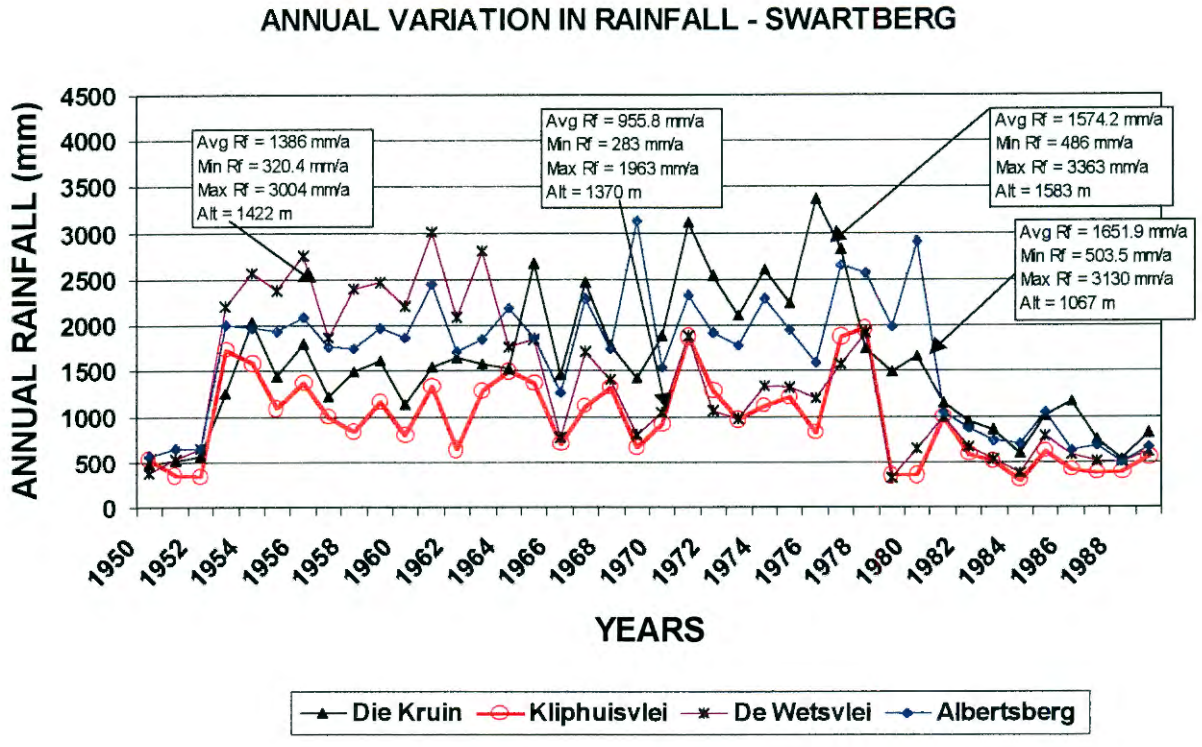

FIGURE 3-6: RAINFALL – KAMMANASSIE MOUNTAINS

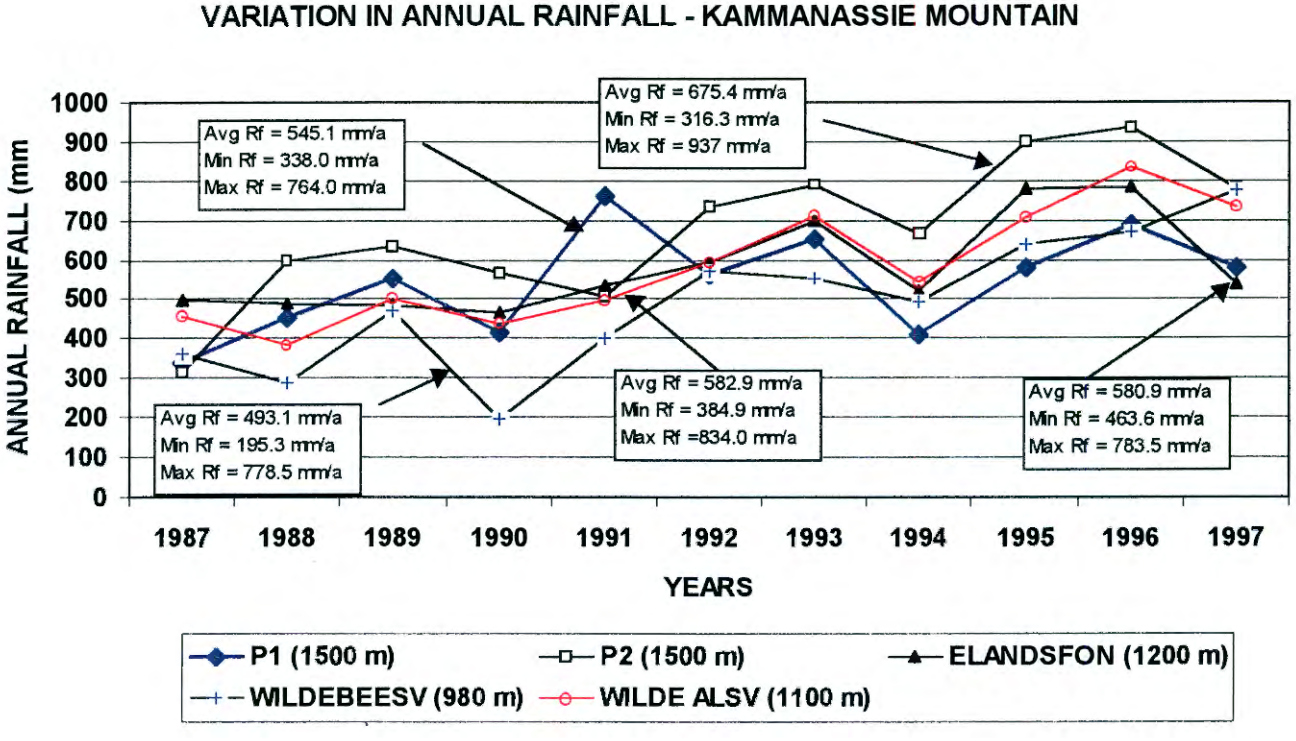

FIGURE 3-7: RAINFALL VARIATION WITH ALTITUDE

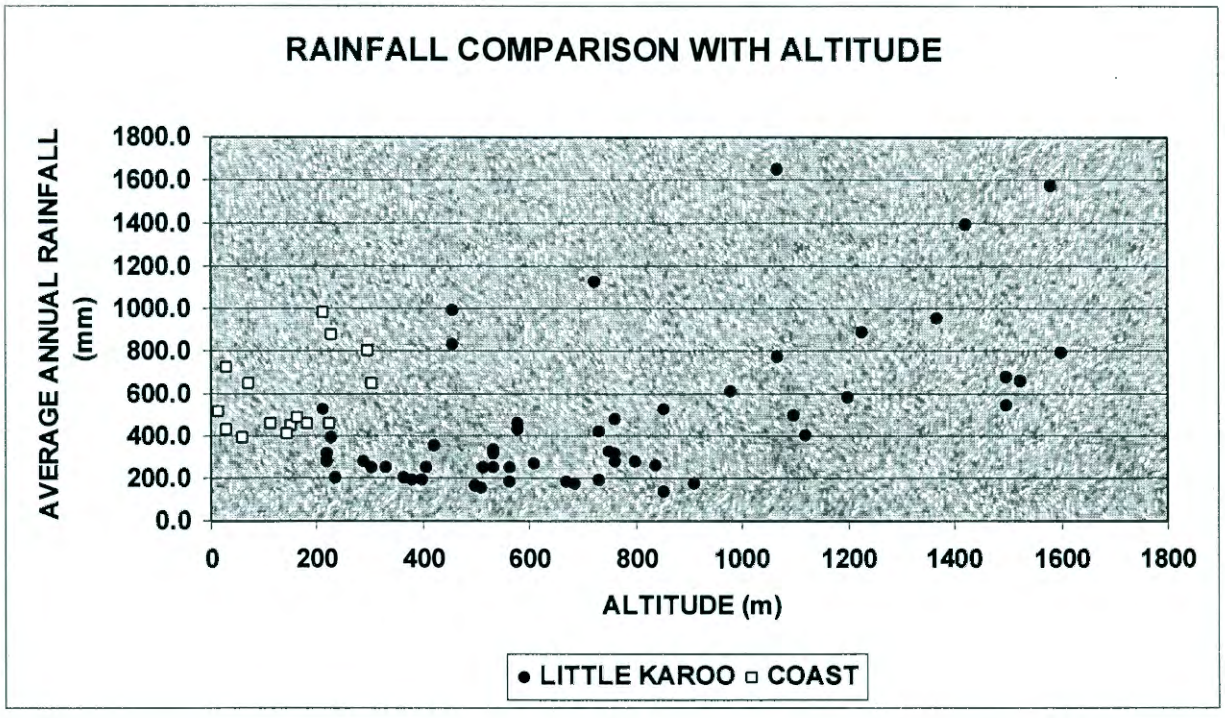

3.5 GEOLOGY AND STRUCTURE

The TMG is a major lithological unit of hydrogeological importance in the Southern and Western Cape region. It is a regional fractured aquifer covering a very large area and a good understanding of fracture styles, geometry and preferred orientation of water-bearing fractures contributing significantly to groundwater flow, and hydrostratigraphic inter-relationships between different lithological units is required.

The depositional and structural development of the geological environments hosting the TMG Aquifers was studied in detail. This section is divided into regional and local geology and structure sub-sections, respectively. The first-mentioned section summarises the regional, larger scale geological features, i.e. sedimentary conditions under which sediments were deposited and regional scale tectonic events (tectonogenis), which impacted on the sedimentary basin after deposition of the sediments. The latter section describes the geology and existing structural relationships of the Kammanassie Mountains on a smaller scale, focussing on the formations of the TMG and associated fracturing and folding styles associated with each formation of the TMG.

3.5.1 Regional geology and structure

The quartzitic sandstone formations of the Table Mountain Group (TMG) are relatively high-permeability aquifers due to a pervasive network of fracture sets, including bedding-parallel fractures, bedding-orthogonal and bedding-oblique jointing at various scales, and fault zones with variable length and displacement characteristics. Any progress towards a full understanding of TMG hydrogeology, therefore, first requires an accurate characterisation of the fractured-rock structure within the aquifers, and a consideration of its implications for permeability, fluid flow, and fluid storage (Hay *et al.*, 1999).

3.5.1.1 Stratigraphy and geological history

Table 3-2 (over page) summarises of the regional stratigraphic units with their associated thickness and lithological compositions. The grey shading of the Schoemanspoort Formation in Table 3-2 indicates its separation from the Cango Group.

A geological map of the regional study area is presented in Figure 3-8. Two N-S geological cross-sections drawn along 22° 33' and 22° 52' East are presented in Figures 3-9 and 3-10, respectively (Chevallier, 1998). The position of the two section lines are indicated A-A' and B-B', respectively, on Figure 3-8.

Basement rocks comprising Maalgaten Granite and a variety of sedimentary and metamorphic rocks belonging largely to the Cango and Kaaimans Groups, respectively. Basement rocks are exposed south of the Outeniqua Mountains and north of the Cango Fault Zone in the south and north, respectively (see cross-sections A-A' and B-B' Figures 3-9 and 3-10, respectively).

The Cape Supergroup attains a thickness of more than 8000 m and consists predominantly of a wedge of quartzitic rocks, thickening to the south, which was deposited along the southern margin of Gondwana. During the deposition of the Cape Supergroup, sedimentary environments varied from terrestrial in the lower parts to shallow marine in the upper parts of the Supergroup.

All the Cape Supergroup rocks comprising the Table Mountain Group (TMG), Bokkeveld and Witteberg Groups are present in the study area. Of the above, only the TMG is of relevance in this study. Therefore its associated sedimentary depositional environment is included.

TABLE 3-1: GEOLOGICAL SUCCESSION IN THE GREATER OUDTSHOORN AREA

SUPER GROUP	SUBGROUP	GROUP	FORMATION	Thickness (m)	LITHOLOGY
					Alluvium, sand, gravel and other unconsolidated deposits as well as calcrete
	Uitenhage		Buffelskloof		Conglomerate, thin sandstone, siltstone and mudstone
			Kirkwood		Conglomerate, siltstone, mudstone
			Enon		Conglomerate, thin sandstone, siltstone and mudstone
Karoo	Beaufort		Teekloof	1000	Mudstone and shale
			Abrahamskraal	2400	Mudstone, siltstone and sandstone
	Ecca		Waterford	800	Sandstone, minor siltstone and shale
			Fort Brown	1000	Shale, thin siltstone and sandstone
			Laingsburg/Rippon	1000	Sandstone, greywacke, siltstone/mottled grey sandstone, shale
			Vischkuil	100	Arenaceous shale, siltstone and thin sandstone
			Collingham	30	Siltstone, chert, sandstone, volcanic ash
	Dwyka			600	Diamictite and shale
Cape	Witteberg	Lake Mentz	Waaipoort	340	Shale, siltstone, thin sandstone
			Floriskraal	80	Sandstone, siltstone, shale and grit
			Kweekvlei	200	Shale
			Witpoort	850	Quartzitic sandstone, minor siltstone
		Weltevrede		800	Micaceous, purple to red brown siltstone, mudstone and shale.
	Bokkeveld	Traka	Adolphspoort	1000?	Siltstone, shale, sandstone
			Karies	1200	Shale
		Bidouw	Waboomberg	200	Siltstone, shale
			Boplaas	100	Sandstone
			Tra-Tra	350	Shale, siltstone
			Hex Rivier	70	Sandstone, siltstone
			Voorstehoek/ Swartkrans	300	Shale, siltstone
			Gamka	200	Sandstone, siltstone
			Gydo	600	Shale, siltstone
	Table Mountain	Nardouw	Baviaanskloof	300	Feldspathic quartz arenite
			Kouga	500	Quartz arenite
			Tchando	400	Brown-weathering arenite, minor siltstone, shale
			Cedarberg	50	Prominent shale marker
			Peninsula	1500	Quartz arenite

Disconformity (break in the geological record).

Cango Group		Schoemanspoort	600	Grit, greywacke, subarkose, conglomerate
	Kansa	Schoongezicht	?	Conglomerate, greywacke, shale
		Gezwindskraal	?	Fine-grained greywacke, shale
	Goegamma	Uitvlugt	?	Cross-bedded greywacke, shale
		Vaartwel	?	Quartz-pebble and conglomerate
		Groenefontein	2400?	Grit, arenite, fine-grained greywacke, shale, limestone lenses
		Matjiesrivier	?	**Kombuys Member**: Limestone, siltstone and shale
			?	**Nooitgedagt**: Limestone, shale, greywacke and subarkose
Cape Granite				Gneissic granite
Kaaimans			85?	Feldspatic Quartzite

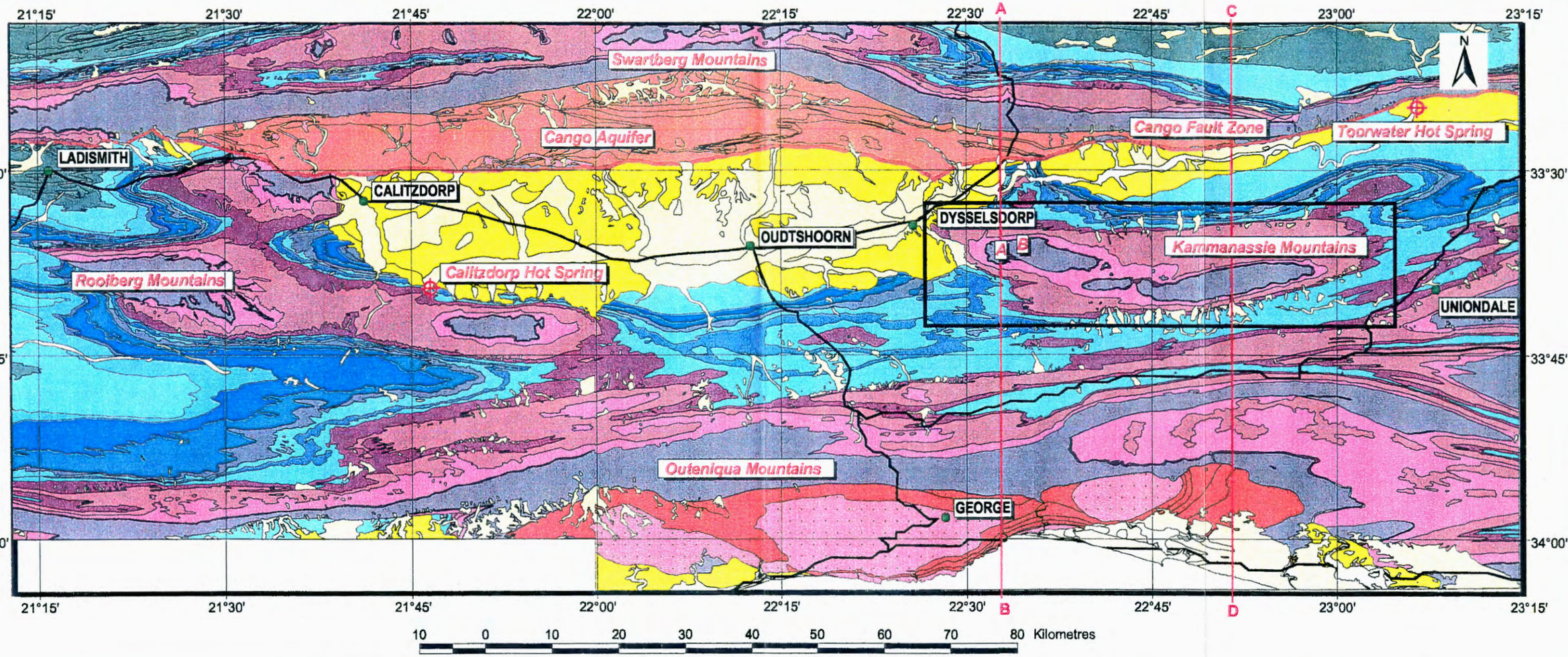

LEGEND

GEOLOGY

Alluvial Deposits

GROUPS

- Uitenhage (Cretaceous)
- Witteberg
- Cape Granite Suite
- Cango
- Kaaimans

BOKKEVELD GROUP

- Adolphspoort
- Boplaas
- Tra-Tra
- Hex River
- Swartkrans
- Gamka
- Gydo
- Karies
- Waboomberg

TABLE MOUNTAIN GROUP

- Baviaanskloof
- Kouga
- Tchando

(TMG) NARDOUW AQUIFER

- Cedarberg C/S
- Peninsula (Peninsula Aquifer)

A—B Section Line

OTHER FEATURES

- Local Study Area
- A Vermaaks River
- B Marnewicks River
- Cango Fault
- Water Bodies
- Major Roads
- Major Towns
- Hotsprings

LOCALITY MAP

ACKNOWLEDGEMENTS

Digital 1:250 000 Geological Data : Council for Geoscience
Digital 1:50 000 Topocadastral Data : Chief Directorate of Surveys and Mapping

WRC Proj. K5/729

GEOLOGICAL MAP - REGIONAL STUDY AREA - KLEIN KAROO

FIGURE 3-8

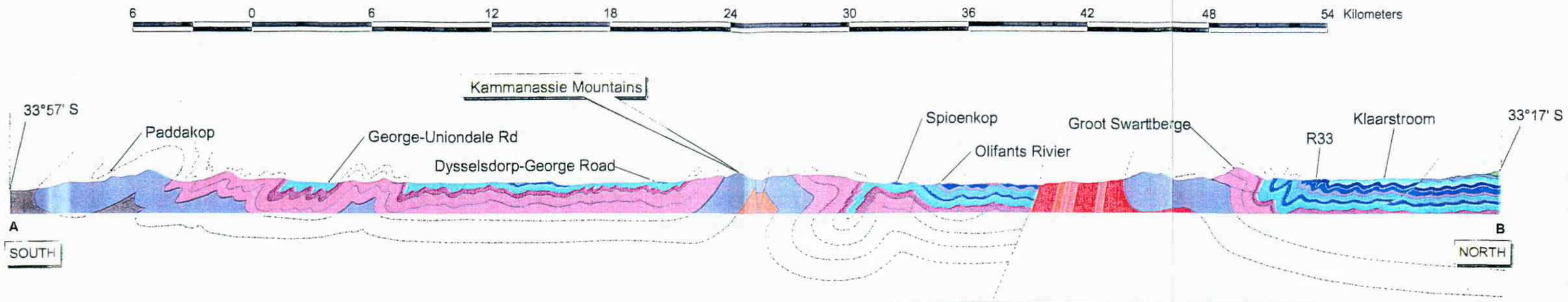

CROSS-SECTION LINE A-B ON FIGURE 3-8
SCALE 1/100 000
PROJECTED STRATIGRAPHY

LEGEND

	Alluvium		
	Enon Formation	UITENHAGIE GROUP	
	Wilpoort Formation	WITTEBERG GROUP	CAPE SUPER GROUP
	Weltevrede Formation		
	Adolphspoort Formation	BOKKEVELD GROUP	
	Boplaas Formation		
	Tra-Tra Formation		
	Hex River Formation		
	Swartkrans Formation		
	Gamka Formation		
	Gydo Formation		
	Baviaanskloof Formation	NARDOUW SUBGROUP	TABLE MOUNTAIN GROUP
	Kouga Formation		
	Tchando Formation		
	Cederberg Formation (C/S)		
	Peninsula Formation		
	Gezwinds Kraal Formation	CANGO GROUP	
	Ullvlugt Formation		
	Vaartwell Formation		
	Groenefontein Formation		
	Undifferentiated		
		KAAIMANS GROUP	

WRC Proj. K5/729	NORTH-SOUTH GEOLOGICAL CROSS-SECTION ALONG 22°33' EAST	FIGURE 3-9

5 0 5 10 15 20 25 30 35 Kilometres

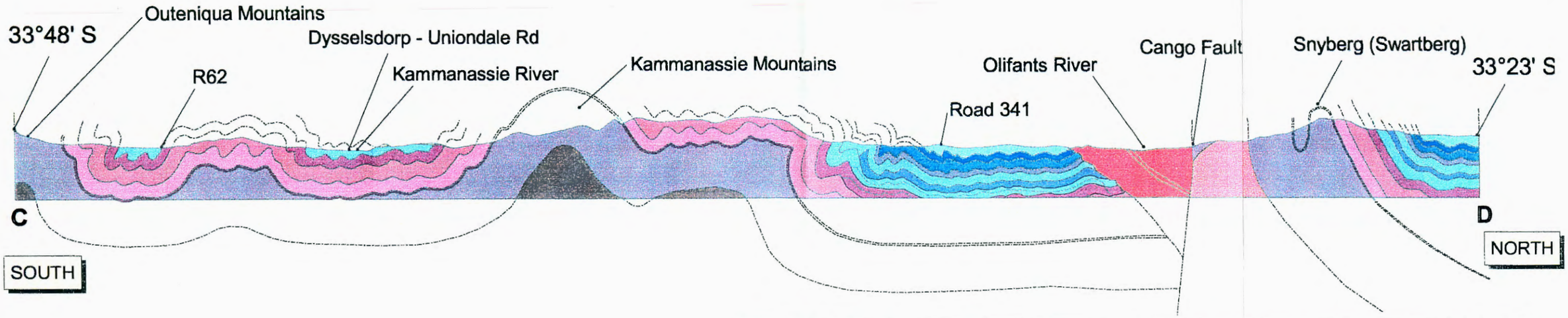

CROSS-SECTION LINE C-D ON FIGURE 3-8
SCALE 1/100 000
PROJECTED STRATIGRAPHY

LEGEND

	Alluvium		
	Enon Formation	UITENHAGE GROUP	
	Witpoort Formation	WITTEBERG GROUP	CAPE SUPER GROUP
	Weltevrede Formation		
	Adolphspoort Formation	BOKKEVELD GROUP	
	Boplaas Formation		
	Tra-Tra Formation		
	Hex River Formation		
	Swartkrans Formation		
	Gamka Formation		
	Gydo Formation		
	Baviaanskloof Formation	NARDOUW SUBGROUP	TABLE MOUNTAIN GROUP
	Kouga Formation		
	Tchando Formation		
	Cedarberg Formation (C/S)		
	Peninsula Formation		
	Gezwinds Kraal Formation	CANGO GROUP	
	Uitvlugt Formation		
	Vaartwell Formation		
	Groenefontein Formation		
	Undifferentiated		
		KAAIMANS GROUP	

WRC Proj. K5/729

NORTH-SOUTH GEOLOGICAL CROSS-SECTION ALONG 22°52' EAST

FIGURE 3-10

The TMG comprises an approximately 3500 m thick sequence of quartz arenite (quartzitic sandstone) and minor shale layers deposited in a shallow, but extensive, predominantly east-west striking basin, changing to a north-west orientation near Worcester (Rust, 1973). A prominent marker band, the Cedarberg Shale, occurs about two-thirds from the bottom of the sequence. The sediments were deposited in a fairly stable continental shelf environment and attain a maximum thickness of 3010 m in the east. Quartz arenite units reflect a prolonged period of eustatic stability with thickness ranging to 1600 m in the shallow marine deposits (Peninsula Formation of the TMG).

A thick succession of conglomerate and sandstone belonging to the Enon Formation (Uitenhage Group) is present, to the south of the Cango Fault Zone (Figure 3-10).

Alluvial valley deposits are associated with the larger river channels while colluvial (slope) deposits produced by sheet-wash, occur on gently sloping surfaces away from the river channels.

3.5.1.2 Regional Structure

The entire geological succession, i.e. the basement rocks, Cape Supergroup and part of the Karoo Sequence were subjected to severe north-south orientated compressive stresses, producing the so-called Cape Fold Belt (CFB) during the Cape Orogeny.

The Cape Fold Belt (CFB) consists of two branches, i.e. a western and southern branch which form the characteristic mountain chain along the southern and part of the western coasts of South Africa, respectively. The western and southern branches of the CFB meet in a 100 km wide syntaxis area, comprising NE-trending folds situated between Ceres and Gansbaai (approximately 200 km to the west of the study area).

In the Southern Cape and Klein Karoo, the southern branch of the CFB comprises a 900 km long gently arcuate belt. The more resistant strata of the group form prominent E-W trending mountain ranges, i.e. Swartberg, Rooiberg, Gamkaberg, Kammanassie and Outeniqua Mountains.

The above-mentioned mountain ranges are separated by synclinal intermontane basins - earlier referred to as a broad valley. The resistant quartzites are exposed in

the cores of anticlinal mountains and form rugged upstanding topography. The intervening broad valleys are open, subdued topographic features, due to the underlying, less resistant Bokkeveld Group sediments. A detailed description of all the deformational stages during the CFB orogenesis can be found in Hälbich (1983).

The compressional deformation during the Cape Orogeny was followed by extensional tectonics, during which the Uitenhage Group was deposited within a number of fault-bounded basins, reaching a thickness of > 2000 m in places (Duvenhage, 1993). Further examples of the extensional tectonics include the following:

- Reverse faults associated with over-folding, during the Cape Orogeny;
- The Cango Fault (CF), a reverse fault on a previous thrust fault plane;
- Several normal faults of post-Cretaceous age.

The Cango Fault Zone (CFZ), previously known as the Swartbergverskuiwing (Du Preez, 1965), is a prominent east-west striking regional structure, dipping approximately 70° to the south. The CFZ starts east of Ladismith and continues past Uniondale (the eastern and western boundaries of the study area) over a distance of more than 220 km. The CFZ has a throw of almost 7000 m and has exposed pre-Cape rocks to the north (see Figures 3-8 to 3-10). This block of pre-Cape rocks, bounded by the Swartberg in the north and Enon Formation in the south, is known as the Cango Inlier.

Several examples of recent tectonic activity (neotectonics), exist in the south-eastern Cape (Andreoli *et al.*, 1989; Hill, 1988; Hattingh and Goedhart, 1997; Hartnady, 1998) and Karoo (Woodford and Chevallier, *in press*). The above-mentioned suggests that an extensional tectonic regime is still prevailing, with extension in a NNE-SSW direction and compression in a WNW-ESE direction.

3.5.1.3 Regional fracture pattern analysis

The results of the lineament mapping and remote sensing by the CGS (Chevallier, 1998) is presented in Maps 1 to 3 (folder in back of report). Map 1 represents the remote sensing results. Maps 2 and 3 represent the regional and local study area lineaments projected onto the satellite images. The lineaments only are shown in Figure 3-11.

From the remote sensing work four major fracture systems (of which the last two is of hydrogeological importance) prevail in the Klein Karoo (Map 2, Folder 1 and Figure 3-11), study area. These are associated with the following events:

- Cape Orogeny: N-S, NW-SE, NE-SW, E-W (thrusting) systems.
- Gondwana break-up (extensional tectonics): development of E-W oblique shears.
- Extension with a right-lateral shear component and reactivation of earlier fractures (E-W, WNW, and N-S).
- Tertiary to present time: continuation of the extensional stress regime in a NNE-SSW direction.

Statistical filtering indicated that two major fracture systems with significantly different characteristics are present in the Klein Karoo, namely an E-W and N-S striking fault system (Figures 3-11 to 3-13).

The E-W striking system consists of long, continuous E-W and WNW trending faults extending across the entire study area, of which only the most prominent faults, with large displacements, are shown on the 1 : 250 000 scale geological maps. The satellite lineament map therefore provides a much more complete representation of the most predominant fracture sets, which are E-W, WNW and ENE trending fracture sets (more fractures and longer extent) in the study area (see Figures 3-11 to 3-13).

The N-S trending fracture system consists of shorter, more discontinuous fractures, which generally correspond to a dense network of NNW-SSE, NNE-SSW trending joints (forming a conjugate) and less prominent N-S trending joints, often not showing any displacements on geological maps or satellite images. These fractures or joints can be very penetrative and form prominent morphotectonic features.

The observed fracture pattern (Figure 3-11) is the combined result of at least two major tectonic events, i.e. the Cape Orogeny (280-220 million years ago) and the fragmentation of Gondwanaland between (200 Ma-123 Ma ago). Most of the E-W trending fractures represent normal faults, with variable components of oblique, often right lateral movement, associated with continental break-up. WNW trending fractures may represent Riedel-shears, and ENE trending fractures the P-shear direction.

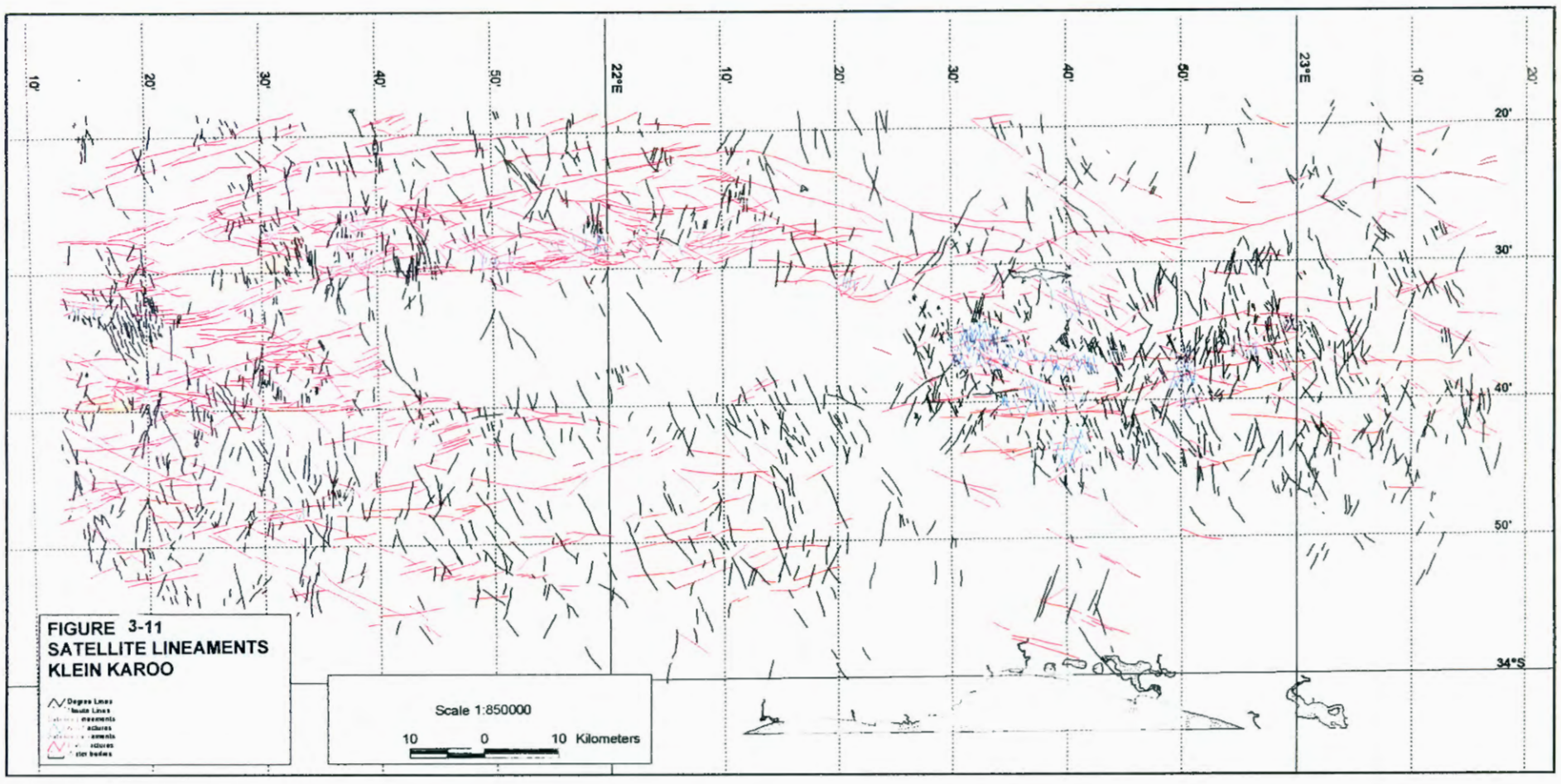

FIGURE 3-11
SATELLITE LINEAMENTS
KLEIN KAROO

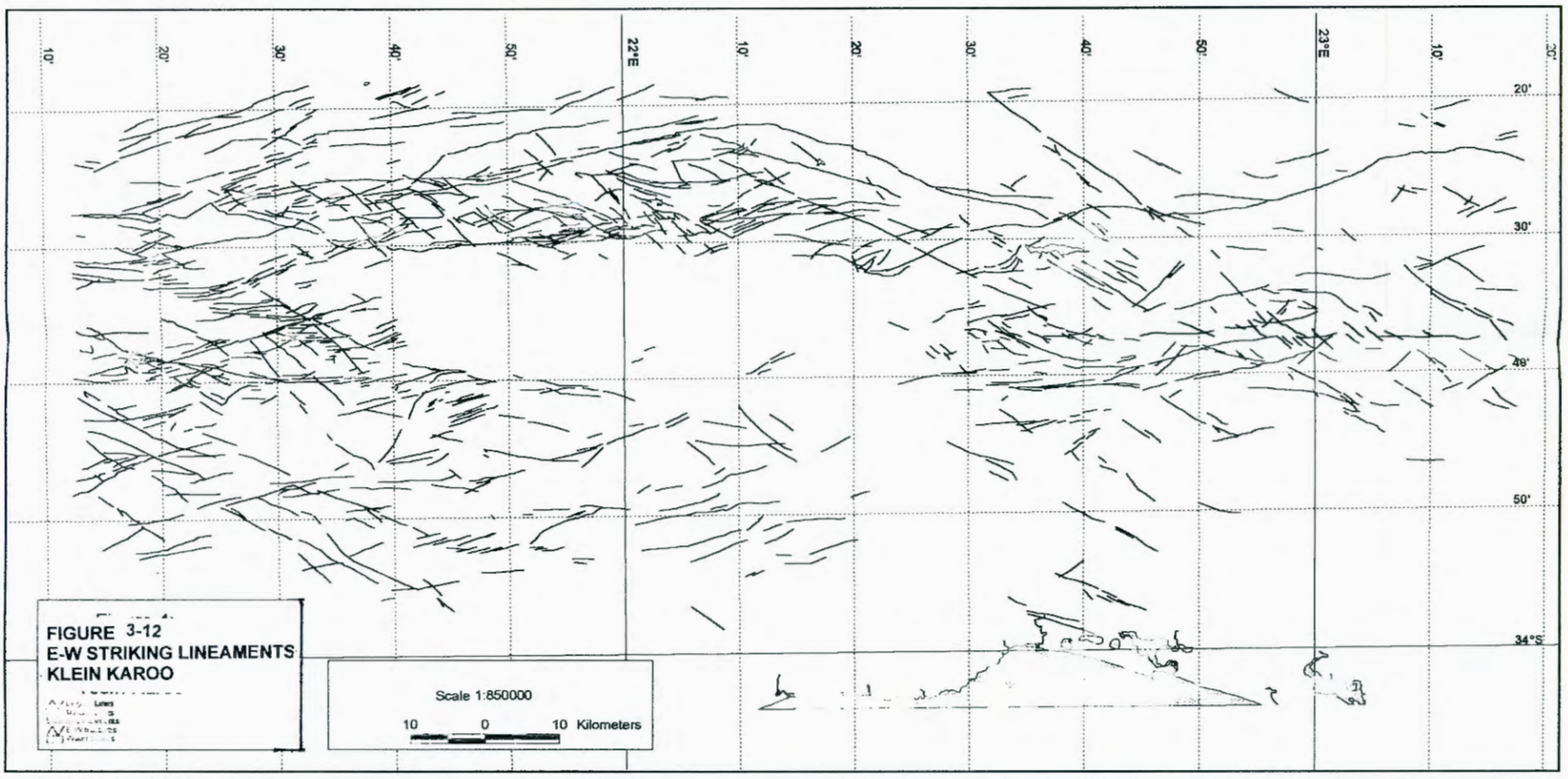

FIGURE 3-12
E-W STRIKING LINEAMENTS
KLEIN KAROO

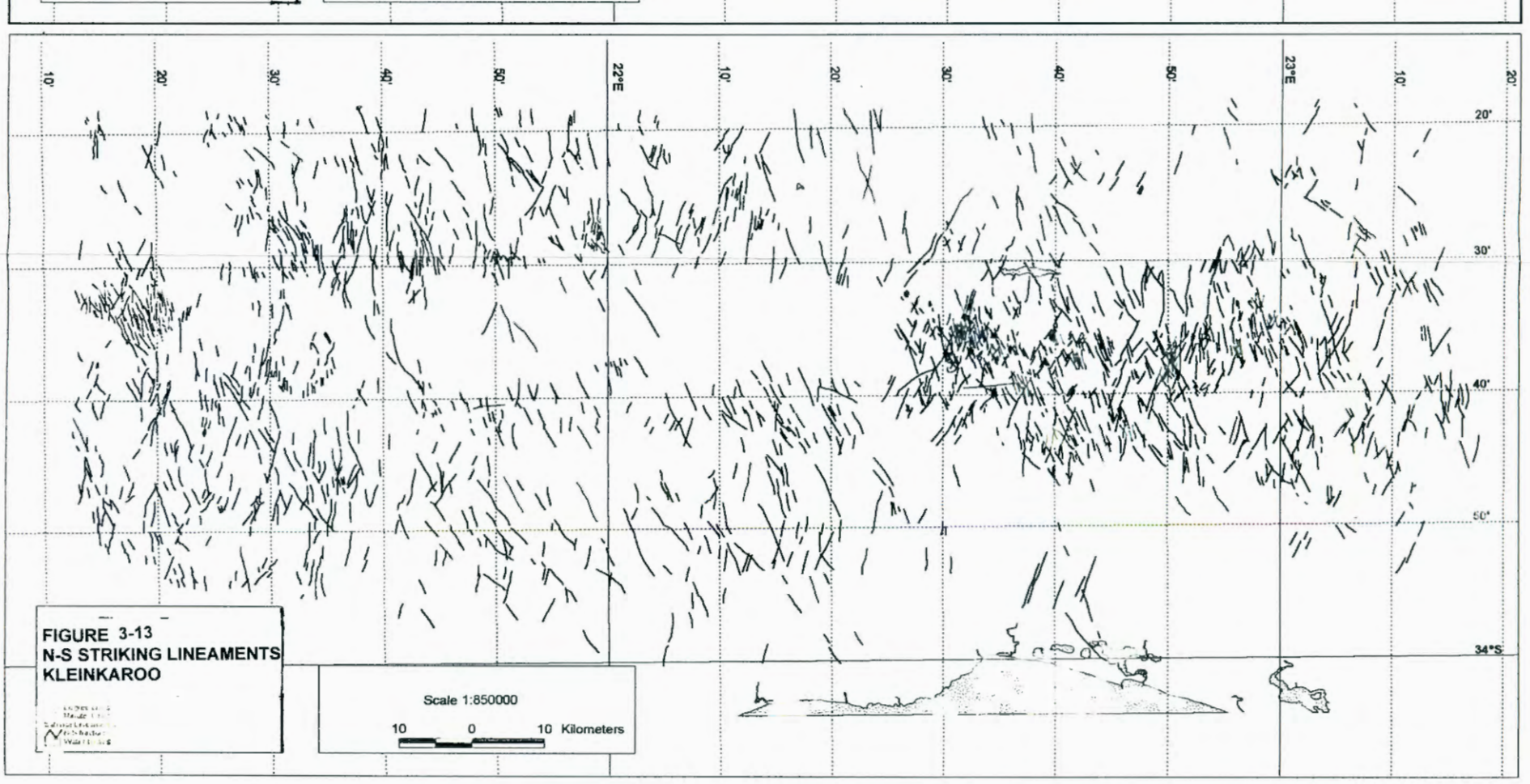

FIGURE 3-13
N-S STRIKING LINEAMENTS
KLEINKAROO

However, the orientation of thrust faults formed during the Cape Orogeny are also E-W trending or parallel / curvilinear with respect to the general trend of the CFB. Recent studies showed that thrust faulting is far more common than originally thought. Extensive field mapping and construction of balanced cross-sections, is the only way to determine the abundance of thrust faulting relative to normal faulting. Normal faulting seems to have controlled the emplacement of dolerite dykes in the Western Karoo and deposition of the Uitenhage Group and even high-level terrace deposits.

North-south trending fractures display large variations in geographic distribution. The Kammanassie and Rooiberg Anticlines have by far the highest density of fractures and joints, of which the majority are most probably related to the Cape Orogeny. The NNW, NNE and NS trending fractures have left a strong overprint over the CFB structures. The above-mentioned fracture sets were later reactivated during the intrusion of dolerite (dykes and sills) and kimberlite (pipes). Some of the lineaments crossing the Uitenhage Group outcrops are older the above-mentioned fractures.

3.5.2 Hydrodynamics of fractured aquifer

TMG ***Aquifers***, i.e. geological units with economically exploitable groundwater quantities, are classified as secondary aquifers, because groundwater flow only takes place in fractures in otherwise impermeable rock. From the several tectonic events described above, extensive folding and faulting gave rise to the secondary porosity. The style of fracturing and folding depends on the matrix lithology (see Section 3.4.2.3 and Section 3.4.3) and regional tectonics and fracture pattern (Section 3.4.1.3).

Fracturing of quartzitic sandstone into breccia and cataclastic rock flour can increase both porosity and permeability of the rock mass considerably. However, recementation of the breccia by secondary silica deposited from silicic solutions and complexes in water circulating through the fractures since the time of its formation, can reduce porosity and permeability further. It is therefore important to differentiate structural geological events producing open and close fracture systems to determine the significant events in terms of groundwater movement.

Further the presence of both vertical and horizontal fractures are of import for groundwater movement. Most of the recharge occurs along the vertical fractures, while the actual groundwater movement is controlled by both vertical as well as horizontal fractures. In most

cases, the greater part of groundwater is stored in the micro-fractures and not in the large macro-fractures (van Tonder *et al., 1998).*

It is therefore necessary to establish which fractures, formed under what tectonic events are most likely to store groundwater, based on their hydrodynamic properties. All the remote sensing, field mapping and satellite lineament data for the local study area is collated in the sections below, to establish the dominant orientations and characteristics of the water-bearing fractures in the TMG.

3.5.2.1 Fracturing styles and orientations

Work by Anderson and Ainslie (1994) and Hartnady and Woodford (1996) indicates that a modern stress field and neotectonics could have an important influence on fractured rock hydrogeology.

Purely based on theorethical considerations, those fracture orientations perpendicular to the direction of regional extension, or those with an acute angle in the direction of maximum compression, are more open and therefore more likely to be permeable for groundwater movement. This relationship still needs to be proven and is further complicated by certain factors, i.e. local and surface stress regimes, i.e. recent uplifts or slope effects.

In the Klein Karoo study area neotectonic observations suggest a modern extensional regime across WNW – trending fractures. These fractures together with E-W trending faults are likely to respond the best to modern stress regimes (Chevallier *et al.*, 1999).

The NNW - trending fractures and less dominant N-S joints is orientated at an acute angle to the direction of maximum compressional horizontal stress. Reactivation in terms of shearing is possible and has already been observed further north in the Karoo sediments. NNW fractures and lineaments are very well developed in the TMG and is likely to be permeable to groundwater movement.

The ENE and NNE – trending fractures are lying with an angle between 40° and 90° to the direction of maximum compression. According to theory, tectonic reactivation will be difficult in this orientation.

From the above it can be concluded that fractures trending NNE-SSW and reactivated fractures in E-W, WNW, N-S orientations are the preferred orientations for groundwater flow.

3.5.2.2 Fracture connectivity

Groundwater movement in fractures is controlled by the fracture characteristics, i.e. connectivity, openness, geometry, etc. which are all the result of the forces, that created them. Fracture characteristics are often very difficult to measure and vary greatly with increasing in situ stress below the surface, which imposes a further complication that needs to be taken into account.

On a regional scale, fracture connectivity is enhanced by fracture sets with broad length distributions, intersecting at high angles (Balberg et al., 1991). Fracture-system geometries and fluid-flow characteristics are controlled by the mechanical nature of the rock mass (Aarset et al., 1997). Well-bedded rocks with mechanical discontinuities at bedding planes (e.g. shale partings) develop strata-bound fracture systems with fractures restricted to single layers. Fractures of this type mostly do not have large variation in length and spacing. Groundwater flow associated with these fracture systems is largely confined to individual beds and thus permeability perpendicular to bedding is low.

Where bedding does not impose a strong mechanical control (largely true in the case of the lithologically uniform TMG layers), non-stratabound fracture systems develop in which fracture spacing is less regular and fracture length distributions are broad. The nature of the fracture connectivity, and thus groundwater flow, in these systems varies with the fracture length distributions and may be dominated by either small or large fractures (Bour and Davy, 1997; Odling, 1997b).

Fracture connectivity plays an important role in the quantification of fracture network geometry and is defined as the ratio of the number of fracture intersections along a fracture plane (3D), or fracture trace (2D) and the volume or area of rock mass under consideration, respectively. If fracture connectivity is above a given threshold value, the flow pattern in a particular fractured rock mass is also considered to be representative at a larger scale for the entire rock mass.

A fractured medium is equivalent to a porous medium if its directional permeability can be modelled by a tensor, i.e. without variable or erratic

permeability. Non-directional and erratic permeability occurs when discontinuous fractures with different orientations cross or meet each other.

The Kammanassie Mega Anticline (area enclosed approximately by 22°25' to 23°15' and 34°30' to 34°45', in Figure 3-11) is divided into four different structural domains (from west to east). Each related to different types of fracturing prevailing in the anticline. Each domain shows a different fracture pattern, which could imply different hydrodynamic properties (Figure 3-14).

Domain 1: Two major and well-developed fracture systems intersect each other. If they all have the same transmissivity it will lead to an erratic directional permeability. Numerous intersections between these joints and the E-W fracture system are indicative of good connectivity.

Domain 2: The NNW overprint is very strong and dominant. Directional permeability is therefore expected. The lesser number of intersections between fractures implies poor connectivity.

Domain 3: This pattern of long continuous fractures of variable directions crossing each other is indicative of erratic directional permeability and good connectivity.

Domain 4: The fractures are discontinuous with no major trend and do not intersect each other. This will contribute to erratic permeability and poor connectivity.

Additional spatial and hydrodynamic analysis of the fracture system, including the following has not been carried out to date, due to budget constraints:

1. Structural analysis of the same area at different scales of observation (this had already been addressed to some extent by Hälbich *et al.*, 1995).
2. Statistical modelling of the fracture system, e.g. polygonisation and discretisation, using different filtering techniques; and
3. Numerical rock flow simulation is required in order to identify different fracture clusters, density of fracture clusters and inter-connecting fracture clusters in order to determine scaling effects on hydraulic conductivity.

FIGURE 3-14: HYDRODYNAMIC PARAMETERS – KAMMANASSIE MOUNTAINS

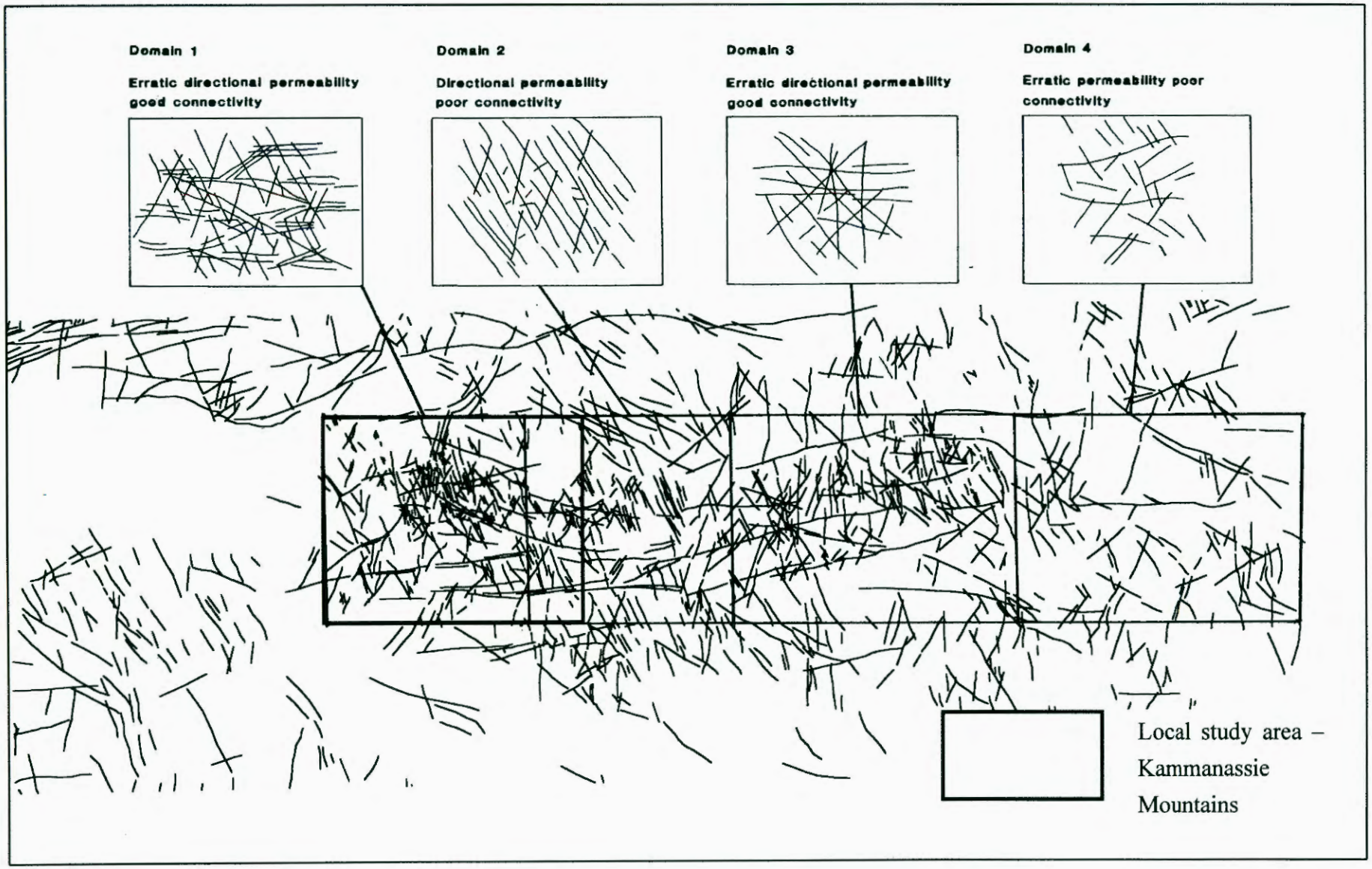

In the absence of the above, only qualitative data interpretation was possible. Qualitative data interpretation only allows discussion of two parameters, i.e. connectivity and directional permeability. It is highly recommended that future studies include statistical modelling of the fracture system and numerical rock flow simulation to quantify fracture systems.

3.5.3 Local geology and structure of the Kammanassie Mountains

Figures 3-15 to 3-17 represents a detailed geological map and cross-sections, covering the local study area around the Kammanassie Mountains.

3.5.3.1 Lithology of the Table Mountain Group sandstones

The TMG is subdivided into six formations, of which only the Peninsula Sandstone Formation, Cedarberg Shale Formation (C/S) and the Nardouw Subgroup are present in the study area.

The Nardouw Subgroup is further subdivided into the Baviaanskloof, Kouga and Tchando Formations (see Table 3-1) based on small lithological differences related to feldspar and shale content. In this study, it is sufficient to refer to the Nardouw Subgroup.

The Peninsula Sandstone Formation is exposed mostly along the mountain crests and comprises two thirds of the total thickness of the TMG (1800 to 2150 m). It is composed of a uniform succession of medium to coarse grained, thickly bedded, grey sandstones, characterised by cross bedding. In places, thin layers of conglomerate are present.

The overlying C/S comprises a 50 to 120 m thick shale layer. It is a good marker horizon because it weathers deeply and to a smooth outcrop, which contrasts with the grey crags of the sandstones above and below. Where fresh, the shale is greenish, extremely fine grained and somewhat sericitic.

The rocks of the Nardouw Subgroup are, in general, more brownish on weathered surfaces and thin intercalations of shale are more plentiful than in the Peninsula Formation. Towards the top, they become more feldspathic. Due to this higher shale content they are less competent than the Peninsula Formation and deformation tends to be more ductile, giving rise to the spectacular fold geometries seen in the mountain road passes that cut through the Nardouw Subgroup.

FIGURE 3-15: SCHEMATIC BLOCK DIAGRAM SHOWING THE 3D GEOLOGY OF THE KAMMANASSIE MOUNTAINS

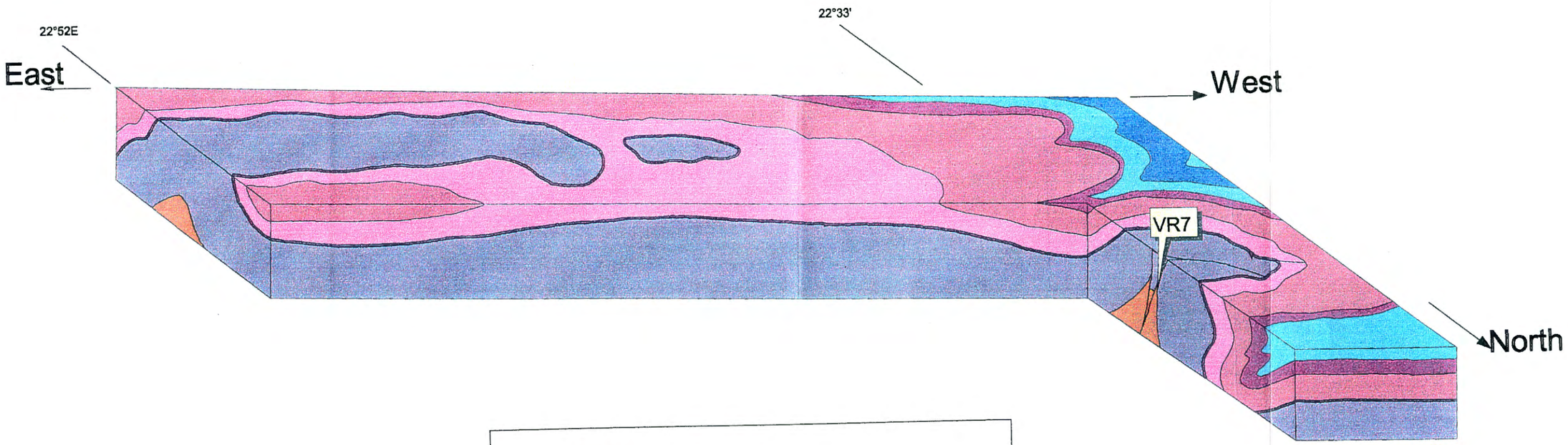

FIGURE 3-16: DETAILED GEOLOGICAL MAPPING OF KAMMANASSIE MOUNTAINS (HÄLBICH ET AL., 1995)

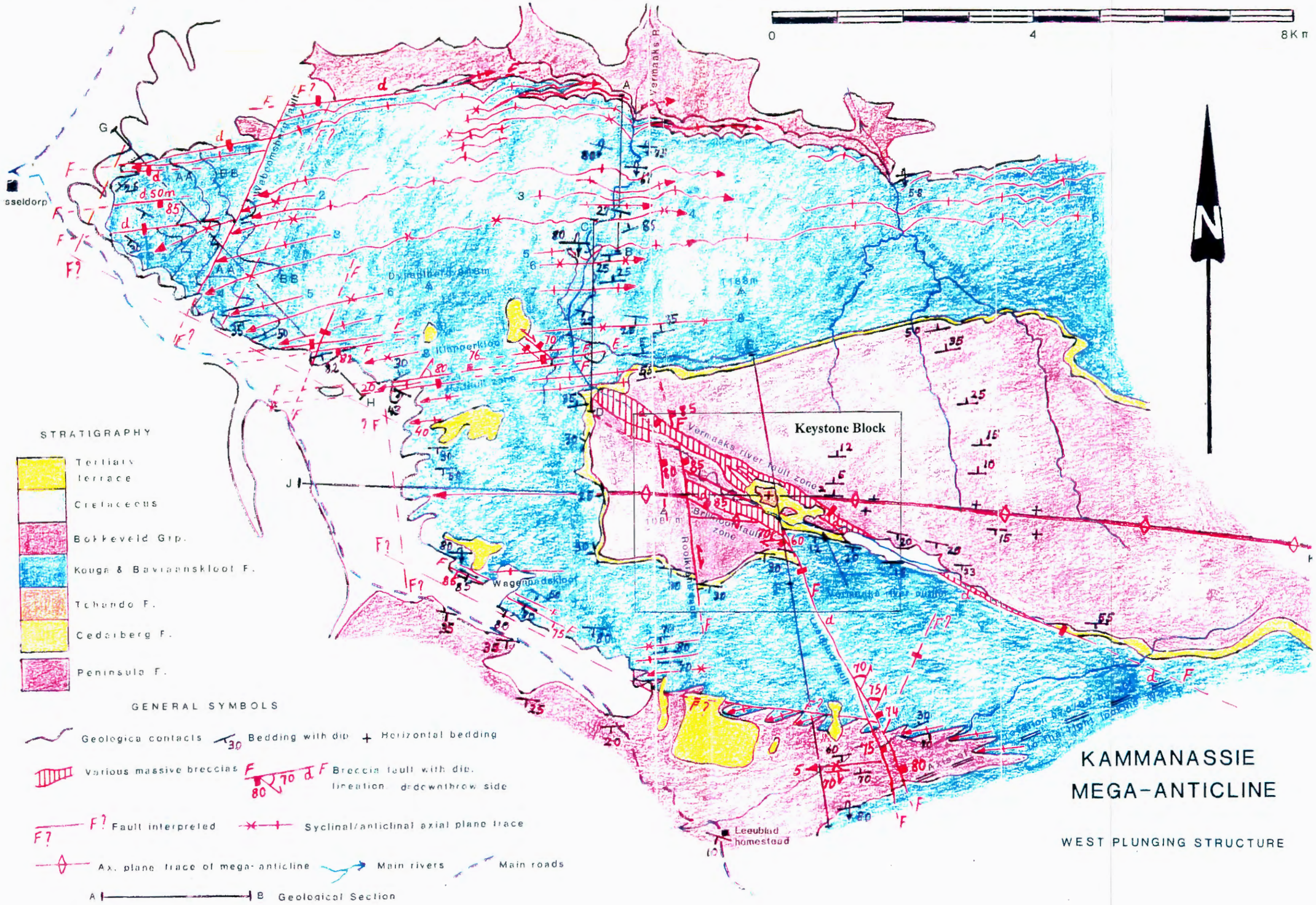

FIGURE 3-17: STRUCTURAL PROFILE – KAMMANASSIE ANTICLINE

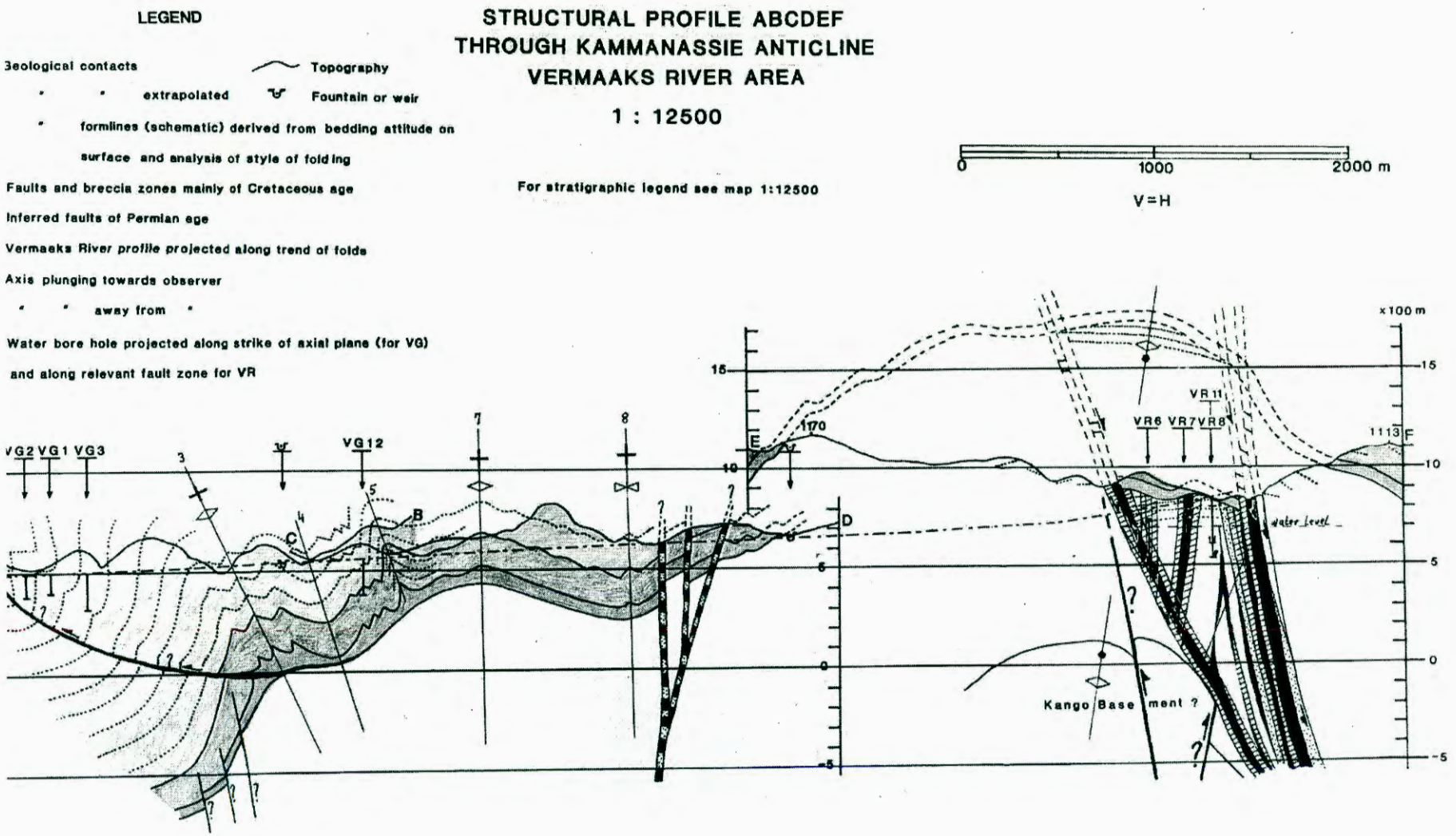

3.5.3.2 Local fracture pattern analysis – Kammanassie Mountains

Detailed remote sensing work by Chevallier *et al.* (1998) has indicated that all three of the fracture types associated with the main tectonic regimes in the Klein Karoo are present in both the regional as well as the local study areas. From Map 2 (Folder 1) it can be seen that the Kammanassie and Rooiberg Anticlines have by far the highest density of fractures and joints, representing good targets for groundwater development and favourable recharge conditions.

A complete hydrodynamic analysis including detailed structural and geometrical analysis of fracture sets at various scales of observation was not possible due to budget constraints. Only fracture density and distribution data, on a regional and local scale, were digitised at a scale of 1 : 50 000 from the satellite lineament map (see Map 2, Folder 1 and Figures 3-11 to 3-13). Field-scale observations were not possible during the remote sensing study. However, field studies carried out by Hälbich, further to the north of the Kammanassie study area in the CFB and in the Great Karoo, indicated that the E-W and N-S fracture systems have different characteristics, in terms of fracture geometries, fracture length and connection. Figures 3-18 A and B represent schematic presentations of the detailed geometry of (A) E-W and (B) N-S trending fracture systems:

1. The E-W trending fault system has an anatomising pattern with an acute angle in-between the three main fractures or joint orientations. Major faults are marked by a concentration of anatomising fractures or joints (Figure 3-18a), with a regular regional distribution.

2. The N-S system comprises three sets of intersecting fractures and master joints with NNW-SSE, NNE-SSW and N-S orientations. Each set of joints has systematic and non-systematic joints perpendicular to each other (Figure 3-18b). The systematic joints dominate and are often long fractures (>1 km), which are easily identified with remote sensing. In general joint spacing and length are proportional to each other, e.g. kilometre-long mega-joints are often kilometres apart, whereas master joints with a length of tens of metres are spaced half a meter or less apart. Non - systematic crosscutting joints are less extensively developed and form links between the prominent joints without intersecting it, resulting in a "step ladder" pattern Figure 5-1b. Non-systematic joints are not easily identified on remote sensing images. The three sets of systematic joints do not seem to correlate with major faults in the study area, and regional fracture density has an irregular distribution. NNW-SSE trending

fractures compose the major fracture orientation in the Kammanassie and the Swartberg Mountains, respectively.

Detailed remote sensing work by Chevallier *et al.* (1998) has indicated that all three of the fracture types associated with the main tectonic regimes in the Klein Karoo are present in all the groundwater augmentation target areas. From Map 2 (Folder 1) it can be seen that the Kammanassie and Rooiberg anticlines have by far the highest density of fractures and joints, representing good targets for groundwater development and favourable recharge conditions.

In terms of groundwater flow relationships, recharge and development an understanding of the fracture orientations, spacing and geometries yielding the best quality and quantity are important.

3.5.3.3 Folding and faulting from field mapping

The Kammanassie Mountains is an eroded remnant of resistant TMG quartz arenites, also referred to as the Kammanassie mega-anticline (Hälbich *et al.*, 1995).

The core of this mega-anticline when compared to the Outeniqua and Swartberg Mountain Ranges constitute one, gently overturned northern limb. A combination of geological cross-sections (Figure 3-9 and 3-10) along the anticlinal hinge of the Kammanassie Mountains, show that the Kammanassie mega anticline comprises of two anticlines with an intervening, very tight syncline only exposed in its lowermost part (Figure 3-16). Anticlinal inter-limb angles are approximately 90°. The axial planes of all the folds in the Peninsula Formation are approximately vertical. In the more feldsphatic formations of the Nardouw subgroup, i.e. the Kouga, Baviaanskloof and the lowermost part of the Bokkeveld Group (Gydo Formation), the folds are overturned. Due to repetition by small-scale folding, the outcrop length of the Kouga Formation is particularly long (Chevallier, *et al.*, 1998).

Hälbich, *et al.* (1995) carried out detailed field mapping along the Vermaaks River Valley and the farm Leeublad to investigate typical fault, fold and contact relationships around the periphery of the Kammanassie mega structure (Figure 3-17). On a less detailed scale, a reconnaissance field survey was carried out in the Marnewicks River Valley and the DECAS area north of the Vermaaks River Valley.

FIGURE 3-18: FRACTURE STYLES/GEOMETRIES

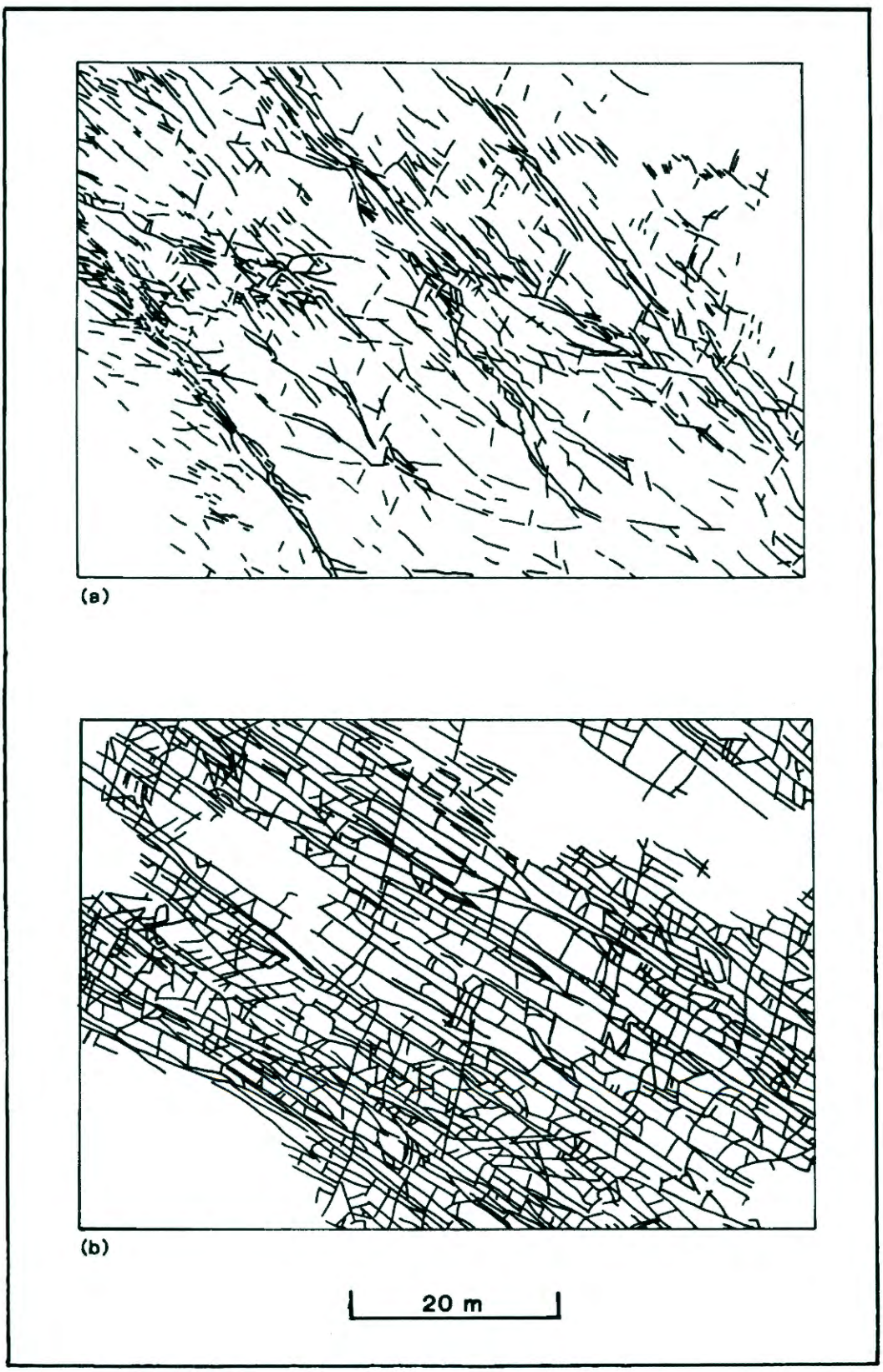

Hälbich, *et al.* (1995) distinguished and identified according to the fold classification system of Ramsay (1967) and Ramsay and Huber (1987) the following folding styles in each of the different TMG formations:

- Nardouw Subgroup rocks north of the Klapperkloof Fault (see Figure 3-16): *Conical folds*, indicative of a component of oblique upward directed shearing during folding along the axial plane of the Kammanassie Anticline;
- Peninsula Formation: *Conical folding* in the core of the mega anticline. *Class 1b, parallel* and *concentric folds*, also *Class 1c.*
- Thick Kouga Formation (Nardouw Subgroup): *Class 1c, rounded*, or *kink folds* with straight limbs. Also *classes 3* and *1b* with and without decollement, respectively.
- Near the Bokkeveld contact, the thin Baviaanskloof Formation (grouped together with Kouga on Figure 3-16, as the formation does not occur with depth in the profile): *Class 2 similar folds.*

Reconstruction of the folds in depth by Hälbich, *et al.* (1995) (see Figure 3-17) necessitates the development of a complex subsidiary anticline to have developed in the Peninsula Subgroup, beneath the Nardouw Subgroup, north of the Klapperkloof faultline. The thickness of the Kouga and Baviaanskloof Formations is estimated to be in the order of 1.25 km.

The C/S acts as a decoupling horizon as marked fold asymmetry develops and the Peninsula beds become steeper. The elevation of the eroded closure of the Kammanassie Anticline was difficult to determine, and estimated to be in the order of 700 to 800 m (see Figure 3-17). Further, the steep angular unconformity between the C/S and Peninsula Subgroup is present as elsewhere in the CFB.

Hälbich *et al.* (1995) distinguished three different types of faulting, based on the morphology:

- A 200 m wide and 9 km long fracture zone occurring along the Vermaaks River Valley (Figure 3-16), to smaller fault lines with sharply defined planes with up to 20 m wide breccia zones. These include the ESE trending Brilkloof, SSE-trending Leeublad and Rooikrans and three E-W-trending Klapperskloof Faults (Figure 3-16).
- Breccia, consisting of rounded and rotated fragments in a fine-grained ground mass.

- Homogeneous mass of a very fine grained cataclasite which is partly recemented and extremely hard.

The differential development of breccias is controlled lithology. A 20 m wide breccia zone in the siliceous Kouga quartzite, dimishes to 2 to 4 m wide in the softer, more feldspathic Tchando Formation, and may even disappear in less competent rocks, i.e. Klapperkloof Faults (Figure 3-16).

Of particular interest from the field mapping of Hälbich *et al.* (1995) was the kinematics of oblique keystone faulting. The high yielding production boreholes of the KKRWSS are drilled into faults of this type. Furthermore, this faulting style has also disrupted the continuous C/S layer, which produces the so-called 'TMG Window areas', such as in the Kammanassie, Rooiberg, Swartberg and Gamkaberg Mountains (see Figure 3-8). In the absence of crosscutting faults, the C/S forms a tight seal between the Peninsula Formation and Nardouw Subgroup representing a no-flow boundary condition. Figure 3-19, adapted from Hälbich *et al.*, 1995, represents a block-diagram (prepared to scale) of the west plunging Kammanassie Anticline.

The following important aspects are summarised from Hälbich, *et al.* (1995) on the kinematics of oblique keystone (wedge-shaped keystone block) faulting:

- The strike and dip measurements within the outlier in the latter compared to those on the outside of the outlier, indicate that the beds have been rotated by 8-10°, viewed left along a strike of 70°00'.

- By assuming the above angle of rotation and an estimated down-throw ranging between 700 and 800 m (derived from stratigraphic evidence of the eroded Kammanassie Anticline closure for the outlier, see Figure 3-17) the rotation occurred 9-10 km east of the maximum position of the Vermaaks River Fault, and 6 km to the south along the Leeublad Fault. Figure 3-19 shows how the effect of faulting diminishes to zero over these distances.

- Rotation of an Y-shaped block in such a rollover mechanism can only develop in the presence of a decoupling horizon in depth, along which the entire block slips southwards in a listric fashion along bedding planes. This is only possible if the Peninsula Formation / basement contact is the first horizon below the C/S. The Cango Fault (Figure 3-8) developed by a similar roll-over mechanism on a much larger scale.

- Blocks 2 and 3 (Figure 3-19) show how throw diminishes rapidly along the bounding faults from the outlier to the northwest. This is explained by the fact that the Vermaaks River Fault became inactive, once it crosses the anticlinal axial plane.

- Blocks 3 and 4 (Figure 3-19) show how the down-throw movement of the Brilkloof Fault was transferred to the crosscutting Rooikrans Fault, which was subsequently transferred to the dormant Vermaaks River Fault. This mechanism caused the down-throw component to diminish rapidly along strike, leading to uninterrupted continuation of the C/S on the northern limb of the west plunging Kammanassie mega anticline.

- During the process of throw transfer, the entire block bounded by the Leeublad, Brilkloof and Rooikrans Faults moved to the south. This movement is recorded by horizontal slip lines found on the Rooikrans fault, as well as displacement of the mega anticlinal axial plane between the Rooikrans and Leeublad Faults respectively in the south (Figures 3-16, 3-17 and 3-19, block 3). Limited southward movement of the southern wall of the keystone (Block 3, Figure 3-19) is expected if a decoupling horizon indeed exists.

Formation of oblique keystone block faulting creates very favourable conditions for groundwater, as in the case of the Vermaaks River Wellfield of the KKRWSS. From this point onwards, the Keystone Block will refer to the area indicated on Figure 3-16.

Hälbich, *et al.* (1995) found the following after measuring joint frequencies and orientations of steeply dipping joints at eight different selected localities in the Nardouw and Peninsula Subgroup and Formation, respectively:

- NW and NE trending open joints are most prominent in the Nardouw Subgroup
- EW trending joints are closed and filled with quartz in the Peninsula Formation, while N to NE and NW trending joints are open.

Further, the spacing of orthogonal joints varies from several decimetres to approximately one metre depending on the thickness of quartzitic layers. Single straight master joints continue from several metres to tens of metres along the same bedding plane.

FIGURE 3-19: BLOCK DIAGRAM INDICATING THE KINEMATICS OF KEYSTONE BLOCK FAULTING

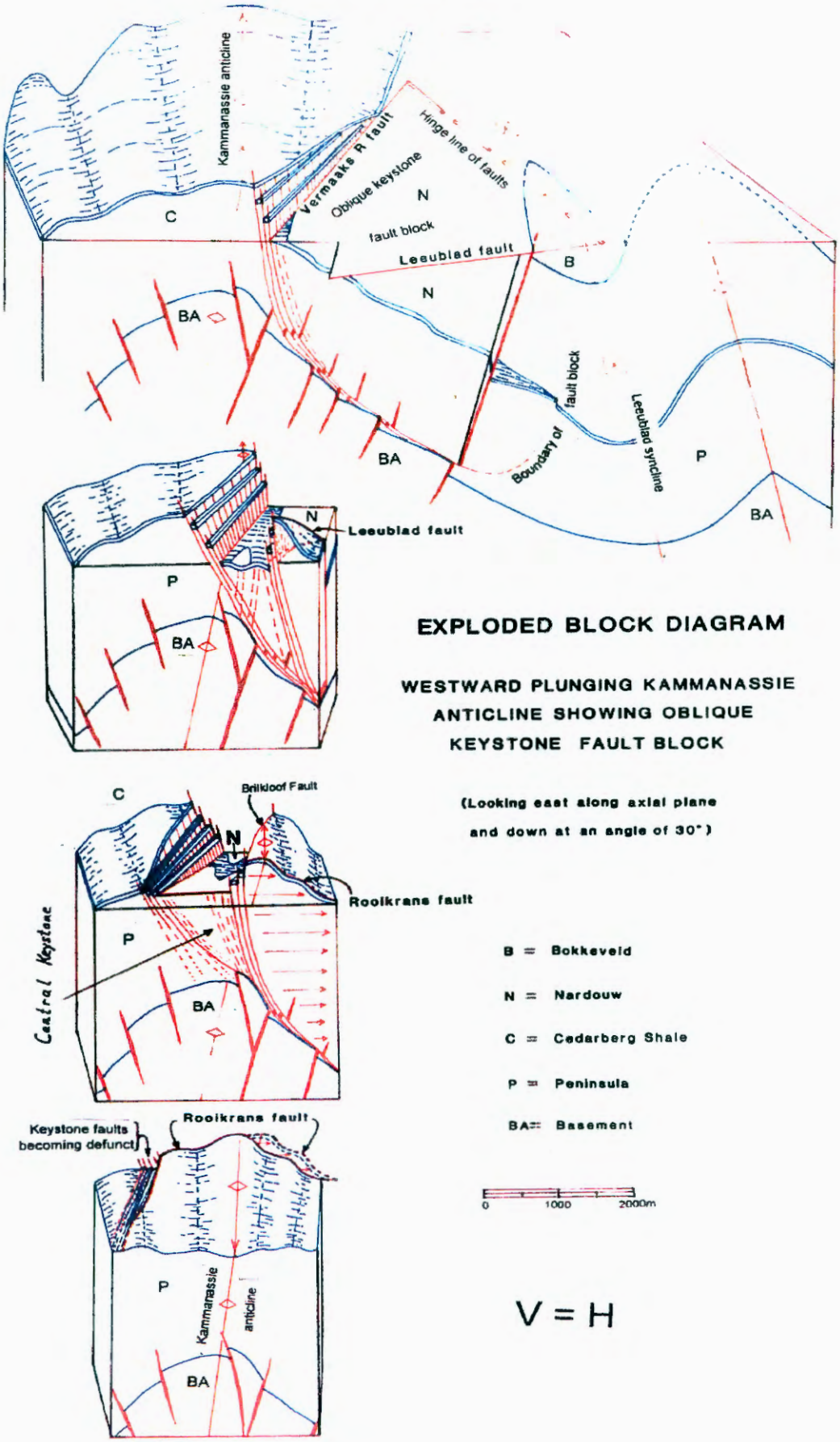

Hälbich, *et al.* (1995) showed that for the Kammanassie Mountains, NW and NE trending open joints are most prominent in the Nardouw Subgroup. In the Peninsula Formation, E-W trending joints are closed and filled with quartz, whereas N to NE and NW trending joints are open.

The spacing of orthogonal joints varies from several decimetres to approximately one metre and depends on the thickness of quartzitic layers. Single straight master joints continue from several metres to tens of metres along the same bedding plane.

Based on the width of open orthogonal joints, Hälbich *et al.* (1995) estimated the secondary porosity of bedding and joint fractures in the Kouga and Peninsula quartzites (Kammanassie Mountains) to be of the order of 0.1 to 1 %. In brecciated and fractured strata porosity is approximately, double that of folded strata, i.e. of the order of 2% and more. The secondary porosity of a massive fault block, i.e. the Vermaaks Keystone Block, is estimated to be of the order of 5 % Hälbich *et al.* (1995).

Secondary porosity along faults increases further to 6 to 7%. Faults are mostly developed in groups of two to three along splays, connected by cross-cutting faults, connecting larger volumes of rock and thereby increasing groundwater storage and flow capacities, i.e. in the Vermaaks River Keystone Block.

Groundwater movement in fractures is controlled by the fracture characteristics, i.e. connectivity, openness, geometry, etc. which are the result of the forces that created them. In an attempt to establish the fracture connectivity across the Kammanassie Anticline, Chevallier (1998) divided the Kammanassie Anticline into four different structural domains (from west to east), each related to different types of fracturing prevailing in the anticline. Each domain shows a different fracture pattern, which could imply different hydrodynamic properties (Figure 3-14).

The width of open joints in the more quartzitic formations (Kouga and Peninsula) is estimated to range between 1 and 10 mm per metre, i.e. 0.1 to 1.0 % (depending on the direction of measurement and the thickness of the strata).

3.6 GEOLOGICAL ORIGIN OF HOT SPRINGS

Andreoli *et al.* (1996) showed the positions of epicenters of post Karoo rock age in South Africa. In general the positions of epicentres seems to correspond well with the localities of hot springs. Hot springs coincide with the position of activation along fractures, and thus providing flowpaths for groundwater to travel upwards from great depths (personal communication, Hartnady).

The hot springs at Calitzdorp and Warmwaterberg are located at the intersection between faults in the TMG and the basal shale layer of the Gydo Formation (Bokkeveld Group). These faults penetrate deep enough into the crust in order to enable groundwater to circulate to great depths to obtain the high temperatures associated with groundwater emanating from hot springs, as required by the geothermal gradient of 35°C/kilometre. Deep regional fault lines feeding hot springs are likely to intersect numerous smaller fractures, which act as feeder zones to the main fracture. In the case of the above-mentioned hot springs, they occur where the ENE-WSW trending faults connect with the NE trending faults near the base of the Bokkeveld Group. In order to estimate the effects of large-scale groundwater abstraction on the flow of hot springs, the groundwater contribution of all fractures feeding the regional structure (resulting in a hot spring) is required to assess groundwater replenishment. This would *inter alia* need much more detailed field information than is currently available.

According to the 1:250 000 Oudtshoorn, the hot spring at Toorwater north of Uniondale, is situated in the Enon Formation. Although detailed information is not available, it is postulated that groundwater rises upwards along an intra-formational fault which cuts deep down into the underlying strata (TMG).

3.7 BOREHOLE INFORMATION

All the relevant information of boreholes sampled during the hydrochemical and environmental isotope surveys in the local study area is summarised in this section. This information is very important for the interpretation of hydrochemical and environmental isotope data.

To improve data interpretation, borehole data are grouped in the following catogories, reflecting the geographic borehole locality:

- Additional monitoring boreholes – Eastern Section KKRWSS
- KKRWSS production borehole data
- Original KKRWSS monitoring boreholes

- Existing boreholes – privately owned land, Kammanassie Mountains.
-

3.7.1 Additional Monitoring Boreholes – Eastern Section KKRWSS

Table 3-2 summarises the drilling results of additional monitoring boreholes.

TABLE 3-2: SUMMARY OF DRILLING RESULTS: ADDITIONAL MONITORING BOREHOLES, EASTERN SECTION

Borehole	Depth (m)	Depth of Water Strike#	Geology (depth in m)	Water Level (m)	Altitude (m)	EC (mS/m)	pH
G40171	50 *(34-40)*	?	0-17 boulders 17-50 Peninsula quarzite	5.085	660.516	12.5	6.2
G40172	16 *(0-16)*	(5.0)	Boulders	5.125	660.416	12.7	5.8
G40173	10 *(0-10)*	(3.0)	0-10 sandstone boulders and fragments in yellow sand matrix	4.925	660.216	26.6	7.2
G40174	147 *(129-135)*	127-133 (13)	0-12 sand and scree 92-147 sandstone and shale Fracture zone : 127 –133 with dark brown Fe staining	105.98	469.66	22.0	7.2
G40175	126	84(5.0)	0-23 Boulders 23-49 C/S layer 49-126 Peninsula quartzite	**Borehole grouted closed and abandoned**			
G40175A	84 *(57-63)*	27 (11) 60(0.75)	0-19 Sand, boulders and scree 19-45 C/S layer 27-30 fractured with quartz vein 48-84 Quartzite, fractured, Fe stained, pyrite quartz veins	Artesian	652.031	13.5	6
G40176	150 *(39-45)* *(116-122)*		0-17 sand and boulders 17-150 sandstone and shale weathering visible up to 119 m, reddish to yellow brown stains	6.71	644.081	13.7	6.1
G40177	150	92(2.4)	0-17 Sand and boulders 17-150 Sandstone (water strike in quartz vein)	51.94	420.036	45	6.85
G40178	120 *(51-57)*	54(8.0)	0-11 weathered sandstone 11-120 sandstone 94-114 faultzone with quartz veins containing pyrite	10.22	535.691	155	7.8

#Water strike yield is indicated within brackets (l/s), screen, if present in italics.

The specific monitoring requirements of the additional monitoring boreholes are as follows (positions are shown on Figure 2-5):

- G40171 to 3 are shallow boreholes drilled on the farm Voorzorg 124, upstream of the C/S layer to monitor the inter-relationships between alluvial and TMG groundwater.
- G40174 was drilled on the farm Rietfontein 142 to monitor the water level responses to abstraction from private abstraction borehole RN1.

- G40175 was drilled to a depth of 126 m on the farm Voorzorg 124, it subsequently collapsed and was grouted. It was replaced by the nearby G40175A, next to abandoned G40175. The purpose of this borehole was to investigate the effectiveness of the C/S layer as an aquitard.
- G40176 was drilled on the farm Voorzorg downstream of the C/S layer.
- G40177 was drilled south of the Bokkraal Wellfield to monitor water level responses to abstraction from the above-mentioned wellfield.
- G40178 was drilled on the southern flanks of the Kammanassie Mountain to monitor long-term water level fluctuations arising from private and commercial abstraction from the Vermaaks River Wellfield.

3.7.2 KKRWSS production borehole data

The best available data set for the Klein Karoo comprises that of the production boreholes of the KKRWSS (summarised in Table 3-3, over page). The positions of the Eastern and Western Section, KKRWSS production boreholes are shown on Figures 3-1 and 2. Figure 2-5 shows the location of the Eastern Sector production boreholes of the KKRWSS in relation to existing boreholes on privately owned land (detail follows in Table 3-5).

All the boreholes were drilled by percussion drilling and originally constructed in a similar way, with 200 mm OD PVC casing and screen. The surface areas of the original PVC screens were very low. Screens have subsequently been replaced with Johnson screens in the Calitzdorp, Varkieskloof, Bokkraal and Droëkloof Wellfields in order to improve borehole efficiencies. The Vermaaks River Wellfields still have the original PVC screens in place. Initially no differentiation was made between boreholes drilled in the Nardouw and Peninsula Subgroup and Formation, respectively. The following production boreholes of the KKRWSS were drilled in the Nardouw Subgroup:

- DL 13 to 17 (Western Section)
- KG1 (Western Section)
- DP 10, 12 and 29 (Varkieskloof Wellfield, Eastern Section)
- DP 28, 15 and 25 (Bokkraal Wellfield, Eastern Section)
- VG3 (Voorzorg – Eastern Section).

Boreholes VR6 to 11 (Vermaaks River Wellfield – Eastern Section) are the only boreholes drilled in the Peninsula Formation. Borehole DP18 is drilled into the alluvial aquifer of the Olifants River.

TABLE 3-3: SUMMARY PRODUCTION BOREHOLE DATA: KKRWSS

Borehole	Depth (m)	Water Level (m)		Fractures/Water Strike (m)*	Depth of pump (m)	Screen Depth (m)	Available Drawdown (m)
		First	Now				
VG3	206.7	6.02	10	110-111(6.0), 190(3.0), 174 (3.0)	148	96.5-206.7	100
VR6	250	34.64	60	228-244(15)	165	108.7-230	170
VR7	177	63.3	90	78-81(8), 129-140(15)	159	53-177	40
VR8	251.3	100.5	125.37	113-117(5) 156-170(4) 234-240(4)	163	89.6-251.3	109
VR11	224.5	125.5	151	139(2) 183-194(8) 200-210(10)	180	18-224.5	49
DP10	210	114.07	90.2	183(7)	180	73-210	93
DP12	192	126.07	102.8	?(20)	180	66-192	20?
DP29	240	120.6	97.09	160-170(2) 185-?(2)			
DP28	246	117.8	94.57	122-124(1.5) 151-160(10) 195-210(11)	170	121-207	40
DP15	224.5	103.8	86.04	110(3) 169(7) 187(11)	180	50-207	100
DP25	203	104.9	83.5	109 166 201	170	9-203	120
DG110	212	110.6	107.57	114-117(1.5) 137 200-203(6)	200	92-212	90
DP18	17	3.6	3.2	4.2-9(15)	14	2-9.4	5
DL13	187	25.2	43.42	?(14.2)		94-187.0	
DL15	137	7.1	53.8	?(33.0)		6.0-137.0	
DL16	169.4	11.53	54.29	?(15)		12.3-169.5	
DL17	248.8	9.8	34.73	26-30(3) 44-48(3) 90-97(2) 130-145(7)		17.3-248.8	
KG1	209	10.8	27.7	20-45(4) 64-70(4) 115-125(2) 140-149(3) 170-180(2)		0-148	

**** First the water strike depth (m), followed by yield, e.g. 110 – 111(6.0)***

The borehole construction effects need to be taken into account when test pumping data are analysed in order to obtain a reliable values for the aquifer parameters, i.e. transmissivity and storativity (see later in Chapter 7). At the time boreholes were drilled and equipped no cognisance was taken that fractured aquifers require a considerable amount of more open screen length in the borehole design.

3.7.3 Original Scheme monitoring boreholes

Table 3-4 below summarises the borehole information of unsuccessful production boreholes of the KKRWSS, which are currently used as monitoring boreholes.

TABLE 3-4: SUMMARY BOREHOLE INFORMATION: UNSUCCESSFUL PRODUCTION BOREHOLES, KKRWSS

Borehole	Depth (m)	Yield (l/s)	Geology	Water Level (m)
DL14	250	0.4	Quartzite	18 (1986)
DL12	185	0.1	Quartzite	9 (1986)
DL11	180	18.2	Quartzite *(50-180)*	43.9 (1987)
WN101	243.5	>2.0	Baviaanskloof Quartzite, shale at 28m 188, 203 m, fractures at 120 m.	4.3 (1989)
VR5	215	15	0-12 boulders; 12-215 Baviaanskloof, shale at 37, 46, 57, 111 m, fractures at 82, 102, 169 and 184-186 m. *(75-215).*	4.3 (1989)
VG12	173	4.7	0-4 boulders; 4-230 Tchando Formation, fractures at 19, 78, 98, 14 and 171-173 *(40-173)*	2.93 (1992)
VG4	113	<2.0	0-2 scree, 2-113 Baviaanskloof	18.2 (1989)
DG107	210	4.1	0-22 boulders, 20-210 Kouga Formation	27 (1987)
DG104	250	5.7	0-8 Enon, 8-250 Kouga Formation	90 (1987)
DP27	249	135-140 (2) 140-195 (10) 240(8)	0-22 Enon 22-249 Baviaanskloof Formation, Fractures at 150 to 155 m, open joints with showing weathering at 241, 242 and 248 m	119 (1992)
DP20	220	0.9	0-18 Enon, 18-220 Baviaanskloof Formation	104.5 (1991)
DP14	167	12	0-6 Enon, 2-30 weathered sandstone, 30 to 167 sandstone	62.5 (1986)
DP13	184.6	30 low quality	Baviaanskloof with shale	112 (1990)

The DG boreholes are drilled near the Droëkloof production borehole DG110. VR5 and WN101 are situated in the Nardouw Aquifer (Baviaanskloof Formation, just south of the Marnewicks v-notch. VG12 is an important monitoring borehole, midway between the VG3 and the Cedarberg shale layer in the Vermaaks River Valley. DP27 is situated near the Varkieskloof production boreholes, and DP13, 14 and 20 near the Bokkraal production boreholes (see Figure 3-1).

Of interest is to note is the high yield, poor quality groundwater intercepted in borehole DP13 in the Bokkraal wellfield. Is this some indication of poor quality groundwater stored in discrete, poorly connected fractures?

3.7.4 Existing boreholes – privately owned land Kammanassie Mountains

One of the amendments of the original terms of reference was to determine the groundwater flow relationships in the Nardouw and Peninsula aquifer on the southern flanks of the Kammanassie Mountains and the potential impact of abstraction from the KKRWSS and existing abstraction on each other *vice versa*.

Table 3-5 (over page) shows the results of a hydrocensus carried out during July 1998. The hydrocensus results are subject to the honesty of farmers and sampling of groundwater to the availability of boreholes. Figure 2-5, show the location of the various boreholes of which information was obtained or /and which was sampled. The results of the sampling analysis are in Tables 1 to 9 and 13 to 15 (Appendix A). Environmental isotope, hydrochemistry, remote sensing and structural geology will be used to characterise the aquifers on the southern flanks of the Kammanassie Mountains and its inter-relationships with the wellfields of the Eastern Section of the KKRWSS.

TABLE 3-5: HYDROCENSUS DATA SOUTHERN KAMMANASSIE MOUNTAINS

FARM	BH	YIELD (l/s)	ANNUAL ABSTRACTION (m3/a)	DEPTH (m)	NOTES
RIETFONTEIN		7.5	236520	75 – 110 – 150	In total 7 boreholes on farm. Borehole drilled deeper, when yield drops, final depth 150 m. At this depth the spring dried out and all the shallow boreholes in the nearby vicinity. Use of this borehole for past 10 year, 365 days a year. Water level at 10 m.
RIETFONTEIN		3.1	32140		Not in use currently. Use as necessary.
RIETFONTEIN		5.0	151000	90 245 242	3 Boreholes in Klapperkloof. Out of use after the flood of 1996.
RIETFONTEIN		0.5	43	30	Drilled in original artesian fountain. High rains of January 1996, spring flow again, last similar rain event in 1981/82 (850 mm of rain).
WAGENPADSNEK	WK3	6.0	197100	75 – 110 – 121	Borehole in use for 15 years for 365 days of the year. Initially drilled deeper from a 3 year period. Water level at 14 m.
LEEUBLAD	Spring	6.3	200000		Spring flow reduces to 5 l/s and increased to 7.5 l/s in low and high rainfall years, respectively. Fountain exists for 150 years, dried up after pumping started at RF2. With the flood of 1996, vegetation washed away and the spring flows again at 3.8 l/s.
LEEUBLAD	LD2	5.0	160000	90	Original yield was 10 l/s, reduced to 5 l/s and lower. Two more boreholes – collapsed. Borehole pumped non-stop
LEEUBLAD		6.2	100000		Only used for stock watering, 30 m deep
LEEUBLAD	LD1				Collapsed in 1984
LEEUBLAD	Springs				Used springs at Wildebeesvlakte – now dry
ROLBAKEN	RF2	6.9	219000	100	Pump installed on 70 m depth. Pump non-stop 365 days a year. Rest water level is 10 m; pumping water level is 50 m. Borehole tested to give 10 l/s. Pumped since 1983.
ROLBAKEN	RF2	6.3	199100	30-84	In 1969, this borehole was artesian at a yield of 3.8 l/s. Tested in 1981 at 10.1 l/s, drilled deeper, pump non-stop. Rest water level is at 5 m, pumping water level at 50 – 60 m
SCHEEPERS-KRAAL	SL2	1.3	20000	160	Brackish water. Use to pump water from a borehole higher up in the mountain for 18 years – damaged by flood – similar scale of abstraction.
KOUTJIE	RF 5,6, 7 RF4	12.6 7.6	50000 100000	90 – 110 110	Several high yielding boreholes. Never pumped at the same time, pumped individually for 3 hours. Boreholes collapsed (only first 20 m cased-off). Water level at 34 m. Water strikes at 72, 88 and 109 m. Above boreholes collapsed in 1996 flood. Replace above with this borehole. Blow-out yield 15 l/s. Water level 38 m.
KOUTIE	RF3	6.3	100000	45 – 75	Drilled on original spring, drilled deeper later, spring stopped flowing.
EILANDS-RIVIER	YR1	2.5	50000	70	Pump for more than 20 years, constant during summer and only to fill dams in winter.
DIEPEKLOOF	DR2	2.5	40000	90	Diesel pump

CHAPTER 4: HYDROCHEMICAL CHARACTERISATION

The positions of the boreholes in the local study area relative to the lineaments are shown on Figure 4-1 over page. According to the structural interpretation, remote sensing and satellite lineament analysis, fractures trending NNE-SSW and certain E-W, WNW and N-S trending fracture orientations are preferred for groundwater flow. Figure 4-1 shows the fracture density, orientations and connectivity around each of the boreholes sampled in the Kammanassie Mountains.

The interpretation of hydrochemistry and environmental isotope data of various existing boreholes and springs (hot and cold) in the Klein Karoo, sampled during several sampling surveys (see Section 2.1) together with the following:

- Interpretation of hydrogeological data
- Remote sensing analysis of satellite images
- Structural interpretation of geological features

are all fundamental in the formulation of the conceptual hydrogeological model for the TMG Aquifers in the Klein Karoo and Kammanassie Mountains. The rationale is to extrapolate the findings of the hydrochemical and environmental isotope data interpretation to other parts of the TMG Aquifer in the Klein Karoo, where no boreholes are currently present.

In this Chapter hydrochemical and environmental isotope data is interpreted together with the above-mentioned. The relevant hydrogeological information on boreholes sampled, is summarised in Section 3.6 (Chapter 3).

The results of the various sampling surveys and groundwater analysis are summarised in Appendix B, Tables B-1 to B-20. The locality of boreholes sampled in relation to the geology are shown on Figure 2-5 and those of the hot springs in Figures 2-3.

4.1 DATA ANALYSIS TECHNIQUES

In order to characterise groundwater of the various TMG Aquifers, the following data interpretation has been carried out on hydrochemical and environmental isotope data:

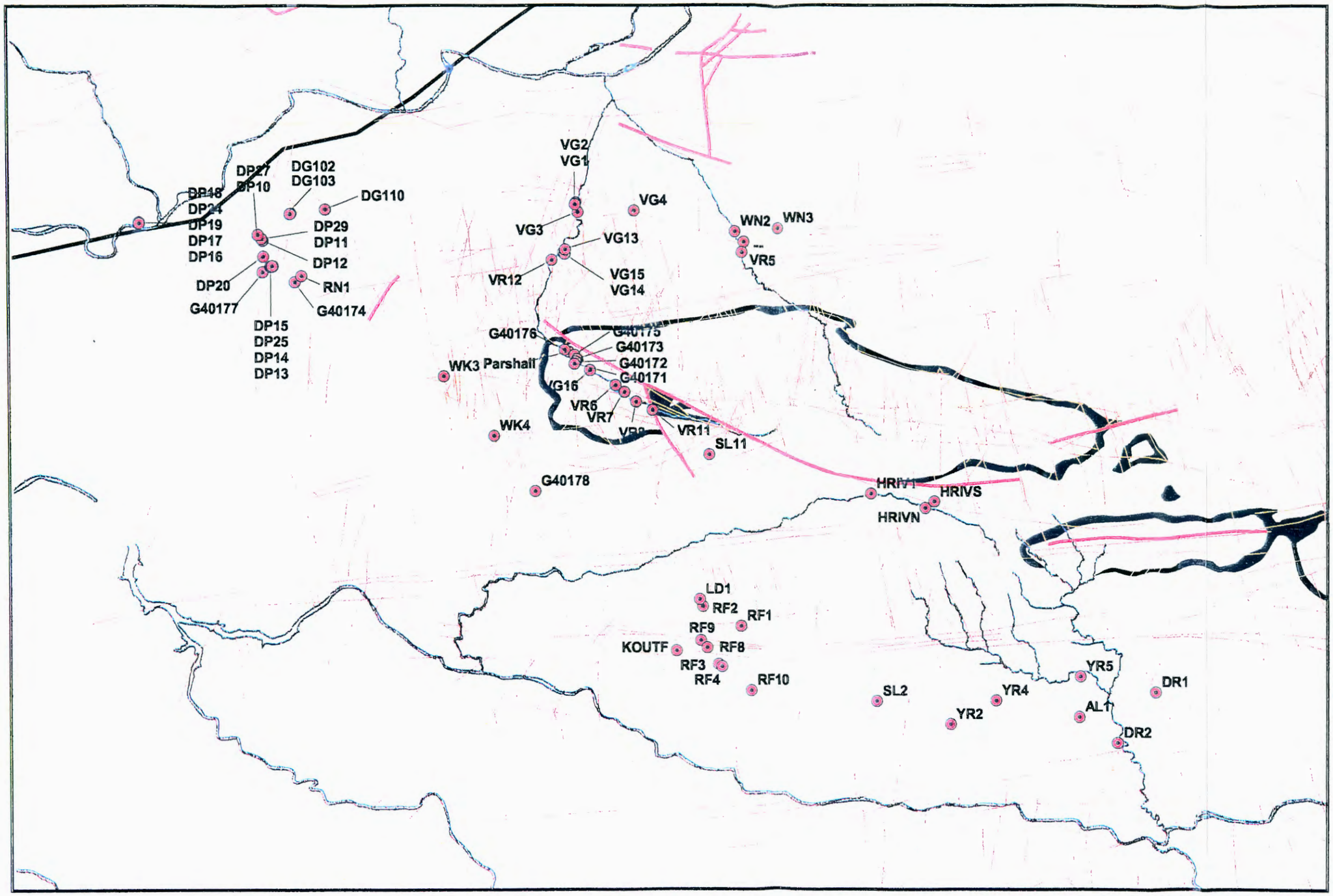

WRC Proj. K5/729	BOREHOLE POSITIONS AND SAMPLING LOCALITIES RELATIVE TO LINEAMENTS KAMMANASSIE MOUNTAINS	Figure No. **4.1**

- Standard tri-linear diagrams, i.e. Piper, Durov, Expanded Durov and SAR diagrams are employed to investigate the use of these diagrams to distinguish between groundwater originating from the Nardouw and Peninsula Aquifer.
- Trace element analysis (see data in Appendix B).
- Various X-Y scatter plots of ionic ratios and / or environmental isotopes are used to investigate dissolution process effects between ion pairs and to fingerprint groundwater types with different flow paths. All the scatter plots are presented in Figures 1 to 36 (Appendix G).
- Composite fingerprint diagrams developed for the Klein Karoo Aquifers represent a type of Schoeller Diagram (see Section 2.5.1.8), showing cumulative dissolved ion concentrations and $\delta^{18}O$ signature of groundwater on the same figure Figures 1 to 19 (Appendix F).
- Interpretation of stable and radioactive environmental isotope data, i.e. $\delta^{18}O$, $\delta^{2}H$ and $\delta^{14}C$, ^{3}H.
- The spatial variation in the following major ions: SO_4, Cl, Si, and EC; as well as environmental isotopes $\delta^{18}O$ and ^{14}C are shown in Figures 1-11 (Appendix F).

To assist data interpretation and colour coding on diagrams representing hydrochemical data, all boreholes or springs with similar geographic or lithologic origin are grouped together. The following preliminary groups are distinguished:

1. Hot springs, i.e. all the TMG hot springs.
2. Cold springs, includes the Vermaaks, Marnewicks and Huis River springs.
3. Nardouw East: production boreholes of the Eastern Sector of the KKRWSS, sited in the Nardouw Aquifer.
4. Nardouw West: production boreholes of the Western Sector of the KKRWSS.
5. Peninsula East: production boreholes of the Eastern Sector of the KKRWSS, sited in the Peninsula Aquifer.
6. TMG artesian, artesian boreholes – G40175A.
7. TMG general, represents the data from the Simonic sampling survey, and is representative of average rainfall sample (seepages). Although this data is included here, not much information was available to enable satisfactory interpretation.
8. Nardouw Private, represents private boreholes drilled in the Nardouw Aquifer, i.e. WK3 and 4, WN2 and 3.
9. Nardouw South essentially includes SBH1 and 2, the only boreholes sampled in the Outeniqua Mountains.
10. "Private South?" represents boreholes drilled on privately owned land on the southern flanks of the Kammanassie Mountains. The groundwater of the above-mentioned

boreholes needs to be characterised in terms of the aquifer it taps. The "?" refers to the the uncertainty of the aquifer tapped.

The main purpose of the above-mentioned grouping of data is to improve visualisation on figures only. Data interpretation aims at definition of the different hydrostratigraphic units, i.e. aquifers and aquitards.

4.2 MACRO ELEMENT DATA ANALYSIS

The groundwater chemistry is determined by the dissolution history of infiltrating rainwater in the aquifer. The lithology of the Peninsula Formation and Nardouw Subgroup varies considerably (Chapter 3). The Peninsula Aquifer is an orthoquartzite composed almost entirely of quartz grains. The Nardouw Aquifer is composed of arcosic sandstones containing feldspars, a variety of clay minerals and other minerals. The major minerals in shale layers (including the C/S layer) are clay minerals, i.e. kaolinite, montmorillonite, illite, chlorite and quartz). The shale layers of the Bokkeveld Aquifer and the C/S contain significant amounts of pyrite. The compositional changes of the host rock should therefore be reflected in the dissolution chemistry of samples taken from the various aquifers.

The groundwater is characterised by low mineralisation (TDS < 300 mg/l), low pH (<6) and low Total Alkalinity (0.5 meq/l). In general the TDS < 50 mg/l and pH ranges between 6 and 7 for the Peninsula Aquifer. For the Nardouw Aquifer TDS values range from < 50 mg/l in the Keystone Block to values between 100 and 300 mg/l elsewhere and pH < 6.

Figures 4-2 to 4-5 represent standard tri-linear diagrams, i.e. Piper, Durov, Expanded Durov and SAR diagrams, respectively. These diagrams are used to evaluate the macro element chemistry of TMG Aquifers and to assess the general application of these diagrams in characterising the different TMG Aquifers.

The following observations are made from Figure 4-2 (Piper diagram):

- Chloride is the major anion in TMG groundwater. This is explained by very little dissolution of host rock minerals and proximity to recharge areas. The groundwater composition is therefore similar to that of rainwater.
- Na and K are the major cations, very little dissolved Ca (low alkalinity).
- Two clusters of groundwater are distinguished, representing the Hot Springs and the boreholes drilled in the TMG, respectively.

- Water originating from hot and cold springs, shallow boreholes drilled in localised structures in the Nardouw Subgroup (DR2, SL2 and VSBH1) and the Bokkeveld shale (G40174), are more mineralised than most boreholes drilled in the TMG Aquifer.
- Water originating from hot springs may represent a mixture, of TMG groundwater from depth mixing with groundwater in the Bokkeveld shale during its upward flow path.
- Although groundwater from the alluvial aquifer (DP18), plots close to TMG groundwater, on the Piper Diagram, it is more mineralised.
- The abandoned artesian monitoring borehole (G40175) plots separately from the main TMG cluster, most probably due to contamination with groundwater from the C/S.

From the above it is concluded that the Piper diagram is not particularly useful to differentiate between groundwater originating from the different TMG Aquifers as similar hydrochemical relationships exists, at variable concentrations, which the Piper diagram is unable to show. The Piper diagram is, however, a very useful diagram to differentiate between groundwater from the TMG Aquifers and other aquifers, i.e. alluvial or limestone.

From the Piper plot, TMG groundwater is classified as a Na/Cl type water, as all other ions are present at very low concentrations. The major ion chemistry of TMG groundwater is not balanced, in that the low alkalinity and pH of the groundwater leads to the conclusion that free CO_2 is present, which needs to be balanced by the dissolution of Mg^{2+} and Ca^{2+}. In thermal springs, unbound CO_2 evolves into mainly Ca^{2+} alkalinity, i.e. shifts to the left in the Piper diagram.

An alternative to the Piper diagram (Figure 4-2) is the Durov diagram (Figure 4-3) and expanded Durov diagram (Figure 4-4). From Figure 4-3 the following observations are made:

- Similar to the Piper plot (Figure 4-2), two groups of groundwater are distinguished, i.e. hot springs and TMG groundwater from boreholes.
- The TMG groundwater clusters around EC and pH values ranging from 5 to 50 mS/m and 4 to 8, respectively.
- DP15 and DP28 have a distinctly lower pH and higher SO_4 content.
- Higher pH and EC are associated with DP18 (alluvial borehole), G40178 (drilled into Bokkeveld) and G40174 (drilled into fracture filled with pyrite and quartz, Nardouw Subgroup).

FIGURE 4-2: PIPER DIAGRAM OF ALL HYDROCHEMICAL DATA

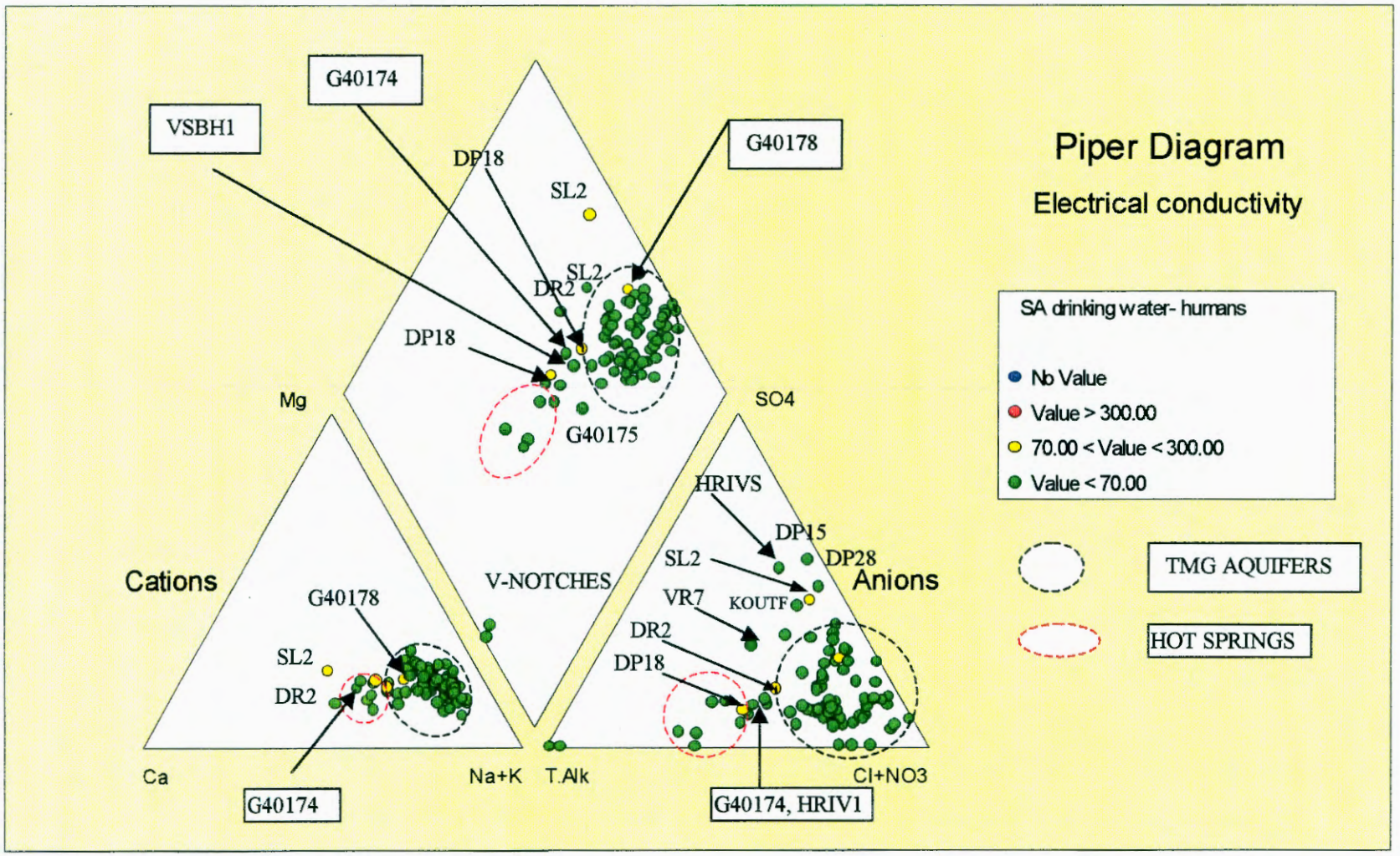

FIGURE 4-3: DUROV DIAGRAM OF ALL HYDROCHEMICAL DATA

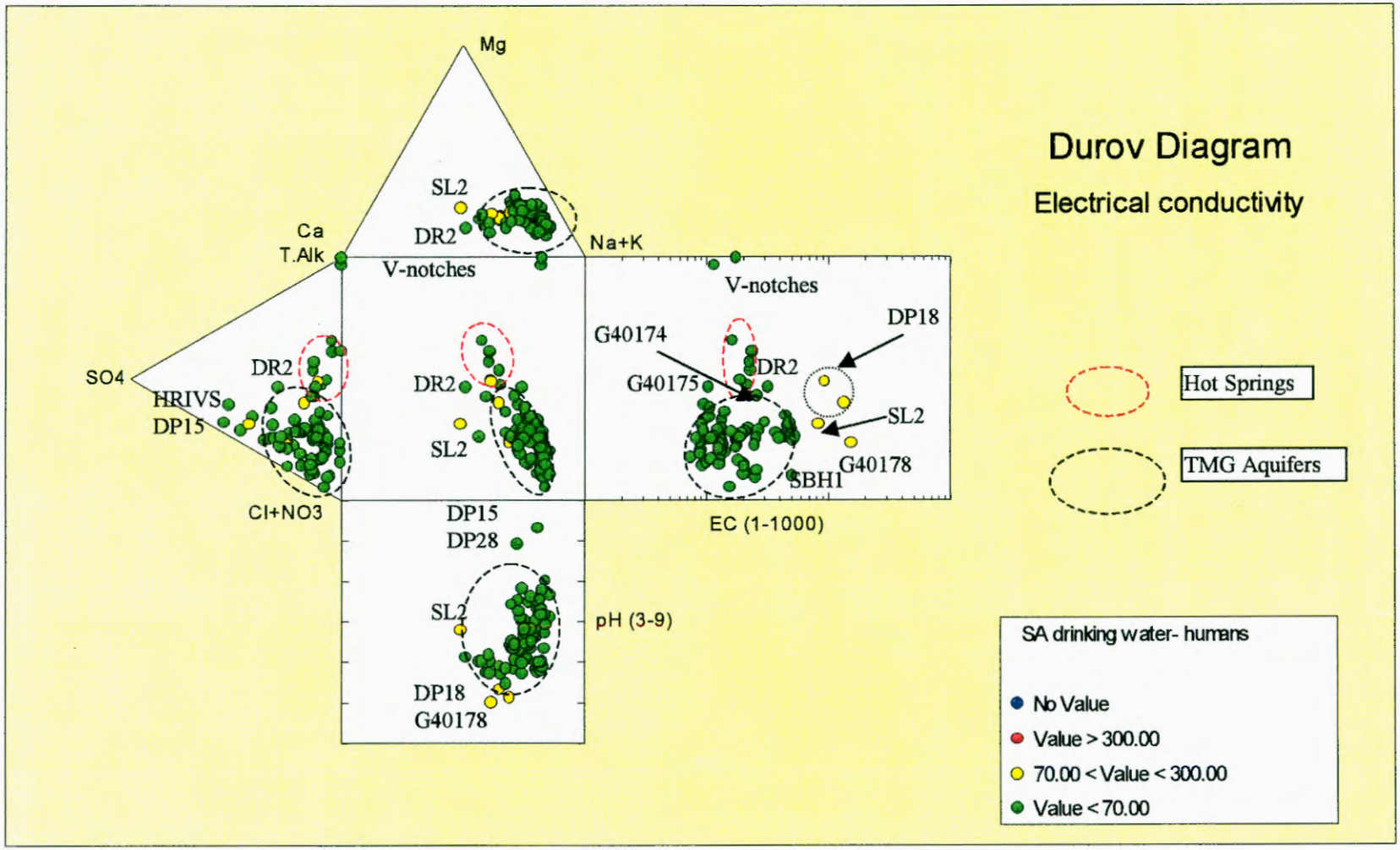

FIGURE 4-4: EXPANDED DUROV DIAGRAM OF ALL HYDROCHEMICAL DATA

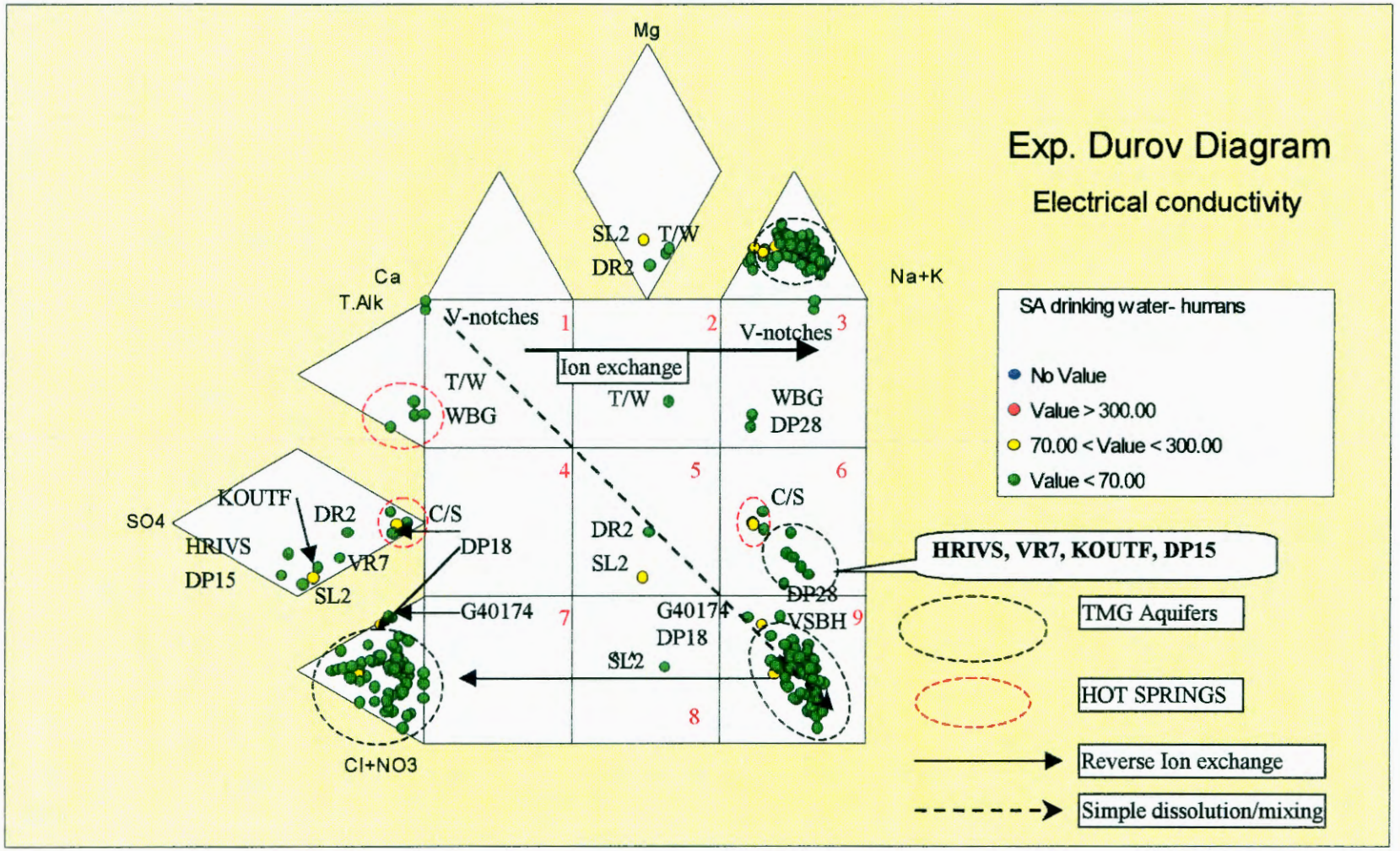

FIGURE 4-5: SAR DIAGRAM FOR LITTLE KAROO TMG HYDROCHEMISTRY DATA

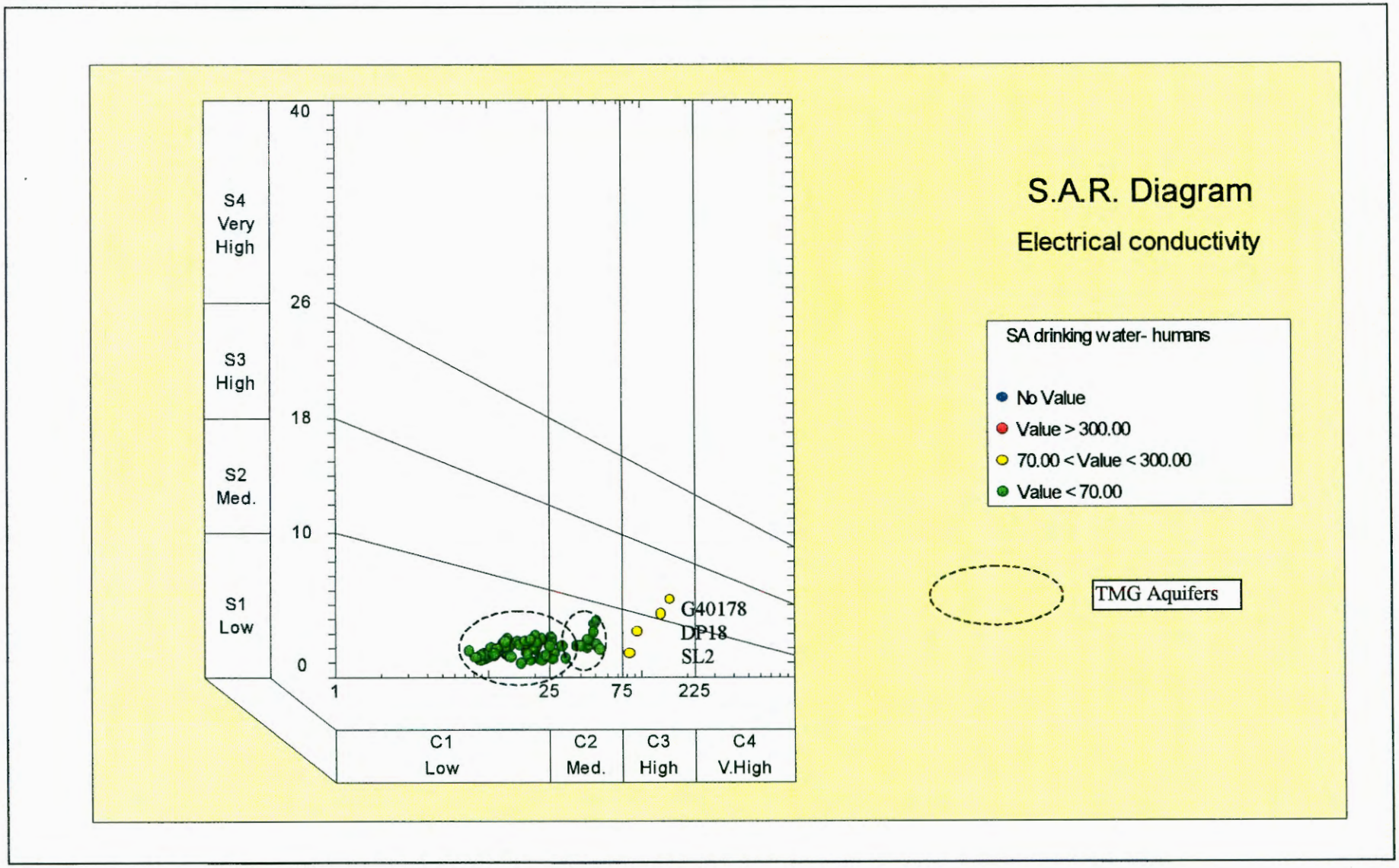

Shallow boreholes drilled into more localised structures, i.e. DR2, SL2 plot distinctly different from TMG groundwater cluster. These boreholes are also situated close to the Bokkeveld contact and has a much higher TDS (> 300 mg/l) compared to other boreholes.

The expanded Durov diagram (Figure 4-4) offers a distinct advantage over the Piper diagram in that nine groundwater fields (indicated by 1 to 9 in red on Figure 4-4) display the different hydrochemical types and processes on the diagram. From Figure 4-4 it is observed that the low alkalinity and TDS of TMG groundwater, complicates interpretation with the expanded Durov diagram, eg samples taken at Vermaaks and Marnewicks V-notches. The hot springs, which generally have higher alkalinity than most of the borehole samples, plot in three distinct fields, i.e.:

1. T/W (Toorwater Spa, near Uniondale) in Field 2: HCO_3^- and Mg^{2+} dominant (or cations indiscriminate field), often indicates water associated with dolomite, more specifically the Cango limestone formation in this case. Ca^{2+} and Na^+ dominance indicates partial ion exchange, which is not the case in the above. Therefore, water released by the Toorwater hot spring, seems to follow a flow path via the Cango Limestone formation.

2. WBG (Warmwaterberg Spa, near Barrydale) in Field 3: HCO_3^- and Na^+ dominant field, which normally indicates ion-exchanged water, although the reduction of SO_4^{2-} at depth can produce H_2S and CO_2 in the case of Na^+ dominant water. Water emanating from the WBG hot spring has most probably undergone ion-exchange reactions in reducing conditions on its flow path through the Bokkeveld shale. Also note that DP28 (Bokkraal Wellfield), the "problem" production borehole of the KKRWSS in terms of its low pH plots close to the WBG hot spring in Field 3.

3. C/S (Calitzdorp Spa) in Field 6: SO_4^{2-} dominates or anions indiscriminate and Na dominate field, is a water type not frequently encountered and most probably indicates mixing. The C/S has the highest temperature 49.6 °C as opposed to 42.3 and 42.5 °C of the T/W and WBG hot springs and the highest DO content (60%) versus almost zero for the other hot springs. The C/S seems to have a long, fast travel path, sampling groundwater from various inter-connected fracture sets. Groundwater ascends rapidly to the surface, with little time for ion exchange with Bokkeveld rocks on its flow path.

From Figure 4-4, most of the TMG Aquifer, borehole data plot in Field 9: Cl^- and Na^+ dominant field, which frequently indicates end-point waters. Unfortunately, the Durov diagram does not allow distinction between Cl^- and Na^+ dominant waters. End-point water is

normally saline water (old brackish water), which is not the case here, even the Bokkeveld groundwater (G40178) is excluded from this category. Ions, eg. Ca^{2+}, Mg^{2+} and HCO_3^- occur in very low concentrations in TMG groundwater, which has a very low overall mineralisation (EC < 10 m/Sm). Mixing occurs along a linear trend within the field and could be indicative of mixing of groundwater in different fracture sets, intercepting groundwater from the various formations, i.e. Peninsula, Nardouw and Bokkeveld.

Similarly to the Piper Diagram (Figure 4-2) boreholes DR2 and SL2 plot differently from the other boreholes, i.e. in Field 5 (no dominant anion or cation) indicative of water exhibiting simple dissolution or mixing.

Figure 4-5 represents the different sodium adsorption ratios (SAR) for the various groundwater samples. Generally, the SAR for TMG groundwater varies from zero to 10 and the salinity from low to medium (hot spring data). The SAR for Bokkeveld and Alluvial groundwater (G40178 and DP18, respectively) is slightly higher (between 10 and 15) and with high salinity.

A major drawback of all tri-linear diagrams is that they do not portray the individual ion concentrations. Schoeller diagrams on the otherhand are based on actual ion concentrations. Most TMG data plots together in one cluster. The distribution of ions within the main field is unsystematic in terms of hydrochemical processes so that the diagram lacks certain logic. It is not possible to differentiate between the different TMG Aquifers, i.e. Nardouw and Peninsula Aquifers on tri-linear diagrams. Further, the low alkalinity and pH of TMG groundwater complicates interpretation of TMG major ion chemistry.

4.3 TRACE ELEMENT DATA ANALYSIS

The trace element data set is incomplete. Unfortunately, samples were wrongly analysed and some were lost on their way to the laboratory. Subsequent re-sampling took place months after the original sampling run and did not include samples for environmental isotope analyses. Subsequent, trace element analyses did not always include the same series of constituents. Therefore, spatial and temporal comparison of trace element data in relation to macro element and environmental isotope data is incomplete and inconclusive. However, a few useful deductions, which need to be confirmed by future sampling programs, are made. Available trace element data are summarised in Tables A-6, -9, -11 and –14 (Appendix A). Figures 1 to 5 (Appendix F) show the spatial variations in Al, Ba, Fe, Mn and Sr. The following observations follow from the above-mentioned figures and tables:

- TMG groundwater does not contain significant concentrations of As, V, Cr, Mo, Pb, Hg or Cd. Therefore, the presence of significant concentrations of any of the above-mentioned are most likely indicative of contamination. The Cd present in DP28 is postulated to be a result of impurities in acid used for remedial action during the borehole rehabilitation program.
- Ba, Al and Sr are the most valuable tracers and are associated with dissolution of silicate minerals (feldspars and clays, respectively).
- Al contents for TMG Aquifers are generally < 0.5 mg/l and seem to be controlled by dissolution of feldspar minerals and formation of Al complexes. The lowest Al content is associated with the Peninsula Aquifer (< 0.02 mg/l), which decreases further with increasing fracture density (Figure 1, Appendix F and Figure 4-3). It is postulated that a decrease in Al concentration is proportional to an increase in permeability because of absence of clay material.
- Ba is a good tracer to distinguish between groundwater from the Nardouw, Peninsula or groundwater from boreholes drilled into the 'Keystone Block' Aquifer, respectively, and is also associated with feldspar dissolution. Ba levels in groundwater from the Peninsula Aquifer are generally <0.002 mg/l, compared to the Nardouw Aquifer where levels are >0.002 mg/l, but <0.050 mg/l. The only exceptions being YR2, DR2 and SBH1, with Ba levels > 0.100 mg/l (most probably due to mixing with groundwater from the nearby Bokkeveld Aquifer). Higher feldspar dissolution of the Nardouw Aquifer, associated with feldspars in shale layers is expected to give rise to higher Ba concentrations in groundwater of this Aquifer.
- Sr commonly replaces Ca and K in feldspar minerals and is the most informative trace element for TMG Aquifers. The Sr concentration is lowest in the Peninsula Aquifer (< 0.003 mg/l). The higher Sr concentration in VR7 is most probably due to dissolution of the keystone fault breccias.
- Ni, Cu, Zn and Co are present in groundwater from some boreholes, and are due to dissolution of minerals containing these trace elements in shales and quartz veins (Hälbich et al., 1995).
- Mn concentration is generally low, (< 0.1 mg/l) and increases towards the Baviaanskloof Formation / Bokkeveld Group contact. Mn concentrations > 2.0 mg/l are reported in G40178, an additional monitoring borehole drilled into the Bokkeveld Group sediments.
- Fe concentration is generally low, (< 0.1 mg/l) and increases towards the C/S contact and weathering of TMG rocks. Further, Fe concentration increases with a decrease in pH and dissolution of pyrite in quartz veins, found in the Nardouw Aquifer, which leads to the sulphate and sulphide formation in an oxidising and reducing chemical environment, respectively. In terms of the iron-bacteriological clogging of boreholes an understanding of the hydrogeology and hydrochemical conditions for the above-mentioned redox reactions is essential.

- Ti is only present in water sampled from the Vermaaks and Marnewicks V-notches and can be attributed to the presence of heavy minerals (rutile) in stream sediments.
- B seems to be an important indicator of flow paths through the Enon, Bokkeveld or alluvial aquifers.

It is recommended that further trace element sampling be carried out. In particular, the dissolution of feldspars and associated trace elements, i.e. Ba, Sr and Al needs to be investigated further. The presence of Ni, Cu, Co and Zn are indicative of the presence of pyrite quartz veining, which is always present in boreholes where iron-reducing bacteriological clogging prevails. In the light of the low EC and TDS values of groundwater in the TMG Aquifers, trace elements can provide a valuable insight in the dissolution chemistry and flow paths of groundwater in the TMG Aquifers. Trace element chemistry may provide valuable insights into the exploitation potential of TMG Aquifers, in terms of providing information on the permeability (feldspar dissolution) and the presence of pyrite quartz veining (potential for iron-reducing bacteriological clogging of boreholes).

4.4 HYDROCHEMISTRY AND ENVIRONMENTAL ISOTOPES

4.4.1 Stable isotope data

Figures 4-6 and 4-7 (over page) represent the $\delta^{18}O$ and $\delta^{2}H$ relationships for ground and rainwater of the Klein Karoo. Figure 4-6 represents all the environmental isotope data available for TMG Aquifers in the Western Cape, while Figure 4-7 represents only the data from the Klein Karoo. TMG West represents groundwater samples taken around the Cape Peninsula and Piketberg, while TMG General represents samples of mountain seepages taken in the Cape Mountains (see Table A-17, Appendix A). All environmental isotope data are summarised in Tables A-3, -7, -12 and -15 (Appendix A). The spatial distribution of $\delta^{18}O$ data is shown in Figure 6 (Appendix F). From Figures 4-6 and 4-7 the TMG data set plots close to the Cape MWL (Diamond, 1997), the Global MWL (Dansgaard, 1964) and the MWL for South Africa (IAEA, 1981). Only two samples have undergone evaporation (Figure 4-6). Figures 4-6 and 7 the following effects are observed:

- The altitude effect: rainfall and mountain seepage samples become progressively lighter (more negative) with increasing altitude. This is in particular true for the lighter signatures of rain samples taken at the Wildebeesvlakte and Parshall rain gauges (Table A-16, Appendix A) as opposed to the rain samples collected at lower altitudes.
- The continental effect: groundwater becomes progressively depleted away from the coast (compare TMG West with Klein Karoo TMG data).

FIGURE 4-6: $\delta^{18}O$ VERSUS $\delta^{2}H$ - TMG AND ALLUVIAL AQUIFERS

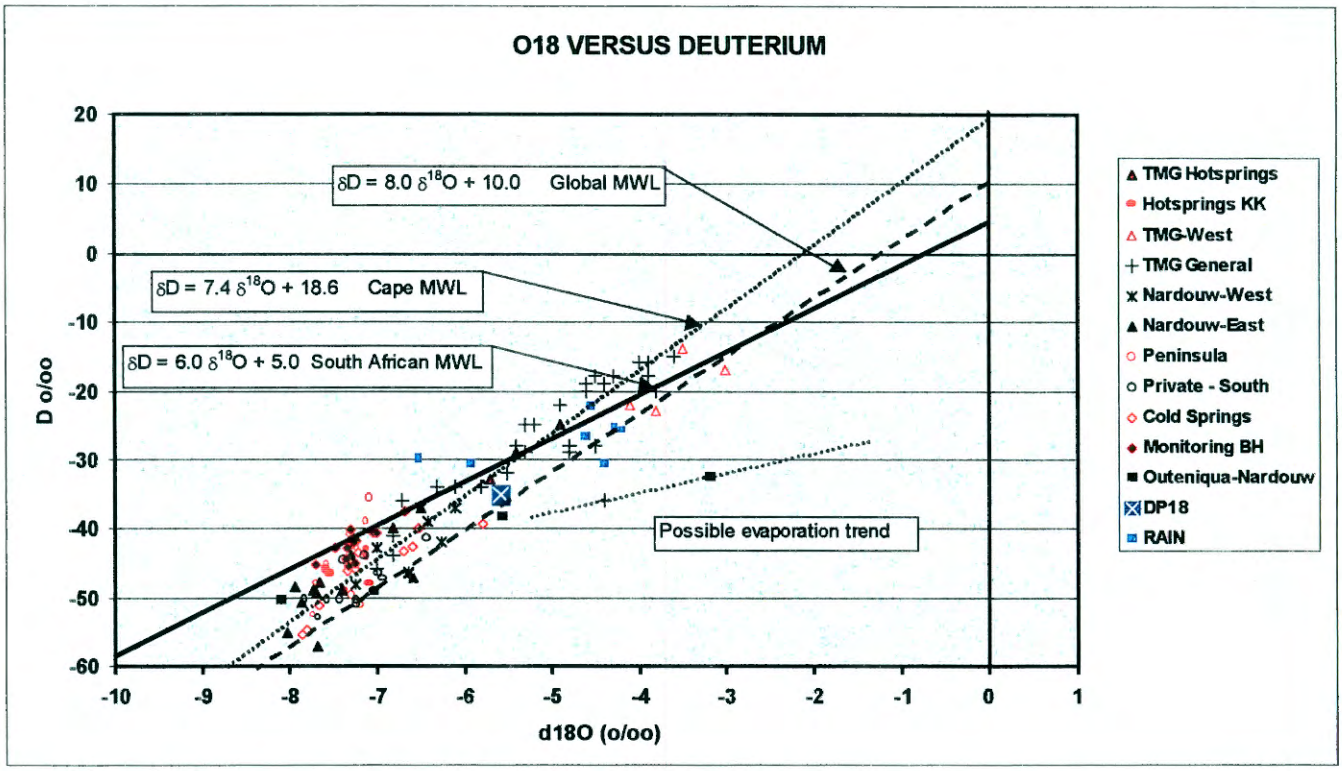

FIGURE 4-7: $\delta^{18}O$ VERSUS $\delta^{2}H$ - KLEIN KAROO TMG AQUIFERS

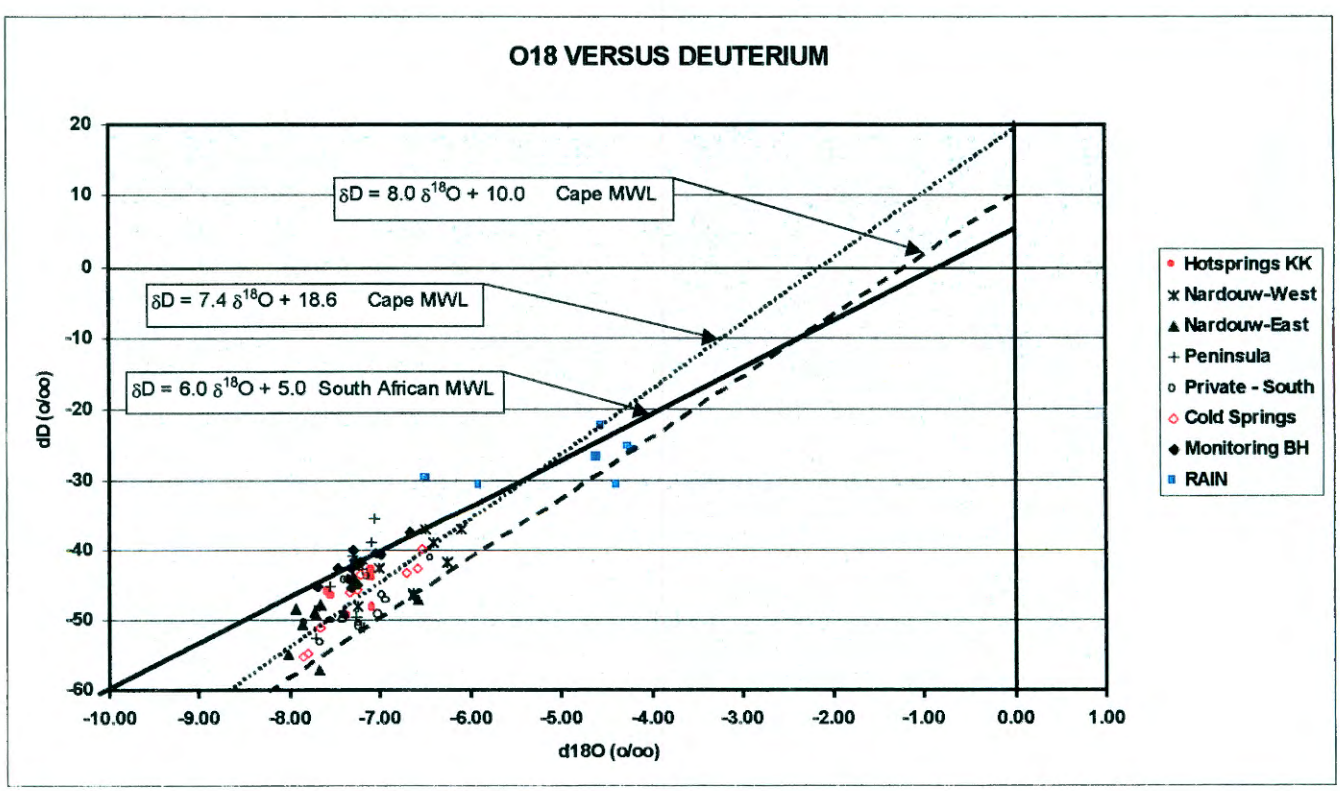

- Rainfall selectivity: TMG Aquifers are more depleted compared to rainfall samples. It is postulated that the major recharging events are associated with heavy frontal rains or snow on mountaintops during spring, which produce depleted signatures. Frontal rains fall mostly during the winter months. Depleted $\delta^{18}O$ signatures are also produced by the one in 20-year flood event, producing rainfall in excess of 200 mm per day. Most of the rainfall originating from thunderstorms evaporates considering the high surface temperatures prevailing during the summer months and seems to contribute significantly less to recharge, than in the case of frontal rains. Recharge during thunderstorms can produce heavier $\delta^{18}O$ signatures due to evaporation occurring before infiltration into the hot soil.
- The hot springs of the Klein Karoo are more depleted than the other TMG Hot Springs in the Western Cape. This is explained by different intake histories. The Klein Karoo hot springs are located far from recharge areas in mountain catchments relative to other hot springs in the Western Cape. Further, other TMG hot springs are situated closer to the ocean and rainfall prevailing in the Western Cape is generally enriched (less negative).

Tables A-3, -7, -12, -15 and 16, Appendix A show that the $\delta^{18}O$ / $\delta^{2}H$ signature of groundwater samples taken during different sampling surveys (same boreholes) varies. This is due to the amount effect, during which a greater amount of precipitation will give a more negative $\delta^{18}O$ signature. Rainfall volume and origin (frontal versus thunderstorm) varies from year to year, with a consequence that recharge of a particular year will have an imprint depending on the rainfall volume and frequency. Comparison of the environmental isotope data for various surveys (Tables A-3 and 7, Appendix A) shows more depleted $\delta^{18}O$ signatures for the July 1997 than those for the same borehole during the January 1996 survey. These differences are postulated to be the result of rainfall selectivity and the amount effect.

The isotopic signature of groundwater is dominated by the imprint of a heavy rainfall event, e.g. that of December 1996 (>200 mm over two days measured at the Wildebeesvlakte rain gauge in the Kammanassie Mountains). A heavy rainfall event such as this, introduces a depleted or 'light' $\delta^{18}O$ signature, where turnover times in the aquifer are fast enough so that groundwater abstraction removes recently recharged water instead of groundwater from storage. On the other hand, groundwater abstraction from storage, in the absence such a flood event leads to a more average $\delta^{18}O$ signature. An increase in Mean Residence Time (MRT) of groundwater in boreholes will therefore indicate that groundwater from storage is being utilised, recharged during historic rainfall events.

4.4.2 Radioactive environmental isotope data analysis

The low pH values of groundwater in the TMG Aquifer indicate that the total dissolved inorganic carbon (TDIC) is mainly in the form of free CO_2 . The narrow range of $\delta^{13}C$ values (-19 to -22 ‰) is evidence of minimal carbonate dissolution. Somewhat higher values of $\delta^{13}C$ are found away from the fracture- bound, steep mountain valleys e.g. Vermaaks River Valley), in groundwater held in local fracture systems and in the much older thermal spring water. This allows the radiocarbon values measured in different sections of the regional system to be compared without necessitating isotopic dilution corrections. (All $\delta^{13}C$ and ^{14}C data are in Tables A-3, A-7, A-15, Appendix A).

Figure 4-8 (over page) is a schematic presentation, showing the ^{14}C values for boreholes above and below the C/S aquitard in the Vermaaks River Valley. ^{14}C values for boreholes above the C/S aquitard range from 75-84 pMC with practically no measurable ^{3}H. Borehole VG3 below the shale band in the Nardouw Aquifer gives a much lower value of 53 pMC. Apart from the similar $\delta^{13}C$, the $\delta^{18}O$ and $\delta^{2}H$ values are almost identical to those above the shale band. This sudden "ageing" suggests that the band acts as an effective aquitard, inhibiting subsurface drainage further downstream of this site. Surface drainage of actively recharged groundwater from above the shale band could also re-infiltrate to recharge groundwater below it. The results further suggest that the water pumped upstream of the C/S Aquitard, in spite of steady drawdown, is largely derived from the Kammanassie Mountain catchment (intermediate flow system) rather than from the regional fracture system. Regional flow paths and recharge from the Outeniqua Mountains at depth can buffer drawdown. However, in order to confirm this, the monitoring network and hydrochemical sampling program needs to be expanded.

A similar situation is encountered for boreholes in smaller valleys to the south and west of the Kammanassie Mountains (see Figures 7, Appendix F, for spatial variation in ^{14}C values). Here too, the residence times of the groundwater, as evidenced by the ^{14}C values, are the only distinguishing features as the hydrochemical and stable isotope signature are similar, suggesting genetic similarity with groundwater in the main valley. A correlation was found between ^{14}C values and fracture systems connecting the water-bearing structure with the recharge areas in the mountains. Highly permeable zones cross-cutting the C/S aquitard produce higher pMC values in the Nardouw Aquifers (70 – 85 pMC), versus values ranging from 40 – 70 pMC in the Nardouw Aquifers in the absence of these fractures, e.g. Vermaaks River. It is postulated that the longer residence times of groundwater in the Nardouw Aquifer are due to slow leakage of groundwater through the C/S Aquitard.

FIGURE 4-8: SCHEMATIC PRESENTATION SHOWING ^{14}C DISTRIBUTION IN GROUNDWATER, VERMAAKS RIVER VALLEY

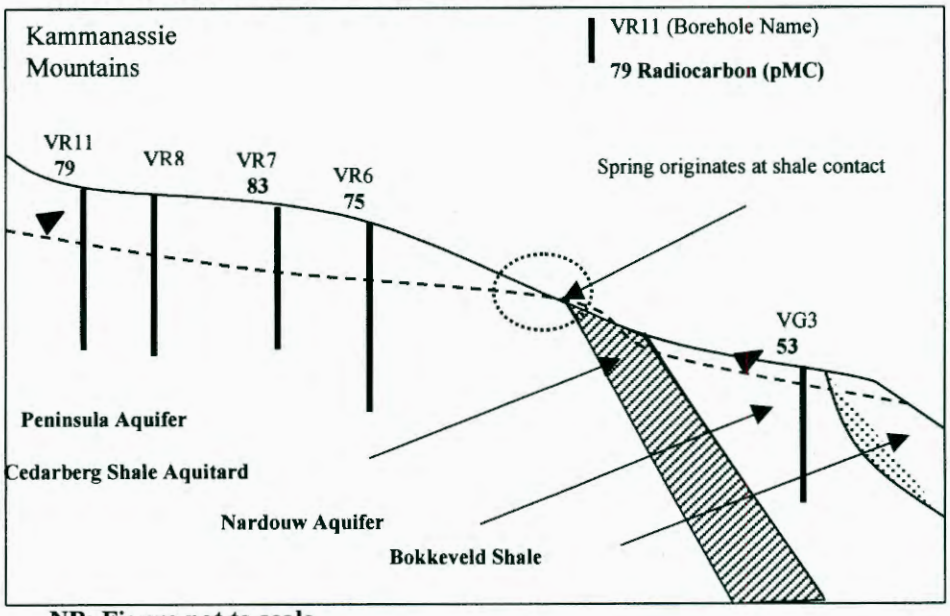

NB: Figure not to scale.

Hot springs are regarded as expressions of deeply circulating regional groundwater but although rising in low-lying terrain, have $\delta^{18}O$ and $\delta^{2}H$ values similar to those observed for the mountain catchments. Figure 6 (Appendix F) shows that most of the boreholes sampled for $\delta^{18}O$ have a fairly depleted $\delta^{18}O$ signature, i.e. < -7 ‰. This is indicative of recharge originating at a higher altitude in the mountains. Boreholes with heavier $\delta^{18}O$ signatures are recharged at a lower altitude. These differences are ascribed to the altitude effect (Verhagen et al. 1991). Hot springs have slightly more positive $\delta^{13}C$ values which, along with the slight shift in hydrochemistry towards higher alkalinity, indicate some development of carbonate chemistry in contact with country rocks. The above and the low pMC values for hot springs in the Klein Karoo (3.9, 11.0 and 25.6 pMC, for the Calitzdorp, Toorwater and Warmwaterberg Spa's, respectively) indicate longer mean residence times of this groundwater (see Figure 4-9). Hot springs are therefore interpreted as surface expressions of groundwater following a regional groundwater flow path.

$\delta^{18}O$ and $\delta^{2}H$ values for most boreholes sampled in the TMG Aquifer indicate that recharge occurs in the mountainous catchments and then flows along various inter-connected fracture sets covering the aquifer. Depending on the fracture geometry, length and characteristics, vertical flow will dominate with intermittent horizontal flow. Some of the recharged groundwater will also leach through the C/S Aquitard to the Nardouw Aquifer and further from the Nardouw to Bokkeveld Aquifers, as indicated by similar $\delta^{18}O$ and $\delta^{2}H$, lower pMC values of groundwater in these aquifers.

Table 4-1 summarises the findings of Weaver *et al.* (1998) during the application of the CFC-dating technique in the TMG Aquifers of the Kammanassie Mountains.

TABLE 4-1: CFC DATING RESULTS – KAMMANASSIE MOUNTAINS, KLEIN KAROO

Borehole	Dissolved Oxygen	pH	Temperature (°C)	Tritium (TU)	CFC (years)	Carbon-14 (pMC)
VR11	5.8	4.3	18.0	0.3 ± 0.1	45	74.6
VR8	4.9	5.0	20.1	0.4 ± 0.1	44	79.3
VR7	5.6	4.5	19.3	1.0 ± 0.2	38	83.0
VR6	5.0	4.5	18.0	0.4 ± 0.1	38	79.4
VG3	4.4	4.5	21.7	1.3 ± 0.2	30	57.0
DP29	0.2	5.5	24.0	0.2 ± 0.1	43	41.2
DP28	0.6	5.1	22.0	0.4 ± 0.1	39	62.3
DP15	0.5	3.7	23.0	-	36	52.0

FIGURE 4-9: EXPONENTIAL MODEL FOR ^{14}C AND ^{3}H SHOWING MRT FOR KKRWSS BOREHOLES IN (TABLE 4-4)

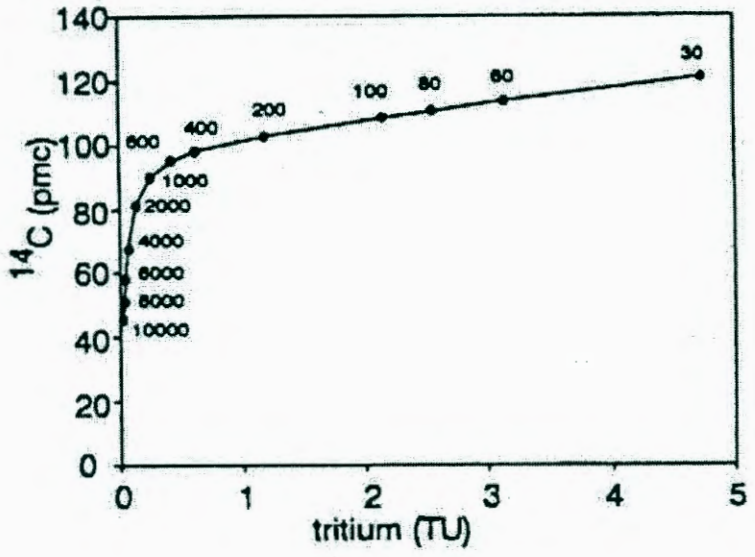

CFC data indicate that the groundwater is < 40 years old as confirmed by ^{3}H analyses (Table 4-1). This contrasts with the ^{14}C ages. This is not surprising, considering the fact that the borehole samples groundwater from different depths and scales of fractures. Any particular sample therefore represents a mixture of recently recharged groundwater and groundwater from storage. This is confirmed if the ^{14}C and ^{3}H data in Table 4-1 are plotted on Figure 4-9. The CFC dating indicates the youngest water, sampled from a much larger area over a longer period of time and moves in the more permeable intermediate scale fractures. The older water is mostly stored in the smaller matrix fractures, which originates

from brittle failure of the rock. The fact that groundwater of recent age is present indicates that the groundwater resource is actively recharged. In the case of VG3, the Nardouw Aquifer in the Vermaaks River Valley downstream of the C/S is most probably recharged by alluvial groundwater. However, the fact that the Vermaaks boreholes (VR boreholes) have been exposed to over-pumping in the past, could have resulted in higher oxygen levels in groundwater, as well as CFC's, which complicates data interpretation. Further, groundwater sampled could have been drawn in from a much shallower level in the aquifer in which case the CFC dating results are not representative for the deeper groundwater.

Table A-3 (Appendix A) also shows that similar environmental isotope compositions for production boreholes DP28 and 15 (only 40 m apart) indicate similar flow paths and origin. The differences in major ion chemistry, particularly sulphate contents of the above-mentioned boreholes are therefore most likely due the presence of iron precipitation and biofouling in these boreholes. Biofouling and clogging of borehole screens are enhanced by bacteria, when oxygen is introduced to a previously reducing environment during pumping of the borehole (see Table A-4, Appendix A).

Comparison of Figures 4-1, 4-13 and Figure 10 (Appendix F) shows that groundwater with the lowest ^{14}C is situated in those parts of the Nardouw Aquifer with the lowest fracture density, generally occurring at low altitudes.

4.4.3 Major ion chemistry and environmental isotopes

Various X-Y scatter plots of ionic ratios and / or environmental isotopes and composite fingerprint diagrams are used to fingerprint groundwater types with different flow paths. All the scatter plots are presented in Appendix G (Figures 1 to 36) and all composite diagrams in Figures 1 to 19 (Appendix H).

Figures 1 to 19 (Appendix H) show composite fingerprint diagrams developed for the Klein Karoo Aquifers. On each composite diagram, the date of sampling is indicated by an alphabetic symbol, representing the sampling season. Sampling surveys carried out during the winter and summer are indicated by the symbols W and S respectively. In those cases where a particular borehole or spring was sampled during more than one sampling survey. One sampling survey was carried out in autumn and is indicated by M.

Where sampling data for more than one season was available, seasonal variation in groundwater fingerprints can be attributed to various reasons, other than variations in rainfall. In general, an enriched $\delta^{18}O$-signature and higher TDS values are associated with summer months. There is too little $\delta^{18}O$ and ^{14}C data to confirm whether differences in $\delta^{18}O$ and

TDS values over seasons are a result of differences in prevailing rainfall conditions or historic recharge events, which are now sampled from storage. The reason for the difference in isotopic signatures is variation in rainfall frequencies, magnitude and origin (amount effect and rainfall selectivity). Frontal rains will result in a more depleted $\delta^{18}O$ signature than in the case of a thunder storm a heavy rain event will be further depleted compared to a small event.

From the composite 'fingerprint diagrams', the following aquifers can be distinguished: Peninsula, Nardouw, Alluvial, Cango Limestone, Enon and Bokkeveld Aquifers. The composite diagrams show that boreholes SL2 and DR2 have similar $\delta^{18}O$ signatures, but different major ion chemistry compared to those of other TMG boreholes (see Figures 1-3 and 10-13, Appendix H and and Figures 1-35, Appendix G). This indicates a similar recharge intake history and different dissolution chemistry resulting from groundwater flow along less fractured, poorly inter-connected fractured rock and mixing with groundwater from the Bokkeveld Group. The remote sensing data (Figure 4-1) show that both SL2 and DR2 are not situated in a densely fractured portion of the aquifer, or in a major lineament. Drilling results show that the above boreholes are situated on isolated NNE and NNW trending structures in the Nardouw Aquifer close to the Bokkeveld Group contact. These shallow, low yielding boreholes are drilled on structures, fed by recharge from the mountain catchment recharge area (as indicated by negative / depleted $\delta^{18}O$ signature of groundwater). The presence of ^{3}H and high ^{14}C indicates that matrix flow is the dominant flow mechanism. It is postulated that groundwater recharge in the mountain areas, flow down-gradient in a poorly connected fractured system as inter-flow.

Figures 13, 17 and 18 (Appendix H) show that Alluvial Aquifers and the Cango Limestone Aquifer have cumulative dissolved ion concentrations > 10 meq/l and more enriched $\delta^{18}O$ signatures (> -6.0 ‰) compared to TMG Aquifers. Groundwater from the TMG Aquifer generally has cumulative dissolved ion concentrations < 10 meq/l and more depleted $\delta^{18}O$ signatures (< -6.0 ‰).

Two groups of hot springs are present in the Western Cape (Figure 19, Appendix H). The first group is constitutes Baden, Brandvlei and Baths hot springs and the second group the Klein Karoo hot springs (Toorwater, Calitzdorp Spa and Brandwater) and the Montagu Spa. Geographically the first group is situated closer to the sea (Atlantic Ocean), whereas the second group is situated more inland.

The Western Nardouw Aquifer (Calitzdorp) has a different fingerprint compared to that of the Eastern Nardouw Aquifer, i.e. higher, dissolved ion concentrations (see Figures 12 and 13 Appendix H), which corresponds to higher alkalinity. The long mean residence time (low

pMC values) and higher TDS values of the Western Nardouw boreholes indicate long turnover times in the aquifer and more concentrated dissolution chemistry, indicating a different lithology and / or flow path. The NE-SW orientation of the structure on which the boreholes are located (Figure 4-1) with few crosscutting NE, NW fractures are signs of poor fracture connectivity with few open fractures for fast groundwater movement. The higher TDS values can the result of a result of matrix flow being the predominant flow process (see next section).

From the $\delta^{18}O$ versus TDS plot (Figures 4-10 and 4-11) it is possible to distinguish between groundwater originating from different aquifers, including the different TMG Aquifers. Although no direct relationship between $\delta^{18}O$ and TDS exists, combination of the information obtained independently from $\delta^{18}O$ and TDS is significant. The $\delta^{18}O$-signature provides information on the recharge area (altitude at which recharge was intercepted), whereas TDS provides information on dissolution processes in the aquifer, flow process and path. The Klein Karoo TMG groundwater typically cluster around $\delta^{18}O$ and TDS values between –6 to –8 ‰ and 0 to 400 mg/l, respectively (Figure 4-10).

FIGURE 4-10: SCATTER PLOT OF $\delta^{18}O$ VERSUS TDS

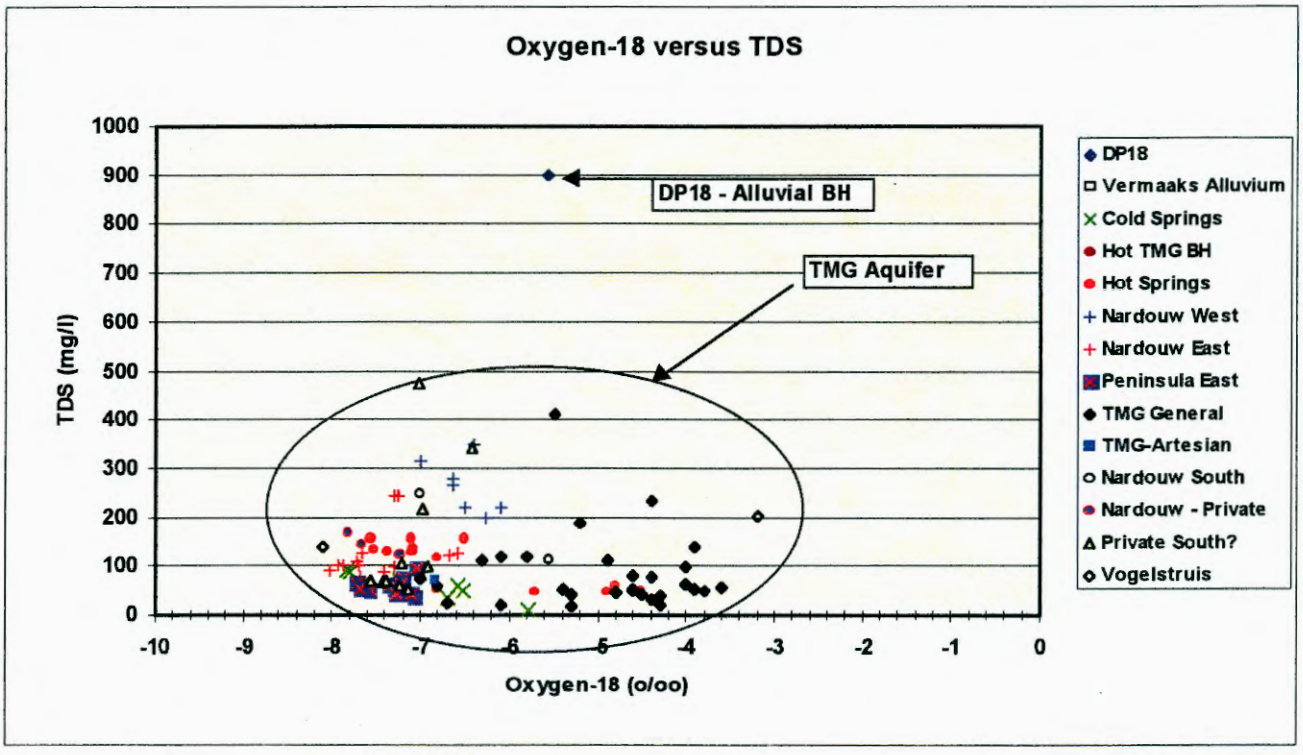

Note that the TMG General samples represents seepage samples and are more enriched than other TMG samples.

FIGURE 4-11: SCATTER PLOT OF $\delta^{18}O$ VERSUS TDS (ZOOM IN)

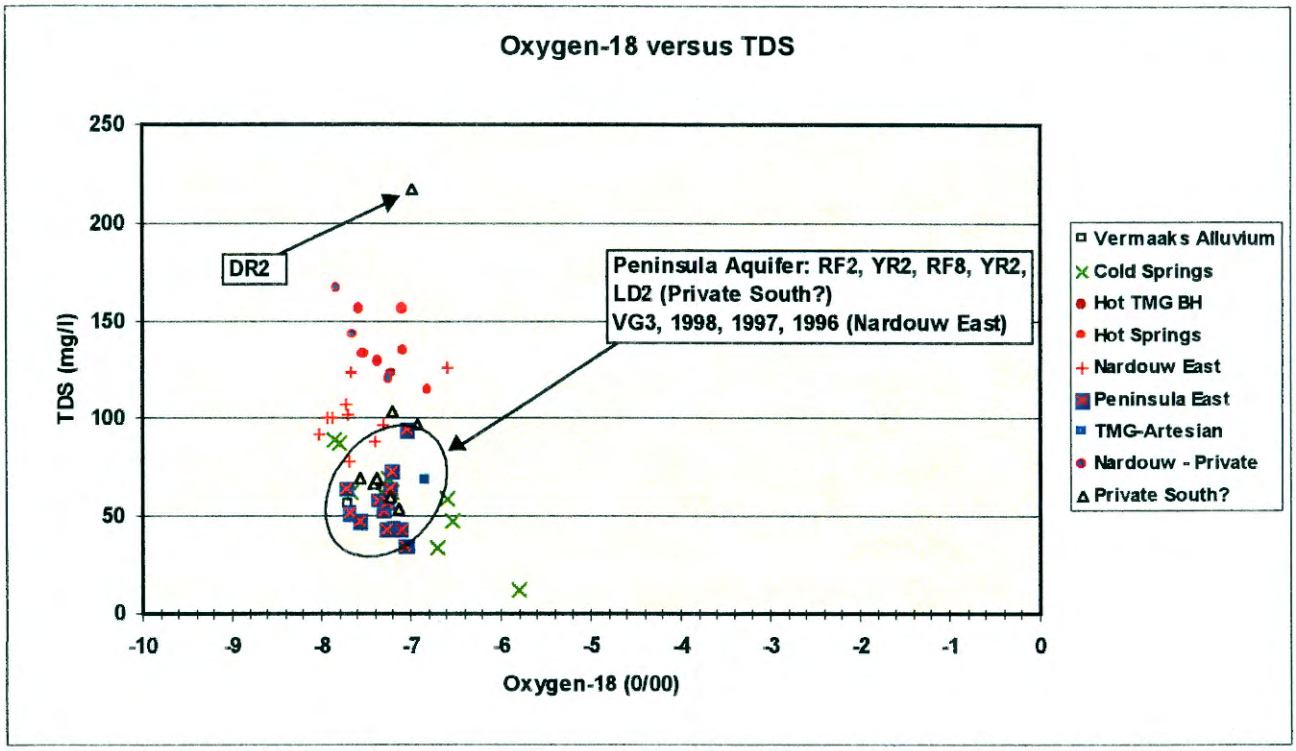

From Figure 4-10, DP18 (Alluvial Aquifer) plots significantly different from TMG Aquifers, eg. more enriched $\delta^{18}O$ signature (-5.6 ‰) and a higher TDS value of 900 mg/l. Further TDS values (in the TMG Aquifer) increase progressively from the Peninsula to Nardouw Aquifers (Figure 4-11). The highest values are associated with the hot springs suggesting that TDS values increase proportional to travel time along flow path (similar for $\delta^{18}O$ and EC, Figures 15 and 16, Appendix G). A similar $\delta^{18}O$ - signature, different TDS-value therefore represents groundwater with the similar recharge altitude, but different flow path. The increase in TDS values is also proportional to the development of alkalinity along the flow path. Figure 4-12 shows how alkalinity increases proportional to mean residence time of groundwater in the TMG Aquifer. This explains the dissolution chemistry of groundwater in the Nardouw Aquifer and Hot Springs far from recharge areas in that the TDS increases proportional to an increase in alkalinity over time.

From Figure 4-12 it is observed that groundwater of most Nardouw East boreholes (production boreholes of the KKRWSS drilled in the Nardouw Aquifer, Kammanassie Mountains, pMC $\leq$ 10 and HCO_3^- < 10 mg/l. The above-mentioned observation indicates that groundwater is locally recharged and aged on the spot. It does therefore not form part of the regional flow system.

Figures 4-11 and 4-12 shows that the $\delta^{18}O$ versus TDS and alkalinity versus ^{14}C relationships for groundwater in Nardouw Aquifer (southern flanks of the Kammanassie Mountains) are almost identical to that of the Peninsula Aquifer. (Indicated as Peninsula East boreholes on Figures 4-11 and 4-12, including boreholes RF2, YR2, RF8, and LD2 on the farms Rolbaken, Ylandsfontein, Koutie and Leeublad, respectively). Remote sensing (Figure 4-1), and geology (Figure 2-5) indicate that although all the above-mentioned boreholes are drilled in the Nardouw Aquifer, it forms part of the highly permeable zone in the Vermaaks 'Keystone Block' (see Figure 3-19). The boreholes in the 'Keystone Block' are therefore in hydraulic connection with the recharge area (Peninsula Aquifer) via a network of inter-connected fractures. Similarly, the $\delta^{18}O$ signature points at recharge intercepted at the same altitude as that of the Peninsula Aquifer and similar TDS values and major ion chemistry suggests similar flow paths.

FIGURE 4-12: SCATTER PLOT OF HCO_3^- VERSUS ^{14}C

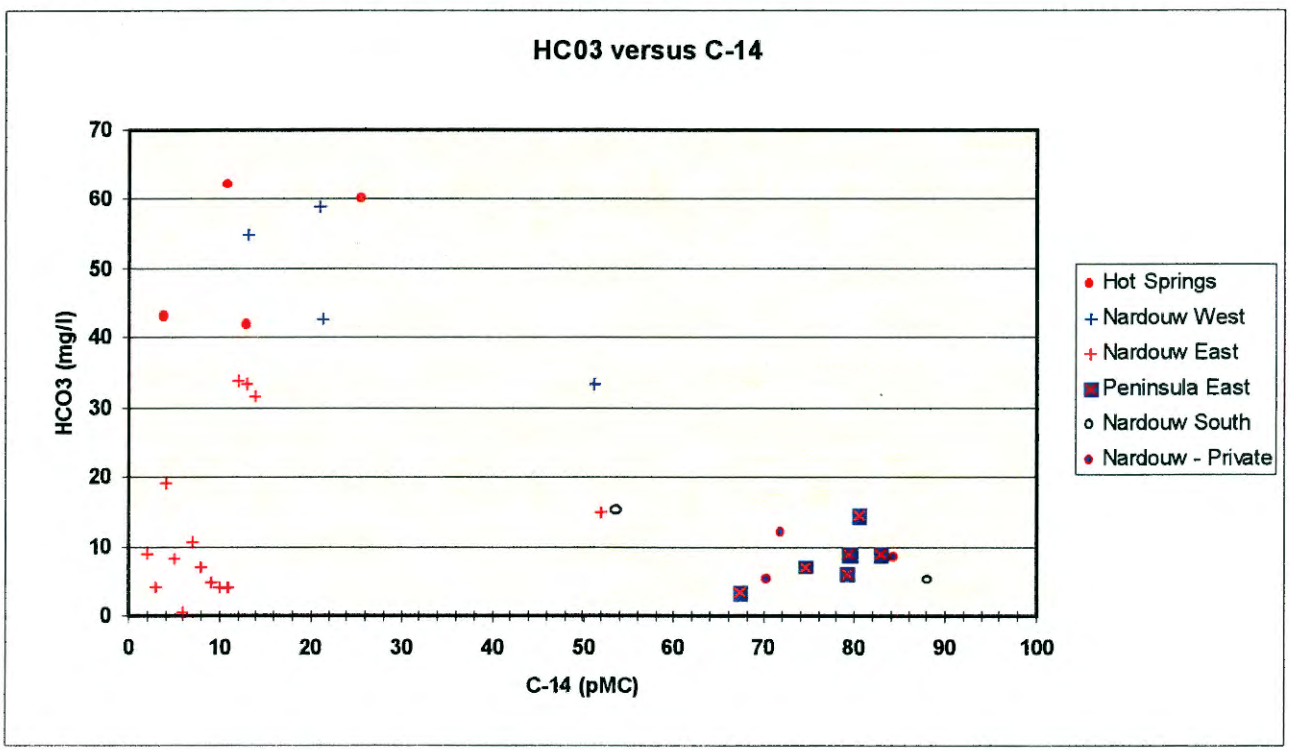

Figure 4-13 shows that ^{14}C values reduce from >70 pMC in the Peninsula and Nardouw Aquifer in the 'Keystone Block' (mean residence time ~1000 years) to >40 pMC (mean residence time ~10 000 years) in the Nardouw Aquifer elsewhere. The ^{14}C values reduce further to < 20 pMC (mean residence time >12 000 years) in the Western Nardouw Aquifer (Calitzdorp) and hot springs. All the samples fall within the same range for $\delta^{18}O$, indicating recharge at the same altitude, i.e. in the mountain catchments. Further, increasing TDS and ^{14}C as well as alkalinity indicate that groundwater follows complicated flow paths along

inter-connected fracture sets to great depths. Deep-seated fractures intercepting groundwater along its flow path allow groundwater to flow to the surface, leading to the presence of Hot Springs. Scatter plots of K^+, F^- and Cl^- versus SiO_2^- indicates that water originating from hot springs is a mixture of groundwater from the Bokkeveld, Nardouw and Peninsula Aquifers. The Toorwater Spa, produces groundwater from the Cango Group limestones, as indicated by its calcium carbonate chemistry.

FIGURE 4-13: SCATTER PLOT OF $\delta^{18}O$ VERSUS ^{14}C

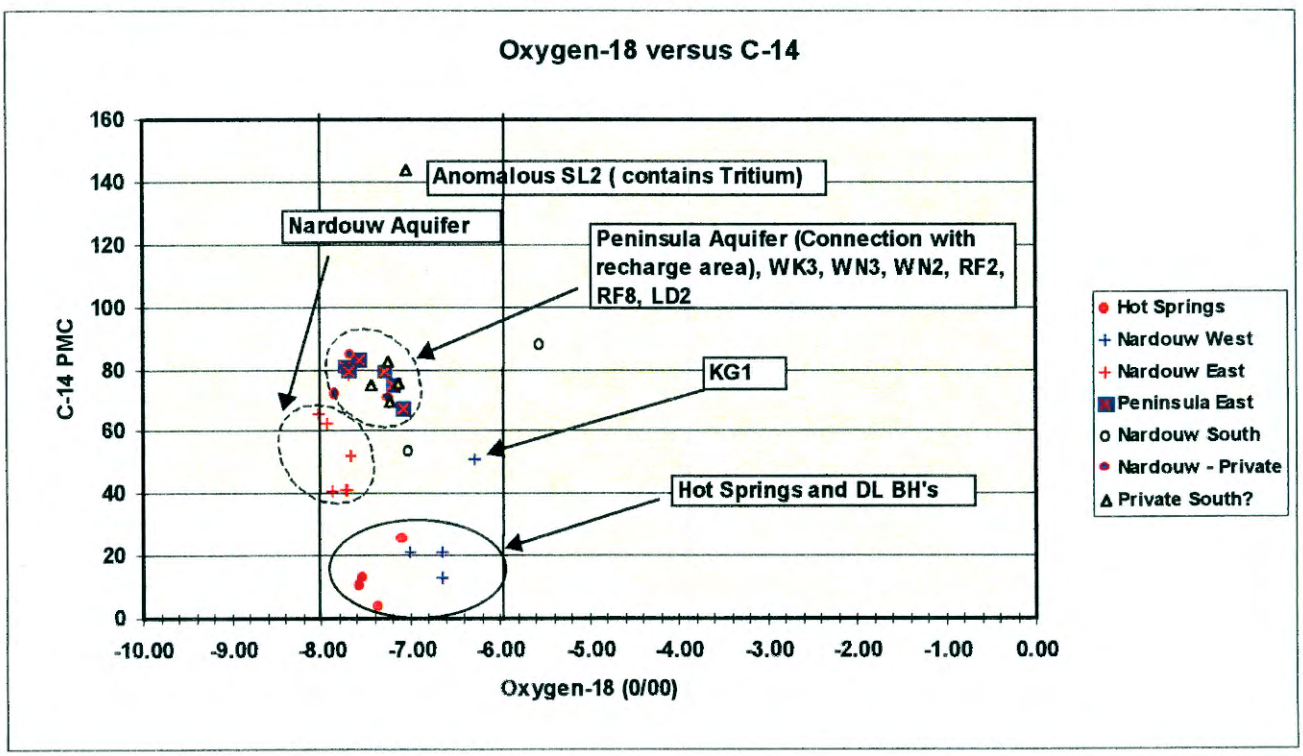

From Figure 4-13 it is possible to distinguish the following five different groups of groundwater:

- Groundwater originating from the Peninsula Aquifer (boreholes VR 6, 7, 8, 11).
- Three types of groundwater originating from the Nardouw Aquifer:
  - Those which are not in direct hydraulic connection with groundwater in the Bokkeveld or Peninsula Aquifers (most boreholes, other than the ones listed).
  - Those which are in hydraulic connection with groundwater in the Bokkeveld Aquifer (all DL boreholes and WK4, WN2, WN3, SL2 and DR2).
  - Those which are in hydraulic connection with the Peninsula Aquifer, along permeable zones (LD2, RF2, RF8 and YR2, on the farms Rolbaken, Ylandsfontein,

Koutie and Leeublad, respectively). The fingerprint of groundwater in the Peninsula and Nardouw Aquifers in the Keystone Block areas is essentially the same. The above indicates that although all the above-mentioned boreholes are drilled in the Nardouw Aquifer, they tap the highly permeable zone in the Vermaaks 'Keystone Block' (see Figure 3-10). The boreholes in the 'Keystone Block' are therefore in hydraulic connection with the recharge area (Peninsula Aquifer) via a network of inter-connected fractures. Similarly, the $\delta^{18}O$ signature indicates at recharge intercepted at the same altitude as that of the Peninsula Aquifer.

- Groundwater originating from the Bokkeveld Aquifer (borehole G40177), see X-Y scatter plots Appendix G.

- Groundwater originating from the Olifants River Alluvial Aquifer (DP18), see X-Y scatter plots Appendix G.

The following observations are made from scatter plots in terms of dissolution processes in TMG Aquifers:

- The $\delta^{18}O$ versus the Na^{+}/ Ca^{2+} scatter plot is useful for deductions on the groundwater flow path in feldspar rocks (Figures 19 and 20, Appendix G). Generally the Na^{+}/ Ca^{2+} ratio increases with increasing feldspar dissolution or distance away from recharge area. The 'Keystone Block' boreholes and the cold springs have the highest Na^{+}/ Ca^{2+} ratio, indicative of feldspar dissolution along its flow path.

- The Cl^{-}/ SO_4^{2-}: versus Na^{+}/ Ca^{2+} scatter plot (Figures 23 and 24, Appendix G) indicates two major groups of water. In the first group simple dissolution of feldspars takes place (most boreholes are included in this group). And a second group where other processes, such iron precipitation and biofouling takes place (also pMC $\leq$ 10 and HCO_3^{-} < 10 mg/l, see Figure 4-12, indicative of locally aged recharge). In the case of the last mentioned group, clogging of borehole screens is expected, resulting from bacteriological activity and a change in redox conditions, resulting from pumping. Boreholes DP15, DP28 (Bokkraal wellfield) and WN2, 3 (Nardouw Aquifer outside the 'Keystone Block') are included in this group. Drilling results around the Bokkraal wellfield indicate the presence of several quartz veins with pyrite, and the interception of 'reducing water', with a strong smell is also frequently reported in drilling records. Dissolved oxygen measurements have also indicated that natural reducing conditions prevail in these boreholes. Pumping of these boreholes introduces oxygen and iron oxidizing bacteria become actively involved, resulting in sulphide oxidation to sulphate, lowering in pH and oxidation of Fe^{2+} to Fe^{3+}.

4.4.4 Multi-component cluster analysis

Multivariate statistical analysis has been successfully applied by Adar *et al.* (1992) to conceptualise and quantify flow relationships together with a mathematical model for the southern Arava Valley (Israel). The above-mentioned study, together with many other similar studies have proved that multivariate principal component and cluster analysis of hydrochemical and environmental isotope data can provide valuable information when applied together with other borehole, aquifer and hydrogeological data.
To evaluate the significance of multivariate statistics, a cluster analysis statistics was carried out on the Klein Karoo, hydrochemical and environmental isotope data, using single and complete linkage with the Euclidian distances method. The results are in Appendix I, and are applied to qualify the hydraulic connection between aquifers and / or different parts of aquifers, based on the clustering of data.

The first two cluster analyses, (Figure 1 and 2, Appendix I) all the Klein Karoo local study area data was used. The only difference between Cluster analysis 1a, b and c and the rest of the analyses is that single linkage between individual borehole analysis is used in the first three analyses and complete linkage in the latter. The results of cluster analyses 1 and 2 are extremely cluttered, however DP18 (alluvial borehole) and G40178 (drilled into Bokkeveld) are significantly different from the rest of the data. Subsequently DP18 and G40178 are excluded (Cluster analysis 1b and 4, Figures 3 and 6, Appendix I) together with all non-Klein Karoo Hot Springs (Cluster analysis 1c, 4, Figures 4 and 6, Appendix I).

Three more cluster analyses were carried out only including borehole information from the Eastern Sector (Cluster analysis 5, Figure 7, Appendix I); the Kammanassie Mountains (Cluster analysis 6, Figure 8, Appendix I) and the Western Sector (Cluster analysis 7, Figure 9, Appendix I).

The following conclusions follow from Cluster analysis 1 to 1c using single linkage, Figures 1, 3 and 4, Appendix I):

- The 'Keystone Block' boreholes (Peninsula and Nardouw Aquifers) group together. Boreholes in the 'Keystone Block' are directly connected to part of the Nardouw Aquifer down-stream of the C/S, outside of the 'Keystone Block' (VG3, DG110, DP25, YR2, WK3, WK4 and the Marnewicks v-notch) and elsewhere.
- DP29, 28 and 15 are directly connected to the Klein Karoo hot springs, which are connected to the Nardouw, Peninsula Aquifers and 'Keystone Block'.
- WN2 and WN3 are connected with the rest of the Nardouw Aquifer, but group separately.

- The Western KKRWSS production boreholes, of the Western Nardouw Aquifer, group separate from the rest of the Nardouw Aquifers.
- SL2 and DL13 group separate from all data.

Although different groundwater types (clusters) can be distinguished from the single linkage cluster analysis, much better results were obtained with complete linkage (Cluster Analysis 4, Figure 6, Appendix I, Figure 4-14, over page). Immediately two groups of groundwater are distinguished, i.e. group A and B (Figure 4-14). Group A contains only boreholes sited in the Nardouw Aquifer. However, Group B also contains boreholes sited in the Nardouw Aquifer. The fact that both Group A and B include boreholes sited in the Nardouw Aquifer suggest that aquifer classification should rather be based on groundwater flow paths (connecting recharge area and abstraction areas), than aquifer lithology. Group A mostly includes the Western KKRWSS production boreholes, borehole SBH1 (Nardouw Aquifer, Outeniqua mountains) SL2 and DR2, two shallow production boreholes sited on local structures (see Figure 4-1) on the southern flanks of the Kammanassie Mountains.

FIGURE 4-14: CLUSTER ANALYSIS SHOWING GROUNDWATER TYPES – KLEIN KAROO TMG AQUIFERS

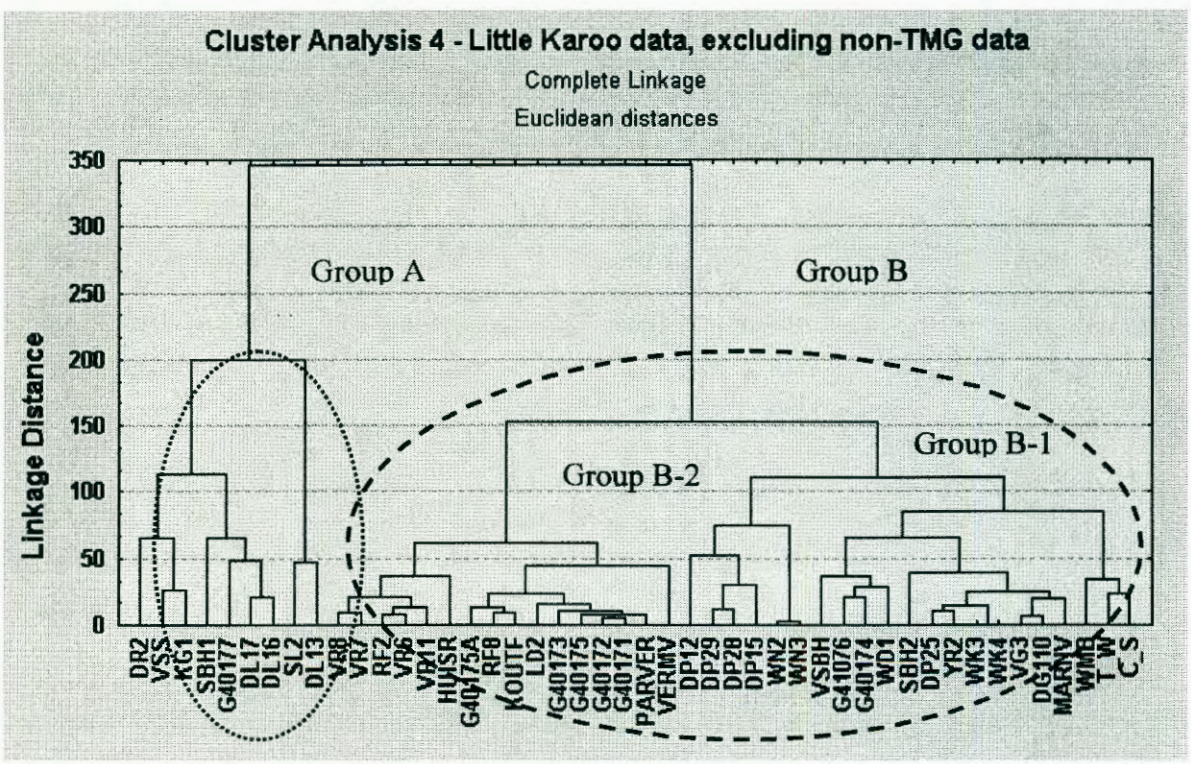

Group B can be subdivided into two broad groups, i.e. subgroup B-1 and B-2. Subgroup B-1 is a combination of boreholes of the Peninsula Aquifer and the other 'Keystone Block' and is

defined as the boreholes connected to the recharge area via an interconnected network of fractures. Subgroup B-2 comprises groups of boreholes sited in the Nardouw Aquifer and is defined as boreholes situated far from the main recharge area. Although no direct inter-connection with the recharge area exists, it still receives indirectly recharge from the main recharge area, via a probably complicated flow path.

The complete linkage between boreholes sited on the Kammanassie Mountains area is shown on cluster analysis 6 and 7 (Figures 7 and 8, Appendix I). The above suggests the following groundwater flow path based on linkage between different clusters: Groundwater travels from the Peninsula Aquifer (recharge area) to the 'Keystone Block' and Nardouw Aquifers, via an interconnected fracture network. Groundwater, which is not replenished in the Nardouw Aquifer travel further until it is intercepted, is a regional structure, returning it to the surface in the form of hot springs.

Cluster analysis 7 (Figure 9, Appendix I) shows only the Western TMG Nardouw Aquifer and the nature of interconnection. WD1 represents a borehole near the Calitzdorp Spa with a groundwater temperature of 39 ° C.

It is significant to note that all the results of the cluster analyses carried out are in line with the findings of all the other hydrochemical interpretations so far. Cluster analyses is therefore a very useful tool, provided that environmental isotope and hydrochemical data are used, to delineate groundwater flow systems.

4.4.5 Variation in chemistry and environmental isotope composition with depth

Comparison of the groundwater samples taken during drilling of the additional monitoring boreholes indicates the following (see results in Tables A-10 to 12, Appendix A):

- In borehole G40175A EC and pH decrease with depth, while the Mn concentration increases three fold from 60 to 84 m, which coincides with a fracture zone in shale with iron stained quartz veins. Over the same interval the SO_4 concentration increases from 9.8 to 12.1 mg/l and $\delta^{18}O$-signature becomes marginally more depleted (–7.0 ‰ (51 m) to –7.2 ‰ (60 m)). From 60 m deeper the $\delta^{18}O$-signature becomes less depleted (–7.0 ‰ at 126 m). Alkalinity reduces steadily from 27 to 8.7 mg/l over a depth range of 51 to 126 m. Take note that a sample taken after borehole completion has the lightest $\delta^{18}O$-signature, i.e. –7.2 ‰.

- In G40176 at 42 m depth Mn contents are very high (0.502 mg/l), which coincides with a possible water strike, in an iron-stained fracture within a shale layer. Further EC (14.2 to 19) and most major cations increase with depth and $\delta^{18}O$ signatures become marginally less depleted (–7.5 ‰ (42 m) to –7.3 ‰ (150 m)).

- From Tables A-10 to 12 (Appendix A) note the difference in composition of samples selected at specific depths during drilling and samples collected after borehole completion. In the latter sample, an average composition for the well is obtained, with an EC of 13.5 mS/m and $\delta^{18}O$ of –7.4 ‰.

- Comparison of $\delta^{18}O$-signatures of G40171 to 3 shows that the top layer of alluvial water are the lightest (-7.7 ‰, G40173) versus the upper part of the Peninsula Aquifer (-7.3‰, in G40171). The bottom alluvial layer has an $\delta^{18}O$ value marginally less than G40171 (–7.2 ‰). The above observation shows that the alluvial aquifer is recharged from below by baseflow, or groundwater stored in the matrix fractures of the TMG Aquifer, which was recharged in the higher altitudes. Mn and Fe contents decrease from 0.157 and 0.25 mg/l respectively in G40173 to Mn below detection limit and Fe of 0.25 mg/l in G40174.

- EC and TDS values increase with depth in G40178 from 109.9 to 155 mS/m and 641 to 1084 mg/l, respectively between 54 and 120 m. The borehole log indicates plenty of quartz veins with pyrite and shale layers. The high values for TDS and EC suggest that the borehole does not intercept the Nardouw Aquifer, but rather samples the Bokkeveld shale. Mn contents are very high and range from 3.4 to 7.2 mg/l (from 54 to 120 m). $\delta^{18}O$ data show that groundwater becomes more depleted with depth, i.e. –7.0 to –7.3 ‰, indicating that the Bokkeveld shale is connected to the recharge areas in the higher altitudes by fractures. This is most probably established by leakage of groundwater from the Nardouw to Bokkeveld Aquifers.

Although the above results are very preliminary, sampling of groundwater for environmental isotope analysis and EC as drilling progresses has been proven to be a valuable source of information.

4.5 TEST FOR THE WORKING HYPOTHESIS

The smallest scale of fractures of the order of tens of metres deep (those striking NW-SE, N-S and NE-SW) corresponds with mechanical failure of rocks near the surface. These fractures facilitate the infiltration of water to shallow depths, leading to the formation of seasonal seepage in mountain ranges at perched water tables during the winter months.

The intermediate scale fractures are related to structural failures along major fault-lines, resulting from folding during the CFB orogenesis, or keystone faulting (Vermaaks River Valley) or later extensional fault movements. These faults penetrate to depths of several hundreds of metres and are restricted to mountain catchments. The largest scale (regional) fractures are associated with deep-seated tectonic movements in the earth's crust, allowing groundwater to circulate towards the surface under artesian pressure from great depths leading to the formation of hot springs. This 'large volume of groundwater' refers to the excess amount of recharged groundwater not flowing out as cold springs or being abstracted. The intermediate and regional groundwater flow paths are also visualised as inter-connected fracture sets along folded bedding planes on catchment and geological basin scales, respectively.

Mazor and Verhagen (1983) investigated the dissolved ions, stable- and radioactive isotopes together with noble gas concentrations in the thermal water of South Africa. Their study included several TMG hot springs, e.g. Calitzdorp Spa, Warmwaterberg, The Baths and others. The dissolved noble gas concentrations, i.e. He, Ne, Ar, Kr and Xe in water samples taken from Klein Karoo hot springs, show abundances similar to that of air saturated water (atmospheric temperatures ranging between 17 and 40 °C). The above favours a meteoric origin of groundwater emanating from TMG hot springs (deep circulation of groundwater) and over-rules any volcanic or magmatic origin. Rainwater infiltrates at air temperatures ranging between 17 and 40 °C and circulates to great depths to reach the high temperatures associated with hot spring water, e.g. 38 to 49°C.

The isotopic signatures of all the hot springs in the Western Cape (regional groundwater flow system), and existing deep boreholes (mixture of intermediate and shallow flow systems) were obtained during various sampling runs. Secondly, seepages emerging in the mountains were sampled along sections through the mountain passes from the coast to the Great Karoo (see Figure 2.3 for the sampling localities). The purpose of seepage sampling was to determine the $\delta^{18}O$ signature of water recharged at a certain altitude. Figure 4-15 (over page) represents the results of these environmental isotope cross-sections through the Cape Mountains, along mountain passes. The results on Figure 4-19 confirm the altitude effect, i.e. progressive depletion of $\delta^{18}O$ in rainfall with increase in the altitude.

Figures 4-16 and 4-17 show the depleted $\delta^{18}O$ signature of the hot springs and deep boreholes, suggesting that water was recharged at a much higher altitude than the elevation of the point of issue of these hot springs. The long flow path required is further confirmed by the low ^{14}C values of the hot springs, ranging between 3.9 and 25.6 pMC, indicative of mean residence times of the order of tens of thousands of years.

FIGURE 4-15: ENVIRONMENTAL ISOTOPE FINGERPRINTING – TOPOGRAPHIC SECTIONS WITH $\delta^{18}O$ VALUES

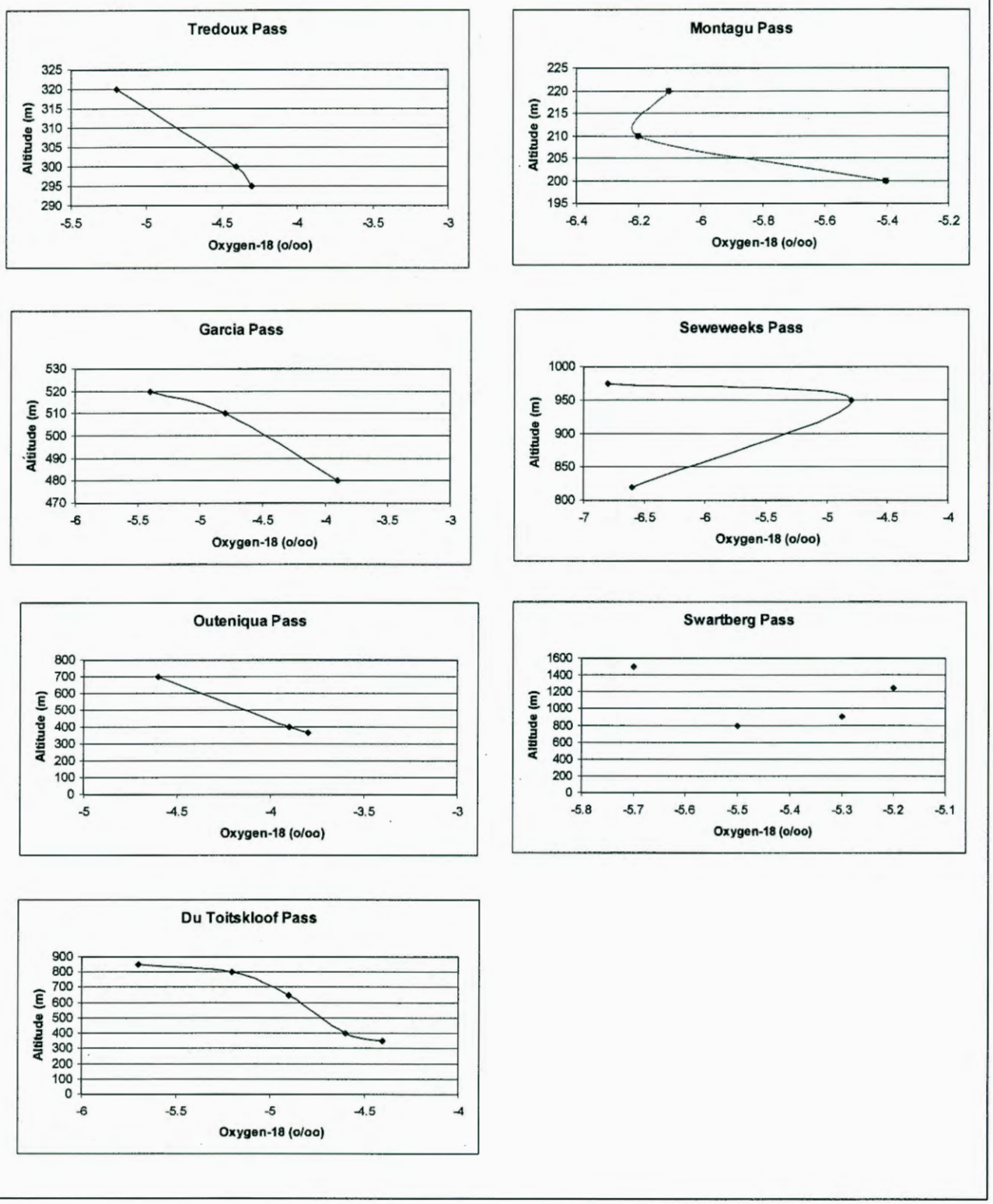

FIGURE 4-16: COMPOSITE DIAGRAM SHOWING FINGERPRINT OF HOT SPRINGS

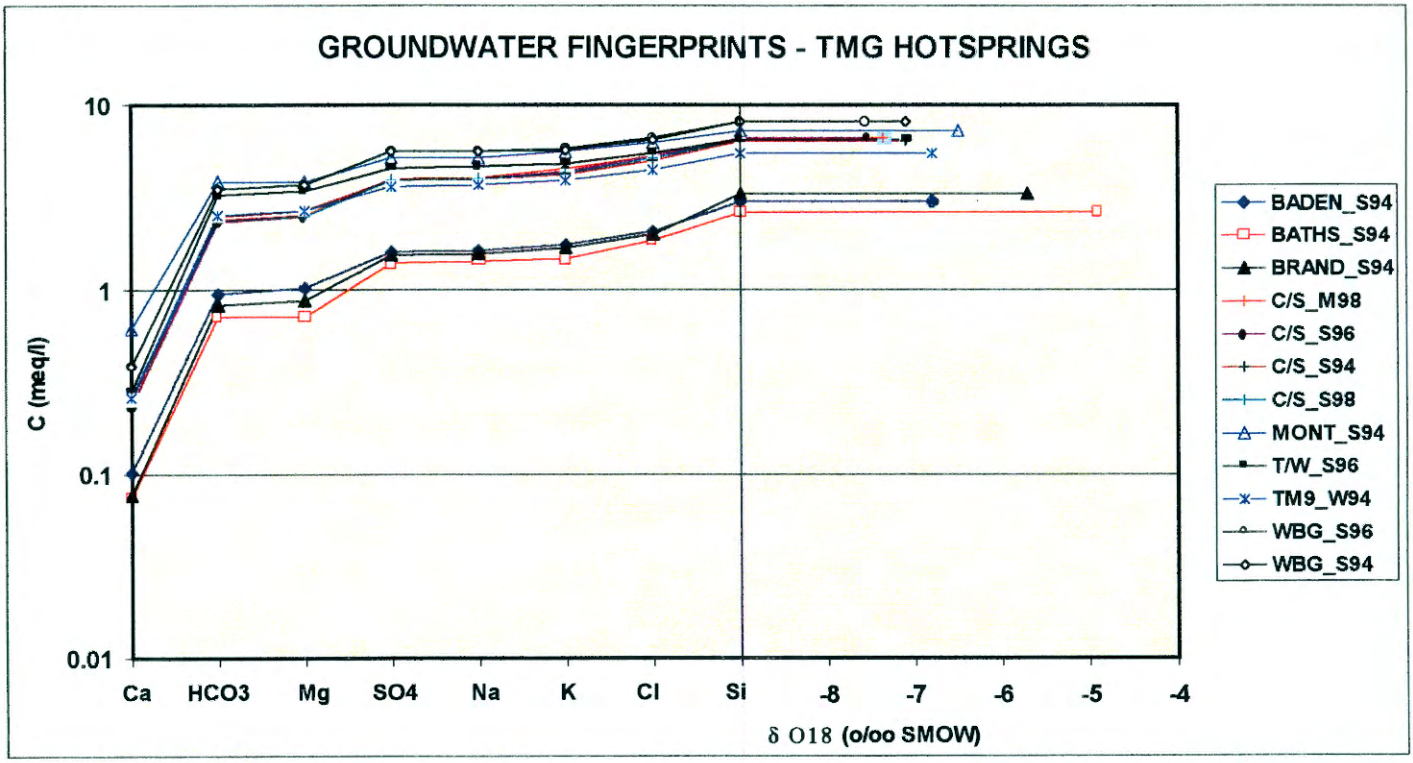

FIGURE 4-17: COMPOSITE DIAGRAM SHOWING FINGERPRINT OF DEEP BOREHOLES IN THE TMG

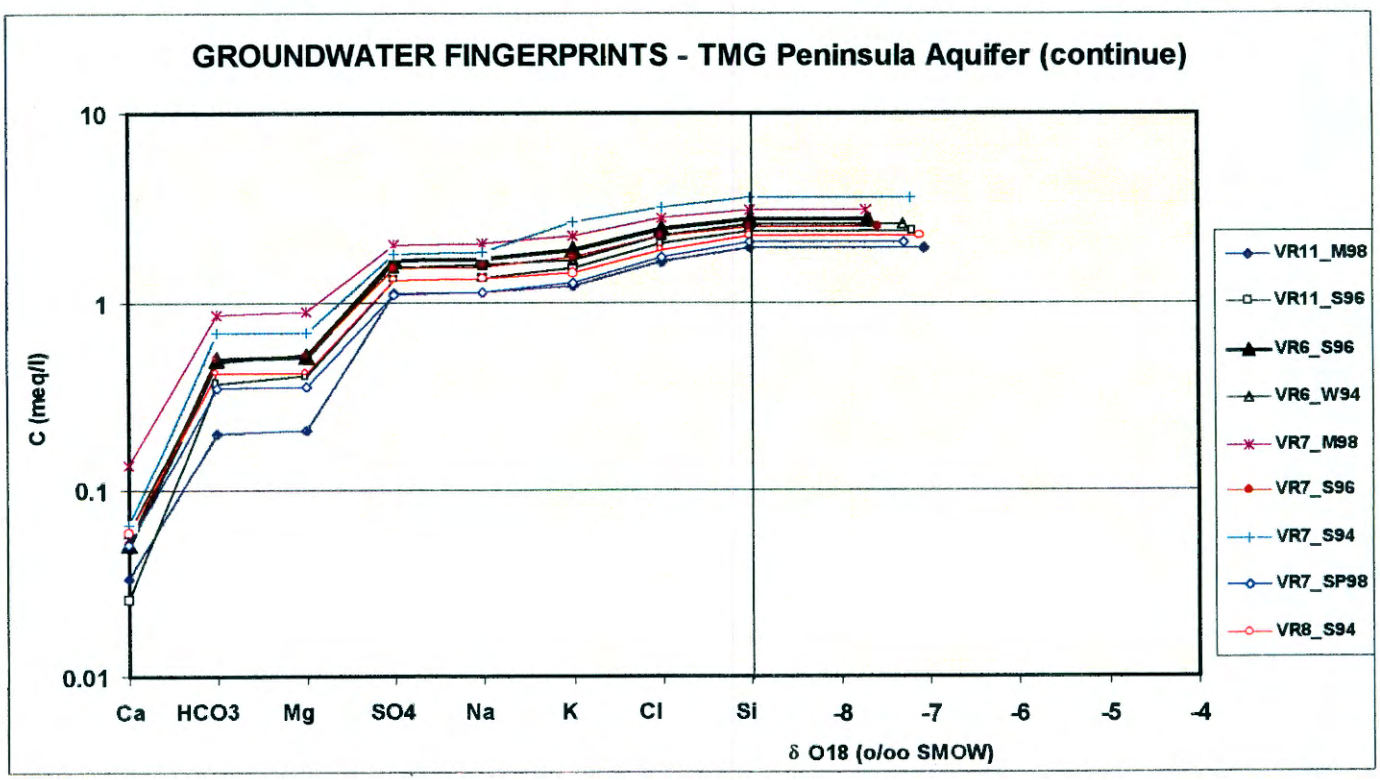

Figure 4-17 also shows the similar 'finger prints' of the hot spring and deep borehole groundwater. The Brandvlei, Baden and Baths (situated near Worcester and Citrusdal, respectively) have 'fingerprints' which differ significantly from the Klein Karoo hot springs due to different recharge histories. The geological interpretation showed that hot springs are situated on localised fractures, occurring at depth, tapping groundwater from a regional flow path.

The $\delta^{18}O$ and ^{14}C signatures of hot springs vary with intake history, degree of interconnection between fracture sets, TMG lithologies, proximity of the hot spring to the recharge area, and / or rainfall origin (rain originating from the Atlantic Ocean).

Comparison of the $\delta^{18}O$ and $\delta^{2}H$ signatures of the hot springs and mountain seepages (Appendix H, Figures 4, 19), confirms that the recharge areas of groundwater emanating at hot springs are at the higher altitudes of the mountain ranges, which confirmed the existence of a regional flow system.

4.6 SUMMARY

Groundwater in the Peninsula Aquifer is characterised by its low mineralisation (TDS < 300 mg/l), low pH (< 6) and very low TAL (<< 0.5 meq/l). The Klein Karoo TMG groundwaters have $\delta^{18}O$ ranging between –6 to –8 ‰ and TDS values < 400 mg/l, respectively.

From the Piper plot, TMG groundwater is classified as a Na/Cl type water, as all other ions are present at very low concentrations. The major ion chemistry of TMG groundwater is not balanced, in that the low alkalinity and pH of the groundwater leads to the conclusion that free CO_2 is present, which needs to be balanced by the dissolution of Mg^{2+} and Ca^{2+}.

In general, all trilinear diagrams, except Schoeller, have the disadvantage that they do not portray the actual ion concentration and that most TMG data clusters together in one area. It is therefore not possible to differentiate between the different TMG Aquifers, i.e. Nardouw and Peninsula Aquifers, on tri-linear diagrams. The distribution of ions within the main field is unsystematic in terms of hydrochemical processes so that the diagram lacks certain logic. The Piper Diagram is, however, a very useful diagram to differentiate between groundwater from the TMG Aquifers and other aquifers, i.e. alluvial or limestone. Further, the low alkalinity and pH of TMG groundwater complicates interpretation of TMG dissolution chemistry. X-Y scatter plots of the following ion pairs and / or environmental isotopes $\delta^{18}O$ and TDS, SO_4^{2-} : Cl^- , HCO_3^- : Cl^- , HCO_3^- versus $\delta^{14}C$ and Na^+: Cl^- and Ca^{2+}: HCO_3^- +

SO_4^{2-} ; Ca^{2+}: Mg^{2+} and Ca^{2+}: $Na^+ + K^+$ ratios are very useful to distinguish groundwater types and dissolution processes. Composite diagrams and multivariate cluster analyses are also useful to characterise the groundwater flow system. Environmental isotopes and hydrochemistry prove to be very important tools in conjunction with hydrogeological and remote sensing data in conceptualisation of the groundwater flow system. With the aid of the above-mentioned data analysis techniques the following different aquifers are distinguished:

- Peninsula Aquifer.
- Three types of Nardouw Aquifers:
  - With no direct hydraulic connection with Bokkeveld or Peninsula Aquifers.
  - In hydraulic connection with Bokkeveld Aquifer.
  - In hydraulic connection with the Peninsula Aquifer, along permeable zones.
- Bokkeveld Aquifer.
- Olifants River Alluvial Aquifer.

It is recommended that further trace element sampling is carried out. In particular, the dissolution of feldspars and associated trace elements, i.e. Ba, Sr and Al needs to be investigated further. The presence of Ni, Cu, Co and Zn is indicative of the presence of pyrite quartz veining, which is always present in boreholes where biofouling and clogging of borehole screens prevails. The low EC and TDS values of groundwater in the TMG Aquifers makes trace elements an important tool in understanding the dissolution chemistry and flow paths of groundwater in the TMG Aquifers. Trace element chemistry may also provide valuable insights into the exploitation potential of TMG Aquifers, in terms of providing information on the permeability (feldspar dissolution) and the presence of pyrite quartz veining (potential for iron-reducing bacteriological clogging of boreholes).

Comparison of the ^{18}O and ^{2}H signatures of the hot springs and mountain seepages confirmed the working hypothesis, i.e. that the recharge areas of groundwater emanating at hot springs are the higher altitudes of the mountain ranges, which confirms the existence of a regional flow system. The ^{18}O and ^{14}C signatures of hot springs vary with intake history, degree of interconnection between fracture sets, TMG lithologies, proximity of the hot spring to the recharge area, and / or rainfall origin.

CHAPTER 5: CONCEPTUAL HYDROGEOLOGICAL MODEL – TMG SUPER AQUIFER KLEIN KAROO SECTION

In this Chapter the individual interpretation from remote sensing, structural, hydrochemistry and hydrogeological data are collated to define the conceptual hydrogeological model for the Klein Karoo Section of the TMG Aquifer.

5.1 AQUIFER DELINEATION

Classical or conventional aquifer delineation, generally includes the following:

- Definition of hydrostratigraphic units, which involves the collation of the following geologic information: geological maps, cross-sections, borehole logs and borings with information of hydrogeologic properties.
- Quantification of the hydrogeological characteristics of each unit, i.e. porosity, permeability, storage and recharge.
- Determination of the hydrogeological inter-connection between different units, if any.

This results in the classification of subsurface layers or zones either as aquitards, aquicludes or aquifers, depending on their water bearing characteristics. Aquifers are further subdivided into confined, unconfined and leaky (semi-confined) aquifers, depending on the nature of bounding layers.

It is generally assumed that hydrostratigraphic boundaries coincide with those of the lithostratigraphic units of a geological sequence. However, the presence of structures such as fractures and faults complicates aquifer definition and may introduce some ambiguities into the hydrostratigraphical classification. For example, where a highly fractured and thus sufficiently permeable fault zone has a sufficiently large stratigraphic throw, it may juxtapose and thus create a leakage junction between two otherwise separate aquifers. A fault could also connect two distinctly different aquifers, previously separated by an aquitard.

Therefore, conventional aquifer delineation does not take high permeability fracture zones cross-cutting several hydrostratigraphic units into account. Neither does it take the hydrogeological characteristics of discrete fracture sets as opposed to the hydrogeological properties of the rock matrix, with the rock being fractured on either regional or local scales, into account. Further, fracturing and faulting can also connect various aquifers and aquitards,

within a geological sequence (eg. Super Group) over a large area, which together constitute a so-called Super Aquifer (Al-Aswat and Al-Bassam, 1997).

In this report, conventional aquifer delineation is adjusted to include aquizones, which are definite structural zones (faults, master joints, even structurally controlled cave systems) of particularly high hydraulic conductivity. Aquizones can be contained within a larger, formally defined aquifer of generally lower permeability or as a limited permeable feature transecting an aquitard unit. Al-Aswad and Al-Bassam (1997) indicate that these may be informally named aquizones, outside of or apart from the formal hydrostratigraphic hierarchy. An example of such an Aquizone is the Keystone Block, shown in Figures 3-16 and 3-18. From this point onwards the area indicated on Figure 3-16 as the Keystone Block refers to the Keystone Block Aquizone.

All the hydrostratigraphic units constituting one stratigraphic sequence are referred to as a Super Aquifer. In this case, the TMG Super Aquifer will include the Nardouw and Peninsula Aquifers and the C/S Aquitard. The most important criteria for aquifer definition in the case of a regional fractured aquifer, such as the TMG Super Aquifer, therefore includes the following:

- Lithology
- Fracture characteristics, and
- Interflow relationships between the different aquifers, aquitards and aquizones within the Super Aquifer, connecting or disconnecting it with the recharge area(s).

Figure 5-1 (over page) shows the entire TMG Super Aquifer in the Western Cape, extending from Clanwilliam in the north-west to Port Elizabeth in the east. Folding and faulting styles vary considerably across the entire TMG outcrop in the Western Cape, based on different thickness of geological successions and its position in the CFB and associated tectonic regimes present in each section. This has not been studied extensively. However, comparison of the following important case studies, shows that significant differences in hydrogeologic characteristics exist in each different section of the TMG Super Aquifer in the Western and Eastern Cape:

- Western TMG Section (A in Figure 5-1), the CAGE study – Hartnady and Hay (2000).
- Hex River – Central TMG Section (B in Figure 5-2), Rosewarne (1984) and Kotze and Rosewarne (1999).
- Agter-Witzenberg and Ceres - Central TMG Section (B in Figure 5-1), Weaver *et al.* (1999).

FIGURE 5-1: REGIONAL EXTENT OF TMG SUPER-AQUIFER (ADAPTED FROM BRINK, 1981)

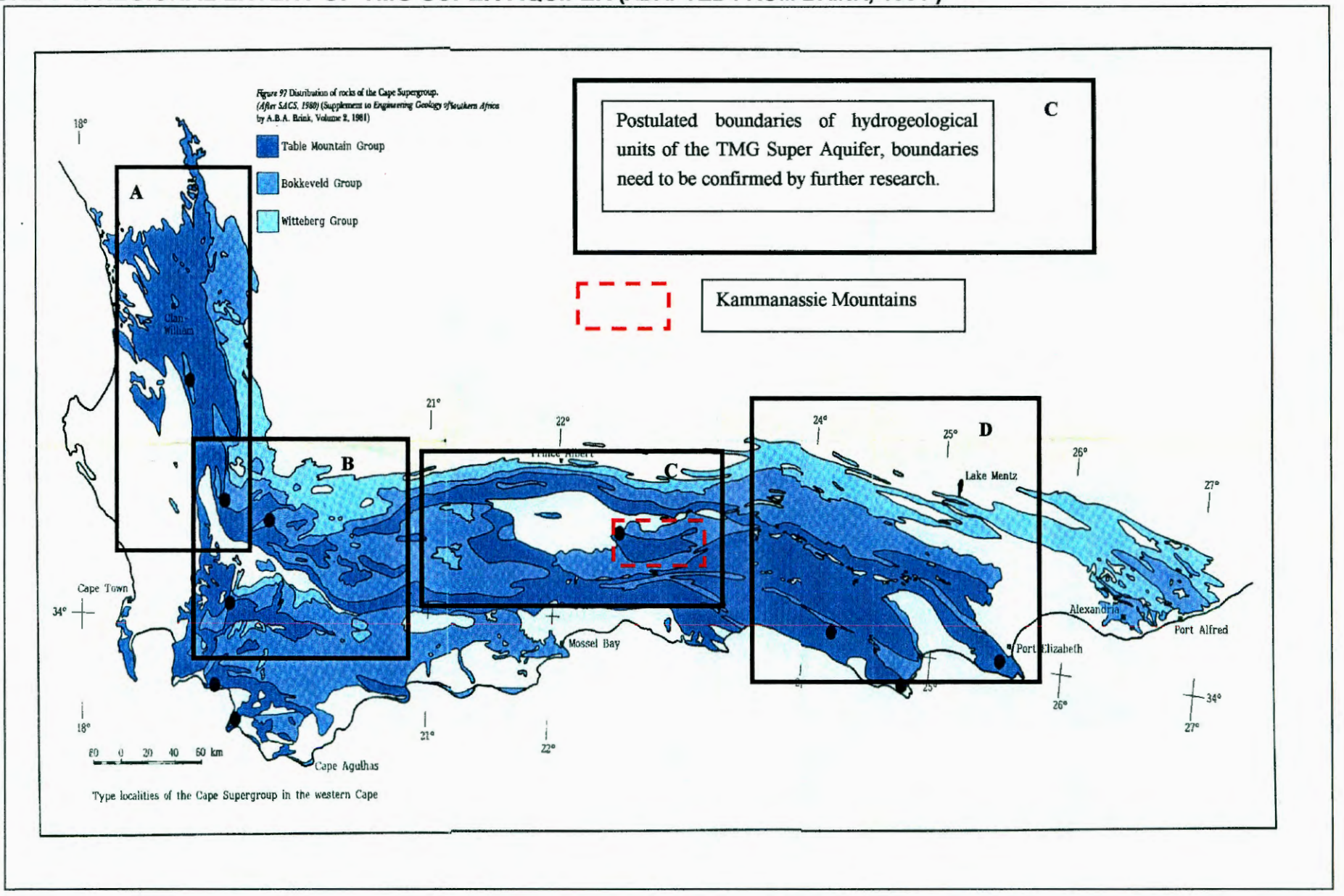

- TMG Aquifer in the Klein Karoo Section (C in Figure 5-1), this study.
- Eastern TMG Section (D in Figure 5-1), Murray (1996).

The above-mentioned case studies indicate that significant differences in: fracturing and faulting styles, lithologic sequences, recharge and natural discharge (springs) prevails in each section of the TMG Super Aquifer. As groundwater flow, quality and quantity are controlled by aquifer characteristics, each section of the TMG Aquifer will therefore have unique characteristics, differentiating it from other parts of the TMG Super Aquifer. In order to manage any section of the TMG Aquifer, a complete understanding of its connection with other parts of the TMG Super Aquifer is required. The different units (sections) of the TMG Super Aquifer must be further investigated in order to calculate the regional water balance, i.e. inflows and outflows to and from individual sections.

5.2 HYDROGEOLOGICAL CHARACTERISTICS OF THE TMG SUPER AQUIFER

The conceptual hydrogeological model for the Klein Karoo Section of the TMG Super Aquifer is formulated herewith covering the following aspects:

- Definition of hydrostratigraphic units
- Aquizones
- Groundwater flow regime and groundwater level distribution
- Types of springs occurring in the TMG Super Aquifer in the Klein Karoo
- Borehole yields.

5.2.1 Definition of hydrostratigraphic units

The following lithologic units constitute the three major hydrogeological units of the TMG Super Aquifer:

- Nardouw Aquifer: Baviaanskloof, Kouga and Tchando Formations
- Cedarberg Aquitard (C/S): the Cedarberg shale layer
- Peninsula Aquifer: the Peninsula Formation quartzites.

Each of the above-mentioned units has unique hydrogeological characteristics, based on its associated lithology, fracturing styles, proximity to recharge areas, etc. All these impact on the water bearing capacity, groundwater quality and yield of a particular unit.

The Peninsula Formation (Peninsula Aquifer) is a pure quartz arenite with a very low primary porosity due to the cementation of individual sand grains. Porosity has been further reduced by low-grade metamorphism associated with the second event of the CFB orogenesis. High temperatures of up to 350° C during the CFB orogenesis resulted in recrystallisation, which closed most of the available pore space. However, increased rock induration led to a higher potential for brittle fracturing during deformation, as well as higher fracture frequencies and thus secondary porosity.

The Nardouw Subgroup (Nardouw Aquifer) contains more silty / shaley interbeds and associated higher feldspar content. The thickness of impervious shale layers in the Kouga and Peninsula Formations varies by one order of magnitude of the stratigraphic thickness. Shale layers have a great impact on the fracturing and folding style of TMG Aquifers, which give rise to large variations in hydraulic conductivity. In general, an increase in shale layers leads to ductile deformation (folding) as opposed to brittle deformation (more fractures) with less shale layers. Clay resulting from the chemical weathering of feldspar can clog secondary groundwater flow paths (fractures) and reduce permeability further.

Field mapping indicates that groundwater movement in the form of seepages is present along most shale intercalations. Based on the increasing degree of iron staining along these contacts and the increasing degree of weathering towards the contact, groundwater movement along shaly contacts takes place, as orthogonal feeder fractures stop there. Permeability in the Nardouw rocks is further enhanced by bedding slip along shaly layers, forming listric thrusts along and obliquely crossing bedding planes.

Based on the width of open orthogonal joints, Hälbich *et al.* (1995) estimated the secondary porosity of bedding and joint fractures in the Kouga and Peninsula quartzites (Kammanassie Mountains) to be in the order of 1 %. In brecciated and fractured strata porosity is approximately, double that of folded strata, i.e. in the order of 2% and more. The secondary porosity of a massive fault block, i.e. the Vermaaks Keystone Block, is estimated to be in the order of 5 % Hälbich *et al.* (1995).

Secondary porosity along faults increases further by one or two factors (6 to 7%). Faults are mostly developed in groups of two to three along splays, connected by cross-cutting faults, connecting larger volumes of rock and thereby increasing groundwater storage and flow capacities, i.e. in the Vermaaks River Keystone Block.

The C/S is an aquitard, which may contain water, but does not transmit significant amounts, unless transected by a fault. This is confirmed by the difference in ^{14}C values up- and down-

stream thereof (see Section 4.1.3.2) and the origin of several springs in the lowest point of the profile, where fractures intersect the Peninsula - C/S contact.

High yielding aquifers in the TMG exist where fractures or faults are confined by aquitards, i.e. shale horizons such as the C/S Formation or the Bokkeveld Group. This gives rise to the so-called TMG window areas (see Figure 3-8).

The sandstones of the Bokkeveld Group in the Klein Karoo are very poor aquifers, as opposed to TMG and Bokkeveld Aquifers in the syntaxis area near Ceres (see B in Figure 5-1). High clay and feldspar contents and long distance from recharge areas, i.e. long residence times of groundwater in the aquifer, result in poorer groundwater quality. Although high yielding boreholes are present in the Bokkeveld Aquifer, groundwater quality is poor (> 500 mS/m) and generally unfit for human consumption.

Apart from regional faults, intense fracturing along fold axial planes also occurs. Where folded and fractured TMG sandstones are overlain by thick confining shale formations, e.g. the Gydo, Swartkrans, Tra-Tra and Adolphspoort Formations of the Bokkeveld Group (Figure 3-8), good targets for further exploitation results. Intersections between fold axial plane fractures and regional faults, overlain by confining shale, are excellent exploration targets.

5.2.2 Aquizones

The geological cross-sections and block-diagrams (Figures 3-14 to 3-17) show that the Peninsula and Nardouw Aquifers of the Kammanassie Mountains are separated by the C/S Aquitard, constituting a tight seal. However, a series of cross-cutting faults, such as the Leeublad, Rooikrans, Brillkloof and Vermaaks River Faults and many other similar faults (indicated on the LANDSAT lineament map, MAP 2, Folder in back of report) provide conduits of preferential flow. These conduits connect the Nardouw and Peninsula Aquifers, thereby enhancing recharge of the Nardouw Aquifer at lower altitudes, as indicated by hydrochemistry and environmental isotope data (see Section 4). This results in good quality groundwater occurring in the Nardouw Aquifer. The groundwater quality in the Nardouw and Peninsula Aquifers is therefore a function of both lithology, as well as the interconnection with the recharge area (primarily Peninsula Aquifer), established by crosscutting fractures.

An example of such an aquizone, consisting of high yielding, good quality groundwater across two hydrogeological units, is in the Keystone Block of the Kammanassie Mountains (see Figure 3-16). The recharge area (Peninsula Aquifer) and the Nardouw Aquifer are interconnected by a network of highly permeable fractures. The Vermaaks River Fault Zone

and the entire Keystone Block constitute an aquizone with hydraulic permeabilities up to three orders of magnitude higher than the surrounding rock mass. Porosity increases from 1% in the massive quartzite of the Nardouw and Peninsula Aquifers (absence of fracturing) to 7% along fractures, with an average porosity of 5% in the Keystone Block Aquizone.

In the absence of permeable aquizones, the hydrogeologic properties of the Nardouw and Peninsula Aquifers are significantly different. The Peninsula Aquifer usually outcrops at higher altitudes and therefore receives more recharge from rainfall and snow. Consequently, groundwater flow paths and residence times are shorter, providing good quality (low TDS) groundwater. These factors and lower the shale content of the Peninsula Aquifer give rise to a more dynamic flow system, resulting from higher recharge and more active flow circulation due to higher permeability. In contrast, the Nardouw Aquifer receives less direct recharge and groundwater has longer travel-times, resulting from leakage from the Peninsula Aquifer through the C/S. Longer travel-times and dissolution of weathered clay increases the TDS of groundwater from Nardouw Aquifers.

In summary, purely based on lithologic considerations the Peninsula Aquifer is the highest yielding TMG Aquifer with the best groundwater quality. The Peninsula Aquifers mostly coincide with the so-called TMG Window Areas (Kammanassie, Swartberg, Gamkaberg and Rooiberg Mountains) outcropping in the high altitudes of the mountain catchments (main recharge areas) and coincides with the DECAS conservation areas. High yielding boreholes with good groundwater quality are possible in the Nardouw Aquifer inside a permeable aquizone, i.e. Vermaaks Keystone Block, at lower altitudes.

5.2.3 Groundwater flow regime and water level distribution

Table 1 (Appendix E) summarises all water level data obtained from various hydrocensus surveys. The reliability of these results depends on the quality of information provided by the farm owners. Most privately owned boreholes generally have very sparse water level data and are equipped with pumps, which do not allow water level measurements (diameter of boreholes too small to allow lowering of a dip meter).

No boreholes are present in the Swartberg TMG (from hydrocensus) and most farmers utilise either surface or spring water. This is not surprising, considering the large amounts of 'surface water' feeding numerous small streams flowing down-gradient to the Olifants River. Most farmers still have servitude water rights dating back to the 1900's.

Only two boreholes were found in the Outeniqua Mountains with water level elevations varying between 525 and 535 mamsl. Most groundwater level and borehole information is

obtained from the Western and Eastern KKRWSS sectors. It is therefore difficult to assess the regional groundwater flow pattern due to the biased data set. Data are almost completely confined to the western portion of the Kammanassie Mountains and a section of TMG outcrop surrounding the Western Scheme section. However, from first principles, the groundwater elevation generally follows the topography. Therefore, existing groundwater elevation data and topographic elevations were used to complete the piezometric contour map (Figure 5-2) showing water level distribution around the Kammanassie Mountains.

Figure 5-3 represents a schematic section, postulating the regional groundwater flow directions for the TMG Aquifer in the Klein Karoo and Kammanassie Mountains. On a regional scale, the Cango Fault Zone (CFZ) is seen as an impermeable zone, based on the low yields of boreholes drilled into the fault and the geological cross-sections (Du Preez, 1965). The CFZ therefore constitutes a no-flow boundary and most groundwater recharged in the Swartberg Mountains is postulated to flow to the north, towards the Karoo rather than to the south (see cross-sections 3-9 and 3-10).

FIGURE 5-3: SCHEMATIC PRESENTATION OF CONCEPTUAL HYDROGEOLOGICAL MODEL

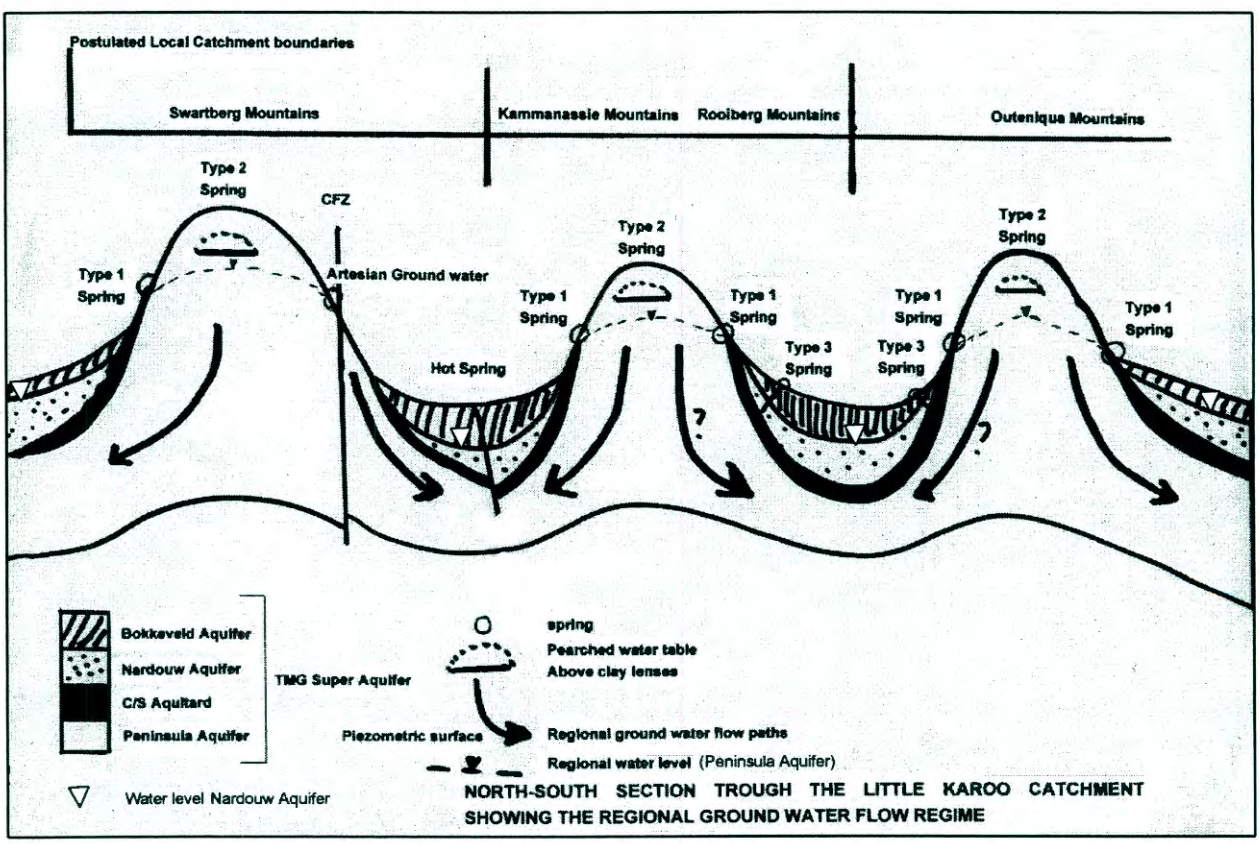

FIGURE 5-2: PIEZOMETRIC CONTOUR MAP – KAMMANASSIE MOUNTAINS

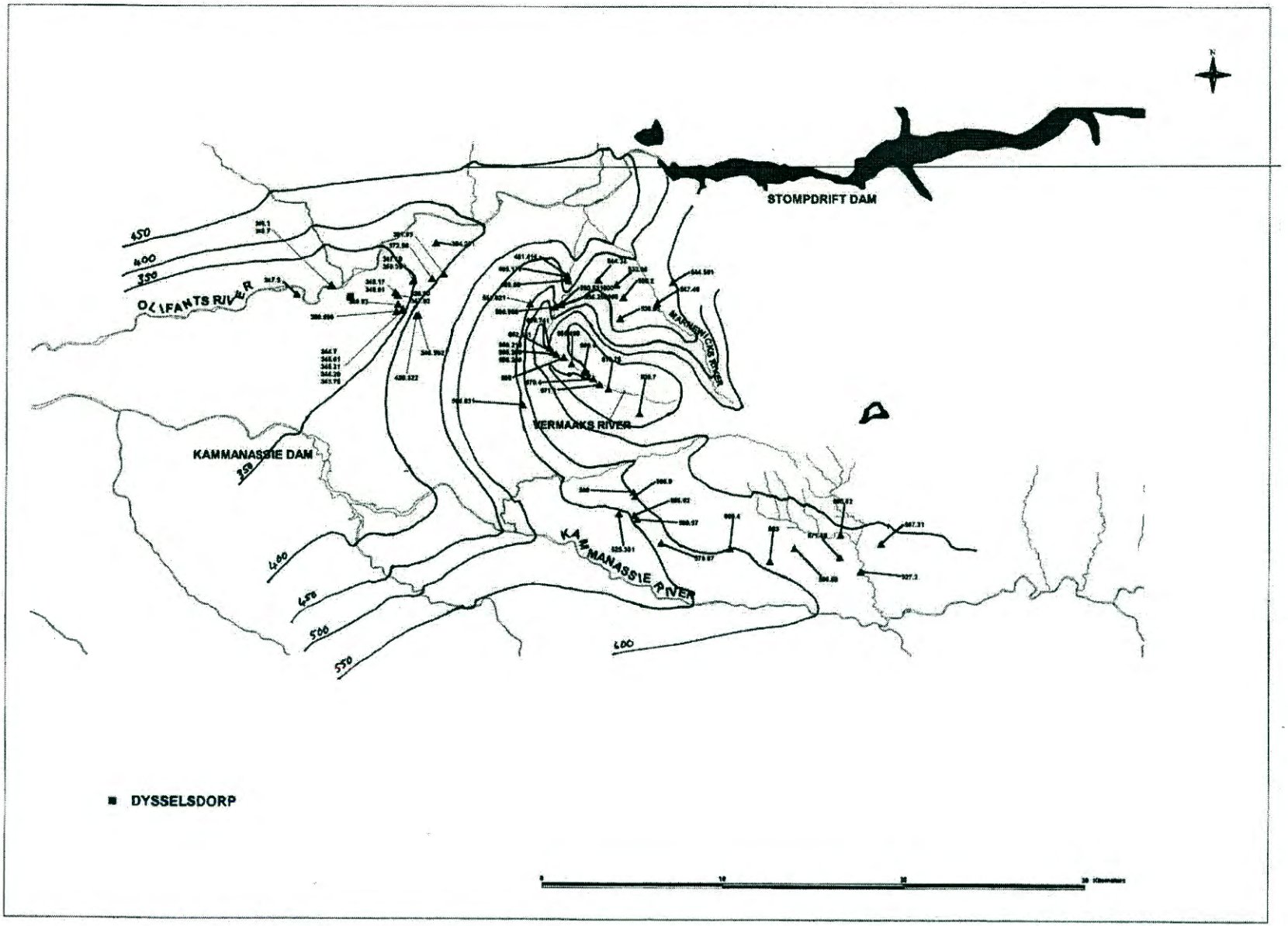

No water level or environmental isotope data are available to estimate whether groundwater flows to the south or north from the Outeniqua Mountains. Piezometric head responses, as well as the lag in responses to recharge on a regional scale are difficult to assess as no water level data outside the Kammanassie Mountains could be found. One of the greatest uncertainties in the present conceptual hydrogeological model is the nature and magnitude of the regional groundwater flux at depth, connecting several local and intermediate catchments, i.e. the Kammanassie, Outeniqua, Rooiberg and part of the Swartberg Mountains. The hydrostatic pressure of this regional flux caused by high recharge in the Outeniqua Mountains in particular, is postulated to buffer the discharge and drop in water levels from the local and intermediate flow systems. (Rainfall in the mountain catchments is between three and six times higher than that of the lower lying, intermediate mountain ranges, e.g. Kammanassie and Rooiberg Mountains.)

Local catchments, coinciding with surface water drainage basins, produce local recharge and surface water runoff in mountain streams. They also partially feed the major regional fractures, which are manifested in the low-yielding thermal springs situated near fracture zones in low-lying areas. An intermediate catchment or groundwater flow system is postulated to represent a mountain range, e.g. Kammanassie Mountains, which includes a combination of surface water catchments as defined by hydrological catchments. However, at depth, several mountain ranges are connected along deep synclinal structures (see Figure 5-3 and geological cross-sections: Figure 3-9 and 3-10), which constitutes the regional flow system. The TMG groundwater flow model developed for the Agter-Witzenberg area, B in Figure 5-1, (Weaver et al., 1999), is also in accordance with the conceptual model developed in this study.

On an intermediate catchment scale, most groundwater recharge takes place in the so-called TMG Window Areas of the Swartberg, Kammanassie and Outeniqua Mountains. After recharge, groundwater flows via interconnected fracture sets down-gradient to great depths and distances, along the folded Peninsula Formation bedding. Similarly, recharge also takes place to a lesser extent in the Nardouw Aquifer, outcropping at lower altitudes. Over time, leakage from the Peninsula to Nardouw to the Bokkeveld Aquifers takes place, resulting in successively longer residence times of groundwater in these aquifers. Crosscutting fractures transecting the C/S Aquitard facilitate direct recharge from the Peninsula to Nardouw Aquifer, by outflow along intermediate scale fractures. This results in shorter residence times and depleted $\delta^{18}O$ signature of groundwater in Nardouw Aquifers, where interconnecting fracture zones such as the Vermaaks and Brillkloof Faults (Figure 3-15) are present. Groundwater flow along folded bedding planes in an E-W direction is possible until crosscutting fractures across bedding planes changes the flow direction.

The regional groundwater flow system is reformulated as deep groundwater flow in the Peninsula Aquifer, along various scales of fractures along the folded TMG bedding, rather than single, large-scale regional fractures. The C/S Aquitard confines groundwater flow until deep-seated fractures (often fairly localised fractures) cutting through the C/S allow groundwater to escape from great depths to the surface in the form of hot springs. It is postulated that fractures transecting the C/S at depths of < 500 m will not lead to the formation of hot springs but rather artesian boreholes with elevated groundwater temperatures, i.e. > 20 ° C).

The wide separation and low yield of the thermal springs suggest limited deep, fracture flow. In order to study the regional flow system, a groundwater monitoring network needs to be expanded to include the Swart, Outeniqua and intermediate mountain ranges, i.e. Kammanassie and Rooiberg Mountains, respectively.

5.2.4 Groundwater storage

In a fractured aquifer the most important controlling factors on groundwater flow are fracture interconnection and openness. The openness of fractures depends on the tectonic regime prevailing during their formation relative to the present tectonic regime. Extensional tectonics generally provides open fractures for groundwater movement. The preferred groundwater flow direction is therefore associated with those fractures striking in the same direction as the extensional tectonic regime. For the TMG Super Aquifer of the Klein Karoo, fractures trending NNE-SSW and reactivated fractures in E-W, WNW, N-S orientations are preferred for groundwater flow.

After recharge has been intercepted by various vertical and horizontal fractures, groundwater flow takes place in vertical as well as horizontal directions, depending on the fracture characteristics. Newly recharged groundwater is temporarily stored in the smallest scale fractures, trending NE-SE, N-S and NE-SW, formed during mechanical failure in the top 100 m of the anticlines. Thereafter, most of the groundwater is stored in smaller fractures, feeding into larger fractures. Depending on the fracture connectivity and the volume of fractured rock, storage is estimated to be approximately 1% in massive quartzites of the recharge area (Peninsula Aquifer). Groundwater movement is primarily vertical in the fractures and will follow the path created by fractures to great depths. The balance of this transport is probably lost through diffuse upward discharge from these zones over wide areas. In the presence of intermediate scale fractures, i.e. the Vermaaks or Brillkloof Faults, storage increases to 7% (determined from joint measurements, Hälbich et al., 1995). Inside an aquizone, bounded by permeable faults, i.e. Keystone Block, storage increases to 5%.

Groundwater is stored in the smallest scale fractures until more recharge and consequent hydraulic pressure (both local and regional) forces stored groundwater downwards into connecting intermediate scale fractures. The Vermaaks River Fault in the Kammanasie Mountains, on which high yielding boreholes such as VR7 are sited, is an example of an intermediate scale fault. Further, excess groundwater flows out as base flow to streams or as leakage through the C/S to the Nardouw Aquifer. The driving force for downward movement of groundwater from storage can also be groundwater abstraction, creating a pressure head, allowing groundwater to flow into connecting intermediate scale fractures. Downward movement will continue with consequent heating of groundwater under the geothermal gradient, until deep-seated fractures penetrating the C/S Aquitard enable groundwater to surface as hot springs (Figure 5-3).

5.3 SPRINGS OCCURING IN THE TMG SUPER AQUIFER

Essentially, three different types of springs occur in the TMG Super Aquifer of the Klein Karoo:

1. Type 1 - Shallow springs emanating at perched water tables across the Peninsula and Nardouw Aquifers of the Cape Mountains. These are not connected to the greater groundwater flow system on any scale, i.e. local, intermediate or regional.

2. Type 2 - Lithologically controlled springs, due to the presence of inter-bedded aquitards. Lithologically controlled springs originate at the contact between an aquifer and aquitard. These springs are connected to the regional water table on a local scale and are buffered by recharge from the intermediate and regional scale flow system. The following three subtypes are differentiated (after Meyer, 2000):

   2.1 Springs emanating from contacts with the C/S Aquitard: Saturation of the Peninsula Aquifer often results in the formation of springs on the Peninsula / C/S contact at suitable topographical levels, from where they overflow onto the Nardouw Aquifer. These springs mostly yield > 5 l/s and are referred to as TMG springs or just springs.

   2.2 Springs emanating at the TMG / Bokkeveld: Although the TMG / Bokkeveld Group contact is a very likely locality for springs, only two examples are known (Meyer, 2000). Generally, springs emerging on the TMG / Bokkeveld Group contact are linked to faults in the TMG and are therefore more representative of a Type 3 spring (see below). These springs appear at low elevations and stopped flowing after abstraction increased along the Kammanassie Mountains and are postulated to be connected with circulating hot water from depth (examples found near Dysselsdorp).

2.3 Springs at unconformities: Originate on the discordant contact between the fractured Peninsula Aquifer and the underlying impervious basement rocks.

3. Type 3 - Fault Controlled Springs (FCS): FCS's mostly represent the hot springs in the Klein Karoo and mostly taps the regional flow system. Meyer (2000) lists eleven FCS's occurring along the CFB curvature, from Citrusdal to Uitenhage in the west and east, respectively. A characteristic of FCS's is the elevated temperatures of groundwater, ranging from > 20° C to > 40 ° C, rising to the surface along fractures intercepting aquitards and aquicludes at depth,.

Type 1 springs are shallow circulating springs, seeping from a network of joints, small, irregular fractures and from bedding planes within the TMG Aquifers, directly above localised aquitards. These seasonal, low yielding features are associated with locally perched water levels and are responsible for the myriad of springs seeping out of the TMG Aquifers during and after rainy weather, often referred to as seeps. Meyer (2000) confirms that these springs are highly seasonal and that flow diminishes with the onset of dry conditions. Groundwater abstraction from any part of the TMG Aquifer will not have any impact on Type 1 springs. These springs will impact vegetation most directly as they have shallow water tables. Fluctuation of rainfall patterns i.e. frequency and volume of rainfall events, has the most significant impact on Type 1 springs.

Types 2 and 3 springs are the most significant in terms of the regional water balance of TMG Aquifers. Several Type 2.1 springs originate on the C/S layer in the Kammanassie-, Gamka-, Rooi- and Swartberg Mountains in the so-called TMG-window areas.

Type 2 springs and fractures surfacing in the narrow mountainous valleys of TMG Mountain catchments provide up to 90% of the stream run-off in the form of baseflow (displaced groundwater). Figure 5-4 is a schematic presentation, showing the difference in water levels on either side of the C/S Aquitard. Positions A and B (Type 2 spring) on Figure 5-4 indicate the lowest topographic positions where TMG baseflow is released into surface water courses.

FIGURE 5-4: SCHEMATIC CROSS-SECTION THROUGH A MOUNTAIN VALLEY TO SHOW TYPE 2 SPRING AND WATER LEVEL RELATIONSHIPS

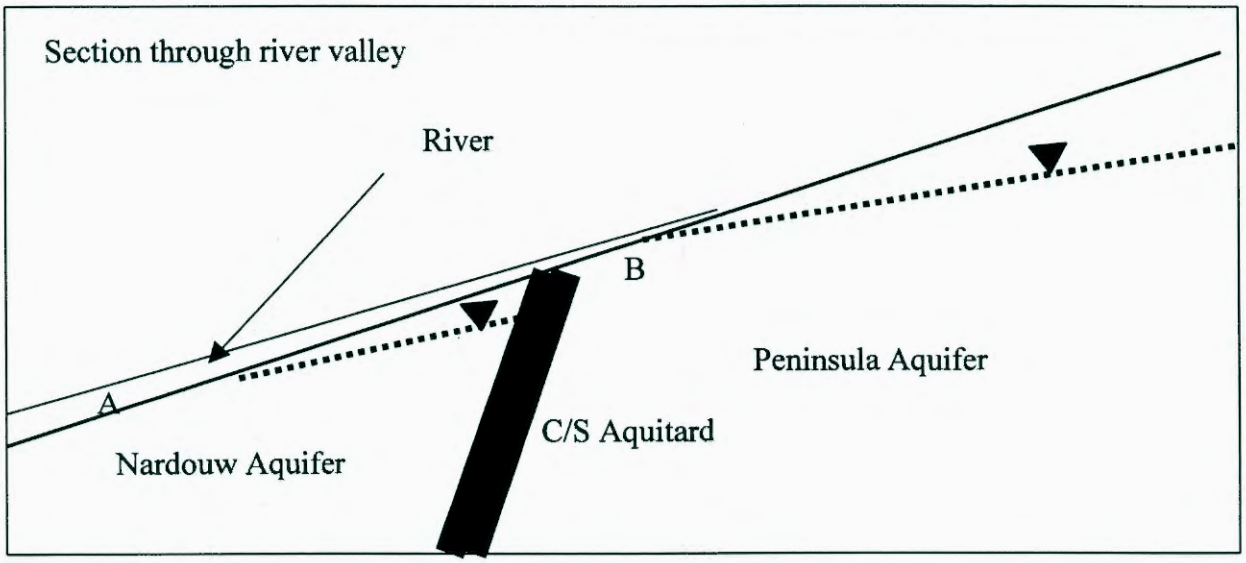

Midgley *et al.* (1994) used stable isotopes in rainfall and streams in the Jonkershoek Valley to determine the relative contribution of 'new water', i.e. rain, during storm flow conditions after heavy rains. Significant differences in the isotopic signatures of rainfall and stream water facilitated the use of a mass balance equation to calculate the component of storm flow. The results indicated that < 5% of storm flow comprised direct run-off. This suggests that rapid response of streamflow to rainfall is a direct consequence of displaced groundwater.

The isotopic content of streams is an approximate long-term average isotope concentration of precipitation in source catchments as well as reflecting a component of evaporative enrichment (Midgley *et al.*, 1994). This is also true for the Vermaaks, Marnewicks and Huis River springs and streamflow. The total groundwater reservoir is therefore large enough to be well buffered to input from rainfall.

Figure 5-5 is a schematic presentation of the Type 2.1 spring. Spring flow generally consists of 90% baseflow, representing groundwater being pushed through the system by incoming rainfall and 10% of surface water. The TMG baseflow originates from groundwater stored in shallow fractures (those caused by brittle failure during folding) in both the Peninsula and Nardouw Aquifers and groundwater released from storage in larger fractures as recently recharged water pushes through the system. The increase in spring flow after rainfall is therefore proportional to recharge elsewhere in the system, i.e. large fractures in the higher altitudes of the mountains, allowing water to exit via near surface fractures in the valleys as interflow. TMG springs represent a mixture of baseflow (result of long term-storage; perennial recharge) and seasonal peaks (interflow), associated with heavy rainfall events (seasonal recharge).

FIGURE 5-5: CONCEPTUAL MODEL – TMG TYPE 2.1 SPRINGS

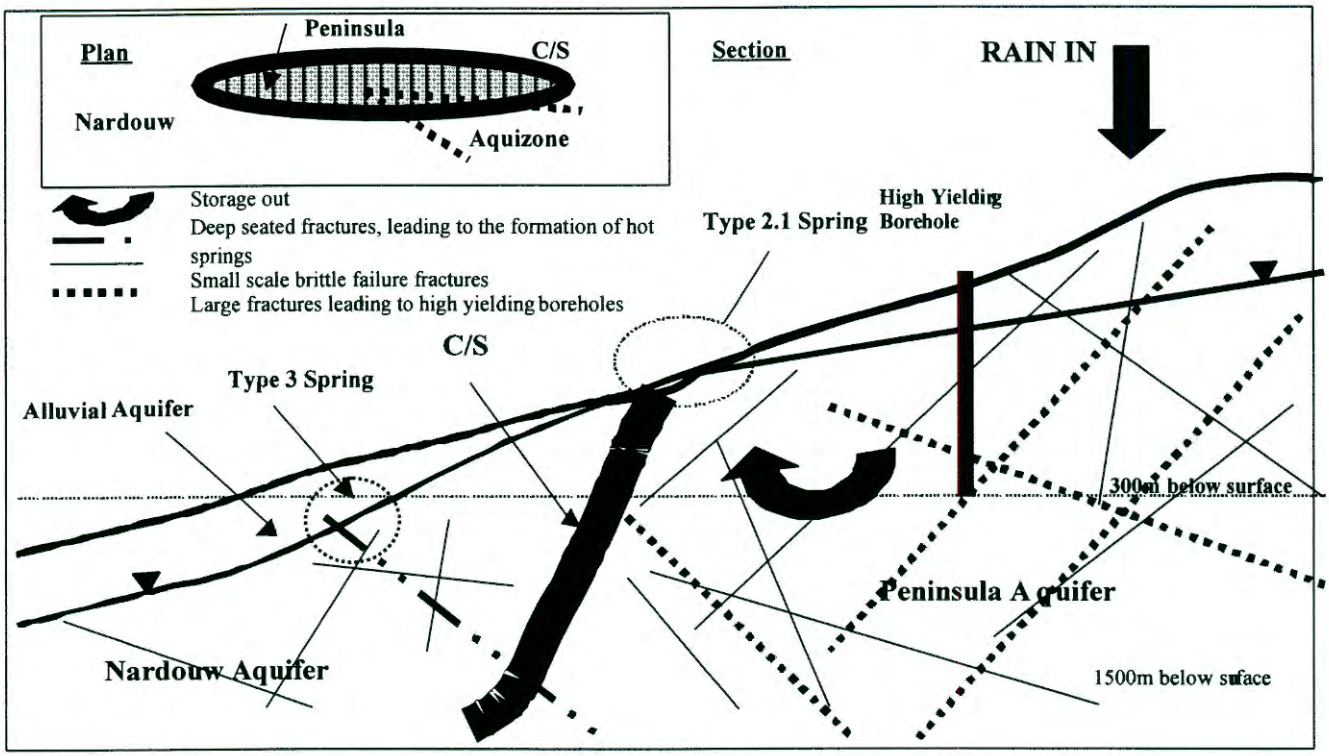

The temperature of Type 3 springs indicates depths of circulation of the order of a few thousand metres. The $\delta^{18}O$ signature of hot springs shows a pronounced depletion in relation to shallow groundwater. This depletion is attributed to the altitude of the recharge area, rainfall selection and recharge from snowmelt. The continuous flow rates and small seasonal variations in flow rates, as well as the extensive ferruginous and silicic spring deposits, suggests considerable age, which is confirmed by ^{14}C data indicating residence times in excess of 30 000 years.

5.4 BOREHOLE YIELDS

Boreholes sited in the TMG Super Aquifer vary in depth from 50 to 300 m, depending on the depth at which the water-bearing fracture is intercepted. Borehole yields generally increase with depth and vary from 5 to 30 l/s. The groundwater is characterised by low mineralisation (TDS < 300 mg/l), low pH (<6) and low Total Alkalinity (0.5 meq/l). Groundwater quality varies according to the host aquifer formation and / or interconnection of the particular part of the aquifer with the recharge area via fracture sets. Borehole efficiencies in the Nardouw Aquifer can be reduced significantly by biofouling and clogging of boreholes screens, which often occur in the presence of pyrite-quartz veining in the vicinity of the Bokkeveld shale contact.

Based purely on lithologic considerations, the Peninsula Aquifer is the highest yielding TMG Aquifer with the best groundwater quality. The Peninsula Aquifers mostly outcrop in the high altitudes of the mountain catchments (main recharge areas) and coincides with conservation areas, which places an environmental constraint on development. However, high yielding boreholes with good groundwater quality occur in the Nardouw Aquifer inside a permeable aquizone, e.g. Vermaaks Keystone Block, at lower altitudes.

5.5 HYDROGEOLOGICAL CONCEPTUAL MODEL FOR KAMMANASSIE MOUNTAINS

The Kammanassie Mountains are postulated to represent an intermediate scale flow system, interconnected to the regional scale flow system of the Outeniqua Mountains at depth, along the folded strata of the Peninsula Aquifer. Hydrochemistry and environmental isotope data have confirmed that most recharge takes place in the higher altitudes where the Peninsula Aquifer occurs and, to a lesser extent, where the Nardouw Aquifer outcrops at lower altitudes. Recharge is then transferred from the Peninsula to the Nardouw Aquifer in one of the following ways:

- Overflow across the C/S layer (Type 2 spring).
- Cross-cutting fractures through the C/S, i.e. the Vermaaks River, Leeublad, Rooikrans Faults and several smaller faults, establishing a direct connection between the Nardouw and Peninsula Aquifers in the Keystone Block Aquizone.
- Outside the Keystone Block Aquizone, leakage of groundwater through the C/S Aquitard recharges the Nardouw Aquifer.
- Flow along bedding planes (shale/quartzite contacts).

Figure 5-6 (over page) shows the positions of local scale flow systems e.g. Vermaaks and Marnewicks, etc. relative to intermediate scale flow systems of the Kammanassie Mountains.

Groundwater quality and yield of TMG Aquifers in the Kammanassie Mountains varies with the lithological unit intercepted, proximity to recharge area and the presence of fractures cross-cutting the C/S Aquitard, forming the Keystone Block Aquizone. This Keystone Block Aquizone connects the Nardouw Aquifer at lower altitudes directly with the recharge areas in the mountains and correlates with remote sensing and lineament mapping. This leads to high yielding, good quality boreholes in the Nardouw Aquifer inside the Keystone Block Aquizone, e.g. boreholes on the farms Leeublad, Rolbaken and Koutie, whereas elsewhere, yields are lower and groundwater quality poorer. Poor fracture interconnectivity and low leakage rates through the C/S Aquitard, leads to longer residence times along the convolute flow paths in the Nardouw Aquifer.

FIGURE 5-6: LOCAL AND INTERMEDIATE SCALE FLOW SYSTEM BOUNDARIES

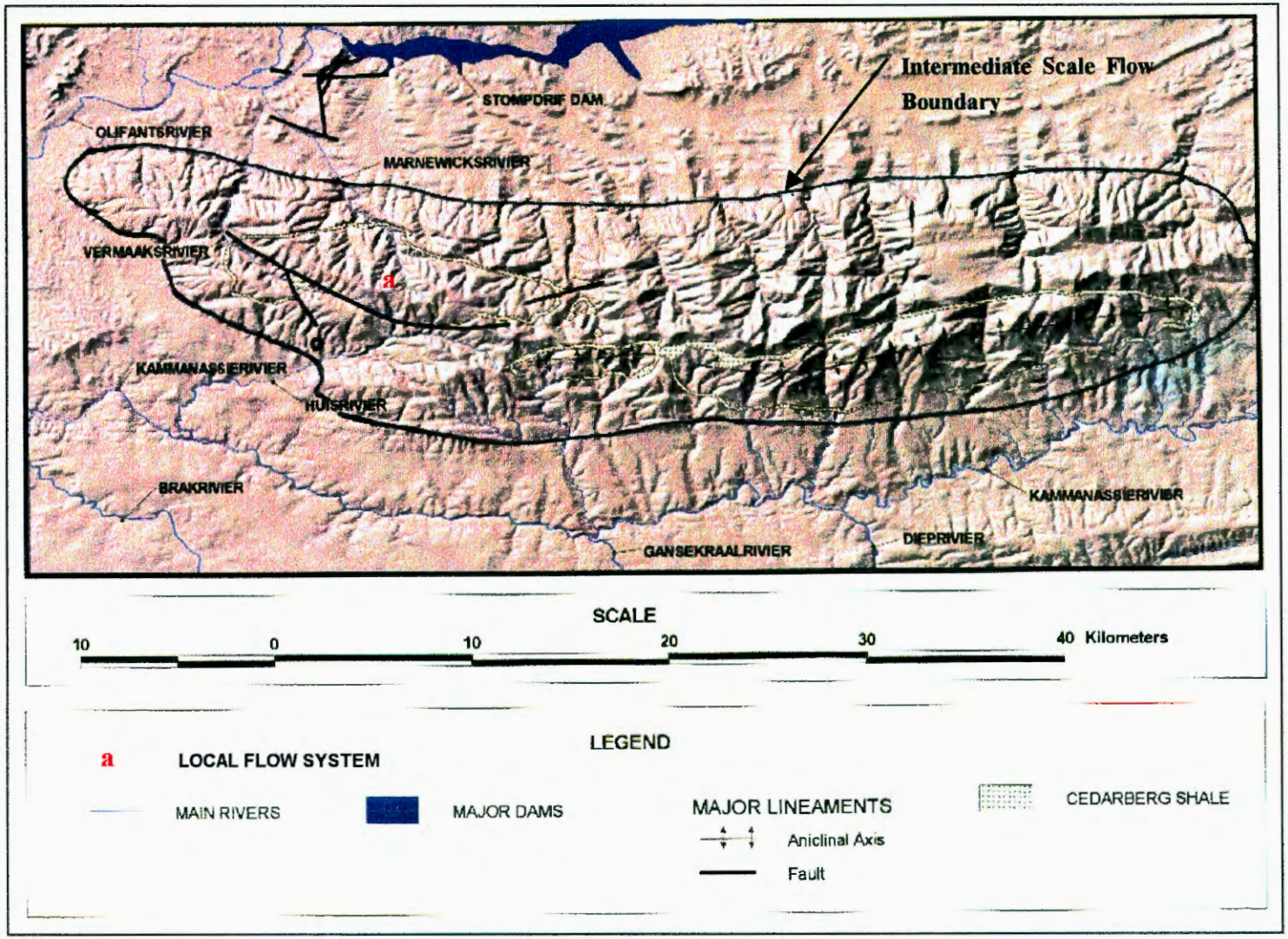

Lower yields (< 5 l/s) and poorer quality water are associated with less densely fractured poorly interconnected parts of the TMG Aquifer, i.e. the Nardouw Aquifer, near the Bokkraal, Varkieskloof and Droëkloof Wellfields.

Thick shale successions in the nearby Bokkeveld Aquifer contain pyrite in a reducing groundwater environment, which leads to iron precipitation, resulting in biofouling and clogging of borehole screens, when oxygen is introduced to the system (from pumping). This process is enhanced by the working of bacteria, resulting in increased precipitation of iron and lowering of the pH, contributing to the so-called 'iron-bacteria problem' experienced in the above-mentioned wellfields.

The major ion chemistry of TMG groundwater is more a function of the style of fracturing, fracture density and interconnection with the recharge area, than the host formation. The groundwater quality and higher yields of boreholes WK3 and 4 (see Figure 2-5) are associated with the good interconnectivity of various fracture sets orientated in NNE, E-W and NNW directions and proximity to the catchment watershed. As indicated before, trace element sampling can provide valuable information regarding the possibility for bacteriological clogging of boreholes. The management of bacteriological clogging of borehole screens and fractures in boreholes requires expensive borehole construction and borehole rehabilitation programs and should be avoided when possible. Warning signs for potential bacteriological clogging in the Klein Karoo are the following:

- Presence of the following trace elements in groundwater: Ni, Cu, Zn and Co, mostly through dissolution of minerals containing these trace elements in shales and quartz veins, which contains pyrite, resulting in natural reducing groundwater conditions.
- Over-pumping of boreholes, where reducing conditions prevail in groundwater.
- Close to Bokkeveld contact.
- No connection with the recharge area.

Isolated fractures in the Nardouw Aquifer near the Bokkeveld contact give low-yielding boreholes with poorer quality groundwater, due to mixing of groundwater from the Nardouw and Bokkeveld Aquifers. This type of Nardouw Aquifer is intercepted in borehole SL2 and DR2. Generally, yields are < 2 l/s and EC values vary between 40 and 50 mS/m with pH < 5 as opposed to the generally low EC values of the Keystone Block Aquizone and Peninsula Aquifer, i.e. <15 mS/m.

The Peninsula Aquifer generally falls directly within the recharge area in the Klein Karoo, constituting the so-called TMG Window Areas. The highest yielding boreholes (10 to

>20 l/s), with the best quality water, are associated with densely fractured areas, connected to the recharge area. These conditions apply in the Peninsula Aquifer and Keystone Block Aquizone where good interconnectivity between fracture sets in a WNW, N-S, NNE and E-W orientation exists, providing high permeability and storage conditions.

Numerous NNW-trending fractures in parts of the Kammanassie Mountains (Vermaaks River Valley) give rise to a strong directional permeability. If these fractures were reactivated during extensional tectonic regimes, they act as valuable feeder zones collecting recharge, which is transferred to more permeable fracture sets trending WNW, NNE and E-W.

Increased exploitation from the highly fractured catchment valleys (Peninsula Aquifer or Nardouw Aquifer in permeable Aquizone), constituting part of local catchments are the most economic solution for groundwater development. Local catchments have groundwater of good quality and yield, buffered by intermediate and regional flow systems. This will clearly have to be at the expense of the baseflow of mountain streams in local catchments and local lowering of water levels. Eventually, the transport of groundwater in regional fractures will be reversed, producing resistance levels in the yield-drawdown relationship. In the light of the present information, this would not appear to have major water quality consequences.

CHAPTER 6: HYDRAULIC PROPERTIES OF AQUIFERS

As every borehole in a fractured rock aquifer reacts differently during pump testing and no generalised methodology for pump test interpretation in fractured aquifers exists, (see Section 2.5.2 for background information on pumping test analysis in fractured aquifers.) It is important to realise the limitations of analytical analyses methods, due to the theoretical assumptions associated with the method. Van Tonder (2000) indicates that in order to analyse a pumping test correctly, the following important characteristics need to be identified:

- The correct geological conceptual model (for application of the correct analytical model).
- Inner boundary conditions (i.e. well bore storage effects (WBS), well bore skin, fracture skin.
- The lateral extent of the fracture or fracture zone.
- Outer boundary conditions (i.e. especially no-flow boundaries but also fixed head boundaries).
- Characteristic flow regimes (the choice of the correct part of the curve to be fitted by looking at the flow dimension that prevails during that specific part of the test).

The identification of characteristic flow regimes is very important for both parameter and sustainable yield estimation. Diagnostic plots (eg. log-log and derivatives) can assist in identifying the different characteristic flow regimes, i.e. WBS, linear, bilinear, semi-radial flow as well as boundary conditions. Figure 2-12 (Chapter 2) shows some of the most important flow characteristics, and how they can be identified from constant rate pumping tests.

Therefore, based on the conceptual model developed for TMG Aquifers and the prevailing characteristic flow regimes, it is possible to select the most suitable analytical model, which is then used to determine the aquifer parameters and sustainable borehole yield. In cases where the fractured aquifer acts as a homogeneous porous aquifer (radial flow), the Theis or Cooper-Jacob methods can be applied for aquifer parameter estimation. In this case the T- and S- values represent the entire aquifer without differentiating between fractures and matrix (van Tonder, 2001).

Based on the current conceptual hydrogeological model developed for TMG Aquifers the available test pumping data for the production boreholes of the Eastern Section of the KKRWSS were analysed in the following way:

- Firstly, all pump test data are captured in the FC spreadsheet (van Tonder and Xu, 1999).
- Based on the diagnostic plots for each borehole, the characteristic flow regime for each aquifer is determined.
- Based on the conceptual hydrogeological model boundary conditions are selected and the influence thereof on the sustainable borehole yield simulated with the FC method. Simultaneously, the influence of nearby production boreholes in the same wellfield is also incorporated.
- For comparison, all data are also analysed with the Cooper-Jacob method in the FC spreadsheet (van Tonder and Xu, 1999).

All the relevant borehole information, i.e. geology, water strikes, borehole construction, depth to water level, etc. for each where pump test data were analysed is summarised in Appendix K-7. All the diagnostic and derivative plots, as well as sustainable yield and risk analysis sheets for each production borehole, are summarised in Figures J-1 to J-58, (Appendix J).

The choice of available drawdown is one of the most critical parameters for sustainable yield estimations. To illustrate the above, the sustainable borehole yield for each production borehole is estimated for the following scenarios of available drawdown:

1. The available drawdown is calculated as the difference between the rest water level and the main water strike (referred to as basic available drawdown scenario).
2. The geometric mean of the final drawdown value of the constant discharge test and the distance to the main water strike (measured from the rest water level). This approach is recommended by van Tonder (2001) for conditions where the main water strike is not reached during the constant yield test (referred to as best available drawdown scenario).

In all cases the extrapolation time is taken as two years and recharge assumed to be zero. The aquifer thickness is taken as 20 m as recommended for fractured aquifers in the manual, which is based on findings in the Karoo Aquifer. Although both the TMG and Karoo Aquifers are fractured aquifers, associated fracture characteristics vary considerably. The FC analysis is very sensitive to changes in aquifer thickness parameter. Sustainable yield calculations include a basic solution, followed by advanced solutions incorporating various boundary conditions and additional boreholes for the basic available drawdown scenario. Thereafter a basic solution for the best available drawdown scenario is carried out. The FC and Cooper Jacob Method are also used to determine the aquifer parameters, i.e. storativity (S) and transmissivity (T) for the Peninsula and Nardouw TMG Aquifers.

For comparison the FC analysis of DP18, an alluvial borehole is included and the complete FC analysis results are in Appendix J. All borehole positions are shown in Figure 3-1.

Constant discharge tests are also evaluated using the Theis or Cooper-Jacob Method (Kruseman & de Ridder, 1994) for each borehole. These methods are designed for confined, porous aquifers, where deviations from the type-curve are noted and data extrapolation carried out to determine a 'safe' abstraction rate (Murray, 1996). The Cooper-Jacob Method in the FC spreadsheet designed by van Tonder and Xu is used for this analysis.

6.1 PENINSULA AQUIFER

The Peninsula Aquifer is postulated to be a purely fractured rock aquifer, i.e. rock mass consisting of large fractures and some matrix blocks with no micro-fissures (van Tonder *et al.*, 1999). The system consists of an interconnected network of fractures and the rock matrix, comprising the blocks surrounded by fractures, is impervious to flow. A good interconnection exists between smaller matrix fractures and larger scale fractures in the highly interconnected Keystone Block Aquizone (see Figures 3-16 and 3-19). Besides excellent inter-connectivity between the various fracture orientations, (MAP 3, Folder 1, remote sensing map) the Peninsula Aquifer mostly outcrops in the higher mountain catchment areas, thus receiving most recharge. The C/S Aquitard confines groundwater flow in the Peninsula Aquifer and represents a boundary condition to flow.

The FC method is used to analyse the aquifer test data of VR6, 7 and 11, representing three of the four existing production boreholes of the Vermaaks Wellfield of the KKRWSS (no pump testing data for VR8). VR6, 7, 8 and 11 are the only four boreholes drilled into the Peninsula Aquifer. The data analysis results for each borehole follows below.

6.1.1 VR7

VR7 is the highest yielding production borehole of the KKRWSS, with a sustainable yield of 20 l/s and is drilled into a highly interconnected fracture system of the Keystone Block Aquizone.

Three constant discharge (CD) tests were carried out at VR7. In 1990, two CD tests were conducted at pump rates of 25 and 35 l/s under similar water level conditions. A third test was conducted in 1997 at a pumping rate of 20.0 l/s, by which time the rest water level had declined to the level of the first of two major water-strikes, i.e. 8 l/s at 76-81 m bgl. The second major water-strike yielded an additional 7 l/s at 129-140 m bgl.

It is interesting to note the variations in calculated T values for VR7 at varying pumping rates and rest water levels (Table 6-1). Woodford (2001) explains the variations in T values by analysis of water level and specific drawdown (Sw/Q) curves from the above tests (see Figure 6-1, after Woodford 2001). From Figure 6-1 it can be seen that local dewatering of the first waterbearing fracture occurred during all three of the tests. The Sw/Q curves (Figure 6-1) show a similar aquifer response for the 1990 and 1997 test, at 25 l/s and 20 l/s, respectively. The early T-value, for the earlier test is somewhat high (Table 6-1). According to Woodford (2001) the 1990 test conducted at a pumping rate of 35 l/s, is in excess of the maximum yield of the borehole, hence the sharp decline in water level in the first 100 minutes. The inflection point and flattening of the drawdown curve after 100 minutes (Figure 6-1) may indicate the presence of a significant water-bearing fracture at 101-103m (Woodford, 2001). (The original drill-logs noted fracturing at 99 and 106m, without an increase in the blow-yield of the borehole.)

The derivative plot shows a horizontal straight line after approximately ten log cycles, indicative of infinite radial flow (Figure J-2, Appendix J). However, a gradient of 0.25 on the log-log diagnostic plot indicates bilinear flow and the absence of a straight-line on the semi-logarithmic plot indicates that the flow is not entirely radial (Figure J-4, Appendix J). A semi-radial flow regime therefore prevails, with a single no flow boundary (from the derivative plot, Figure J-2, Appendix J).

FIGURE 6-1: BOREHOLE VR7 - WATERLEVEL AND SW/Q VARIATIONS DURING CONSTANT DISCHARGE TESTS (ADAPTED FROM WOODFORD, 2001)

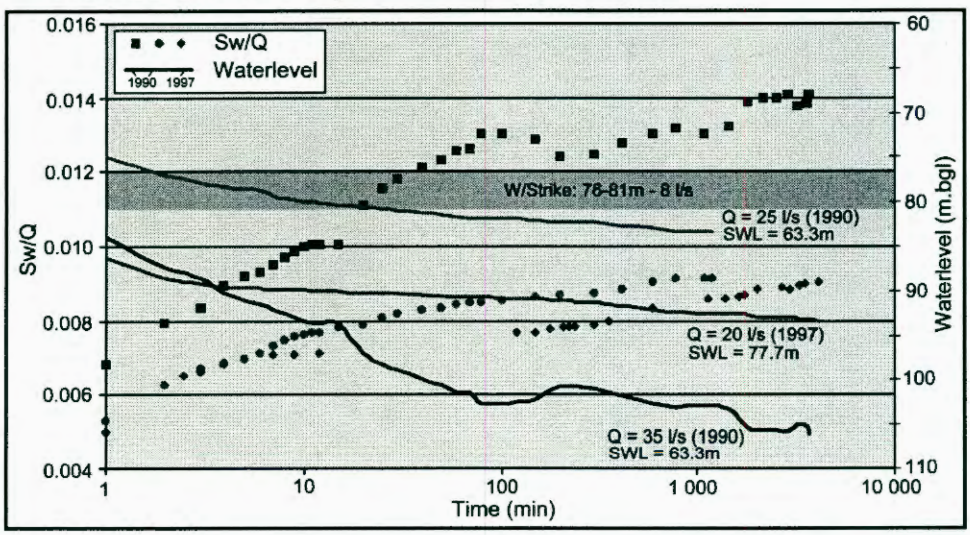

If the rule of thumb for radial flow conditions is applied, the transmissivity (T) of the aquifer is estimated as follows:

T = 1.22 Q

$$= 0.183 * 1728 = 2108 \text{ m}^2/\text{d}$$

where Q is the yield in m^3/d.

The T versus time plot (Figure J-3, Appendix J), shows that T initially increases up to 400 m^2/d, but reduces to 150 m^2/d after 600 minutes of pumping, whereafter it stabilises. Further, the characteristic kink signifying double porosity is present, indicating matrix / fracture flow.

Results show that the main fracture (boundary condition to flow) supplying water to this borehole has not been intercepted and that VR7 taps an interconnected, highly fractured portion of matrix fractures in the Keystone Block Aquizone. From the above analysis, it is postulated that a yield of up to 50 l/s would be obtained from a deeper borehole (with a larger diameter), drilled close to VR7. The fracture interconnection is so good, that the typical sinusoidal waveform (Figure J-2, Appendix J), showing interception of fractures at various scales, is not observed on the derivative plot. The matrix of fractures therefore almost acts as a continuum.

Table 6-1 summarises the results of sustainable yield calculations for the following scenarios (Figures J-5 to J-10, Appendix J), using a basic available drawdown of 40 m:

- Basic Solution, excluding boundary conditions or additional borehole effects (Figures J-5 and J-6, Appendix J).
- Advanced Solution 1: includes a single barrier boundary 2200 m from the borehole, representing the C/S layer (Figures J-7, Appendix J).
- Advanced Solution 2: includes two parallel boundaries (16 000 and 2 200 m from VR7, respectively), representing the C/S window area (Figure J-8, Appendix J).
- Advanced Solution 3: same as advance solution 2, but includes two additional boreholes, representing VR6 and 8[1], yielding 6.0 and 7.4 l/s respectively, each situated 400 m away from VR7 (Figure J-9, Appendix J).
- Worse case scenario: closed square boundary 4000 m radius from VR7 and two boreholes (VR6 and 8) as in advanced solution 3 (Figure J-10, Appendix J).

[1] Pump testing by GCS indicated that pumping from VR6, 7 and 8 influences each other.

TABLE 6-1: RESULTS OF FC-METHOD ANALYSIS OF VR7

	Basic Solution	Advanced Solution 1	Advanced Solution 2	Advanced Solution 3	Worst Case Scenario	Cooper-Jacob
Effective BH radius	7.2					7.2
T_{early} (m^2/d)	168.0					276.2
T_{late} (m^2/d)	144.0					
S_{late}	1.1×10^{-3}					1.6×10^{-12}
Yield range (l/s)	36.6 – 15.2					
Yield 68% Risk (l/s)	24.7	29.2	28.0	23.0	3.9	
Yield 95% Risk (l/s)	13.6	26.5	25.0	20.0	-3.4	
Recommended Yield (l/s)	**20**	**25.0**	**26.0**	**20.0**	**1.0**	

The Cooper-Jacob solution for VR7 (Figure J-11, Appendix J) indicates a T-value of 276 m^2/d, storativity of 1.6×10^{-12} and effective borehole radius of 7.2 m.

6.1.2 VR6

The derivative plot of VR6 (Figure J-16, Appendix J) has a typical sinusoidal waveform, i.e. the derivative decreases at the position of a fracture. After dewatering of the fracture, the derivative increases again. The diagnostic plots (J-14, Appendix J) indicate a bilinear flow pattern (0.25 slope of Theis plot and a straight line on the square root with time plot).

In comparison to VR7, the T-value is considerably lower (compare Figures J-3 and J-17, Appendix J). It increases to a maximum value of 30 and 60 m^2/d at the interception of two fractures (sets of fractures). The T values remain constant below 10 m^2/d after 100 minutes. The S value is approximately 1.5×10^{-4}.

Only a basic solution is carried out for the VR6 data set and the results are as follows:

- $T_{early} = 29.0\ m^2/d$
- $T_{late} = 7.0\ m^2/d$
- $S_{late} = 1 \times 10^{-3}/d$
- Yield range : 14.5 – 3.9 l/s
- Yield 68% risk = 7.8 l/s
- Yield 95% risk = 7.4 l/s
- Recommended Yield = 7.0 l/s.

The Cooper-Jacob solution for VR6 (Figure J-19, Appendix J) indicates a T-value of 17 m^2/d, storativity of 2.7×10^{-7} and effective borehole radius of 26 m.

6.1.3 VR11

The derivative plot of VR11 (Figure J-24, Appendix J) also follows a sinusoidal waveform pattern, indicative of the interception of various fractures, similar to that of VR6. The semi-log diagnostic plot (Figure J-22, Appendix J) shows radial flow periods, intermittent with steeper gradient segments where matrix flow dominates (as indicated by the step between fault segments). The flat line of the log-log diagnostic plot (Figure J-22, Appendix J) shows bilinear flow (leakage from matrix to fracture).

Table 6-2 summarises the sustainable yield simulations for the following (Figures J-27 to J-29, Appendix J):

- Basic solution, excluding boundary conditions or additional borehole effects (Figure J-27, Appendix J).
- Advanced Solution 1: includes two parallel boundaries (16 000 and 2 200 m away from borehole, respectively), representing the C/S window area. One additional borehole yielding 7.4 l/s, 400 m from borehole VR11 (VR8, as indicated by pump test results) is also simulated (Figure J-28, Appendix J).
- Advanced Solution 2: includes two perpendicular boundaries 2000 and 1800 m from the borehole, representing the C/S of the Keystone Block as well as one borehole, representing VR8, yielding 7.4 l/s respectively, situated 400 m from VR11 (Figure J-28, Appendix J).

TABLE 6-2: RESULTS OF FC METHOD ANALYSIS OF VR11

	Basic Solution	Advanced Solution 1	Advanced Solution 2	Cooper-Jacob
Effective BH radius	10.3			10.3
T_{early} (m2/d)	112.0			160.0
T_{late} (m^2/d)	90.0			
S_{late}	1.1×10^{-3}			4.3×10^{-9}
Yield range (l/s)	23.9 – 9.9			
Yield 68% Risk (l/s)	21.8	23.0	18.4	
Yield 95% Risk (l/s)	14.06	21.0	16.6	
Recommended Yield (l/s)	12	15.0	15.0	15.4

The T value averages around 50 m2/d for the first 30 minutes (Figure J-23, Appendix J), whereafter it increases to 190 m2/d for approximately 300 minutes and then decreases again to 100 m2/d.

The Cooper-Jacob solution for VR11 (Figure J-26, Appendix J) indicates a T-value of 161 m^2/d, storativity of 4.3×10^{-9} and effective borehole radius of 10 m.

6.2 NARDOUW AQUIFER

The Nardouw Aquifer has a scale effect introduced by the lower fracture frequency and more ductile nature of the formations due to the presence of thicker shale layers. The scale effect refers to the different scale of heterogeneity introduced by micro-fractures in the matrix blocks themselves and the intersecting of a network of interconnected fractures subdividing the matrix blocks. Alternatively, the rock is also referred to as a fractured porous rock (van Tonder *et al.*, 1999).

The Nardouw Aquifer outcrops at lower altitudes and receives much less direct recharge than the Peninsula Aquifer. Considerable amounts of indirect recharge (groundwater inflow from a neighboring compartment) are possible via fracture systems connecting the Peninsula and Nardouw Aquifers, i.e. Keystone Block Aquizone. A large part of the aquifer is confined below a thick layer of Bokkeveld shale.

Test pumping analysis, with the FC Method is carried out for DP28 and 15.

6.2.1 DP28

The derivative plot (J-31, Appendix J) for DP28 is significantly different from that of the Peninsula Aquifer boreholes. The plot follows a single wide-open sinusoidal wave, representing the dewatering of a single fracture. The semi-logarithmic diagnostic plot (Figure J-33, Appendix J) indicates that a boundary is reached, whereafter matrix flow dominates. Similarly, the log-log plot and cartesian plots also indicate that the fracture position is reached. Table 6-3 summarises the sustainable yield simulations for the following scenarios (Figures J-35, J-37 and J-38, Appendix J):

- A basic solution excluding any boundary conditions (Figure J-35, Appendix J).
- Advanced solution 1 incorporating the C/S layer 6000 m away and the influence of DP25 (6 l/s) and DP15 (9 l/s), each 50 m away from DP28 (Figure J-37, Appendix J).
- Advanced solution 2 including the above-mentioned two boreholes and a single boundary 100 m away from DP25, representing the main fracture (Figure J-38, Appendix J).

The high yields obtained from advanced solution 1 (Figure J-35, Appendix J) indicate that the boundary condition assumption is likely to be incorrect. The C/S Aquitard is therefore too far away to be an important boundary condition to flow in the Nardouw Aquifer and the position

of the main fracture is the controlling factor (see advanced solution 2, Figure J-38, Appendix J).

TABLE 6-3: RESULTS FC METHOD ANALYSIS OF DP28

	Basic Solution	Advanced Solution 1	Advanced Solution 2	Cooper-Jacob
Effective BH radius	13.8			13.8
T_{early} (m^2/d)	265.0			216.0
T_{late} (m^2/d)	104.0			
S_{late}	2.2×10^{-3}			1.8×10^{-6}
Yield range (l/s)	22.4 – 9.5			
Yield 68% Risk (l/s)	17.0	22.9	17.2	
Yield 95% Risk (l/s)	10.0	21.3	16.0	
Recommended Yield (l/s)	10.0	15.0	10.0	21.1

T values average at 70 m^2/d and increase to a maximum value of 200 m^2/d over the central portion of the test (400 to 2000 minutes). The results indicate a fracture of limited extent, which is dewatered after approximately 400 minutes of pumping, whereafter, matrix flow becomes increasingly important (Figure J-32, Appendix J).

The Cooper-Jacob solution (Figure J-36, Appendix J) indicates a T-value of 216 m^2/d, storativity of 1.8×10^{-6} and effective borehole radius of 14 m.

6.2.2 DP15

The derivative plot (Figure J-41, Appendix J) shows an initial, radial flow period followed by a sinusoidal wave form indicative of fracture interception. Very little early data are available to make deductions on early flow behavior.

From Figure J-42 (Appendix J), T values average 100 m^2/d for the largest part of the test duration. However, a high yielding fracture is intercepted after 9 minutes of pumping, resulting in an increase of the T-value (1600 m^2/d). This is the first example where T and S values decrease and increase, respectively, with time. The above indicates the increased importance of matrix flow with time, or limited extent of major fractures.

The diagnostic log-log plot (Figure J-43, Appendix J) confirms the above and shows leakage from the matrix. DP15 is placed better than DP28 in terms of exploiting the fracture system. Two simulations are carried out with the FC Method, i.e. a basic solution, excluding boundary conditions and one advanced solution incorporating the other Bokkraal boreholes, DP25 and 28, yielding 12 and 9 l/s respectively.

The following results are obtained from sustainable yield calculations for the basic solution:

- $T_{early} = 66.0\ m^2/d$
- $T_{late} = 43.0\ m^2/d$
- $S_{late} = 2.1 \times 10^{-3}/d$
- Yield range : 22.5 – 9.5 l/s
- Yield 68% risk = 23.0 l/s
- Yield 95% risk = 19.0 l/s
- Recommended Yield = 15.0 l/s.

The Advanced solution gave:

- Yield 68% risk = 11.1 l/s
- Yield 95% risk = 10.8 l/s
- Recommended Yield = 10.0 l/s

The Cooper-Jacob solution (Figure J-45, Appendix J) indicates a T-value of 86 m^2/d, storativity of 1.7×10^{-6} and effective borehole radius of 28 m.

6.2.3 VG3

The derivative plot (Figure J-60, Appendix J) shows an initial, radial flow period followed by a sinusoidal wave form indicative of fracture interception. The derivative plot shows the interception of a good fracture network.

From Figure J-62 (Appendix J), T values average 12 m^2/d for the largest part of the test duration. However, a slightly higher yielding fracture is intercepted after 9 minutes of pumping, resulting in an increase of the T-value (20 m^2/d). The T and S remain constant, with time. The above indicates a good interconnected fracture network.

The diagnostic log-log plot (Figure J-63, Appendix J) confirms the above and clearly shows radial flow conditions. Only one simulation is carried out with the FC Method, i.e. a basic solution.

The following results are obtained from sustainable yield calculations for the basic solution:

- $T_{early} = 43.6\ m^2/d$

- T_{late} = 13.3 m^2/d
- S_{late} = 2.2 x 10^{-3}/d
- Yield range : 3.9 – 11.2 l/s
- Recommended Yield = 5.0 l/s.

The Cooper-Jacob solution (Figure J-61, Appendix J) indicates a T-value of 20.6 m^2/d, storativity of 2.8 x 10^{-6} and effective borehole radius of 2.5 m.

6.3 ALLUVIAL BOREHOLE – DP18

The derivative plot (Figure J-52, Appendix J) for DP18 is very similar to that of the fractured aquifers. However, the sinusoidal waveform of the derivative does not indicate fractures but heterogeneities in unconsolidated material, or boundary conditions, i.e. the constant head river boundary.

From Figure J-53 (Appendix J) the average T-value is approximately, 250 m^2/d, but initial increases in T values to between 500 and 1000 m^2/d are observed (most probably a coarse gravel layer). S-values increase in a step-like fashion with time from 1 x 10^{-6} to 1 x 10^{-3}. The semi-log diagnostic plot (Figure J-54, Appendix J) indicates that a flow boundary is reached.

The Cooper-Jacob solution for DP18 (Figure J-56, Appendix J) indicates a T-value of 342 m^2/d, storativity of 9.3 x 10^{-7}, effective borehole radius of 32 m and a recommended borehole yield of 13.2 l/s.

The Basic FC solution (Figure J-57, Appendix J) indicates the following:

- T_{early} = 119.0 m^2/d
- T_{late} = 70.5 m^2/d
- S_{late} = 5.5 x 10^{-4}/d
- Yield 68% risk = 1.3 l/s
- Yield 95% risk = 1.1 l/s.

Initially, it seems that the FC method is not very applicable to primary aquifers. This is particularly true if the performance of this borehole over the past 10 years (see later, in Wellman Appendix K) is investigated. DP18 yielded between 10 and 12 l/s continuously on a sustainable basis with minimal drawdown over the past nine years of abstraction. However,

the poor results are self-explanatory if a fixed head boundary (representing the Olifants River) is included 50 m from DP18 in the advanced solution. The sustainable borehole yield increases to 10 l/s, which confirms the long-term field results. The FC method therefore emphasises the importance of the constant head boundary (river) in determining the sustainable yield of this aquifer. A further important question that needs to be answered, in terms of DP18 is: "Exactly where does this high yielding, good quality water in DP18 come from?" From the Olifants River alluvial aquifer or a palaeochannel situated in the Cango River? Isotope analysis confirmed that it is not TMG groundwater seeping into the river.

6.4 SUMMARY

Table 6-4 summarises the hydraulic properties of the TMG Aquifers in the Klein Karoo areas.

TABLE 6-4: HYDRAULIC PROPERTIES OF THE TMG AQUIFERS IN THE KLEIN KAROO AREA

Borehole	CD Pump Rate (l/s)	Yield FC (l/s)	RWL (m.bgl)	FC-Method Transmissivity (m^2/day)		Storativity*	Geological Formation
				Early Time	Late Time		
VR6	15.4[A]	7	46.9	29 (17)	7	1.0×10^{-3} (1.6×10^{-7})	Peninsula
VR7	20.0[A]	20	78.0	168 (276)	144	1.1×10^{-3} (1.6×10^{-12})	Peninsula
	25.0[B]		63.3	424 (229)	161	2.2×10^{-3}	
	35.0[B]		63.3	182 (191)	39	2.2×10^{-3}	
VR11	8.3[B]	12	125.5	112 (161)	90	1.1×10^{-3} (4.3×10^{-9})	Peninsula
VG3	8.8[B]	5	7.1	43.6 (20.6)	13.3	2.2×10^{-3} (2.8×10^{-6})	Nardouw
DP28	20.2[A]	10	101.0	265 (216)	10	2.2×10^{-3} (1.8×10^{-6})	Nardouw
DP15	-	15	90.0[B]	66 (86)	43	2.1×10^{-3} (1.7×10^{-6})	Nardouw

Note:
( ) – Cooper -Jacob Method (Van Tonder & Xu, 1999).
* – Obtained from late time-drawdown data.
RWL – Rest waterlevel.
A – Pump test conducted in 1997.
B – Pump test conducted in 1990.

SVF-Method Storativity = 5.5×10^{-3} (Van Tonder & Xu, 1999)
Murray (1996) in Woodford (2001): Borehole VR11
Drawdown Late-T = 103 m^2/day.
Drawdown Early-T = 18 m^2/day.
Recovery T = 18 m^2/day.
$S_F = 2.0 \times 10^{-5}$ $S_M = 5.6 \times 10^{-4}$

In most cases, the estimated T and sustainable yield values obtained from the Cooper-Jacob method are higher than those obtained from the FC-method. The FC method provides far more realistic estimates for S than the unrealistically low values obtained from the Cooper-Jacob method. The FC Method is a good method to determine aquifer parameters for secondary and primary aquifers, if the boundary conditions of the system are known.

The FC analysis results for the Peninsula Aquifer show that no major fracture is intercepted in VR6 and 11 and flow represents mainly matrix flow originating from various scales of brittle fracturing of the Peninsula Aquifer. On the contrary, VR7 intercepts a much higher yielding, interconnected fracture system. However, the main water-bearing feature (boundary condition) has not been intercepted during testing. Around the Keystone Block Aquizone (along the Rooikrans, Vermaaks and Brillkloof Faults), T values range between 150 and 200 m^2/d, respectively. These values are consistent with T estimates for the Boschkloof Wellfield near Citrusdal (Hartnady and Hay, 2000). T values of the brittle matrix reduces from 100 to 10 m^2/d (averaging around 50 m^2/d) in an ellipsoidal geometry away from these fracture zones. True radial flow conditions are not found, in which case T values are expected to increase to 1000 m^2/d and more.

In the Nardouw Aquifer, matrix flow is more predominant. The remote sensing data indicated a lower fracture density and poor connection with the recharge zones. Fractures may have T values up to 200 m^2/d, eg. DP28, but they are of limited extent and with long ground water residence times, as indicated by the Carbon-14 ages. Average matrix transmissivity is estimated to be 50 m^2/d in the vicinity of fractures and considerably less in the absence of fracturing, possibly < 1 m^2/d.

The derivative plots for the Peninsula Aquifer deviate from those observed in Karoo and Nardouw Aquifers. In both the last-mentioned cases, matrix flow is more predominant and of a different style than that in the Peninsula Aquifer. This is not surprising considering the difference in fracturing styles of the above-mentioned aquifers. The higher clay content of the Nardouw and Karoo Aquifer rocks and consequent ductile nature, gives rise to intense micro-fracturing across different layers, providing typical double porosity with larger-scale fracturing also present. On the contrary, the brittle nature of the Peninsula Aquifer rocks can provide very high yielding boreholes with almost radial flow conditions.

Table 6-5 summarises the results of FC and Cooper-Jacob analysis carried out using the geometric mean of the final drawdown of constant discharge test and the distance to the main water strike. The available drawdown used in Table 6-4 (difference between the rest water level and the main water strike) is also shown in Table 6-4. Comparison of the results in Tables 6-4 and 6-5 show the following:

- The selection of available drawdown has a great impact on the sustainable yield.
- The Cooper-Jacob method in the new FC spreadsheet gives very reliable sustainable yield estimates for fractured aquifers.

- In general early T values are higher and late T values lower, using more conservative (lower), estimates for available drawdown.
- The available drawdown selection does not impact on S values.
- Cooper-Jacob late T estimates are higher than those of the FC Method.
- For both available drawdown scenarios, unreasonable S estimates are obtained with the Cooper-Jacob method.
- Unrealistic low sustainable yield estimates (with the FC method) show that more complex boundary conditions are required, for better yield estimates eg. in the case of DP18 and VG3.

TABLE 6-5: SUMMARY – SUSTAINABLE YIELD AND AQUIFER PARAMETERS, USING BEST AVAILABLE DRAWDOWN ESTIMATE

Borehole	AD (m) *	Sustainable Yield (l/s) – CJ #	Sustainable Yield (l/s) - FC	Early T (m^2/day)	Late T (m^2/day)#	S #
VR6	104 (170)	7.6	4.4	30	6 (23)	1.1×10^{-3} (4.4×10^{-9})
VR7	25 (40)	13.0	13.3	209	144 (172)	1.1×10^{-3} (2.4×10^{-7})
VR11	27 (49)	12.5	10.7	111	90 (177)	1.1×10^{-3} (4.4×10^{-9})
VG3	68 (100)	5.5	2.6	43	5 (28)	2.2×10^{-3} (2.3×10^{-8})
DP15	38 (100)	6.7	5.9	49	33 (78)	1.1×10^{-3} (5.4×10^{-10})
DP28	100 (40)	21	19.4	265	104 (124)	2.2×10^{-3} (2.3×10^{-4})
DP18	6 (5)	10.6	0.5	113	70 (657)	2.2×10^{-3} (6.3×10^{-10})

- Basic drawdown used for FC and Cooper-Jacob simulations in Table 6-4.
- # All values in brackets, represents the results for the Cooper-Jacob method in latest FC spreadsheet, using best available drawdown estimate.

The above confirms the conclusions of van Tonder (2001), in that the most reliable sustainable yield is obtained when the position of the main water strike is reached during the constant discharge test. By using the final drawdown of the constant discharge test as the available drawdown, a conservative estimate for sustainable yield is usually simulated. For shallow water strikes, the geometric mean final drawdown and position of the main water strike is preferred for available drawdown, where the main water strike is not reached during the test. For very deep water strikes, where the final drawdown is still far above the main water strike, the geometric mean, could lead to an over-estimation of the sustainable yield (as illustrated by DP28, Table 6-5).

6.5 BOREHOLE EFFICIENCY CALCULATED FROM STEP DRAWDOWN TEST RESULTS

Woodford (2001) shows the following from the analysis of step drawdown, test data, carried out at VR11 in the Vermaaks River Wellfield in 1991 and 1997, respectively:

- The 1997 test was carried out at lower water level conditions. The rest water level was 141.7 m.bgl (1991) as opposed to 125.5 m.bgl in 1997, and a fracture yielding 2 l/s at 139 m was dewatered.
- The hydraulic efficiency of VR11 was significantly lower in 1991 when compared to the 1997 test, despite the fact that the fracture at 139 m.bgl was still saturated (see SW/Q curves in Figure 6-2, adapted from Woodford, 2001). This is probably due to the gradual 'development' of the borehole over time after pumping started in 1993 as opposed to the 1991 test, which was carried out on an undeveloped borehole directly after completion of the drilling.
- The step-drawdown test will indicate at what discharge rate the water level has 'stabilised' in the short-term above 148 m.bgl (Figure 6-2A, adapted from Woodford, 2001). The geological log indicates the presence of a fracture at this depth that 'may be water-bearing'.

FIGURE 6-2: BOREHOLE VR11 –WATER LEVEL AND SW/Q VARIATIONS DURING STEP-DRAWDOWN TESTS CONDUCTED IN 1991 AND 1997 (ADAPTED FROM WOODFORD, 2001)

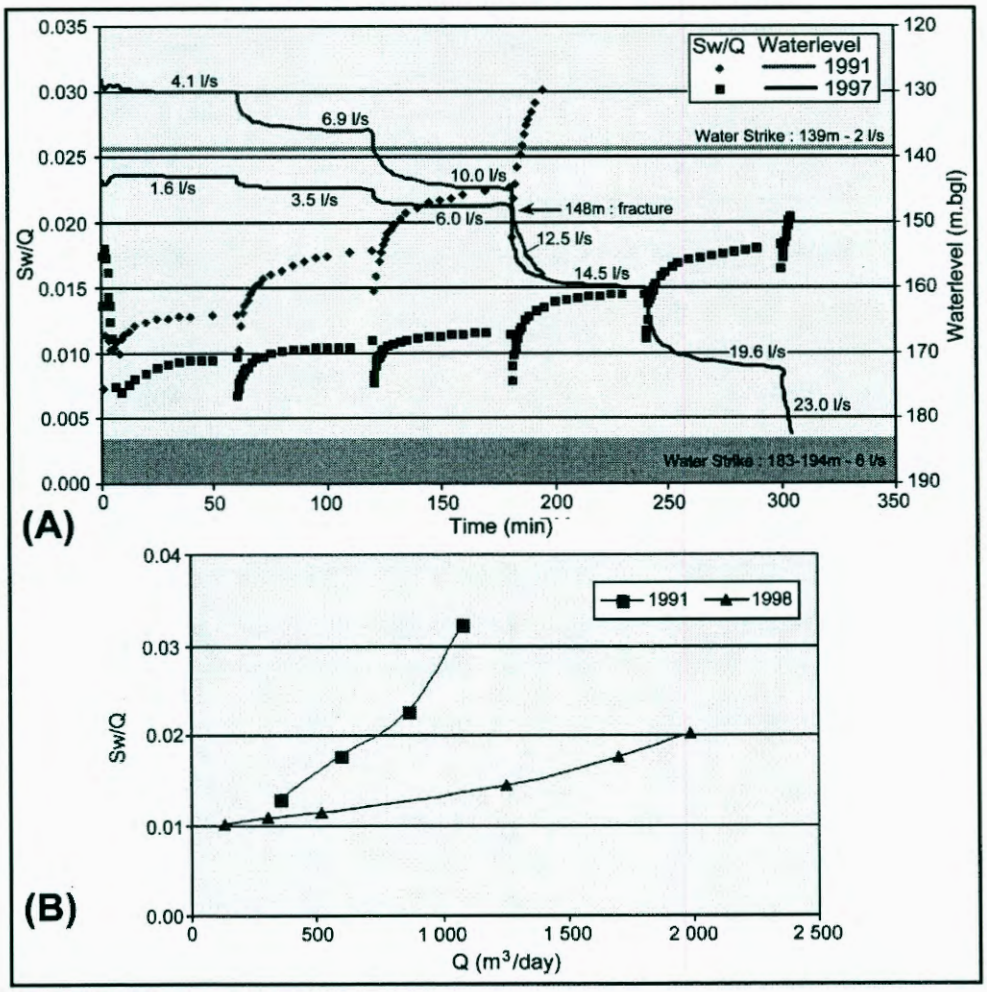

Woodford (2001) has shown the values of a properly executed step drawdown test, where the full discharge capacity of the borehole has been tested. This involves increasing the pumping rate gradually to draw the water level down to the depth of the last, major water strike. Step drawdown tests are also useful to determine the effectiveness of borehole screens and rehabilitation. Woodford shows how a nine-stage step drawdown test was used to test borehole efficiency before and after screen replacement and rehabilitation.

Table 6-6 summarises the borehole efficiencies calculated from step drawdown tests carried out at the production boreholes of the Eastern Sector of the KKRWSS. From Table 6-6 it can be seen that boreholes efficiency is low in boreholes where matrix flow plays a role (Nardouw Aquifer). The prevailing flow regime, i.e. fracture versus matrix flow, has major implications for borehole construction, i.e.matrix flow will require a more effective screen.

All the boreholes except the VR boreholes have highly effective Johnson screens. The VR boreholes are equipped with highly ineffective PVC screens. The borehole performance over time and test pumping analyses, show that irrespective of the poor screen, the Peninsula Aquifer has higher borehole efficiencies, as indicated by the borehole performance over time and test pumping analysis. The efficiency of borehole drilled in the Peninsula Aquifer seems to increase over time with borehole development. The above is explained by the presence of less shale formations in the Peninsula Aquifer and prevailing oxidizing groundwater redox conditions, leading to the absence of bacteriological clogging of the boreholes (see Figure 6-3 for an example).

It is relevant to note that the production boreholes of the Varkieskloof, Bokkraal and Droëkloof Wellfields are not good examples of typical Nardouw Aquifer boreholes. They are all situated on an over-folded sequence of Nardouw and Enon Group sediments with thick shale layers, containing pyrite-quartz veins and low pH groundwater in natural reducing conditions.

The transmissivity of TMG fractured aquifers, is high and screens should be avoided as far as possible to prevent turbulent flow conditions. The effectiveness of the boreholes in the Peninsula Aquifer can be doubled by using limited screens lengths only, to protect the pump. A borehole such as VR7 can easily yield > 35 l/s, as indicated by test pumping. However, the diameter of VR7 restricted testing to a pump that can only handle 35 l/s. Further, the low surface area of the screens installed reduced borehole efficiency to 76% at 35 l/s.

TABLE 6-6: BOREHOLE EFFICIENCIES FROM STEP DRAWDOWN TEST DATA

Borehole	Pumping rates (l/s)	Borehole efficiency (%)
DP25	7.0	75.0
	11.3	65.0
	19.0	52.0
	26.0	44.0
DP12	2.4	83.0
	5.4	69.0
	9.2	57.0
	15.5	44.0
	20.8	37.0
	27.1	31.0
DP29	6.1	23.0
	8.3	18.0
	11.1	14.0
DP15	1.7	34.0
	3.6	20.0
	6.9	11.0
	9.4	9.0
DP18	5.7	36.0
	11.1	23.0
	16.7	16.0
	20.0	14.0
DG110	1.9	87.0
	4.0	75.0
	6.0	67.0
	9.6	56.0
	14.6	45.0
	17.7	41.0
DP28	4.4	82.0
	9.4	68.0
	16.8	55.0
	24.9	45.0
	27.7	42.0
VR11	4.1	51.0
	6.9	38.0
	10.0	30.0
	12.5	26.0
VR7	2.8	97.0
	6.5	94.0
	9.8	91.0
	15.3	86.0
	20.2	83.0
	25.9	79.0
	35.0	74.0
VR6	2.4	77.0
	5.0	62.0
	6.7	55.0
	8.6	48.0
	14.3	36.0
	20.8	28.0
VR8	4.2	56.0
	9.5	46.0
	16.0	33.0
	22.0	27.0

In bold – Nardouw boreholes were matrix flow dominates

FIGURE 6-3: EXAMPLES OF IRON-BACTERIOLOGICAL CLOGGING OF BOREHOLE EQUIPMENT

A

B

A represents the clogged pump-inlet of DP28 and B the clogged rising main of private borehole VG2

In the Nardouw Aquifer borehole, construction is more complex, in that the boreholes are prone to collapse in the absence of screens. On the other hand, with screens, the borehole efficiencies are low, even with Johnson screens, due to biofouling and clogging of borehole screens, related iron precipitation and the working of bacteria.

Dissolved oxygen measurements indicate that groundwater is reducing in all those boreholes where biofouling and clogging of borehole screens occur. Inefficient borehole screens and over-pumping lead to turbulent ground water flow in boreholes during pumping, thereby introducing oxygen to a former reducing environment and causing a change in redox conditions, leading to the deposition of minerals and bacteriological growth. Turbulence only happens if the screen entrance velocity, (v), is too high. Therefore if the pumping rate is kept low so that $v < 3$ cm/s, no turbulence occurs. Introduction of oxygen also accelerates the working of bacteria, which speeds up the biofouling process, while the screen provides an increased surface area for deposition. The bacteria are most probably part of the depositional environment during the deposition of the TMG sequence and are present in both the Peninsula and Nardouw Aquifers. The activity of bacteria is controlled by the redox conditions and pH. The low borehole efficiencies in the Nardouw Aquifer are a combination of biofouling and clogging of screens and inefficient borehole screens.

CHAPTER 7: WATER BALANCE

The water balance for the local scale flow sytem of the Vermaaks River catchment and Keystone Block Aquizone within the intermediate scale flow system Kammanassie Mountains is calculated based on the conceptual hydrogeological model formulated in Section 5.4. Thereafter, exploitation potential of the Vermaaks River Wellfield is estimated by a water balance calculation. The water balance takes all the sources (groundwater recharge) and sinks (groundwater outflows from the system) into account, i.e. spring flow and groundwater abstraction. Evapotranspiration losses are already accounted for in the groundwater recharge equation.

For the water balance calculation, various methodologies are applied to determine recharge for the intermediate and local scale catchments. Further detailed aquifer testing analyses are carried out and integrated with recharge calculations in order to fine-tune water balance estimations for the local catchment and to estimate the wellfield capacity of the Vermaaks River Wellfield. Figure 7-1 shows the boundaries of the Kammanassie Mountains catchment, which is taken as the lowest elevation of the Baviaanskloof Formation. The catchment is further subdivided into the following hydrogeological units (surface area of outcrop):

- Peninsula Aquifer outcrops (TMG Window Areas):

    1. Unit 1: Vermaaks Window – 40.6 km^2
    2. Unit 2: Small Window – 7.3 km^2
    3. Unit 3: Large Window – 64.6 km^2

    TMG Window Areas cover a total surface area of 113.4 km^2

- Cedarberg Shale Aquitard outcrop – **17.1 km^2**

- Nardouw Aquifer – **500.2 km^2**

Kammanassie Mountains covers a total surface area of 630.7 km^2

FIGURE 7-1: KAMMANASSIE MOUNTAINS CATCHMENT AREA

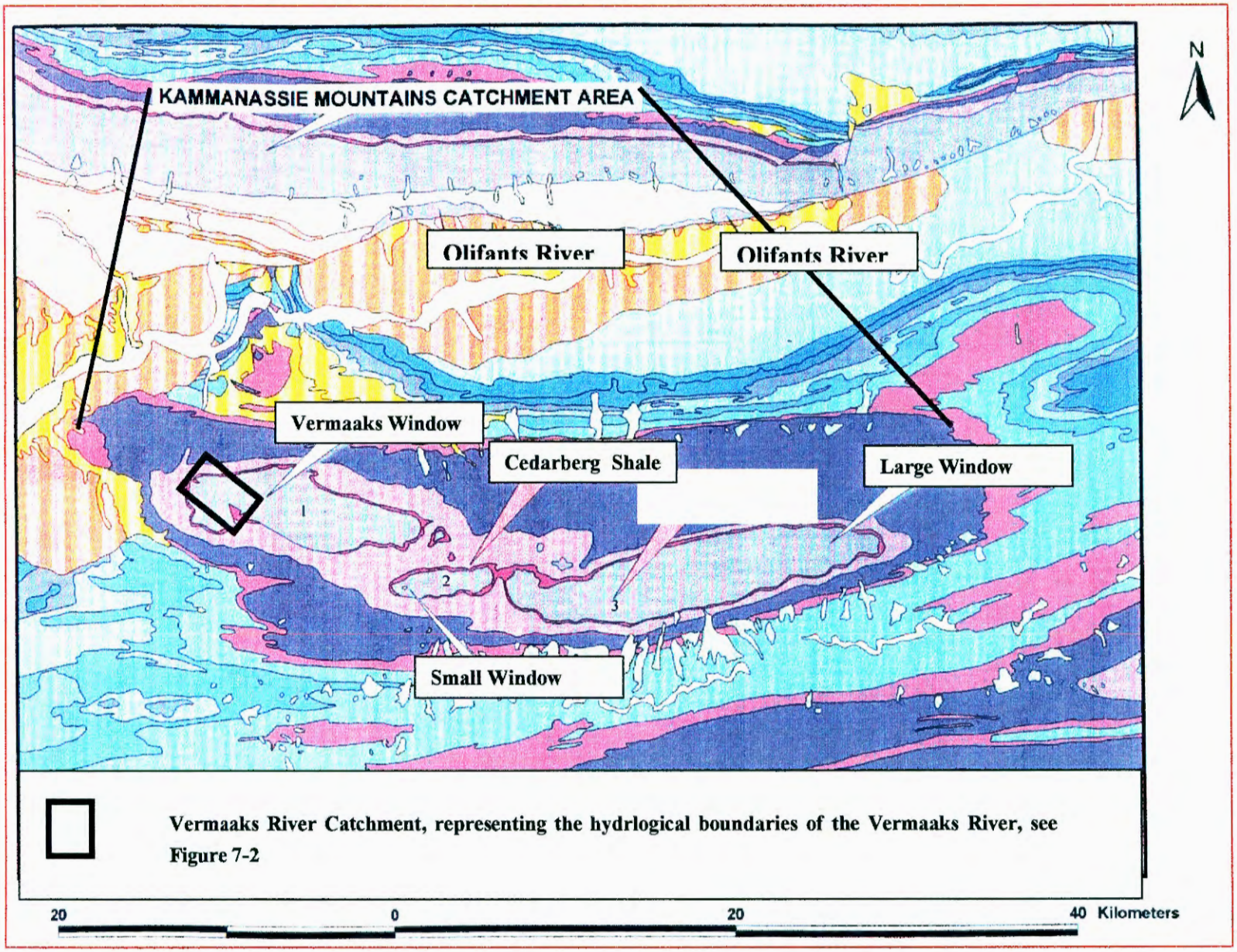

Figure 7-2 shows the Vermaaks River local scale catchment (after Woodford, 2000), which represents the hydrological catchment of the Vermaaks River and covers an area of 10.85 km^2. The C/S Aquitard is presented in Figure 7-2 as the thick red-brown surfaces.

FIGURE 7-2: THE VERMAAKS RIVER LOCAL CATCHMENT AREA

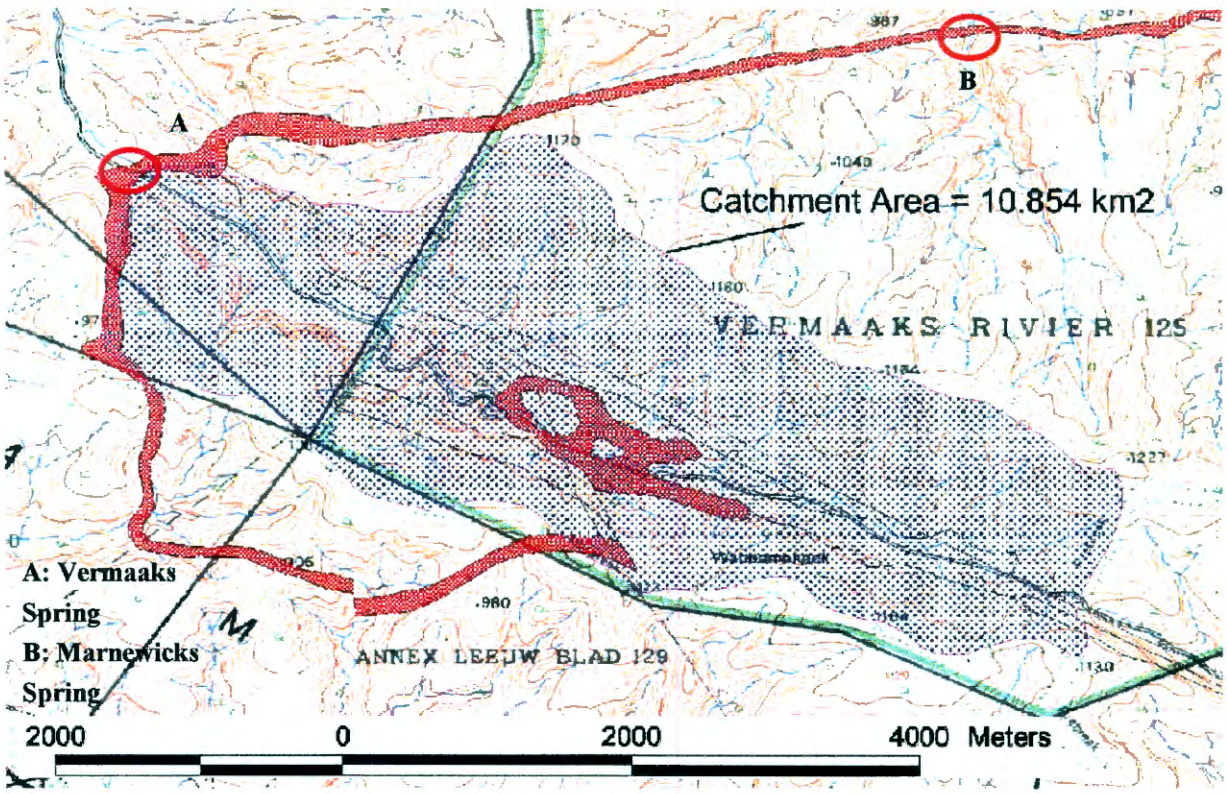

The annual rainfall variations for the Klein Karoo are shown in Figures 3-4 to 3-6. From the above-mentioned, average annual, rainfall figures associated with each of the aquifers of the Kammanassie Mountains are as follows:

- Nardouw Aquifer: 350 mm based on long-term rainfall records for Le Roux Station Rain Gauge and rainfall figures measured at Dysselsdorp, and
- Peninsula Aquifer: 600 mm (Kammanassie Mountain Rain Gauges).

In order to calculate the water balance for the Kammanassie Mountains, it was assumed that recharge is the only source to the system and spring flow and groundwater abstraction the only losses from the system. Recharge and losses from the system (spring flow and abstraction) are calculated. Recharge estimation methodologies make use of the long-term hydrogeological and climatological monitoring information in the Vermaaks River Aquifer Unit. All the recharge estimates, including qualified "expert guesses", are summarised in the newly developed Recharge Excel Spreadsheet (van Tonder *et al.*, 2000) in order to determine the average recharge figure for the Nardouw and Peninsula Aquifers. Thereafter, the safe

yield of the wellfield, obtained from the analysis of aquifer test data, are compared to the results obtained from recharge estimates. The location of the Vermaaks River Wellfield production boreholes are shown in Figures 7-28 and 2-5).

7.1 DISCHARGE FROM THE SYSTEM

The major outflows (losses or discharge) from the Kammanassie Mountains are springflow and groundwater abstraction. The total discharge from the Kammanassie Mountains and local scale Vermaaks River catchment and Keystone Block Aquizone are accordingly calculated in the next two sections. The relevance of the Keystone Block Aquizone is that the Vermaaks River Wellfield and several other boreholes tap this hydrogeological unit.

Groundwater abstraction in the Kammanassie Mountains takes place from four wellfields of the KKRWSS (DWAF) and various boreholes on privately owned land. The cumulative annual abstraction from all the above sources is calculated to determine an estimate for the total amount of groundwater lost to abstraction per annum.

7.1.1 Groundwater abstraction from the LKRWSS

Figure 7-3 (over page) and Table 7-1 summarises the total annual abstraction from the five wellfields of the Eastern Sector of the KKRWSS for the period January 1993 to February 2000. From Figure 7-3, annual abstraction for the Eastern Sector Wellfields never exceeded 1.1×10^6 m^3/a, which is considerably less than the design capacity of the Eastern Sector of the KKRWSS, i.e. 3.3×10^6 m^3/a.

Further, the largest proportion of abstraction takes place from the Vermaaks River Wellfield, situated in the Peninsula Aquifer. Therefore, the present operation is considerably different from the original design. For example, the bulk of the yield (> 60%) is drawn from the Peninsula Aquifer, whereas it was originally planned to draw only 40 % (Table 1, Appendix D) from this aquifer.

Table 7-1 shows the total annual, groundwater abstraction figures for all the KKRWSS, Eastern Sector Wellfields (the actual values presented in Figure 7-3).

TABLE 7-1: TOTAL GROUNDWATER ABSTRACTION, KKRWSS EASTERN SECTOR

	1993	1994	1995	1996	1997	1998	1999	Av
Vermaaks	409885	472467	323043	325400	510292	624680	556714	460354
Voorzorg	69113	122688	65816	95475	84958	111903	125411	96481
Varkieskloof	104557	96811	175185	147113	71679	66895	28375	98659
Bokkraal	220429	157261	195671	200940	52631	18082	21355	123767
Olifants	160658	148416	147955	168040	167241	162120	75266	147099
Droekloof	73645	49071	32293	59087	64042	21233	24480	46264
TOTAL	1038286	1046714	939963	996055	950843	1004913	831601	972625

FIGURE 7-3: ANNUAL ABSTRACTION FROM WELLFIELDS OF THE KKRWSS (ABSTRACTION FOR 2000 UP TO FEBRUARY)

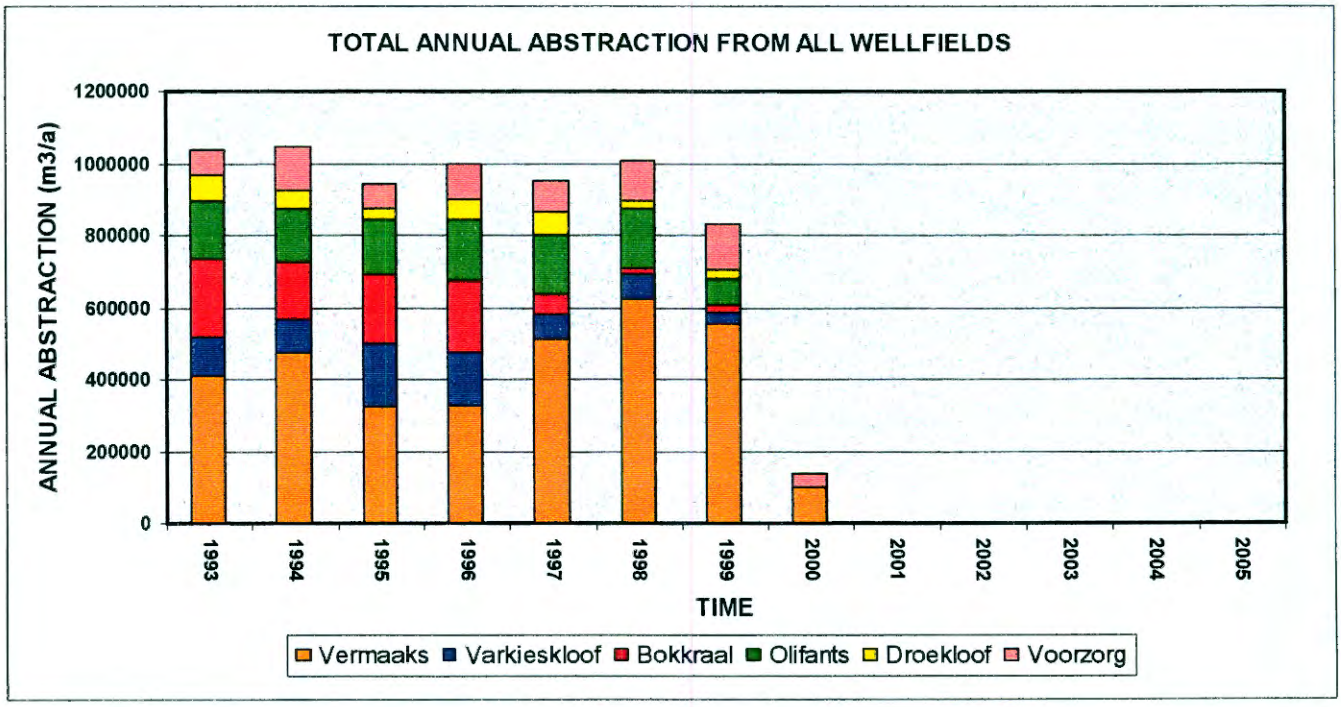

Figures 7-4 to 7-7 represents the annual abstraction from individual boreholes in the Vermaaks Rivier, Voorzorg, Varkieskloof, Bokkraal, Droëkloof and Olifants River Wellfields. The following is observed from the above-mentioned figures:

- Abstraction from the Varkieskloof, Bokkraal and Droëkloof Wellfields (utilizes Nardouw Aquifer) progressively reduces every year. This is partly due to the fact that the boreholes were out of action for most of 1999 and 2000, due to screen replacements and borehole rehabilitation.
- Most abstraction is from the Vermaaks River (utilizes Peninsula Aquifer) and Olifants River (Alluvial Aquifer) Wellfields, in particular boreholes VR7 and DP18.

FIGURE 7-4: TOTAL ABSTRACTION VARKIESKLOOF

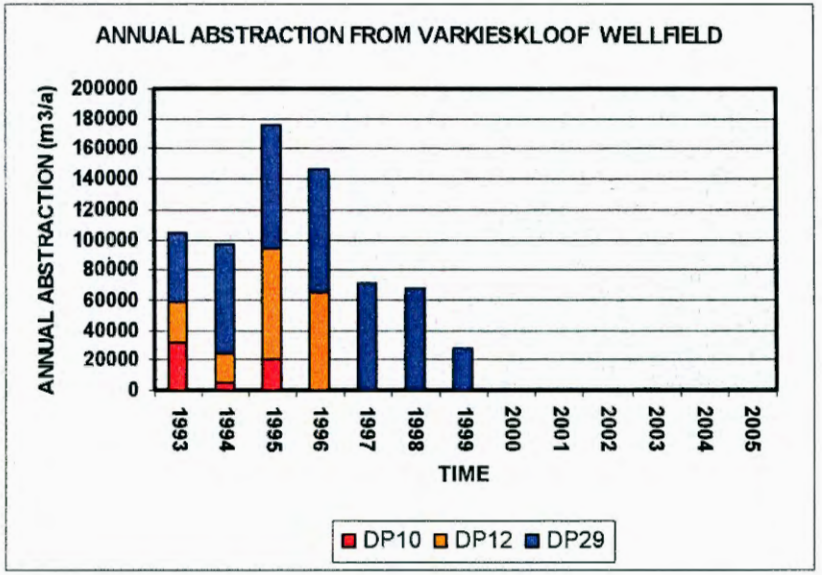

FIGURE 7-5: TOTAL ABSTRACTION DROËKLOOF &OLIFANTS RIVIER

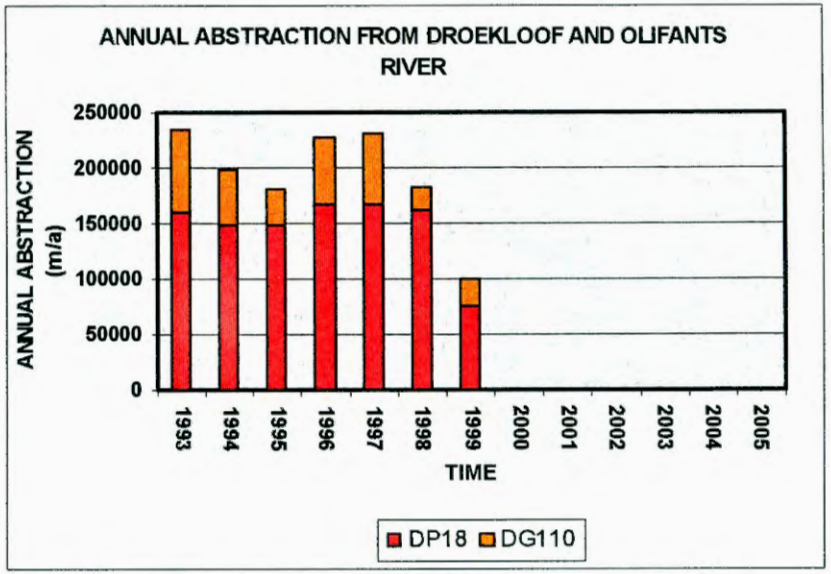

FIGURE 7-6: TOTAL ABSTRACTION VERMAAKS

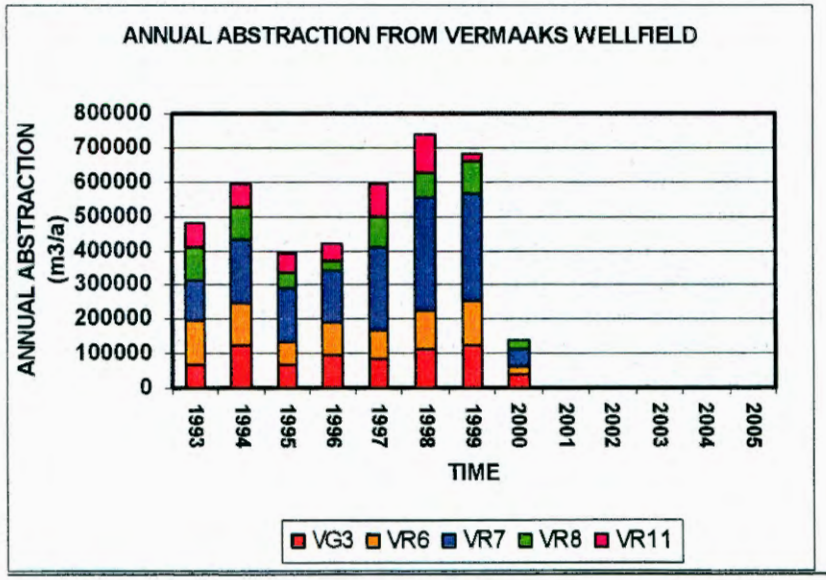

FIGURE 7-7: TOTAL ABSTRACTION BOKKRAAL

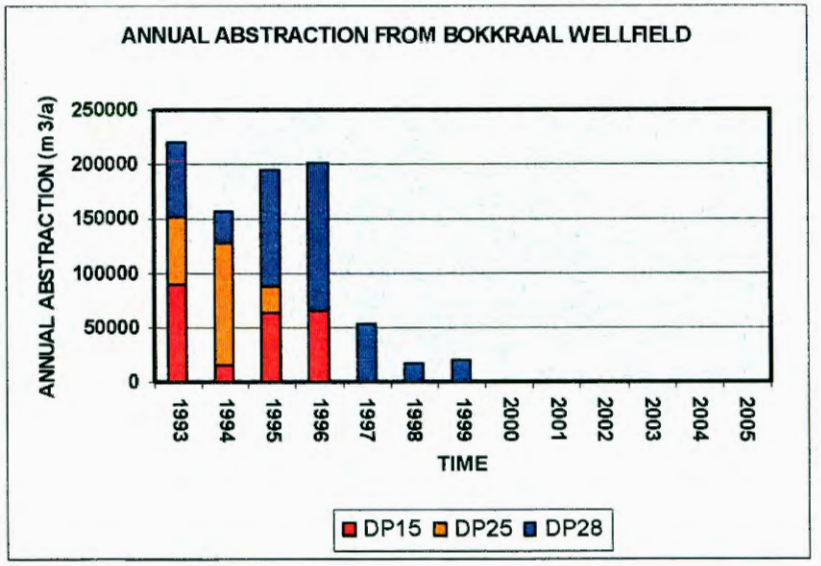

As the Alluvial Aquifer does not form part of the Kammanassie Mountains water balance, it is excluded from the further calculations.

For the water balance calculation, the 1998 groundwater abstraction figures, rather than the average abstraction figures (Table 7-1) are used for the following reasons:

- The current groundwater abstraction scenario (data not incorporated herewith) favours groundwater abstraction from the Vermaaks River Wellfield more than the Bokkraal, Droëkloof and Varkieskloof Wellfields. Therefore, the greater proportion of the Eastern Sector groundwater originates from the Vermaaks and Voorzorg Wellfield.
- Groundwater quality problems and borehole rehabilitation programs interrupted abstraction from the Varkieskloof, Droëkloof and Bokkraal Wellfields, resulting in low abstraction totals from these boreholes.

As seen in Figure 7-4 and Table 7-1, approximately 1.0 x 10^6 m^3/a groundwater is abstracted from the Eastern Sector wellfields of the KKRWSS. From the above-mentioned 0.38 x 10^6 m^3/a and 0.63 x 10^6 m^3/a is utilised from the Nardouw Aquifer (Varkieskloof, Bokkraal, Droëkloof and Voorzorg) and Peninsula Aquifer (Vermaaks Wellfield), respectively.

7.1.2 Other groundwater abstraction in the Kammanassie Mountains

Table 7-2 (over page) summarises the annual abstraction for all boreholes sited in the TMG Aquifer of the Kammanassie Mountains on privately owned land. These figures are obtained from a hydrocensus carried out along the Southern and flanks of the Kammanassie Mountains and abstraction figures obtained from the KKRWSS. All the borehole localities are shown in Figure 2.5.

Table 7-2 shows the following:

- That almost double the amount of groundwater is abstracted on privately owned properties in and around the Kammanassie Mountains compared to that of the Eastern Sector of the KKRWSS.
- Out of a total annual private abstraction figure of 1.6 x 10^6 m^3/a, 0.9 x 10^6 m^3/a of groundwater comes from the Keystone Block Aquizone.
- The total annual abstraction from the Peninsula Aquifer is 0.63 x 10^6 m^3/a.
- The total annual abstraction from the Nardouw Aquifer is 2.0 x 10^6 m^3/a.

- The total annual abstraction from the Keystone Block Aquizone is 1.6 x 10^6 m^3/a.

The total annual abstraction for the Kammanassie Mountains, including the boreholes on privately owned land and the KKRWSS, is estimated to be of the order of 2.6 x 10^6 m^3/a.

TABLE 7-2: SUMMARY OF ABSTRACTION FIGURES FROM THE KAMMANASSIE MOUNTAINS CATCHMENT FOR 1998

Farm / Wellfield	Aquifer	Annual Abstraction (m^3/a)	Notes
Rietfontein	Nardouw	419 703	After flood 1998 < 151000 (m^3/a)
Welgevonden	Nardouw	73 500	Estimated on 7 l/s for 8 hours per day
Wagenpadsnek	Nardouw	197 100	
Leeublad	Nardouw (Aquizone)	260 000	Spring yielding 5-7.5 l/s stopped to flow after drilling of borehole RF2
Rolbaken	Nardouw (Aquizone)	418 100	RF2 next to spring yield 6.9 l/s
Koutie	Nardouw (Aquizone)	250 000	Potential for double the current abstraction
Eilandskraal	Nardouw	50 000	
Scheeperskraal	Nardouw	20 000	Next to Bokkeveld contact
Diepekloof	Nardouw	40 000	Next to Bokkeveld contact
TOTAL PRIVATE ABSTRACTION AQUIZONE = 928 000 (m^3/a)			
TOTAL PRIVATE ABSTRACTION = 1 628 403 (m^3/a)			
Total KKRWSS East	Nardouw and Peninsula	1 000 000	
KKRWSS	Nardouw	380 233	Only eastern Section, including VG3
KKRWSS	Peninsula	626 680	Excluding VG3
TOTAL ABSTRACTION FROM PENINSULA = 626 680 (m^3/a)			
TOTAL ABSTRACTION FROM NARDOUW = 2 008 636 (m^3/a)			
TOTAL ABSTRACTION KAMMANASSIE MOUNTAINS = 2 735 316 (m^3/a)			
TOTAL ABSTRACTION FROM AQUIZONE = 1 554 680 (m^3/a)			

7.1.3 Springflow

Table 7-3 and Figures 7-8 (over page) summarise the spring flow measured in the Vermaaks and Marnewicks Springs, both Type 2.1 springs (see Section originating 5.3). The positions of the above-mentioned springs are shown on Figure 7-2. The Marnewicks' spring originates

approximately 40 m lower in the profile, than the Vermaaks Spring and the data record is complete for the period March 1991 up and until December 1999.

Although a watershed separates the two surface water drainage basins of the Vermaaks and Marnewicks River systems, both springs drain from the same groundwater compartment, delineated by the C/S Aquitard (Figures 2-5 and 7-2). Spring flow mimics the rainfall and spring discharge is a function of both seasonal and annual rainfall. The average annual flow for the Vermaaks and Marnewicks Springs, together with annual abstraction from the Vermaaks River Wellfield (excluding Voorzorg, i.e. VG3) is presented in Table 7-3.

From Table 7-3 it can be seen that, the Marnewicks spring flow varies only with variation in rainfall, whereas the Vermaaks River spring flow varies with groundwater abstraction and rainfall. In general, the rainfall over the past three years has considerably fewer peak rain events in excess of 100 mm (Figure 7-8) than previously.

TABLE 7-3: SUMMARY OF AVERAGE ANNUAL SPRING FLOW FROM THE VERMAAKS AND MARNEWICKS SPRINGS

YEAR (Calendar)	Annual abstraction (m^3/a) *(l/s)	Annual Rainfall (mm) Wildebeesvlakte	AVERAGE ANNUAL FLOW V-NOTCH (l/s)	
			Vermaaks (l/s)	Marnewicks (l/s)
1992	0 (0.0)*	571.1	18.2	No data
1993	409885 (13.0)	552.0	10.1	No data
1994	472467 (15.0)	492.5	6.0	12.5
1995	323043 (10.2)	641.3	6.2	12.3
1996	325400 (10.3)	673.0	6.1	13.4
1997	510292 (16.2)	778.5	9.9	15.9
1998	624680 (19.8)	367.0	4.6	10.6
1999	556714 (17.7)	401.0	3.5	10.6
TOTAL	**3223481 (102)**	**4476.3**	**64.6**	**75.4**

Rainfall events recharge fractures in the Peninsula Aquifer across the Kammanassie Mountains and forces groundwater to exit in the form of baseflow in streams in order to accommodate the rainwater. This effect is further buffered by recharge in the Outeniqua Mountains with a lagged response (regional flow system). The C/S acts as a no-flow boundary and causes overflow once the Peninsula Aquifer is saturated. Groundwater abstraction in the Peninsula Aquifer, removes water from storage and at the same time gives way to newly recharged groundwater. Depending on the prevailing rainfall scenario, groundwater abstraction may reduce spring flow over time, if the rate abstraction exceeds the

natural recharge rate. The reduction in spring flow can be short or long-term, depending on the variation in rainfall and the recharge capacity of the peak rain event every 5 to 10 years.

FIGURE 7-8: MONTHLY SPRING FLOW VERSUS RAINFALL

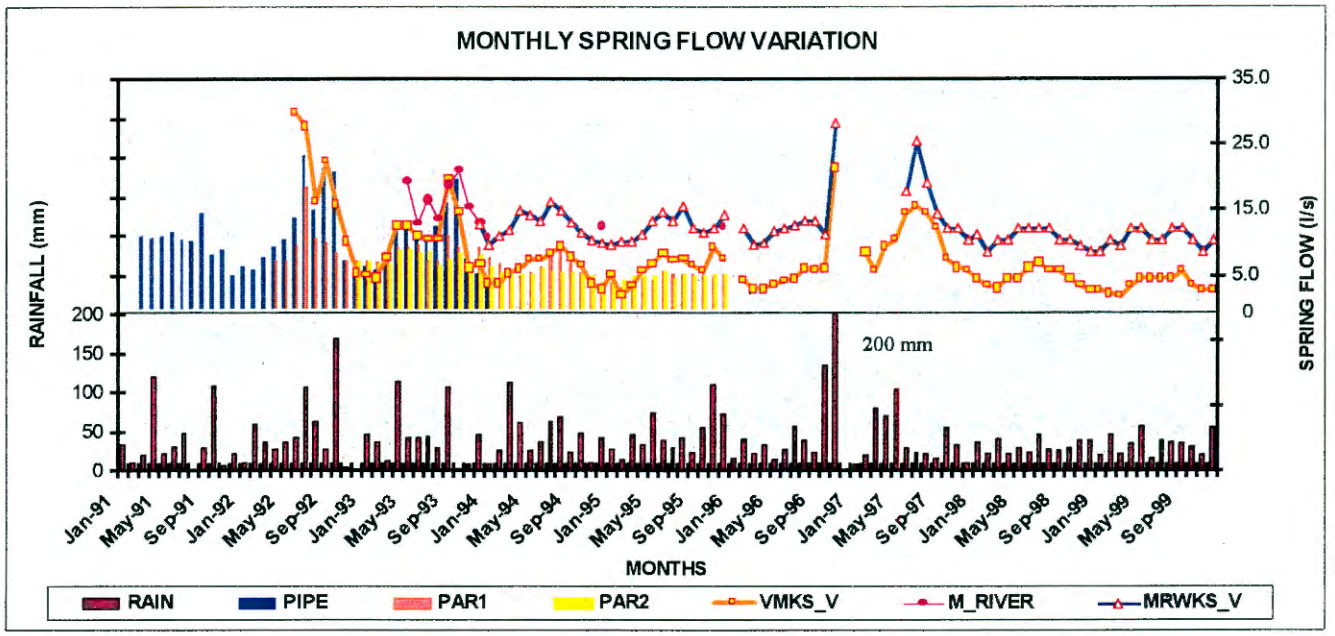

Analysis of spring flow and rainfall data shows that recharge is significantly more from a single rain event of 100 mm, compared to that of five rain events with a cumulative total of 100 mm, based on daily rainfall data (obtained from Weather Bureau). In most cases, the peak rain events, occurred over a period of 2 to 4 days.

Midgley et al. (1994) showed that high stream flows during peak rainfall events are due to higher groundwater released as baseflow, rather than surface water run-off. Significant rain events recharge the Peninsula Aquifer only once every five to 10 years. In the absence of abstraction, the Peninsula Aquifer is saturated and most recharged groundwater will essentially flow away, as incoming water replaces groundwater ejected from storage. Thus, controlled abstraction over a five to 10 year period could create enough storage to accommodate the peak rain events and reduce run-off significantly. However, it is noted that a long lag between rainfall and recharge can be expected over a period much longer than the rainfall event itself.

Abstraction has taken place from four production boreholes upstream of the C/S Aquitard in the Vermaaks River Wellfield since 1993. Annual abstraction from the wellfield is approximately 0.5 x 10^6 m^3/a (15.8 l/s). As spring flow was not monitored prior to the start of groundwater abstraction, it is difficult to determine the potential reduction in spring flow

as a result of abstraction. Over the period 1993 to 1999, rainfall and spring flow varied between 370 and 780 mm/a and 3.5 and 10.1 l/s, respectively. Over the same period groundwater abstraction yielded between 10 and 20 l/s. Therefore groundwater abstraction yields much more groundwater, than what was accessible / available, prior to abstraction, at the expense of a proportion of spring flow. However, over the long-term the possibility exists that spring flow may reduce further, indicative that the aquifer storage contribution to abstraction is increasing over time, if abstraction exceeds recharge and water levels decline.

Whittingham (1969) summarised stream flow data collected in the Klein Karoo for 1969. From rainfall records, of rain gauges in the Swartberg Mountains, 1969 represents a below average rainfall year (1423 mm, relative to the 20-year average of 1574 mm). It is therefore postulated that the spring flow estimate of Whittingham represents a below average flow figure for the Vermaaks Spring. Whittingham reports a minimum summer flow of 10 l/s for the old Vermaaks weir (not onto bedrock). Unfortunately, no flow measurements are available for the Marnewicks River. The best estimate for minimum flow of the Vermaaks Spring, prior to abstraction from the Vermaaks River Wellfield, is of the order of 10 l/s (0.32 x 10^6 m^3/a).

Based on a yield of 10 l/s for the Vermaaks River spring, groundwater abstraction over the period 1993 to 1999 yields approximately 14 l/s more groundwater, at the expense of a 6 l/s proportion of spring flow for the same period. However, if abstraction is controlled over the long-term the possibility exists that spring flow can increase over time, indicating that the aquifer storage contribution to abstraction is decreasing over time, if abstraction is less than recharge and water levels rise. Unfortunately, the opposite is also true.

In the absence of complete spring flow records, from before the start of groundwater abstraction, spring flow yields were estimated from available flow records for the Kammanassie Mountains and personal experience. Spring flow figures of 10, 12 and 40 l/s are postulated for the Vermaaks, Marnewicks and Huis River systems, yielding 62 l/s (2.0 x 10^6 m^3/a) in total. Of this spring flow total, the Vermaaks and Huis River systems drain the Keystone Block Aquizone, yielding 50 l/s (1.6 x 10^6 m^3/a).

7.1.4 Total Discharge from the Kammanassie Mountains

The total outflow from the Kammanassie Mountains hydrogeological unit can now be estimated, as follows:

- Total groundwater abstraction from the Nardouw Aquifer: 2.0 x 10^6 m^3/a.

- Total groundwater abstraction from the Peninsula Aquifer: 0.6 x 10^6 m^3/a.
- Total spring flow (Peninsula Aquifer only): 2.0 x 10^6 m^3/a.

From the above, the total outflow from the Kammanassie Mountains is estimated to be 4.6 x 10^6 m^3/a, of which 1.6 x 10^6 m^3/a drains from the Keystone Block Aquizone.

7.2 RECHARGE

Bredenkamp (1995) concluded that the best recharge estimates for any catchment are obtained by comparison of the results obtained from various methodologies. Therefore, the following methodologies are applied to determine recharge for aquifers of the Kammanassie Mountains:

- Baseflow
- Cumulative Rainfall Departure (CRD) Method
- Area related method
- Carbon-14 storage calculation
- Chloride mass balance method
- Saturated Volume Fluctuation (SVF) method
- Equal Volume (EV) method
- Recharge spreadsheet (van Tonder *et al.*, 2000)
- GIS raster approach (Woodford, 2001)

A brief summary of theory and rationale of each approach is given in Section 2.1.5.5.

7.2.1 Baseflow

The average annual baseflow from experimental TMG mountain catchments (Jonkershoek, Zachariashoek after Bredenkamp *et al.,* 1995*)* reveals a linear relationship with rainfall above a threshold value (of rainfall0. The same applies to the average annual total flow and flood flow components. The average total run-off for different regions is also linear to average annual rainfall. From 55 to 60% of the total run-off constitutes baseflow in the TMG catchments (Bredenkamp *et al.,* 1995), which is controlled by the status of groundwater levels in the catchments. However, Midgley *et al.* (1994) showed that up to 90% of the peak flows after rain events are TMG baseflow in the Jonkershoek catchments (see Section 5.3).

The following average run-off and baseflow figures for the Vermaaks and Marnewicks River catchments is estimated from the regional rainfall and run-off relationships (for Jonkershoek, Zachariashoek after Bredenkamp *et al.*, 1995*)*:

- Runoff: Rainfall measured for the Kammanassie Mountains varies between ~500 and 675 mm/a (Figure 3-6). From the regional rainfall versus run-off relationship, this yields run-off ranging between 50 and 150 mm.
- Base flow: Similarly, baseflow is estimated to range between 50 and 200 mm/a. Therefore, recharge ranges between 10 and 30 % of annual precipitation, respectively.

Recharge for the Jonkershoek catchment is estimated to be approximately 18% of the average monthly rainfall in excess of a threshold figure of about 66 mm. Similarly, recharge is 20% above a 66 mm threshold for the hydrograph separation method. This implies that if rainfall is less than 66 mm per month, recharge will be considerably less, if any. On the contrary, baseflow can increase to more than 90% in peak rain events. Based on the above relationship, recharge for the Kammanassie Mountains is calculated. The results are summarised in Table 7-4. The position of the Marnewicks and Vermaaks River Valleys are shown on Figures 2-5 and 3-1.

TABLE 7-4: RECHARGE IN MM/A FOR THE KAMMANASSIE – BASED ON HYDROGRAPH SEPARATION METHOD (JONKERSHOEK)

CATCHMENT	FORMULA	AV_RF = 500 mm/a	AV_RF = 675 mm/a
JONKERSHOEK	RE = 0.66(RF – 565)	RF too low	72.6
	RE = 0.28(RF-714)	RF too low	RF too low
ZACHARIASHOEK	RE = 0.5(RF–540)	RF too low	67.5
	RE = 0.47(RF-445)	28.9	108.1
EQUAL VOLUME	RE = 0.2(RF-66)	86.8	121.8
RECHARGE RANGE (%)		5-17 %	10-18%

RE = Recharge and RF = Rainfall

Figure 7-9 shows the relationship between rainfall and stream flow for the Vermaaks River. The intercept of the regression line with the y-axis equals baseflow in the absence of recent rainfall and represents previous recharge events. A value of approximately 100 mm equals 4.5 l/s or 15 to 25% annual recharge for rainfall ranging between 500 and 675 mm/a.

Similarly, the streamflow versus rainfall relationships for the Marnewicks v-notch indicates baseflow the order of 143 mm (9.7 l/s) or recharge ranging between 21 and 28 % for rainfall

ranging between 675 and 500 mm/a, respectively. Figure 7-10 shows the rainfall versus streamflow relationship for the Marnewicks v-notch. Note that the Marnewicks v-notch is not constructed onto basement drains a larger catchment and contains no abstraction boreholes upstream of the C/S Aquitard.

FIGURE 7-9: RAINFALL VERSUS STREAM FLOW – VERMAAKS RIVER V-NOTCH

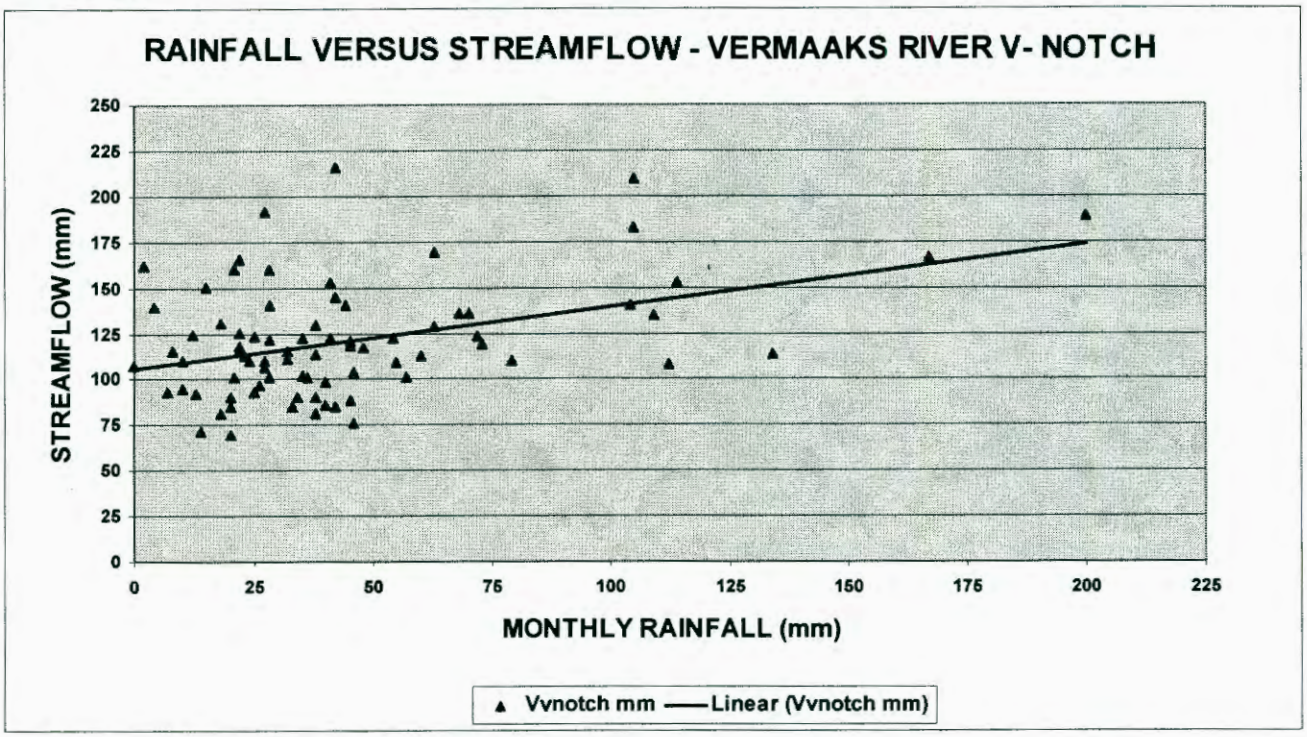

FIGURE 7-10: RELATIONSHIP BETWEEN STREAMFLOW AND RAINFALL – MARNEWICKS V-NOTCH

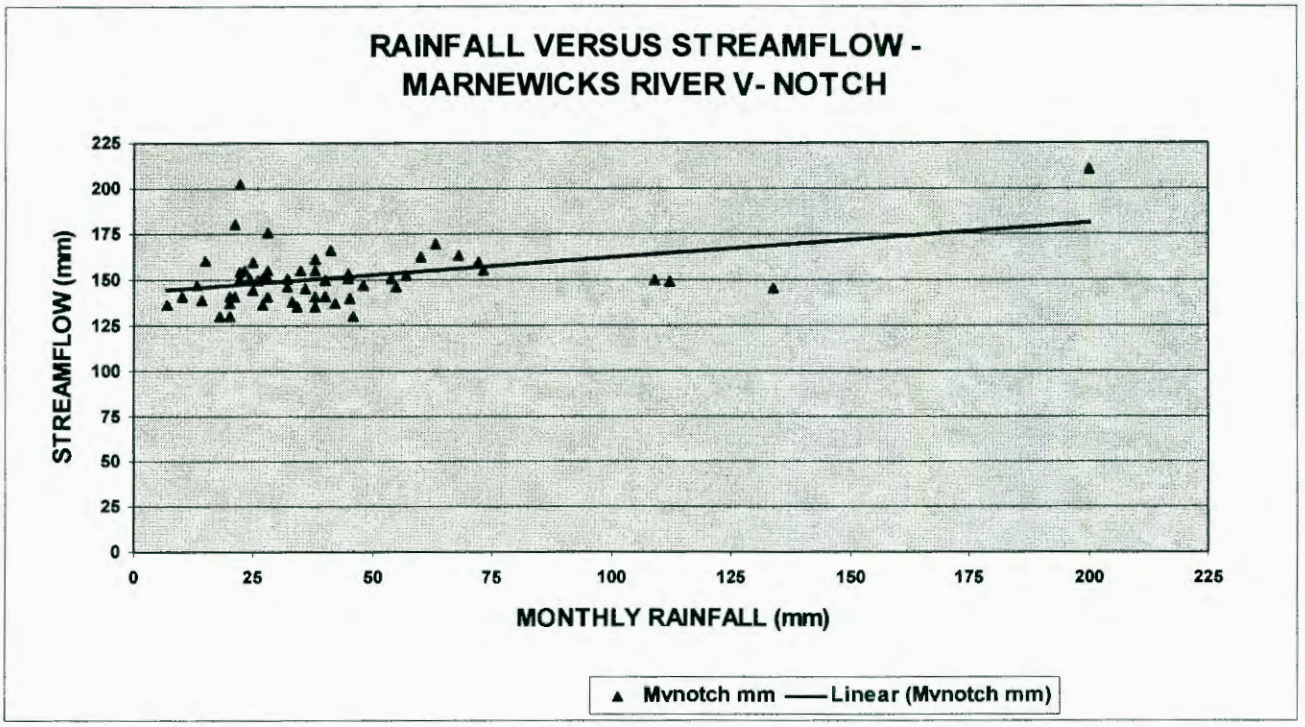

However, from Figures 7-9 and 7-10, the monthly rainfall masks the correlation between rainfall and streamflow. The regression line is not unique, as its slope will change considerably, if one value is removed. Much better results are expected, if daily springflow and rainfall figures are used.

7.2.2 CRD Method

The CRD-method effectively simulates water level variations over time for given rainfall figures. The simulated curve is then calibrated with measured water levels. The CRD method is used to simulate variations of the groundwater table for production boreholes in the Vermaaks River Valley (VG3, VR6, 7, 8 and 11) with and without groundwater abstraction. Rainfall data of the Wildebeesvlakte rain gauge are used (see Figure 3-6). Note that VG3 is situated down-gradient from the C/S Aquitard and falls outside the Vermaaks River local catchment (see Figure 4-8).

Based on a simple analysis of rainfall records, CRD series is generated stochastically by incorporating the effects of a long and short-term memory of rainfall events and abstraction for the following scenarios:

- 3, 6, 12, 24 and 36-month rainfall average values as the short-term memory of the Klein Karoo system.
- For the long-term reference value, the moving average rainfall values for 1 and 3 years preceding a specific month as well as the long-term average mean monthly rainfall (40 mm/month).
- The effect of abstraction is incorporated by subtracting ineffective rainfall, i.e. rainfall lost to abstraction (this required manipulation of the CRD curve to improve the simulated fit). This method still needs to be verified by theory. (Bredenkamp *pers. Comm, 1999*).

The mathematical relationship used for the simulation of CRD curves (after Bredenkamp *et al.* (1995) is presented in Equation 11, page 51.

The best fit between simulated and measured data are obtained with a three month short-term memory for the Vermaaks River system and a long-term memory representing the average long-term monthly rainfall figure, for the Wildebeesvlakte Rain Gauge (CRD 3,av).

Figures 7-11 to 7-15 represent simulated (CRD 3,av) versus measured water levels for production boreholes VG3, VR6, 7, 8 and 11 of the Vermaaks River Wellfield, using the Bredenkamp Formula (Equation 12, page 52). The simulated CRD curve for each of the

above boreholes incorporating the effect of pumping by trial and error adjustment of the k factor, are also shown on each figure. All the above-mentioned figures use groundwater level data from April 1993 until April 1999 and rainfall data from January 1987, to April 1999.

The following observations are made from Figures 7-11 to 7-15:

- Initially, water levels follow the trend of the CRD(3,av) curve closely, whereafter a regressing trend causes a deviation from the simulated and measured water levels.
- The effect of pumping can be simulated by subtracting ineffective rainfall (k-factor).

Table 7-5 summarises the total cumulative abstraction from each production borehole, changes in water levels and rainfall for the period April 1993 to April 1999 to make quantitative deductions from the above relationships possible. The corresponding CRD for the above period for each borehole is also summarised in Table 7-5 (red from the secondary y-axis in the Figures 7-11 to 7-15).

TABLE 7-5: SUMMARY HYDROGEOLOGICAL INFORMATION FOR BOREHOLES VG3, VR6, 7, 8 AND 11

Borehole	Cumulative Abstraction (m^3)	Cumulative Rainfall (mm)	CRD (mm)	Change in Water level (m)**	Relationship between Rainfall and CRD***
VG3	415725	2044*	-100	0.0	5%
VR6	648151	3146	-600	-15.0	19%
VR7	1246235	3146	-500	-20.0	16%
VR8	428419	3146	-400	-21.5	13%
VR11	482077	3146	-600	-28.5	19%
Total VR	2804882"				

* Rainfall taken for VG3 rain gauge (data from August 93 to April 99)

** Change in water level measurements over time (negative, indicates drop in water level0

*** The CRD is expressed as a percentage of the cumulative rainfall measured.

"The cumulative totals are for a 6 year period

It is postulated that the negative CRD values indicate the recharge that was removed by abstraction from storage. This postulation is supported by the regressing trend in water levels and deviation between simulated and measured water levels on Figures 7-11 to 7-15. Annual recharge of the Vermaaks River Wellfield (VR boreholes) is therefore in the order 13 to 19% less than the total annual abstraction, equaling:

$Re = (1 - 0.13) * 2.8 \times 10^6 / 6 = 0.41 \times 10^6\ m^3/a$

Or, $Re=(1 - 0.19) * 2.8 \times 10^6 / 6 = 0.38 \times 10^6\ m^3/a$

FIGURE 7-11: MEASURED VERSUS SIMULATED WATER LEVEL FLUCTUATIONS FOR VG3 (CRD METHOD)

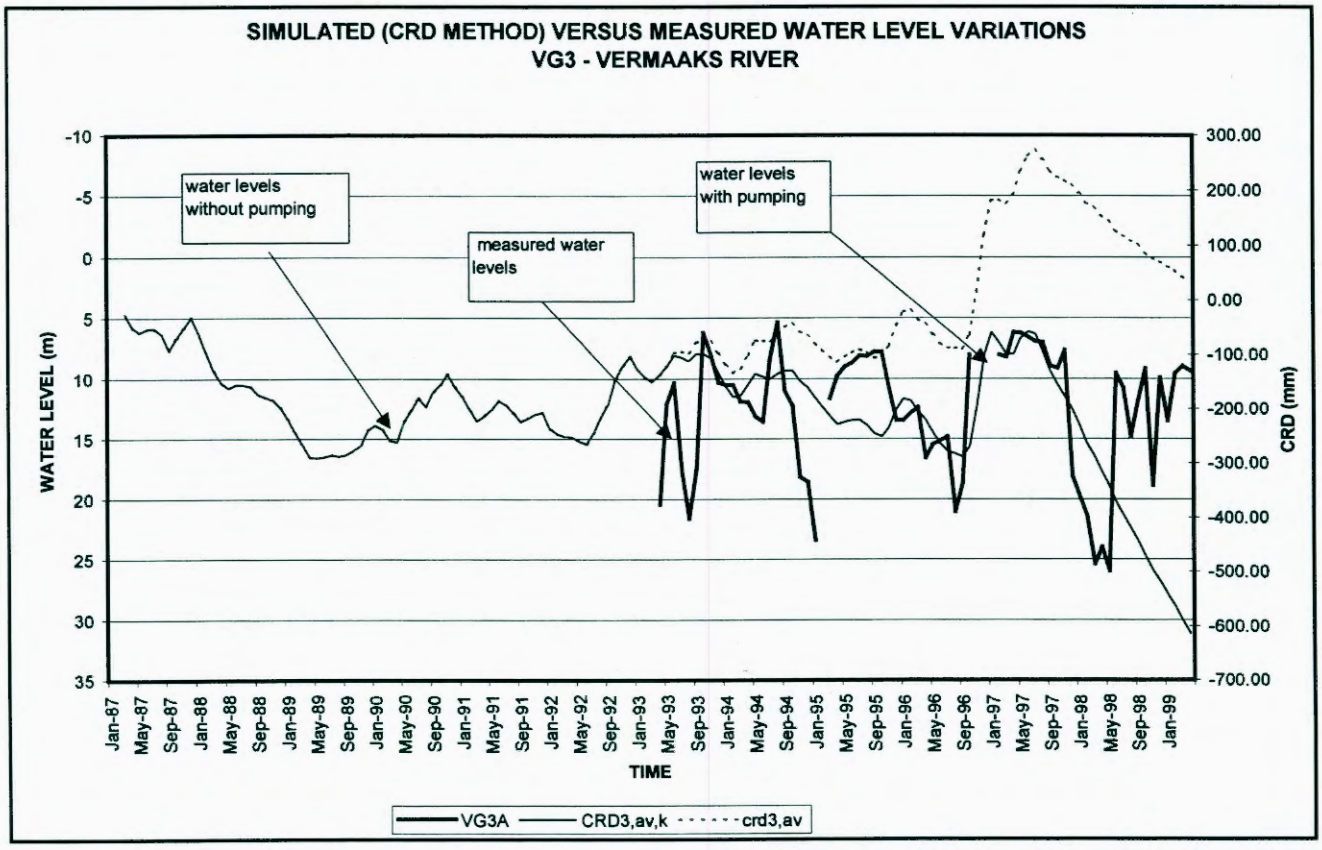

FIGURE 7-12: MEASURED VERSUS SIMULATED WATER LEVEL FLUCTUATIONS FOR VR6 (CRD METHOD)

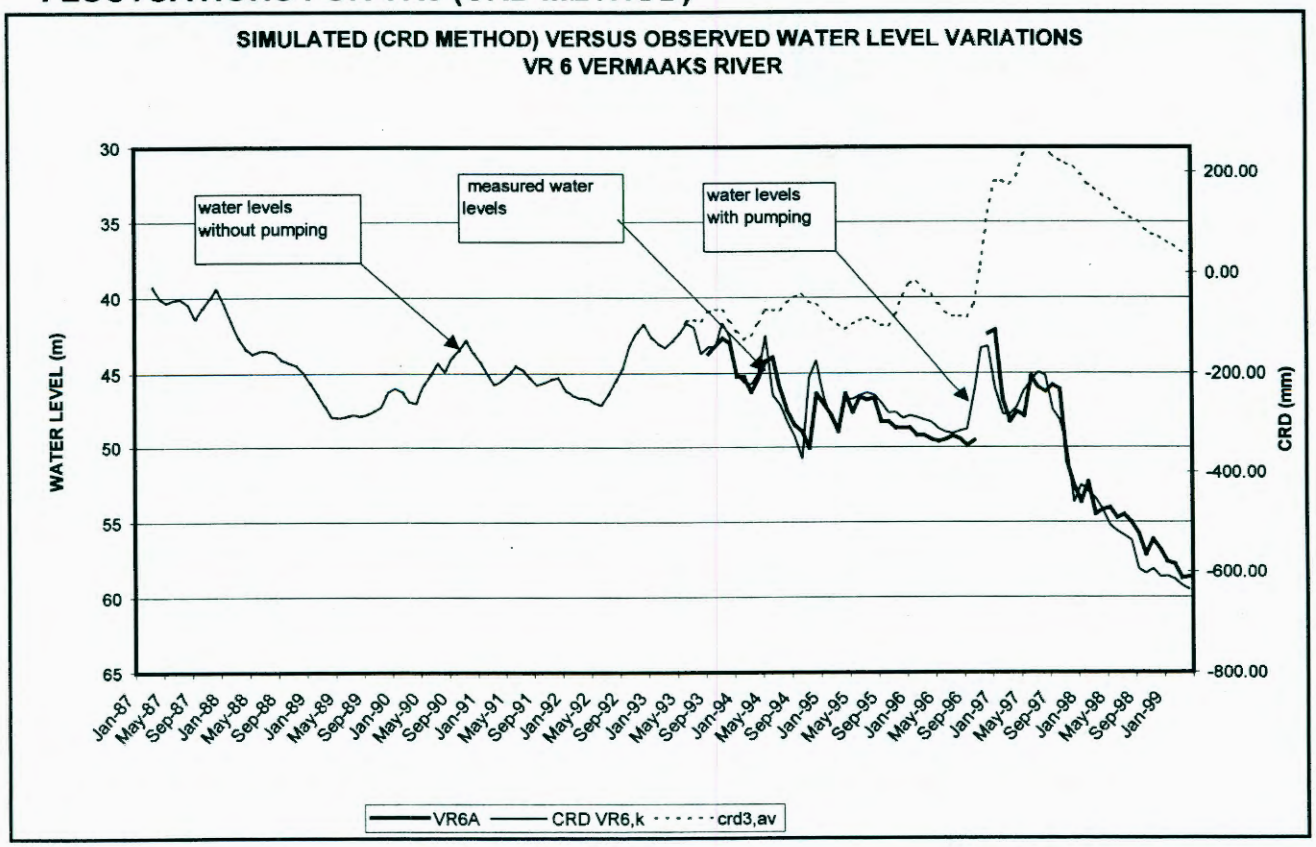

FIGURE 7-13: MEASURED VERSUS SIMULATED WATER LEVEL FLUCTUATIONS FOR VR7 (CRD METHOD)

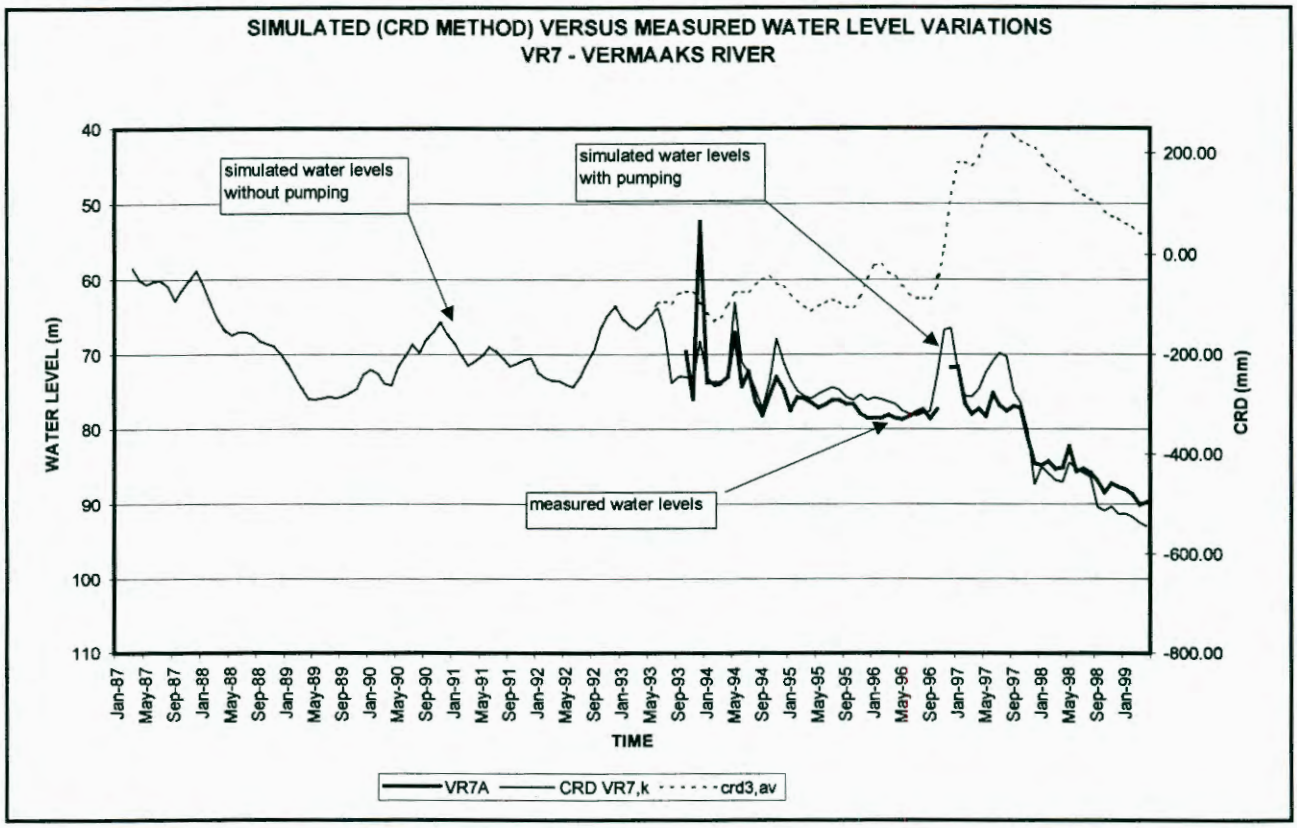

FIGURE 7-14: MEASURED VERSUS SIMULATED WATER LEVEL FLUCTUATIONS FOR VR8 (CRD METHOD)

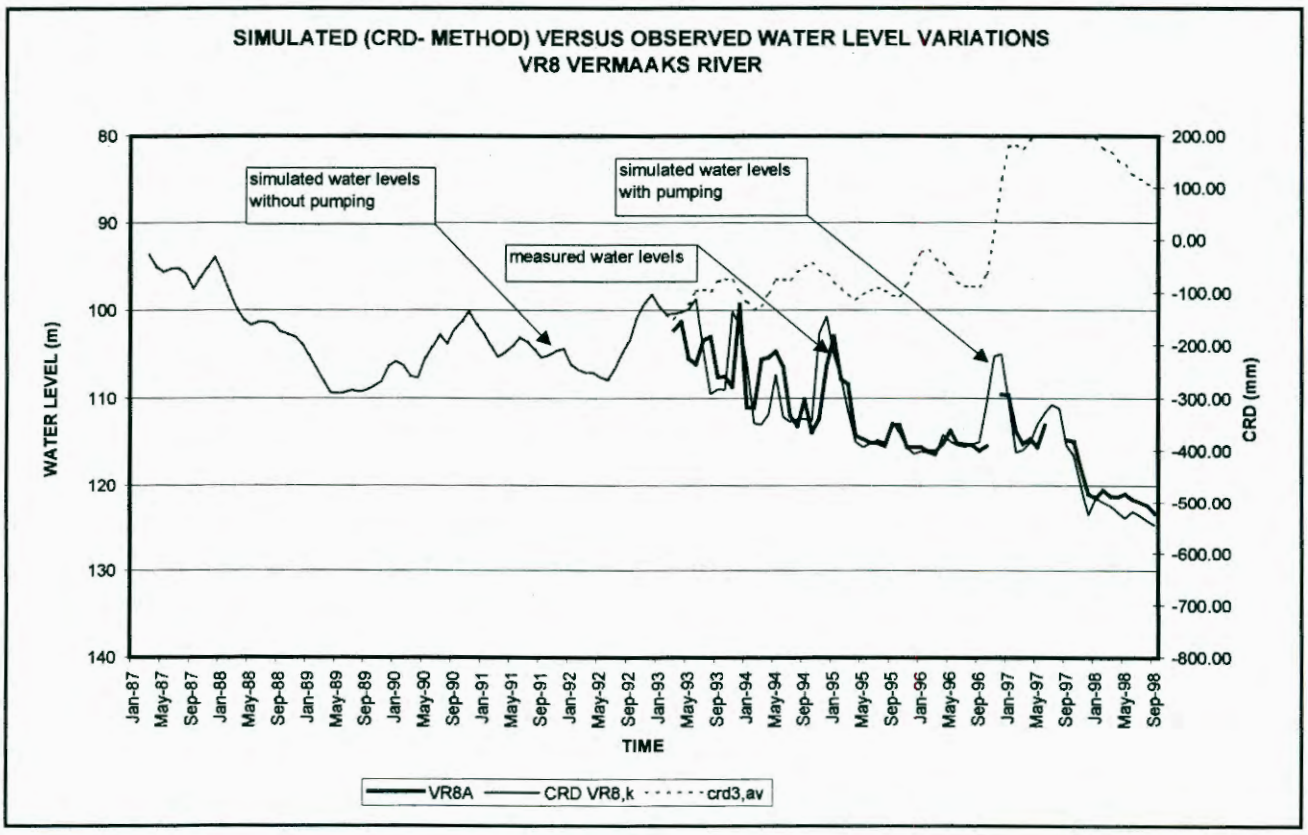

FIGURE 7-15: MEASURED VERSUS SIMULATED WATER LEVEL FLUCTUATIONS FOR VR11 (CRD METHOD)

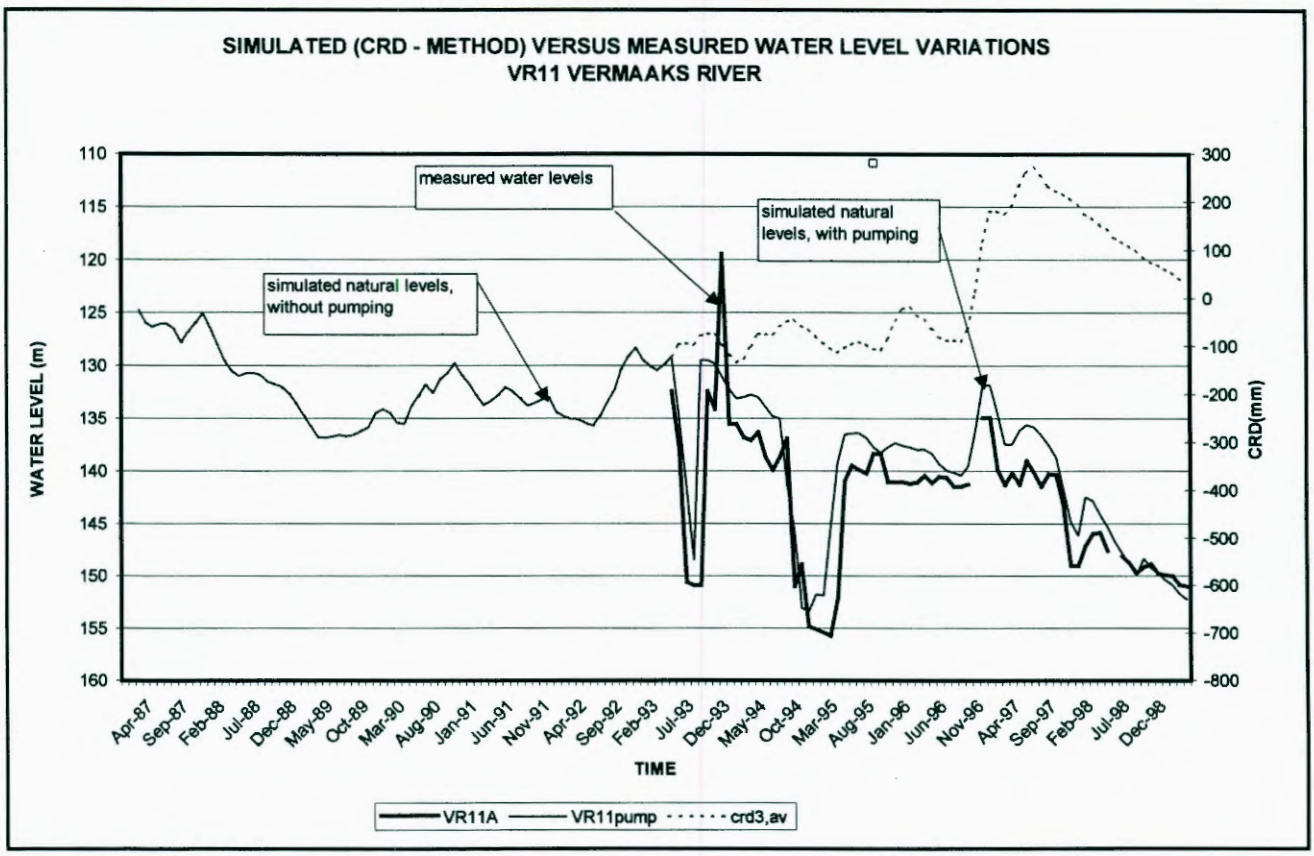

The above recharge estimation is not the sustainable aquifer yield, but only the sustainable wellfield capacity that will not lead to any further drop in water levels.

Figures 7-16 and 7-17 represent CRD simulations, using the latest modification of the CRD method (Equation 14, page 53, after Xu and van Tonder, 2000). The Recharge Excel spreadsheet (developed by Xu and van Tonder, 2000) is used to simulate recharge for the Peninsula and Nardouw Aquifers, respectively. For simulation of recharge of the Peninsula Aquifer, the average water level of the Vermaaks River Wellfield (i.e. boreholes VR6, 7, 8 and 11) and the rainfall data from the Wildebeesvlakte rain gauge are used. Alternatively, the simulation of recharge for the Nardouw Aquifer used the average water level calculated for the Bokkraal, Varkieskloof, Droëkloof Wellfield and VG3 borehole(s) and rainfall data measured at Purification Works East Rain Gauge.

The CRD simulation for the Peninsula Aquifer (Figure 7-16) indicates annual recharge of the order of 14.4 % for cut-off rainfall values of 10 mm/month (rainfall < 10 mm/month will not contribute significantly to recharge). This yields annual recharge of 86.4 mm/a for rainfall of 600 mm.

FIGURE 7-16: CRD SIMULATION FOR THE PENINSULA AQUIFER

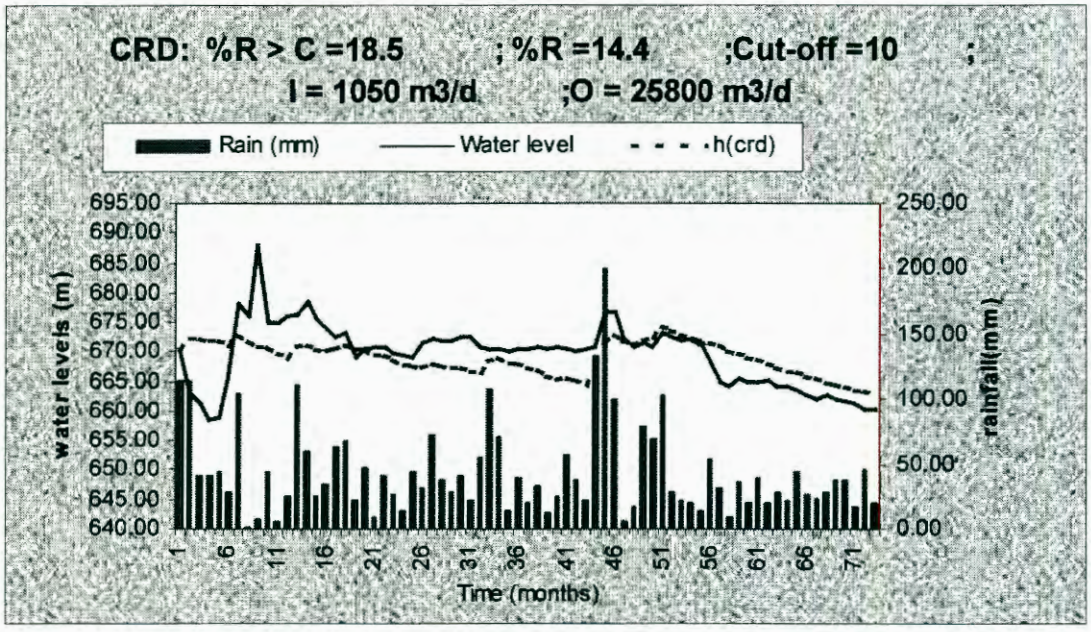

The CRD simulation for the Nardouw Aquifer (Figure 7-17) indicates annual recharge in the order of 3.2 % for cut-off rainfall values of 9 mm/month (rainfall < 9 mm/month will not contribute significantly to recharge). This yields annual recharge of 11.2 mm/a for rainfall of 350 mm.

FIGURE 7-17: CRD SIMULATION FOR NARDOUW AQUIFER

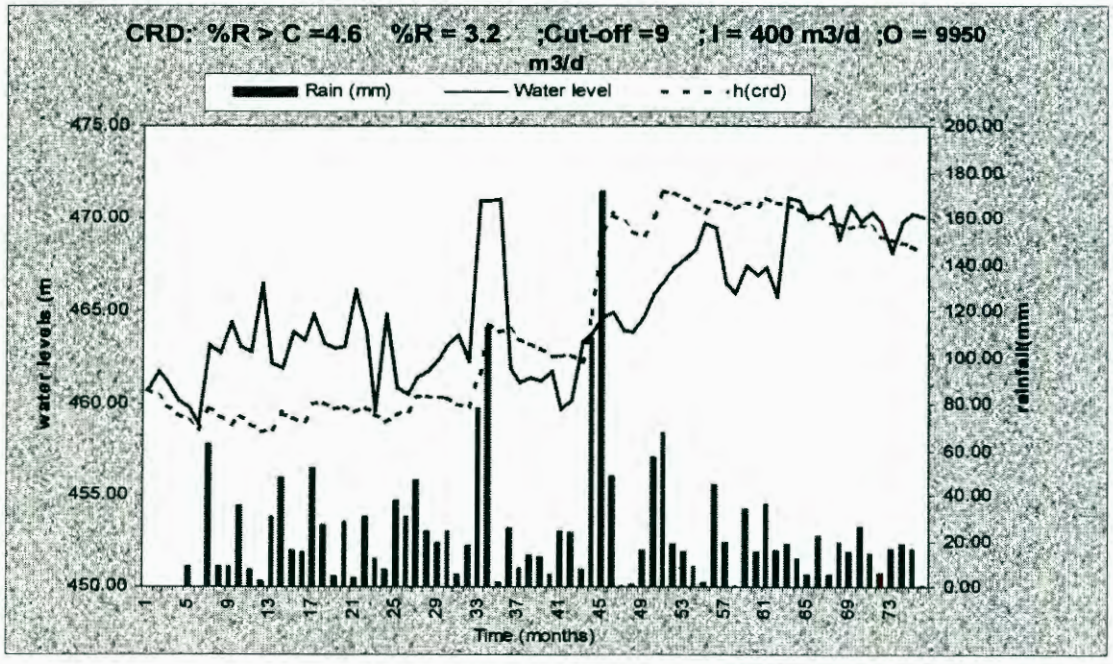

7.2.3 Area related method

Dörhöfer and Josopait (1981) developed a very practical method for recharge estimation over large areas, including hard and soft-rock aquifers for groundwater management in Lower Saxony, Germany. This method seems to be very applicable to the Klein Karoo and takes the differences in soil type, depth to water table, topography, precipitation and vegetation into account for different parts of the catchment area.

The method simply applies a series of transparent overlays for evapotranspiration, direct disharge (A/A_u) onto a diagram for determining the recharge stage for the various parts of the catchment. Figure 7-18 (adapted from Dörhöfer and Josopait, 1981) represents the relationship between evapotranspiration (ET) and grain size shown by lysimeter results. Based on the soil and vegetation types, the ET stage is determined by drawing a straight line from x-axis (soil type) until it intercepts the relevant 'vegetation type line' from which the corresponding ET stage is read on the Y-axis.

FIGURE 7-18: EVAPORATION (ET) AND GRAIN SIZE RELATIONSHIP SHOWN BY LYSIMETER RESULTS (ADAPTED FROM DÖRHÖFER AND JOSOPAIT, 1981)

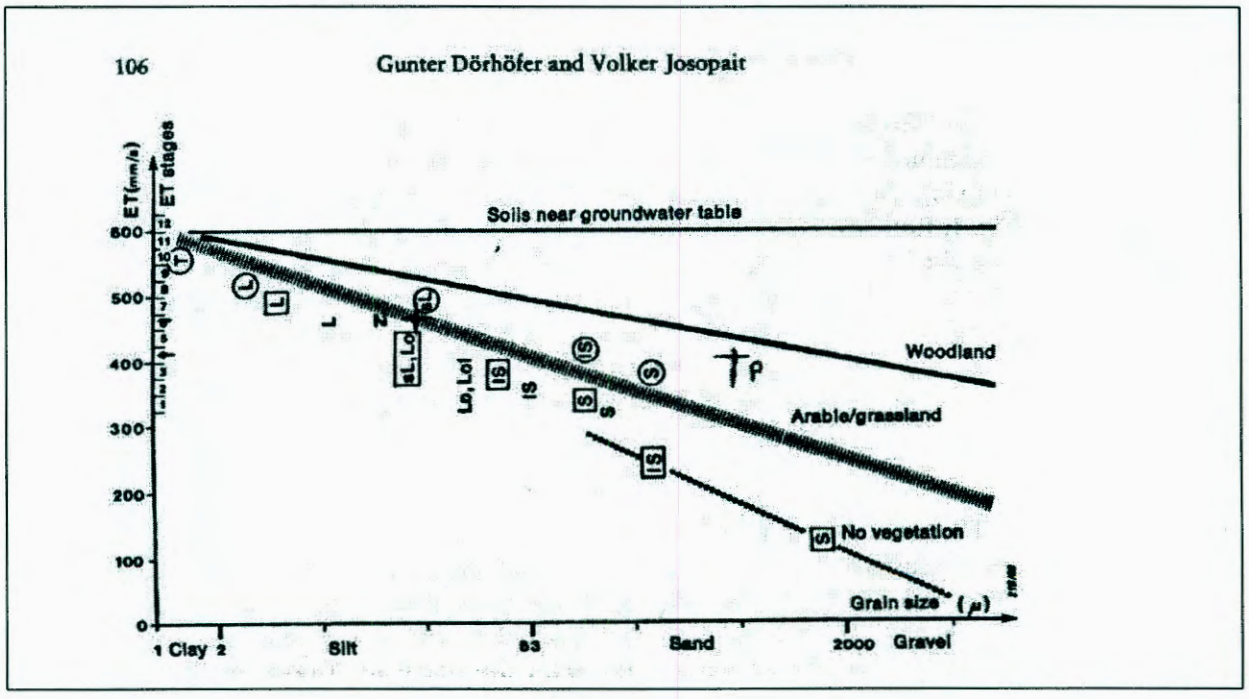

After assessment of the ET, A_d needs to be determined. This is the sum of the surface run-off and inter-flow and is important in mountainous catchments. Dörhöfer and Josopait (1981) derived a series of characteristic lines (A/A_u) representing direct discharge for different topographic conditions (see Figure 7-19). These were based on the assumption that direct

discharge (A_d) increases proportional to precipitation, similar to groundwater discharge (A_u) and total discharge (A). From Figure 7-19 the direct discharge stage for each part of the catchment is determined.

FIGURE 7-19: TRANSPARENT OVERLAY WITH A/A_u CHARACTERISTIC LINES
(ADAPTED FROM DÖRHÖFER AND JOSOPAIT, 1981)

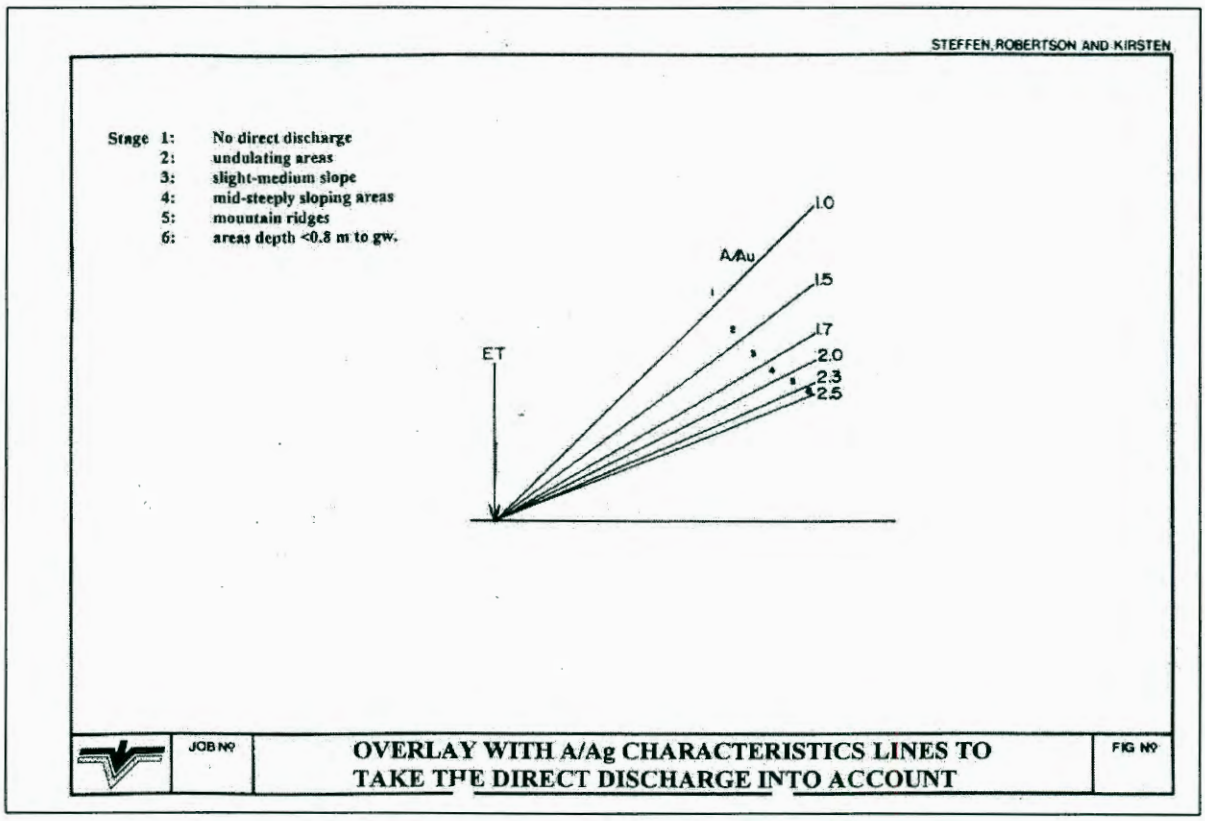

The total discharge A of each sub-area is determined by the difference between precipitation and evaporation. The direct discharge A_d is separated by means of the A/A_u relation, producing the groundwater discharge A_u which corresponds to the groundwater recharge rate G (use Figure 7-19).

The groundwater recharge rate G is the difference between mean annual precipitation N, evaporation ET and direct discharge A_d (Dörhöfer and Josopait, 1981):

$$G = N - ET - A_d \quad \text{..... Equation 16}$$

Recharge for each sub-area of the catchment is determined as follows:

- Place the A/A_u overlay (Figure 7-19) on the recharge diagram (Figure 7-20) so that the x-axes of both diagrams overlap and arrow on the ET overlay are in the center of the applicable ET stage.
- Find the rainfall figure of the area of concern on the x-axis
- Draw a perpendicular line from that point (x-axis) that will intersect the characteristic line for the A/A_u stage of the area.
- Draw a horizontal line from the A/A_u line intersection to the y-axis.
- Intercept of this line with y-axis represents the relevant recharge rate for the area of concern.

FIGURE 7-20: DIAGRAM FOR DETERMINATION OF RECHARGE STAGES

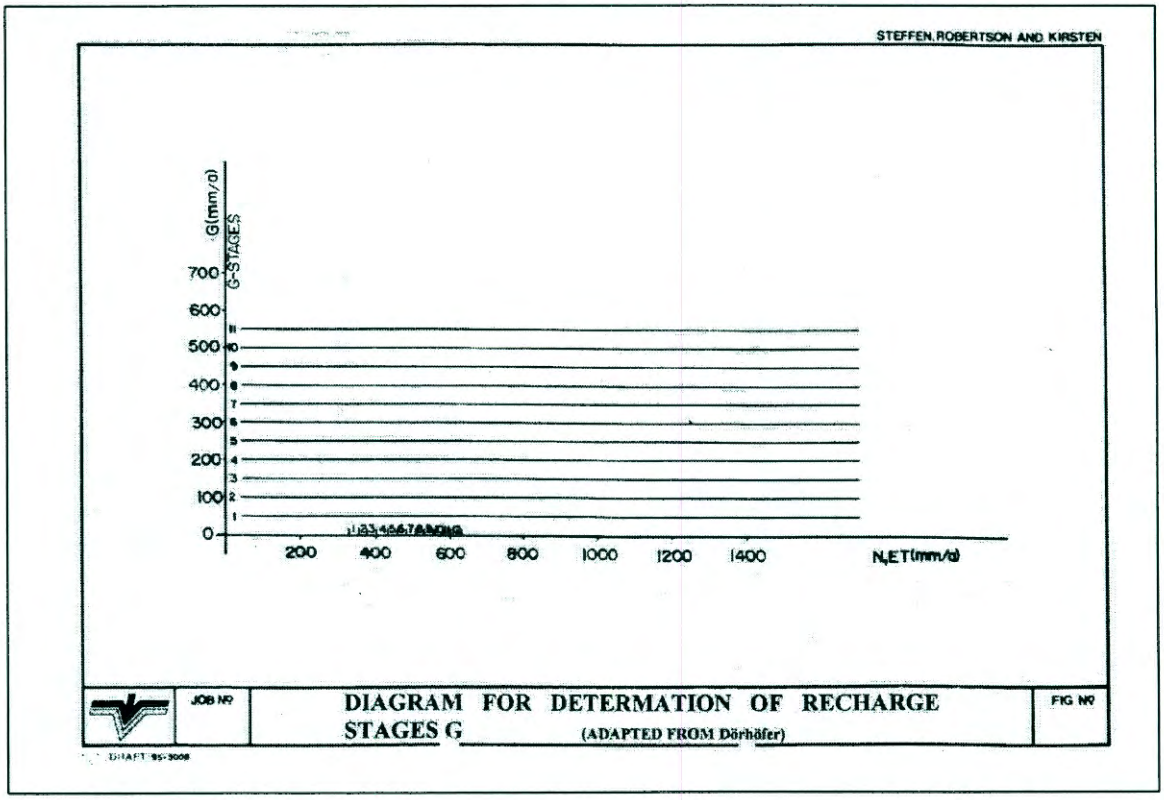

The above approach is applied for the Nardouw and Peninsula Aquifers of the Kammanassie Mountains. Table 7-6 summarises the input criteria for each of the above-mentioned aquifers, represented sub-areas, with different characteristics.

The area related method for recharge estimation was originally developed for wet conditions in Europe and not semi-arid areas, i.e. Klein Karoo. It is therefore not a useful method for recharge estimation in areas with an annual rainfall < 500 mm/a. However, the estimate for the Peninsula Aquifer of the order of 15% of annual rainfall seems reasonable.

TABLE 7-6: SUMMARY – CRITERIA USED FOR AREA RELATED RECHARGE CALCULATION

	Peninsula Aquifer	Nardouw Aquifer
Rainfall (mm)	600	350
Soil type	Coarse Sand	Silt
Vegetation	Between grass and woodland	Arable / Grassland
ET Stage	4	6
Direct discharge stage	5	3 to 4
Recharge Rate (mm/a)	90 (15%)	Not possible

7.2.4 Storage assessment with ^{14}C data

The Vermaaks River Wellfield was pumped at a combined average rate of 5 x 10^5 m^3/a over a six year period with a very moderate drawdown. Figure 4-8 shows a schematic cross-section across the Kammanassie Mountains, showing the Vermaaks River Wellfield. For the purpose of this calculation, it is conservatively assumed that this withdrawal equals the annual recharge rate (see water level variations, Appendix K-7, for boreholes VR6, 7, 8 and 11) .

Tritium in samples from production boreholes lies at or below the limit of detection (0.2±0.2 TU). CFC data from the Vermaaks River boreholes (Weaver and Talma 1999) are consistent with tritium. It can therefore be assumed to a first approximation that the pumped water does not contain significant amounts of thermonuclear radiocarbon.

Assuming that the system as a whole can be regarded as phreatic, the mean residence time (MRT) of the groundwater (Verhagen et al. 1991; Gieske 1995) is given by:

$$MRT = 8270 \{(A_0/A) - 1\} \quad \text{.....Equation 17}$$

where A_0 is the initial (recharge) value and A the measured value of radiocarbon.

In the absence of carbonate dissolution (Section 4.1.3.2) A_0 is taken conservatively to lie in the range of 90-95 % of atmospheric. This gives values for MRT as shown in Table 7-7 (Kotze *et al.*, 2000):

TABLE 7-7: MRT VALUES FOR VERMAAKS WELLFIELD BOREHOLES

Borehole	Measured ^{14}C A (pMC)	Initial (Est.) ^{14}C A_0 (pMC)	MRT (years)
VR 6	79.4	90 - 95	1100 –1600
VR 7	83.0	90 - 95	700 – 1200
VR 11	74.6	90 - 95	1700 – 2300
MEAN			1200 –1700

Hälbich and Greeff (1995) arrived at a figure of 1.2 x 10^{10} m^3 for the rock volume, which could be tapped by the Vermaaks River Wellfield. They also estimated the total fracture porosity ranging between 1 and 7 %, with the maximum of 7 % representing the porosity of faultzones, i.e. Vemaaks and Brilkloof. A figure of 5% is estimated for the Vermaaks Keystone Block Aquizone. These figures give storage volumes of 1.2 to 6.0 x 10^8 m^3 (porosities of 1 and 5% respectively) and 8.4 x 10^9 m^3 (porosity 7%) tapped by the Vermaaks River Wellfield. The recharge rate (R) is calculated, using the estimated ranges of radiocarbon-based mean residence times and of porosities (Verhagen, 2000):

$R = V / MRT$ ..... Equation 19

$= (0.7 – 5.0) \times 10^5 \ m^3/a$

For porosities between 1 and 5 % and MRT between 1200 and 1700 years.

Similarly the recharge rate of 4.9 to 7.0 x 10^6 m^3/a is calculated for the faultzones using Equation 19, with the same MRT values and a porosity of 7%. As the faultzones occur over very narrow zones, the high porosity values of the faults can provide over-estimations of the recharge rate. Therefore the porosity of the Keystone Block Aquizone is postulated to be more applicable, i.e. 5%.

Therefore the withdrawal rate at balance, or effective recharge rate RE:

$RE = 5 \times 10^5 \ m^3/a$

Corresponding to the upper limit of estimated recharge (R).

As substantial amounts of groundwater are likely to drain out of aquifer storage over and above the abstraction from the wellfield, RE, and therefore the discrepancy between the

figures, could be greater than these figures suggest. The MRT values based on radiocarbon values are unlikely to be significantly less than the range calculated above.

It is therefore concluded that the porosity of the entire catchment feeding the wellfield is of the same order as the estimate from structural considerations for aquizones and, therefore, considerably higher, than previously accepted (Kotze *et al.*, 2000).

7.2.5 Chloride mass balance method

The chloride mass balance method is one of the best methods for recharge estimation in semi-arid areas. Unfortunately the detection limits for chloride analysis of rainwater samples taken during this investigation were too high with the consequence that the chloride concentrations measured in all but one sample were below detection limit (see Table A-16, Appendix A).

A chloride value of 20 mg/l is measured in a rain sample collected from the rain gauge at DP25 (Nardouw Aquifer). The corresponding chloride value in a nearby borehole DP15, is 46 mg/l, which gives the following recharge estimation (Figure 7-21), using Recharge spreadsheet (van Tonder *et al.*, 2000):

FIGURE 7-21: RECHARGE CALCULATION USING CHLORIDE MASS BALANCE METHOD

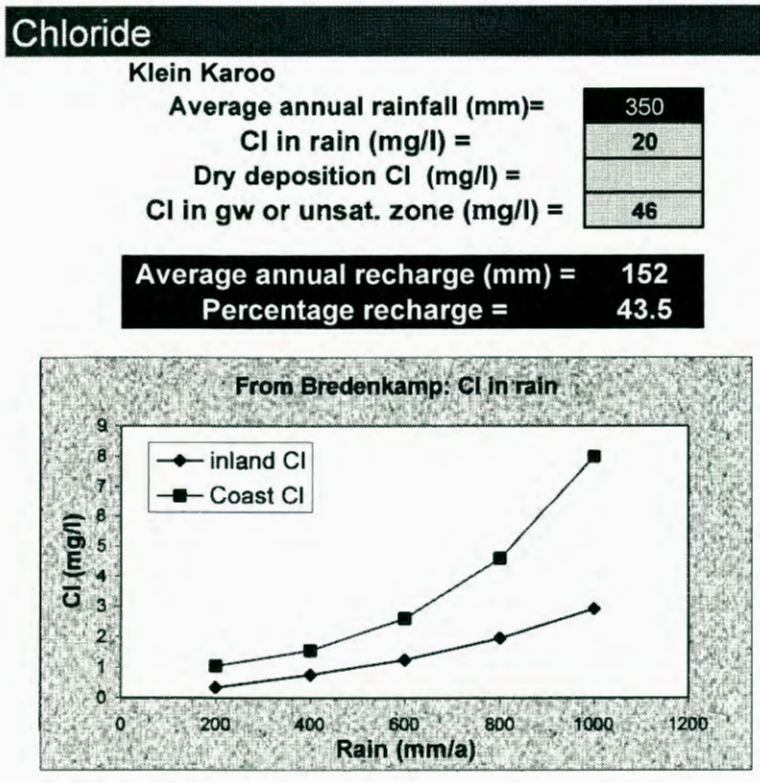

From the Cl in rain relationship (Bredenkamp et al., 1995), the above chloride measurement of 20 mg/l appears highly suspect.

Bredenkamp *et al.* (1995), estimated recharge to be in the order of 35% for the Zachariashoek catchment. This was based on chloride concentrations of 4.2 and 11.8 mg/l in rain and streamflow, respectively and a mean annual precipitation of 1063 mm/a.

The applicability of the chloride mass balance method in mountain catchments is debatable, as this method assumes that all rainfall infiltrates and run-off is a minimum. In mountain catchments, with substantial run-off, groundwater is stored temporarily as interflow, which flows out to streams during later rain events.

Sampling of rain, spring and groundwater for chloride is essential for recharge calculations for semi-arid areas and a network for chloride monitoring on at least a quarterly basis needs to be put in place in the valley areas. On the other hand, the chloride method is applicable only if substantial groundwater drainage can be demonstrated.

7.2.6 SVF Method

The Saturated Volume Fluctuation (SVF) method after van Tonder (1989) is used to simulate the recharge for the Nardouw and Peninsula Aquifers in the Kammanassie Mountains, with the use of the RECHARGE Excel spreadsheet (van Tonder *et al.*, 2000).

Similarly to the CRD-method, the average water level and total abstraction for the Vermaaks River Wellfield are calculated, using the water level and abstraction data for VR6, 7, 8 and 11. For the Nardouw Aquifer the average water level and total abstraction for the Varkieskloof, Bokkraal, Droëkloof and VG3 borehole are calculated. The results of the SVF simulations for both aquifers, using the above information, follows in Figures 7-22 and 7-23. In both cases, data from April 1993 to April 1999 are used.

FIGURE 7-22: SVF RECHARGE SIMULATION FOR THE NARDOUW AQUIFER

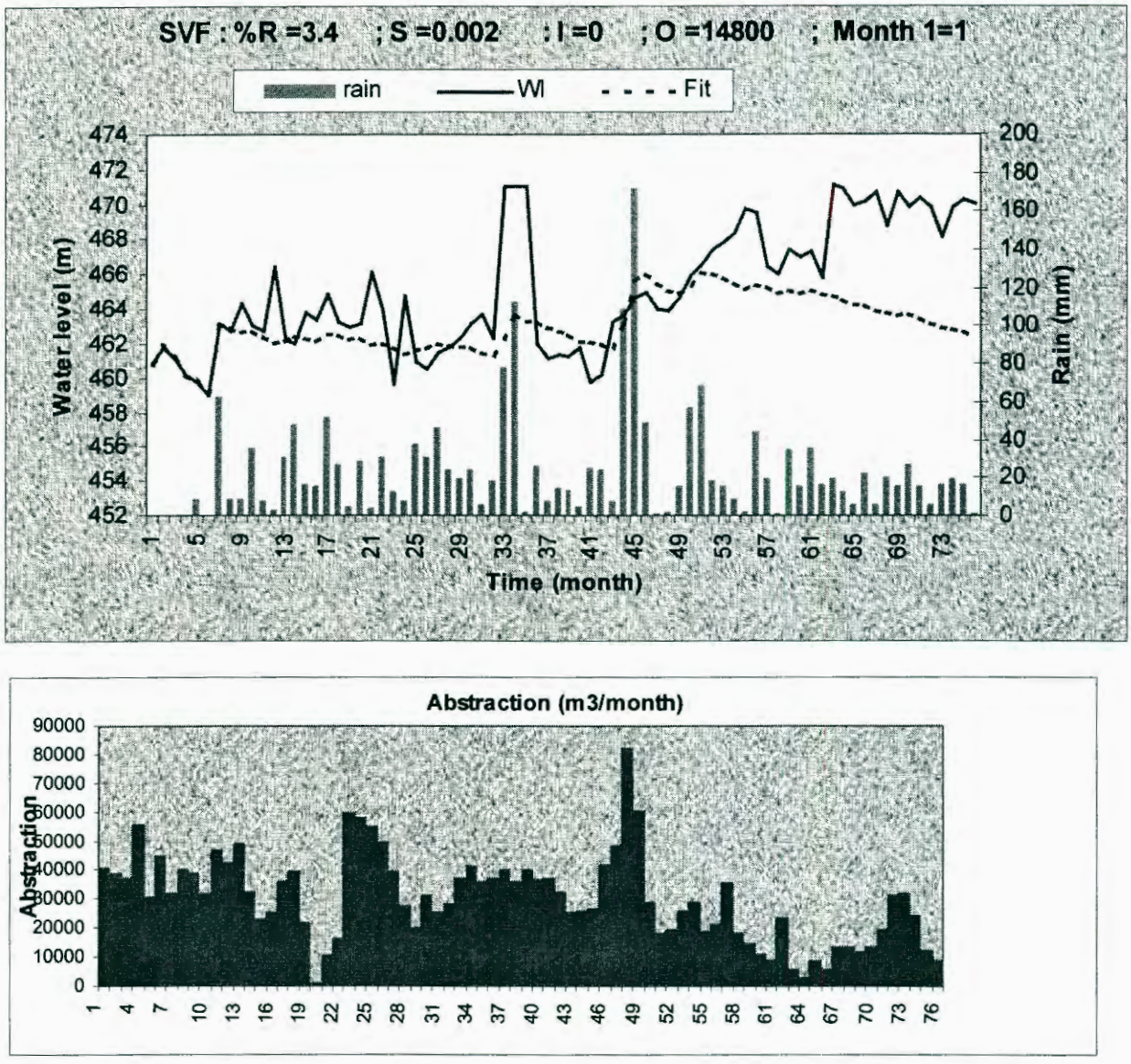

From Figure 7-22, the recharge and storativity for the Nardouw Aquifer are in the order of 3.4% of annual precipitation and 0.002, respectively. The SVF simulation corresponds well with the measured water levels up and until month 50, from where the simulated curve deviates from the measured water level curve. Analyses of the groundwater abstraction data show a significant decline in abstraction from the above-mentioned wellfields in the Nardouw Aquifer, resulting in water level recovery from storage.

Figure 7-23 shows the SVF recharge simulation for the Peninsula Aquifer. In general, a good fit between simulated and measured water levels is found for the Peninsula Aquifer. A recharge and storage of 16% of annual precipitation and 0.0055, respectively is found.

FIGURE 7-23: SVF RECHARGE SIMULATION FOR THE PENINSULA AQUIFER

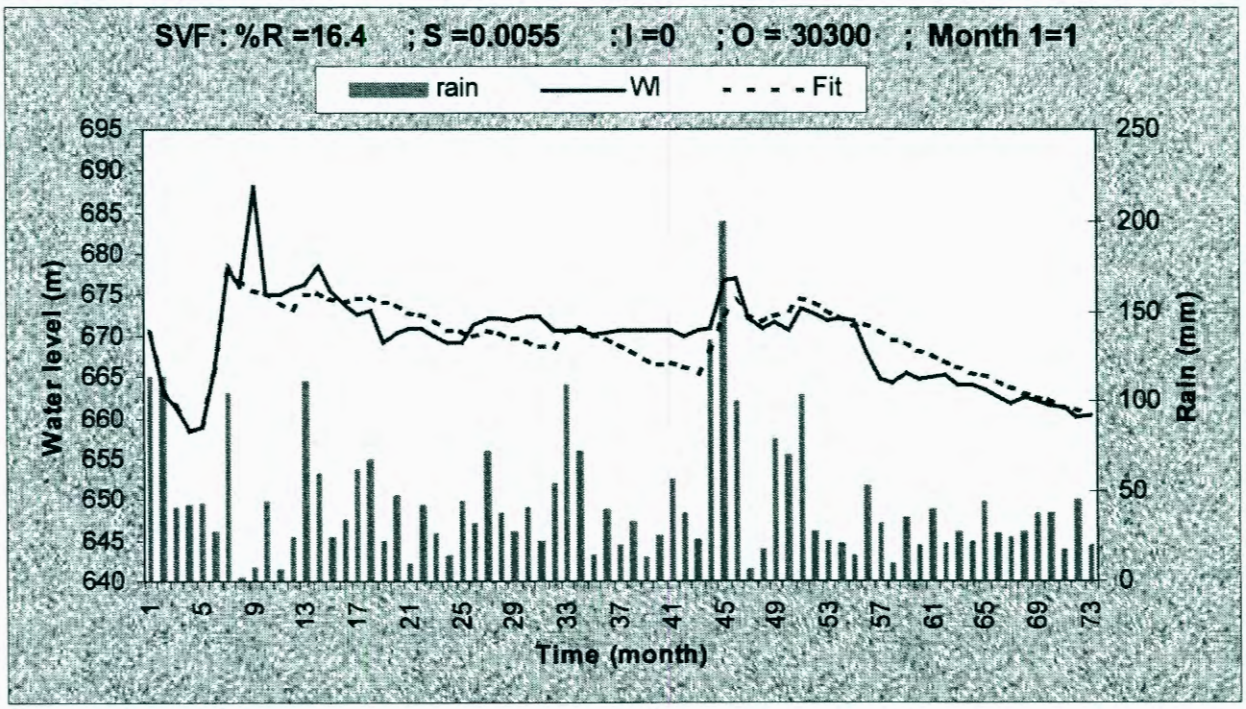

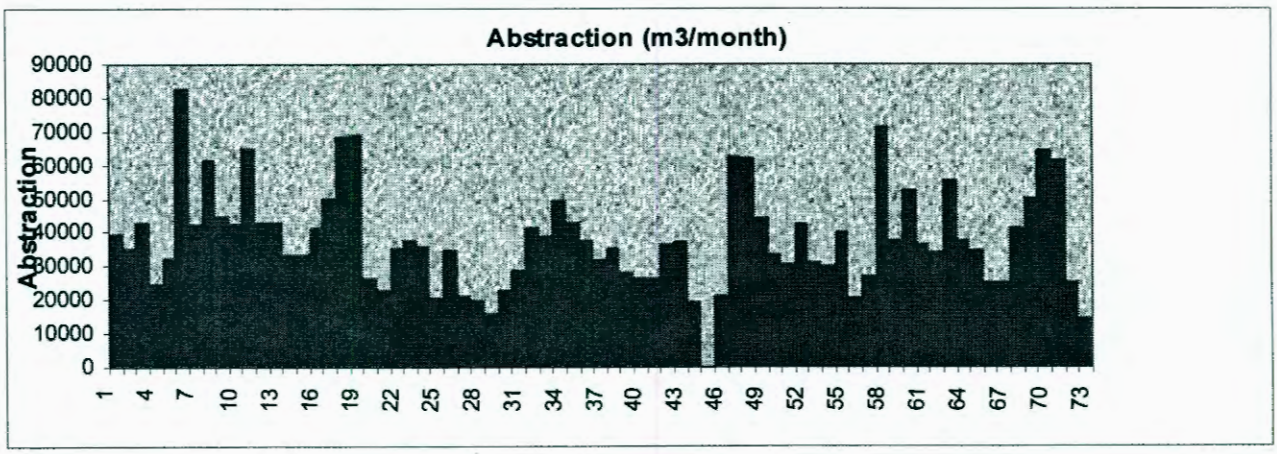

7.2.7 EQUAL VOLUME Method

Recharge and storativity are calculated for the Peninsula and Nardouw Aquifers using the same data set as before (in Sections 5.5.1.2 and 5.5.1.6) by applying the Equal Volume (EV) Method (van Tonder, 1999).

Figures 7-24 and 7-25 summarise the results of the EV Method, using the RECHARGE spreadsheet (van Tonder *et al.*, 2000). A recharge estimate of 3.1 % of annual precipitation and a storativity value of 0.00095 is estimated for the Nardouw Aquifer (Figure 7-24).

FIGURE 7-24: RECHARGE AND STORATIVITY FOR THE NARDOUW AQUIFER USING THE EQUAL VOLUME METHOD.

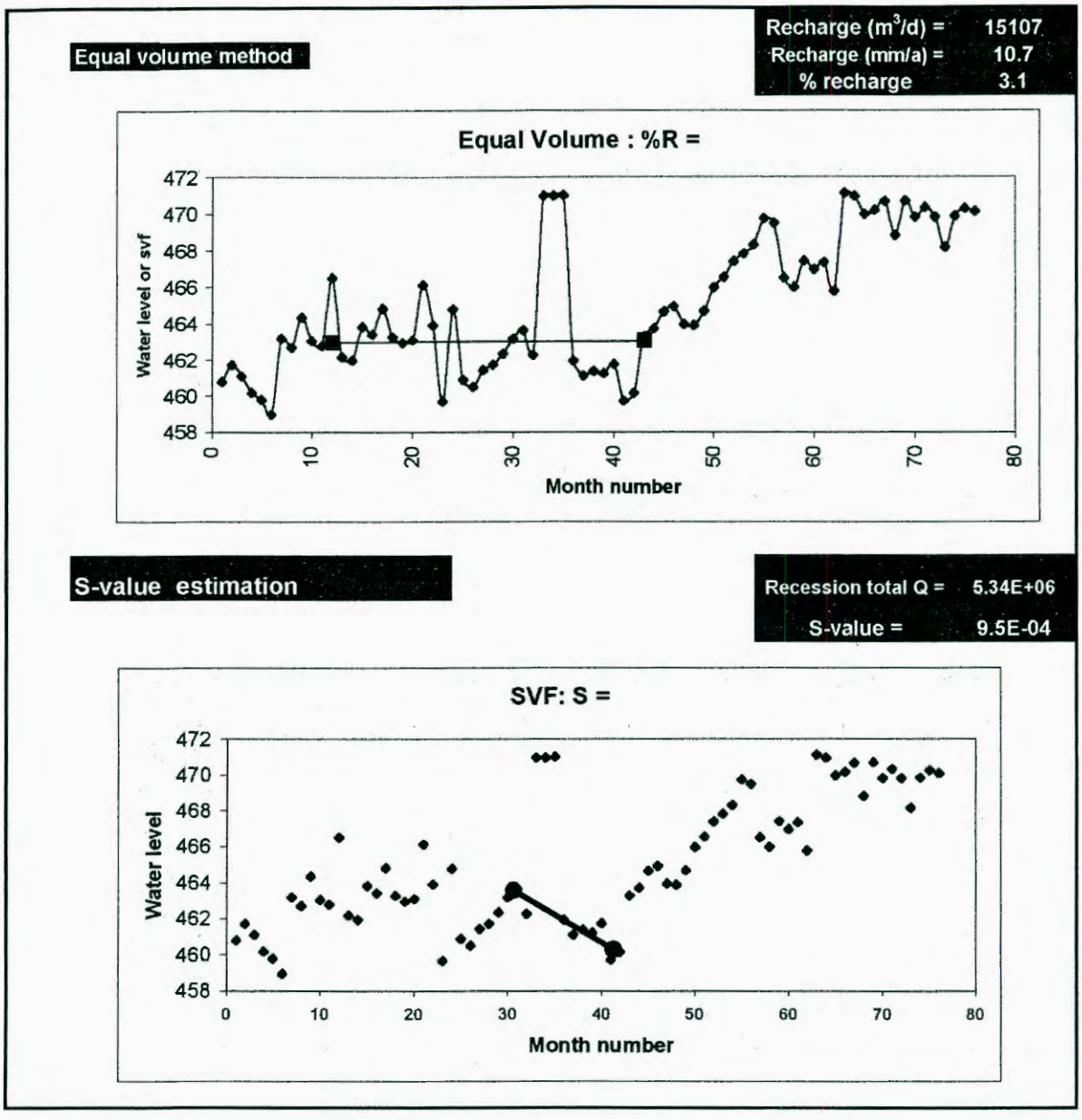

FIGURE 7-25: RECHARGE AND STORATIVITY FOR THE PENINSULA AQUIFER USING THE EQUAL VOLUME METHOD.

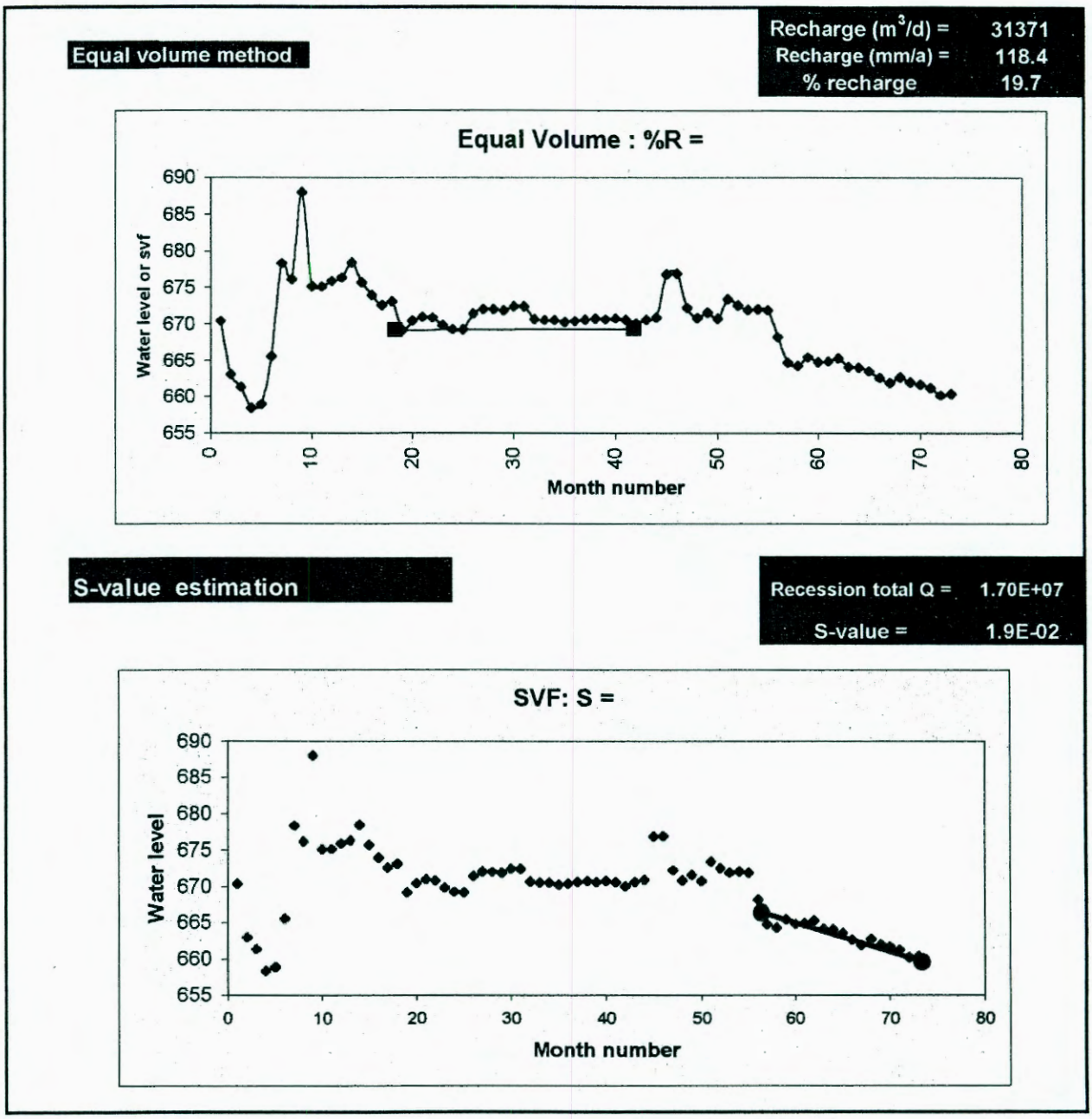

A recharge estimate of 19.1 % of annual precipitation and a storativity value of 0.019 is estimated for the Peninsula Aquifer (Figure 7-25).

7.2.8 RECHARGE Spreadsheet

The latest EXCEL spreadsheet 'RECHARGE', developed by van Tonder *et al.* (2000) is used to calculate recharge, first for the Nardouw and then the Peninsula Aquifers of the Kammanassie Mountains.

The RECHARGE spreadsheet is a user-friendly way to calculate recharge for a wide range of methodologies, included in the spreadsheet as macros. Besides the SVF, CRD and EV methods, a series of characteristic maps from which qualified guesses of recharge are made, by simply reading the relevant variable for the area of concern from a map, are also included in the spreadsheet. The selected value is then entered into a matrix in the spreadsheet, which calculates the recharge figure. Qualified guesses of recharge are obtained by using existing data, expert opinions and interpolation of known values, including the following:

- Recharge from soil and vegetation data
- Recharge from geological data
- Vegter's recharge map
- ACRU Recharge by Roland Schultz (1997)
- Harvest Potential Map
- Expert guesses, including the relevant case studies carried out recently in similar hydrogeological conditions / near vicinity.

The results of all available qualified guesses and recharge calculations are summarised in a matrix, from which the average annual recharge for each aquifer is calculated, by applying a weight to each estimate, according to certainty.

Figures 7-26 and 7-27 summarise the recharge estimations for all methodologies applied for the Peninsula and Nardouw Aquifers, respectively. Although, an average recharge rate of 7.8 % of annual precipitation is suggested for the Nardouw Aquifer (Figure 7-26), a rate of 19 mm/a (or 5.4%) of precipitation is used, as the qualified guesses are over-estimations, which artificially elevate the recharge average. This yields 9.5 million m^3/a recharge for the Nardouw Aquifer of the Kammanassie Mountains over an area of 500.2 km^2.

For the Peninsula Aquifer (Figure 7-27) an average recharge rate of 13.6 % of annual rainfall is suggested. However, a recharge rate of 84 mm/a (or 14.0%) of annual rainfall is used, as the suggested value is low when compared to the results of the SVF, CRD and EV methods, which are based on observed data. This yields 9.5 million m^3/a annual recharge for the Peninsula Aquifer of the Kammanassie Mountains over an area of 113.4 km^2.

FIGURE 7-26: RECHARGE SUMMARY FOR NARDOUW AQUIFER

Summary of Recharge

Klein Karoo

Method	mm/a	% of rainfall	Certainty (Very High=5 ; Low=1)
Cl	152.2	43.5	2
SVF: Equal Volume	10.7	3.1	4
SVF: Flt	11.9	3.4	4
CRD	11.2	3.2	4
Qualified Guesses :			
Soil	37.5	10.7	3
Geology	8.3	1.5	3
Vegter	32.0	9.1	1
Acru	40.0	11.4	1
Harvest Potential	75.0	21.4	1
Expert's guesses	56.0	16.0	1
Base Flow (minimum Re)	75.0	21.4	1
^{2}H displacement method	1.0	0.3	3
Carbon 14 method	6.2	1.8	1
EARTH Model	10.2	2.9	4
Groundwater Flow Model			1
Average recharge	27.4	7.8	
Recharge =	19.0	5.4	

= 9.5038 Mm^3/a

= 26037.81 m^3/d

= 301.36 L/s

Area (Km^2) =	500.2
Annual Rainfall (mm) =	350

FIGURE 7-27: RECHARGE SUMMARY FOR PENINSULA AQUIFER

Summary of Recharge

Klein Karoo

Method	mm/a	% of rainfall	Certainty (Very High=5 ; Low=1)
Cl	66.7	11.1	1
SVF: Equal Volume	118.4	19.7	4
SVF: Flt	98.4	16.4	4
CRD	86.4	14.4	4
Qualified Guesses :			
Soil	163.7	27.3	3
Geology	23.0	4.2	3
Vegter	32.0	5.3	3
Acru	50.0	8.3	3
Harvest Potential	100.0	16.7	3
Expert's guesses	87.2	14.5	3
Base Flow (minimum Re)	75.0	12.5	4
^{2}H displacement method	16.0	2.7	1
Carbon 14 method	11.9	2.0	2
EARTH Model	143.4	23.9	2
Groundwater Flow Model			0
Average recharge	84.0	14.0	
Recharge =	84.0	14.0	

= 9.5256 Mm^3/a

= 26097.53 m^3/d

= 302.05 L/s

Area (Km^2) =	113.4
Annual Rainfall (mm) =	600

Note the ^{2}H displacement method, calculates recharge, based on the deviation of a data point from the meteoric water line (for a given data set).

7.2.9 GIS Raster based approach

Woodford (2001) applied a GIS raster-based approach (see Section 2.5.3.3) to estimate the annual volumes of recharge to the Vermaaks River Groundwater Unit (see Figures 7-1, 7-2 and 7-28). He determined the annual volumes of rainfall recharge to this unit (10.85 km^2) from 25x25m cells of mean annual precipitation and its statistical coefficient of variation (Schultze, 1997), as well as terrain slope (Table 7-8, adapted from Woodford, 2001).

TABLE 7-8: ESTIMATED MEAN, MAXIMUM AND MINIMUM RAINFALL RECHARGE TO THE VERMAAKS RIVER GROUNDWATER UNIT (ADAPTED FROM WOODFORD, 2001)

Recharge	Units			Recharge Rate (% of MAP)
	m^3/a	m^3/d	l/s	
Mean	206 072	565	6.5	3.8
Maximum	259 675	711	8.2	4.8
Minimum	133 787	367	4.2	2.5

The calculated rainfall recharge in $m^3/km/a$, based on interpolation of the Recharge rates presented in Table 7-8 is presented in Figure 7-28. The positions of the production boreholes of the Vermaaks River Wellfield (Eastern Section of the KKRWSS) are also shown Figure 7-28.

From Figure 7-28, Woodford (2001) derived a recharge estimate of 0.25 million m^3/a for the Vermaaks River local catchment. This estimate is considered very conservative, giving the low recharge rates applied. The entire Vermaaks River catchment falls inside the Vermaaks Window (Figure 7-1) and taps the Peninsula Aquifer. Therefore recharge is estimated to be 1.04×10^6 m^3/a, considering a recharge rate of 14%, surface area of 10.85 km^2 and annual rainfall of 600 mm/a. When rainfall is 500 mm, which it was for the greater part of abstraction from the Vermaaks Wellfield, recharge is only 0.76×10^6 m^3/a.

Consideration of the hydrogeologic catchment for recharge calculation is considered a simplistic approach for fractured aquifers, such as the TMG in the Kammanassie Mountains. The C/S Aquitard is the only boundary condition to flow and should be used as the aquifer boundary when calculating the surface area of the aquifer for recharge calculations. Other approaches will yield very conservative recharge estimates.

FIGURE 7-28: VERMAAKS RIVER WELLFIELD AND RAINFALL RECHARGE TO VERMAAKS RIVER CATCHMENT (ADAPTED FROM WOODFORD, 2001)

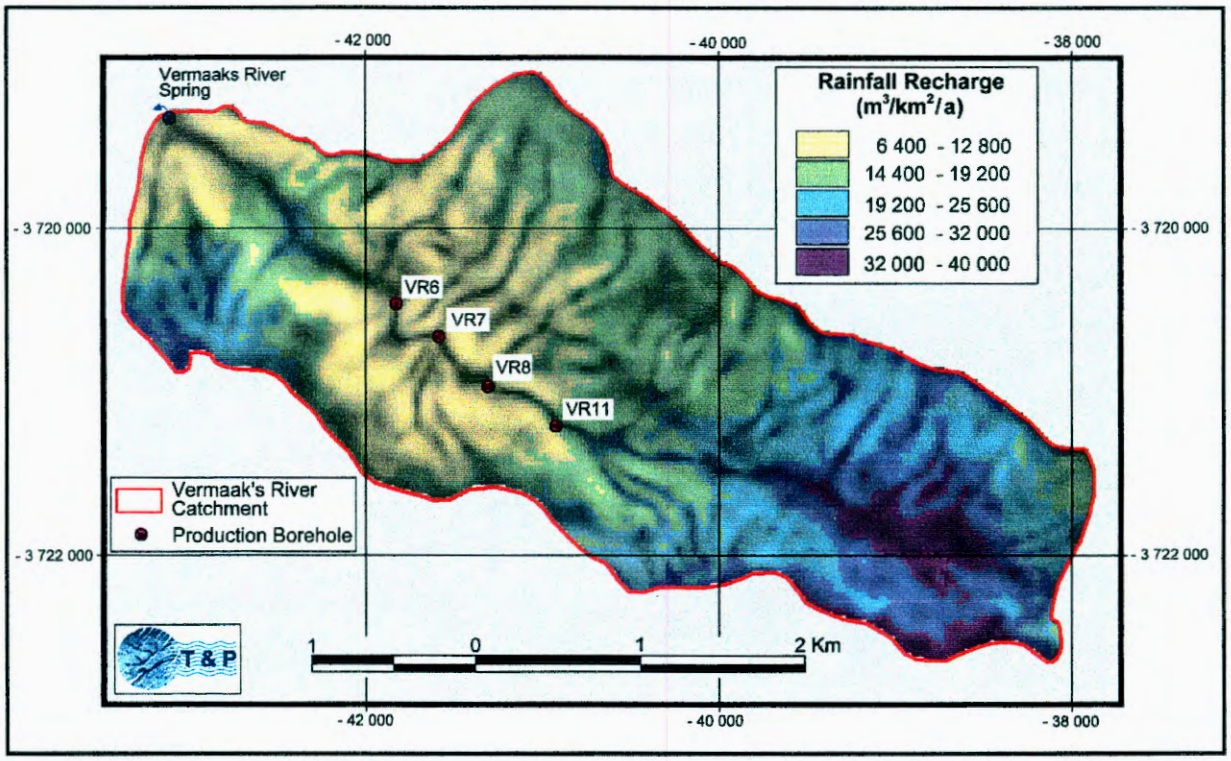

7.2.10 Total inflows - Recharge

Recharge calculations, using various recharge methodologies indicate that the average recharge rates for the Nardouw and Peninsula Aquifers of the Kammanassie Mountains are 5.4 and 14 %, respectively. This yields 9.5 million m^3/a recharge each (combined recharge of 19 million m^3/a) for the Nardouw Aquifer and Peninsula Aquifers of the Kammanassie Mountains over an area of 500.2 and 113.4 km^2, respectively.

The CRD and ^{14}C storage calculation give recharge estimates of 0.4 and > 0.5 million m^3/a, respectively, for that portion of local scale Vermaaks River catchment, exploited by the Vermaaks River Wellfield.

7.3 WATER BALANCE CALCULATION

A water balance calculation is first carried out for the aquifers of the Kammanassie Mountains (intermediate scale catchment). Secondly the amounts of groundwater available in the Vermaaks River hydrologic catchment (local scale) and the Keystone Block Aquizone (local scale) are calculated.

Strictly speaking, not all of the balance between recharge and discharge is available for further allocation, since some of it flows to rivers and springs, the vegetation needs groundwater and possible outflows to other groundwater compartments occurs. Therefore, the reserve approach to recharge estimation in the RECHARGE Excel spreadsheet (after van Tonder and Xu, 2000) was used. The reserve approach considers all the above factors and indicates how much groundwater is available for further allocation after all the above criteria and more are taken into account. As not much is currently known about the environmental groundwater requirements, rough estimates are entered into the reserve spreadsheet.

Considering the existing groundwater abstraction (2.0 million m^3/a) and recharge (10.0 million m^3/a) from and to the Nardouw Aquifer of the Kammanasie Mountains, respectively, the balance of 8.0 million m^3/a groundwater is still available for utilisation. The additional groundwater allocation for abstraction is therefore estimated using the Reserve approach in Figure 7-29.

FIGURE 7-29: WATER BALANCE CALCULATION FOR THE NARDOUW AQUIFER USING THE RESERVE APPROACH

Groundwater Reserve

Klein Karoo	Million m^3/a
Recharge =	10.004
Groundwater Abstraction(excluding BHN) =	2
Basic Human Need (BHN) from GW =	2
Ecology and IFR Requirement =	2
Groundwater flux towards rivers =	2.0000
Groundwater outflow from area =	5.0000
Amount allowed to be intercepted from outflow	2.0000
Groundwater Inflow into area =	0.5000
Extra GW allocation possible =	1.5040

GW RECHARGE	10.0040	1.5040	Extra GW Allocation	3.5040
		2	Existing Abstraction	
		2	Basic Human Need	Reserve = 6.5000
		2	Ecology + IFR	

Area (km^2) = 500.2
Rainfall (mm/a) = 350

Level of confidence	
Confidence Level	Criteria
Very high (+ 75%)	Aquifer response to pumping monitored and quantified. Detailed informarion from exploration of the catchment. Extrapolation of info from similar GW regimes elsewhere which are well understood
High (65 - 75%)	Aquifer response to pumping observed Detailed informarion from exploration of the catchment. Extrapolation of info from similar GW regimes elsewhere which are well understood
Medium (40 - 65%)	Detailed info from exploration of the catchment. Extrapolation of info from similar GW regimes elsewhere are understood
Low (20 - 40%)	Limited on-site data. Extrapolation of info from similar GW regimes reasonably well understood
Very Low (< 20%)	No on-site data; based on national-scale maps. Extrapolation of info from similar regimes reasonalby well understood

Enter confidence Level	Medium

From Figure 7-29 it can be concluded that approximately 1.5 million m^3/a of groundwater is available for allocation in the Nardouw Aquifer, if the assumptions for groundwater inflow (from Peninsula Aquifer), ecology requirement and flux to rivers are correct. Based on the

conceptual hydrogeological model and the presence of highly permeable aquizones, much more groundwater could be available for allocation in the Nardouw Aquifer.

The same approach was followed for the Peninsula Aquifer. Figures 7-30 and 7-31 summarise the recharge estimations and water balance calculation, using the groundwater reserve approach, respectively.

The balance of groundwater still available for allocation in the Peninsula Aquifer is estimated with the Reserve approach (Figure 7-30). If the existing groundwater abstraction from the Peninsula Aquifer (0.7 million m^3/a) in the Kammanassie Mountains is subtracted from the annual recharge (9.5 million m^3/a) a considerable amount of groundwater seems to be available for further use.

FIGURE 7-30: WATER BALANCE CALCULATION FOR THE PENINSULA AQUIFER USING THE RESERVE APPROACH

Groundwater Reserve

Klein Karoo	Million m^3/a
Recharge =	9.5256
Groundwater Abstraction(excluding BHN) =	0.8
Basic Human Need (BHN) from GW =	
Ecology and IFR Requirement =	2
Groundwater flux towards rivers =	2.0000
Groundwater outflow from area =	2.0000
Amount allowed to be intercepted from outflow	0.5000
Groundwater Inflow into area =	1.0000
Extra GW allocation possible =	6.2256

GW RECHARGE	9.5256	6.2256	Extra GW Allocation	Reserve = 7.0256
		0.8	Existing Abstraction	
		0	Basic Human Need	
		2	Ecology + IFR	

Area (km^2) = 113.4
Rainfall (mm/a) = 600

Level of confidence	
Confidence Level	Criteria
Very high (+ 75%)	Aquifer response to pumping monitored and quantified. Detailed informarion from exploration of the catchment. Extrapolation of info from similar GW regimes elsewhere which are well understood
High (65 - 75%)	Aquifer response to pumping observed Detailed informarion from exploration of the catchment. Extrapolation of info from similar GW regimes elsewhere which are well understood
Medium (40 - 65%)	Detailed info from exploration of the catchment. Extrapolation of info from similar GW regimes elsewhere are understood
Low (20 - 40%)	Limited on-site data. Extrapolation of info from similar GW regimes reasonably well understood
Very Low (< 20%)	No on-site data; based on national-scale maps. Extrapolation of info from similar regimes reasonalby well understood

Enter confidence Level	Medium

It is observed from Figure 7-30 that approximately 6.2 million m^3/a is still available for allocation in the Peninsula Aquifer, if the assumptions for groundwater inflow (from Peninsula Aquifer), ecology requirement and flux to rivers is correct.

The water balance of the Vermaaks Window and the of the Peninsula Aquifer (indicated as Unit 1 on Figure 7-3) is calculated as follows (see Figure 7-26):

- The surface area of the Vermaaks Unit is 40. 6 km^2.
- The recharge rate for the Peninsula Aquifer is 14 % of an average annual rainfall of 600 mm.
- From the above the annual recharge for the Vermaaks Window equals 3.4 x 10^6 m^3/a.
- The annual abstraction from the Vermaaks River Wellfield is approximately 0.7 x 10^6 m^3/a (maximum).
- The average annual flow of the Vermaaks, Marnewicks and Huis Springs are taken as 10, 12 and 40 l/s respectively, totalling 62 l/s (1.32 x 10^6 m^3/a). Of this total 30% is TMG baseflow, giving a total of 0.4 x 10^6 m^3/a for the baseflow component to streams.
- The difference between recharge, abstraction and baseflow of 2.2 x 10^6 m^3/a, minus the allocation for vegetation, is left for allocation. If the baseflow is taken as 90% (Midgley et al., 1994), 1.5 x 10^6 m^3/a minus the allocation for vegetation is left for allocation.

However, the Vermaaks Window is in hydraulic connection with the Nardouw Aquifer in the Keystone Block Aquizone, according to the conceptual hydrogeological model. Therefore, the water balance for the Keystone Block Aquizone also needs to be considered as follows:

- Hälbïch *et al.* (1995) has shown that the surface area of the Keystone Block Aquizone is 1.2 km^2 (i.e. 600 m base and 2000 m length).
- The Keystone Block consists of the Nardouw Aquifer. The recharge for the Keystone block equals 0.024 x 10^6 m^3/a, considering a recharge rate of 5% of annual rainfall (350 mm/a) over an area of 1.2 km^2.
- Annual abstraction from the Aquizone is 1.55 x 10^6 m^3/a (including abstraction from the Vermaaks Wellfield, see Table 7-2).
- Recharge – Abstraction = 0.024 – 1.55 = -1.53 x 10^6 m^3/a.
- The water levels in the Keystone Block Aquizone boreholes vary between 20 and 40 m below surface on the privately owned land. It is postulated that the recharge deficiency of 1.53 x 10^6 m^3/a is balanced by an inflow from the Vermaaks Window.

Not enough groundwater level data are available for the boreholes on privately owned land in the Keystone Block Aquizone. It is therefore difficult to assess what the impact of abstraction on the southern flanks of the Kammanassie Mountains in the Keystone Block Aquizone is on the regional water level and *vice versa*.

The maximum available groundwater in the Vermaaks Window, taking the outflow to the Keystone Block Aquizone into account, is therefore of the order of 0.5 x 10^6 m^3/a, including a component for vegetation and the environment. Figure 7-26 shows a suggested water balance scenario for the Vermaaks Window, based on the reserve concept. The water balance in Figure 7-26 allows for the following:

- 0.5 x 10^6 m^3/a for baseflow (flux to streams)
- 0.5 x 10^6 m^3/a for the environment
- 0.7 x 10^6 m^3/a for abstraction from the Vermaaks Wellfield and
- 2.0 x 10^6 m^3/a groundwater outflow to the Keystone Block Aquizone.

From the above balance, 0.71 x 10^6 m^3/a of groundwater is still available for allocation.

FIGURE 7-31: PROPOSED WATER BALANCE FOR THE VERMAAKS WINDOW

Groundwater Reserve

Klein Karoo	Million m^3/a
Recharge =	3.4104
Groundwater Abstraction(excluding BHN) =	0.7
Basic Human Need (BHN) from GW =	
Ecology and IFR Requirement =	0.5
Groundwater flux towards rivers =	0.5000
Groundwater outflow from area =	2.0000
Amount allowed to be intercepted from outflow	0.5000
Groundwater Inflow into area =	0.0000
Extra GW allocation possible =	0.7104

GW RECHARGE	3.4104	0.7104	Extra GW Allocation	Reserve 1.4104
		0.7	Existing Abstraction	
		0	Basic Human Need	
		0.5	Ecology + IFR	

Area (km^2) = 40.6
Rainfall (mm/a) = 600

Level of confidence	
Confidence Level	Criteria
Very high (+ 75%)	Aquifer response to pumping monitored and quantified. Detailed information from exploration of the catchment. Extrapolation of info from similar GW regimes elsewhere which are well understood
High (65 - 75%)	Aquifer response to pumping observed Detailed information from exploration of the catchment. Extrapolation of info from similar GW regimes elsewhere which are well understood
Medium (40 - 65%)	Detailed info from exploration of the catchment. Extrapolation of info from similar GW regimes elsewhere are understood
Low (20 - 40%)	Limited on-site data. Extrapolation of info from similar GW regimes reasonably well understood
Very Low (< 20%)	No on-site data; based on national-scale maps. Extrapolation of info from similar regimes reasonalby well understood

Enter confidence Level	Medium

Therefore, from the water balance calculation in Figure 7-31 it seems that groundwater inflows minus outflows, gives a surplus of 0.7 x 10^6 m^3/a. If this is the case, then why did:

- The water levels drop between 15 and 28.5 m in the Vermaaks River Wellfield over the period 1993 to 1999; and

- The spring flow measured at the Vermaaks River spring, decline from more than 10 l/s to 4 l/s over a seven year period of groundwater abstraction from the Vermaaks River Wellfield?

The above indicates that some of the assumptions are wrong. Out of the total amount of groundwater recharge in the Vermaaks Window (3.4 x 10^6 m^3/a), 2.0 x 10^6 m^3/a is postulated to represent outflow to the Keystone Block Aquizone. A further, 0.7 x 10^6 m^3/a is abstracted in the Vermaaks River Wellfield, leaving 0.7 x 10^6 m^3/a for baseflow and vegetation. From the above and Figure 7-31, the outflow to the Keystone Block Aquizone and the baseflow could possibly be under-estimated, i.e.:

- If baseflow is increased to 1.2 x 10^6 m^3/a (90% of total stream flow, after Midgley et al., 1994), there is a deficit of 0.7 x 10^6 m^3/a.
- If the amount allowed to be intercepted from the outflow to the Keystone Block Aquizone is reduced from 0.5 x 10^6 m^3/a to 0.0, the deficit reduces further to 1.2. x 10^6 m^3/a.

The results of the above scenario are presented in Figure 7-31 and represents a deficit of 0.5 x 10^6 m^3/a (15.9 l/s) in the water balance for the Vermaaks Window. Bearing in mind that only 0.9 x 10^6 m^3/a is abstracted from the Nardouw Aquifer of the Keystone Block Aquizone (see Table 7.2), an outflow component of 2.0 x 10^6 m^3/a is possibly to high. However, to improve this estimate, the monitoring network in the Keystone Block Aquizone needs to be expanded, to obtain water level and abstraction figures over time.

The water balance of the Vermaaks River catchment (Figure 7-32) is calculated as follows for a rainfall of 600 mm/a:

- Recharge is 1.04 x 10^6 m^3/a (33 l/s)
- Abstraction is 0.7 x 10^6 m^3/a (22 l/s)
- Spring flow is 0.13 x 10^6 m^3/a (4 l/s)

The above indicates a surplus of 0.21 x 10^6 m^3/a (7 l/s) of groundwater still available for groundwater abstraction. However, some of this water drains to the Keystone Block Aquizone, which is why groundwater levels are declining. The sustainable yield of the Vermaaks River Wellfield is estimated between 0.4 and 0.5 x 10^6 m^3/a, considering that spring flow has already declined by 0.19 x 10^6 m^3/a (6 l/s). However, the sustainable yield of the Vermaaks River Wellfield is estimated to be only of the order of 0.3 to 0.4 x 10^6 m^3/a if rainfall is 500 mm and recharge only 0.76 x 10^6 m^3/a.

FIGURE 7-32: PROPOSED WATER BALANCE FOR THE VERMAAKS WINDOW

Groundwater Reserve

Klein Karoo	Million m^3/a
Recharge =	3.4104
Groundwater Abstraction(excluding BHN) =	0.7
Basic Human Need (BHN) from GW =	
Ecology and IFR Requirement =	1.2
Groundwater flux towards rivers =	1.2000
Groundwater outflow from area =	2.0000
Amount allowed to be intercepted from outflow	0.0000
Groundwater Inflow into area =	0.0000
Extra GW allocation possible =	-0.4896

GW RECHARGE	3.4104	-0.4896	Extra GW Allocation	0.2104
		0.7	Existing Abstraction	
		0	Basic Human Need	
		1.2	Ecology + IFR	

Area (km^2) = 40.6
Rainfall (mm/a) = 600

Level of confidence	
Confidence Level	**Criteria**
Very high (+ 75%)	Aquifer response to pumping monitored and quantified. Detailed information from exploration of the catchment. Extrapolation of info from similar GW regimes elsewhere which are well understood
High (65 - 75%)	Aquifer response to pumping observed Detailed information from exploration of the catchment. Extrapolation of info from similar GW regimes elsewhere which are well understood
Medium (40 - 65%)	Detailed info from exploration of the catchment. Extrapolation of info from similar GW regimes elsewhere are understood
Low (20 - 40%)	Limited on-site data. Extrapolation of info from similar GW regimes reasonably well understood
Very Low (< 20%)	No on-site data; based on national-scale maps. Extrapolation of info from similar regimes reasonalby well understood

Enter confidence Level	**Medium**

A sustainable yield of 0.4 to 0.5 x 10^6 m^3/a for the Vermaaks River Wellfield is in line with the aquifer storage, calculated from the carbon-14 mean residence time of groundwater in the aquifer. The above considers the long-term average storage and not average annual variations in rainfall. In the long-term, groundwater abstraction of 0.4 to 0.5 x 10^6 m^3/a is sustainable and will not deplete the aquifer, provided that abstraction elsewhere in the Keystone Block Aquizone (private properties on the Southern Flanks of Kammanassie Mountains) remains constant with time. However, many opportunities for further development exist in the Kammanassie Mountains, outside the Keystone Block Aquizone.

CHAPTER 8: AQUIFER MANAGEMENT

The following aquifer management tools are used and considered for data analysis in order to design an aquifer management plan for the Kammanassie Mountains and Vermaaks River Wellfield respectively:

- Aquifer testing – Flow Characteristic (FC) Method and Cooper-Jacob
- Recharge and water balance
- The WELLMAN Package - Wellfield management spreadsheet
- The TMGMAN - Management Plan for TMG Aquifers.

The results are discussed below.

8.1 AQUIFER TESTING

Woodford (2001) shows that a coherent conceptual model describing the flow dynamics of the Table Mountain Group (TMG) fractured-rock aquifer systems is a prerequisite to successfully apply existing methods of aquifer test analysis to obtain accurate and useful information on their hydraulic properties.

The KKRWSS provides a classical example where conventional aquifer testing techniques and simplistic analytical methods were applied in the past to evaluate the field data. Aquifer testing was mainly aimed at providing estimates of the 'safe-yield' of the production borehole and information required for the design of the pump equipment (Mulder, 1995 and, Jolly, 1998). The hydraulic parameters calculated are not used in further quantitative analysis, as the reliability of the information is generally doubted.

Table 8-1 (over page) summarises the recommended pumping rates for the production boreholes of the Eastern Section of the KKRWSS, based on simplistic pump testing analysis (1993 to 1998), considering only the capacity of the production borehole itself and not the aquifer. Table 8-1 also shows the results of more detailed aquifer test analysis in the last column (see Chapter 6).

TABLE 8-1: SUMMARY RECOMMENDED PUMPING RATES OF PRODUCTION BOREHOLES, EASTERN SECTOR KKRWSS FROM PUMP TEST ANALYSIS

WELLFIELD	BOREHOLE NUMBER	RECOMMENDED PUMPING RATES (l/s)					
		Feb 1993[A]	Nov 1993[A]	Feb 1995[A]	1995[B]	1998[C]	2001[D]
VERMAAKS	VR6	12 (20)	8 (15)	8 (10)	3.0	-	7.4 (4.4)
	VR7	30 (40)	20 (30)	20 (30)	5.0	11 (25)	20 (13.3)
	VR8	15 (25)	10 (20)	10 (20)	5.0	-	#
	VR11	15 (25)	8 (15)	8 (15)	7.0	6 (10)	15.4 (10.7)
	TOTAL	72 (110)	46 (80)	46 (75)	20.0	17 (35)	42.4
VOORZORG	VG3	8 (10)	4.6 (10)	4.5 (10)	3	2 (6)	5 9 (2.6)
BOKKRAAL	DP15	5.8 (20)	5.8 (12)	6 (10)	5	-	5.7 (5.9)
	DP25	9 (20)	9.8 (15)	7 (15)	7	-	#
	DP28	8 (20)	8.3 (25)	9 (20)	9	7*	21.1 (19.4)
	TOTAL	22.8 (60)	23.9 (52)	22 (45)	21	7	
DROëKLOOF	DG110	8 (16)	3.5 (12)	3.5	3	2 (6)	#
OLIFANTS RIVIER	DP18	9.5 (14)	9.8 (14)	11 (14)	11	10	13.2 (0.5)
VARKIESKLOOF	DP10	12 (14)	9.5 (15)	3.5	-		#
	DP29	10 (10)	3 (8)	5.5 (8)	3	-	#
	DP12	5.8 (12)	5.8 (8)	5.5 (8)	-	5*	#
	TOTAL	27.8 (36)	18.3 (31)	14.5 (16)	3	5*	

NOTE:

A Mulder (1995).

B Kotze (1995).

C Jolly (1998).

D Kotze (2001), current study.

- Mulder's February 1993 recommendations are based upon the evaluation of step-drawdown and constant-discharge aquifer-tests conducted in 1990-91.
- Mulder's November 1993 and 1995 recommendations are based upon the evaluation of the 1990 aquifer-test data and monitoring of groundwater-levels and abstraction.
- Kotze's (1995) recommendations are based upon step-drawdown and constant discharge tests conducted in 1990, as well as the monitoring of groundwater-levels and abstraction; and assumption that enough groundwater needs to be released to ensure that Vermaaks Spring continue to flow.
- Jolly's recommendations are based upon step-drawdown and constant discharge tests conducted in 1997, as well as the monitoring of groundwater-levels and abstraction.
- Kotze's (2001) recommendations are based upon step-drawdown and constant discharge tests conducted in 1990 and 1997, using the FC analysis method for two different available drawdown assumptions. This is very preliminary, the final figures including the water balance follows in Section 7. The values in brackets represent the best available drawdown estimate (geometric mean).

10(20) Represent continuous and peak pumping rate.

* ONLY IN THE SUMMER

■ Alternative borehole use, i.e. either VG3 or DG110 for two months of the year (2 l/s) and combined use for one month of the year (6 l/s).

\# No data found for re-analysis with FC method

From Table 8-1 the pumping rates of boreholes and wellfield have been adjusted 5 times (Mulder, March and November 1993, Kotze, 1995 and Jolly, 1998) without consideration of conceptual hydrogeological model, recharge and water balance. Specific aspects that were not addressed in the absence of a conceptual hydrogeological model, in any of the above pumping rate adjustments are the following:

- Differences in management scenarios between the Nardouw and Peninsula Aquifers. Only one of the KKRWSS wellfields, i.e. the Vermaaks River Wellfield, is situated in the Peninsula Aquifer. The other wellfields are situated in the Nardouw Aquifer, which requires a different borehole construction and pumping scenario, i.e. a lower yield over a longer time to avoid iron-bacteriological clogging of borehole screens.

- Interconnectivity between boreholes and wellfields: Typical examples are the Varkieskloof and Bokkraal Wellfields, where three or more boreholes are sited on the same structure and fall within each others' radius of influence. Re-testing by Jolly (1998) confirmed that the following boreholes are inter-connected in the following wellfields:

  - In the Vermaaks River Wellfield: VR6, 7 and 8.
  - In the Bokkraal Wellfield: DP15, 25 and 28.

- Simplistic pump test analysis, without consideration of aquifer characteristics or a water balance, show that high pumping rates could be achieved at relatively little drawdown, in many of the production boreholes of the KKRWSS (especially in the Vermaaks River Wellfield), Jolly (1998), and the FC Method, see last column of Table 6-2.

In the absence of a water balance study, Jolly (1998) recommended that pumping be done on a continual basis at lower rates than currently pumped for the following reasons:

- To minimise drawdown interference between boreholes.
- A lower pumping rate is assumed to be more sustainable, because abstraction will be less than aquifer replenishment and the chances of turbulent flow conditions are reduced.
- To allow more efficient pump use and to minimise electricity use (This depends on the size of pump installed. A large pump is more efficient at higher pumping rates, therefore a considerable saving can be made by replacing the large pumps in the Nardouw Aquifer production boreholes with smaller ones, operating more cost-effectively at lower rates).
- Reduce the potential for iron-bacteria build-up.
- To simplify wellfield management by eliminating starting and stopping pumps at predetermined intervals.

- To reduce the number of production boreholes within each other's radius of influence in each wellfield.

Based on the above considerations Jolly (1998) recommended a revision of the pumping schedule for, currently in use at the KKRWSS (see second last column in Table 6-2). Although Jolly (1998) considered both the Eastern and Western Sector, only the Eastern Sector is included here (see Table 6-2):

- Three boreholes are to be pumped continuously (VR11, VR7 and DP18).
- Two boreholes to be pumped continuously during the summer months only (DP12 and DP28).
- Two boreholes to be used on an *ad hoc* basis to keep the reservoirs full (VG3 and DG110).

The above schedule specifically set the production figures very conservatively to meet the current demand, which is 50 l/s in the summer and 25 l/s in the winter months. No distinction is made between those wellfields tapping the Nardouw and Peninsula Aquifers. Further, accurate recharge figures and a water balance calculation are still outstanding, without which, a proper estimate of sustainable yield cannot be made.

Jolly (1998) concludes that pumping test results indicate that in addition to the above further 41 l/s, representing a maximum of up to 91 l/s can be obtained from the boreholes. Of the above, VR7 and VR11 can continuously yield 25 l/s and 10 l/s, adding 18 l/s to the supply.

Table 6-2 shows that testing of individual boreholes within a wellfield or aquifer unit does not take into account the interference effects of other production boreholes. Simple summation of all the 'safe-yield' estimates from these analyses will obviously result in an overestimation of the supply potential.

At present the borehole characteristics and yields are very well established, but the impacts of groundwater abstraction on spring flow and the environment are not quantified. Therefore based on the conceptual hydrogeological model and water balance the relationship between recharge from rainfall, abstraction and spring flow is quantified. A management decision should then be made on the relative importance of spring flow or abstraction from deep boreholes.

In order to achieve the above objective, more sophisticated methods of data analysis is required to determine the exploitation potential of the Eastern Sector of the KKRWSS

8.2 WELLMAN

WELLMAN is an Excel spreadsheet specifically designed for management of the boreholes and wellfields of the KKRWSS and other similar schemes in TMG Aquifers. All the hydrogeological information of the KKRWSS production and observation boreholes is linked into a single Excel spreadsheet by macros. An example of the output of WELLMAN is in Appendix K-1, while Figure 8-1 is the title page of the WELLMAN spreadsheet.

FIGURE 8-1: WELLMAN TITLE PAGE

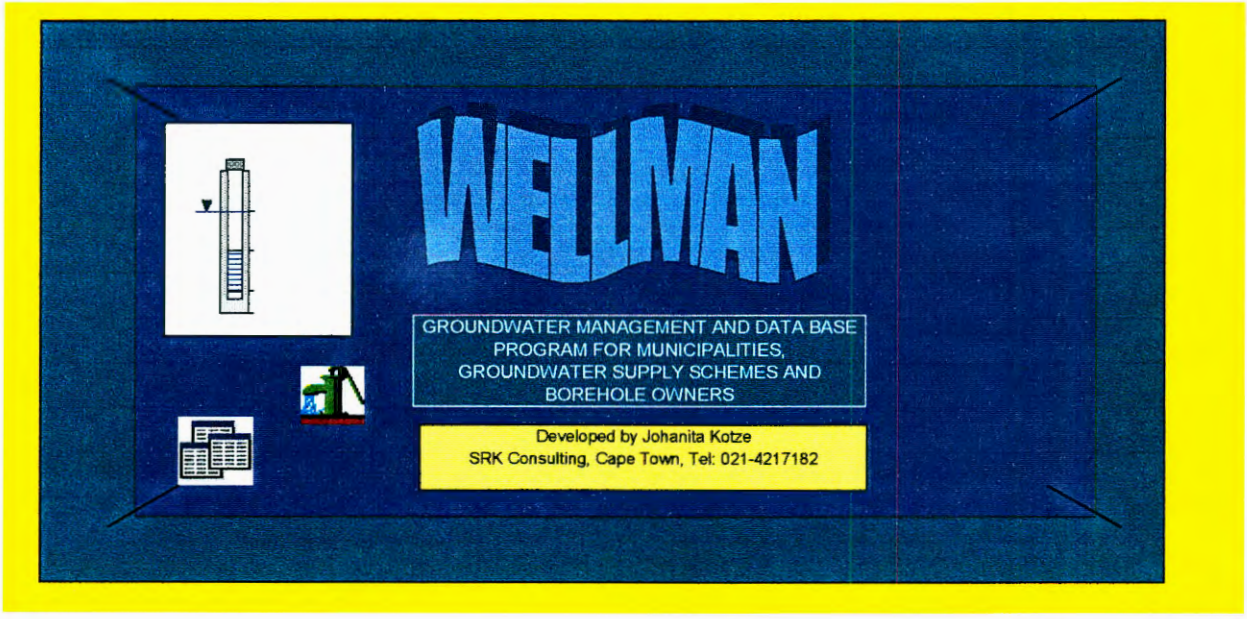

WELLMAN is a user-friendly Excel spreadsheet containing a Main Menu Sheet (Figure 8-2) with sub-menus (incorporated by simple macro's in the spreadsheet). By simply selecting any of the white buttons shown in Figure 8-2, one can move directly to the relevant data or figures.

:

- Selected borehole / wellfield of the Eastern Sector of the KKRWSS, i.e. 'Go to BH1 to 13' and 'Go to Wellfield1 to 4' on the main menu (Figure 8-2).
- Observation boreholes, see Figure K-1I (Appendix K-1).
- Map showing borehole and wellfield localities in and around the Kammanassie Mountains, see Figure K-1O (Appendix K-1).
- Rainfall data for Wildebeesvlakte Rain Gauge, see Figure K-1G (Appendix K-1).
- Total Annual abstraction for the Eastern Sector of the KKRWSS, see (Figure K-3E, Appendix K-3).
- Spring flow for the Vermaaks and Marnewicks Springs, see Figure K-1Q (Appendix K-1)
- Environmental isotope data, see Figure K-1R (Appendix K-1).

- 'Go to borehole': Boreholes 1 to 13 represent all the production boreholes of the Eastern Sector of the KKRWSS, see Figure K-2A to H (Appendix K-2).
- 'Go to wellfield': Wellfields 1 to 4 represent all the wellfields of the Eastern Sector of the KKRWSS, see Figures K-3A to D (Appendix K-3).

Appendix K-1 contains examples of all the main features incorporated in the WELLMAN spreadsheet.

FIGURE 8-2: MAIN MENU – WELLMAN SPREADSHEET

Main Menu sheet

Region	Little Karoo		OBS_wl	MAP	Rainfall	Title page	Annual Abstraction	Springflow	Isotopes
District	Oudtshoorn								
Water Board	Overberg			Tel. Number	044 2724634				
	Enter BH Number								
Example	Example			This is an example					
Borehole 1	VG3	Go to BH 1		Production Borehole - Voorzorg, Vermaaks Wellfield					
Borehole 2	VR6	Go to BH 2		Production Borehole - Upper Vermaaks River Valley - Vermaaks Wellfield					
Borehole 3	VR7	Go to BH 3		Highest Yielding Production Borehole - Vermaaks Wellfield					
Borehole 4	VR8	Go to BH 4		Production Borehole - Upper Vermaaks River Valley - Vermaaks Wellfield					
Borehole 5	VR11	Go to BH 5		Production Borehole - Upper Vermaaks River Valley - Vermaaks Wellfield					
Borehole 6	DP10	Go to BH 6		Production Borehole - Varkieskloof					
Borehole 7	DP12	Go to BH 7		Production Borehole - Varkieskloof					
Borehole 8	DP29	Go to BH 8		Production Borehole - Varkieskloof					
Borehole 9	DP15	Go to BH 9		Production Borehole - Bokkraal					
Borehole 10	DP25	Go to BH 10		Production Borehole - Bokkraal					
Borehole 11	DP28	Go to BH 11		Production Borehole - Bokkraal					
Borehole 12	DG110	Go to BH 12		Production Borehole - Droëkloof					
Borehole 13	DP18	Go to BH 13		Production Borehole - Olifants River "Brug"					
	Enter Wellfield Name								
Wellfield 1	VERMAAKS	Go to Wellfield 1		Production Boreholes VG3, VR6, VR7, VR8 and VR11					
Wellfield 2	VARKIESKLOOF	Go to Wellfield 2		Production Boreholes DP10, DP12 and DP29					
Wellfield 3	BOKKRAAL	Go to Wellfield 3		Production Boreholes DP15, DP25 and DP28					
Wellfield 3	DROEKLOOF&OLIFANTS	Go to Wellfield 4		Production Boreholes DP18 and DG110					

Two important features of WELLMAN are that data are entered only once. Further, all data are captured in a suitable format, which allows simple copy and paste commands to enter the information into other formatted spreadsheets, eg. RECHARGE and FC (after van Tonder and Xu, 1999 and 2000, respectively).

The following important data for the Eastern Sector of the KKRWSS are presented in Appendices:

- All observation well data are summarised in Figures K-4A to H (Appendix K-4).
- All geological information is summarised in Figures K-6A to K (Appendix K-6).
- All management subroutines from the 'Go to borehole' routine is summarised in Figures K-5A to M (Appendix K-5).

If 'Go to BH1 to 13' (Figure 8-2) is selected, all the relevant borehole information for the borehole selected is summarised on one sheet (Figure 8-3). New macro's enable the following selections (white buttons on Figure 8-3):

- Data: a spreadsheet summarising all the rest and pumping water levels, time of pumping and abstraction volume for each month for the selected borehole (see Figure K-2A, Appendix K-2).
- Chemistry: spreadsheet summarising all the macro and selected trace element analysis for each month, to produce a concentration versus time plot for selected constituents (Figure K-2B and E, Appendix K-2).
- Environmental isotope data for selected borehole (Figure K-2C, Appendix K-2).
- Geology for selected borehole (Figure K-1D, Appendix K-2).
- Pump test data for selected borehole (Figure K-2F, Appendix K-2).
- Management (Equal Volume calculation) for selected borehole (Figure K-2H, Appendix K-2).

All the subroutines of each 'Go to Borehole' submenu of the main menu are presented in Appendix K-2.

8.2.1 Determining the sustainable yield of a borehole with WELLMAN

The borehole summary sheet (Figure 8-3) contains all the necessary information to manage each of the KKRWSS production boreholes. The water level versus abstraction and recommended yield graphic (Figure 8-3) shows the effect of increasing abstraction on rest and pumping water levels. (The recommended yield is the recommendations estimated from pump test analysis in the past, summarised in Table 8-1). The position of the pump inlet, available drawdown and the pumping water level are also shown on Figure 8-3. Therefore, comparison of the effect of any given abstraction on water levels can be investigated. All relevant information, including the following, is also summarised above the graph:

- Location, owner
- Geological formation, depth of water strikes, main water strike position, blow-out yield
- Borehole design: screen depths, diameter, type of screen, depth of borehole, depth of pump installation, type of pump installed
- Recommended yield from from various sources.

FIGURE 8-3: EXAMPLE OF THE GO TO BH1 SUBMENU

BH number	VG3	Wellman Groundwater Management and Data base program							
Wellfield	Vermaaks								
Municipality	Overberg	Y	42820.8	Main water strike (m) =	190	Recommended Q (l/s) =	2.5	216	m3/d
Owner	DWAF	X	3715464.4	BH depth (m) =	206.7	Q (FC-Method)			
Geological formation	TMG - NAR	Altitude	497.3	Use of water	Domestic	Q (Thels-Method)	3	259	m3/d
Topo map sheet #		Drilled	15/4/89	Depth of pump instal	148	Q (Guess)			
Screen Type	PVC	IWL (m)	6.02	Blow Yield (l/s) =	12	Q (Equal Volume)	2.0	173	m3/d
Screen Depth	96.5 - 150	Diameter	208	Other water strikes (m)=	110, 174	KW of pump			
Screen Depth	150 - 206.7	Diameter	168	Pump	submersible	Max. Q of pump (l/s)	4	346	m3/d

Other comments:
Borehole is situated in a closed boundary (Average distance = 1 km)

DATA | CHEM | EN_ISO | Geology | Pump test | Manage | Main

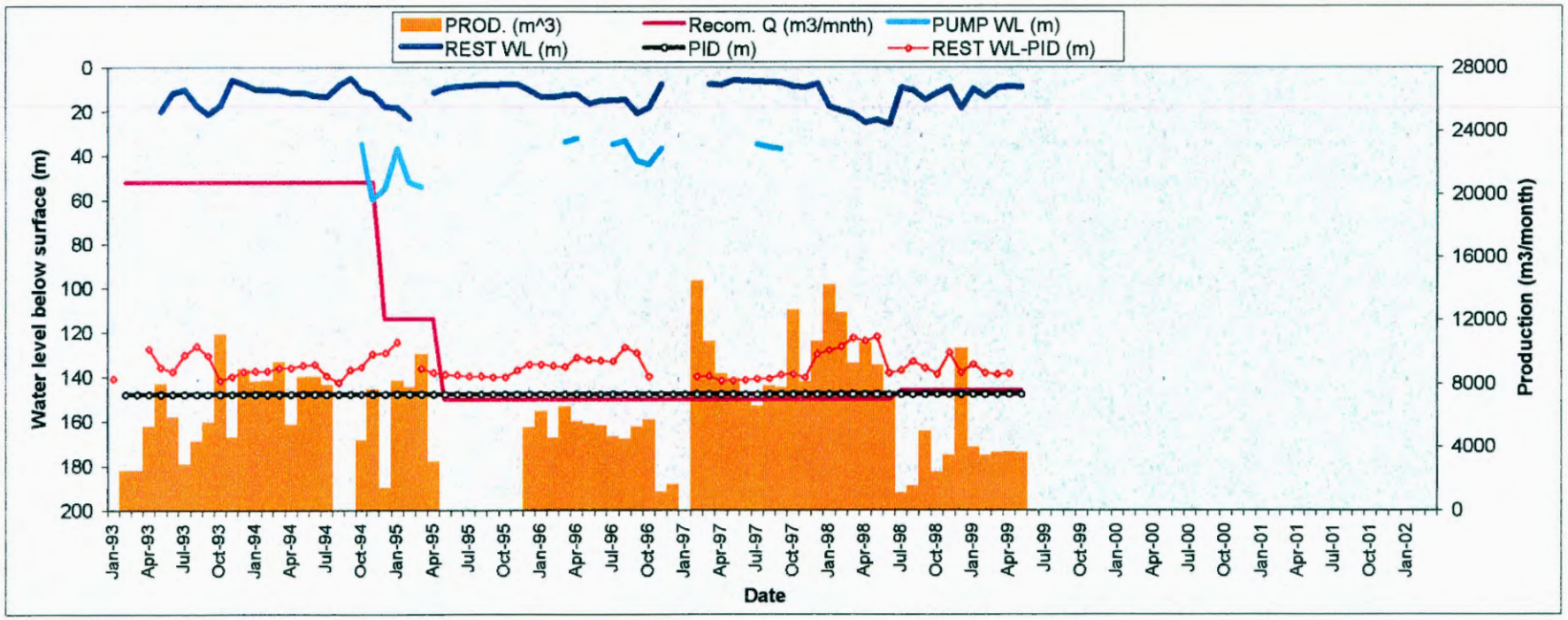

The recommended pumping rate from the various test pumping analysis methods is also summarised for each borehole in the summary section above the graphics. Appendix K-7 contains the Go to Borehole 1-13 sheets for all production boreholes of the Scheme. The Equal Volume method was also applied to determine the sustainable yield for each borehole (Appendix K-5).

The Go to Wellfield sub-menu (from Figure 8-3) summarises the annual abstraction from each wellfield (see Appendix K-3).

The major advantage of WELLMAN is that it summarises all relevant borehole and other hydrogeological information of each borehole and wellfield in a user-friendly spreadsheet. By simply selecting a borehole and pressing the "Go To BH" button, a graphical display of pumping and rest water level data in relation to depth of pump intake and monthly abstraction, versus recommended abstraction can be visualised (Figure 8-3).

From Figure 8-3, it is observed that lowering of the rest water levels takes place over time, when a certain monthly abstraction (referred to herewith as threshold) is exceeded. By simple visual inspection, the maximum, monthly abstraction volume to avoid unacceptable lowering of the rest water level is determined. At the same time, the depth of pump intake and available drawdown is also visible. The rainfall over time can also be looked at by simply selecting the "Rainfall" submenu, from the main menu interface (Figure 8-2). Because each graph shows the actual and recommended monthly abstraction, it is easy to evaluate whether the managing agent complies to instructions. The presence of the pumping and rest water levels makes it possible to evaluate the pump efficiency and could indicate the onset of bacteriological clogging in the production boreholes in the Nardouw Aquifer. In the case of the Vermaaks River Wellfield, which is connected to a spring, the spring flow figures are also summarised in the same spreadsheet to evaluate the impact of abstraction on spring flow.

In terms of management of fractured aquifers, the ultimate management system is an adequate groundwater level and rainfall monitoring network. During the early stages of developing a groundwater monitoring network in such aquifers, the water balance, conceptual hydrogeological model and recharge mechanisms are unknown. The only way to start understanding the aquifer flow systems and conceptual model is to evaluate the available data. The WELLMAN spreadsheets provide an easy way to evaluate aquifer performance based on the 'real' data, by simply taking groundwater variations and abstraction over time into account for as long a period as possible (preferably > 36 months). Furthermore, WELLMAN represents the 'real world situation', where groundwater abstraction from several boreholes in the same wellfield is imprinted in the water level reaction. Therefore, although the WELLMAN solution offers individual borehole displays, it incorporates

pumping from all the boreholes in the unit, e.g. for the Vermaaks River Wellfield, the WELLMAN solution incorporates pumping from all four boreholes at the recommended rate (Table 8-2). One way to ensure sustainable development of TMG Aquifers is to complete a comprehensive aquifer test analysis, backed by preliminary recharge calculations for the development of a new wellfield. At a later stage, as water level, abstraction and rainfall data become available over time, the aquifer management plan can be fine-tuned by WELLMAN.

Analyses of the information displayed on Figure 8-3 for the Vermaaks River Wellfield, referred to as the WELLMAN method of analysis, shows the following:

- Abstraction of approximately 6500 m^3/month or 215 m^3/d (2.5 l/s), has a negligible impact on the rest water level over time. This is valid for the rainfall conditions that prevailed over a 74 month period (April 1993 to March 1999).
- The maximum abstraction that could be tolerated over short periods (at the most one month) followed by periods of no pumping for recovery, is 346 m^3/d (4 l/s).
- Using the same data the Equal Volume method gives 173 m^3/d (2 l/s) and the Theis method 259 m^3/d (3 l/s).
- Note how the new recommendation contrasts with earlier yield recommendations, i.e. 8, 4.6 and 4.5 l/s (see Table 8-1).

8.2.2 Recommended pumping rate for Eastern Sector KKRWSS Production boreholes

The WELLMAN method of analysis is carried out for each production borehole of the Eastern Sector of the KKRWSS. For each of the above-mentioned boreholes a WELLMAN summary sheet similar to Figure 8-3 is designed (Appendix K-7). All these WELLMAN summary sheets are summarised in Table 8-2. The positions of all the production boreholes in Table 8-2 is shown in Figure K-1O (Appendix K-1) and in Figure 3-1.

Table 8-2 summarises the recommended sustainable yield for each of the production boreholes of the Eastern Sector of the KKRWSS, based on the following analysis methods:

- FC Method (see Sections 6.2.1, 6.2.2 and 6.2.3 and Table 8-1)
- Cooper-Jacob Method (see Sections 6.2.1, 6.2.2 and 6.2.3 and Table 8-1)
- Equal Volume Method (after van Tonder and Xu, 2000) in WELLMAN
- WELLMAN Method of analysis.

Based on the WELLMAN method of analysis (described in Section 8.3.2) the sustainable and maximum yields for each of the production boreholes of the Eastern Sector of the KKRWSS

is determined (Appendix K-7). The results from the WELLMAN method of analysis are compared with the recommended borehole yields obtained from the FC, Cooper-Jacob and Equal Volume Methods, respectively. The recommended yields, summarised in Table 8-2 are based on continuous pumping over a 24 hour day.

TABLE 8-2: SUMMARY OF RECOMMENDED SUSTAINABLE BOREHOLE YIELDS: EASTERN SECTOR PRODUCTION BOREHOLES

METHOD AND RECOMMENDED SUSTAINABLE YIELD (m^3/d) AND (l/s)						
	Aquifer	***FC Method m^3/d (l/s) #**	**Cooper-** ****Jacob Method** **m^3/d (l/s)**	**Equal Volume Method** **m^3/d (l/s)**	**Recommended Yield WELLMAN** **m^3/d (l/s)**	**Max Yield WELLMAN** **m^3/d (l/s)**
VERMAAKS UNIT						
VR6	Peninsula	639 (7.4) 360 (4.4)	657 (7.6)	230 (2.7)	216 (2.5)	302 (3.5)
VR7	Peninsula	1728 (20.0) 1149 (13.3)	1123 (13)	546 (6.3)	864 (10.0)	1296 (15.0)
VR8	Peninsula	-		175 (2.0)	259 (3.0)	432 (5.0)
VR11	Peninsula	1331 (15.4) 925 (10.7)	1080 (12.5)	202 (2.3)	259.2 (3.0)	346 (4.0)
VOORZORG UNIT						
VG3	Nardouw	434 (5.0) 225 (2.6)	475 (5.5)	173 (2.0)	216 (2.5)	346 (4.0)
VARKIESKLOOF UNIT						
DP10	Nardouw	950.4 (11.0)		34 (0.4)	174 (2.0)	216 (2.4)
DP12	Nardouw	-		163 (1.9)	259.2 (3.0)	346 (4.0)
DP29	Nardouw	-		222 (2.6)	259.2 (3.0)	518 (6.0)
BOKKRAAL UNIT						
DP15	Nardouw	950.9 (11.0) 510 (5.9)	579 (6.7)	165 (1.9)	432 (5.0)	518 (6.0)
DP25	Nardouw	-		147 (1.7)	259.2 (3.0)	518 (6.0)
DP28	Nardouw	1382.4 (16.0) 1676 (19.4)	1814 (21)	326 (3.8)	432 (5.0)	778 (9.0)
DROëKLOOF UNIT						
DG110	Nardouw	-		134 (1.6)	172.8 (2.0)	216 (2.5)
OLIFANTS RIVER UNIT						
DP18	Alluvial	864 (10.0) 43 (0.5)	916 (10.6)	463 (5.4)	518.4 (6.0)	1038 (12.0)

- No test pumping data could be found

Red values represent sustainable yield using geometric mean of final drawdown of constant yield test and main water strike

* Advance FC solution using available drawdown = difference between main water strike and rest water level.

** Use Cooper –Jacob method in FC Spreadsheet.

Comparison from Tables 8-1 and 8-2 shows that the highest yield estimates for boreholes are obtained simplistic pump test interpretation, without consideration of aquifer characteristics. From Table 8-2, the FC Method gives the highest recommended yield for all boreholes where this method is applied incorrectly. If the correct available drawdown is entered into the FC spreadsheet (values in red, in Table 8-2), the results are comparable with those of the Wellman method of analysis. The Equal Volume Method gives the lowest yields. The

Cooper-Jacob method gives values between the Equal Volume and FC Method values, but slightly over-estimates the yields of boreholes where matrix flow occurs predominantly. The main difference between the FC and Cooper-Jacob analyses is that it uses short-duration pump test data compared to the other methods (72 hours versus 74 months), which uses long-term water level, abstraction and rainfall data. In the case of pump test analysis, the test pump rate also influences the results.

Table 8-2 shows that thorough pump test analysis with the FC spreadsheet is an excellent method in the absence of long-term water level and abstraction data to determine the sustainable yield of a borehole, provided that:

The end drawdown of the constant discharge test is used as the available drawdown input value, when the main water strike was reached during the constant discharge test. If the position of the main water strike was not reached during the constant discharge test, use the geometric mean of the final drawdown and main water strike for relatively, shallow water strikes. Careful in the case of deep water strikes, when the geometric mean could lead to an over-estimate of sustainable yield (van Tonder, 2000).

8.2.2.1 Recommended yield: Vermaaks River Wellfield

Groundwater abstraction for the period April 1993 to March 1999 from the Vermaaks Unit, is estimated to be of the order of 1252 m^3/d and the recommended yield is 1598 m^3/d (see Table 8-2). For the above-mentioned period, the average monthly rainfall was 40 mm, compared to the long-term average for the Kammanassie Mountains of 50 mm / month. This gives 7396 m^3/d (2.7 x 10^6 m^3/a) recharge, if a recharge rate of 14% of annual rainfall is assumed. This is considerably less than the recharge estimate of 3.4 x 10^6 m^3/a, using a long-term average rainfall figure of 600 mm/a for the Kammanassie Mountains (Chapter 7, Section 7.3).

From Table 8-1, pump test analysis results without consideration of the aquifer boundaries and water balance seem to provide an over-estimation of borehole yield, as the borehole yield and not the aquifer yield is considered. A sustainable yield of 1598 m^3/d is estimated for the Vermaaks River Wellfield with the Equal Volume method and WELLMAN based on the analysis of long-term groundwater level, abstraction and rainfall data,. Up to March 1999 the current abstraction of 1252 m^3/d from the Vermaaks River Spring has already led to a substantial decline

in springflow (at least 6 l/s, see Section 7.3) and water levels (approximately 20 m).

The Wellman and Equal Volume Methods used groundwater abstraction and water level data for the period April 1993 to March 1999 (74 months). For the same period 2932 and 1890 mm of rainfall was measured at the Wildebeesvlakte and Dysselsdorp Purification Works' rain gauges, which yields the following rainfall per km^2 for the Peninsula and Nardouw Aquifers, respectively:

- Peninsula Aquifer: 2.932 x 10^6 m^3 / 74 months / km^2 = 1321 m^3/d rain / km^2, of which 185 m^3/d / km^2 is recharged, assuming a recharge rate of 14%.

- Nardouw Aquifer: 1.890 x 10^6 m^3 / 74 months / km^2 = 851 m^3/d rain / km^2, of which 43 m^3/d / km^2 is recharged, assuming a recharge rate of 5 %.

- The Vermaaks Window = 40 km^2, which yields 40 x 185 = 7396 m^3/d (85.6 l/s) recharge.

- Spring flow (Vermaaks, Marnewicks and Huis Rivier) 5357 m^3/d (62 l/s) of which 30 % is base flow (TMG groundwater), giving 1607 m^3/d.

Based on a recharge rate of 7396 m^3/d (85.6 l/s), annual abstraction of 1252 m^3/d (14.5 l/s) and 1607 m^3/d (18.6 l/s) baseflow to springs, a surplus of 4537 m^3/d (52.5 l/s) is calculated. However, why does the groundwater level drop 20 m and spring flow in the Vermaaks River Spring decline by 520 m^3/d (6 l/s)? It is postulated that one or more of the following explains the above discrepancy:

- The Vermaaks River Wellfield does not have access to the groundwater supply of the entire Vermaaks Unit, i.e. the catchment size is considerably smaller than 40 km^2.
- The Vermaaks River Wellfield forms part of the Keystone Block Aquizone. Groundwater outflow from the Vermaaks Window recharge area along the Keystone Block is postulated to be at least 2542 m^3/d (29.5 l/s, or 0.93 x 106 m^3/a, see Table 7-2) to recharge the Nardouw Aquifer of the Keystone Block. This would then compensate for the current abstraction in southern part of the Kammanassie Mountains (Table 7-2 and Section 7.3). It is however expected that the magnitude of this outflow component is even bigger.

- Base flow constitutes more than 30% of total flow in streams. Midgley et al. (1994) shows that approximately 90% of the flows in streams in TMG catchments are groundwater. This gives a total spring flow volume of 4821 m^3/d (55.8 l/s).

Considering the above, the water balance is as follows:

- Recharge is 7396 m^3/d (85.6 l/s) for the Vermaaks Window.
- Outflow to the Keystone Block Aquizone, is 2542 m^3/d (29.5 l/s).
- Groundwater abstraction Vermaaks Wellfield, is 1252 m^3/d (14.5 l/s).
- Baseflow to the Vermaaks, Marnewicks and Huis Rivier systems, is 4821 m^3/d (55.8 l/s).
- Water In – Water Out = 7396 – (2542 + 1252 + 4821) = -1219 m^3/d (14.1 l/s).

If the above postulation is correct, the above water balance shows that approximately 1219 m^3/d (14.1 l/s) of groundwater is taken from storage, resulting in the drop in water levels and decline in springflow.

If the catchment boundaries of that part of the Peninsula Aquifer feeding the Vermaaks Wellfield is taken as the Vermaaks River catchment (Figure 7-2), recharge is estimated as follows:

- Catchment size of 10.85 km^2
- Recharge allocation of 185 m^3/d / km^2.
- Recharge = 185 * 10.85 = 2007 m^3/d (23.2 l/s)

The latest average flow measured for the Vermaaks Spring is estimated to be approximately 346 m^3/d (4 l/s) and abstraction equals 1252 m^3/d (14.5 l/s), leaving, 346 m^3/d (4 l/s). The system shows declining water levels, which means that the recharge assumption of 14 % (or 185 m^3/d/ km^2) is wrong, or the assumption that the Vermaaks Wellfield taps only the hydrologic catchment of the Vermaaks River is wrong. If the recharge rate is calculated backwards, to eliminate the surplus, recharge is estimated to be 10.4% (or 137 m^3/d/ km^2), which is far lower than estimated (see Section 7-26). It is postulated that any catchment size smaller than the TMG Window area will give wrong recharge estimates, as the only boundary condition is the C/S Aquitard. Further, the

outflows to the Nardouw Aquifer of the Keystone Aquizone needs to be considered.

Taking into account the results of the water balance study, pump testing interpretation and the borehole characteristics, the total recommended yield of the Vermaaks River Wellfield is 1555 m^3/d (18 l/s). From test pumping results only VR7 and VR11 can be pumped simultaneously. A pumping schedule of 15 l/s for VR7 and 3 l/s for VR11 is recommended on a continuous basis. The other boreholes, i.e. VR6 and VR8, can be maintained as monitoring and standby boreholes, at yields of 2.5 and 3.0 l/s, respectively. It is also possible to pump only VR7 at 18 l/s continuously.

The reason why 15 l/s is allowed for VR7 and not 10 l/s as indicated by the WELLMAN method of analysis, is because this method considers simultaneous pumping from all boreholes in the WELLFIELD. VR6 and 8 are excluded, freeing more capacity, which is allocated to VR7.

8.2.2.2 Recommended yields : other TMG wellfields of Eastern Sector of KKRWSS

From re-testing and borehole reconstruction and rehabilitation work carried out by Jolly (1998), the major issues in the above-mentioned wellfields, are:

- The presence of iron-bacteriological clogging, reducing the borehole efficiencies. Therefore, continuous pumping at low pumping rates is preferred to minimise the chances for iron-bacteriological clogging.
- All three boreholes in the Bokkraal and Varkieskloof Wellfields, respectively, are sited on the same lineament and all the boreholes in each of the above wellfields fall within each other's radius of influence. It is therefore only possible to pump one borehole at a time in the Bokkraal and Varkieskloof Wellfields.

Based on the recharge calculations for the total Nardouw Aquifer, significant amounts of groundwater are still available for abstraction. Of the above-mentioned wellfields, only the Bokkraal Wellfield is located close to nearby abstraction on the farm Waaikraal. Based on the limitations listed above, the yields of the Varkieskloof, Bokkraal and Droëkloof Wellfields are limited in terms of the available recharge. This is also illustrated by the steep rise in water levels over the past two years (see Appendix K-7).

It is recommended that DP28 and DP12 be pumped on a continuous basis at 5 and 3 l/s, respectively, giving a total yield of 8 l/s (691 m^3/d) for the Bokkraal and Varkieskloof Wellfields. DG110 can yield 2.0 l/s on a continuous basis. The total capacity of the Droëkloof Wellfield is therefore 173 m^3/d. The total capacity of the Bokkraal, Varkieskloof and Droëkloof Wellfields is therefore 10 l/s (864 m^3/d).

8.2.2.3 Recommended yield: Voorzorg Wellfield

The Voorzorg Wellfield is composed at present of only one borehole, VG3, situated downstream of the C/S Aquitard. Considering recharge and the fact VG3 is the only borehole in an approximately 8 km strip downstream from the C/S, and provided that VG2 (privately owned borehole) is not in operation, the following recommendation is made:

That VG3 is pumped on a continuous basis at 2.5 l/s (216 m^3/d). For not more than thirty days continuously, VG3 can yield 4.0 l/s (346 m^3/d), provided that it is allowed to recover afterwards for the same number of days it was pumped at the higher rate.

8.2.2.4 Recommended yield: Olifants River Wellfield

No water balance was carried out for this wellfield as DP18, the only production borehole, is drilled into the alluvial aquifer of the Olifants River. However, from Table 8-2 the following yields are recommend for DP18:

- The WELLMAN method of analysis: 6 l/s (518 m^3/d) and a maximum yield of 12 l/s (1038 m^3/d).
- The FC method: 10 l/s (864 m^3/d).
- Theis method: 11 l/s (950 m^3/d).

Based on the performance of this borehole, continuous pumping at a rate of 10 l/s (864 m^3/d) is recommended. Pumping for short periods, not longer than 30 days continuously, is permitted at 11 l/s (950 m^3/d), on the condition that the borehole is allowed to recover thereafter.

8.2.2.5 Capacity of the Eastern Sector KKRWSS

The Eastern Sector of the KKRWSS has a design capacity (estimated from test pumping carried out in 1994 by DWAF (Mulder, 1995) of 9000 m^3/d (3.3 x 10^6 m^3/a) based on peak demand. In the original scheme design, groundwater was abstracted from 13 production boreholes in six wellfields (Figure 3-1). Of these, the following wellfields abstract water from the Nardouw Aquifer, with the number of boreholes per wellfield given in brackets: Varkieskloof (3), Bokkraal (3) and Droëkloof (1). The Vermaaks River (5) wellfield taps the Peninsula Aquifer. One borehole taps the alluvial aquifer of the Olifants River.

Recent changes to the KKRWSS management by Jolly (1998) are based on borehole efficiency, considerations around iron-reducing bacteria and an assumption that all TMG Aquifers are the same. Neither water balance considerations, nor the conceptual hydrogeological model, are taken into account. Further, production figures were set conservatively to meet the current demand, which is 50 l/s in summer and 25 l/s in the winter months (approximately 1.18 x 10^6 m^3/a). Jolly (1998) states that test pumping results indicated that a maximum of up to 91 l/s (1.43 x 10^6 m^3/a) could be obtained from the boreholes.

Evaluation of long-term water level variations over time, the conceptual hydrogeological model and water balance indicates that the following can be obtained from the wellfields:

- Vermaaks River Wellfield: VR7 and VR11 – 1555 m^3/d
- Bokkraal Wellfield: DP28 - 432 m^3/d
- Varkieskloof Wellfield: DP12 - 259 m^3/d
- Droëkloof Wellfield: DG110 - 173 m^3/d
- Voorzorg Wellfield: VG3 - 216 m^3/d
- Olifants River Wellfield: DP18 - 864 m^3/d

The above gives a total capacity of 3499 m^3/d or 1.27 x 10^6 m^3/a from seven boreholes out of the 13 drilled. The capacity could be substantially more if it was not for the iron-bacteriological clogging, in all the wellfields exploiting the Nardouw Aquifer.

8.3 RADIUS OF INFLUENCE OF BOREHOLES

In order to determine the radius of influence of a production borehole, the Dupuit Equation, frequently used to calculate the dewatering requirements for an open pit mine, is used.

- **Background**

In order to quantify groundwater flow to open pit workings, the "equivalent borehole approach" is commonly used to obtain a preliminary estimate of inflow volume. This technique assumes that dewatering of an excavation is effected by use of an imaginary borehole, fully penetrating the entire saturated thickness of the aquifer. Water is pumped out at a uniform discharge rate in order to maintain the piezometric level in the aquifer below the final pit floor. The excavation itself is assumed to represent a large diameter borehole.

The Peninsula Aquifer of the TMG Window Areas is considered as an unconfined aquifer in which linear and steady state flow to the 'pit' is calculated by the modified **Dupuit equation**:

$$Q = \frac{\pi K(H^2 - h^2)}{\ln R/r} \qquad \text{.....Equation 20}$$

where,

Q: pit inflow (m^3/s)
K: hydraulic conductivity (m/s)
H: hydraulic head above final pit floor (m) at distance R
h: hydraulic head above final pit floor at distance r
R: radial extent of drawdown (m), based on $R=3000 \times H \times (K)^{1/2}$
r: equivalent borehole radius (m)

The radial extent term was used to calculate the radius of influence for the Peninsula Aquifer boreholes in the Vermaaks River Wellfield. The hydraulic conductivity was calculated from the FC analyses interpretation and H is interpreted as the drawdown in the pumping borehole. Due to poor borehole construction and biofouling and/or clogging of borehole screens impacting on the boreholes in the Varkieskloof, Droëkloof and Bokkraal wellfields, they are excluded in these calculations. The above Nardouw Aquifers are not considered typical Nardouw Aquifers, based on hydrochemical considerations and most probably intersect Bokkeveld shale with quartz veins containing pyrite, providing the low pH, sulphide oxidizing environment.

- **Limitations of the Dupuit Equation**

These calculations are based on the following assumptions and conditions:

- The aquifer is unconfined.
- The aquifer is of infinite areal extent.
- The aquifer is isotropic.
- The aquifer is homogeneous and of uniform thickness over the area influenced by the pump test.
- Prior to 'mining', the water table is horizontal over the area that will be influenced by drawdown.
- The aquifer is pumped at a constant rate.
- The 'mine' penetrates the entire aquifer and thus receives water from the entire saturated thickness of the aquifer.
- The Dupuit assumptions are satisfied, if (1) the velocity of flow is proportional to the tangent of the hydraulic gradient instead of the sine, as it is in reality and (2) the flow is horizontal and uniform everywhere in a vertical section through the axis of the imaginary borehole.

- **Radius of influence calculations**

Table 8-3 summarises the relevant information required to calculate the radius of influence of the Vermaaks and Voorzorg boreholes. The 'best' Nardouw Aquifer borehole is the VG3 borehole in the lower portion of the Vermaaks River Valley. Although this borehole is recharged by TMG groundwater in the alluvium of the river, this is the best data set. From Table 8-3 the radius of influence in the Nardouw Aquifer varies between 10 to 106 m for rest and pumping conditions, respectively.

In the Varkieskloof and Bokkraal Wellfields, groundwater abstraction during 1998 and 1999 was considerably less than previously, as most boreholes were out of action during screen replacements and rehabilitation programs. In the absence of abstraction, rest water levels rose between 20 and 30 m, leading to an 'inverse cone of depression', in terms of H. However, a quick calculation of the radius of influence for DP28, using T = 200 m^2/d and H = 10 and 20, for rest water level and pumping conditions, respectively, for times before the water level recovery started, give a radius of influence of 128 and 255 m, for pumping and non-pumping conditions, respectively. Based on the above, boreholes in the Nardouw Aquifer, should be spaced at least 1 km apart. From the above two of the boreholes in each of the Bokkraal and Varkieskloof Wellfields are redundant and should be used as standby and monitoring boreholes.

TABLE 8-3: SUMMARY – RADIUS OF INFLUENCE, VERMAAKS AND VOORZORG PRODUCTION BOREHOLES

BH	Depth (m)	Initial wl (m)	Saturated Thickness (m)[1]	H_{rest} (m) [2]	$H_{pumping}$ (m) [3]	T (m^2/d)[4]	K (m/d)[5]	K (m/s)	Radius (m)[6]
VG3	207	6	201	3	33	20	0.1	$1.5x10^{-6}$	10 (106)[7]
VR6	250	35	215	24	39	20	0.09	$1.0x10^{-4}$	75 (121)
VR7	177	63	114	27	37	180	1.6	$1.9x10^{-5}$	346 (475)
VR8	251	101	150	24	34	20	0.1	$1.2x10^{-6}$	89 (127)
VR11	225	126	99	25	35	50	0.5	$5.9x10^{-6}$	181 (326)

Boreholes VR6, 7, 8 and 11 are each 400 m apart and VR6 is approximately 2200 m from the C/S Aquitard. Table 8-3 indicates that the current cone of depression of VR6, 7 and 8 overlaps, which is further exaggerated for pumping conditions. For pumping conditions the cone of depression of VR8 and VR11 also overlaps. This is not surprising, as pump testing by Jolly in 1998, indicated that VR6, 7 and 8 are interconnected.

Table 8-3 shows that the cone of depression for abstraction from the Vermaaks River Wellfield is not likely to expand further than a radius of 1.05 km from VR7. The cone of depression has the shape of an elongated ellipsoid along the Vermaaks River Valley, with the centre of the cone being VR7.

In the Vermaaks River Wellfield the borehole spacings are too small, and the rate of drawdown in the cone is largely exaggerated by drawdown cones of the four boreholes intercepting each other, leading to faster drawdown. A borehole spacing of 2 km apart seems to be adequate. In the current configuration groundwater is mined over a small surface area, creating high groundwater flow gradients towards the cone to fill up the gap, as seen with the fast recovery of boreholes once the pumps are switched off. The most economical solution would be to use VR6, 8 and 11 as monitoring and/or standby boreholes and to pump VR7 at 18.0 l/s.

---

[1] The saturated thickness is simply taken as the saturated portion of the aquifer that can bedewatered.

[2] Difference between initial water level, after borehole was drilled in 1993, and rest water level measured in March 1999.

[3] Difference between pumping water level and initial water level.

[4] Transmissivity calculated by FC Method.

[5] Hydraulic conductivity calculated by T/ saturated thickness.

[6] Radius of influence calculated for each borehole using the Dupuit relationship $R = 3000 * H * (K)^{1/2}$

[7] 10 (106) represents the radius of influence for VG3 for the current rest water level and pumping water level conditions respectively.

8.4 TMG MANAGEMENT PLAN

In order to manage or develop any part of the TMG Aquifer (Figure 5-1, page 49) a holistic view of all components of the conceptual hydrogeological model and their interaction needs to be understood. The following aspects need to be considered in order to improve management of TMG Aquifers (TMGMAN):

1. The TMG Super Aquifer as presented in Figure 5-1 (page 49) needs to be divided into hydrogeological compartments, in terms of the following:

   - Remote sensing and satellite lineament analysis, together with geological interpretation, is required to define the aquifer geometry and to define permeable aquizones, linking different lithological units.
   - The lithology of the host aquifer, i.e. Nardouw versus Peninsula Aquifer.
   - Definition of the conceptual hydrogeological model for each section of the TMG Super Aquifer.
   - Based on the conceptual hydrogeological model for each section of the Super Aquifer, a preliminary water balance calculation needs to be carried out. This requires that recharge and outflows (abstraction and springflow) for each Section of the TMG Super Aquifer must be determined.

2. The impact of abstraction on baseflow in streams and vegetation needs to be addressed. Abstraction will sooner or later impact spring flow and the minimum spring flow requirement that will minimise impact on the environment needs to be defined.

3. It must be anticipated that with the growth in water demand, groundwater abstraction from the TMG Aquifers in the Western Cape will become increasingly important. A monitoring borehole network should be put in place in each of the Sections of the TMG Super Aquifer to collect information to improve our understanding of the dynamics of the system. It is proposed that such monitoring networks include the following:

   - Network of monitoring boreholes sited on permeable structures, identified by remote sensing and lineament mapping, across the aquifer under consideration, to clarify all aspects of the conceptual model.
   - Monthly water level measurements at monitoring boreholes.
   - Environmental isotope and hydrochemical sampling carried out on at least an annual basis.
   - Adequate distribution of rainfall gauges.
   - Sampling of rainwater for Cl and $\delta^{18}O$.

- Determine recharge from relationship of Cl in groundwater for areas outside the mountain catchments and rainwater, and ^{14}C and ^{3}H, mean residence times.
- Carry out a spring survey and characterise the springs in the study area.
- Capture all the information in a data base such as Wellman.
- Conduct pumping tests and determine the aquifer parameters.

4. During development of a wellfield the following needs to be considered:

- Use remote sensing and satellite lineament mapping to site boreholes.
- Nardouw Aquifers at lower altitudes in the absence of pemeable connections to the recharge zones in the mountains can pose all sorts of management problems, such as iron-bacteriological clogging of borehole screens.
- Identify potential highly permeable aquizones, connected to the Nardouw Aquifer at lower altitudes with the recharge areas.
- Characterise fracture styles, geometry and density, providing pathways for recharged ground water in the mountains to flow in folded bedding planes to lower elevations in aquizones.
- Determine from first principles the radius of influence for boreholes, i.e. 2 km spacing required for boreholes in the Peninsula Aquifer and 1 km for the Nardouw Aquifer.
- Do not equip boreholes where reducing conditions prevail in the groundwater, as these are ideal conditions for iron-reducing bacteriological clogging of borehole screens.
- Avoid siting of boreholes upstream of the C/S Aquitard and but rather target permeable aquizones at lower altitudes.
- Establish a good spring flow record, before abstraction commences.
- Carry out pump testing and apply comprehensive aquifer testing analysis techniques, using the FC spreadsheet in conjunction with a water balance to determine the sustainable yield of boreholes and wellfields.
- Verify and update pump test analyses results later with groundwater monitoring data.
- Use hydrochemistry and environmental isotopes in conjunction with satellite lineament mapping to characterise the groundwater flow paths.
- Characterise environmental concerns in the study area and try to minimise negative impacts by selecting better pumping targets, based on the conceptual hydrogeological model.

Based on the history of the management problems experienced by the KKRWSS, the principles of TMGMAN will assist wellfield management in the TMG Aquifers of the Little

Karoo and elsewhere. TMGMAN includes the aquifer characteristics, recharge and pump test analyses results, in order to obtain a holistic aquifer management scenario. It is recommended that the principles of TMGMAN be expanded into an ARCVIEW and ACCESS database for the TMG Super Aquifer in order to simplify regional management of the aquifer.

CHAPTER 9: CONCLUSIONS

The main conclusions following on from this research are:

- The TMG is a regional fractured aquifer, covering a large area in the Western Cape. A good understanding of the fracture styles, geometry and preferred orientation of water-bearing fractures contributing significantly to groundwater flow together with a good understanding of the hydrostratigraphic inter-relationships between different lithological units, is essential in aquifer conceptualisation. In order to manage TMG Aquifers optimally the conceptual hydrogeological model and water balance need to be understood.

- Geology, remote sensing, satellite lineament mapping and analysis, with the combined use of environmental isotopes and hydrochemistry in conjunction with hydrogeological data, are indispensable tools in the formulation of the conceptual hydrogeological model for the TMG Aquifer.

- Extensional regimes prevailed across WNW trending fractures in the Little Karoo. The afore-mentioned fractures and E-W trending faults are likely to respond best to modern stress regimes. Reactivation along NNW-trending fractures and N-S trending joints is also possible. NNW trending fractures and lineaments are well developed in the TMG and are likely to be permeable to ground water movement, i.e. the receiving environment for ground water recharge providing secondary porosity.

- Interpretation of hydrochemical data with trilinear diagrams, except the Schoeller diagram, is not very useful to differentiate between the different TMG Aquifers, i.e. Nardouw and Peninsula Aquifers, due to the low mineralisation of groundwater from these aquifers. The Piper Diagram is, however, a very useful diagram to differentiate between groundwater from the TMG Aquifers and other aquifers, e.g. alluvial or limestone.

- TMG groundwater is classified as a Na/Cl type water on the Piper Diagram, as all other ions are present at very low concentrations. The major ion chemistry of TMG groundwater is not balanced, in that the low alkalinity and pH of the groundwater leads to the conclusion that free CO_2 is present, which needs to be balanced by the dissolution of Mg^{2+} and Ca^{2+}. In thermal springs, unbound CO_2 evolves into mainly Ca^{2+} alkalinity, i.e. shifts to the left in the Piper diagram.

- X-Y scatter plots of the ion pairs and / or environmental isotopes $\delta^{18}O$ and TDS, SO_4^{2-} : Cl^- , HCO_3^- : Cl^- , HCO_3^- versus $\delta^{14}C$ and Na^+: Cl^- and Ca^{2+}: HCO_3^- + SO_4^{2-} ; Ca^{2+}: Mg^{2+} and Ca^{2+}: Na^+ + K^+ ratios are very useful to distinguish groundwater types and dissolution processes in TMG Aquifers.

- The following types of groundwater are distinguished in the Kammanassie Mountains of the Klein Karoo, based on significantly differing hydrochemical and environmental isotope signatures and analysis of structural geology:

  - Peninsula Aquifer.
  - Three types of groundwater originating from the Nardouw Aquifer: (1) those which are not in direct hydraulic connection with groundwater in the Bokkeveld or Peninsula Aquifers, (2) those which are in hydraulic connection with groundwater in the Bokkeveld Aquifer, and (3) those which are in hydraulic connection with the Peninsula Aquifer in permeable aquizones.
  - Groundwater originating from the Bokkeveld Aquifer.
  - Groundwater originating from the Olifants River Alluvial Aquifer.

- Groundwater in the Peninsula Aquifer is characterised by its low mineralisation (TDS < 300 mg/l), low pH (< 6) and very low TAL (<< 0.5 meq/l). The Klein Karoo TMG groundwaters typically cluster around $\delta^{18}O$ and TDS values between –6 to –8 ‰ and < 400 mg/l, respectively.

- Compared to TMG Aquifers, the sandstones of the Bokkeveld Aquifer are generally poor aquifers in the Klein Karoo, with poor groundwater quality, although yields > 10 l/s do occur.

- Due to the low total dissolved inorganic carbon of the ground water, it is necessary to extract 300 L or more ground water in the field for radio carbon analysis, made possible by the polyethylene bag method of precipitation. Because of the largely unbound dissolved inorganic carbon in TMG groundwater, no corrections need to be applied for storage estimations.

- The sudden "ageing" of ground water from above and below the C/S in the Vermaaks River Valley (from 75-84 to 53 pMC), apart from similar $\delta^{13}C$, $\delta^{18}O$ and $\delta^{2}H$ values indicates that the C/S acts as an effective aquitard, inhibiting subsurface drainage further down-stream.

- Trace element chemistry has the potential to provide valuable insights into the exploitation potential of TMG Aquifers, in terms of providing information on the permeability (feldspar dissolution) and the presence of pyrite-quartz veining (potential for iron-bacteriological clogging of boreholes).

- The presence of Ni, Cu, Co and Zn is indicative of the presence of pyrite quartz veining, which is always recorded in borehole logs where iron-bacteriological bacteriological clogging prevails.

- Comparison of the $\delta^{18}O$ and $\delta^{2}H$ signatures of the hot springs and mountain seepages confirmed the working hypothesis, i.e. that the recharge areas of groundwater emanating at hot springs are the higher altitudes of the mountain ranges. The $\delta^{18}O$ and ^{14}C signatures of hot springs vary with intake history, degree of interconnection between fracture sets, TMG lithologies, proximity of the hot spring to the recharge area, and / or rainfall origin.

- Conventional aquifer delineation is not appropriate for the regional fractured TMG Aquifers, as hydrostratigraphic boundaries do not coincide with those of the lithostratigraphic units of a geological sequence. Fractures and faults complicate aquifer definition and may introduce some ambiguities into the hydrostratigraphical classification. For example, where a highly fractured and thus sufficiently permeable fault zone has a sufficiently large stratigraphic throw, it may juxtapose and thus create a leakage junction between two otherwise separate aquifers. A fault could also connect two distinctly different aquifers, previously separated by an aquitard, or high permeability fracture zones can crosscut several hydrostratigraphic units.

- Conventional aquifer delineation is adjusted to include aquizones, which are definite structural zones (faults, master joints, even structurally controlled cave systems) of particularly high hydraulic conductivity, crosscutting several lithologic sequences. Aquizones can be contained within a larger, formally defined aquifer of generally lower permeability or as a limited permeable feature trans-secting an aquitard unit. An example of such an aquizone is the Vermaaks Keystone Block referred to as the Keystone Block Aquizone.

- The TMG Super Aquifer of the Western Cape is defined as the TMG outcrop extending from Clanwilliam in the north-west to Port Elizabeth in the east and can be divided into four distinct sections, based on significantly different folding and faulting styles, resulting from different thickness of geological successions, their position in the CFB and

associated tectonic regimes present in each section. The four sections of the TMG Super Aquifer include the Western, Central, Klein Karoo and Eastern TMG Sections.

- The TMG Super Aquifer consists of the Peninsula and Nardouw Aquifers separated by the C/S Aquitard. The Peninsula Aquifer consists of a highly fractured quartz arenite. The Nardouw Aquifer consists of an arcosic sandstone with silty / shaley interbeds. The porosity of bedding and joint fractures is of the order of 1%, as opposed to 5% in permeable aquizones, i.e. Vermaaks Keystone Block Aquizone and up to 7% along major fault zones, i.e. Vermaaks River Fault Zone.

- The following three types of springs occur in the TMG Super Aquifer:

  - Type 1: shallow springs emanating at perched water tables. These are not connected to the regional groundwater table and will not be impacted by groundwater abstraction.
  - Type 2: lithologically controlled springs, due to the presence of inter-bedded aquitards, i.e. Type 2.1 at Peninsula - C/S contact, Type 2.2 TMG – Bokkeveld contact and Type 2.3 at unconformities.

  - Type 3: fault controlled springs, representing hot springs mostly.

The C/S is an aquitard, as indicated by significant differences in ^{14}C values stream-up, down-stream of it, and forms the characteristic TMG Window areas across the Cape Mountains. The C/S Aquitard acts as a confining layer for groundwater in the Peninsula Aquifer with depth and leads to the formation of cold springs at the C/S - Peninsula Formation contact (Type 2.1). Fractures trans-secting the C/S layer at great depth lead to the formation of hot springs (Type 3 springs).

- The following three scales of groundwater flow systems are distinguished:

  - Local scale, representing a TMG Window area, e.g. Vermaaks Window.
  - Intermediate scale, representing a mountain range, e.g. Kammanassie Mountains.
  - Regional scale representing groundwater flow along the folded bedding of the TMG Super Aquifer.

- Numerous NNW-trending fractures in parts of the Kammanassie Mountains (Vermaaks River Valley) give rise to a strong directional permeability. These fractures act as important feeder zones collecting recharge, which is transferred to more permeable fracture sets trending WNW, NNE and E-W.

- The regional groundwater flow directions and fluxes are not well understood. The wide separation and low yield of the thermal springs in the Klein Karoo, suggests limited deep fracture flow. The regional flow component is visualised in this study as flow at depth along the folded bedding of the Peninsula Aquifer, rather than regional fractures.

- The Cango Fault Zone is postulated to be a no-flow boundary and groundwater entering the Peninsula Aquifer in the Swartberg Mountains is postulated to flow in a northerly direction along the folded bedding towards the TMG underlying the Great Karoo. The Peninsula Aquifer outcropping in the Kammanassie, Rooiberg and Outeniqua Mountains is connected at depth along the folded bedding. In the absence of borehole and water level information, it was not possible to determine the magnitude and direction of the major regional groundwater flow component.

- Increased exploitation from the highly fractured catchment valleys (Peninsula Aquifer or Nardouw Aquifer in permeable Aquizone), constituting part of local catchments is the economic solution for groundwater development. Local catchments have groundwater of good quality and yield, buffered by intermediate and regional flow systems. This will clearly have to be at the expense of the baseflow of mountain streams in local catchments and local lowering of water levels. Eventually, the transport of groundwater in regional fractures will be reversed, producing resistance levels in the yield-drawdown relationship. In the light of the present information, this would not appear to have major water quality consequences. Exploitation of regional scale fractures can be considered in other sections of the TMG Super Aquifer.

- Based on lithological considerations, the highest yielding (10 l/s to > 20 l/s), best quality groundwater is found in the Peninsula Aquifer on WNW, N-S, NNE and E-W trending fractures, falling directly within the recharge area, constituting the so-called TMG-window areas.

- Groundwater yield and quality in the Nardouw Aquifer depends on its connection with the recharge area. Far from the recharge area, close to the Bokkeveld contact, groundwater contains very little dissolved oxygen, due to reducing conditions, which together with quartz-pyrite veining in the Bokkeveld results in iron-bacteriological clogging of borehole screens. This Nardouw Aquifer type was encountered in the Bokkraal, Varkieskloof and Droëkloof Wellfields. It is not feasible to drill boreholes deeper than 100 m in this aquifer considering the costs associated with rehabilitation and construction of boreholes. Further, the prevailing flow conditions and geological formation requires specialised borehole design and equipping with Johnson screens.

Further, to manage the iron-bacteriological clogging of screens, continuous pumping at low rates is preferred, reducing annual capacity from these boreholes considerably.

- The best groundwater targets in the Klein Karoo are associated with the Nardouw Aquifer located in permeable aquizones, directly connected with the recharge area. High yielding, good quality groundwater is available outside the recharge area employing deeper boreholes, with limited environmental impacts on spring flow reduction within the mountain catchments. Alternatively drilling of deep boreholes through the Nardouw into the Peninsula Formation outside mountain catchments can also provide good targets and needs to be tested.

- Pump test analysis with FC spreadsheet is an excellent method in the absence of long-term water level and abstraction data to determine the sustainable yield of a borehole, provided that it is done correctly, including identifying the following characteristics:

  - Correct conceptual hydrogeological model
  - Inner boundary conditions, i.e. WBS effects, well bore skin, fracture skin and lateral extent of the fracture or fracture zone
  - Outer boundary conditions, i.e. no flow boundaries and fixed head boundaries
  - Characteristic flow regimes
  - Selection of the most suitable analytical model
  - Understand the limitations of the method of analysis and analytical model
  - Apply practical knowledge and experience
  - If the FC method is used, make sure that available drawdown is selected correctly.

- The end drawdown of the constant discharge test is used as the available drawdown input value, when the main water strike was reached during such a constant discharge test. If the position of the main water strike was not reached during the constant discharge test, use the geometric mean of the final drawdown and main water strike for relative, shallow water strikes. Care should be taken in the case of deep water strikes, when the geometric mean could lead to an over-estimation of sustainable yield (van Tonder, 2000).

- Verify the sustainable yield estimations from the FC spreadsheet with continued monitoring and further data analysis methods, such as WELLMAN, the Equal Volume and SVF methods.

- In most cases, the estimated T and sustainable yield values obtained from the Cooper-Jacob method are higher than those obtained from the FC-method. The latest Cooper-

Jacob method in the FC spreadsheet gives similar results to the basic FC solution, if the available drawdown is selected correctly. The FC method provides far more realistic estimates for S than the unrealistically low values obtained from the Cooper-Jacob method. The FC Method is a good method to determine aquifer parameters for secondary and primary aquifers, if the boundary conditions of the system are known.

- The FC analysis results for the Peninsula Aquifer show that fracture flow is more predominant in the Peninsula Aquifer. T values range between 150 and 200 m^2/d for the Peninsula Aquifer of the Kammanassie Mountains.

- In the Nardouw Aquifer, matrix flow is predominates. Although fractures may have T values up to 200 m^2/d, e.g.DP28, they are of limited extent and with long groundwater residence times, as indicated by the Carbon-14 ages. Average matrix transmissivity is estimated to be 50 m^2/d in the vicinity of fractures and considerably less in the absence of fracturing, possibly < 1 m^2/d.

- Step drawdown test analysis provides an excellent tool to evaluate borehole and screen efficiencies as well as the success of rehabilitation programs.

- The KKRWSS provides a classic example of where application of conventional aquifer testing techniques and simplistic analytical methods in the past have lead to over-estimation of the groundwater resource. Aquifer testing was mainly aimed at providing estimates of the 'safe-yield' of the production boreholes and information required for the design of the pump equipment. Consequently, the recommended pumping rates for the KKRWSS had to be reduced five times.

- Analysis of total groundwater abstraction figures for the Kammanassie Mountains indicates that:

  - The amount of groundwater abstracted on privately owned properties in and around the Kammanassie Mountains is double that of the Eastern Sector of the KKRWSS.
  - The total annual abstraction on privately owned properties is 1.6×10^6 m^3/a, of which 0.9×10^6 m^3/a, comes from the Keystone Block Aquizone.
  - The total annual abstraction from the Peninsula Aquifer is 0.63×10^6 m^3/a.
  - The total annual abstraction from the Nardouw Aquifer is 2.0×10^6 m^3/a.
  - The total annual abstraction for the Kammanassie Mountains is estimated to be of the order of 2.6×10^6 m^3/a.

- The total annual abstraction from the Keystone Block Aquizone is 1.5 x 10^6 m^3/a.

- Midgely *et al.* (1994) have shown with the aid of stable isotopes that < 5% of storm flow in TMG catchments is comprised of direct run-off, suggesting that the rapid response of streamflow to rainfall is a direct consequence of displaced groundwater. Water balance calculations show that baseflow represents more than 30% of annual precipitation in a catchment.

- The best estimate for minimum flow of the Vermaaks Spring, prior to abstraction from the Vermaaks River Wellfield, is of the order of 10 l/s (0.32 x 10^6 m^3/a). Spring flow figures of 10, 12 and 40 l/s are postulated for the Vermaaks, Marnewicks and Huis River systems, yielding 62 l/s (2.0 x 10^6 m^3/a) in total. Of this spring flow total, the Vermaaks and Huis River systems drain the Keystone Block Aquizone, yielding 50 l/s (1.6 x 10^6 m^3/a).

- Groundwater abstraction of 14 l/s (0.6 x 10^6 m^3/a), over the period 1993 to 1999 from the Vermaaks River Wellfield, resulted in a decline of flow from the Vermaaks River Spring of 6 l/s (0.2 x 10^6 m^3/a) over the same period of time.

- Recharge calculations, using various recharge methodologies, indicate that the average recharge rates for the Nardouw and Peninsula Aquifers of the Kammanassie Mountains are 5.4 and 14 %, respectively. This yields 9.5 million m^3/a annual recharge each (combined recharge of 19 million m^3/a) for the Nardouw Aquifer and Peninsula Aquifers of the Kammanassie Mountains over an area of 500.2 and 113.4 km^2, respectively.

- The sustainable yield of the Vermaaks River Wellfield is estimated between 0.4 and 0.5 x 10^6 m^3/a, considering that spring flow has already declined by 0.19 x 10^6 m^3/a (6 l/s). However, the sustainable yield of the Vermaaks River Wellfield is estimated to be only of the order of 0.3 to 0.4 x 10^6 m^3/a, if rainfall is 500 mm and recharge only 0.76 x 10^6 m^3/a. In the long-term, abstraction in the range of 0.4 to 0.5 x 10^6 m^3/a is sustainable, if abstraction elsewhere in the Keystone Block remains constant.

- The porosity of bedding and joint fractures in the Nardouw and Peninsula Aquifers are in the order of 1%, as opposed to 5% and more in brecciated and fractured strata, i.e. Keystone Block and Faultzones. From the porosity and the mean residence time of

groundwater in the Vermaaks River Wellfield, the storage of the Keystone Block Aquizone, which the wellfield utilises is in the order of 0.5×10^5 m^3/a.

- Recharge estimations, based on hydrologic catchment boundaries, under-estimates the hydrogeological potential of a groundwater unit. The boundary condition, i.e. C/S Aquitard, needs to be used instead to determine the catchment size.

- Water balance calculations for the Vermaaks River Wellfield show that groundwater outflow along permeable aquizones needs to be considered.

- Annual abstraction from the KKRWSS has never exceeded 1.1×10^6 m^3/a as opposed to the designed capacity of 4.7×10^6 m^3/a. The major reasons for this are:

  - Simplistic initial pump test analysis, only considering the borehole capacity and not the aquifer capacity.
  - Out of the 18 production boreholes, 13 are sited in the Nardouw aquifer, where iron-bacteriological clogging requires continuous pumping at low yields.
  - 60% of the boreholes are drilled within each other's radius of influence.
  - A water balance study was not carried out and the impacts on the flow of the Vermaaks River spring from abstraction of the nearby Vermaaks Wellfield not considered.
  - Lack of a conceptual hydrogeological model, defining the groundwater flow relationships, characteristics of the aquifers and long-term sustainable aquifer yield.

- A user-friendly Excel spreadsheet "WELLMAN" has been developed for the management of wellfields and boreholes in the TMG. Various macros in the spreadsheet link a series of worksheets containing rainfall, water level, abstraction, springflow, geological logs test pumping and depth of pump inlet information.

- Evaluation of long-term water level variations over time, the conceptual hydrogeological model, WELLMAN and water balance indicates that the following can be obtained from the wellfields:

  - Vermaaks River Wellfield: VR7 and VR11 – 1555 m^3/d
  - Bokkraal Wellfield: DP28 - 432 m^3/d
  - Varkieskloof Wellfield: DP12 - 259 m^3/d
  - Droëkloof Wellfield: DG110 - 173 m^3/d
  - Voorzorg Wellfield: VG3 - 216 m^3/d
  - Olifants River Wellfield: DP18 - 864 m^3/d
  - Maintain a flow of 4 l/s (346 m^3/d) at the Vermaaks River Spring.

- The total capacity of the Eastern Sector of the KKRWSS is estimated to be 3499 m^3/d or 1.27 x 10^6 m^3/a from seven boreholes out of the 13 drilled.
- The radius of influence for boreholes in the Nardouw and Peninsula Aquifers is 1 and 0.5 km respectively.

CHAPTER 10: REFERENCES

Al-Aswat, A.A and Al-Bassam, A.M. (1997). *Proposed hydrostratigraphical classification and nomenclature: application to the Palaeozoic in Saudi Arabia.* J. Afr. Earth Sci., 24 (4) 497-510.

Adar, E. M., Rosenthal, E., Issar, A.S. and Batelaan, O. (1992). *Quantitative assessment of the flow pattern in the southern Arava Valley (Israel) by environmental tracers and a mixing cell model:* Journal of Hydrology 136 (1992), pp 333 – 352.

Andersen N.J.B. and Ainslie L.C. (1994). *Neotectonic reactivation - an aid to the location of groundwater.* Afr. Geo. Rev. 1, 1-10.

Andreoli M.A.G., van der Vlugt R., Norman N., von Veh M.W. and Andersen N.J.B. (1989). *Interpretative geological map of the pre-Tertiary basement between Gansbaai and Waenhuiskrans - Arniston, S. Cape (1/100 000).* Atomic Energy Corporation of South Africa, Limited.

Andreoli, MAG, Doucoure, M, Van Bever Donker, J, Brandt, D and Andersen, NJB (1996). *Neotectonics of southern Africa- a review.* Africa Geoscience Review, Vol. 3, No.1., pp1-16.

Bands, D.P., Bosch, J.M., Lamb, A.j., Richardson, D.M., van Wilgen, B.W., van Wyk, D.B. &Versfeld, D.B. (1992) *Jonkershoek Forestry Research Centre – Pamplet 384.* Issued by the Forestry Branch of the Department of Environmental Affairs.

Berkowitz, B. (1992) *Modelling groundwater flow and pollution in dry regions.* Course in Groundwater Modelling, Ben Gurion University of the Negev, Israel.

Bosch, J.M. (1979). *Treatment effects on annual and dry period streamflow at Cathedral Peak.* South African Forestry Journal No 108, March 1979.

Braune, E. and Reynders, A.J. (1998) *"Past achievements and future challenges for groundwater in South Africa".* GEOCONGRESS 98, July, Pretoria, South Africa.

Bredenkamp, D.B. (1992). *Estimation of the yield of the Polfontein compartment.* Technical Report GH3783, Directorate Geohydrology, Dept. Water Affairs.

Bredenkamp, D.B., Botha, L.J., van Tonder, G.J., van Rensburg, H.J. (June 1995). *Manual on quantitative estimation of groundwater recharge and aquifer storativity based on practical hydrological methods.* Water Research Commission Report, TT 73/95.

Brink, A.B.A. (1981). *Engineering Geology of Southern Africa.* Everton Book Press, 247pp.

Brown, L., Smart, M. and Cluver, G. (2001) *The impact of groundwater abstraction on ecosystems in the Kammanassie Nature Reserve and Environs.* WRC Project K4/470 (ongoing).

Chevallier, L. (1999). *Regional structural geological interpretation and remote sensing, Little Karoo.* WRC Project K8/324.

Chevallier L. and Woodford A.C. (2000*) Morphotectonics and mechanism of emplacement of the dolerite rings and sills of the western Karoo South Africa.* S.Afr. J.Geol. (ongoing).

Clark I. and Fritz, P. (1997). *Environmental isotopes in hydrogeology.* Lewis Publishers, New York, pp328.

Craig, H. (1961b). *Standards from reporting concentrations of deuterium and oxygen-18 in natural waters.* Science 133:1833-4.

Craig, H. and Keeling, M. (1963). *The isotopic geochemistry of water and carbon in geothermal areas,* In: E. Tongiorgi, (Ed.), *Nuclear Geology on Geothermal Areas. Spoleto. 1963.* Consiglio Nazionale delle Ricerche, Laboratorio di Geologia Nucleare, Pisa: 17-53.

Dansgaard, W (1964). *Stable isotopes in precipitation.* Tellus 16: 436-68.

De Beer, C.H. (1990). *Simultaneous folding in the western and southern branches of the Cape Fold Belt.* S. Afr. J. Geol., **93**(4), 583-591.

De Beer, J.H. (1983), *Geophysical studies in the southern Cape Province and models of the lithosphere in the Cape Fold Belt.* Spec. Publ. geol. Soc. S. Afr., **12**, 57-62.

De Laat, P.J. M. and Savenije, H.H.G. (1996). *Principles of Hydrology.* International Institute for Infrastructural, Hydraulic and Environmental Engineering, The Netherlands, course notes (HH273/96/1).

Department of Water Affairs (1986). *Yield analysis – Terms and procedure.* Report PCOOO/0016886.

Domenico, P.A. and Schwartz, F.W. (1990). *Physical and chemical hydrogeology.* John Wiley and Sons, New York, 824 pp.

Dörhöfer, G. and Volker, J. (1981). *A method for determining area-related rates of groundwater recharge.* Volume 14, Natural resources and development. A biannual collection of recent German contributions, Hannover, Germany.

Drever, J.I. (1997). *The geochemistry of natural waters: Surface and Groundwater Environments. 3rd Ed.*, Prentice Hall, New Jersey, 436 pp.

Dunkle, S.A., Plummer, L.N., Busenberg, E., Phillips, P.J., Denver, J.M., Hamilton, P.A., Michel, R.L. and Coplen, T.B. (1993). *Chlorofluorocarbons (CCl3F and CCl2F2) as dating tools and hydrologic tracers in shallow groundwater of the Delmarva Peninsula, Atlantic Coastal Plane, United States.* Water Resources Research, Vol. 29, No. 12, 3837-3860.

Duvenhage, A.W.A, Meyer, R. and de Raath, C.J (1993). *A geoelectrical survey in the Oudtshoorn area to identify potential drilling targets for groundwater.* CSIR Division of Earth, Marine and Atmospheric Science and Technology, Report No. EMAP-C-93042.

Duvenhage, A.W.A and Meyer, R.(1992). *The reinterpretation of Schlumberger deep resistivity soundings from the Oudtshoorn Cretaceous basin and an evaluation of the applicability of other geoelectrical techniques to identify target areas in the Table Mountain Group for groundwater exploration.* EMATEK, CSIR, Report No. EMA-C-92023.

Du Preez, J.W. (1965) *Verslag oor boorgate op die Swartbergverskuiwing in die Oudtshoorn Vallei tussen Schoemanshoek en Georgida.* Unpublished Geological Survey of SA report, Reference 205/B/3876, (also GH3909, DWAF).

DWAF – Directorate Geohydrology (1994): *Notes from discussion with Prof. Issar at the Institute for Groundwater Studies (IGS), Bloemfontein: 1-2 February 1994.*

Diamond, R. (1997). *Stable isotopes of the thermal springs of the Cape Fold Belt.* Unpubl. MSc thesis, Univ. Cape Town, 81 pp.

Freeze, R.A. and Cherry, J.A. (1979). *Groundwater.* Prentice-Hall, 604 pp.

Friedli, H., Lotscher, H., Oeschger, H., Siegenthaler, U. and Stauffer, B. (1986). *Ice core record of the $^{13}C/^{12}C$ ratio of atmospheric CO_2 in the past two centuries.* Nature, 324:237-238.

Fu, L., Milliken, K.L. and Sharp, J.M. (Jr) (1992). *Permeability variations in liesegang-banded Breathitt Sandstone (Pennsylvanian) diagnetic controls.* Geol. Soc. America Abs. with programs (Ann.Mtg.), Vol. 24, 254 pp.

Gallegos, D. J., Thoma, S.G. and Smith, D.M. (1992). *Impact of fracture coatings on the transfer of water across fracture faces in unsaturated media.* IN: Proceedings of the 3rd Annual International High-Level Radioactive Waste Management Conference, Las Vegas, NV, pp 738-745.

Garrels, R.M. and Christ, C.L. (1965). *Solutions, minerals, and equilibria.* Freeman, Cooper, and Company, San Francisco, 450 pp.

Gat, J.R. and Tzur, Y. (1967). *Modification of the isotopic composition of rainwater by processes which occur before groundwater recharge.* In Isotopes in Hydrology, IAEA Veina, 49 –60.

Gat, J.R. and Carmi, I. (1970). *Evolution of the isotopic composition of atmospheric waters in the Mediterranean Sea area.* J. Geophys. Res 75:3039-48.

Gat, J.R. (1981). *Palaeoclimate conditions in the Levant as revealed by the isotopic composition of palaeowaters.* Israel Meteorol. Research Papers 3: 13-28.

Gat, J.R. (1996). *Oxygen and hydrogen isotopes in the hydrologic cycle*. Unpublished paper, Dept. of Environmental Sciences and Energy Research, Weizmann Institute of Science, 76100 Rehovot, Israel.

Gieske, A. (1995). *Hydrodynamics of 14C analysis in unconfined aquifers.* Groundwater '95. Ground Water Recharge and Rural Water Supply. GWD/BWA Conference, Midrand. Paper 17.

Gringarten, A.G. (1982) *Flow test evaluation of fractured reservoirs.* Special paper 189, Geological Society of America. 27 p.

Hem, J. D. (1985). *Study and interpretation of the chemical characteristics of natural water.* 3 rd ed. US, Geol. Survey Water Supply paper 2254.

Hälbich, I.W. (1983.) *A tectogenesis of the Cape Fold Belt.* Spec. Publ. geol. Soc. S. Afr., **12**, 165-175.

Hälbich, I.W., Fitch, F.J. & Miller, J.A. (1983). *Dating the Cape Orogeny.* Spec. Publ. geol. Soc. S. Afr., **12**, 149-164.

Hälbich, I.W. and Greef, G.J. (1995). *Final report on a structural analysis of the west plunging nose of the Kammanassie Anticline.* Geology Department, University of Stellenbosch, Consulting report to DWAF, Directorate Geohydrology.

Hartnady C.J.H. and Woodford, A., (1996) *A feasibility investigation of the relationship between near-surface neotectonic crustal stress and groundwater occurrence in a Karoo fractured-rock aquifer.* Research proposal to the Water Research Commission.

Hartnady C.J.H. (1998). *A review of the earthquake history and seismotectonic interpretation of the kingdom of Lesotho,* IN: Melis and Duplessis consulting Engineers (eds), Review of the current stage of knowledge of the seismotectonic setting of Lesotho and its significance in predicting seismic design parameters for the Katse and Mohale Dams and further phases of the LHWP. *Lesotho Highlands Water Project contract No 1028., Workshop in Maseru, 25 May, 1998.* 37pp.

Hartnady, C.J. & Hay, E.R. (2000): ***CAGE STUDY***, Final report in preparation for the Department of Water Affairs & Forestry.

Hattingh, J. & Goedhart M.L. (1997*) Neotectonic control on drainage evolution in the Algoa basin, southeastern Cape Province.* S. Afr. J. Geol., **100**, 43- 52.

Hill R.S. (1988) *Quaternary faulting in the South Eastern Cape Province.* S. Afr. J. Geol. **91**, 399 - 403.

Huntoon, P.W. (1993). *The influence of Laramide foreland structures on modern ground-water circulation in Wyoming artesian basins.* IN: Snoke, A.W., Steidtmann, J.R., and Roberts, S.M., eds., Geology of Wyoming: Geological Survey of Wyoming Memoir No.5, pp 756-789.

IAEA, Conference Notes on: The First International Symposium On Application of Tracers in Arid Zone Hydrology. Vienna, Austria, 1994.

Issar, A.S. (1994). *Proposals for the study of regional groundwater flow in South Africa, with reference to the Transvaal and Northern Cape dolomite, The Table Mountain Sandstones and the Karoo Basin and a proposal to study the impact of climate change on the hydrological balance in South Africa.* Department of Water Affairs and Forestry, Technical Report No GH3833, March 1994.

Issar, A.S. (1995). *Report No3: On the regional hydrogeology of South Africa.* Consulting report to DWAF: Directorate Geohydrology, July 1995.

Issar, A.S. (1996). *Report No4: On the regional hydrogeology of South Africa.* Consulting report to DWAF: Directorate Geohydrology, August 1996, Technical Report No GH3895.

Jolly, J. (1998). *Klein Karoo Rural Water Supply Scheme – Critical evaluation of existing management and monitoring systems.* Groundwater Consulting Services Report 96-W11-52.

Kendall, K.N. and McDonell, J. (1995). *Isotope tracers in catchment hydrology.* Elsevier.

Kirchner, J. and Willemink, H. (1984). *Grondwaterstudie Oudthsoorn-omgewing Fase Een.* Instituut vir Grondwater Studies, Universiteit van die Oranje Vrystaat.

Kirchner, J., van Tonder, G.J. and Lukas, E. (1991). *The exploitation potential of Karoo aquifers.* Water Research Commission contract, 170/2/91.

Kirchner, J. and G.J. van Tonder (1995). *Proposed guidelines for the execution, evaluation and interpretation of pumping tests in fractured-rock formations.* Water SA, Vol.21 No.3, July 1995.

Konikow, L.F. (1994). *Numerical models of groundwater flow and transport.* IN: Manual on Mathematical Models in Isotope Hydrogeology, IAEA, Viena, Austria.

Konikow, L.F., & Patten, E.P., Jr. (1985). *Groundwater forecasting.* IN: Hydrological forecasting, (Anderson, M.G., Burt, T.P., Eds), John Wiley and Sons Ltd., New York, 221-270.

Kotze, J.C., (1993) *Pumptesting methods for fractured rock aquifers.* Unpublished Masters Thesis, IGS, UOFS, Bloemfontein.

Kotze, J.C., (1995) *Interim report on the performance of the Klein Karoo Rural Water Supply Scheme.* Department Geohydrology, Department Water Afairs and Forestry, Technical Report GH 3858, Pretoria.

Kotze, J.C., ***(1996)*** *Hydrogeological summary of actions of hydrogeological importances since 28 July 1995.* Department Geohydrology, Department Water Afairs and Forestry Report GH 3880, Pretoria, 1996.

Kotze, J.C. and Rosewarne, P.N. (1996). *Little Karoo Scheme – Hydrogeological Overview.* SRK Consulting Report No 230827/1 for Department of Water Affairs and Forestry.

Kotze, J.C. and Rosewarne, P.N. (1999). *Klein Karoo Rural Water Supply Scheme Augmentation Study – Groundwater Investigation.* SRK Consulting Report No 248547 for Department of Water Affairs and Forestry.

Kotze, J.C. and Rosewarne, P.N. (1999). *Hex Vallei – Twee Rivieren Irrigation Boards – Groundwater flow modelling of the Sanddrif and Amanderl River catchments.* SRK Consulting Report No 239303/1.

Kotze, J.C., Verhagen, BTh and Butler, M. (2000). *An aquifer model based on chemistry, isotopes and lineament mapping: Little Karoo, South Africa.* IN: Proceedings of the XXX IAH Congress on groundwater: Past Achievements and Future Challenges Cape Town / South Africa, A.A. Balkema, Rotterdam (ed Oliver Sililo).

Kruseman, G.P. and De Ridder, N.P.(1991). *Analysis and evaluation of pumping test data. 2nd. Ed.* International Institute of Land Reclamation and Improvement, Wageneningen, The Netherlands. 377p

Kumbrein, W.C. & Graybill, F.A. (1965). *An introduction to statistical models in geology.* McGraw-Hill, New York, 475 pp.

Lerner, D.N., Issar, A.S. and Simmers, I. (1990). *Groundwater recharge – A guide to understanding and estimating natural recharge.* IAH Publication, Volume 8.

Lock, B.E. (1980). *Flat plate subduction and the Cape Fold Belt of South Africa.* Geology, **80**, 35-39.

Mazor, E. and Verhagen, B.Th., (1983). *Dissolved ions, and radioactive isotopes and noble gases in thermal waters of South Africa.* Journal of Hydrology, 63 (1983) pp 315-329.

Mazor, E. (1991). *Applied chemical and isotopic groundwater hydrology.* Open University Press, Buckingham.

Merlivat, L. & Contiac M. (1975). *Study of mass transfer at the air-water interface by an isotopic method,* J. Geophys. Res. 84:5029-33.

Meyer, P.S. & Dyasan, B. (1989). *Voorgestelde grondwaterwaarnemings-program voortspruitend uit 'n hidrosensus in die Dysselsdorp- en Kammanassiebergebied.* Department of Water Affairs and Forestry, Tegnical Report No GH3653.

Meyer, P.S., and Dyason, B., (1989). *Voorgestelde grondwaterwaarnemingsprogram voortspruitend uit 'n hidrosensus suidwes van Calitzdorp.* DWAF, Technical Report GH3662, Augustus 1989.

Meyer, P.S. (1990). *Boorplekkeuses vir die tweede boorfase van die Klein Karoo Landelike Watervoorsieningskema.* Department of Water Affairs and Forestry, Tegnical Report No GH3679.

Meyer, P.S. (2000). *Springs in the Table Mountain Group, with special reference to fault controlled springs.* IN: Table Mountain Sandstone Aquifer Handbook *(in preparation).*

Midgley, J.J. and Scott, D.F., (1994). *The use of stable isotopes of water (D and ^{18}O) in hydrological studies in the Jonkershoek Valley.* Water SA Vol. 20, No. 2, April 1994.

Mulder, M.P. (1991). *Klein Karoo Landelike Waterskema – Vermaaksriviervallei: Water Balans.* Department of Water Affairs and Forestry, Technical Report No 33738.

Muskat, M. (1937) *The flow of homogeneous fluids through porous media.* McGaw-Hill, New York.

Moench, A.F. (1984) *Double-porosity models for a fissured groundwater reservoir with fracture skin.* **Water Resour. Res. 20** 831-846.

Mulder, M.P. (1995). *Grondwatervoorsiening vir Klein Karoo Landelike Waterskema.* Department of Water Affairs and Forestry, Technical Report No 3854, Volume I and II.

Murray, E.C. (1996): *Guidelines for assessing borehole yields in Secondary Aquifers.* Unpublished M.Sc. Thesis, Univ. of Rhodes, Grahamstown.

Newton, A.R. (1973). *A gravity folding model for the Cape Fold Belt.* Trans. geol. Soc. S. Afr., 76(2), 145-152.

Neuman, S.P. (1994). IN: *The Flow-Characteristic Method of analyzing pumping-tests.* Pump Test Workshop held February 1999, CSIR, Stellenbosch (van Tonder and Xu, 1994).
Pearse, A.J., Steward, M.K. and Sklash, M.G., (1986). *Storm run-off generation in humid headwater catchments. 1. Where does the water come from?* Water Resour. Res. 22(8) 1263-1272.

Ramsay, J.G. (1967). *Folding and fracturing of rocks.* Mc.Graw-Hill, 568 pp.

Ramsay, J.G. and Huber, M.I. (1987). *The techniques of modern structural geology, Vol.2. Third edition,* Academic Press, London, 700 pp.

Remson, I., Hornberger, G.M., Molz, F.J., (1971). *Numerical methods in subsurface hydrology. John* Wiley New York, NY, 389pp.

Rautenbach, C.J. de W. (1998). *The unusual rainfall and sea surface temperature characteristics in the South Africa region during the 1995/96 summer season.* Water SA Vol. 24 No.3.

Rosewarne, P.N. (1984). *The hydrogeology and hydrogeochemistry of the aquifer of the Hex River Valley. Report MSc Thesis, Rhodes University.*

Rosewarne, P.N. (1988). *Feasibility study on large scale groundwater abstraction from the Table Mountain Group sandstones.* Proposal to WRC.

Rust, I.C. (1973). *The evolution of the Palaeozoic Cape Basin, southern margin of Africa.* In: Nairn, A.E.M. & Stehli, F.G. (eds.), The ocean basins and margins, Vol. 1: The South Atlantic, 247-276. Plenum Publishing Corporation, New York.

Schultze, R.E. (1997). *South African Atlas of Agrohydrology and Climatology.* Water Research Commission, Technical Report TT82/86, Pretoria.

Scott, D.F. and Le Maitre, D.C. (January 1998). *The interaction between vegetation and groundwater: Research Priorities for South Africa.* Water Research Commision Report No 730/1/98.

Scott, D.F., Le Maitre, D.C and Fairbanks, D.H.K. *Forestry and streamflow reductions in South Africa: A reference system for assessing extent and distribution.* Water SA Vol. 24 No.3.

Sharp, J.M. (1993) *Fractured aquifers / Reservoirs: Approaches, problems and Opportunities.* **Memoires of the XXIV Congress of IAH**: Hydrology of Hard Rocks, Oslo, Norway.

Smakhtin, V.Y., Watkins, D.A., Hughes, D.A., Sami, K. and Smakhtina, O.Y. (1998). *Methods of catchment-wide assessment of daily low-flow regimes in South Africa.* Water SA Vol. 24 No.3.

Steenkamp, G. (1996). *Fractured rock aquifers.* Unpublished Masters Thesis, IGS, UOFS, Bloemfontein.

Streltsova, T.D. (1976) *Hydrodynamics of Groundwater Flow in a Fractured Formation.* Water Resour. Res. 12 405-413.

Theis, C.V. (1935): *The relation between lowering of the piezometric surface and the rate and duration of discharge of a well using groundwater storage.* Transactions of the American Geophysical Union, Vol. 16, p519-524.

Tsang and Tsang, Y.W. and Tsang, C.F. (1987). *Channel flow in fractured media.* Water Resources Research, Vol. 23, pp 467-479.

Turner, J.V., Macpherson, D.K. and Stokes, R.A. (1987). *The mechanisms of catchment flow processes using natural variations in Deuterium and Oxygen-18.* J. Hydrol. 94, pp 143-162.

Van der Voort (1996). *Flow in Karoo Aquifers.* Unpublished masters thesis, UOFS.

Van Tonder, G.J. (1984). *PC-Program SVF.* Unpublished report. Institute of Groundwater Studies, UOFS, Bloemfontein.

Van Tonder G.J., Kunstmann H. and Xu Y. (1998) *Estimation of the sustainable yield of a borehole including boundary information, drawdown derivatives and uncertainty propagation,* pumptest course notes, UWC.

Van Tonder G.J. and Xu, Y. (1999). *A guide for the interpretation of pumping tests and estimation of sustainable yields of boreholes in fractured-rock aquifers.* Department of Water Affairs and Forestry, Technical Report No GH3927.

Van Tonder G.J., Janse van Rensburg, H., Staats, S., Cogho, V.E., Elphinstone, C.D., Viviers, M.I., Meyer, R., Watson, A.G. and Bredenkamp, D.B. (1999). *The development of risk analysis and groundwater management techniques for Southern African Aquifers.* WRC Report No 378/1/99, Water Research Commission, Pretoria.

Van Tonder, G. & Xu, Y., (1999): *The Flow-Characteristic method of analyzing pumping-tests.* Pump Test Workshop held February 1999, CSIR, Stellenbosch.

Van Tonder, G & Xu, Y., (2001). *A guide for the estimation of groundwater recharge in South Africa.* Presented at the Recharge Workshop at the University of Pretoria, June 2001.

Van Tonder, G. (2001). *Chapter 3: Guideline for pumping test analyses in fractured aquifers.* IN: Manual on pumping test analysis in fractured aquifers (unpublished).

Vegter, J.R. (1995). *An explanation of a set of national groundwater maps. Report No TT74/95,* Water Research Commission.

Verhagen, B. Th., Geyh, M.A., Fröhlich, K. and Wirth, K. (1991). *Isotope hydrological methods for the quantitative evaluation of groundwater resources in arid and semi-arid areas.* Research Report, Fed. Ministry for Econ. Coop. Of the Fed, Republic of Germany.

Verhagen, B. Th. (1997). *Use of environmental isotopes in the characterisation of the Table Mountain Sandstone Aquifer, South Africa.* Progress Report to the International Atomic Energy Agency, Research Contract 8983/RO/Regular Budget Fund.

Verhagen, B. Th. (2000). *Environmental isotope hydrology: Principles and application to the geohydrology of the Karoo Basin.* Karoo Aquifer Handbook, WRC, in preparation.

Vogel, J.C. (1970). *Carbon-14 dating of groundwater.* Isotope hydrology 1970, Proc. Symp. IAEA, 9-13 March 1970, 225-237.

Visser, J.N.J. (1991). *Discussion and author's reply to: 'Simultaneous folding in the western and southern branches of the Cape Fold Belt' by C.H. de Beer. SA J. Geol., 93(4), 583-591.* SA J. Geol., **94**(5/6), 392-395.

Visser, J.N.J. (1992). *Basin tectonics in south-western Gondwana during the Carboniferous and Permian.* In: De Wit, M.J. & Ransome, I.G.D. (eds.), Inversion tectonics of the Cape Fold Belt, Karoo and Cretaceous Basins of Southern Africa, 109-115. Balkema, Rotterdam.

Wang, J.F. & Anderson, M.P. (1982). *Introduction to Groundwater modelling.* Freeman, San Francisco, CA, 237 pp.

Whittingham, J.K, (1969). *Water Resources in the Grobbelaars river catchment, tables of springs and boreholes.* DWAF Technical Report No GH1458.

Weaver, J.M.C., Talma, A.S. and Cavé, (1996). *Geochemistry and isotopes for resource evaluation in the fractured rock aquifers of the Table Mountain Group.* WRC Report No K5/731, Water Research Commission, Pretoria.

Yurtsever, Y. (1975). *Worldwide survey of stable isotopes in precipitation.* Rep. Isotope Hydrology Section, IAEA, 40pp.

Woodford A. and Chevallier L. (1998). *Regional characterisation and mapping of Karoo fractured aquifer systems - An integrated approach using a geographical information system and digital image processing.* Water Research Commission Project report K5/653.

Woodford A. (2001) *Interpretation and applicability of pumping-tests in Table Mountain Group Aquifers.* IN: TMG handbook (*op cit).*

Ek verklaar dat die proefskrif wat hierby vir die graad PhD Geohidrologie aan die Universiteit van die Oranje Vrystaat deur my ingedien word, my selfstandige werk is en nie voorheen deur my vir 'n graad aan 'n ander universiteit / fakulteit ingedien is nie. Ek doen voorts afstand van outeursreg in die proefskrif ten gunste van die Universiteit van die Oranje Vrystaat.

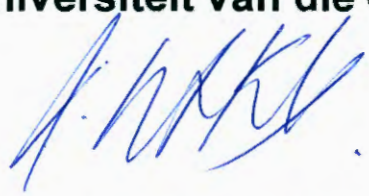

Johanita Christelle Kotze

OPSOMMING

Die Tafelberg Groep Akwifeer is regionale waterdraer, wat strek oor groot dele van die Wes- en Oos-Kaap Provinsies. Ten einde die doeltreffende bestuur en ontwikkeling van die Tafelberg Groep Akwifeer te bewerkstellig word 'n holistiese benadering, wat al die verskillende komponente asook hul onderlinge interaksie in die geohidrologiese konseptuele model, in ag te neem.

Om die bestuur van die Klein Karoo Landelike Watervoorsienings Skema in die Klein Karoo te verbeter is 'n geohidrologiese konseptuele model vir die Tafelberg Groep Akwifeer in die Klein Karoo ontwikkel. Die konseptuele model is gegrond op die struktuur geologiese kartering, remote sensing, lineament kartering vanaf satellietfoto's, omgewings isotope en hidrochemie te same met geohidrologiese data.

Die geohidrologiese konseptuele model toon aan dat die Tafelberg Groep Akwifeer bestaan uit die Nardouw en Peninsula Akwifere, geskei van mekaar deur die Sederberg Skalie Akwitard. Die Pensinsula Akwifeer is hoofsaaklik 'n gefraktuurde kwartsareniet, met 'n transmisiwiteit wat varieer tussen 150 en 200 m^2/d. Fraktuurvloei as die hoof vloei meganisme. Die Nardouw Akwifeer, het 'n transmissiteit wat varieer tussen <1 en 50 m^2/d, in die afwesigheid en teenwoordigheid van frakture onderskeidelik en bestaan uit 'n arkosiese sandsteen, afgewissel met slik en skalie tussen lae.

Beduidende verskille in ^{14}C isotoop waardes in grondwater stroom-op en –af van die skalie band onderskeidelik, dui aan dat die S/S 'n akwitard is wat 'n digte seël tussen die Peninsula en Nardouw Akwifere vorm, in die afwesigheid van frakture, en vorm die sg. Tafelberg Groep Venster areas in die Kaapse Berge. Die Sederberg Skalie Akwitard laat grondwater in die Peninsula Akwifeer onder druk verkeer met diepte en gee aanleiding to die formasie van standhoudende fonteine by die Sederberg Skalie / Peninsula kontak. Frakture wat die Sederberg Skalie laag op groot dieptes onderbreek, gee aanleiding tot die oorsprong van warmwaterbronne. Seisonale fonteine vorm tydens die reënseisoen bokant verhewe watertafels, wat bo lokale skalie lae vorm. Hierdie fonteine is baie afhanklik van reënval aanvulling en is nie verbind met die regionale watertafel nie, en sal ook nie deur grondwater onttrekking beinvoled word nie.

Hierdie studie het bewys dat grondwater aanvulling (ongeveer 14% van jaarlikse reënval), grotendeels plaasvind in die sg. Tafelberg Groep Venster areas, in die hoogs gefraktuurde lokale berg opvanggebiede. Vanaf die aanvullingsgebied vloei grondwater deur middel van 'n netwerk van gekonnekteerde frakture stroom-af langs die geplooide sandsteen lae tot op groot dieptes. Die aangevulde grondwater word tydelik gestoor in kleinskaalse NO-SO, N-S and NO-SW strekkende frakture, wat gevorm is deur die meganiese verbrokkeling van die boonste 100 meter van rots. Verdere aanvulling forseer die water afwaarts na intermediêre skaal frakture óf oormatige water ontsnap as basisvloei na die bergstrome, óf grondwater onttrekking vind plaas.

Veel minder direkte aanvulling vind plaas in die geval van die Nardouw Akwifeer (6 % van jaarlikse reënval) as gevolg van laer reënval, op laer hoogte bo seespiëel waar die akwifeer hoofsaaklik dagsoom. In 'n mindere mate word die Nardouw Akwifeer ook aangevul deur die syfering van water deur die Sederberg Skalie Aquitard.

Drie verskillende skale van grondwater vloeisisteme word geonderskei, nl: lokaal, intermediêr en regionaal, wat onderskeidelik gedefineer word as, Tafelberg Groep Venster (binne die skalie band), 'n bergreeks en grondwater beweging langs die geplooide Tafelberg Groep laagvlakke (verskeie bergreekse).

Die regionale vloei sisteem en die omvang daarvan is huidiglik nog ongedefinieerd. Die wyd verspreiding en lae vloei volumes van warmwaterbronne in die Klein Karoo dui op beperkte diep grondwater sirkulasie. Die regionale grondwater vloei word verder, eerder gevisualiseer as vloei tot op groot dieptes langs die geplooide laagvlakke in die Peninsula Akwifeer as langs regionale frakture, wat wel die geval is elders in die Tafelberg Groep regionale akwifeer. Verder postuleer die studie dat die Kango Verskuiwingszone ondeurdringbaar is en as 'n geen vloei grens vir grondwater vloei beskou word.

Die hoogsgefraktuurde lokale berg-opvangsgebiede, gevorm deur nou valleie, is die mees ekonomiese oplossing vir grondwater ontwikkeling. Lokale grondwater opvangsgebiede lewer grondwater van goeie gehalte en lewering wat gebuffer word deur die aanvulling in intermediêre en regionale vloei sisteme. Ontginning van lokale opvangsgebiede sal onvermydelik ten koste van basisvloei van bergstrome in lokale opvangsgebiede, asook gepaardgaande verlaging van watervlakke, geskied. Oor die langtermyn sal die buffering van regionale en intermediére aanvulling die effek van grondwater ontrekking teenstaan.

Die beste teikengebiede vir grondwater-ontwikkeling in die Tafelberg Groep Akwifeer van die Klein Karoo is die voorkoms van hoogs deuratende akwizones in die Nardouw Akwifeer wat met die aanvullingsgebied verbind is. Boorgate met hoë lewering en goeie grondwater kwaliteit is ook moontlik buite die aanvullingsgebied, ten koste van dieper boorgate, deur die Nardouw en Bokkeveld formasies tot binne in die Peninsula Akwifeer. Beide bg. opsies sal die omgewings impakte op fonteinvloei in bergopvanggebiede aansienlik beperk, mits onttrekking nie aanvulling oorskrei nie.

Hierdie navorsing het bewys dat volgehoue standhoudende ontwikkeling van Tafelberg Groep Akwifere slegs moontlik is, indien die geohidrologiese konseptuele model en waterbalans van die akwifeer verstaan word. Alhoewel boorgate met hoë lewering dikwels moontlik is in deurlatende fraktuurzones met hoë porositieite en deurlatenheid, lei eenvoudige interpretasie van pomptoets data, sonder die inagneming van die geohidrologiese konseptuele model of waterbalans tot grootskaalse oorskatting van die boorgatlewering en boorgatveld potensiaal. Dit lei tot ooronttrekking en gevolglike ongewenste omgewings impakte en oorkapitaliseering van groundwater skemas.

SUMMARY

The Table Mountain Group Aquifer is a regional fractured aquifer, covering a large area of the Western and Eastern Cape Provinces. In order to manage or develop any part of the TABLE MOUNTAIN GROUP Super Aquifer, a holistic view of all components of the conceptual hydrogeological model and their interaction needs to be understood.

A conceptual hydrogeological model is formulated for the Table Mountain Group Aquifers of the Klein Karoo, based on the interpretation of geological mapping, remote sensing, satellite lineament mapping, environmental isotopes and hydrochemistry in conjunction with hydrogeological data.

This conceptual hydrogeological model shows that the Table Mountain Group Super Aquifer consists of the Nardouw and Peninsula Aquifers separated by the Cederberg Shale Aquitard. The Peninsula Aquifer consists of a highly fractured quartz arenite, with transmissivity ranges between 150 and 200 m^2/d and fracture flow is the main flow mechanism. Matrix flow occurs in the Nardouw Aquifer, which consists of arkosic sandstones with silty / shaley interbeds, with transmissivity ranging between 50 m^2/d in the vicinity of fractures and < 1 m^2/d in the absence of fractures.

.

The Cederberg Shale is an aquitard, as indicated by significant differences in ^{14}C values in groundwater up and down-stream of it and forms the characteristic Table Mountain Group Window areas across the Cape Mountains. The Cederberg Shale Aquitard acts as a confining layer for groundwater in the Peninsula Aquifer with depth and leads to the formation of cold springs at the Cederberg Shale - Peninsula Formation contact. Fractures transsecting the Cederberg Shale layer at great depth leads to the formation of hot springs. Seasonal springs form above perched water tables, above localised clay layers in the rainy season, which are very dependent on rainfall recharge and not connected to the regional groundwater flow system and will therefore not be affected by groundwater abstraction.

This research has confirmed that most recharge takes place in the Peninsula Aquifer (14% of annual rainfall) which outcrops in the so-called Table Mountain Group Window Areas in the highly fractured mountainous local catchments. From here it travels via inter-connected fracture sets down-gradient to great depths and distances. Groundwater recharge is stored temporarily in the smaller scale NE-SE, N-S and NE-SW trending fractures that formed during mechanical failure in the top 100 m of the anticlines. The major movement is downwards in these fracture sets. Groundwater is stored in these fractures until either more recharge forces it further downwards into connecting intermediate scale fractures, or excess groundwater is released as baseflow to streams or by groundwater abstraction. Minor recharge (6% of annual recharge) also takes place in the Nardouw Aquifer, where it outcrops below the Cederberg Shale Aquitard, but to a lesser extent, due to lower rainfall at lower altitudes. Further recharge in the Nardouw Aquifer also results from leakage through the Cederberg Shale Aquitard.

Three scales of groundwater movement takes place in the Table Mountain Group Aquifer, i.e. local, intermediate and regional scale, representing the Table Mountain Group Window areas, a mountain range and groundwater flow along the folded bedding of the Table Mountain Group Super Aquifer, respectively.

The regional groundwater flow directions and fluxes are not well understood. The wide separation and low yield of the thermal springs suggest limited deep flow. The regional flow component is visualised in this study as flow at depth along the folded bedding of the Peninsula Aquifer, rather than regional scale fractures, which is possible elsewhere in the Tabel Mountain Sandstone Aquifer. The Cango Fault Zone is postulated to be a no-flow boundary.

Increased exploitation from the highly fractured catchment valleys, constituting part of local catchments are the most economic solution for groundwater development. Local catchments have groundwater of good quality and yield, buffered by intermediate and regional flow systems. This will clearly have to be at the expense of the base-flow of mountain streams in local catchments and local lowering of water levels. Eventually, the transport of groundwater in regional fractures will be reversed, producing resistance levels in the yield-drawdown relationship. In the light of the present information, this would not appear to have major water quality consequences.

The best groundwater targets in the Klein Karoo are in the Nardouw Aquifer and comprise permeable aquizones, directly connected with the recharge area. High yielding, good quality groundwater is available outside the recharge area at the expense of deeper boreholes, drilled through the Bokkeveld and Nardouw Formations into the Peninsula Aquifer, with limited environmental impacts on spring flow reduction in the mountain catchments themselves.

The research confirmed that sustainable development of Table Mountain Group Aquifers are only possible if the conceptual hydrogeological and water balance is understood. In permeable fracture zones high yielding boreholes are possible, resulting from the high porosity and permeabilities along these zones. Simplistic interpretation of pump test data, without acknowledgement of aquifer boundary conditions and recharge can lead to the over-estimation of borehole yields, resulting in over-abstraction and consequent negative environmental impacts and poor returns on capital investments in groundwater schemes.

APPENDIX A: HYDROCHEMISTRY DATA

TABLE A-1: SUMMARY FIELD DATA – SIMONIC, KOTZE, VERHAGEN – JANUARY 1996

Borehole	Location	LAT	LONG	Depth	Elevation	WL	Yield	TEMP	pH	DO(%)	TAL	EC
VR6	Vermaaks River	33.3643	22.3248	250	718.3	48.7	8.6	19.5	4.8	55		9
SL2	Scheeperskraal	33.4152	22.371	153	610		1.3			12	1.2	47.5
DL17	Danielskraal	33.3409	22.2125	248.8	291.7	33.36	8	23.4	6.05	80	1	34.5
T/W	Toorwater Spa	33.2356	23.0916	0				42.3	6.2	5	1.2	45.5
P1	Parshall1, Vermaaks	33.57777	22.5355	0			5.5	27		95		5.62
WBG	Warmwaterberg Spa	33.4557	20.54	0				42.5	6.55	0	1	12
C/S	Calitzdorp Spa			0				49.6	6.65	59	1.1	18
VR11	Vermaaks River	33.3711	22.3332	210	812.2	141	8.3	20.9	4.75	53	0.2	6.9
VR7	Vermaaks River	33.3654	22.3304	173	748.9	78.5	20	19.3	5.2	51	0.2	7.2
RF2	Rolbaken	33.4021	22.342	116	600	37.41	10.1	20.4	5.05	7	0.2	10
RF1	Rietfontein	33.404	22.3457	85		13.51	10	20.4	4.75	68	0.2	13
DL13	Danielskraal	33.56743	21.63809	185	261.8	44.31	7	24	6.45	6	1.3	40.5
DP12	Varkieskloof	33.3423	22.2715	192	468.5	120.58	6.5	23.2	5.5	0	0.9	15.5
DP29	Bokkraal	33.3427	22.2714	240	463.1	115.8	6	24	6	0	0.5	14.5
VG3	Voorsorg	33.3402	22.322	206.7	497.3	13.44	6.1	21.8	6.1	47		14.3
DP18	Olifants River	33.3402	22.322	18	351.1	2.4	9.1	20.7	6.75	0	4.2	83
DP28	Varkieskloof	33.3453	22.2125	246	459.1	115.03	11	23.5	4.95	0	0.35	13.5
DL16	Danielskraal	33.3358	22.2124	279.4	279	32.75	2.5	23.7	6.55	1	1.35	33.5
DP15	Bokkraal	33.3453	22.2644	207	451.1	105.89	9	23.3	3.6	0	0	21
LD2	Leeublad	33.4014	22.3417	90	620		5	23.5	5.5	65	0.2	10
WN2	Welgevonden				527.6				5.55	41	0.35	22

TABLE A- 2: FE AND MN CONCENTRATIONS, ADAPTED FROM SRK REPORT 230827

Borehole	Fe (mg/l)	Mn (mg/l)	SO4 (mg/l)
VR11	0.285	<0.001	<4
VR7	0.182	<0.001	6
VR8	0.208	<0.001	8
DL15	3.414	0.796	20
DL13	0.574	0.034	22
VR6	0.175	<0.001	7
DL16	3.746	0.643	20
DP18	0.574	0.34	113

TABLE A-3: ENVIRONMENTAL ISOTOPE ANALYSIS – JANUARY 1996 SAMPLING SURVEY Verhagen, Kotze and Simonic

NAME	DATE	C-14	T	C-13	O-18	D
		pMC	TU	o/oo	o/oo	o/oo
C/S	96/01/31	13		-14.5	-7.53	-46.6
DL13	96/01/31	21		-11.9	-7	-42.7
DP12	96/01/31		0.3		-6.58	-47.3
DP15	96/01/31	52		-19.7	-7.66	-47.8
DP18	96/01/31	114.2	3.2	-13.1	-5.57	-35.1
DP28	96/01/31	62.3	0.4	-20.3	-7.93	-48.6
DP29	96/01/31	41.2	0.1	-18.8	-7.72	-48.9
LD2	96/01/31		0		-7.38	-44.5
RF2	96/01/31	75.4	0.1	-21	-7.13	-44
SL2	96/01/31		0.2		-6.43	-41.4
T/W	96/01/31	25.6		-17.3	-7.08	-48
VR11	96/01/31	74.6	0.3	-20.6	-7.18	-51.1
VR6	96/01/31	79.4	0.4	-21.3	-7.68	-48.1
DL17	96/01/31	21.7		-18.3		
VR7	96/01/31	83	0	-20.8	-7.56	-45.2
v-notch	96/01/31		0.5		-7.33	-46.2
m-vnotch	96/01/31		0.5		-7.24	-45.8
WBG	96/01/31	11		-14.6	-7.57	-46
WN2	96/01/31	72	0.3	-19.7	-7.82	-50.4

TABLE A-4: MACRO ELEMENT CHEMISTRY – 1996 SAMPLING SURVEY KOTZE, VERHAGEN AND SIMONIC

Name	DATE	EC	TDS	pH	Ca	Mg	Na	K	TAL	SO4	Cl	NO3	F	PO4	Si	NH4
C/S	96/01/31	21.5	133	7.3	9	4	17	9.4	42	9	34	0.04	0.4	0.005	17.7	<0.04
DL13	96/01/31	49.5	313	7.2	12	8	66	16.2	59	24	115	0.05	0.5	<0.005	5.3	0.07
DL15	94/8/5	44.5	229	7.2	12	10	37	14.2	36	20	90	0.04	0.4	0.019	4.5	<0.04
DL16	94/8/5	46.7	254	7.3	12	9	47	14.3	50	20	91	0.04	0.5	0.02	4.9	<0.04
DP12	96/01/31	22.2	126	6.4	5	4	32	4.3	19	16	41	0.04	0.4	0.051	5	<0.04
DP15	96/01/31	30.2	124	3.7	3	3	21	3.7	4	60	32	0.04	0.1	0.005	5	<0.04
DP18	94/8/5	135	899	7.7	71	29	170	3.9	213	113	249	0.69	0.6	0.021	4.5	<0.04
DP28	96/01/31	18	100	5.9	3	3	22	3.6	9	18	39	0.04	0.2	0.009	5.4	<0.04
DP29	96/01/31	20.8	107	6.4	5	4	25	4.2	15	14	36	0.04	0.2	0.008	4.9	<0.04
LD2	96/01/31	14.3	69	6	3	2	21	1.1	9	4	31	0.19	0.1	0.006	4.1	<0.04
RF1	96/01/31	13.3	76	5.9	2	2	22	1.7	10	4	33	0.25	0.1	0.008	4.7	<0.04
RF2	96/01/31	11.9	54	5.7	2	2	17	0.5	6	4	25	0.17	<0.1	0.005	4.3	<0.04
SL2	96/01/31	54.4	341	7	36	11	49	14.2	57	26	136	0.04	0.2	0.008	10.3	0.13
T/W	96/01/31	16.5	135	7	11	4	14	7.9	60	4	22	0.04	0.3	0.043	15.1	0.05
VR11	96/01/31	9.5	44	5.9	1	2	11	1.6	7	4	19	0.11	<0.1	0.013	4.4	<0.04
VR6	96/01/31	11.5	52	6	2	2	14	1.2	9	4	21	0.26	<0.1	0.034	4	<0.04
VR7	96/01/31	9.5	48	6.2	2	2	12	1.2	9	4	18	0.23	0.1	0.012	3.7	<0.04
VR8	96/01/31	8.9	45	5.9	2	2	9	1.2	4	8	22	0.04	0.3	0.018	3.8	<0.04
v-notch	96/01/31	17.5		7	3	3	25	2.2	9			<0.04	0.1	0.042	5	<0.04
m-vnotch	96/01/31	11.5		7.1	2	2	16	1.6	7			0.34	0.1	0.029	4.1	<0.04
WBG	96/01/31	23.9	157	7.3	15	3	23	9.6	62	4	28	0.04	0.2	0.008	21.4	<0.04
WN2	96/01/31	25.9	167	6.2	9	5	35	8.5	12	40	55	0.08	0.2	0.007	7.5	<0.04

TABLE A-5: MACRO ELEMENT CHEMISTRY – SAMPLING SURVEY JULY 1997, KOTZE AND BUTLER

S_NO	H-NO	DATE	TDS	pH	Na	Mg	Ca	F	Cl	NO3	SO4	P	TAL	Si	K	NH4
RF2	97009982	19970711	69	5.72	16.4	1.9	2	0.06	25.8	0.169	6	0.005	12.6	4.49	0.29	0.026
RF2	97011095	19970711	57	5.7	16.1	2	1.7	0.06	23.7	0.148	3.4	0.005	7	4.82	0.36	0.011
VV-notch																
VParshall	97011071	19970711	62	6.19	16.1	2.5	2.1	0.06	24.2	0.497	3.9	0.023	8.8	4.74	0.63	0.004
VParshall	97010005	19970711	67	6.2	16	2.4	2.6	0.06	25.8	0.458	5.1	0.03	9.9	4.34	0.51	0.022
MV-notch	97011058	19970710	77	6.93	19.7	3	2.2	0.06	29.9	0.082	9.3	0.003	9.1	4.78	1.11	0.014
MV-notch	97009970	19970710	87	7.14	20	2.6	2.1	0.07	31.4	0.071	14.8	0.017	12.4	4.39	1	0.022
C/S																
VG3																
LB2	97011083	19970711	67	5.84	18.6	2.2	2.4	0.06	27.5	0.186	3.2	0.002	10.1	4.72	0.35	0.011
LB2	97009994	19970711	74	5.91	18.4	2.2	2.9	0.06	29.1	0.204	5.4	0.005	11.9	4.38	0.26	0.021
VR8																
DL13																
VR11																
DL16																
DL17																
VR7																
KG1																
DP29																
DG110	97011174	19970711	91	5.53	21.3	4	3.6	0.13	42.8	0.052	10.5	0.001	5.6	5.25	1.33	0.006
DG110	97011010	19970711	102	5.54	24.6	3.9	4	0.16	47.5	0.093	10.2	0.006	8.1	5	1.31	0.017

TABLE A-6 : TRACE ELEMENT CHEMISTRY – JULY 1997 SAMPLING SURVEY– KOTZE AND BUTLER

S_NAME	T	Al	Fe	Mn	Be	Cd	Co	Cr	Cu	As	Hg	B	Mo	Ni	Pb	Ti
RF2																
VV-notch	13.4	<0.02	0.191	<0.001		<0.002		<0.003	<0.002	<0.05		<0.003	<0.005	<0.006	<0.015	
VV-notch	13.4	<0.02	0.191	<0.001		<0.002		<0.003	<0.002	<0.05		<0.003	<0.005	<0.006	<0.015	
V Parshall																
M V-notch																
Calitzdorp Spa	29.4	<0.02	0.284	2.848		<0.002		<0.003	<0.002	<0.05		<0.003	<0.005	<0.006	<0.015	
VG3	15	0.044	<0.003	0.216		<0.002		<0.003	<0.002	<0.05		<0.003	<0.005	<0.006	<0.015	
LB2																
VR8	22.7	<0.02	<0.003	<0.001		<0.002		<0.003	<0.002	<0.05		<0.003	<0.005	<0.006	<0.015	
VR8	22.7	<0.02	0.018	<0.001		<0.002		<0.003	<0.002	<0.05		<0.003	<0.005	0.006	<0.015	
DL13	20	<0.02	0.492	0.36		<0.002		<0.003	<0.002	<0.05		0.143	<0.005	<0.006	<0.015	
VR11	18.8	<0.02	<0.003	<0.001		<0.002		<0.003	<0.002	<0.05		<0.003	<0.005	<0.006	<0.015	
VR11	18.8	<0.02	0.029	<0.001		<0.002		<0.003	<0.002	<0.05		<0.003	<0.005	0.006	<0.015	
DL16	20.4	<0.02	0.155	0.339		<0.002		<0.003	<0.002	<0.05		<0.003	<0.005	<0.006	<0.015	
DL17	17.6	<0.02	0.269	0.735		<0.002		<0.003	<0.002	<0.05		<0.003	<0.005	0.008	<0.015	
VR7	20.3	<0.02	<0.003	<0.001		<0.002		<0.003	<0.002	<0.05		<0.003	<0.005	<0.006	<0.015	
VR7	20.3	<0.02	0.143	0.02		<0.002		<0.003	<0.002	<0.05		<0.003	<0.005	0.006	<0.015	
KG1	22.4	<0.02	0.066	0.847		<0.002		<0.003	<0.002	<0.05		<0.003	<0.005	<0.006	<0.015	
DP29	23.3	<0.02	1.605	0.581		<0.002		<0.003	<0.002	<0.05		<0.003	<0.005	0.006	<0.015	
DP29	23.3	<0.02	0.088	0.643		<0.002		<0.003	<0.002	<0.05		<0.003	<0.005	0.006	<0.015	
DG110	20	<0.02	0.825	0.313		<0.002		<0.003	<0.002	<0.05		<0.003	<0.005	<0.006	<0.015	

TABLE A-7 : ENVIRONMENTAL ISOTOPE DATA – JULY 1997 SAMPLING SURVEY – KOTZE AND BUTLER

Lab No.	Location	Tritium (TU)	Carbon 14 (pMC)	Oxygen 18 (‰)	Deuterium (‰)	Radon
WKK 24	Rolbaken	0.0±0.2		-7.56	-50.3	3
WKK 25	Vermaaks V Notch	1.6±0.2		-7.84	-55.3	
WKK 26	Vermaaks Partial	0.5±0.1		-7.66	-51.2	5
WKK 27	Marnewicks V Notch	1.6±0.2		-7.79	-54.8	
WKK 28	Calitzdorp Spa	0.0±0.1	3.9±1.6	-7.36	-49.7	
WKK 29	VG 3	1.3±0.2	78.1±2.5	-7.68	-57.1	4
WKK 30	LB2	0.0±0.1	75.0±1.6	-7.42	-50.3	2
WKK 31	VR 8	0.4±0.1	79.3±2.5	-7.27	-49.7	2
WKK 32	DL 13	0.9±0.2	53.3±2.0	-7.24	-48.2	
WKK 33	VR 11	0.0±0.1	67.4±2.2	-7.06	-49.5	
WKK 34	DL 16	0.2±0.2	13.1±1.6	-6.63	-46.5	
WKK 35	DL 17	0.3±0.1	21.3±1.6	-6.63	-46.4	
WKK 36	VR 7	1.0±0.2	80.6±2.5	-7.71	-52.7	1
WKK 37	KG 1	0.2±0.1	51.2±2.0	-6.26	-41.9	
WKK 38	DP 29	0.0±0.2	40.6±2.0	-7.87	-50.8	
WKK 39	DG 110	0.0±0.2	41.0±2.0	-7.7	-49.5	

TABLE A-8: MACRO ELEMENT CHEMISTRY - RESAMPLING BY DWAF MARCH 1998

S_NO	H-NO	DATE	TDS	pH	Na	Mg	Ca	F	Cl	NO3	SO4	P	TAL	Si	K	NH4
T/W	98004396	19980330	133	6.83	15.4	3.2	10.9	0.21	24.6	0.001	11.9	0.015	47.1	15.09	9.27	0.014
VV-notch	98004451	19980331	89	7.03	24.8	2	3.8	0.07	33.8	0.008	7.6	0.008	13.5	5.66	0.33	0.01
VR7	98004610	19980331	64	7.18	13.6	1.6	5.4	0.06	19.4	0.12	4.5	0.01	14.4	4.14	1.7	0.016
LD2	98004712	19980331	58	6.15	18.5	1.4	2.2	0.06	26.4	0.179	4.1	0.007	3.1	4.12	0.44	0.008
RF2	98004591	19980331	54	7.03	16.7	1.3	3	0.05	22.6	0.143	3.6	0.009	4.7	4.34	0.65	0.011
VG3	98004402	19980331	89	5.37	26.7	2.6	2.3	0.07	41.3	0.669	10.2	0.008	2.1	5	0.58	0.014
VR11	98004694	19980331	35	6.69	10.9	1	1.3	0.05	14.6	0	2.1	0.008	3.4	4.26	0.37	0.011
DG110	98004669	19980401	88	5.71	25.3	2.9	3.8	0.18	42.6	0.008	8.6	0.007	3.2	4.64	0.84	0.026
KG1	98004463	19980402	198	6.68	38.1	8.1	12	0.23	78.6	0.005	11.2	0.008	33.2	5.17	9.59	0.01
DL16	98004700	19980402	278	6.93	57.3	8.6	13.2	0.3	94.2	0.006	22.5	0.007	54.8	5.75	15.18	0.011
DL15	98004645	19980402	238	6.96	43	10.1	13.3	0.27	89.5	0.005	14.7	0.005	42.6	5.17	14.81	0.01
DL17	98004580	19980402	266	6.69	47.9	11.9	15.7	0.26	98.9	0.001	24.6	0.007	42.7	5.7	14.43	0.009
C/S	98004554	19980402	130	7.11	17.6	3.4	9.2	0.29	26.8	0.008	12	0.008	43.3	17.81	7.85	0.012

TABLE A-9: TRACE ELEMENT CHEMISTRY – RESAMPLING BY DWAF – MARCH 1998

S_NAME	T	Al	Fe	Mn	Be	Cd	Co	Cr	Cu	As	Hg	B	Mo	Ni	Pb	Ti
T/W		<0.02	0.113	1.74		<0.002		<0.003	<0.002	<0.05		<0.003	<0.005	<0.006	<0.05	
VG3		0.026	<0.003	0.143		<0.002		<0.003	<0.002	<0.05		<0.003	<0.005	<0.006	<0.05	
VV-notch		<0.02	0.011	<0.001		<0.002		<0.003	<0.002	<0.05		<0.003	<0.005	<0.006	<0.05	
KG1		<0.02	0.248	1.114		<0.002		<0.003	<0.002	<0.05		<0.003	<0.005	<0.006	<0.05	
C/S		<0.02	0.508	2.5		<0.002		<0.003	<0.002	<0.05		<0.003	<0.005	<0.006	<0.05	
DL17		<0.02	<0.003	<0.001		<0.002		<0.003	<0.002	<0.05		0.017	<0.005	<0.006	<0.05	
RF2		<0.02	<0.003	<0.001		<0.002		0.003	<0.002	<0.05		<0.003	<0.005	<0.006	<0.05	
VR7		<0.02	<0.003	<0.001		<0.002		<0.003	<0.002	<0.05		<0.003	<0.005	<0.006	<0.05	
DL15		<0.02	<0.003	0.577		<0.002		<0.003	<0.002	<0.05		0.031	<0.005	<0.006	<0.05	
DG110		<0.02	0.128	3.222		<0.002		<0.003	<0.002	<0.05		<0.003	<0.005	<0.006	<0.05	
VR11		<0.02	<0.003	<0.001		<0.002		<0.003	<0.002	<0.05		<0.003	<0.005	<0.006	<0.05	
DL16		<0.02	<0.003	0.322		<0.002		<0.003	<0.002	<0.05		0.077	<0.005	<0.006	<0.05	
LD2		<0.02	<0.003	<0.001		<0.002		<0.003	<0.002	<0.05		<0.003	<0.005	<0.006	<0.05	
MV-notch		0.121	0.123	<0.001		<0.002		<0.003	<0.002	<0.05		0.005	<0.005	<0.006	<0.05	
DP28		3.67	0.647	1.797		0.1		<0.003	<0.002	<0.05		0.004	<0.005	0.507	<0.05	
WBG		0.022	0.902	0.958		<0.002		<0.003	<0.002	<0.05		0.02	<0.005	<0.006	<0.05	

TABLE A-10: MACRO ELEMENT CHEMISTRY – MONITORING BOREHOLES VERMAAKS RIVER

Sample	H-NO	DATE	EC	TDS	pH	Na	Mg	Ca	F	Cl	NO3	SO4	P	TAL	Si	K	NH4
G40174 147M	97017656	19970918	22.7	121	7.28	20.8	3.1	12.2	0.16	32.2	0.232	10.6	0.019	31.7	4.69	1.94	0.189
G40175 51M	97026013	19971106	17.7	94	6.97	14.5	1.8	9.8	0.09	21.9	0.011	11.7	0.015	27	4.57	1.12	0.023
G40175A 23M	97026025	19971106	16.8	96	7.06	15.2	1.6	9.7	0.1	22.5	0.007	14.8	0.016	25.3	4.46	1.06	0.018
G40175A 27M	98006265	19980123	14.1	78	6.78	13.5	2.3	3.2	0.11	22	0.195	8.7	0.019	20.9	4.44	1.43	0.305
G40175A 60M	98006277	19980127	12.1	73	6.71	11.9	1.5	3.5	0.08	16.9	0.008	9.8	0.013	21.6	2.27	2.55	0.021
G40175A 84M	98006319	19980203	11	67	6.55	12.7	2.1	3.5	0.08	21.3	0.02	12.1	0.006	10.6	4.16	1.82	0.019
G40175B 115M	97026001	19971106	11.8	57	6.2	13.8	1.6	2	0.07	20.9	0.006	8.6	0.023	7.1	4.43	1.08	0.025
G40175C 126M	97025999	19971112	12.4	60	6.63	13.4	1.7	2.3	0.07	20.8	0.015	9.6	0.032	8.7	4.55	1.15	0.029
G40176 42M	98006289	19980204	14.2	69	6.99	14.1	2	2.9	0.07	23.2	0.211	7.3	0.009	13.9	2.62	1.07	0.066
G40176A 119M	98006290	19980206	18.2	111	7.43	15.5	2.2	10.1	0.05	22.7	0.401	12.3	0.07	35.6	5.01	3.03	0.084
G40176B 150M	98006307	19980207	19	109	7.16	15.1	2.2	11.2	0.11	21.5	0.014	8.1	0.02	39.3	5	2.74	0.031
G40177 92M	98006253	19980210	45	245	6.85	40.4	7.1	17.7	0.22	85.3	0.005	39.1	0.007	33.2	2.1	14.1	0.019
G40177B 150M	98006344	19980218	37.6	245	7.56	40.9	6.9	17.7	0.24	85.6	0.065	37.8	0.008	33.9	2.13	14.62	0.043
G40178 54M	98006320	19980219	109.9	641	6.92	135.2	27.6	37	0.31	230.1	0.013	115.4	0.011	73.7	15.16	4.86	0.374
G40178 120M	98006332	19980220	155	1084	7.89	232.8	43.1	73.4	0.46	395.2	0.021	220.5	0.017	88.8	13.85	9.67	0.111
G40171	98010852	19980513	13.6	64	6.59	14.3	2.1	3.8	0.08	20.6	0.317	5.6	0.031	12.9	4.39	0.59	0.008
G40172	98010864	19980513	13.3	64	6.45	15.6	2.3	2.5	0.08	21.6	0.39	8.3	0.053	9.4	4.4	0.74	0.017
G40173	98010876	19980513	12.9	56	6.31	14.6	2	2.2	0.07	20.5	0.171	5.6	0.016	8.2	4.03	0.74	0.001
G40175A	98010888	19980513	13.2	57	6.18	13.6	2.4	2.4	0.09	19.7	0.098	10.8	0.014	5.1	4.59	0.99	0.012
G40176	98010890	19980513	13.5	58	6.37	13.7	2.4	2.9	0.09	19.1	0.223	7	0.03	9	4.63	0.8	0.041

TABLE A-11: TRACE ELEMENT CHEMISTRY – MONITORING BOREHOLES VERMAAKS RIVER

Sample	Date	H-NO	Fe	Mn	Be	Cd	Co	Cr	Cu	As	Hg	B	Mo	Ni	Pb	Ti
G40174 147M	18-Sep-97															
G40175 51M	06-Nov-97	97026050	<0.003	0.114		<0.002		<0.003	<0.002	<0.05		<0.003	<0.005	<0.006	<0.015	
G40175A 23M	06-Nov-97	97026062	0.306	0.139		<0.002		<0.003	<0.002	<0.05		<0.003	<0.005	<0.006	<0.015	
G40175A 27M	23-Jan-98	98006368	<0.003	0.093		<0.002		<0.003	<0.002	<0.05		<0.003	<0.005	<0.006	<0.015	
G40175A 60M	27-Jan-98	98006370	<0.003	0.309		<0.002		<0.003	<0.002	<0.05		<0.003	<0.005	<0.006	<0.015	
G40175A 84M	03-Feb-98	98006411	<0.003	0.507		<0.002		<0.003	<0.002	<0.05		<0.003	<0.005	0.013	<0.015	
G40175B 115M	06-Nov-97	97026049	<0.003	0.17		<0.002		<0.003	<0.002	<0.05		<0.003	<0.005	<0.006	<0.015	
G40175C 126M	12-Nov-97	97026037	0.068	0.196		<0.002		<0.003	<0.002	<0.05		<0.003	<0.005	<0.006	<0.015	
G40176 42M	04-Feb-98	98006381	<0.003	0.502		<0.002		<0.003	<0.002	<0.05		<0.003	<0.005	<0.006	<0.015	
G40176A 119M	06-Feb-98	98006393	<0.003	<0.001		<0.002		<0.003	<0.002	<0.05		<0.003	<0.005	<0.006	<0.015	
G40176B 150M	07-Feb-98	98006400	0.224	0.023		<0.002		<0.003	<0.002	<0.05		<0.003	<0.005	<0.006	<0.015	
G40177 92M	10-Feb-98	97006356	<0.003	2.14		<0.002		<0.003	<0.002	<0.05		<0.003	<0.005	<0.006	<0.015	
G40177B 150M	18-Feb-98	98006423	<0.003	1.741		<0.002		<0.003	<0.002	<0.05		<0.003	<0.005	<0.006	<0.015	
G40178 54M	19-Feb-98	98006447	<0.003	3.442		<0.002		<0.003	<0.002	<0.05		<0.003	<0.005	<0.006	<0.015	
G40178 120M	20-Feb-98	98006435	<0.003	7.2		<0.002		<0.003	<0.002	<0.05		0.041	<0.005	<0.006	<0.015	
G40171	01-May-98	98011030	0.136	<0.001		<0.002		<0.003	<0.002	<0.05		0.041	<0.005	<0.006	<0.015	
G40172	01-May-98	98011042	0.136	<0.001		<0.002		<0.003	<0.002	<0.05		0.041	<0.005	<0.006	<0.015	
G40173	01-May-98	98011054	0.248	0.157		<0.002		<0.003	<0.002	<0.05		0.041	<0.005	<0.006	<0.015	
G40175A	01-May-98	98011066	<0.003	0.186		<0.002		<0.003	<0.002	<0.05		0.041	<0.005	<0.006	<0.015	
G40176	01-May-98	98011078	<0.003	0.013		<0.002		<0.003	<0.002	<0.05		0.041	<0.005	<0.006	<0.015	

TABLE A-12: ENVIRONMENTAL ISOTOPE DATA – MONITORING BOREHOLES – VERMAAKS RIVER

Lab No	Sample	Date	O18	DEUT
March Series				
G4487	G40174 147M	18-Sep-97	-6.7	-38
G4488	G40175	06-Nov-97	-7.0	-41
G4489	G40175A 23M	06-Nov-97	-7.1	-39
G4490	G40175A 27M	23-Jan-98	-7.2	-39
G4491	G40175A 60M	27-Jan-98	-7.2	-39
G4492	G40175A 84M	03-Feb-98	-7.0	-38
G4493	G40175B 115M	06-Nov-97	-7.0	-40
G4494	G40175C 126M	12-Nov-97	-7.0	-40
G4495	G40176 42M	04-Feb-98	-7.5	-43
G4496	G40176A 119M	06-Feb-98	-7.3	-43
G4497	G40176B 150M	07-Feb-98	-7.3	-46
G4498	G40177 92M	10-Feb-98	-7.3	-45
G4499	G40177B 150M	18-Feb-98	-7.3	-40
G4500	G40178 54M	19-Feb-98	-7.0	-41
G4501	G40178 120M	20-Feb-98	-7.3	-42
May series				
G4502	G40171	01-May-98	-7.2	-42
G4503	G40172	01-May-98	-7.3	-42
G4504	G40173	01-May-98	-7.7	-45
G4505	G40175A ARTESIAN	01-May-98	-7.3	-42
G4506	G40176	01-May-98	-7.4	-44

TABLE A-13: MACRO ELEMENT CHEMISTRY –SAMPLING SURVEY, JUNE 1998 - KOTZE

S_NO	H-NO	DATE	EC	TDS	pH	Na	Mg	Ca	F	Cl	NO3	SO4	P	TAL	Si	K	NH4
SBH1	98014602	19980617	50.8	246	5.96	62.9	7.8	7.7	0.12	130.6	0.041	10.5	0.007	15.1	9.2	7.57	0.074
SBH2	98014614	19980617	25.5	110	5.85	30.8	4.1	2.9	0.13	56.2	0.35	5.6	0.007	5.1	5.56	2.62	0.001
HUISRIV1	98014626	19980618	9.7	48	7.28	11.2	1.8	1.3	0.12	15	0.106	8	0.008	8.3	2.98	0.35	0.009
HUISRIVN	98014638	19980618	9.3	34	7.22	10.9	1.6	1.1	0.11	13.8	0.113	4.7	0.008	1.1	3.05	0.48	0.02
HUISRIVS	98014640	19980618	9.6	59	6.72	10.5	2.4	2.4	0.1	11.1	0.115	23.5	0.015	5.6	3.17	1.16	0.038
V/S BH	98014651	19980619	26.4	138	6.59	17.7	6.7	5.7	0.18	36.8	0.007	13.9	0.009	36.7	6.38	12.49	0.041
V/Sfontein	98014663	19980619	37.7	203	6.86	53.5	7	3.2	0.15	80.2	0.14	22.6	0.01	28.7	0.27	0.95	0.002
WK4	98014675	19980622	26	121	5.47	31.3	4.4	3.5	0.12	58	0.513	13.6	0.041	5.4	5.02	1.08	0.04
VG3	98014687	19980623	20.6	92	5.23	23.6	3.3	2.4	0.11	38.9	0.906	18.3	0.008	0.6	4.74	0.82	0.07
DR2	98014699	19980624	32.3	217	6.9	25.9	4.8	26.2	0.25	43.5	0.011	45.8	0.024	49.3	9.56	9.71	0.034
WN3	98014705	19980625	25.1	143	5.76	30.1	4.6	8.7	0.15	50.8	0.088	31.6	0.012	8.5	7.69	6.46	0.067
MEIRINP	98014717	19980626	3	12	6.83	3.6	0.6	0.6	0.1	4.1	0.012	2.7	0.008	0.1	1.46	0.24	0.006
SL2	98014729	19980701	83.7	473	6.23	54.9	19.9	57.4	0.13	126.7	0.007	158.6	0.008	34.1	13.5	13.18	0.011
YR2	98014730	19980630	18.1	97	5.6	19.4	3.1	7	0.1	31.5	0.083	20.1	0.029	8.7	7.32	4.7	0.05
KOUTIEF	98014742	19980629	10.7	62	6.69	11.8	2.1	2.1	0.09	15.2	0.003	19.3	0.033	6.4	7.27	2.93	0.105
WK3	98014754	19980702	17.4	104	5.84	23.8	3.4	2.6	0.09	39.8	0.249	24.1	0.041	6.1	5.05	1.61	0.005
RF8	98014766	19980629	10.4	60	5.33	14.8	1.6	1.7	0.09	19.9	0.205	15.7	0.011	3.9	4.7	0.62	0.003

TABLE A-14 – TRACE ELEMENT CHEMISTRY SAMPLING SURVEY JUNE 1998 - KOTZE

S_NO	H-NO	DATE	Al	Fe	Mn	Cd	Cr	Cu	As	B	Mo	Ni	Pb	Sr	Ba	V	Zn
SL2	98014894	19980617	<0.02	<0.005	3.085	<0.005	<0.005	<0.005	<0.03	<0.005	<0.07	<0.007	<0.03	0.558	0.152	<0.005	0.079
VG3	98014857	19980617	0.059	0.009	0.247	<0.005	<0.005	0.011	<0.03	<0.005	<0.07	0.031	<0.03	0.039	<0.002	0.018	0.032
WK4	98014845	19980618	<0.02	<0.005	0.043	<0.005	<0.005	<0.005	<0.03	<0.005	<0.07	<0.007	<0.03	0.009	<0.002	<0.005	<0.005
RF8	98014948	19980618	<0.02	<0.005	<0.001	<0.005	<0.005	<0.005	<0.03	<0.005	<0.07	<0.007	<0.03	0.007	<0.002	<0.005	<0.005
WK3	98014936	19980618	<0.02	<0.005	0.421	<0.005	<0.005	<0.005	<0.03	<0.005	<0.07	<0.007	<0.03	0.012	0.01	<0.005	<0.005
WN3	98014870	19980619	<0.02	<0.005	0.803	<0.005	<0.005	<0.005	<0.03	<0.005	<0.07	<0.007	<0.03	0.095	0.016	<0.005	0.016
SBH1	98014778	19980619	<0.02	<0.005	0.575	<0.005	<0.005	<0.005	<0.03	<0.005	<0.07	<0.007	<0.03	0.102	0.123	<0.005	<0.005
SBH2	98014780	19980622	<0.02	<0.005	<0.001	<0.005	<0.005	<0.005	<0.03	<0.005	<0.07	<0.007	<0.03	0.029	0.028	<0.005	0.064
DR2	98014869	19980623	<0.02	<0.005	0.947	<0.005	<0.005	<0.005	<0.03	<0.005	<0.07	<0.007	<0.03	0.216	0.107	<0.005	0.007
MeiringP	98014882	19980624	<0.02	<0.005	<0.001	<0.005	<0.005	<0.005	<0.03	<0.005	<0.07	<0.007	<0.03	<0.001	<0.002	<0.005	<0.005
YR1	98014912	19980625	<0.02	<0.005	0.18	<0.005	<0.005	<0.005	<0.03	<0.005	<0.07	<0.007	<0.03	0.058	0.048	<0.005	<0.005
KoutieFon	98014924	19980626	<0.02	<0.005	<0.001	<0.005	<0.005	<0.005	<0.03	<0.005	<0.07	<0.007	<0.03	0.11	<0.002	<0.005	<0.005
V/S BH	98014821	19980701	<0.02	<0.005	2.596	<0.005	<0.005	<0.005	<0.03	<0.005	<0.07	<0.007	<0.03	0.052	0.042	<0.005	0.422
V/S Fon	98014833	19980630	0.197	0.006	<0.001	<0.005	<0.005	<0.005	<0.03	<0.005	<0.07	<0.007	<0.03	0.035	<0.002	<0.005	<0.005
Huis R 1	98014791	19980629	0.064	0.009	<0.001	<0.005	<0.005	<0.005	<0.03	<0.005	<0.07	<0.007	<0.03	0.006	<0.002	<0.005	<0.005
HuisRS	98014810	19980702	<0.02	<0.005	<0.001	<0.005	<0.005	<0.005	<0.03	<0.005	<0.07	<0.007	<0.03	0.011	<0.002	<0.005	<0.005
HuisRN	98014808	19980629	0.087	0.025	<0.001	<0.005	<0.005	<0.005	<0.03	<0.005	<0.07	<0.007	<0.03	0.005	<0.002	<0.005	<0.005

TABLE A-15: ENVIRONMENTAL ISOTOPE DATA – SAMPLING SURVEY JUNE 1998 – KOTZE

Laboratory Number	Location	Oxygen-18 (o/oo)	Deuterium (o/oo)	Carbon-14 (pMC)	tritium (TU)
WKK 40	Scheeperskraal			143.9	0.3±0.4
WKK 41	VG 3	-8.02	-55.1	65.7±2.3	
WKK 42	WK4	-7.23	-50.9	70.4±2.3	
WKK 43	RF8	-7.23	-40.8	82.4±2.4	
WKK 44	WK3	-7.21	-50.6	68.2±2.3	
WKK 45	WN3	-7.65	-53.2	84.4±2.5	
WKK 46	SBH 1	-7.01	-49.5	53.7±2.2	
WKK 47	SBH 2	-5.55	-38.4	88.1±2.5	
WKK 48	Diep R	-6.98	-46.5		
WKK 49	Meiringspoort	-5.79	-39.3		
WKK 50	YR 1	-6.93	-47.4		
WKK 51	Koutie Fontein	-6.59	-43.5		
WKK 52	V/S BH	-8.10	-50.6		
WKK 53	V/S Spring	-3.19	-32.6		
WKK 54	SL2	-7.03	-49.1		
WKK 55	Huis R Sping	-6.58	-42.6		
WKK 56	Huis R 1	-6.52	-39.9		
WKK 57	Huis R Nardouw	-6.69	-43.3		

TABLE A-16: ENVIRONMENTAL ISOTOPE AND CHLORIDE ANALYIS OF RAIN SAMPLES TAKEN IN THE LITTLE KAROO

Lab Number	**Rainfall Location**		**Oxygen-18** (o/oo)	**Deterium** (o/oo)	**Chloride** mg/l
WKK 58	DL 13 25 Aug 98 15h03	Rain	-4.38	-30.7	<10
WKK 59	Wildebeesvlakte 25 Aug 98	Rain	-6.49	-29.8	<10
WKK 60	VG 3 25 Aug 98	Rain	-4.21	-25.8	<10
WKK 61	DP 25 25 Aug 98	Rain	-4.25	-25.4	20
WKK 62	V Keep 25 Aug 98	Rain	-4.54	-22.4	<10
WKK 63	KG 1 25 Aug 98	Rain	-4.61	-26.7	<10
WKK64	Parshall 25 Aug 98	Rain	-5.90	-30.7	<10
	Parshall 5 Dec 95	Rain	-4.50	-28	

TABLE A-17: ENVIRONMENTAL ISOTOPE DATA – SIMONIC, DWAF

SERNAME	SUBNAME	SAMDATE	O18	DEUT
CAPE SPRINGS	101 VLAKFONTEIN MIDDELBURG	04/25/94	-3.9	-24
CAPE SPRINGS	134 JOUBERTINA BH HE2	05/04/94	-6.3	-36
CAPE SPRINGS	139 MORESTER BH NF12A	05/05/94	-4.3	-22
CAPE SPRINGS	8021 BURGERSVILLE SPR	04/19/94	-3.8	-23
CAPE SPRINGS	8043 CRADOCK	04/22/94	-7.0	-46
CAPE SPRINGS	8090 MURRAYSBURG	04/20/94	-4.4	-36
TMS	TM1 KNYSNA MUNICIPAL FORES	07/04/94	-4.4	-19
TMS	TM2 YZERNEK COMMONAGE	07/04/94	-4.6	-19
TMS	TM3 KRANTZBOSCH FOREST RES	07/04/94	-4.9	-22
TMS	TM4 UITVLUGT	07/04/94	-5.2	-25
TMS	TM5 ANNEX VLUGT	07/04/94	-5.7	-29
TMS	TM6 KRANZ BERG	07/04/94	-6.1	-31
TMS	TM7 GOLD DIGGINS	07/04/94	-7.2	-41
TMS	TM8 GOLD DIGGINS	07/04/94	-7.3	-44
TMS	TM9 NOITGEDACHT	07/04/94	-6.8	-41
TMS	TM9B NOITGEDACHT	07/04/94	-6.9	-38
TMS	TM10 VOET PADSBERG	07/05/94	-5.8	-34
TMS	TM11 DE WETS VLEY	07/05/94	-6.1	-34
TMS	TM12 ALBERT BERG	07/05/94	-5.3	-29
TMS	TM13 NOOITGEDAGT	07/05/94	-5.5	-32
TMS	TM14 MALGASKRAAL	07/06/94	-3.6	-15
TMS	TM15 MALGASKRAAL	07/06/94	-3.9	-16
TMS	TM16 NORTH STATION	07/06/94	-4.6	-20
TMS	TM17	07/06/94	-7.2	-43
TMS	TM18 DANIELS KRAAL	07/06/94	-6.5	-37
TMS	TM19 DANIELS KRAAL	07/06/94	-6.4	-39
TMS	TM20 KLEINBERG	07/06/94	-6.1	-37
TMS	TM21 TOWERKOP STAATBOS	07/06/94	-6.8	-44
TMS	TM22 TOWERKOP STAATBOS	07/06/94	-4.8	-29
TMS	TM23 TIGERKLOOF	07/06/94	-6.7	-36
TMS	TM24 KRISTAL KLOOF	07/07/94	-5.4	-28
TMS	TM25 KRISTAL KLOOF	07/07/94	-3.8	-20
TMS	TM26 THE CAMP	07/07/94	-3.9	-18
TMS	TM27 PLAAS	07/07/94	-4.0	-16
TMS	TM28 PLAAS	07/07/94	-4.3	-18
TMS	TM29 NORTH STATION	07/07/94	-4.5	-18
TMS	TM30 NORTH STATION	07/07/94	-5.3	-25
TMS	TM31 FARM	07/08/94	-6.1	-34
TMS	TM32 ROODEBERG	07/08/94	-6.3	-34
TMS	TM33 GOREE	07/08/94	-5.5	-25
TMS	TM34 GEVONDEN	07/08/94	-3.8	-24
TMS	TM35	07/08/94	-4.5	-21
TMS	TM36 DU TOIT KLOOF POORT	07/08/94	-4.7	-23
TMS	TM37 DU TOIT KLOOF POORT	07/08/94	-4.2	-17
TMS	TM38 DU TOIT KLOOF POORT	07/08/94	-4.7	-22

TABLE A-18: MACRO ELEMENT CHEMISTRY – TMG SAMPLING PROGRAM – SIMONIC, DWAF

S_NO	H-NO	DATE	TDS	pH	Na	Mg	Ca	F	Cl	NO3	SO4	P	TAL	Si	K	NH4
TM1	94013287	19940704	232	5.92	64.8	10.3	2.7	0.2	124.6	0.041	16.4	0.04	9.1	4.28	1.91	0.028
TM2	94013299	19940704	48	5.8	12.4	1.8	1.3	0.19	23.1	0.03	4.6	0.02	3.2	2.44	0	0.011
TM3	94013305	19940704	113	6.25	31	3.6	2.8	0.18	54.9	0.515	5.5	0.024	10.7	3.05	0	0.036
TM4	94013317	19940704	188	6.39	48.6	5.9	7.7	0.18	99.7	0.058	6.9	0.034	15	3.32	0	0
TM5	94013329	19940704	73	6.29	18.9	2.1	2.2	0.18	36.6	0.025	5.3	0.111	6.1	3.74	0	0.001
TM6	94013330	19940704	33	6.11	8.2	1.3	0.9	0.18	14.3	0.024	3	0.044	4.3	2.18	0	0
TM7	94013342	19940704	75	6.6	16.3	2.5	3.9	0.18	32	0.041	4.7	0.079	12.1	3.69	0.13	0.028
TM8	94013354	19940704	80	6.18	18	3.1	2.5	0.17	37.7	0.02	3.5	0.027	9.7	3.72	2.82	0.001
TM9	94013366	19940704	115	6.86	11.6	3.4	10.1	0.31	21.5	0.029	5	0.02	45.6	13.86	6.95	0.021
TM10	94013378	19940705	117	7.12	9.9	5.6	13.3	0.59	15	0.025	14.7	0.061	47.5	2.27	0.16	0.008
TM11	94013380	19940705	20	7.52	1.9	0.8	0.9	0.3	4.1	0.033	5.6	0.12	4.7	0.98	0	0.002
TM12	94013391	19940705	19	6.86	1.5	0.9	1.1	0.23	3.7	0.038	6.3	0.107	3.8	0.65	0	0.038
TM13	94013408	19940705	410	7.74	18.9	10.7	69.6	0.25	27.2	0.363	14.8	0.081	218.7	4.6	0.24	0.008
TM14	94013410	19940706	55	4.72	10.8	2	2	0.23	21.1	0.042	11.7	0.142	4.9	1.97	0	0.075
TM15	94013421	19940706	52	5.24	11.4	2.2	1	0.21	22.8	0.037	8.2	0.109	4.9	3.03	0	0.027
TM16	94013433	19940706	53	5.95	13	2.3	1.2	0.19	26.6	0.035	5.1	0.098	3.5	2.72	0	0.027
TM17	94013445	19940706	62	6.19	13.1	2.2	2.3	0.2	24.4	0.311	5.1	0.113	10.7	3.88	0.28	0.021
TM18	94013457	19940706	219	7.19	36.2	8.2	11.6	0.37	80.6	0.046	14.8	0.039	43.7	4.91	13.05	0.004
TM19	94013469	19940706	349	7.28	70.6	11.3	15.7	0.76	131.3	0.027	26.9	0.032	62.4	5.47	15.93	0.013
TM20	94013470	19940706	219	7.24	41.8	9.2	11.7	0.53	92.4	0.025	20.6	0.039	28	4.71	8.4	0.01
TM21	94013482	19940706	59	6.6	13	2.2	1.5	0.33	25.2	0.03	10.2	0.105	5.1	4.71	0.02	0.036
TM22	94013494	19940706	45	6.99	8.8	2.7	1.4	0.24	20.8	0.04	5.8	0.105	4	2.41	0	0.018
TM23	94013500	19940706	23	6.58	2.8	1.1	1.3	0.22	5.8	0.075	2.8	0.161	6.5	3.65	0	0.011
TM24	94013512	19940707	52	6.59	12.5	2.2	1	0.21	24.4	0.027	7	0.094	3.8	2.73	0	0.006
TM25	94013524	19940707	49	7.42	11.8	1.9	1.4	0.19	21.9	0.035	5.1	0.084	5	2.57	0	0.016
TM26	94013536	19940707	140	5.72	4.7	1	4.7	0.19	11.2	0.038	96.9	0.134	17.2	1.45	0	0.051
TM27	94013548	19940707	62	6.02	12.8	2.3	1.8	0.19	24.3	0.033	12.7	0.099	5.8	3.57	0.5	0.052
TM28	94013550	19940707	38	6.02	8.1	1.6	0.7	0.49	15.2	0.042	6.3	0.095	4.4	3.57	0	0.052
TM29	94013561	19940707	41	6.08	10.2	1.9	0.6	0.26	19.4	0.029	4.4	0.073	3.3	3.35	0	0.011
TM30	94013573	19940707	43	6.78	10.7	2.1	0.8	0.22	20.1	0.045	3.7	0.106	3.6	3.57	0	0.023
TM31	94013585	19940708	117	7.27	33.1	3.9	2.9	0.21	63.9	0.058	7	0.079	4.5	4.67	0.27	0.038
TM32	94013597	19940708	111	7.8	19	6	4	0.26	39	<0.04	6	0.102	27	5.1	3.6	<0.04

TABLE B-18 (CONTINUE)

S_NO	H-NO	DATE	TDS	pH	Na	Mg	Ca	F	Cl	NO3	SO4	P	TAL	Si	K	NH4
TM33	94013603	19940708	97	7.3	23	5	1	0.26	44	<0.04	7	0.073	13	3.5	<0.03	<0.04
TM34	94014279	19940708	21	7.8	3	<1	<1	0.17	6	0.06	<4	0.012	6	1.4	<0.3	<0.04
TM35	94014280	19940708	20	7.3	3	<1	<1	0.5	5	<0.04	<4	0.012	7	0.9	<0.3	<0.04
TM36	94014267	19940708	21	7.2	2	<1	1	0.2	5	<0.04	<4	0.01	7	1.4	<0.3	0.05
TM37	94014280	19940708	29	7.8	5	<1	2	1.08	7	<0.04	5	0.012	6	0.6	<0.3	<0.04

APPENDIX B: BACKGROUND INFORMATION

B-1: BACKGROUND INFORMATION : CARBON-13 AND 14

- **Evolution of Carbon in groundwater**

Most fresh groundwater originates as meteoric water, in most cases infiltrating through the soils into the geosphere (Clark *et al.,* 1997). In infiltrating through soil groundwater dissolved inorganic carbon (DIC) increases along the way by solution of CO_2, and evolves through the weathering of carbonate and silicate parent material.

As carbonate acidity is "consumed" by weathering, the pH increases and the distribution of dissolved inorganic species shifts towards bicarbonate (HCO_3^-) and carbonate (CO_3^{2-}). The groundwater generally approaches equilibrium with calcite, whose solubility will control pH and the equilibrium of carbonate species.

At the same time, labile organic matter from the soil can be dissolved. Oxidation of dissolved organic matter (DOC) is initially caused by aerobic bacteria, using O_2. If the supply of DOC is exhausted before the is O_2 consumed, then the redox conditions will not evolve much further unless an another electron donor in the system is found, i.e. ferrous iron materials, sulphides, etc.. If an excess of DOC accompanies the groundwater below the water table and beyond the influence of atmospheric O_2, then anaerobic bacteria will consume it using electron acceptors, i.e. NO_3^-, Fe^{3+}- oxyhydroxides or SO_4^{2-}. Ultimately, methanogenic reactions can take place. The redox evolution is accompanied by mineral dissolution and precipitation reactions that affect the mass balance of dissolved solids and the distribution of isotopes.

All sources of carbon are linked through these acid-base and redox reactions, which are most often mediated by bacteria. Bacterial involvement is important for two reasons:

1. Bacteria derive their energy from redox reactions and therefore act as catalysts, speeding up reactions that are otherwise kinetically impeded;
2. Bacteria are isotopically selective, preferring to break the weaker, light-isotope bonds. Bacteria mediated reactions are then accompanied by large isotope fractionations.

An understanding of the distribution of isotopes in the carbon cycle begins with a look at carbonate geochemistry. Carbonate geochemistry involves acid-base reactions and the determination of carbonate equilibria and state of mineral saturations (references include

Garrels and Christ, 1965, Freeze and Cherry, 1979, Drever, 1997, Dominco and Schwartz, 1990 and Stumm and Morgan, 1996).

A detailed summary of carbonate geochemistry is available in Clark *et al.* (1997).

- **Atmospheric and soil CO_2**

The atmosphere is the smallest global reservoir of carbon, with an average concentration of 360 ppmv (or partial pressure of $10^{-3.5}$). The short-term natural CO_2 concentration is largely controlled by biologic activity (photosynthesis and respiration) in the oceans and continents. Long-term variations are controlled by tectonism and weathering. The $\delta^{13}C$ of atmospheric CO_2 was approximately –6.4 ‰ (Craig and Keeling, 1963; Friedli *et al.,* 1986), but is now decreasing due to the burning of fossil fuels.

When water infiltrates to the sub-surface, it equilibrates with soil CO_2. Bacterial oxidation of vegetation soils together with respiration of CO_2 in the root zone maintains CO_2 levels between 1000 and 100 000 ppmv ($P_{CO_2} \sim 10^{-3}$ to 10^{-1}). These levels are considerably higher than the ~ 360 ppmv of CO_2 in air today. Solution of soil CO_2 produces carbonic acid, which lowers pH and increases the weathering capacity of groundwater. The amount of carbon dioxide that can dissolve will depend on the geochemistry of the recharge environment: the temperature and initial pH of the water, as well as the partial pressure of soil CO_2.

- **Dissolution of soil CO_2 and carbonate speciation**

When $CO_{2(g)}$ diffuses into water, it forms four main species of dissolved inorganic carbon (DIC), i.e. dissolved or aqueous CO_2 ($CO_{2(aq)}$), carbonic acid or hydrated CO_2 (H_2CO_3), bicarbonate or dissociated carbonic acid (HCO_3^-) and carbonated or the second dissociation species of carbonic acid CO_3^{2-}.

Their distribution, or relative concentration, is a function of pH.

The concentrations of HCO_3^- and CO_3^{2-} together comprise carbonate alkalinity. The formal definition of alkalinity is the concentration of dissolved species which act as proton (H^+) acceptors and buffer pH, eg. Groundwater with a high HCO_3^- concentration will consume

acidity generated, by reversing the two dissociation reactions. The following species dominates at various pH ranges

- At low pH: H_2CO_3;
- At pH ranging between 6.4 and 10.3: HCO_3^-;
- At very alkaline conditions (high pH): CO_3^{2-}.

- **pH buffering and mineral weathering**

The higher the CO_2 concentration in the soil atmosphere, the lower will be the initial groundwater pH. The low pH is then buffered by mineral weathering in the soil and upper bedrock. Calcite dissolution is perhaps the most common and effective buffering reaction. The alteration of silicate minerals to clays also consumes H^+, although these reactions proceed more slowly.

Carbonate dissolution depends on the CO_2 concentration in the soil (the higher CO_2 concentration, the greater will be the amount of calcite dissolved) and the degree of "openness" between the groundwater and the soil atmosphere.

Under open system conditions, calcite dissolution proceeds with a constant supply of soil CO_2. Open system conditions are typical of the unsaturated zone where gas and aqueous phases coexist. Under closed system conditions, the groundwater infiltrates through the soil and reaches the saturated zone before it begins dissolving calcite. Here the groundwater is closed off from the source of CO_2. The fixed concentration of CO_2 gained in the soil is not replenished as carbonate dissolution proceeds, and so the amount of dissolution and the final DIC concentration will be lower. Closed system conditions are typical of recharge areas where infiltration to the water table is fast.

Weathering of silicate minerals has a different effect on the carbonate system. The DIC is derived solely from the CO_2 consumed by the alteration of feldspars such as albite, anorthite to kaolinite. In such reactions, the only change to the carbonate system is the associated increase in pH, which shifts the distribution of DIC species to the HCO_3^- field. For saturated conditions (open system), additional CO_2 will be dissolved from the soil zone, while below the water table (closed system) the extent of the reaction is limited, due to unavailability of CO_2. However, in both cases, the DIC is derived solely from the soil CO_2.

- **Carbon-13 in the Carbonate System**

Carbon-13 is an excellent tracer of carbonate evolution in groundwater, because of the large variations in the various carbon reservoirs.

B-2: BACKGROUND INFORMATION : OXYGEN-18 AND DEUTERIUM

- **Processes in the atmosphere**

In the water cycle 90% of the atmospheric water flux takes place over the oceans and is referred to as the marine part (Gat, 1996). Although the isotopic composition of marine precipitation varies greatly depending on various factors, it is in general heavier (enriched in ^{18}O) than continental precipitation. As marine air progresses from the coast to the continents, different marine air parcels will mix and homogenise, resulting in precipitation, which is closely aligned along the so-called meteoric water lines (MWL). These are straight-lines with a formula:

$\delta\ ^{2}H = 8\ \delta\ ^{18}O + d$ …… **equation 1**

Where d has been named the 'deuterium excess' parameter by Dansgaard (1964). The Global Meteoric Water Line (GMWL) is one such meteoric water line with d = 10 ‰ (Craig 1961b). The further removed from the vapour source, the more depleted (lighter, or enriched in ^{16}O) the delta values of precipitation on each of the meteoric water lines becomes. Dansgaard (1964) recognised four parameters, which determine this depletion in the isotopic values, namely:

- The ***temperature effect***: The isotopic composition of precipitation depends on the temperature at which oceanic water is evaporated into air and even more important the temperature of condensation at which clouds and rain or snow are formed. This effect makes it possible to distinguish between winter and summer rainfall events recharging an aquifer in areas (with summer and winter rainfall prevailing) where rainfall is not strongly seasonal.
- The ***altitude effect***: during an orographic rain event, the rain will become progressively isotopically lighter as clouds ascend the mountain range, the 'lightest rain' will therefore fall on the highest part of the mountain. A depletion in $\delta^{18}O$ of –0.26 ‰ / 100 m was measured in the Swiss Alps (Mazor, 1991).

- The ***continental effect*** (distance from the coast), i.e. the clouds become progressively more isotopically depleted (more negative δ-values) away from the coast. Isotopically heavy rain falls first, with remaining residual air masses becoming progressively lighter.
- The ***latitude effect*** – progressive isotopic depletion in the air masses away from the equator.
- The ***amount effect***: The greater the amount of precipitation, the more negative the $\delta^{18}O$ signature, in general. Rainfall intensity may also play a role.

All the above are related to the rain-out of moisture from the atmosphere as a result of cooling of the air mass and the temperature of condensation in the air mass (Yurtzever, 1975). Different air / sea interaction conditions at the source result in a series of parallel meteoric water lines (each of slope 8). The 'd' parameter in each case relates to the moisture source (Gat 1981), particular the moisture deficit above the interface of the air-masses' origin (Merlivat & Contiac, 1975). Particular regional MWL relating to local effective moisture sources have been recognised, such as the eastern Mediterranean – MWL with d ~ 20 ‰ (Gat & Carmi, 1970) and the Western Australian line with d ~ 14 ‰, etc. Recent investigations in the Western Cape Mediterranean region by Diamond (1997) has established the Western Cape MWL at:

$\delta\ ^{2}H = 7.38\ \delta\ ^{18}O + 18.6$ …….…… **equation 2**

Further, the estimated mean rain line for Southern Africa (IAEA, 1981) is:

$\delta\ ^{2}H = 6\ \delta\ ^{18}O + 5$ ……..…… **equation 3**

The isotopic signature of rain is therefore a function of isotopic exchange between falling raindrops and ascending air in the cloud and the temperature at the cloud base (Gat, 1996), erasing the very depleted signatures. The only exceptions to the above, where no isotopic exchange occurs, applies to snow, hail and precipitation originating from strongly convective systems, resulting in very depleted isotopic signatures.

An additional process, which can affect the isotopic composition of precipitation, is evaporation of falling raindrops beneath the cloud base, leading to enrichment of the heavy isotope species. The δ-values will lie on evaporation lines, which deviate from the MWL, in that their slope is generally less than 8.

As seasons change, the isotopic signature of rainfall at any site will reflect two basic changes in the rain pattern, namely:

- The change in source characteristics over the ocean due to the seasonal change in ocean temperature and air-sea interaction conditions, which primarily affects the 'd' value;
- Secondly the different degrees of rainout during the different seasons, as dictated by the temperature along the air mass trajectory, result in seasonal changes. Further, the evaporative enrichment from falling raindrops, the admixture of re-evaporated moisture, or the effects of snow and hail are also different for different seasons.

- **Processes associated with precipitation infiltration**

The figure below shows the evolution of δ ^{2}H and δ ^{18}O associated with infiltrating rain water.

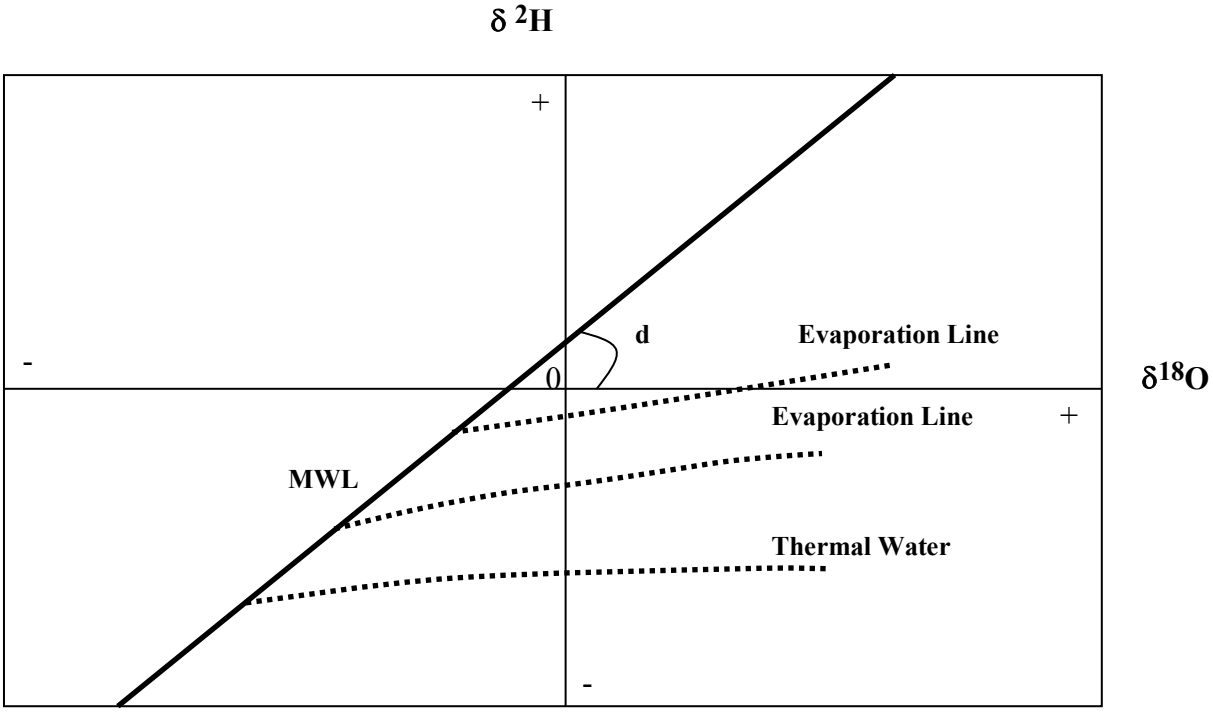

As rain falls to the surface, a number of processes, take place, which modify the isotope composition of precipitation. These processes depend on a combination of factors relating to the terrain and rain event characteristics (e.g. amount, intensity ad intermittence) respectively. In semi-arid areas, such as in the Little Karoo, plant cover is limited and direct evaporation from temporary surface water impoundments that appear after stronger rains are expected to produce the largest isotopic signal. Gat and Tzur (1967) calculated the change in isotopic composition of infiltrating water for the climatic conditions of Israel to be < 1 ‰ $\delta^{18}O$ for soils with an infiltration capacity of < 2 mm/h in summer versus ~ 2 ‰ δ ^{18}O for the same soils in winter. These effects could be described as rainfall infiltration selectivity, due to isotopic variations during storm events (Verhagen and Butler).

In general, any open water bodies, i.e. a dam or river will be enriched in the heavy isotope species (^{18}O), as a result of isotopic fractionation accompanying evaporation.

- **Processes taking place in groundwater**

The isotopic composition of groundwater tends to reflect the isotopic composition of rain water from which it is derived and the times spend in the unsaturated zone. If it was recharged by direct infiltration via preferred pathways with minimum hold-up in the soil cover, the isotopic signature of groundwater is very similar to the isotopic composition of the infiltrating precipitation. Therefore the isotope composition of groundwater is a very useful tool for identifying recharge areas (utilizing the geographic effects on the isotopic composition of rain, such as the altitude effect), tracing mixing patterns and in particular the intrusion of lake or seawater, which are enriched in heavy isotopes. Various recharge events (different rainfall events), small and large scale, direct and indirect, will each imprint a distinguishable stable isotopic signature on the recharged groundwater.

Environmental stable isotopes can to a very good approximation be regarded as conservative tracers throughout the groundwater system. Isotopic exchange between groundwater and the host rock becomes noticeable, at elevated temperatures of more than 80°C, resulting in an 'oxygen shift' towards more positive $\delta^{18}O$ values. However, extrapolation of the isotopic composition of such water (at constant $\delta^{2}H$) makes it possible to identify the meteoric origin of geothermal water.

B-3: THEORETICAL MODELS FOR FRACTURED AQUIFERS

Explanations for flow in fractured aquifers can be found in various theoretical models. The summary provided below is partly adapted from reading material provided by Prof G. van Tonder on a pump test analysis course for fractured aquifers. It is considered a very complete summary available of theoretical models for fractured aquifers.

Muskat (1937) was one of the firsts who analysed the flow in fractured media. Gringarten (1982) found from a comprehensive literature survey that three main approaches are generally followed in theoretical models for fractured aquifers, i.e.:

- The deterministic approach, which is based on an accurate and detailed description of individual fracture systems, and is mainly used for small-scale problems in geotechnical engineering;

- The double-porosity medium approach, which assumes a uniform distribution of matrix blocks and fissures throughout the aquifer (including single-fractured models and multi-porosity / multi-permeability models);
- The equivalent homogeneous aquifer approach, which considers only main trends of the pressure behaviour of the fissured aquifer and tries to relate them to a known model of lower complexity.

Theoretical models generally form the basis of type curves methods derived by various researchers for the analysis of pumping test data of fractured aquifers. For a complete description of all the different models, the reader is referred to Kotze (1993) and Kruseman and De Ridder (1991). A short summary of the most important theoretical models follow below:

- **The Double-porosity** concept was introduced Barenblatt *et al*. (1960) and has been used extensively in the petroleum field. Two approaches that differ in the manner, by which flow from a block to a fissure occurs, have been taken. The first approach assumes that flow occurs under pseudo-steady state conditions (Warren and Root, 1963); in the other approach, the flow occurs under transient conditions from the block to the fracture (Kazemi, 1969). Although the pseudo-steady state approach simplifies the mathematical computations, it ignores some of the physics of the problem. This implies that the transient approach is clearly superior from a theoretical standpoint.

  Bourdet and Gringarten (1980) showed that the double-porosity behaviour of a fractured aquifer only occurs in a restricted area around the pumped borehole. Outside that area (i.e. for λ-values greater than 1,78), the drawdown behaviour is that of an equivalent porous medium. A simplified method of application of the Bourdet-Gringarten method is as follows. It is based on matching both the early- and late-time data with the Theis-curve, which yields values of Tf and Sf and Tf and Sf+Sm respectively (subscripts f and m, denotes the transmissivity –T and Storativity – S, respectively). For this reason, a typical field pumping test curve will just look like the Theis curve and it is thus very tempting to use the Theis model to fit the field data.

- **The fracture skin** concept was introduced by Moench (1984) - a thin skin of low-permeability material deposited on the surfaces of the blocks, which serves to impede the free exchange of fluid between the blocks and the fracture. The effect of fracture skin in double-porosity systems is to delay flow from the blocks to the fractures and gives rise to pressure responses that are similar to those predicted under conditions of pseudo-steady state flow (Moench, 1984). According to Moench, by reducing gradients of hydraulic head

in the compressible blocks, fracture skin provides theoretical justification for the pseudo-steady state flow approximations used in the Warren and Root (1963) model.

B-4: NUMERICAL MODELLING

- **What is modelling?**

A model is a simplified representation of a real system or process. A hydrogeological conceptual model is a hypothesis of how a system or process operates (Konikow, 1994). The idea can be expressed quantitatively as a mathematical model.

Mathematical models are abstractions that replace objects, forces and events by expressions that contain mathematical variables, parameters and constants (Krumbein, *et al.,* 1965). Differently put, a mathematical model should be understood to be a mathematical process (operation) which, when applied to an **input** data sequence, results in and **output** data sequence. It is assumed to describe the processes for which the model is used. Most often, simplification of reality is necessary in order to obtain solutions.

- **Different types of groundwater models**

Currently there are three types of mathematical modelling formulations that can be used for quantitative interpretation of hydrogeological data:

1. Deterministic, distributed-parameter, numerical models: are based on conservation of mass, momentum and energy, i.e. on a balance of the various fluxes of these quantities. Deterministic models imply the solution of the classical advective-dispersive equation for prescribed initial and boundary conditions;
2. Linear lumped-parameter models or analytical models, based on systems analyses approach (transport process is represented by a convolution integral. Based on different system response functions, three subgroups can be distinguished namely, piston-flow, exponential and dispersive models;
3. Discrete-state compartmental simulation models, which can be considered as a quasi-physical, distributed parameter-modelling approach.

The research presented herein attempted to use a deterministic mathematical model.

- **Deterministic Models**

Deterministic models describe cause and effect of relations. The accuracy of such deterministic models and its predictions depends a great deal upon how closely the concepts underlying the governing processes reflect the real processes that are controlling the system's behaviour. Heterogeneity, or variability in aquifer properties, is characteristic of all geologic systems and is now believed to play a key role in the processes of groundwater flow and solute transport. Therefore, it is often preferable to apply distributed-parameter models, which allow the representation of variable system properties.

Deterministic groundwater models generally require the solution of partial differential equations. Partial differential equations, describing groundwater flow and transport, can be solved mathematically by using either analytical or numerical solutions. The advantages of an analytical solution, when it is possible to apply, one are that it usually provides an exact solution to the governing equation and is often relatively simple and efficient to obtain.

In general, obtaining the exact analytical solution to the partial differential equation requires almost unrealistic idealisation of the properties and boundaries of the flow system. In the simulation of most field problems, the mathematical benefits of obtaining an exact analytical solution are outweighed by the errors introduced by the simplifying assumptions made of complex field conditions, which are required during the analytical approach (Konikow *et al.*, 1994).

Alternatively, for problems where the simplified analytical models no longer describe the physics of the situation, the partial differential equations can be solved numerically. In doing so, the continuous variables are replaced with discrete variables that are defined at grid blocks (or nodes). The continuous differential equation (governing equation(s)), describing the hydraulic head or solute transport everywhere in the system, is replaced by a finite number of algebraic equations that defines the hydraulic head or concentration over specific points in space and time (discretized format). Within the discretized format, approximation of the variable's internal properties, boundaries and stresses in the system is impossible. Deterministic, distributed parameter, numerical models relaxed the idealised conditions of analytical or lumped parameter models and can therefore be more realistic and flexible for the simulation of field conditions when applied properly. Due to changes in the state of a groundwater system over time and space, the governing equations are normally

written to give the change in dependent variables with respect to both time and location.

- **Classes of numerical methods**

Two major classes of numerical methods are acceptable for solving the groundwater flow equation, i.e. finite difference and finite element methods. Comprehensive applications of these numerical methods in groundwater problems can be found in Remson, *et al.* (1971) and Wang, *et al.* (1982). Both of these numerical approaches involve subdivision of the area of interest into a number of smaller areas (cells or elements), constituting a grid. Each of the cells or elements is associated with node points (at either the cell centres or peripheries). These two methods differ from each other in the way in which the first derivative of the partial differential equations are approached:

- Finite difference: Solves the first derivative in governing equation as difference equations (differences between values of variables at adjacent nodes, both in space and time, with respect to the interval between those adjacent nodes);
- Finite element: Uses assumed functions of the dependent variables and parameters to evaluate equivalent integral formulations of the partial differential equations.

In both these numerical methods, the discretisation of the space and time dimensions allows the continuous-boundary value problem for the solution of the partial differential equation to be reduced to the simultaneous solution of a set of algebraic equations. These equations can then be solved using either iterative or direct matrix methods.

Each of the numerical methods has its advantages and disadvantages, but there are very few groundwater problems for which either is clearly superior. Table 2-1 overpage summarises the differences between the two methods:

TABLE B-1: COMPARISON OF FINITE DIFFERENCE AND ELEMENT METHODS

Constraint	Finite Difference	Finite Element
Conceptually and mathe-matically	▪ Are simpler and easier to program for a computer	▪ Make use of more sophis-ticated mathematics
Grid Construction and input requirements	▪ Simple rectangular grid, easy data input; ▪ Difficult to simulate irregular aquifer boundaries or parameter zones within aquifer	▪ Flexible finite element grid, allows close spatial approximation of irregular aquifer boundaries, or parameter zones within the aquifer; ▪ Difficult to construct and specification of input data;
Accuracy	▪ Not always very accurate	▪ More accurate numerically for some problems

APPENDIX C: RAINFALL DATA

TABLE C-1 : ANNUAL RAINFALL FORESTRY RAIN GAUGES – KAMMANASSIE MOUNTAINS

KAMMANASIE MOUNTAIN - FORESTRY RAIN GAUGES										
	P1 (1500 m)		P2 (1500 m)		ELANDSFON (1200 m)		WILDEBEESV (980 m)		WILDE ALSV (1100 m)	
	YTOT	STOT	YTOT	STOT	YTOT	STOT	YTOT	STOT	YTOT	STOT
1987	338	453	316.3	426.1	499.7	458.7	361	384.5	458.8	546.4
1988	450	424.9	599.1	506.5	489.7	298.5	286.8	340.8	384.9	331.3
1989	553.4	610.7	634.5	773.8	482	650.4	469	353.3	502.3	619.2
1990	415.1	717.4	567	478.2	463.6	398.7	195.3	325	440.2	352.5
1991	764	504	506	649	536.5	630	404	502.1	497.5	627
1992	559.5	621.2	736	768	592	772	571.1	559	594.2	799.7
1993	654.7	552	788	796.5	700.5	475	552	581.5	711.5	553
1994	412.5	510.3	664.8	768	522	740	492.5	547.3	543.5	605.5
1995	579.7	444.9	900.6	683.4	781	545	641.3	495	709	567
1996	687.3	878.3	937	1169.3	783.5	867.5	673	1051.5	834	1073.5
1997	582		779.6		539.5		778.5		736	
AVG	**545.1**	**571.7**	**675.4**	**701.9**	**580.9**	**583.6**	**493.1**	**514.0**	**582.9**	**607.5**

Unreliable information / missing data

TABLE C-2: WEATHER BUREAU RAIN GAUGES - LITTLE KAROO REGION

	STATION	PLACE	LAT	LONG	ALT	DATE FROM	DATE TO	LENGTH OF RECORD	YEARS _AVG YTOT	AVG YTOT	A_MIN	A_MAX	YEARS _ AVG STOT	AVG_ STOT	S_MIN	S_ MAX
1	*00100362	Heidelberg	34.1000	21.0333	145	1966	1998	32	30	407.6	215.7	646.3	30	406.6	204.0	667.6
2	*0010456X	Riversdal	3.1000	21.2666	116	1877	1981	104	71	452.8	245.4	686.1	68	442.0	221.3	759.9
3	*0010742X	Stilbaai-Bos	34.3666	21.4166	30	1924	1998	74	65	428.7	224.2	709.5	65	439.8	237.0	625.5
4	*00110659	Diepkloof	34.0833	21.5500	225	1949	1998	49	41	458.8	274.4	809.3	43	459.2	240.6	813.2
5	*0011132X	Albertinia - Pol	34.2000	21.5833	183	1924	1998	74	65	455.8	213.5	894.4	66	453.4	188.5	779.5
6	*00114517	Herbertsdale	34.0166	21.7666	152	1886	1998	112	31	443.2	252.3	747.8	29	449.9	189.0	726.4
7	*00122517	Cape St Blaize	34.1833	22.1500	60	1880	1998	118	55	386.5	183.8	717.8	53	392.5	157.5	684.2
8	*00123032	Sandhoogte	34.0500	22.1833	163	1927	1998	71	52	481.5	291.9	961.5	52	480.2	262.4	894.7
9	*00123938	Great Brakriver	34.0500	22.2333	15	1900	1985	85	72	511.3	185.9	895.5	71	498.9	260.0	827.5
10	*00140634	Knysna-TNK	34.0500	23.0500	30	1880	1998	118	75	722.1	477.6	1154.2	75	745.7	478.9	1652.1
11	*00143930	Harkerville Bos	34.0500	23.2333	213	1888	1998	110	84	977.3	344.8	1695.7	88	979.7	365.4	1485.0
12	*0014633	Plettenbergbaai	34.0500	23.3666	73	1891	1998	107	71	651.0	376.5	1183.3	68	658.9	301.7	1063.9
13	*00265105	Garcia-Bos	34.0000	21.8333	305	1936	1998	62	58	644.7	405.6	1031.6	57	642.7	380.4	969.4
14	*00268244	Van Wyksdorp - Pol	33.7333	21.4666	305	1969	1998	29	28	250.3	123.9	441.8	28	254.0	110.1	487.6
15	*00273021	Calitzdorp - Pol	33.5333	21.6833	238	1877	1998	121	104	198.7	53.9	429.2	99	199.5	75.7	438.2
16	*00278760	Welbedag	33.6000	22.0000	564	1920	1998	78	63	180.7	57.1	379.3	59	185.2	52.5	389.0
17	*00280833	Ruitersberg	33.8833	22.0500	1229	1940	1998	58	40	886.2	492.6	1994.7	40	892.2	499.3	1914.5
18	*00281504	Mosselbaai - Kwepertuin	34.0000	22.0833	213	1928	1998	70	57	527.1	254.5	1039.2	54	543.2	256.0	946.2
19	*00283355	Oudtshoorn - TNK	33.5833	22.2000	332	1878	1998	120	107	245.2	114.2	457.7	102	246.4	106.5	469.0
20	*00284075	Groot Doring Rivier	33.7833	22.2333	533	1926	1998	72	62	245.8	121.0	539.1	61	250.7	70.9	550.9
21	*00284159	Jonkersberg - Bos	33.9166	22.2333	457	1919	1998	79	73	991.5	634.7	1862.6	72	991.7	549.5	2299.0
22	*0028771X	Herold	33.8500	22.4333	579	1924	1998	74	68	459.8	196.4	978.2	67	468.7	186.2	959.4
23	*00287842	Dysseldorp	33.5666	22.4500	424	1993	1998	5	4	348.2	253.4	455.6	4	362.8	270.5	549.5
24	*00288428	Le Roux - SAR	33.5333	22.4833	408	1912	1992	80	49	246.3	112.4	390.3	43	247.4	109.9	492.0
25	*00292945	Bergplaas - Bos	33.9000	22.6666	457	1924	1998	74	73	830.2	522.5	1565.2	72	830.2	468.9	1415.2
26	*0029542X	Rooi Rivier	33.5333	22.8166	564	1923	1998	75	75	247.1	83.7	491.7	74	247.7	78.0	540.7
27	*00296247	Karatara-Bos	33.9000	22.8500	297	1928	1998	70	64	801.0	509.7	1424.4	64	803.7	496.0	1346.7
28	*00301890	Uniondale	33.6500	23.1166	750	1989	1998	9	8	324.5	208.5	428.9	8	337.6	158.0	506.9
29	*00302198	Uniondale TNK	33.6500	23.1333	762	1889	1979	90	88	315.2	68.3	714.1	85	323.3	74.0	611.6
30	*00302657	Buffelsnek - Bos	33.9166	23.1500	724	1890	1998	108	93	1127.9	756.1	1670.8	93	1114.3	759.0	1619.9

TABLE C-2 (CONTINUE) : WEATHER BUREAU RAIN GAUGES - LITTLE KAROO REGION

	STATION	PLACE	LAT	LONG	ALT	DATE FROM	DATE TO	LENGTH OF RECORD	YEARS _AVG YTOT	AVER AGE YTOT	A_MIN	A_MAX	YEARS _ AVG STOT	AVG_ STOT	S_MIN	S_MAX
31	*00305240	Welgelegen	33.7333	23.3000	853	1972	1998	26	25	527.1	277.5	957.0	26	522.3	284.5	1022.6
32	*00460598	Ladismith - Buffelsvlei	33.4833	21.0333	381	1920	1998	78	64	190.7	73.0	364.9	63	195.8	41.9	359.9
33	*00464795	Ladismith TNK	33.4833	21.2666	533	1878	1998	120	112	316.6	138.0	553.3	112	313.1	135.1	584.8
34	*00465925	Ladismith - Zandrivier	33.3666	21.3333	1120	1985	1998	13	10	403.1	276.3	543.4	10	424.7	294.8	689.4
35	*00468097	Zoar - Col	33.4833	21.4500	515	1964	1998	34	32	244.9	103.0	479.9	32	244.7	74.5	649.7
36	*00472057	Matjiesvlei - Gamka Bo	33.4166	21.6166	610	1961	1998	37	35	262.3	112.8	513.2	35	263.6	89.2	532.0
37	*00473599	Calitzdorp Dam	33.4833	21.7000	366	1923	1998	75	63	201.4	48.7	522.0	62	199.7	49.3	570.3
38	*00474367	Weltevreden	33.2666	21.7500	511	1934	1998	64	61	154.5	49.7	313.8	61	155.2	36.1	364.3
39	*00475498	Prins Albert - Slagterspoort	33.1500	21.8166	500	1990	1998	8	7	162.7	90.5	258.6	6	176.9	86.1	253.8
40	*00477167	Kruis Rivier	33.4333	21.9000	579	1928	1998	70	69	423.9	256.9	731.9	68	424.8	219.2	793.6
41	*00477651	Damaskus	33.2500	21.9333	910	1953	1998	45	44	174.5	58.2	344.0	44	177.9	70.0	373.4
42	*00480432	Prins Albert TNK	33.2166	22.0333	686	1877	1998	121	100	170.6	56.5	352.9	98	171.3	41.8	409.5
43	*00480516	De Wetsvlei	33.3500	22.0333	1525	1950	1998	48	46	655.4	302.0	1183.0	46	657.3	252.0	1226.5
44	*00480795	Swartberg Bos	33.3166	22.0500	1600	1948	1998	50	42	794.4	437.1	1324.3	41	802.6	416.5	1357.2
45	*00480831	Matjies Rivier	33.3833	22.0500	732	1930	1998	68	66	418.2	153.2	888.8	65	420.6	178.3	906.5
46	*00481429	Albertberg	33.3666	22.0833	1067	1950	1998	48	44	771.6	424.5	1396.6	45	774.0	478.5	1231.8
47	*00485046	Raubenheimerdam	33.4000	22.2833	762	1991	1998	7	4	473.2	360.1	653.6	4	432.7	326.6	570.1
48	*00490500	Klaarstroom - Pol	33.3333	22.5333	732	1910	1998	88	83	194.0	33.4	452.4	81	196.3	35.5	460.1
49	*00490608	De Rust - Pol	33.5000	22.5333	533	1914	1998	84	72	329.4	153.8	637.3	66	328.4	136.8	602.6
50	*00493723	Rondawel	33.2000	22.7166	853	1912	1998	86	70	138.0	21.1	360.4	66	143.0	38.6	326.4
51	*00502304	Tuintjies Kraal	33.3000	23.1333	672	1910	1998	88	59	184.8	40.7	455.5	52	188.2	75.4	443.2
52	*00503278	Rondekop	33.4500	23.1833	762	1972	1998	26	25	274.3	123.3	499.0	24	271.4	132.4	556.1
53	*00506888	Rooiklip	33.4666	23.3833	800	1986	1998	12	11	278.0	180.6	463.7	11	285.6	121.2	554.3
54	*00508872	Willowmore	33.2833	23.5000	840	1877	1998	121	76	261.5	98.3	659.9	72	263.6	85.5	630.3
55	*00227591	Worcester	33.6500	19.4333	221	1880	1998	118	118	272.0	127.4	480.1	117	272.7	107.6	462.4
56	*00241970	Montagu	33.7833	20.1167	223	1883	1998	115	83	310.9	126.8	562.5	77	315.9	107.6	639.1
57	*00254148	Barrydale-Pol	33.9000	20.7333	290	1925	1998	73	69	277.0	93.6	568.7	69	281.3	147.8	522.6
58	*00630053	Citrusdal	32.4167	19.0167	230	1965	1998	33	26	390.4	241.0	334.0	25	395.5	99.3	687.0
59	*00272446	Calitzdorp Werke	33.5667	21.6500	400	1993	1998	5	3	194.8	133.3	229.8	3	194.8	171.6	237.9
60	*00288381	George	33.9667	22.4667	229	1877	1998	121	105	879.9	561.0	1656.1	105	872.8	490.1	1564.1

TABLE C-3 : FORESTRY RAIN GAUGES

	STATION	PLACE	LAT	LONG	ALT	DATE FROM	DATE TO	LENGTH OF RECORD	YEARS _AVG YTOT	AVER AGE YTOT	A_MIN	A_MAX	YEARS _ AVG STOT	AVG_ STOT	S_MIN	S_MAX
57	Die Kruin	Swartberg	33.3600	22.0400	1583	1950	1989	39	39	1574.2	486.2	3363.0				
58	Kliphuisvlei	Swartberg	33.3400	21.9100	1370	1950	1989	39	39	955.8	283.0	1963.0				
59	De Wetsvlei	Swartberg	33.3400	22.0400	1422	1950	1989	39	39	1386.0	320.4	3004.0				
60	Albertberg	Swartberg	33.3600	22.0900	1067	1950	1989	39	39	1651.9	503.5	3130.0				
61	Elandsvlakte	Kammanassie	33.6575	22.7569	1200	1950	1997	47	47	580.9	463.6	783.5			298.5	867.5
62	Perdevlakte P1	Kammanassie	33.6078	22.8581	1500	1950	1997	47	47	545.1	338.0	764.0			424.9	878.3
63	Perdevlakte P2	Kammanassie	33.6286	22.8522	1500	1950	1997	47	47	675.4	316.3	937.0			426.1	1169.3
64	Wildealsvlei	Kammanassie	33.6536	22.6692	1100	1950	1997	47	47	493.1	195.3	778.5			325.0	1051.5
65	Wildebeesvlakte	Kammanassie	33.6253	22.5806	980	1950	1997	47	47	607.5	195.3	778.5			331.3	1073.5
66	Buffelsklip	Kammanassie	33.5689	22.8911	700	1950	1997									

FIGURE C-1: AVERAGE RAINFALL DISTRIBUTION FOR LITTLE KAROO – RAINFALL INCREASE PROPORTIONAL TO ALTITUDE

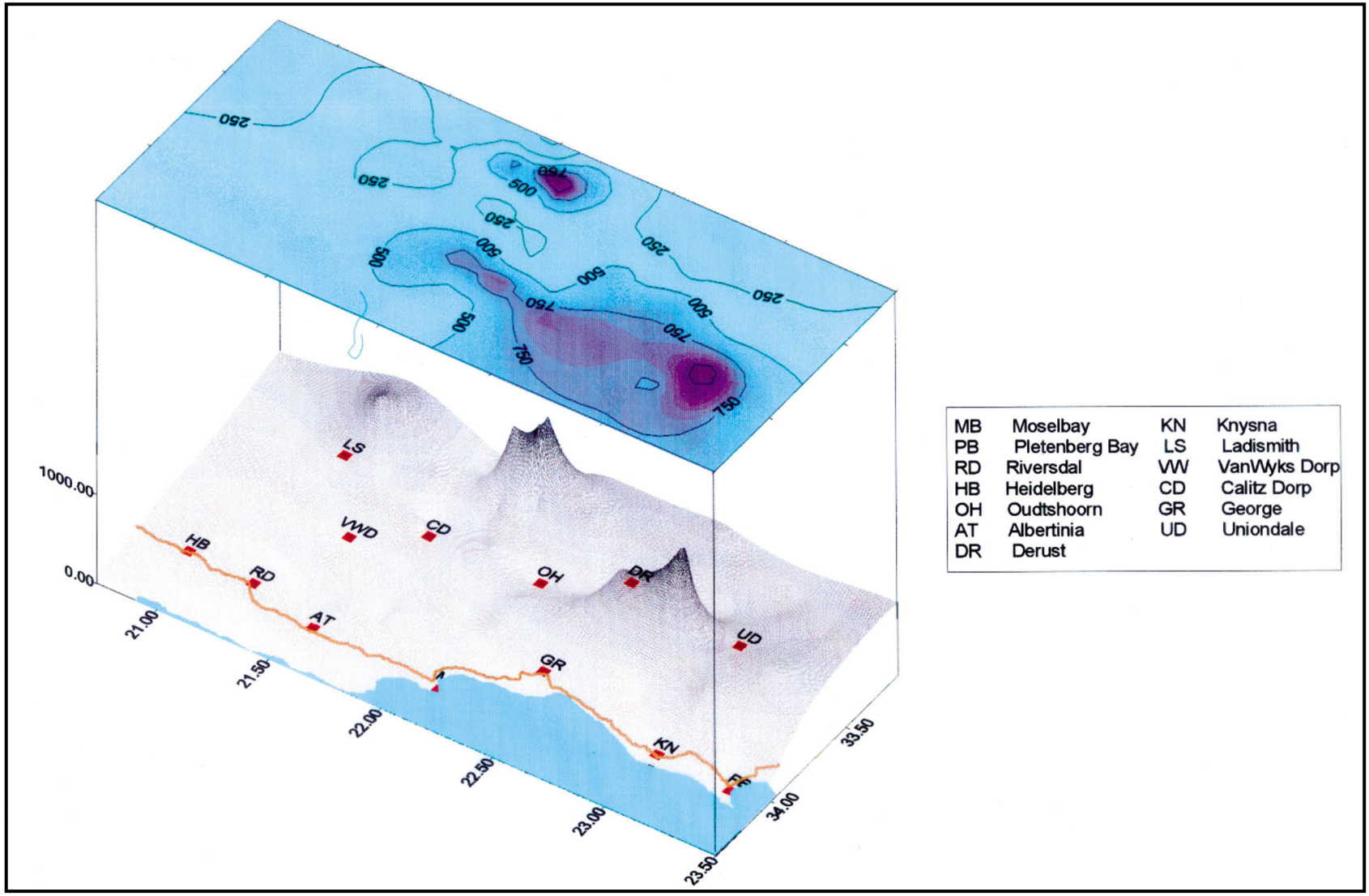

APPENDIX D: WELLFIELD CAPACITIES

TABLE D-1: KKRWSS WELLFIELD CAPACITIES

PRODUCTION BOR																			
NAME		BOREHO						SUMMARY: RECOMMENDED ABSTRACTION R											
CURRENT	OLD	CONSTRUCTION																	
		DEPTH	DEPTH OI			GROUND WATER		MAX											
		DRILLEI	299mm	COLLAR	CURRENT	REST LEV		TOLERABL	FEB 19			NOV 199			FEB 1995 (MULD			APRIL 1995 (KOTZE)	
			PVC	HEIGHT	TRANSDUC			DRAWDOW			PEAK			PEAK			PEAK		
			CASING	(MAMSL)	DEPTH	WATER	DATE				ABS			AB			AB		
						LEVEL	MEASURE	(M)	M3/D	L/S	L/S	M3/D	L/S	L/S	M3/D	L/S	L/S	M3/D	L/S
DP10	D3C	237	208	456.5	166	342.4	08/1990	170	1040	12	14	800	9.25	15	190	3.5	GEEN		
DP12	D3B	192	186	468.5	174	341.2	08/1990	180	500	5.8	12	500	5.8	8	300	5.5	8		
DP15	D4B	207	207	451.1	177	347.3	08/1990	180	500	5.8	20	500	5.8	12	320	6	10	360	5
DP18	D8D	18	16	351.1	9	347.5	06/1990	11	820	9.5	14	850	9.8	14	600	11	14	600	11
DP25		203	203	449.1	177	341.3	10/1991	180	780	9	20	850	9.8	15	450	7	15	530	5
DP28		246	210	459.1	167	341.7	10/1991	170	690	8	20	720	8.3	25	700	9	20	580	9
DP29		240	240	463.1	175	339.1	10/1991	180	865	10	10	260	3	8	300	5.5	8	300	3
DG110		212	212	488.5	177	374.7	10/1991	180	690	8	16	300	3.5	12	190	3.5	GEEN	230	3
						TOT_ABS DYSSELSD			5885	68.1	126	4780	55.25	109	3050	51	75		
VG3	D13	206.7	148.7	497.3	144	491.1	10/1990	148	690	8	10	400	4.6	10	400	4.5	10	230	3
VR6	D23	250	230	718.3	162	684.8	10/1990	165	1035	12	20	700	8.1	15	700	8	10	430	3
VR7	D20	177	151.5	748.9	146	686.7	10/1990	150	2600	30	40	1700	19.7	30	1700	20	30	670	5
VR8	D21	251	164.8	786.7	152	686.7	10/1990	163	1300	15	25	865	10	20	850	10	20	530	5
VR11		224.5	214	812.2	176	686.1	10/1991	180	1300	15	25	690	8	15	700	8	15	500	7
						TOT_ABS VERMAAKS			6925	80	120	4355	50.4	90	4350	50.5	85		
DL13	C3	185	132.7	261.8	117	235.6	09/1991	120	1166	7.5	14	600	6.9	25	600	7	25	150	3.5
DL15	C5	137	136.5	285.6	117	284.43	09/1991	120	520	6	14	700	8.1	20	700	8	20		7
DL16	C6	169	132.8	279	122	285.1	10/1990	125	430	5	20	300	3.5	20	300	3.5	15	150	3
DL17	C7	249	149.5	291.7	137	282.7	10/1990	140	1300	15	25	865	10	25	200	3	GEEN	150	3
KG1	C8	209	148	242	137	227.5	10/1990	140	1300	15	25	1300	15	25	1000	11	25		6
						TOT_ABS CALITZDOR			4716	48.5	98	3765	43.5	115	2800	32.5	85		
						TOTAL ABS - SCHEME			17526	196.6	344	12900	149.15	314	10200	134	245		

APPENDIX E: WATER LEVEL DATA

TABLE E-1 : WATER LEVEL DATA

BH	LONG	LAT	Y	X	ALT	DATE	WL_ELV
AL1	33.70194	22.67416			605	1995	571.55
CP2	33.55642	22.33792			247.878	1994	212.58
CP3	33.55278	21.66083	124348.2	3714597	247.878	1995	215.24
DG102	33.56748	22.46139			476.4	1992	347.1
DG103	33.56737	22.46168			469.6	1995	359.35
DG104	33.56389	22.47667			493.2	1995	391.93
DG110	33.56611	22.47083	49135.5	3715404	488.5	1995	372.58
DL1	33.57242	22.37466			301.9	1997	290.94
DL11	33.55944	21.6575	124656.6	3715336	277.7	1995	196.4
DL12	33.56111	21.65528	124859.1	3715532	257.9	1995	217.7
DL13	33.56389	21.65028	125315.3	3715847	261.8	1995	217.49
DL14	33.56694	21.64361	125945.7	3716187	276.1	1995	254.74
DL15	33.56722	21.63806	126462.8	3716235	285.6	1995	261.65
DL16	33.56583	21.64333	125971.8	3716071	279	1995	246.25
DL17	33.56889	21.63194	127010.5	3716432	291.7	1995	258.34
DL2	33.57083	21.625			303.4	1994	259.12
DP10	33.57278	22.45278	50790.8	3716159	456.5	1995	348.17
DP11	33.57409	22.45394			463.7		329.9
DP12	33.57444	22.45417	50673.2	3716325	468.5	1995	347.92
DP13	33.58111	22.45667	50440.3	3717071	458.9	1995	344.74
DP14	33.58139	22.45639	50462.3	3717091	451.4	1995	345.61
DP15	33.58139	22.45611	50468.5	3717093	451.1	1995	345.21
DP16	33.56984	22.42106			351.2	1994	334.25
DP17	33.56997	22.42091			349.1	1995	346.1
DP18	33.56972	22.42083	53753.1	3715823	351.1	1995	348.7
DP19	33.56969	22.4211			350.8	1995	346.2
DP20	33.57861	22.45417	50654,0	3716804	448.8	1995	345.93
DP24	33.56944	22.42083	53764.2	3715792	350.7	1995	349.26
DP25	33.58152	22.45625			449.1	1995	344.2
DP27	33.57306	22.45278	50784	3716166	458.3	1995	349.91
DP28	33.58111	22.45667	50426.1	3717073	459.1	1995	343.75
DP29	33.57389	22.40389	50701.4	3716277	463.1	1995	347.3
DR1	33.69528	22.69444			639.7	1995	587.21
DR2	33.70889	22.68444			545	1995	527.2
GA1	33.55889	21.66028	124397.9	3715267	245.73	1995	203.58
GA2	33.55889	21.66028	124402.6	3715263	245.645	1995	214.945
KG1	33.54889	21.65722	124688.9	3714161	242	1995	218.29
LD2	33.67055	22.57138			618	1995	598
RF10	33.695	22.58527			605	1995	579.87
RF2	33.6725	22.57222			624.9	1995	595.9
RF8	33.68361	22.57333			615	1995	589.57
RF9	33.68166	22.57166			590	1995	555.62
RN1	33.58389	22.46417	49719.65	3717364	468.562	1995	349.592
RY10	33.54889	22.47278	48964.97	3713497	426.331	1995	384.251
RN105	33.58417	22.46306	49838.47	3717405	460.112	1997	420.322
SL11	33.63173	22.57405			589.8	1991	529.7
SL2	33.69777	22.61944			610	1995	605.4
VG1	33.565	22.53806	42887.57	3715234	490.759	1995	485.179
VG12	33.57972	22.53167	43458.92	3716880	563.826	1995	560.966
VG2	33.56444	22.53806	42869.18	3715190	489.966	1995	481.416
VG3	33.56694	22.53861	42820.8	3715464	497.3	1995	483.86
VG4	33.56667	22.55333	*	*	559.8	1995	544.33
VR11	33.61972	22.55861	40941.7	3721305	812.2	1995	810.76
VR5	33.57778	22.58278	38720	3716638	549.5	1995	547.48
VR6	33.61167	22.54639	42082.9	3720432	718.3	1995	669.6
VR7	33.61472	22.55111	41648	3720761	748.9	1995	670.4
VR8	33.6175	22.55417	41351.5	3721066	786.7	1995	671.1

TABLE E-1 : WATER LEVEL DATA (CONTINUE)

BH	LONG	LAT	Y	X	ALT	DATE	WL_ELV
VVERMAAKS					530		
VMARNEWICKS					540		
PARSHALL					590		
WK3	33.58537	22.56429			578.7	1995	529.95
WK4	33.6275	22.51583	44906.22	3722179	658.921	1995	584.631
WN101	33.56889	22.5625	*	*	534.3	1995	532.06
WN2	33.57512	22.56597			527.6	1995	508.2
YR2	33.70388	22.63944			615	1995	583.9
YR4	33.6975	22.65166			620	1995	580.59
YR5	33.69111	22.67444			660	1995	650.82
WN3	33.56778	22.59056	37993.16	3715520	563.781	1999	544.581
G40171	33.60278	22.5325	43387.17	3719435	660.516	1999	655.216
G40172	33.60278	22.5325	43387.05	3719429	660.416	1999	655.266
G40173	33.60278	22.5325	43387.07	3719423	660.216	1999	655.286
G40174	33.58472	22.94583	5009.63	3717351	469.666	1999	362.856
G40175A	33.60167	22.53056	43561.01	3719314	652.031	1999	652.031
G40176	33.59972	22.52917	43678.19	3719097	644.081	1999	636.741
G40177	33.58222	22.45333	50735.26	3717181	420.036	1999	368.696
G40178	33.68083	22.56417	40414.5	3728069	535.691	1999	525.331
VG13	33.57833	22.535	43163.47	3716721	553.871	1995	550.531
VG14	33.57861	22.535	43151.26	3716754	555.736	1995	554.256
VG15	33.57806	22.51944	43059.63	3716690	556.101	1995	551.621
VG16	33.60722	22.54028	42654.53	3719919	691.006	1996	665.406
SBH1	-33.8094	22.57139			545	1998	525
SBH2	-33.7836	22.71			555	1998	535

APPENDIX F: SPATIAL VARIATION IN CHEMISTRY

FIGURE F-1: SPATIAL VARIATION OF ALUMINIUM IN GROUNDWATER – LITTLE KAROO

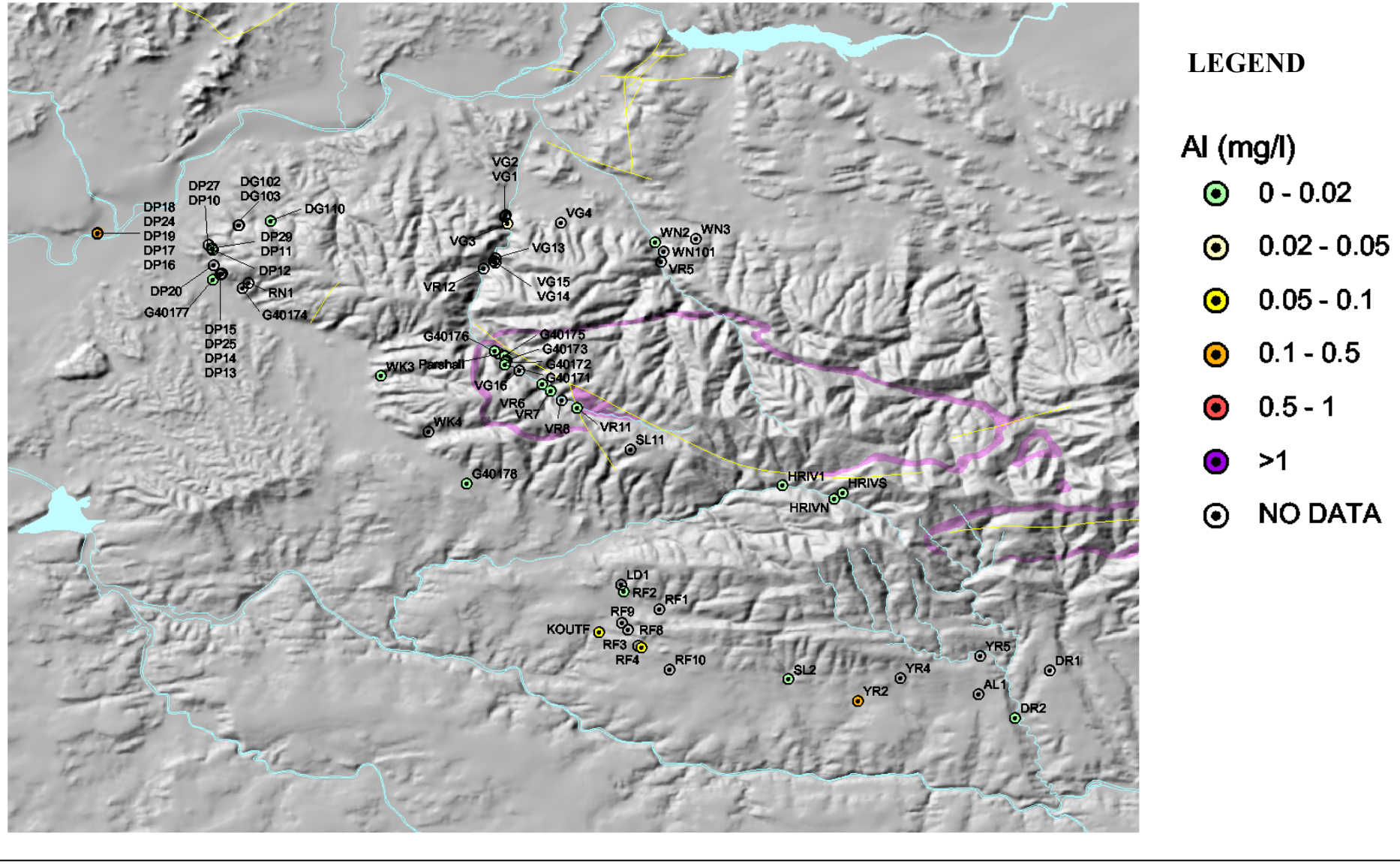

FIGURE F-2: SPATIAL VARIATION OF BARIUM IN GROUNDWATER – LITTLE KAROO

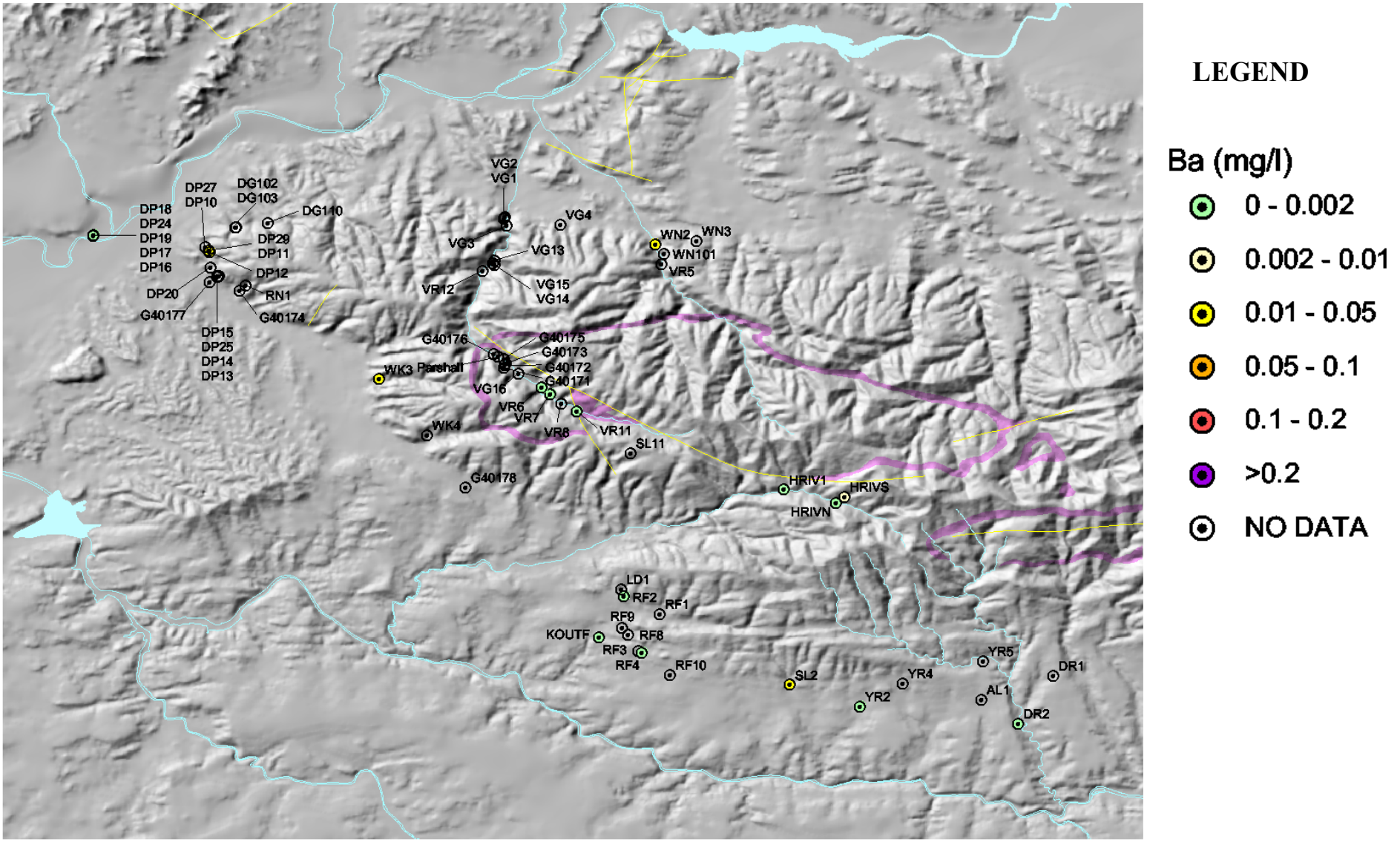

FIGURE F-3: SPATIAL VARIATION OF STRONTIUM IN GROUNDWATER – LITTLE KAROO

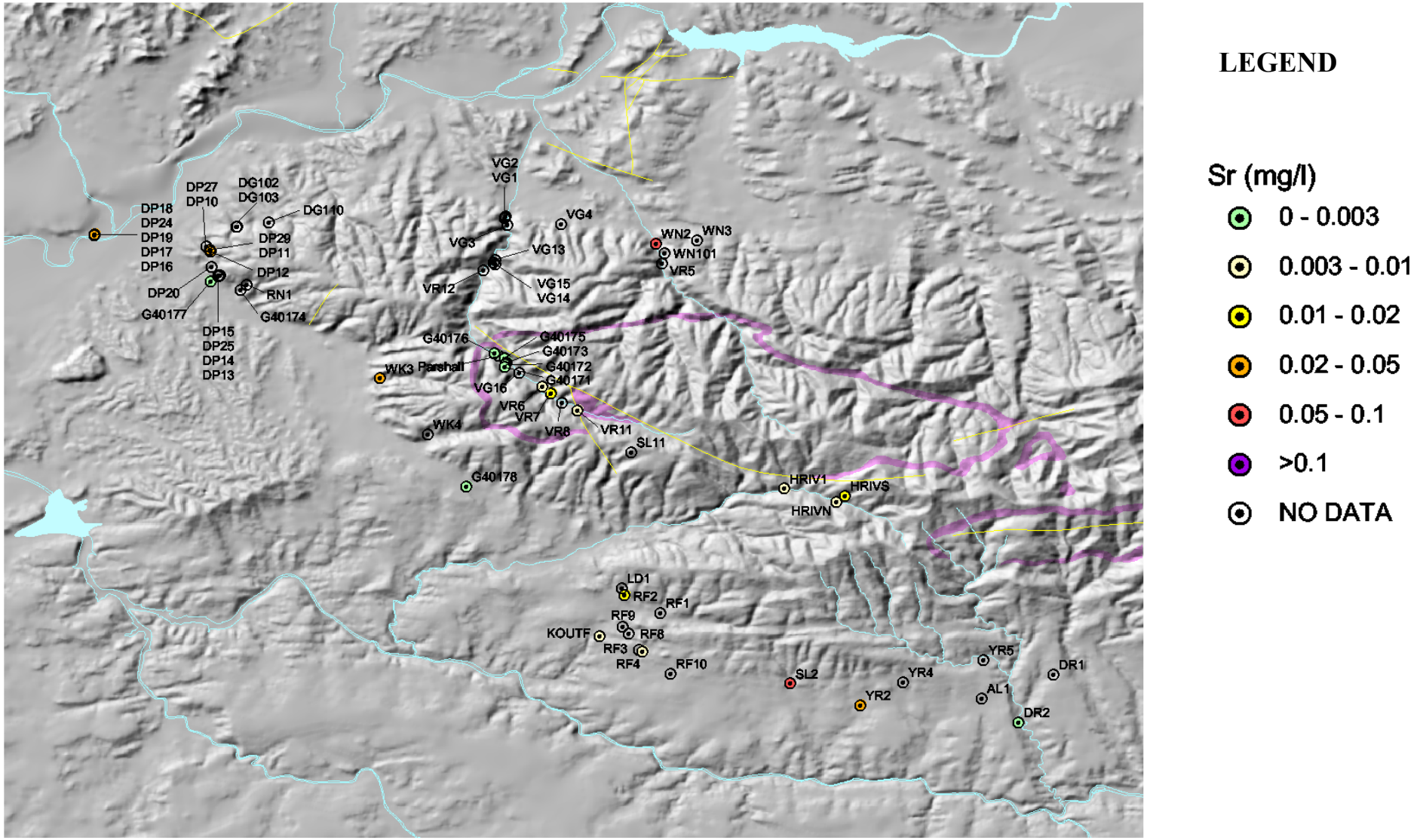

FIGURE F-4: SPATIAL VARIATION OF MANGANESE IN GROUNDWATER – LITTLE KAROO

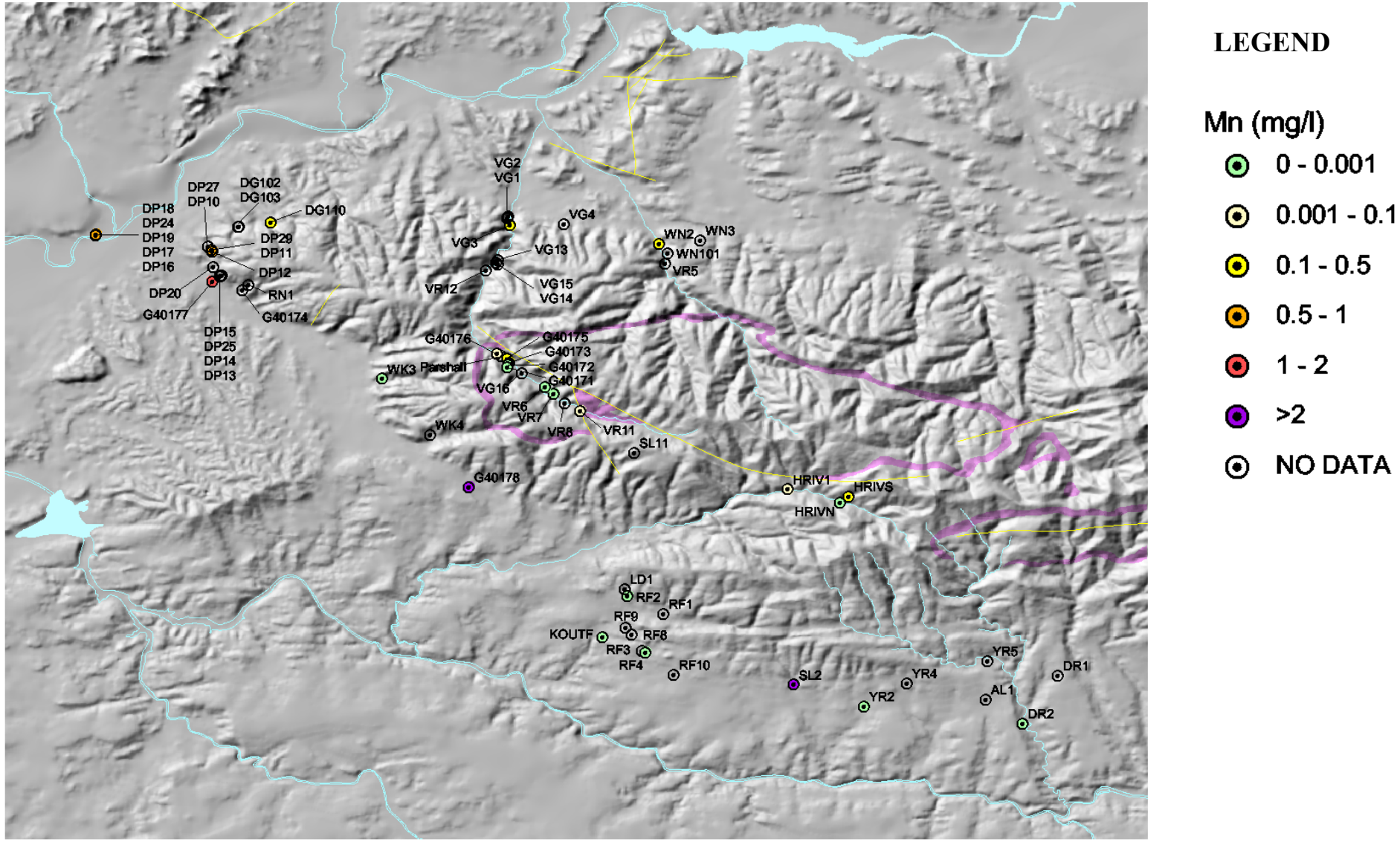

FIGURE F-5: SPATIAL VARIATION OF IRON IN GROUNDWATER – LITTLE KAROO

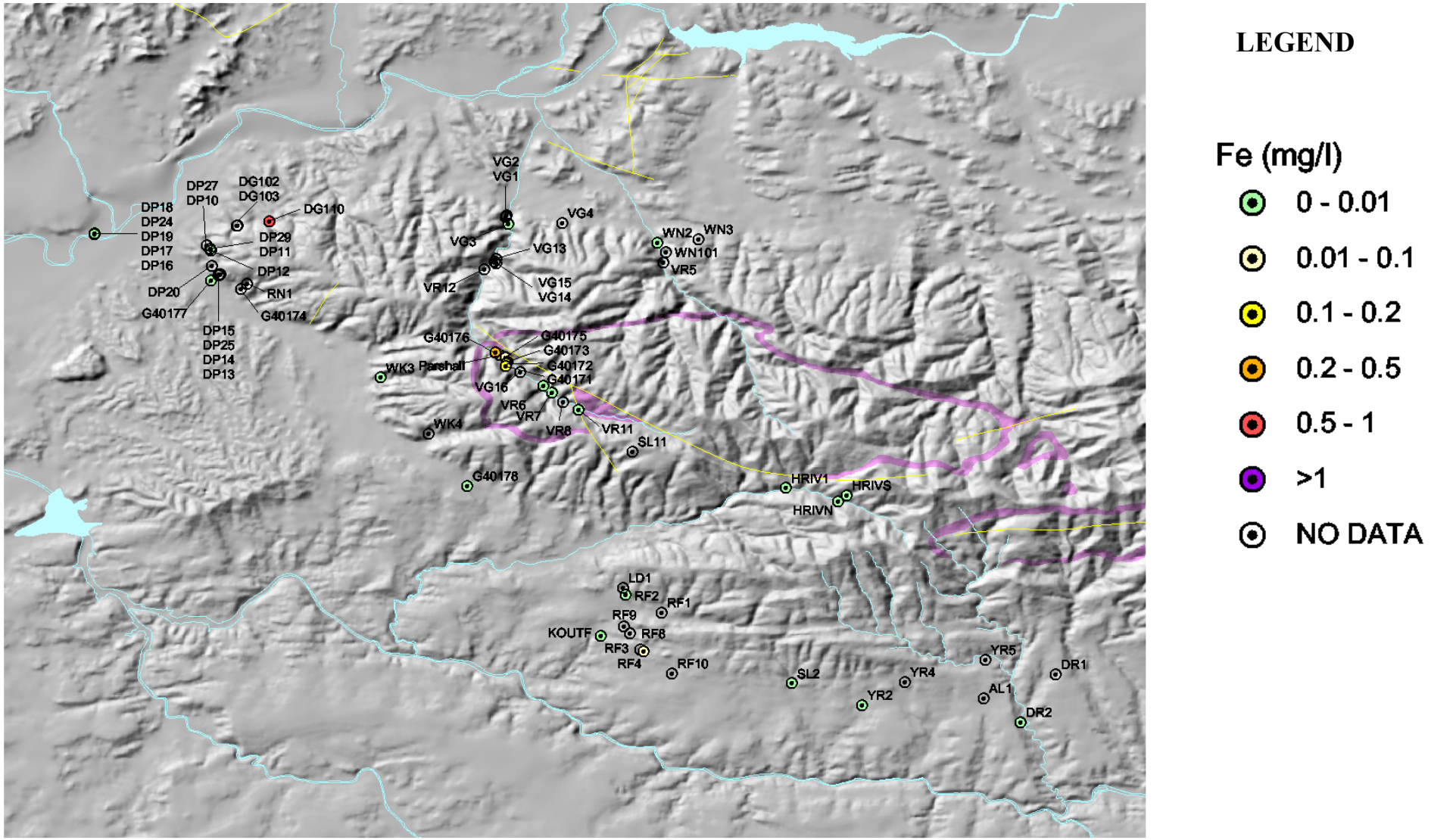

FIGURE F-6: SPATIAL VARIATION OF OXYGEN-18 IN GROUNDWATER – LITTLE KAROO

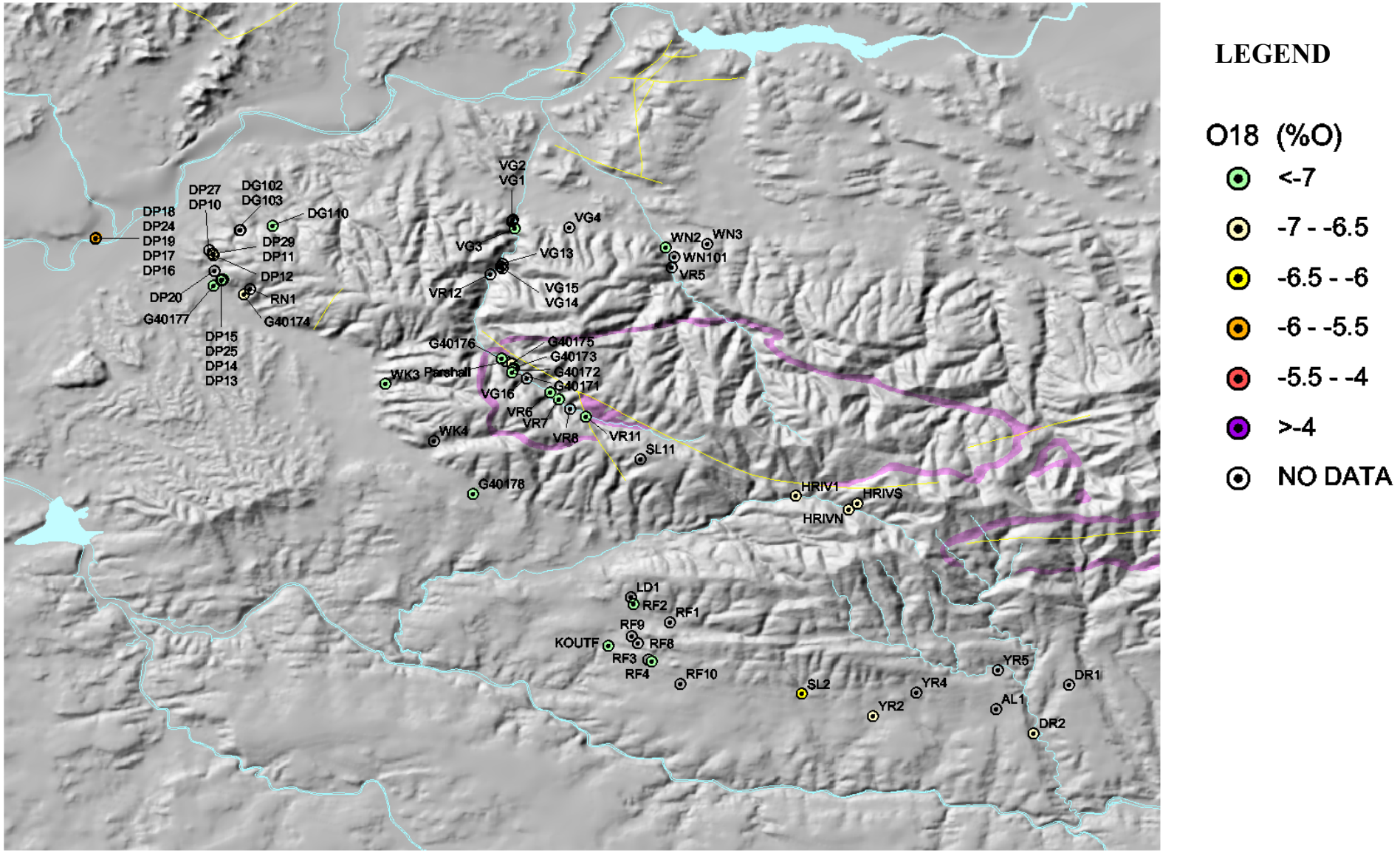

FIGURE F-7: SPATIAL VARIATION OF CARBON-14 IN GROUNDWATER – LITTLE KAROO

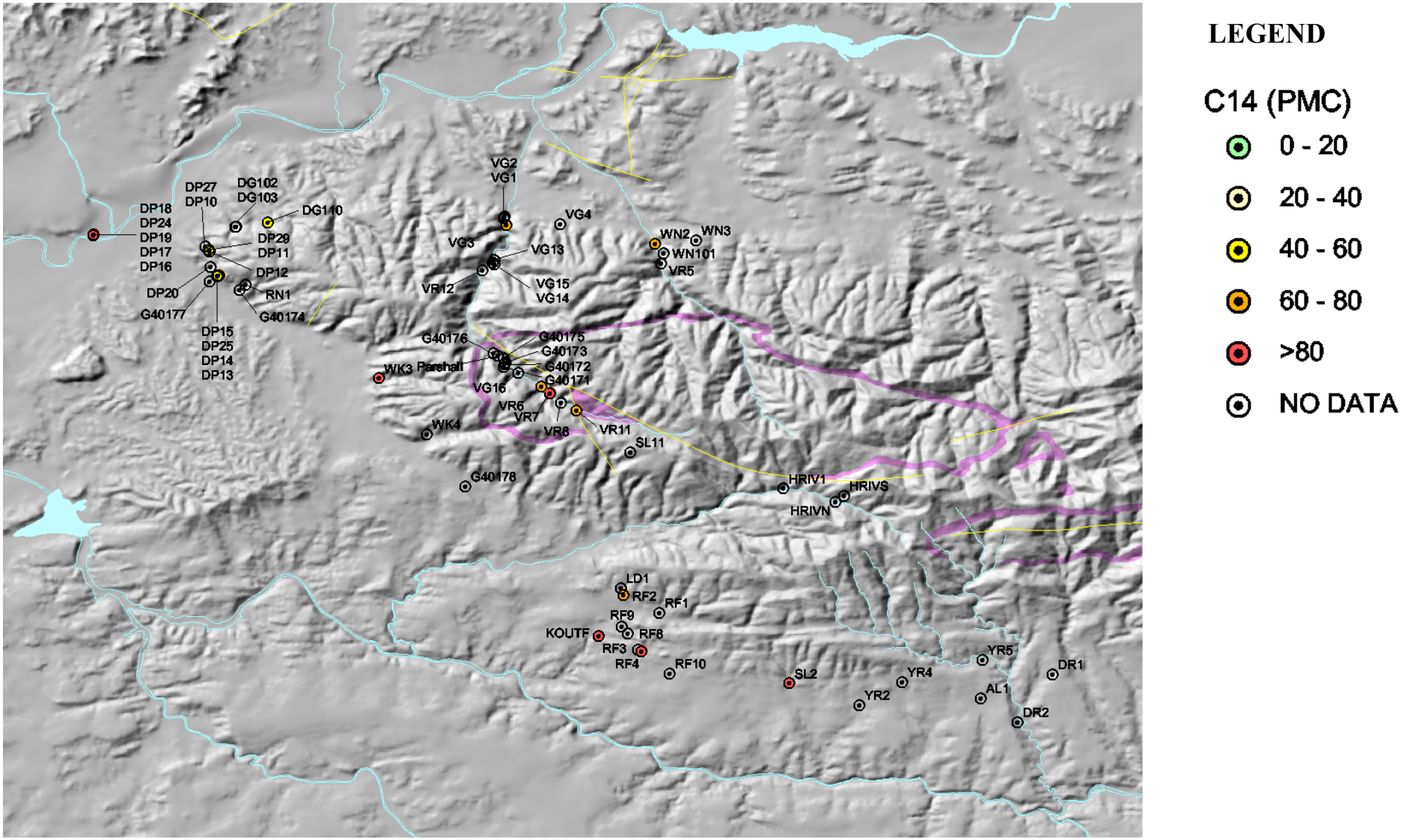

FIGURE F-8: SPATIAL VARIATION OF SULPHATE IN GROUNDWATER – LITTLE KAROO

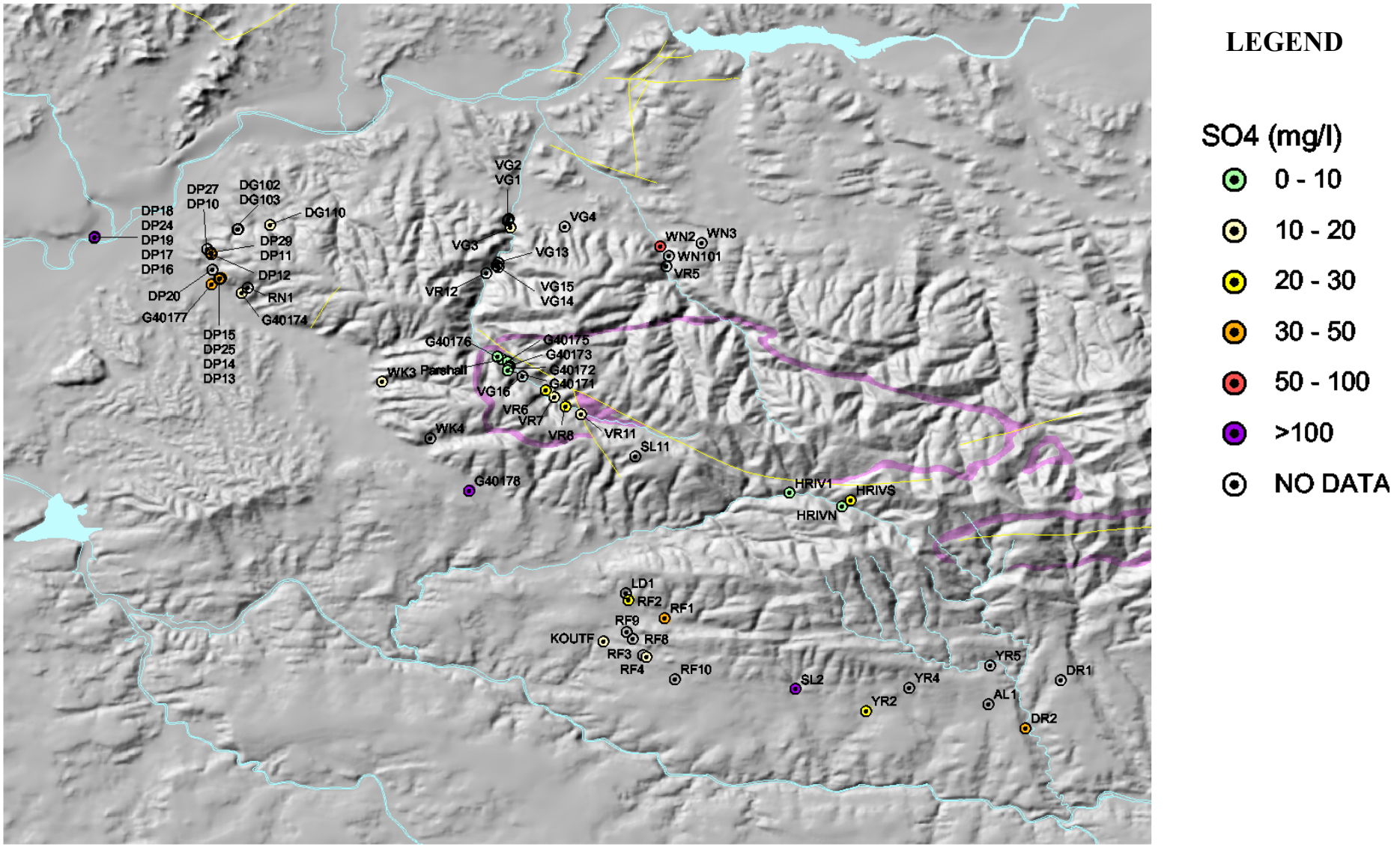

FIGURE F-9: SPATIAL VARIATION OF SILICON IN GROUNDWATER – LITTLE KAROO

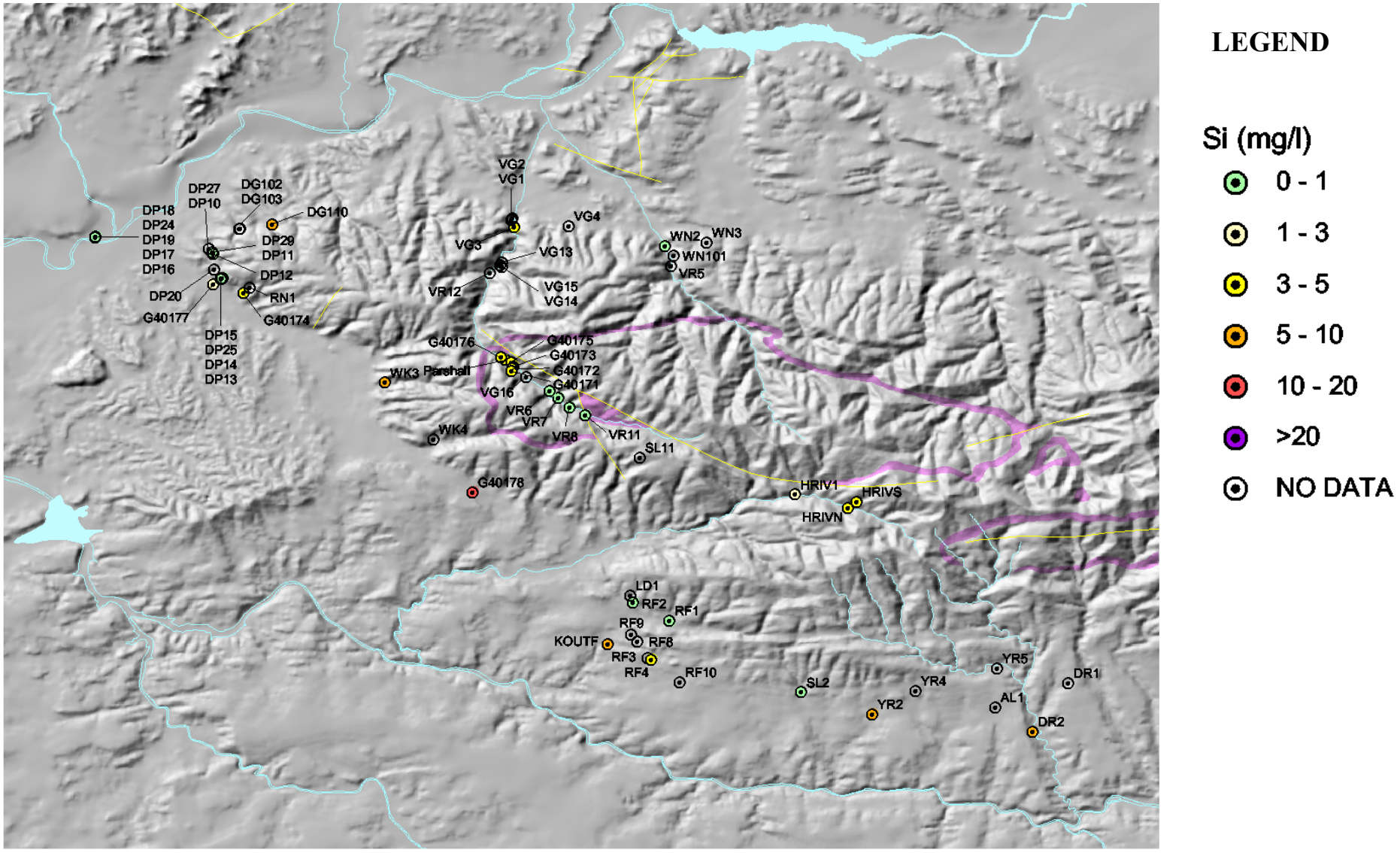

FIGURE F-10: SPATIAL VARIATION OF ELECTRIC CONDUCTIVITY IN GROUNDWATER – LITTLE KAROO

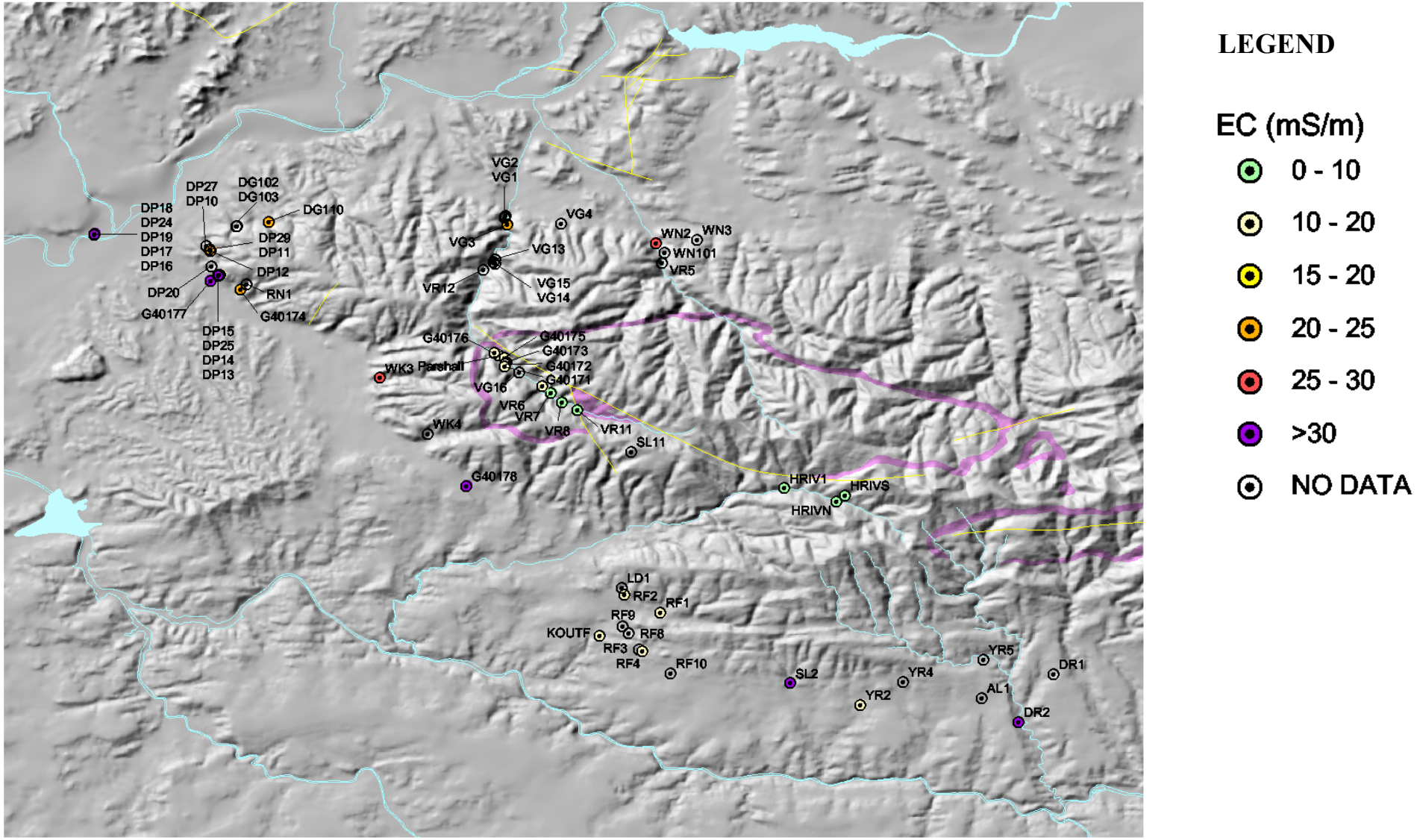

FIGURE F-11: SPATIAL VARIATION OF CHLORIDE IN GROUNDWATER – LITTLE KAROO

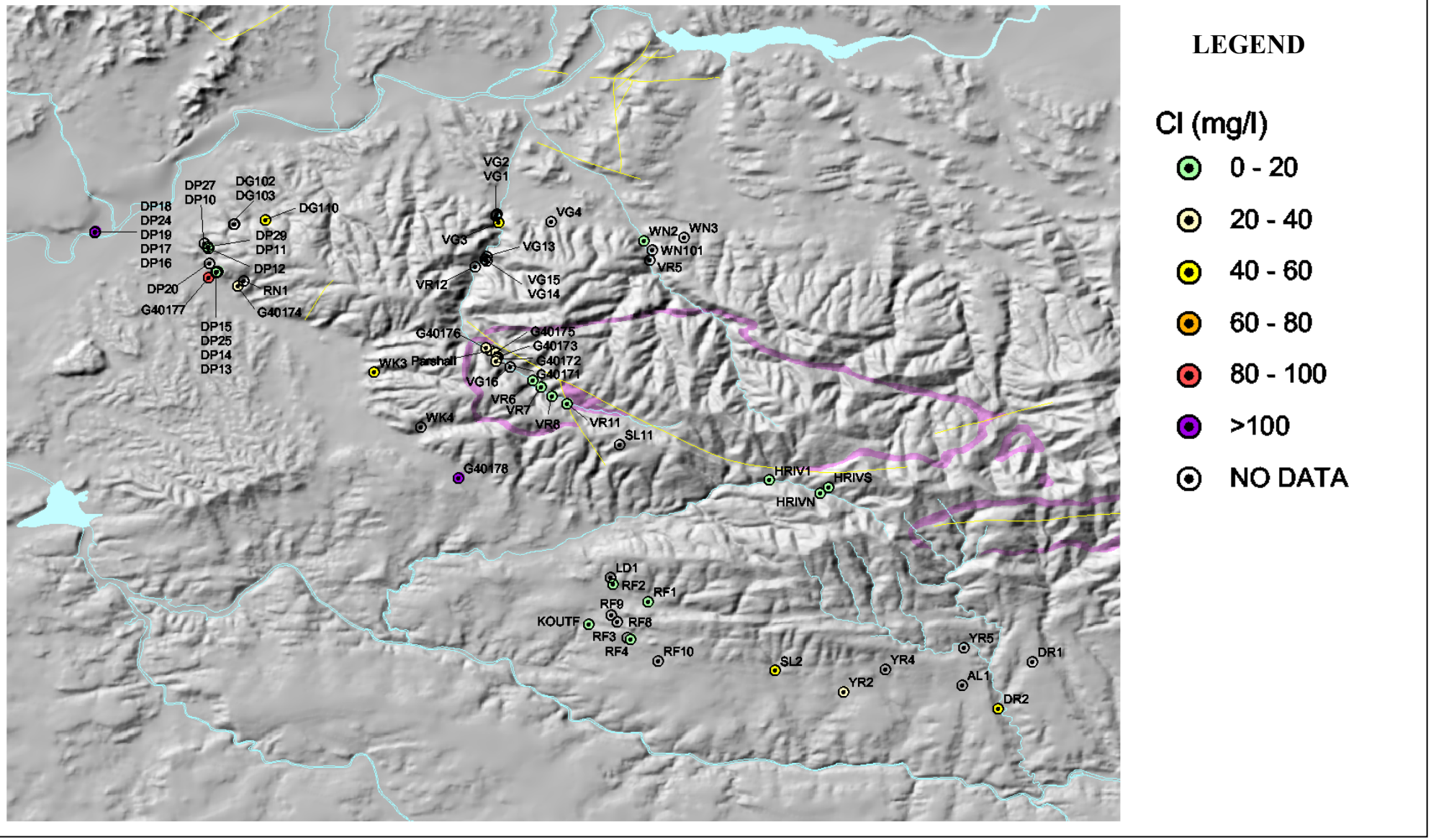

APPENDIX G: X-Y SCATTER PLOTS

FIGURE G-1 : X-Y SCATTERPLOT OF MAJOR IONS Ca AND Mg

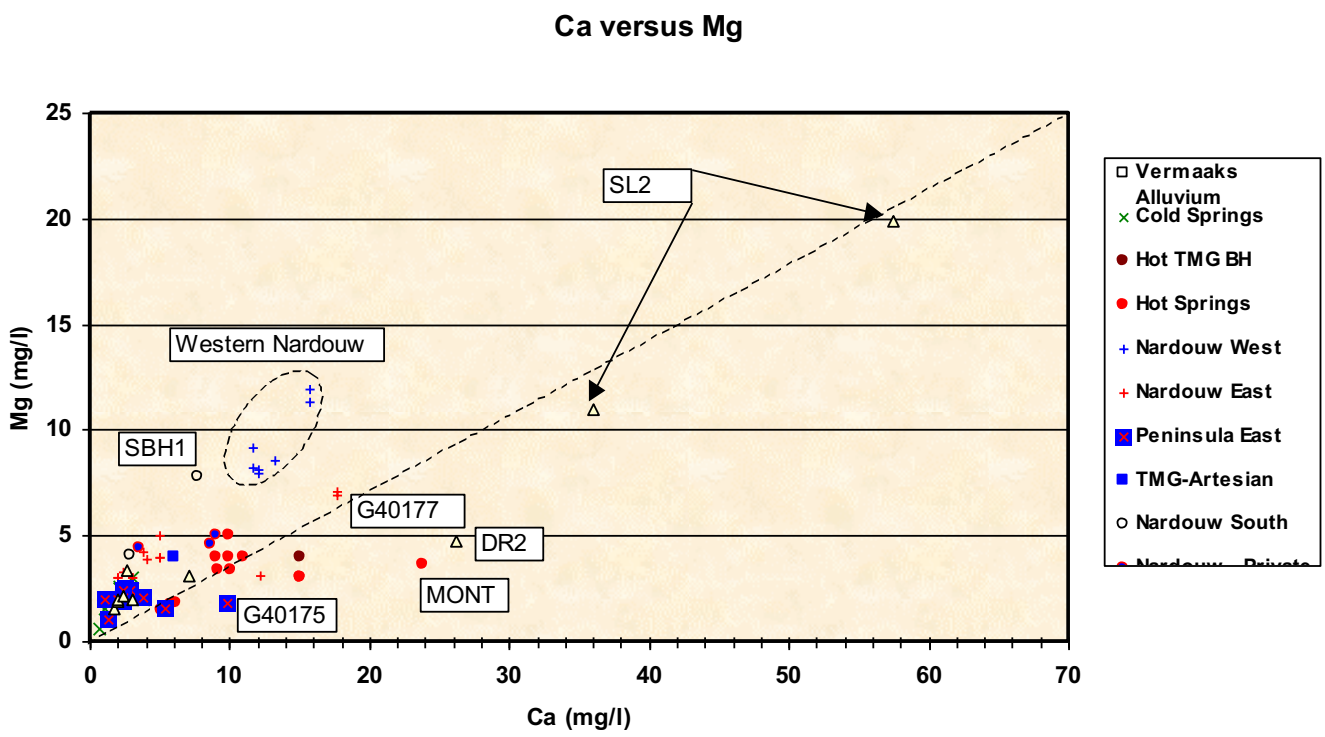

FIGURE G-2 : X-Y PLOT OF MAJOR IONS Ca AND Na + K

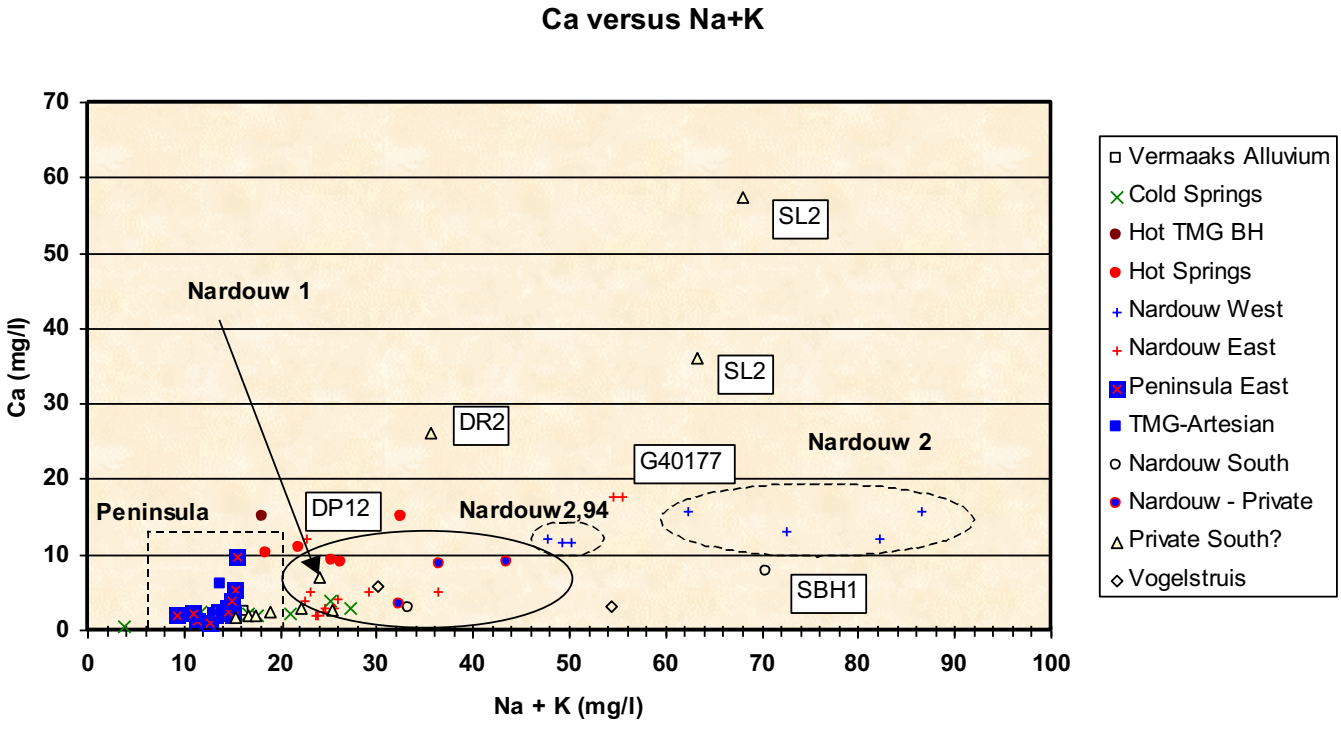

FIGURE G-3 : X-Y SCATTERPLOT OF MAJOR IONS Na AND Cl

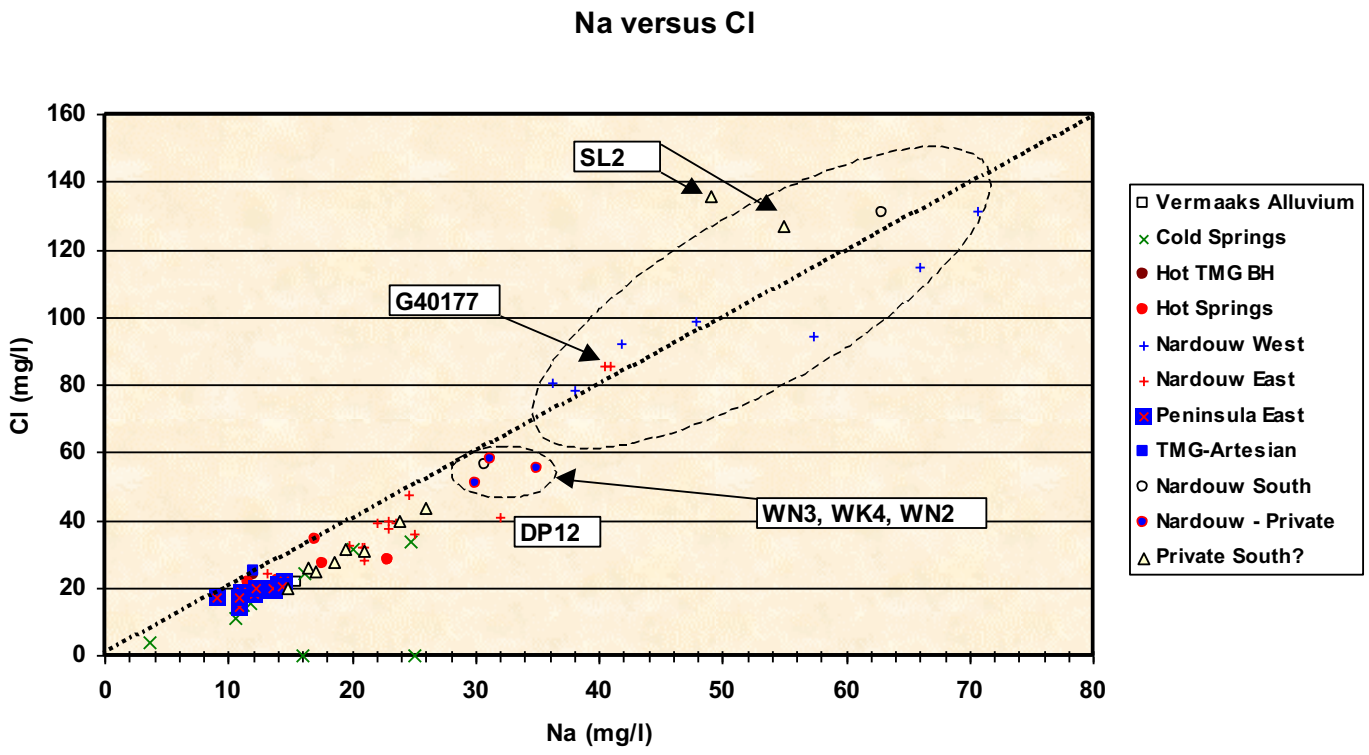

FIGURE G-4 : X-Y PLOT OF MAJOR IONS Ca AND HCO3 + SO4

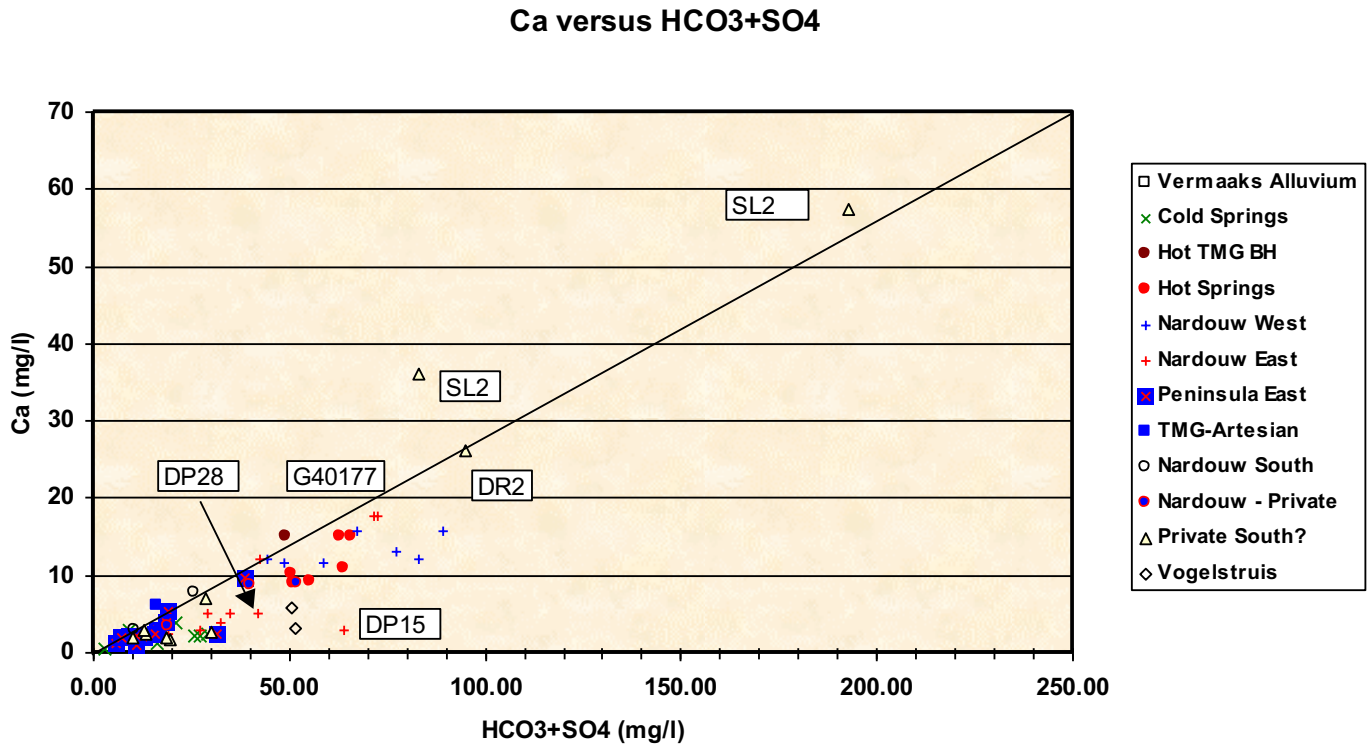

FIGURE G-5 : X-Y SCATTERPLOT OF MAJOR IONS Na AND Ca +Mg

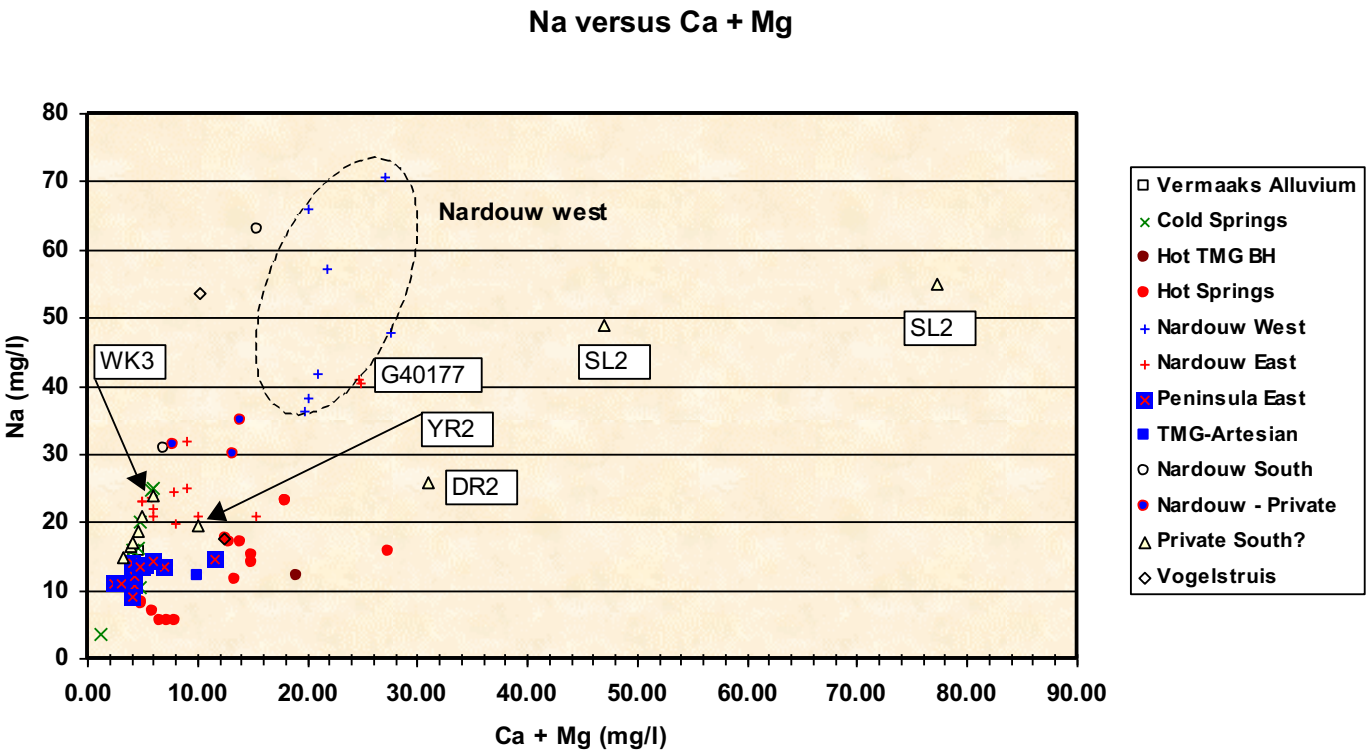

FIGURE G-6 : X-Y PLOT OF MAJOR IONS HCO3 AND Cl

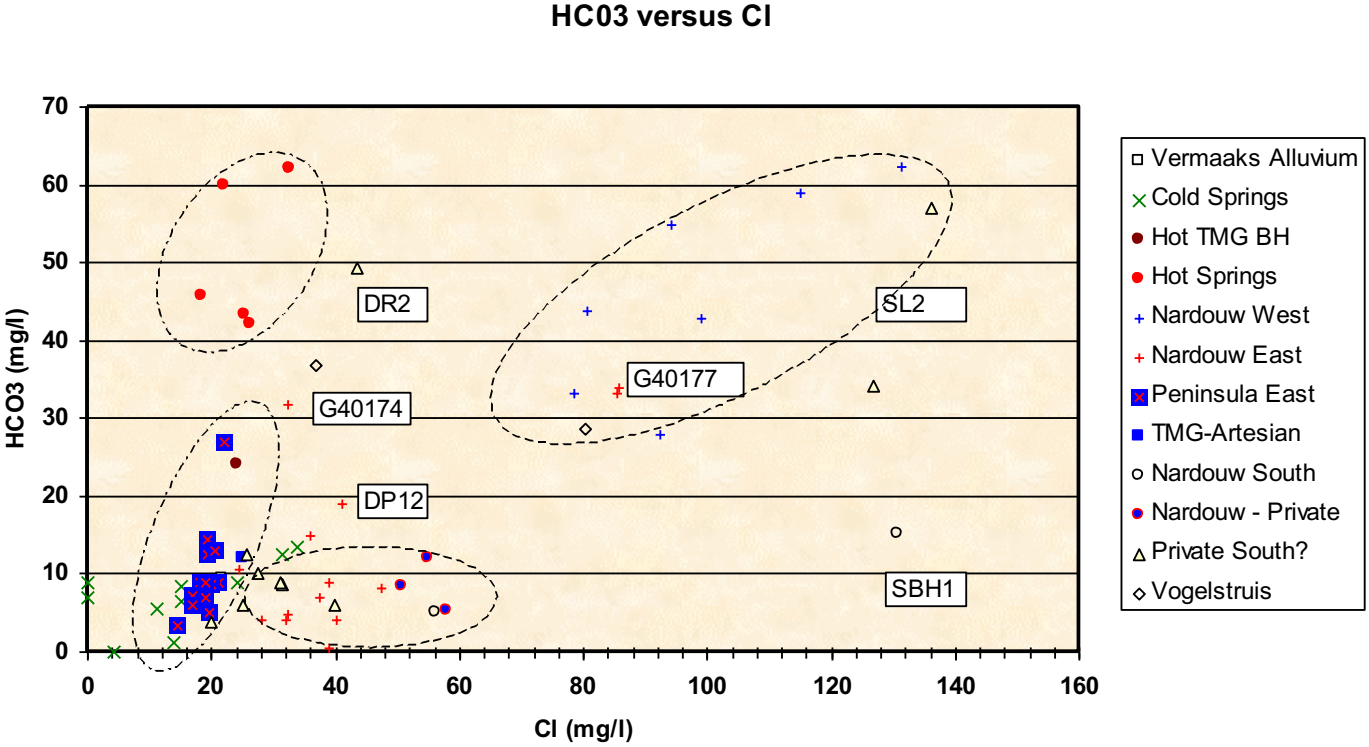

FIGURE G-7 : X-Y SCATTERPLOT OF MAJOR IONS Ca AND Mg

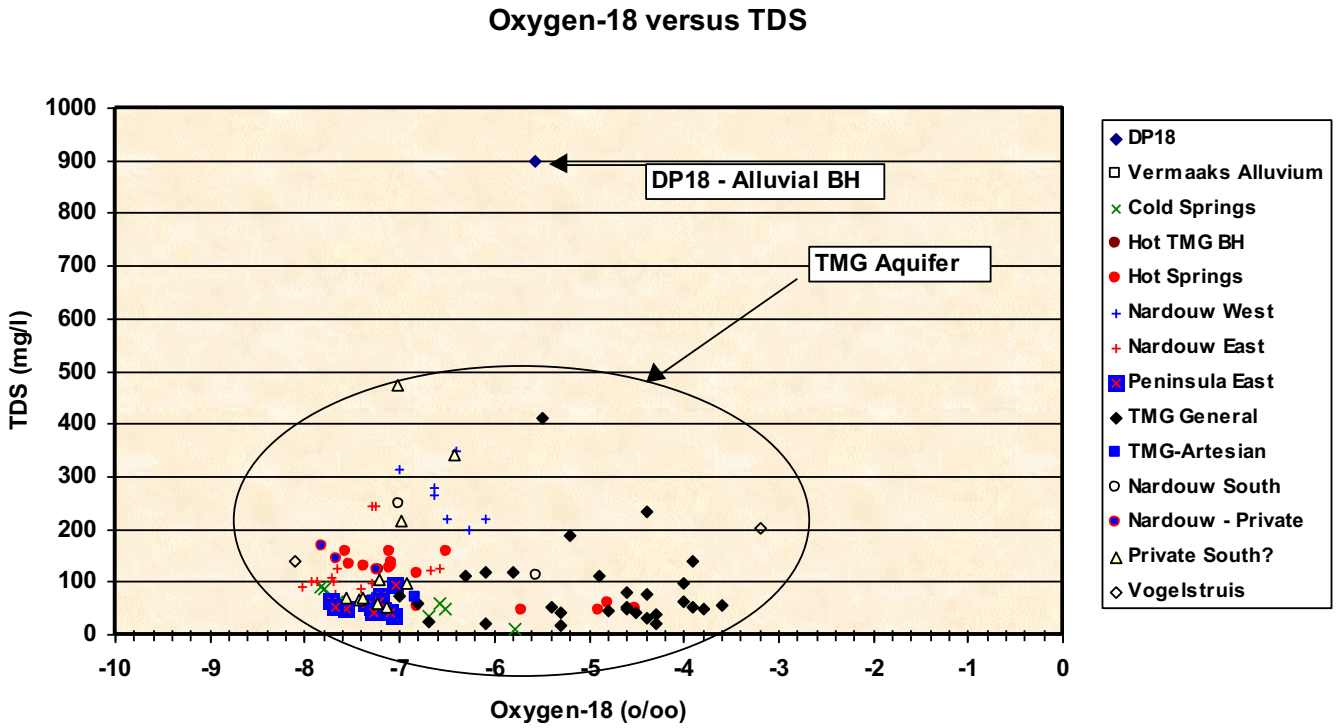

FIGURE G-8 : X-Y PLOT OF MAJOR IONS O-18 AND TDS

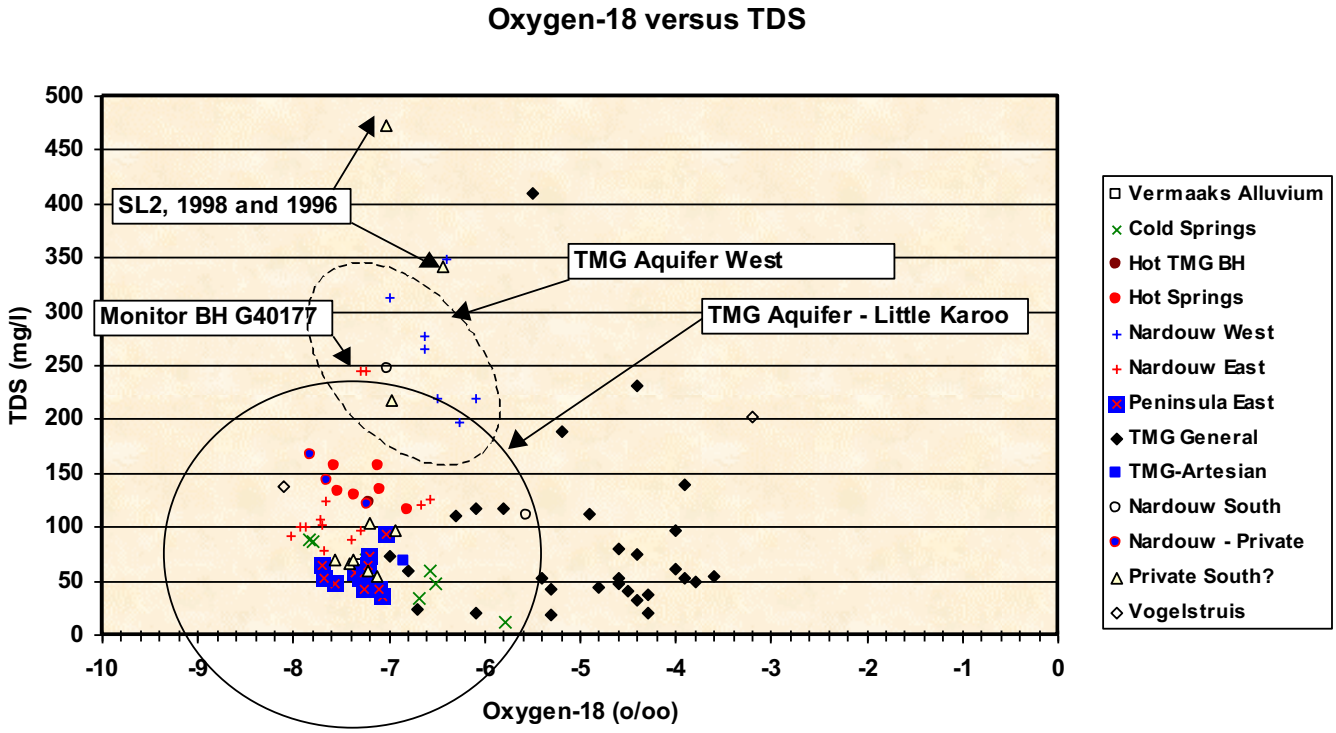

FIGURE G-9 : X-Y SCATTERPLOT OF MAJOR IONS Ca AND Mg

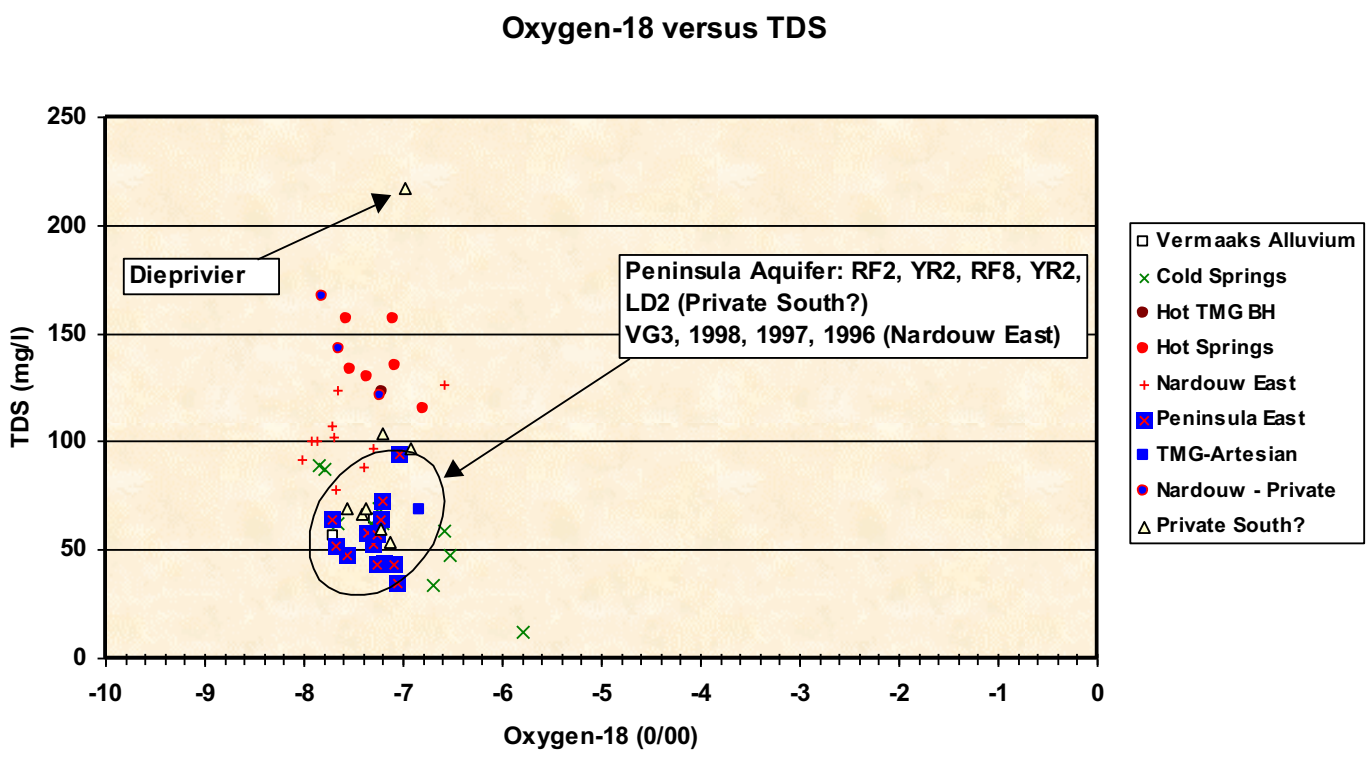

FIGURE G-10 : X-Y SCATTER PLOT O-18 VERSUS C-14

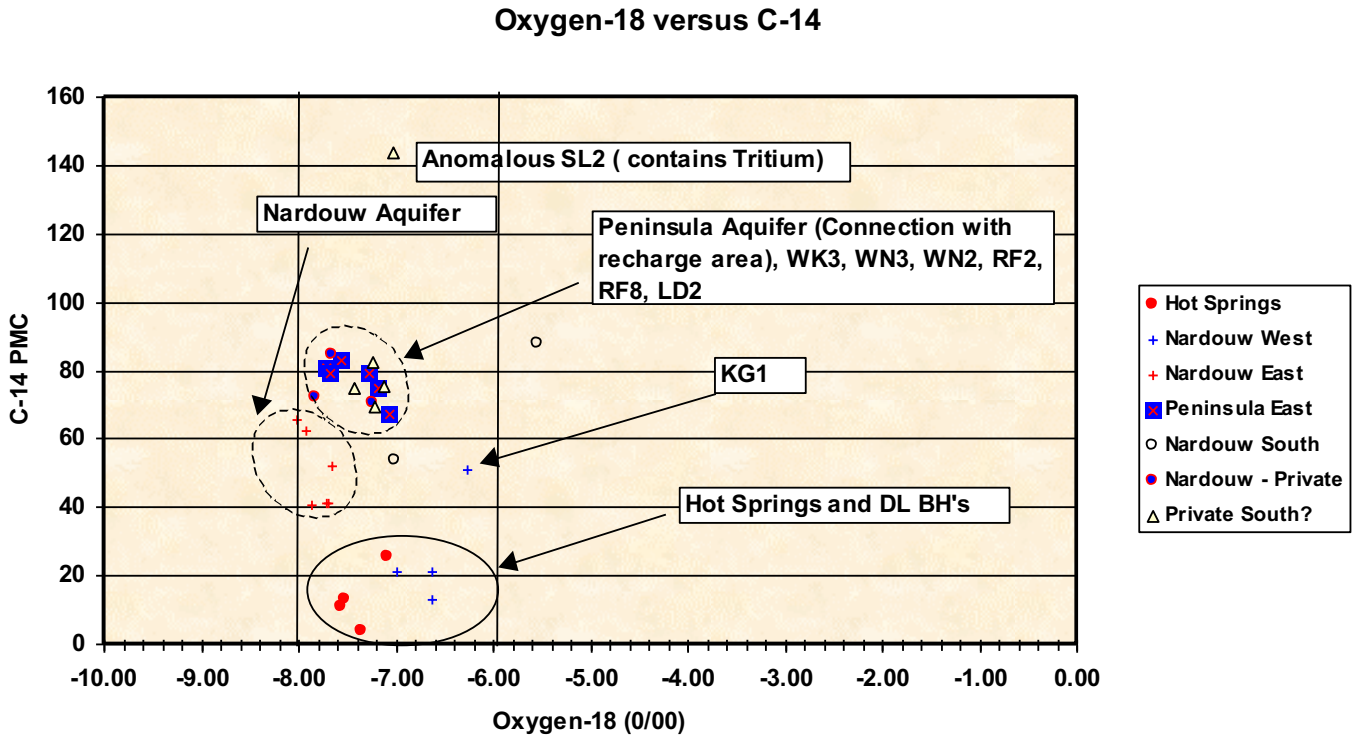

FIGURE G-11 : X-Y PLOT OF MAJOR IONS SiO2 AND F

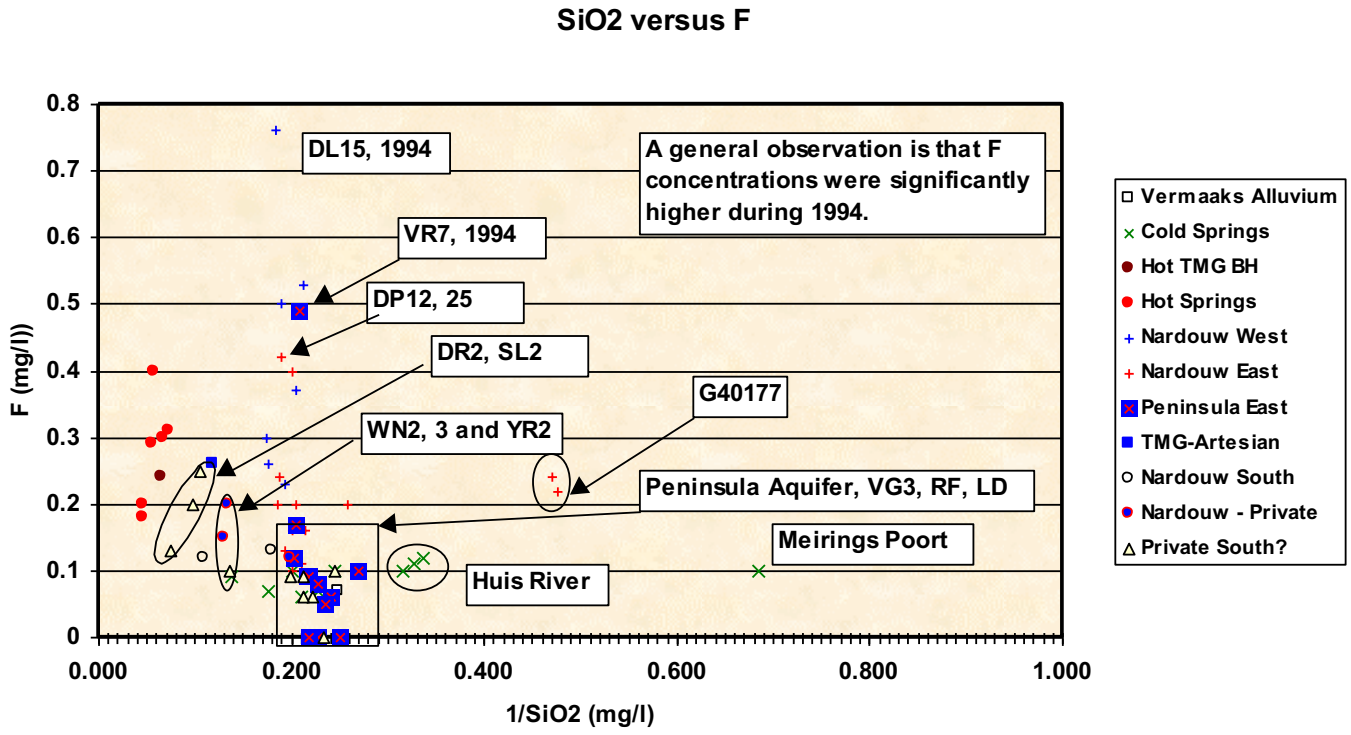

FIGURE G-12 : X-Y PLOT OF MAJOR IONS SiO2 AND K

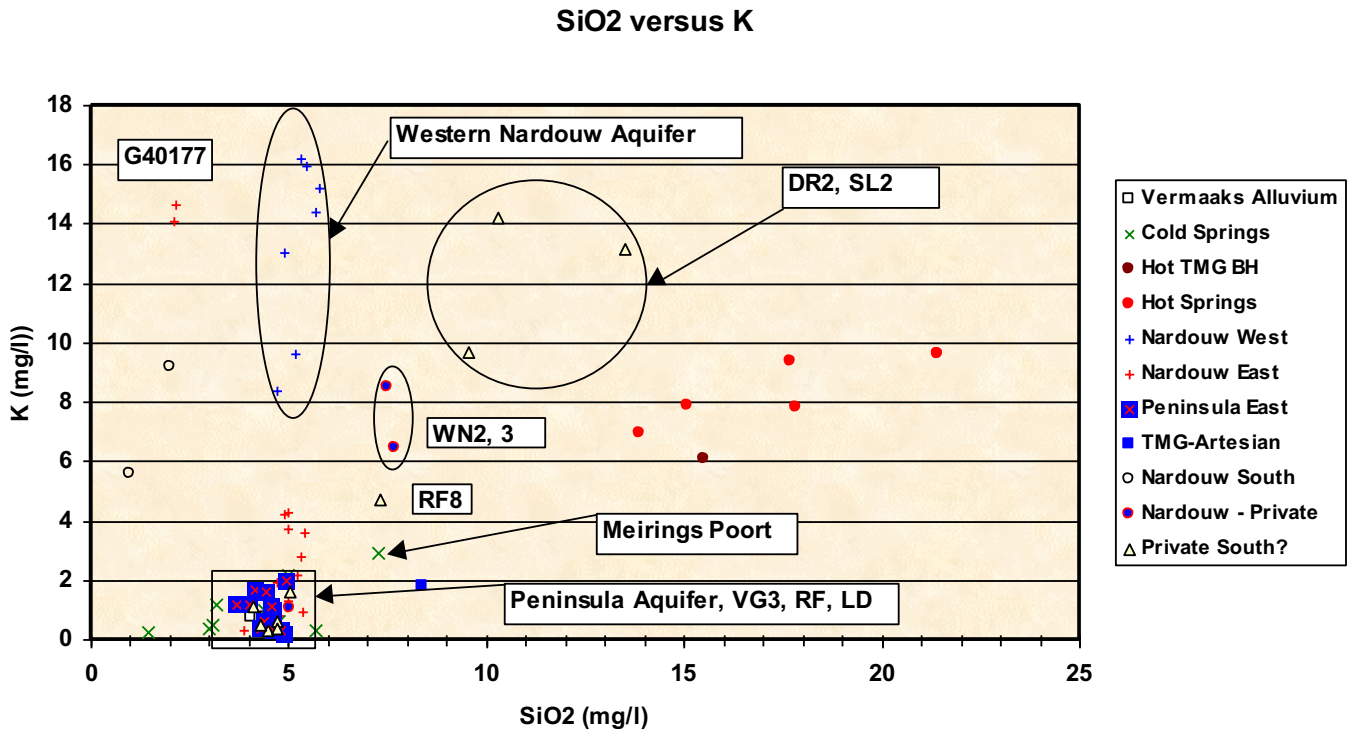

FIGURE G-13 : X-Y PLOT OF MAJOR IONS O18 AND Cl

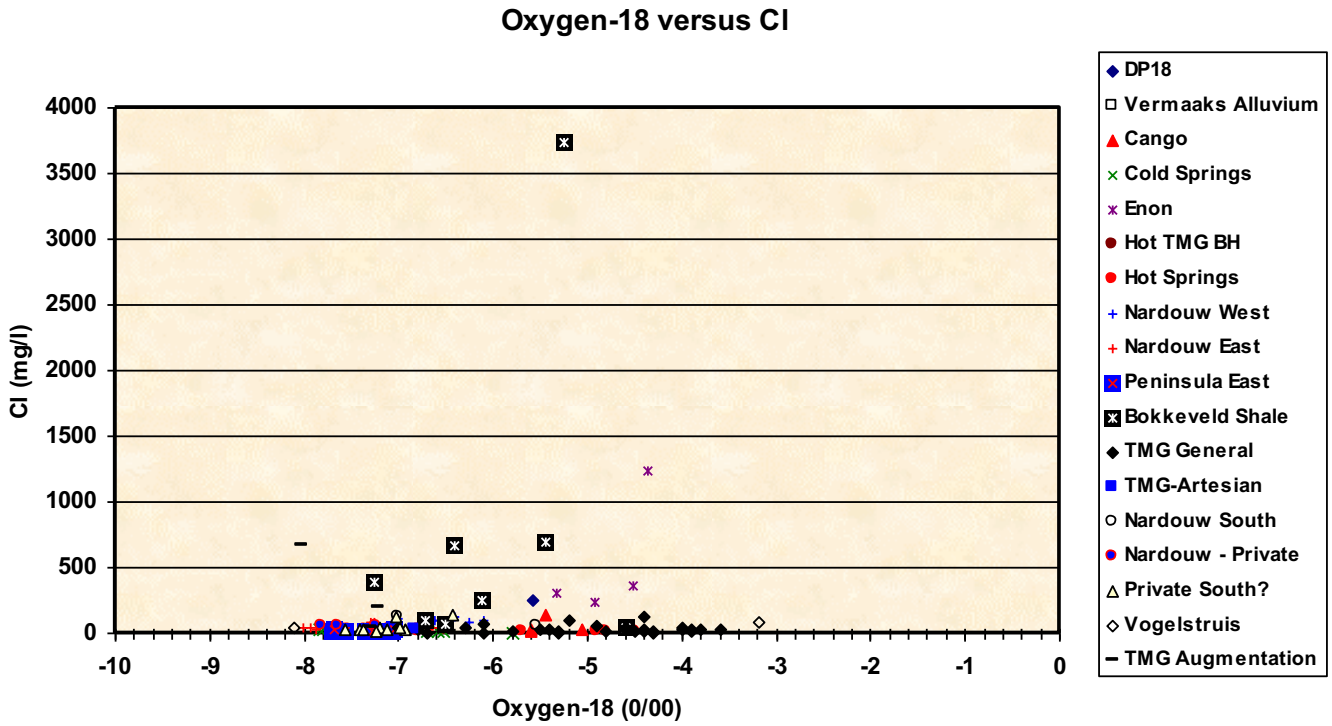

FIGURE G-14 : X-Y PLOT OF MAJOR IONS O18 AND Cl

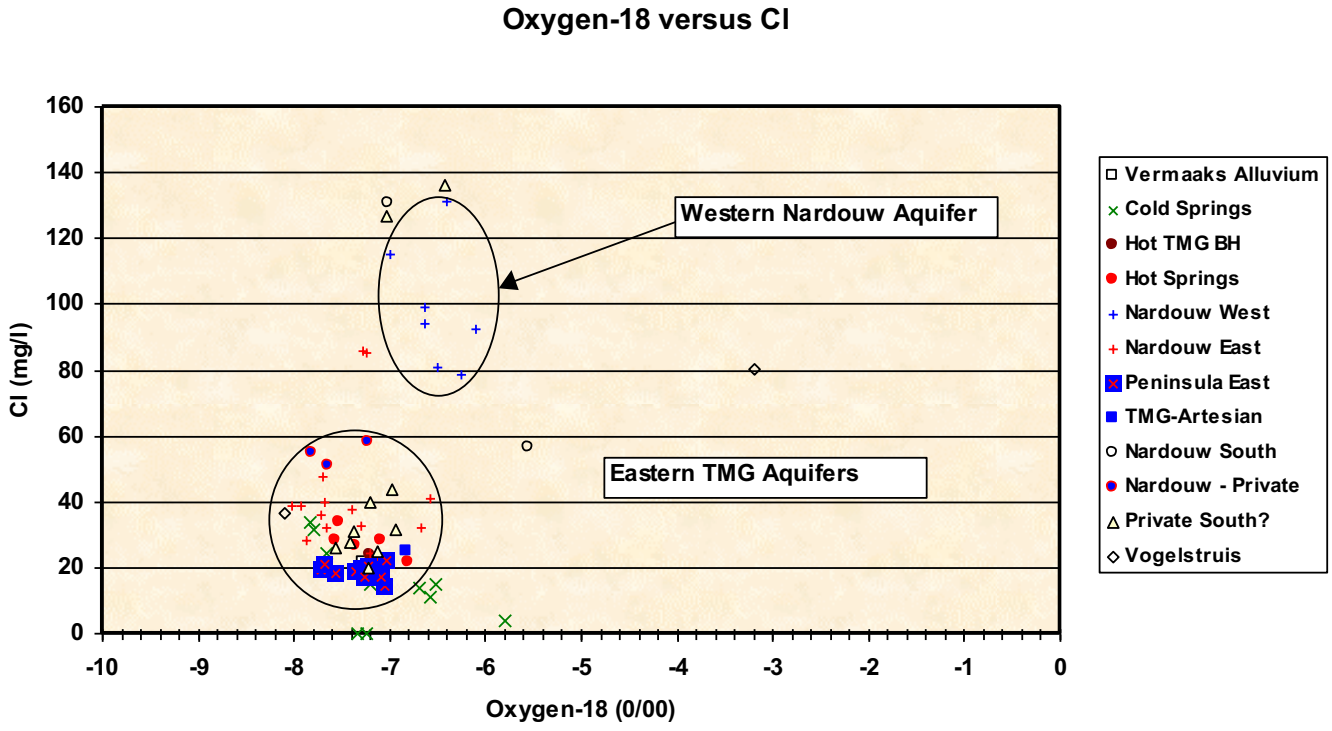

FIGURE G-15 : X-Y PLOT OF MAJOR IONS O-18 AND EC

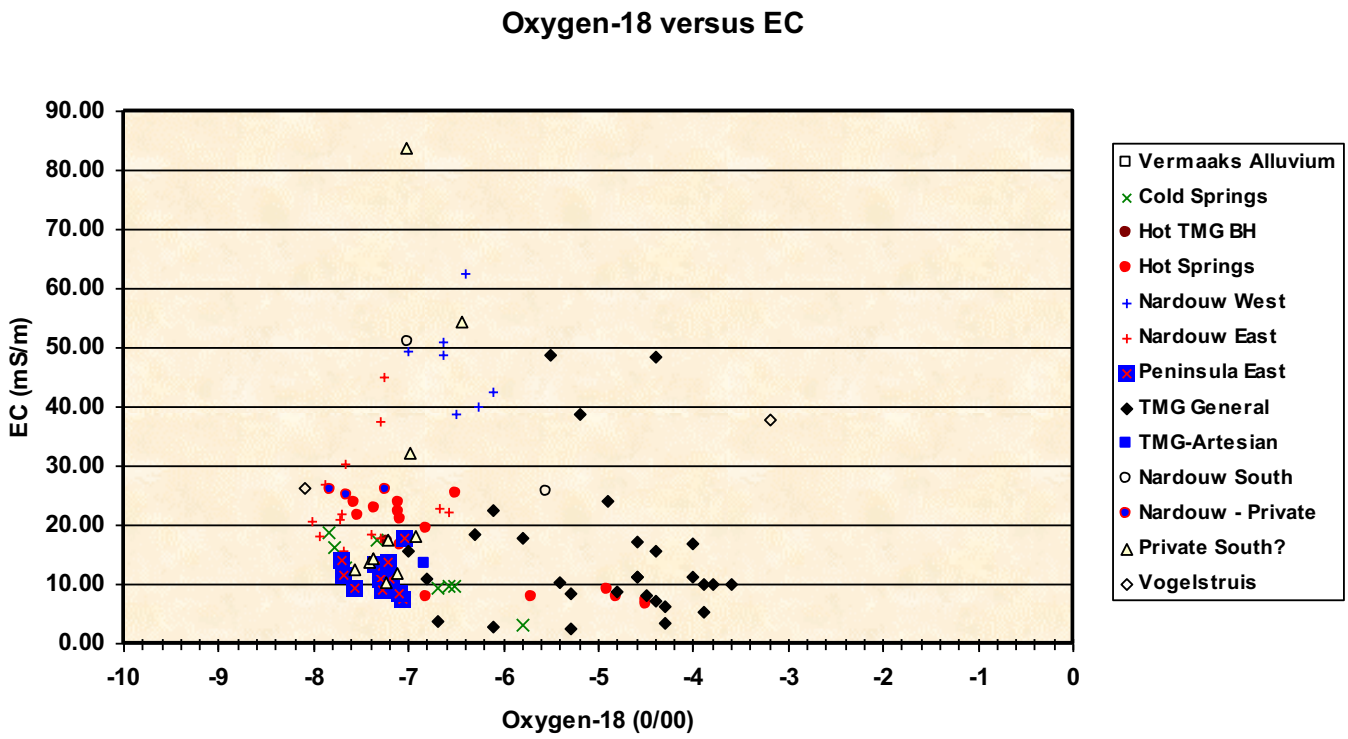

FIGURE G-16 : X-Y PLOT OF MAJOR IONS O-18 AND EC

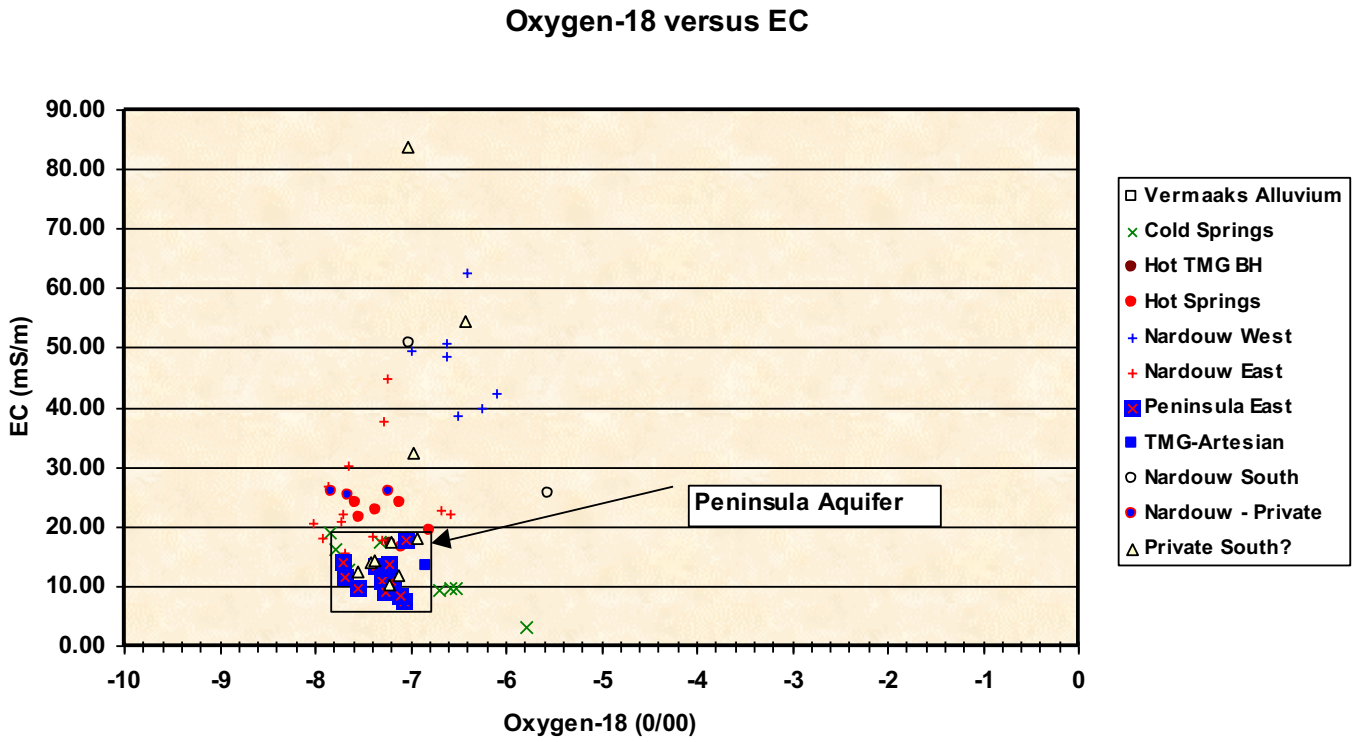

FIGURE G-17 : X-Y PLOT OF MAJOR IONS F AND K

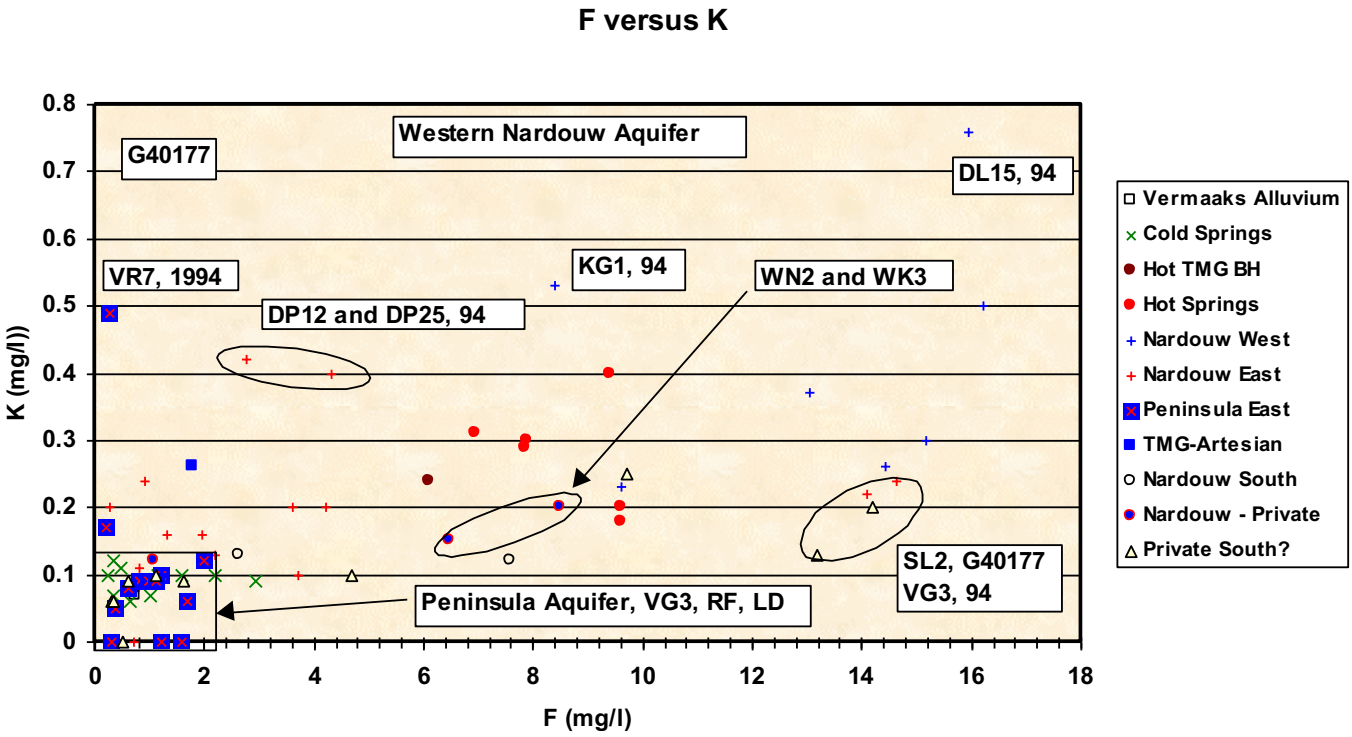

FIGURE G-18: X-Y PLOT OF MAJOR IONS F AND K

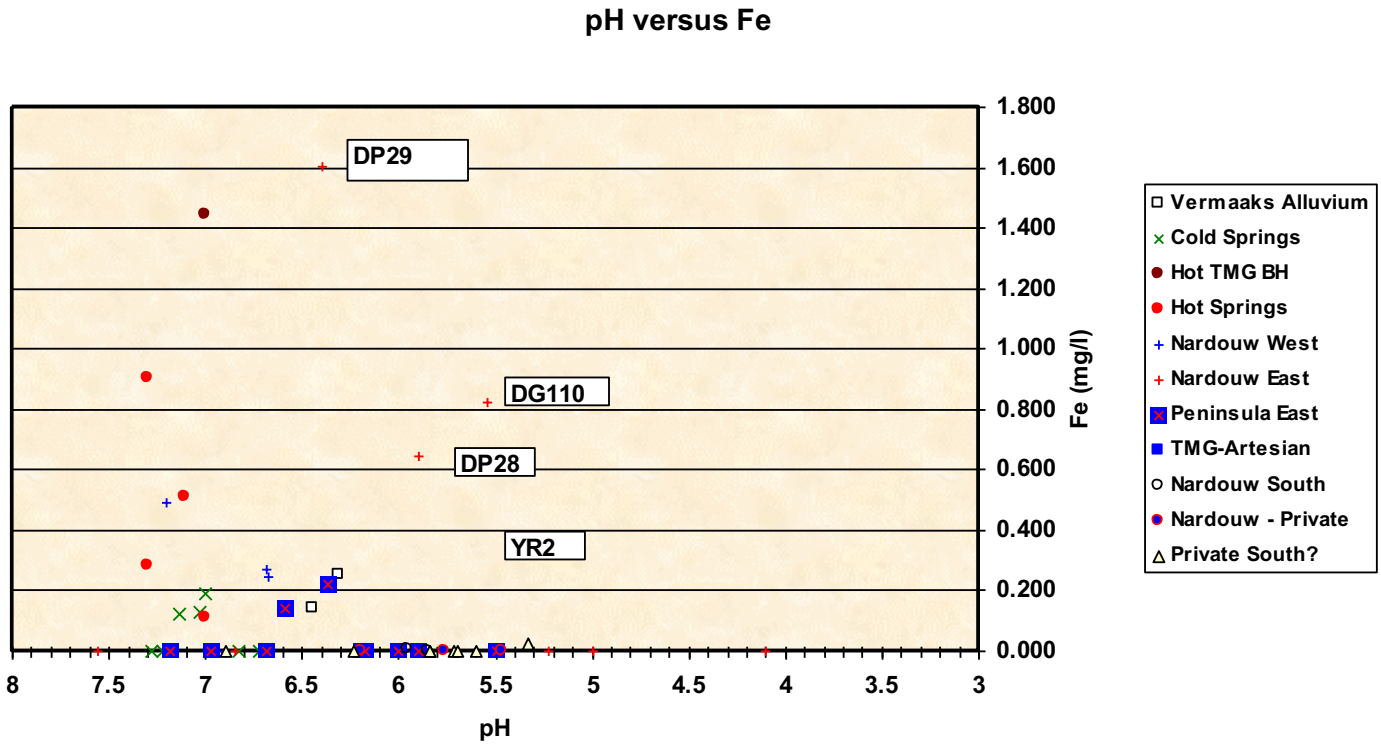

FIGURE G-19 : X-Y PLOT OF MAJOR IONS O18 AND Na/Ca Ratio

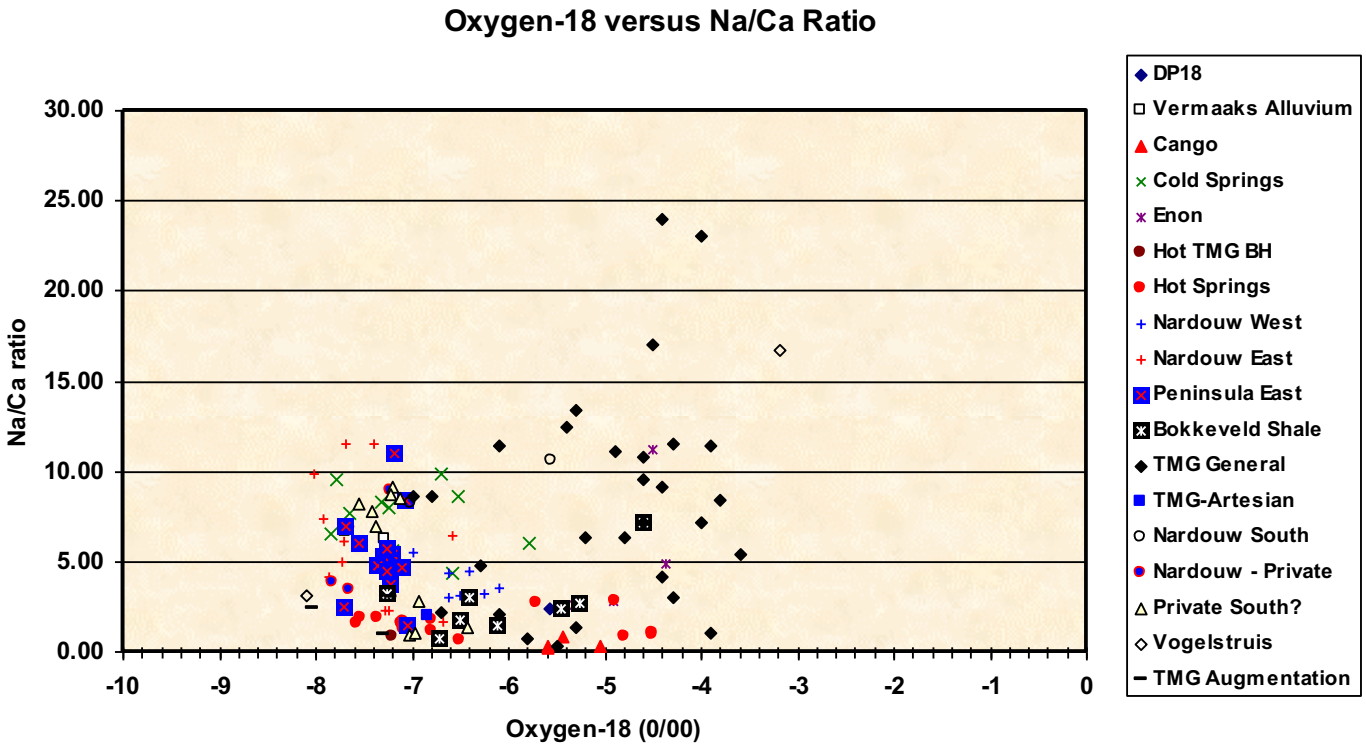

FIGURE G-20 : X-Y PLOT OF MAJOR IONS O18 AND Na/Ca Ratio

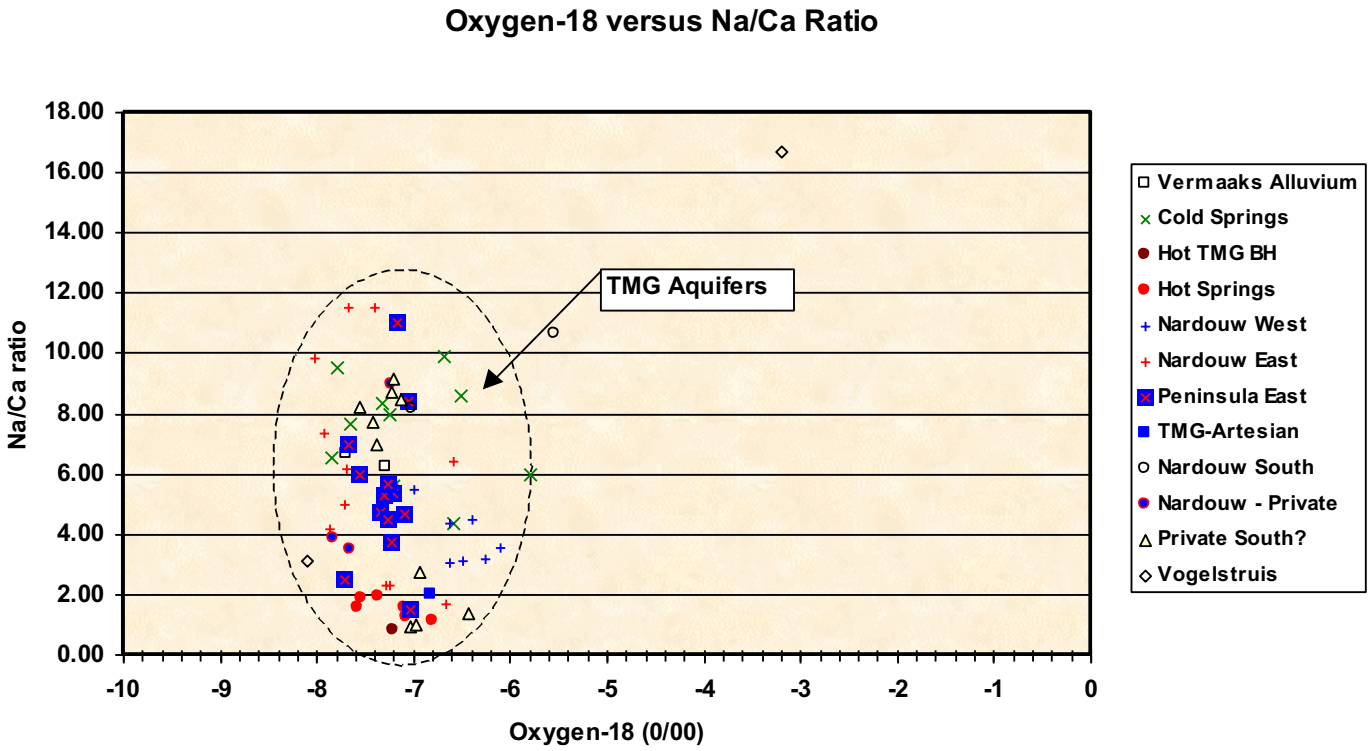

FIGURE G-21 : X-Y PLOT OF MAJOR IONS O18 AND Cl/SO4 Ratio

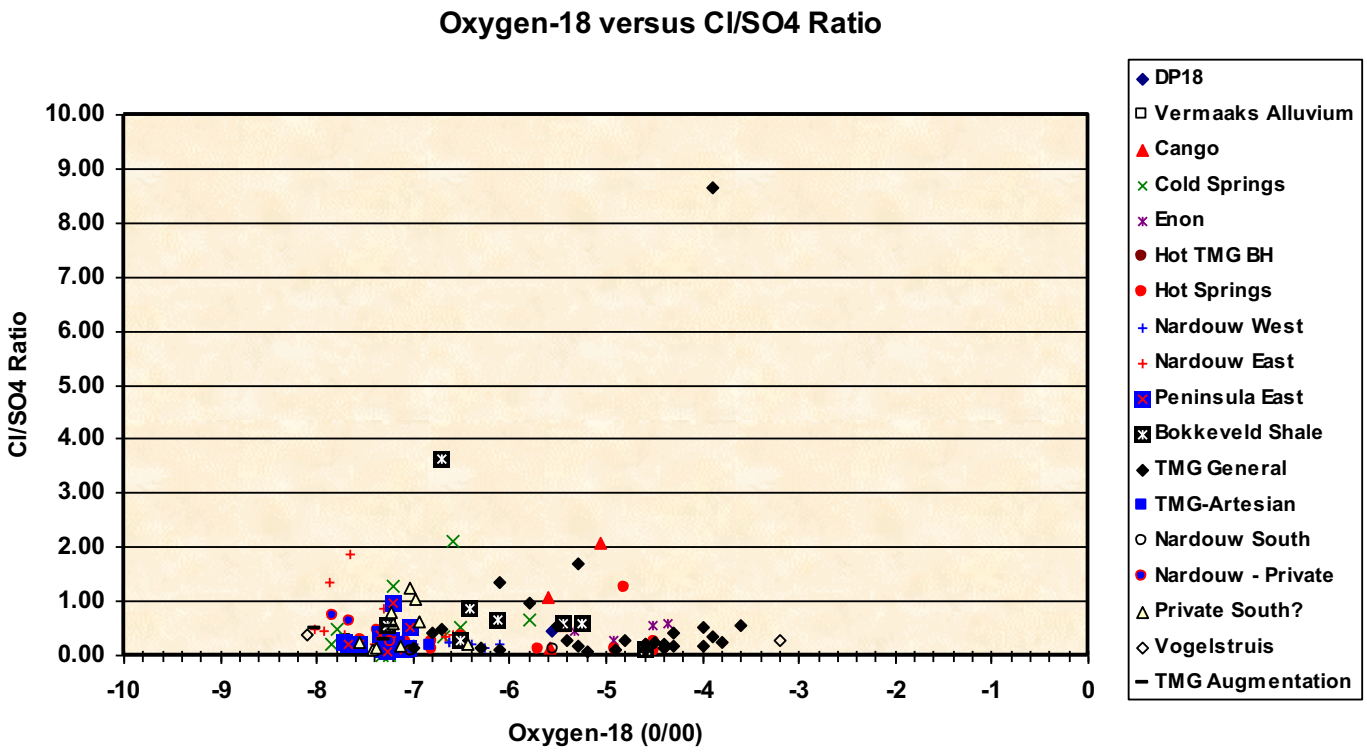

FIGURE G-22 : X-Y PLOT OF MAJOR IONS O18 AND Cl/SO4 Ratio

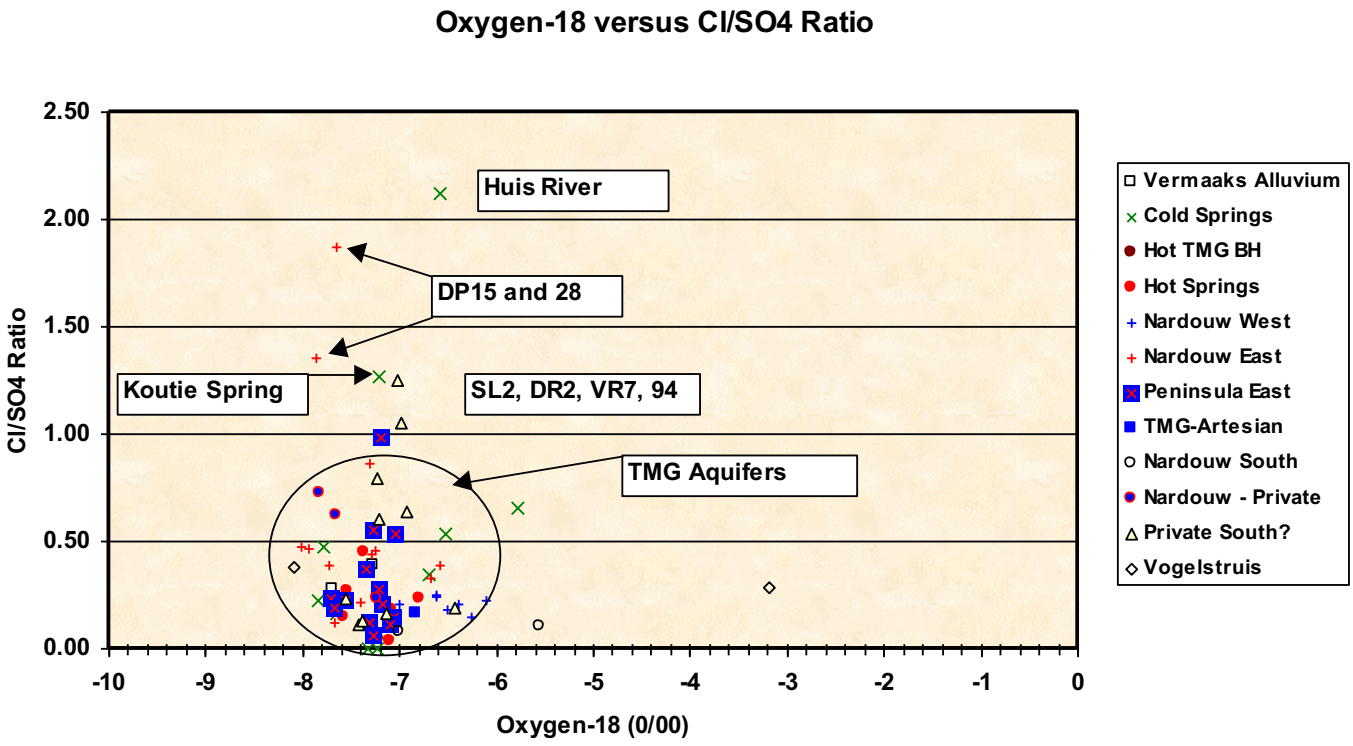

FIGURE G-23 : X-Y PLOT OF MAJOR IONS Na/Ca AND Cl/SO4 Ratio

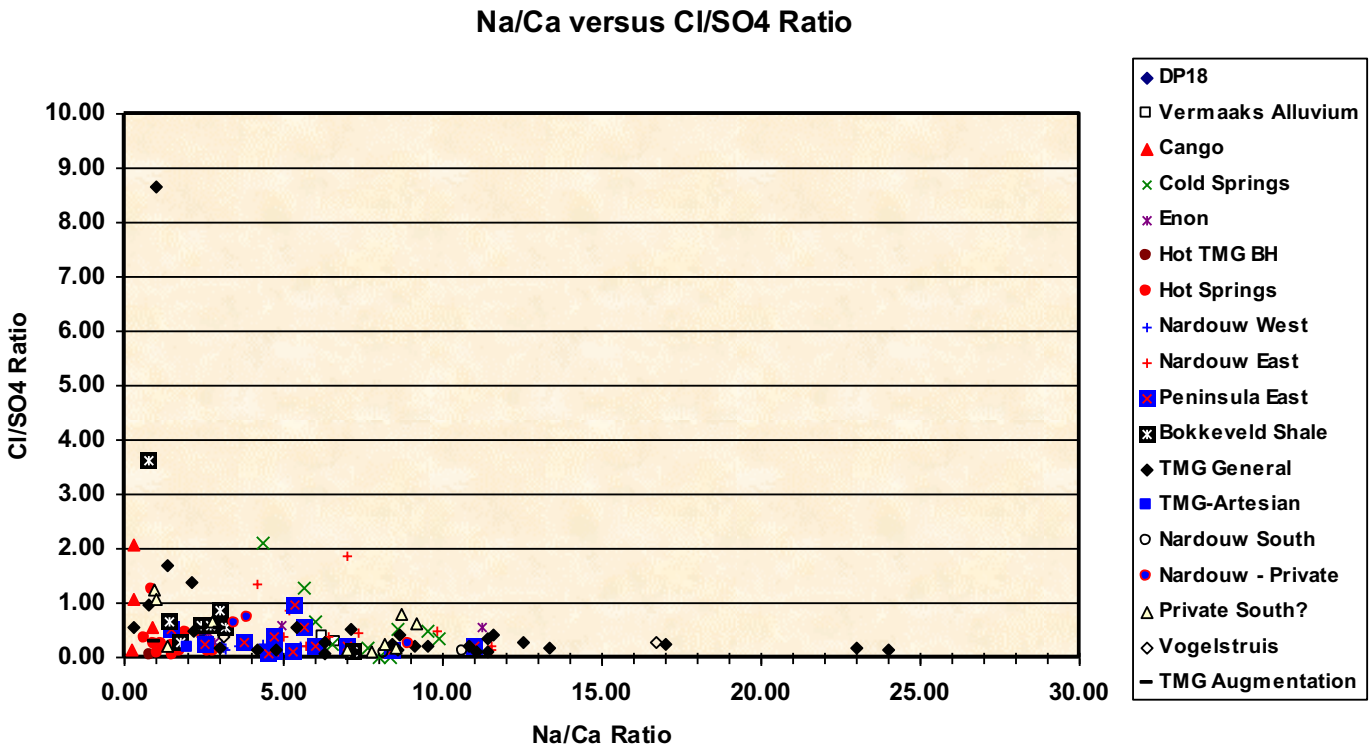

FIGURE G-24 : X-Y PLOT OF MAJOR IONS Na/Ca AND Cl/SO4 Ratio

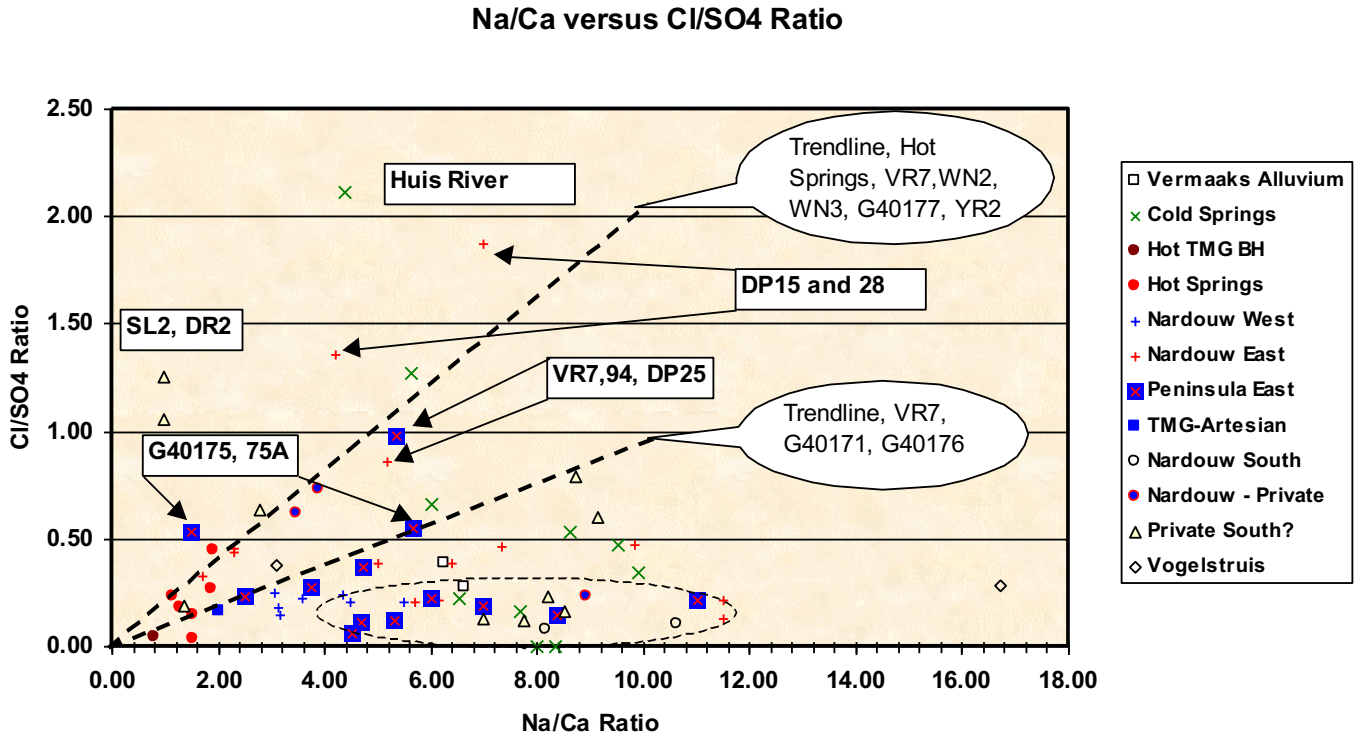

FIGURE G-25 : X-Y PLOT OF MAJOR IONS O-18 AND Si Ratio

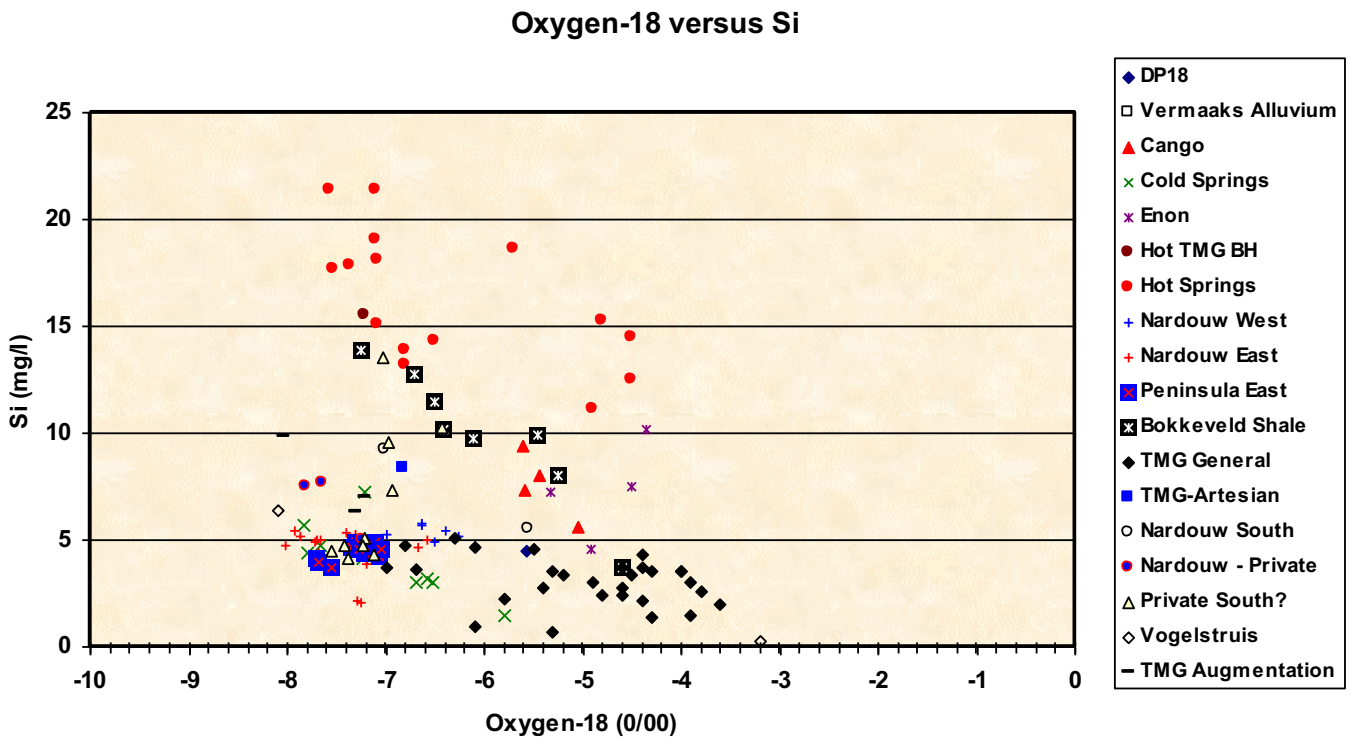

FIGURE G-26 : X-Y PLOT OF MAJOR IONS O-18 AND Si Ratio

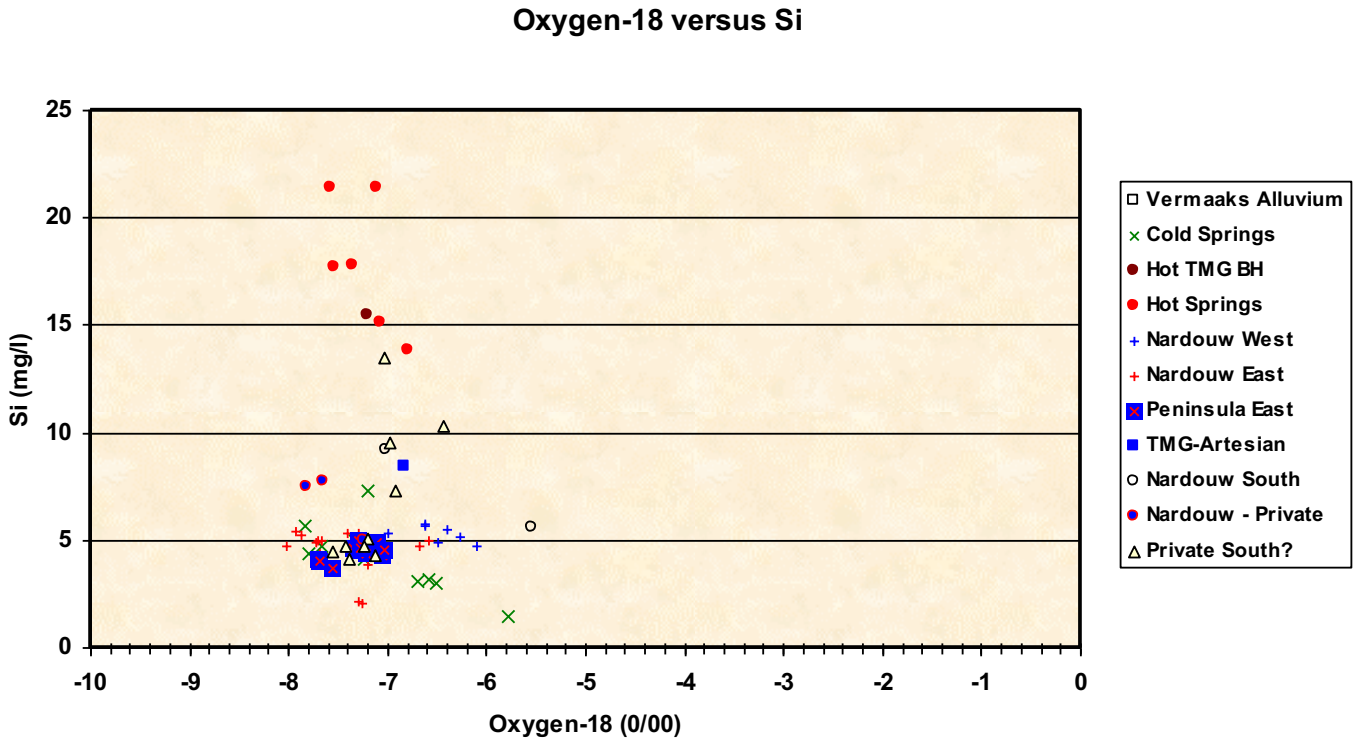

FIGURE G-27 : X-Y PLOT OF MAJOR IONS pH AND Cl/SO4 Ratio

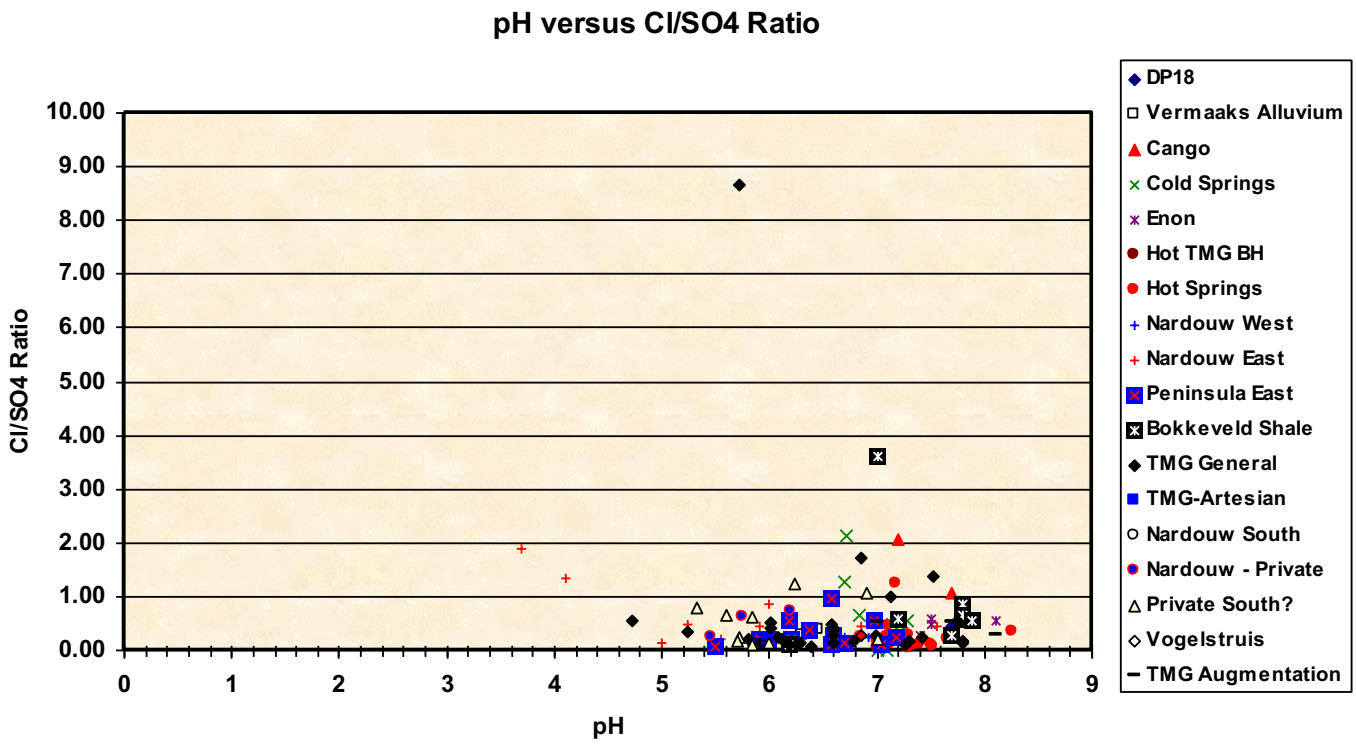

FIGURE G-28 : X-Y PLOT OF MAJOR IONS pH AND Cl/SO4 Ratio

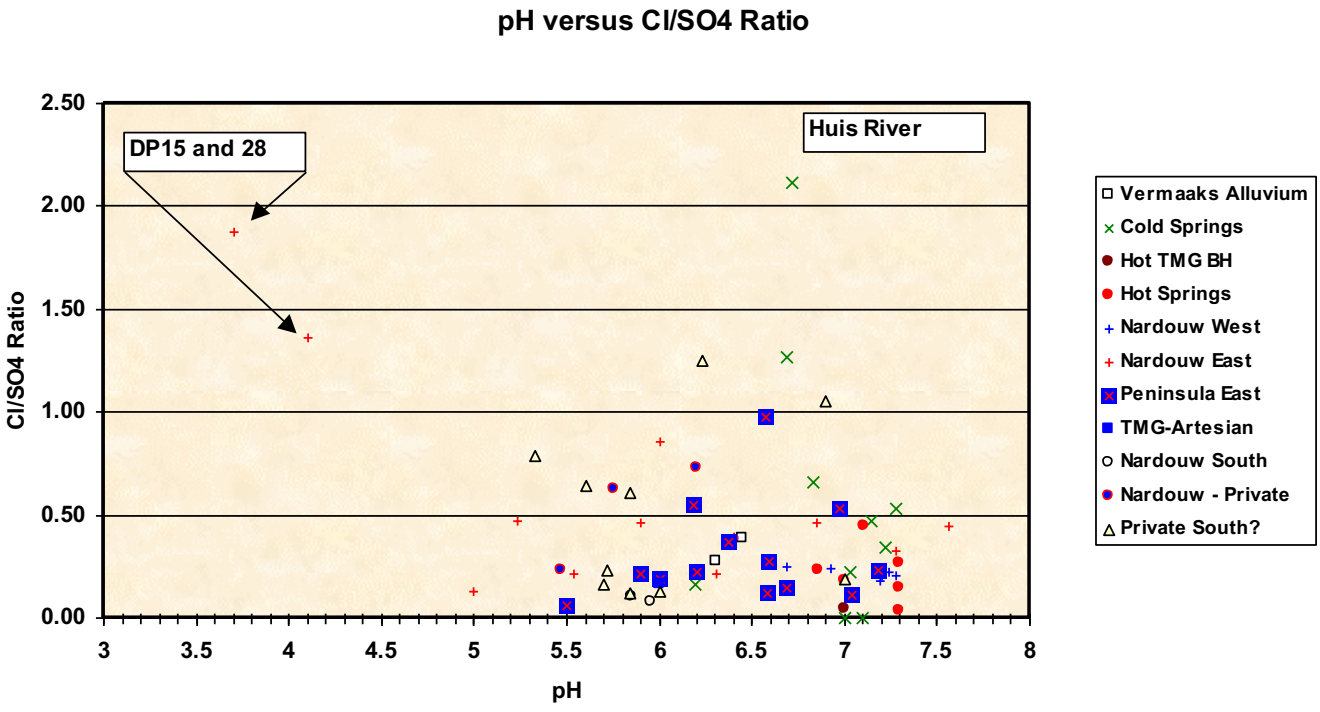

FIGURE G-29 : X-Y PLOT OF MAJOR IONS pH AND Na/Ca Ratio

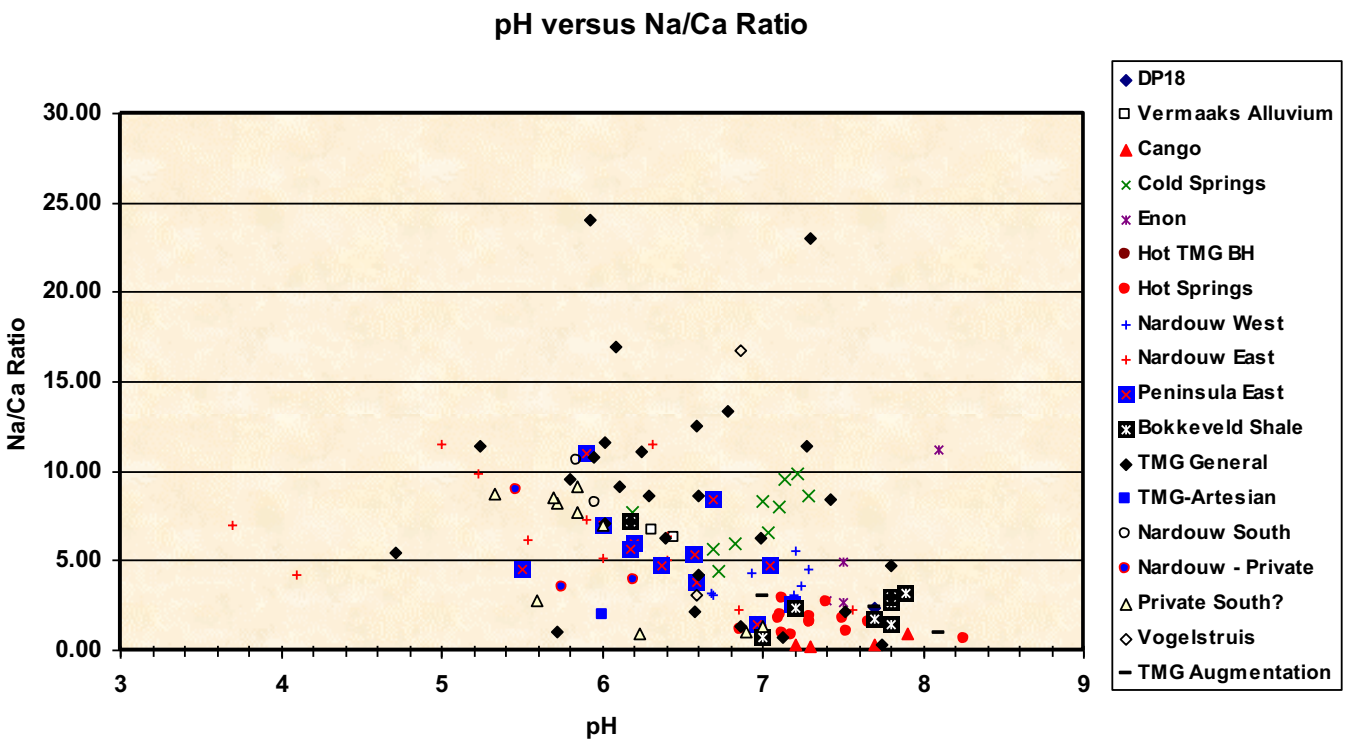

FIGURE G-30: X-Y PLOT OF MAJOR IONS pH AND Na/Ca Ratio

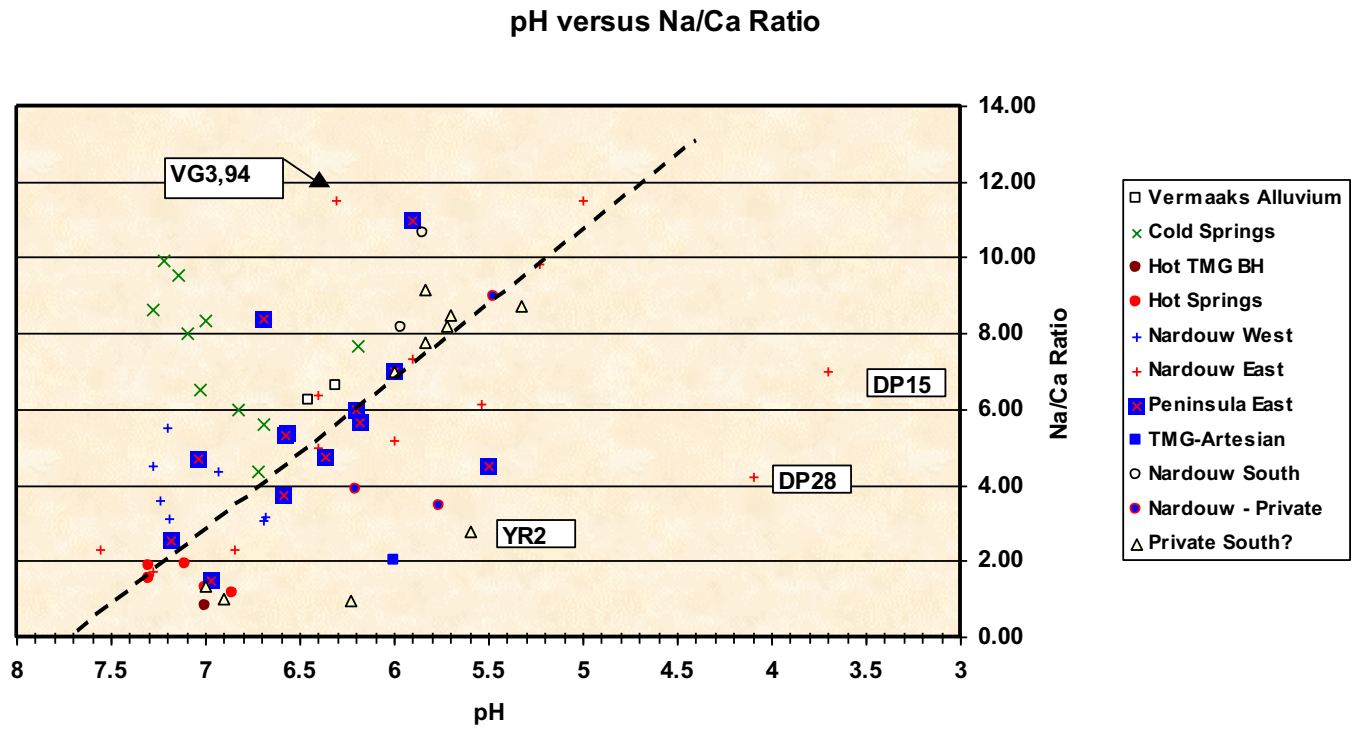

FIGURE G-31 : X-Y PLOT OF MAJOR IONS pH AND Mn

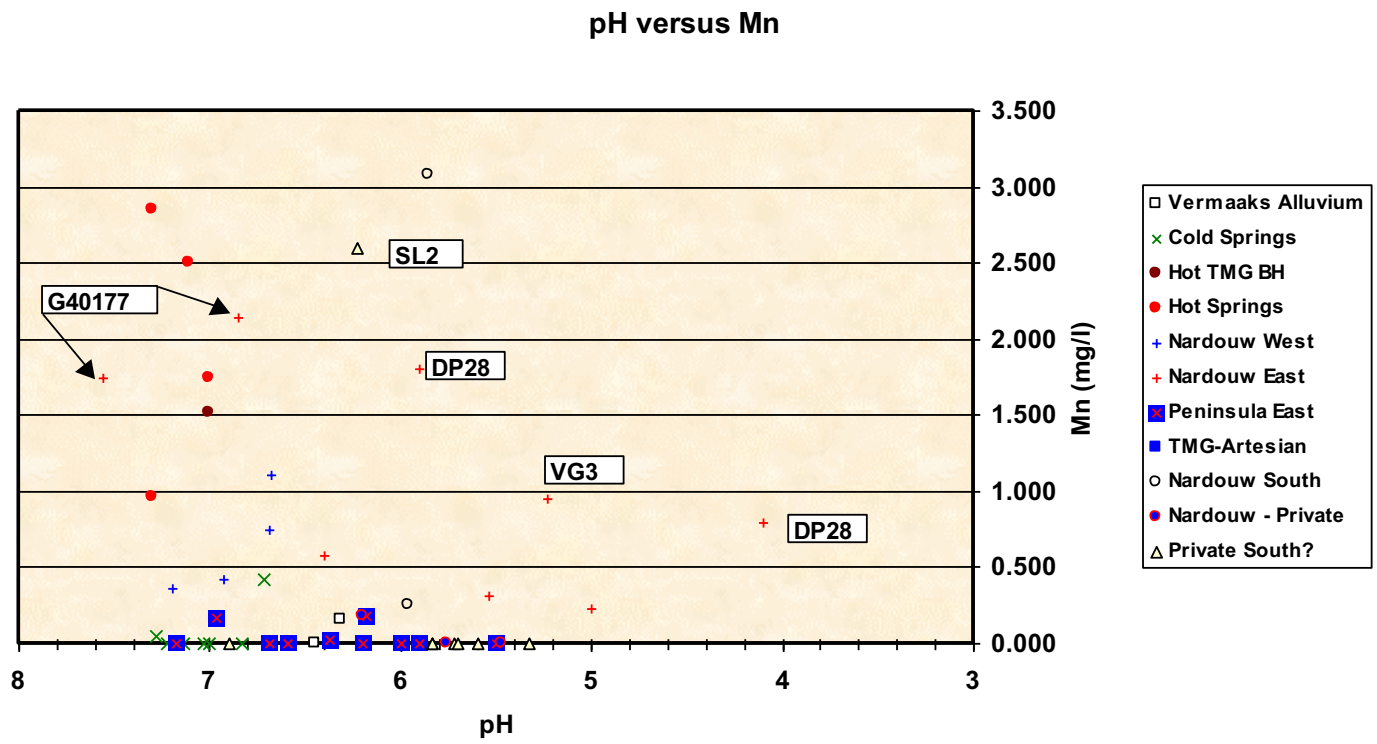

FIGURE G-32: X-Y PLOT OF MAJOR IONS Mg AND Cl

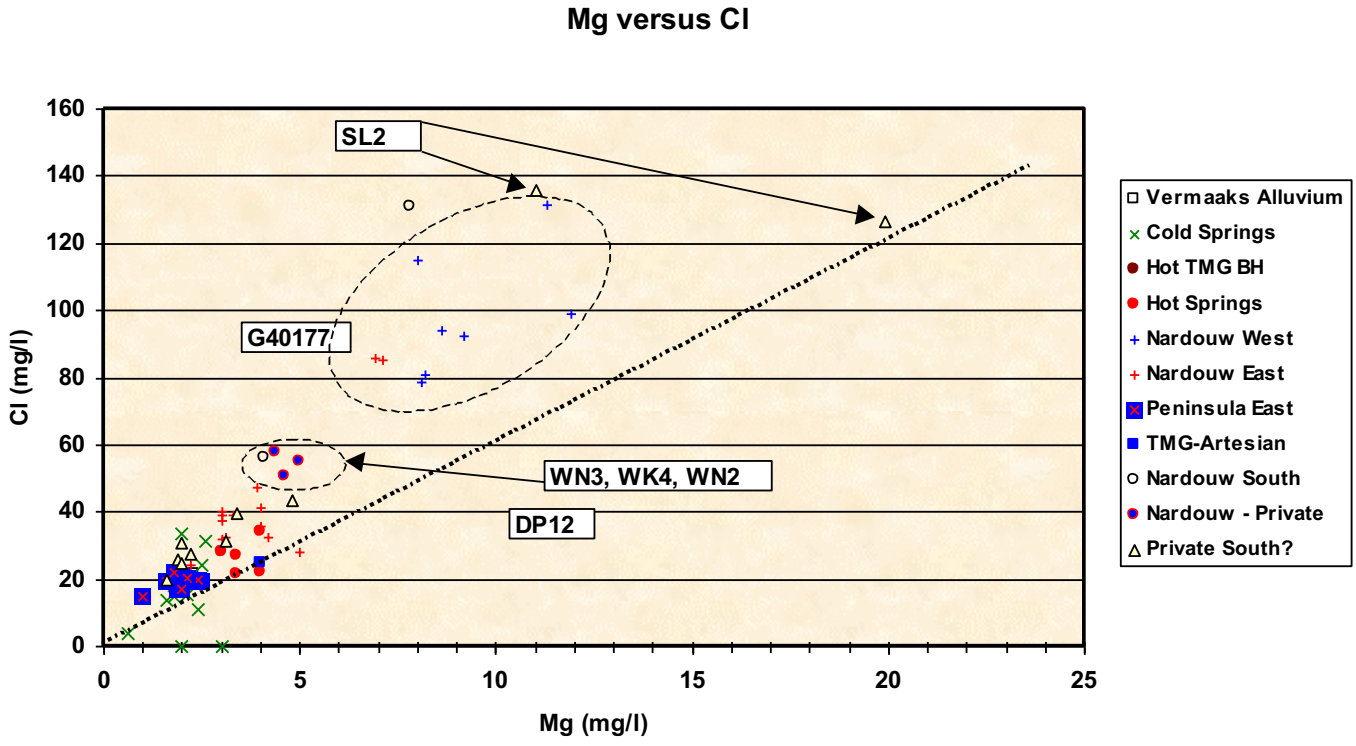

FIGURE G-33 : X-Y PLOT OF MAJOR IONS SO4 AND Cl

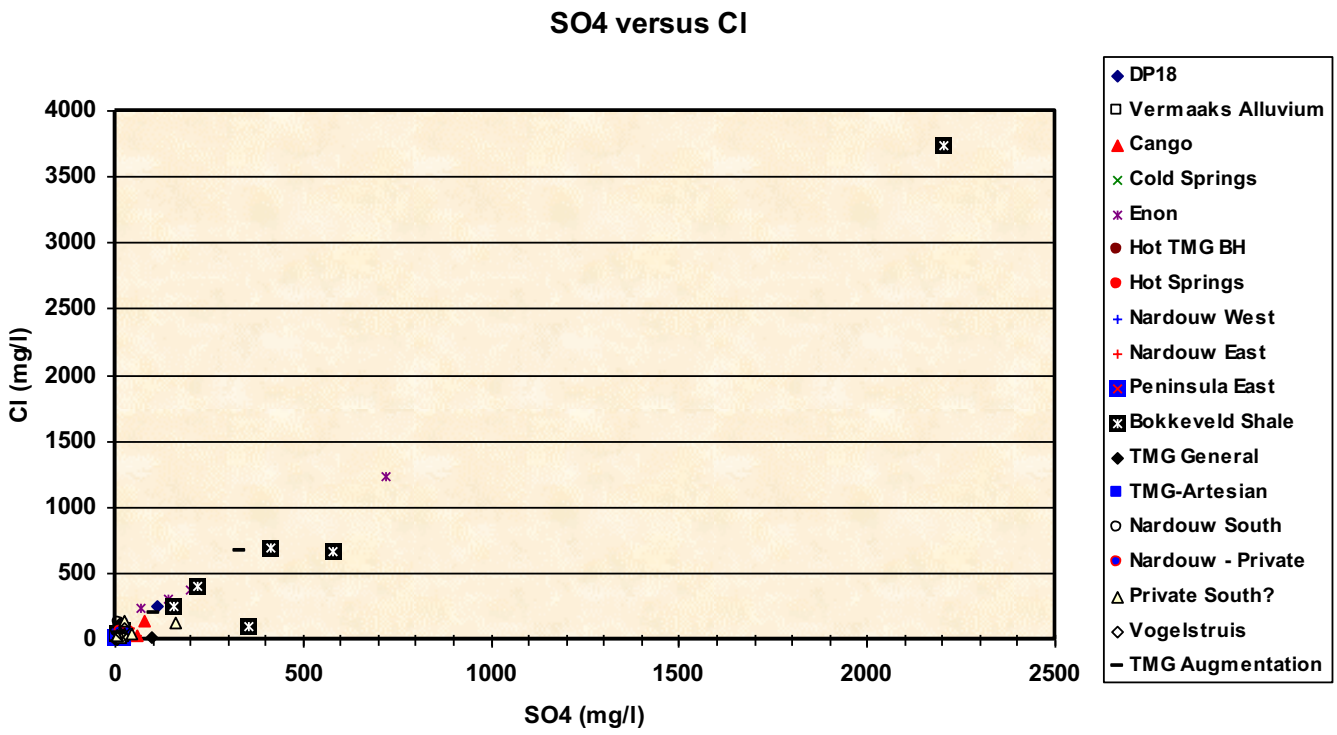

FIGURE G-34 : X-Y PLOT OF MAJOR IONS SO4 AND Cl

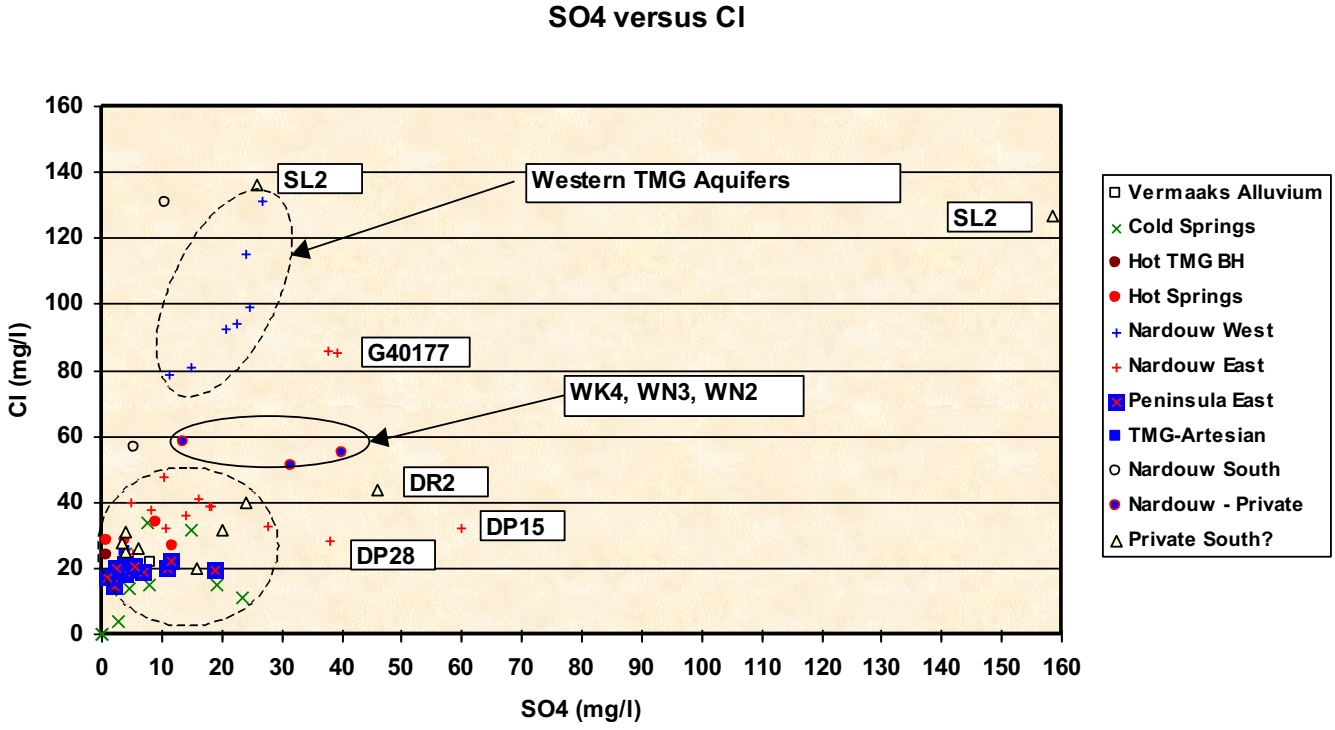

FIGURE G-35 : X-Y PLOT OF MAJOR IONS Na AND Cl

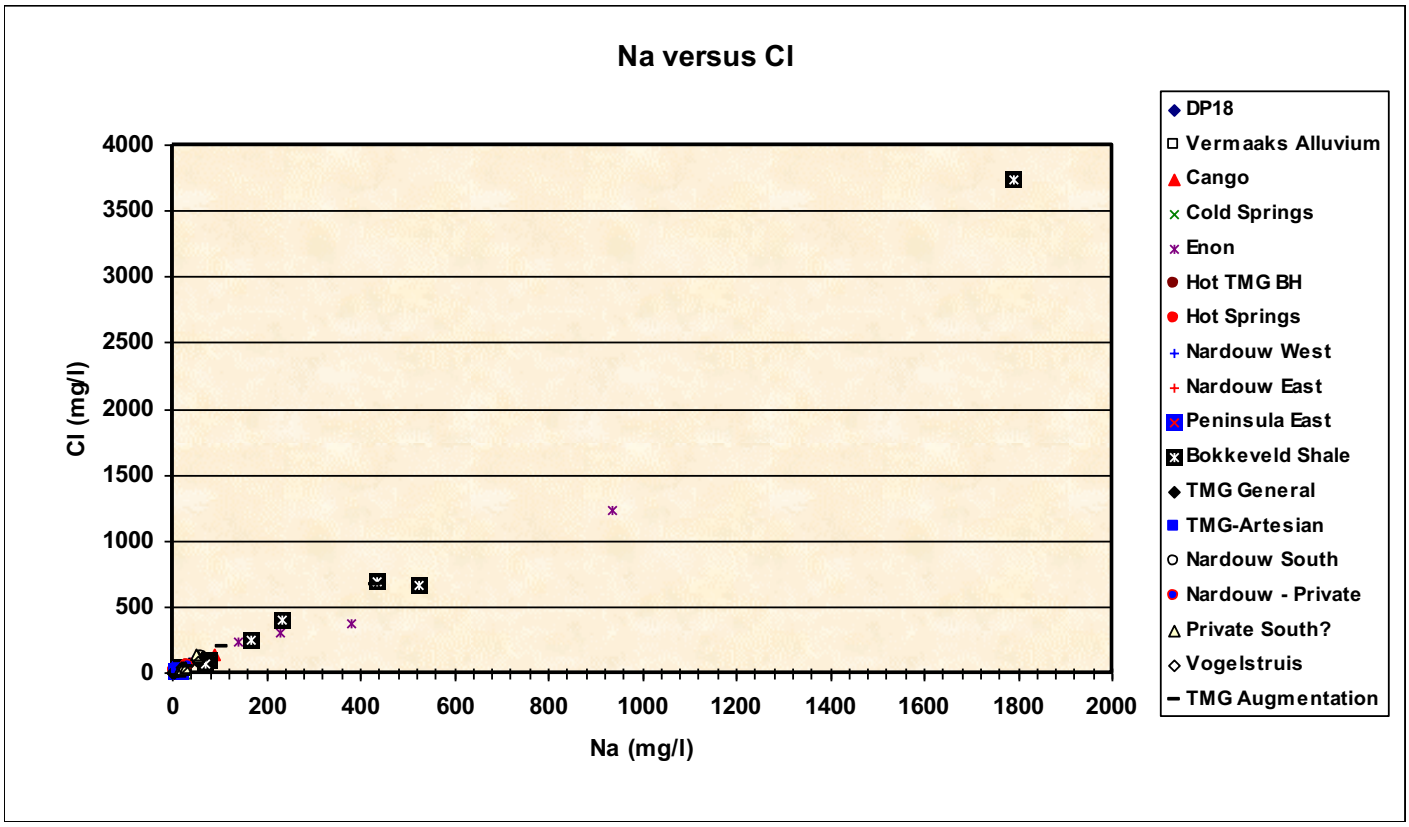

FIGURE G-36 : X-Y PLOT OF MAJOR IONS Na AND Cl

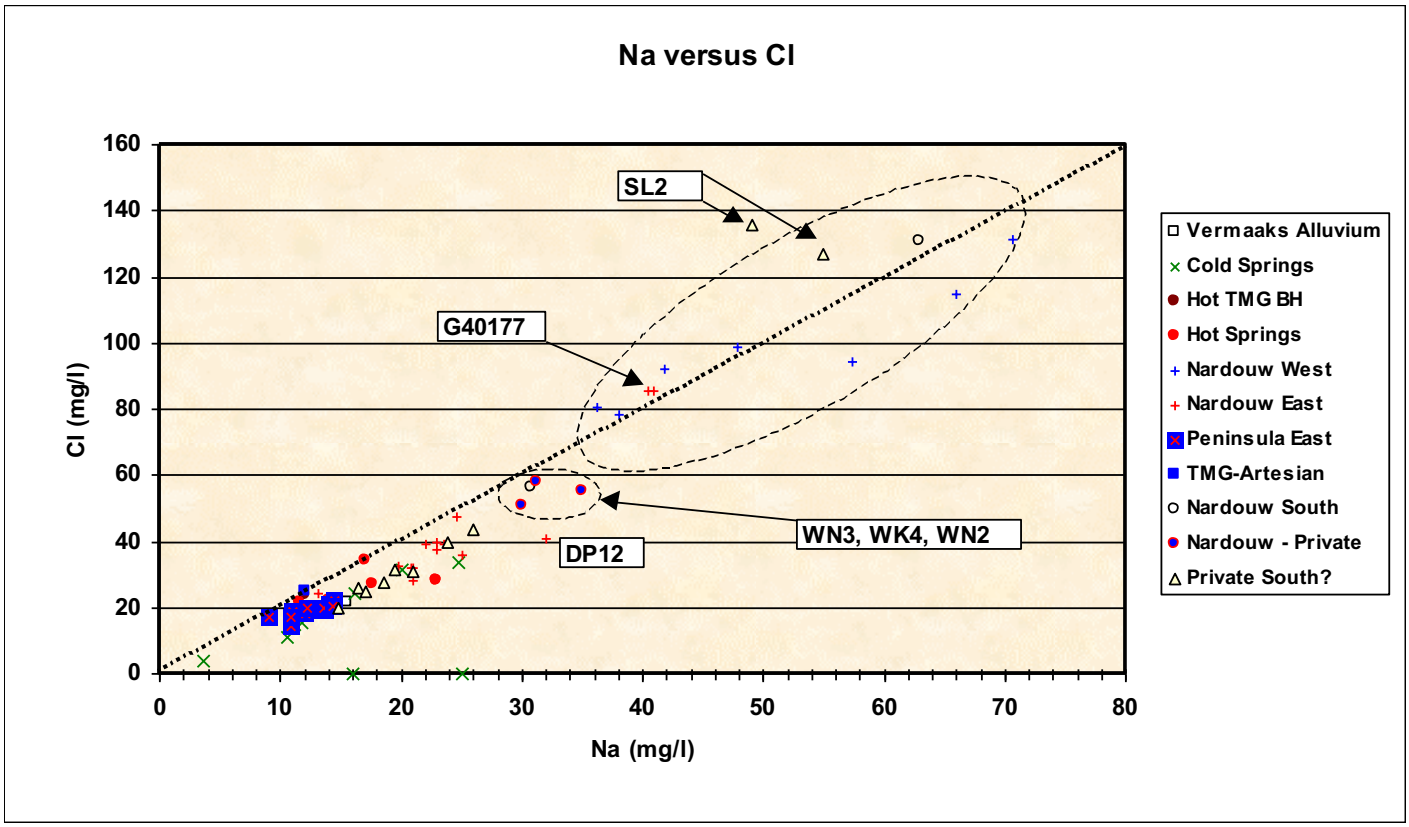

FIGURE G-37 : X-Y PLOT pH AND Fe

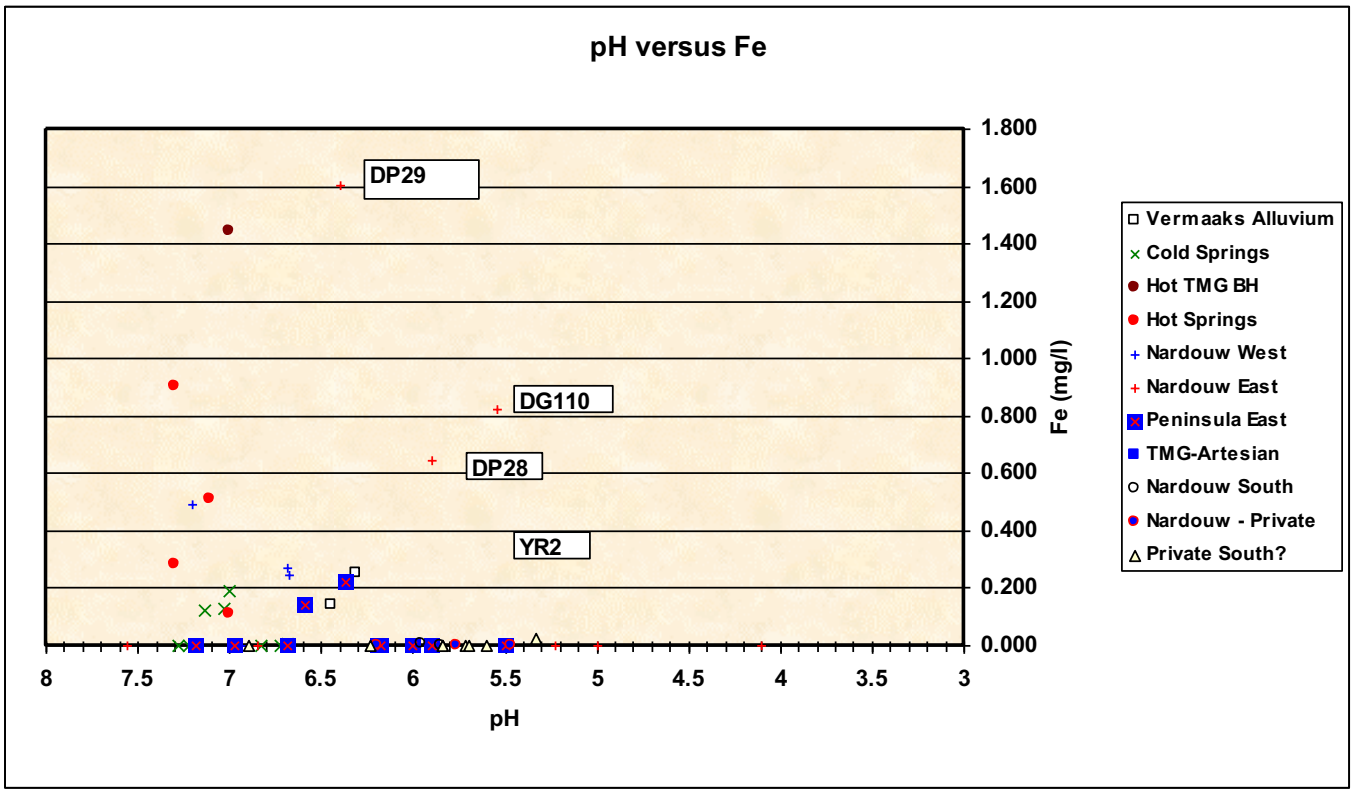

APPENDIX H: COMPOSITE DIAGRAMS

FIGURE H-1: COMPOSITE DIAGRAM – TMG KAMMANASSIE PRIVATE BOREHOLES

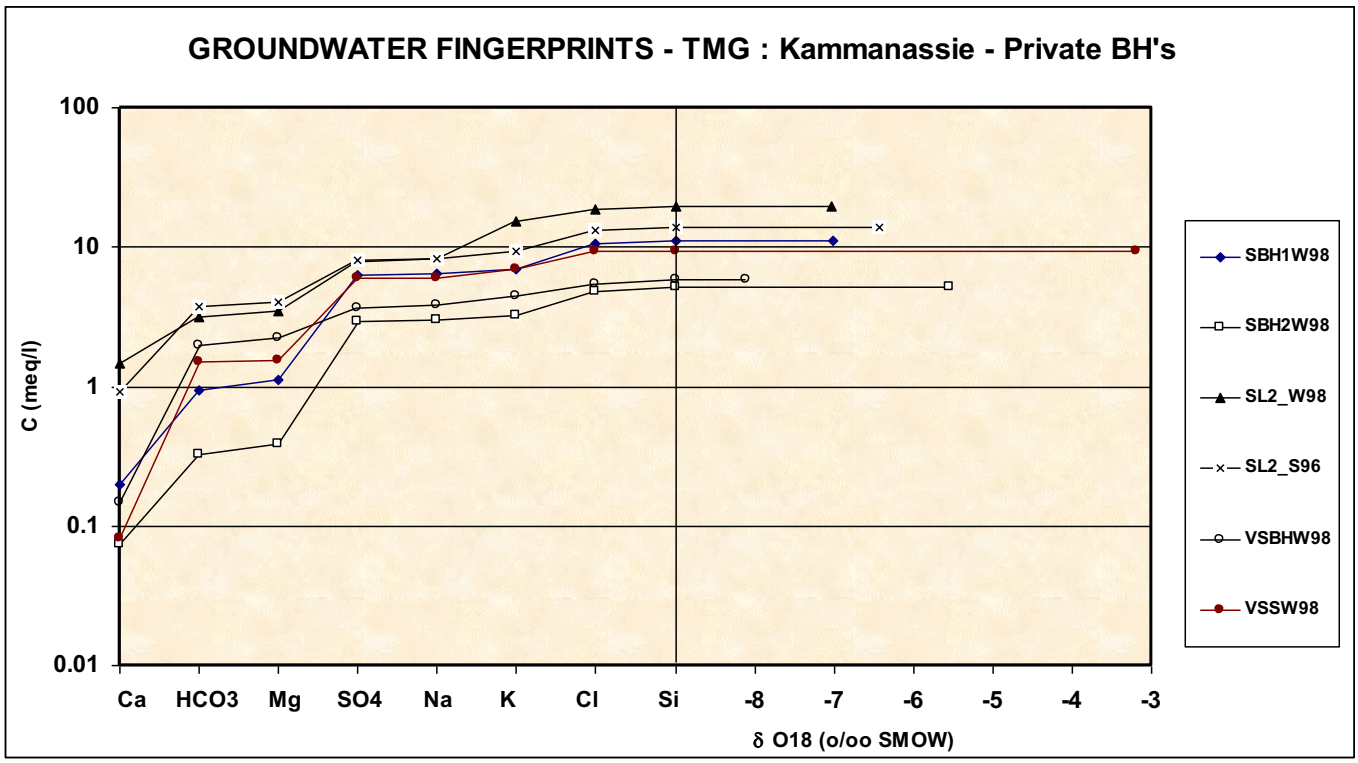

FIGURE H-2: COMPOSITE DIAGRAM – TMG KAMMANASSIE PRIVATE BOREHOLES

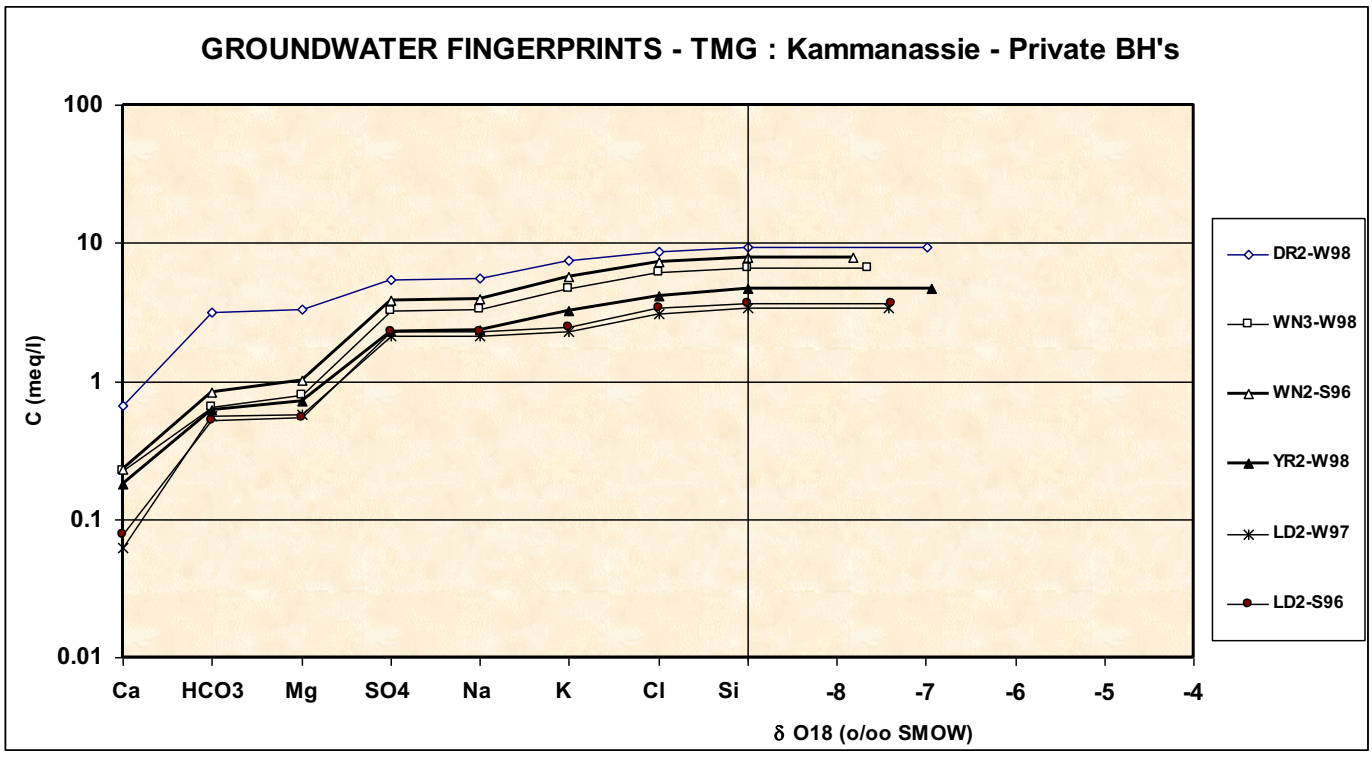

FIGURE H-3: COMPOSITE DIAGRAM – TMG KAMMANASSIE PRIVATE BOREHOLES

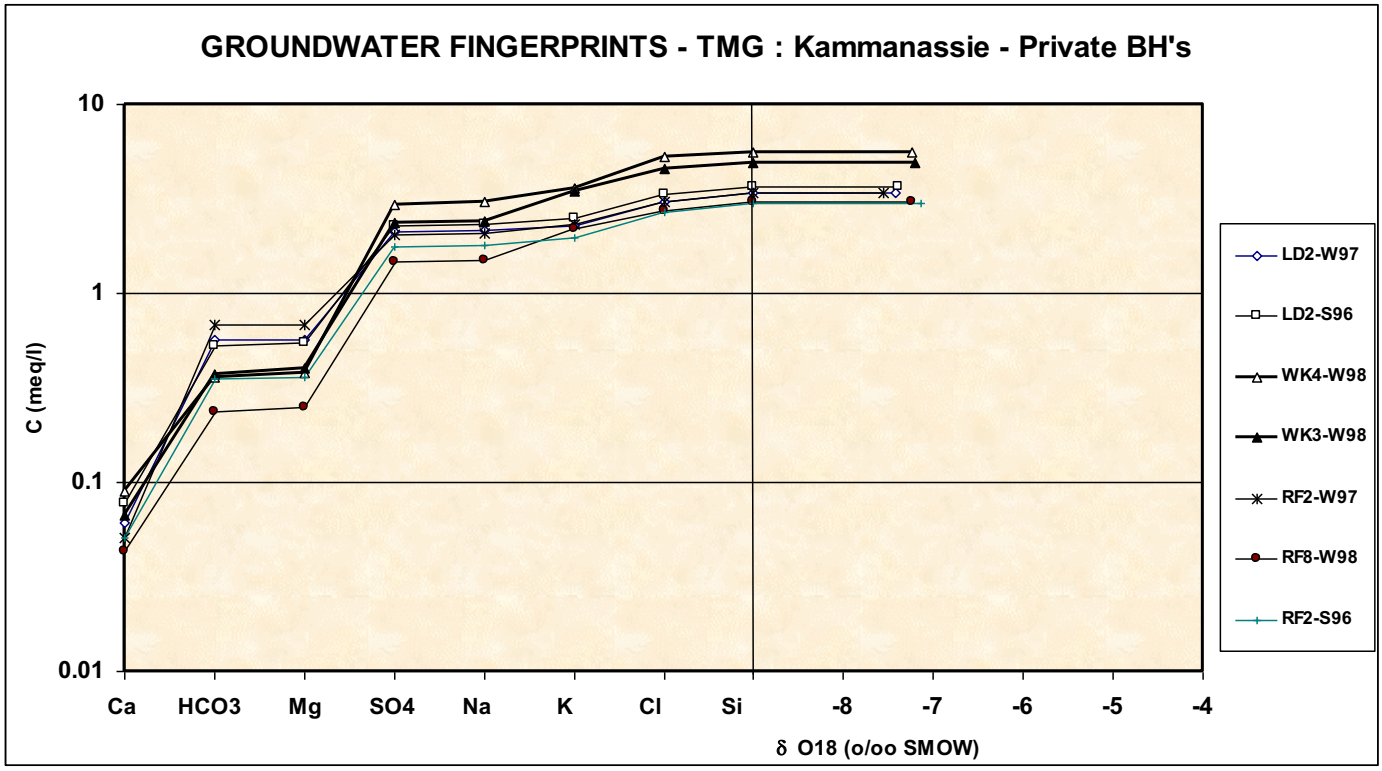

FIGURE H-4: COMPOSITE DIAGRAM – TMG : COLD SPRINGS

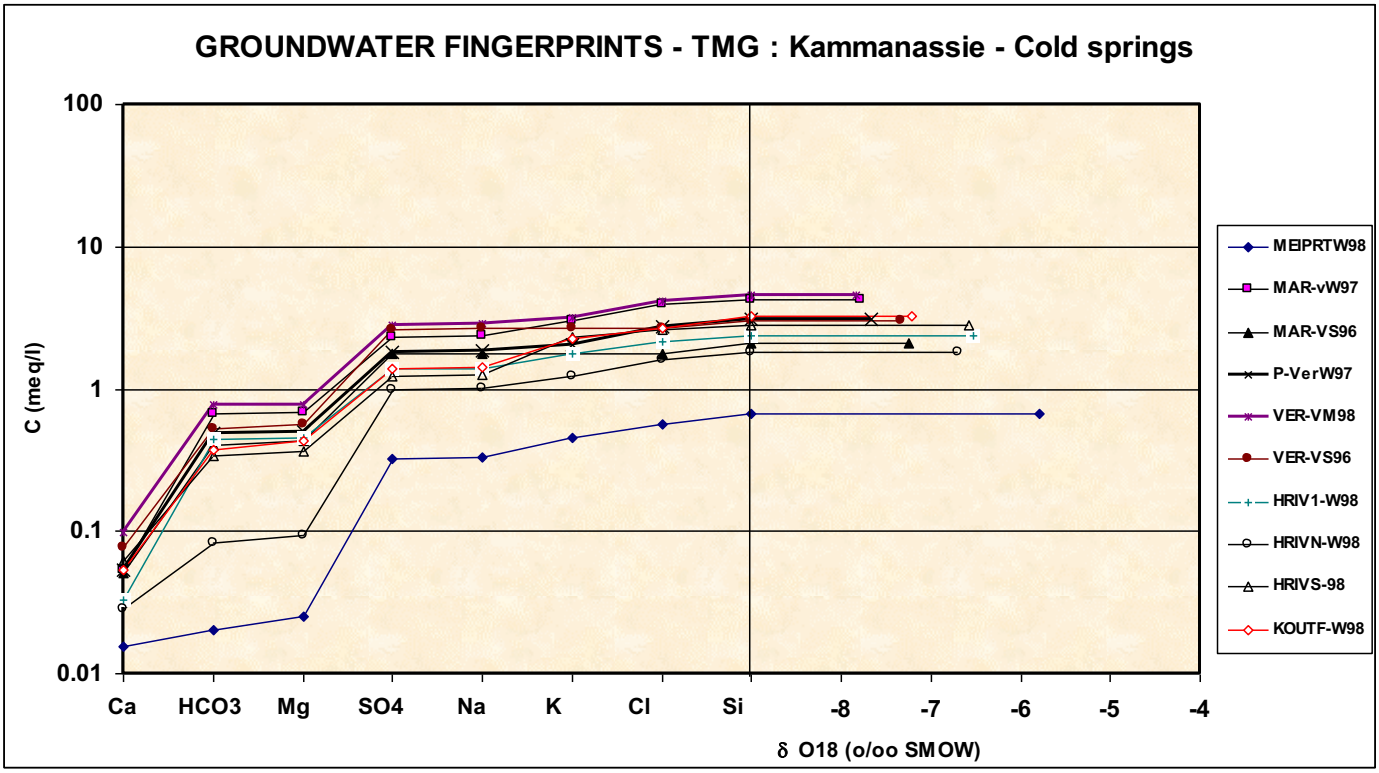

FIGURE H-5: COMPOSITE DIAGRAM – TMG GENERAL (SEEPAGES)

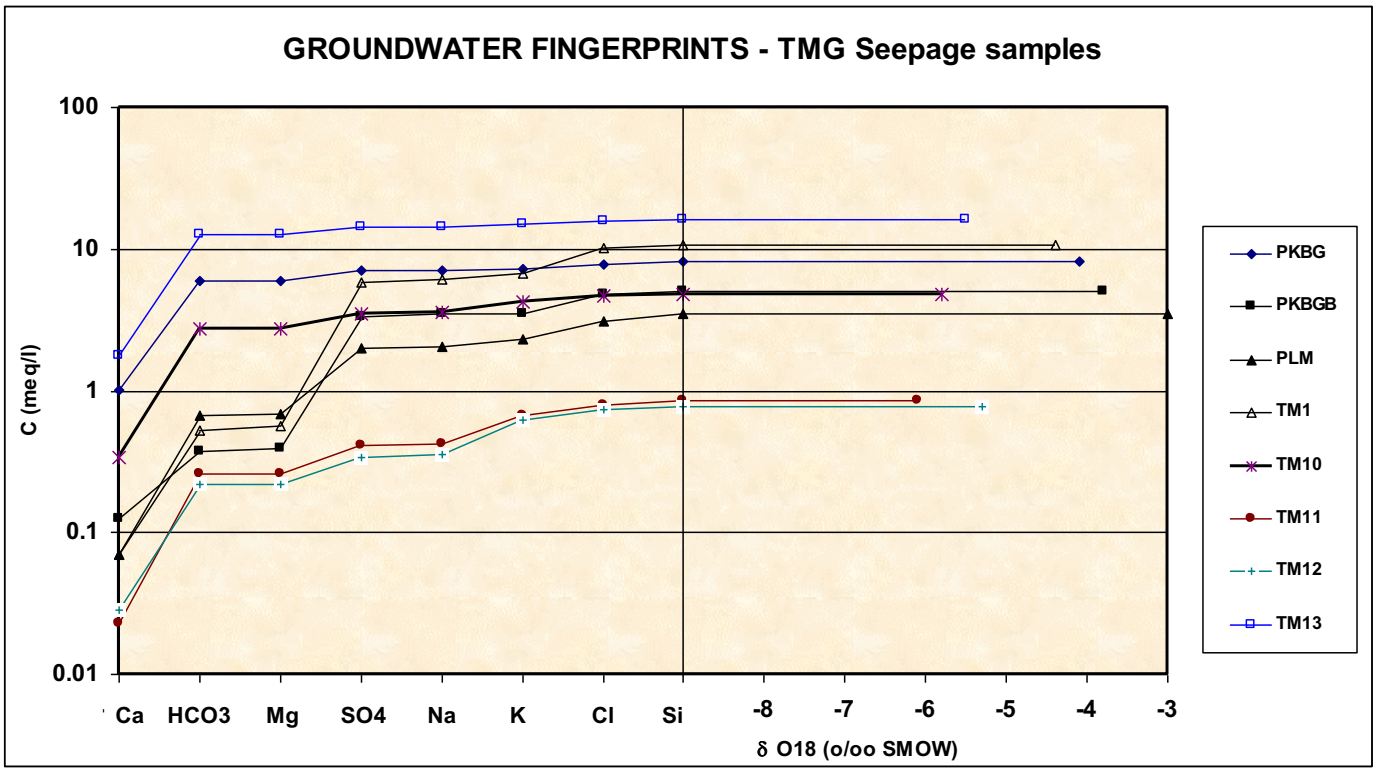

FIGURE H-6: COMPOSITE DIAGRAM – TMG GENERAL (SEEPAGES)

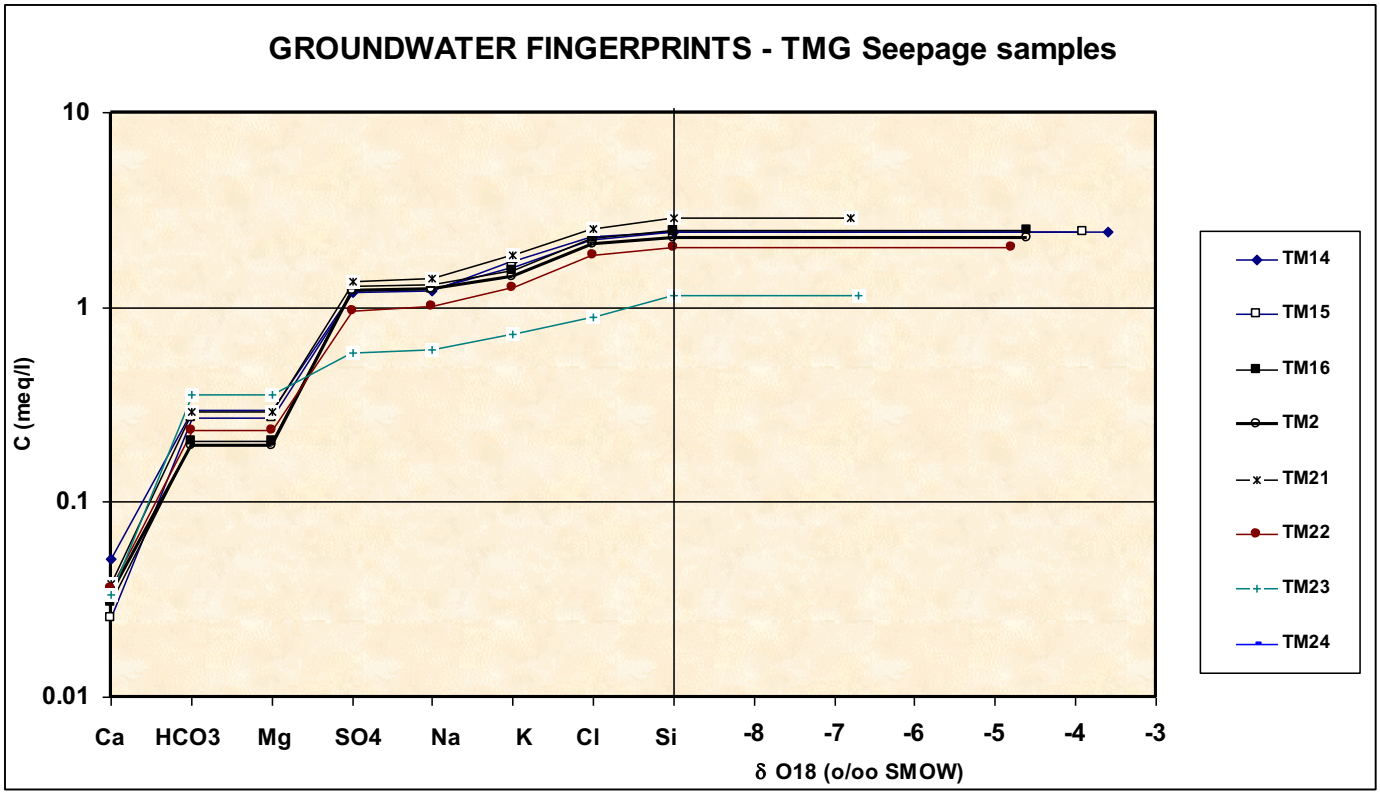

FIGURE H-7: COMPOSITE DIAGRAM – TMG GENERAL (SEEPAGES)

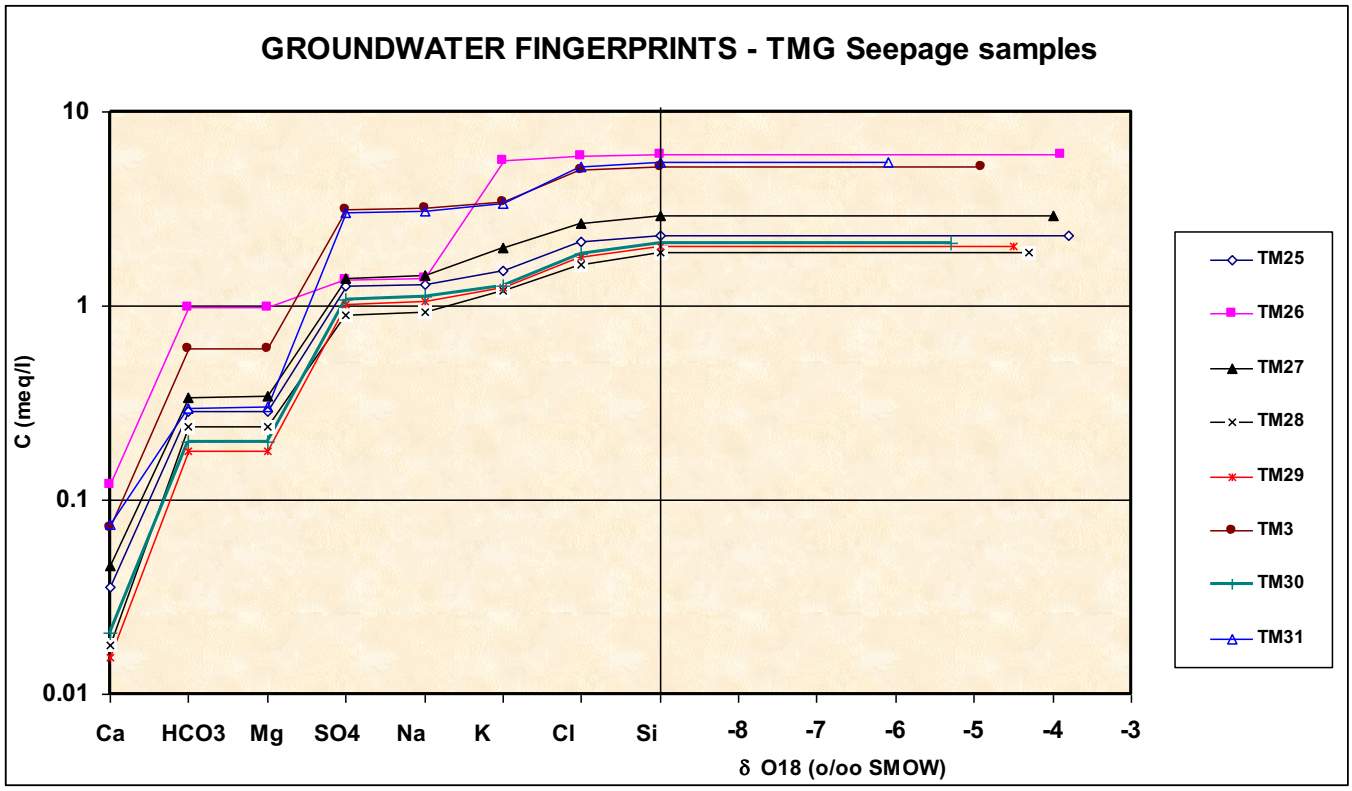

FIGURE H-8: COMPOSITE DIAGRAM – TMG GENERAL (SEEPAGES)

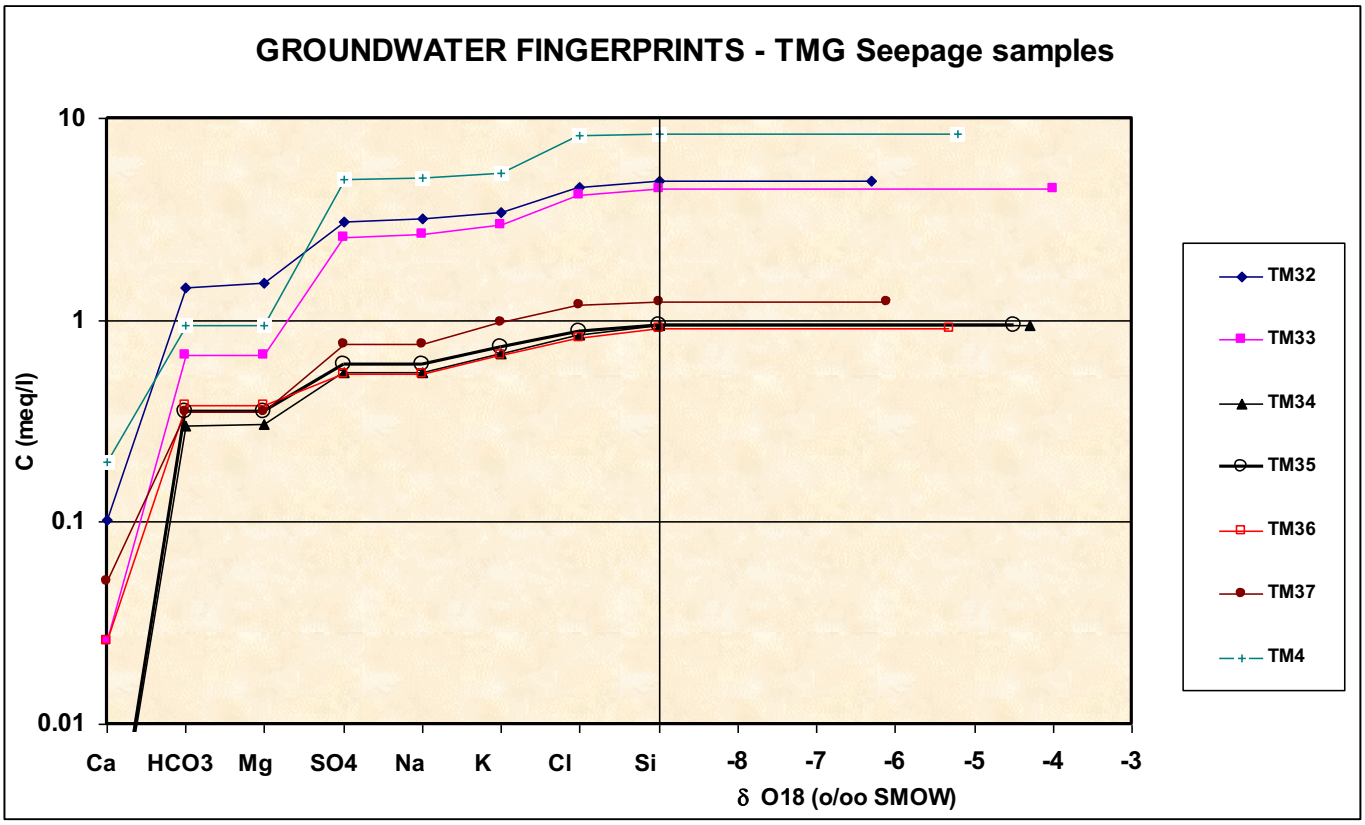

FIGURE H-9: COMPOSITE DIAGRAM – TMG GENERAL (SEEPAGES)

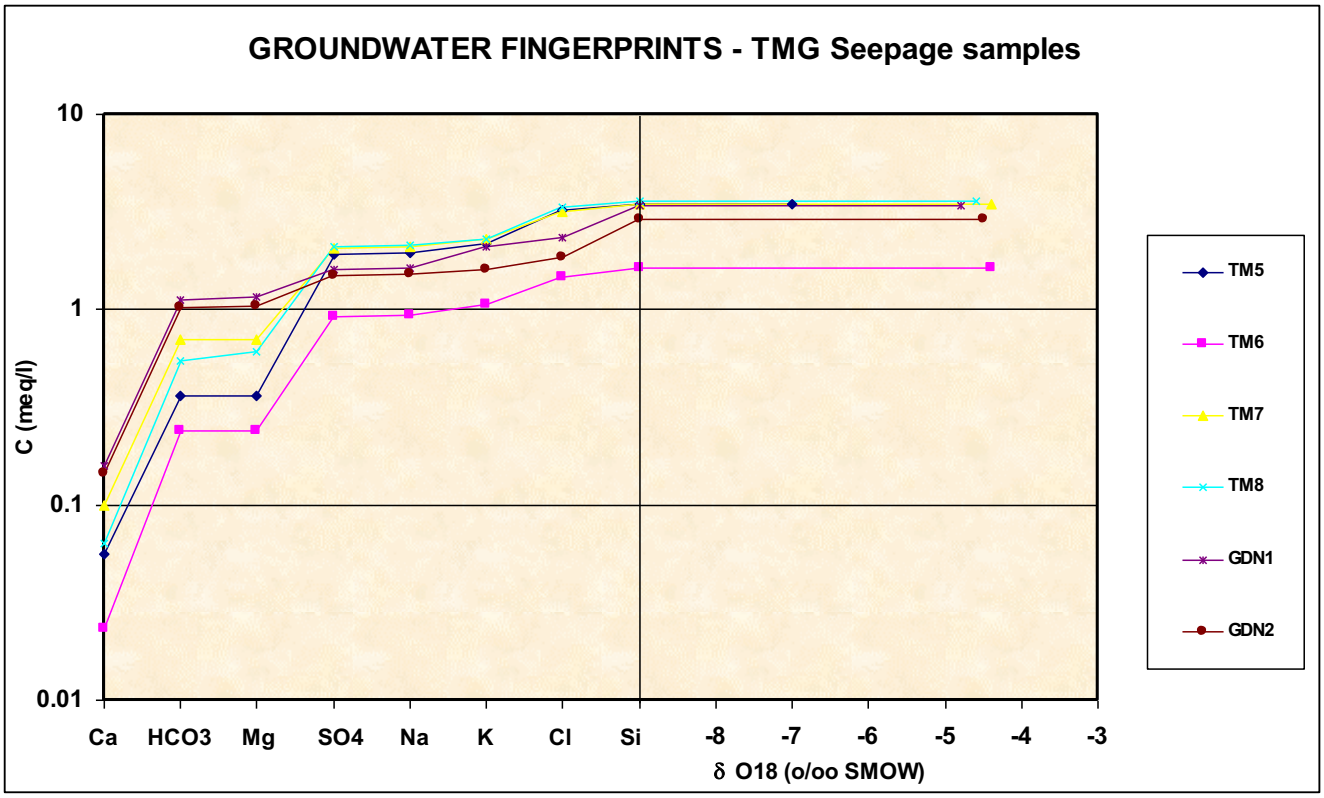

FIGURE H-10: COMPOSITE DIAGRAM – TMG : TMG AQUIFERS

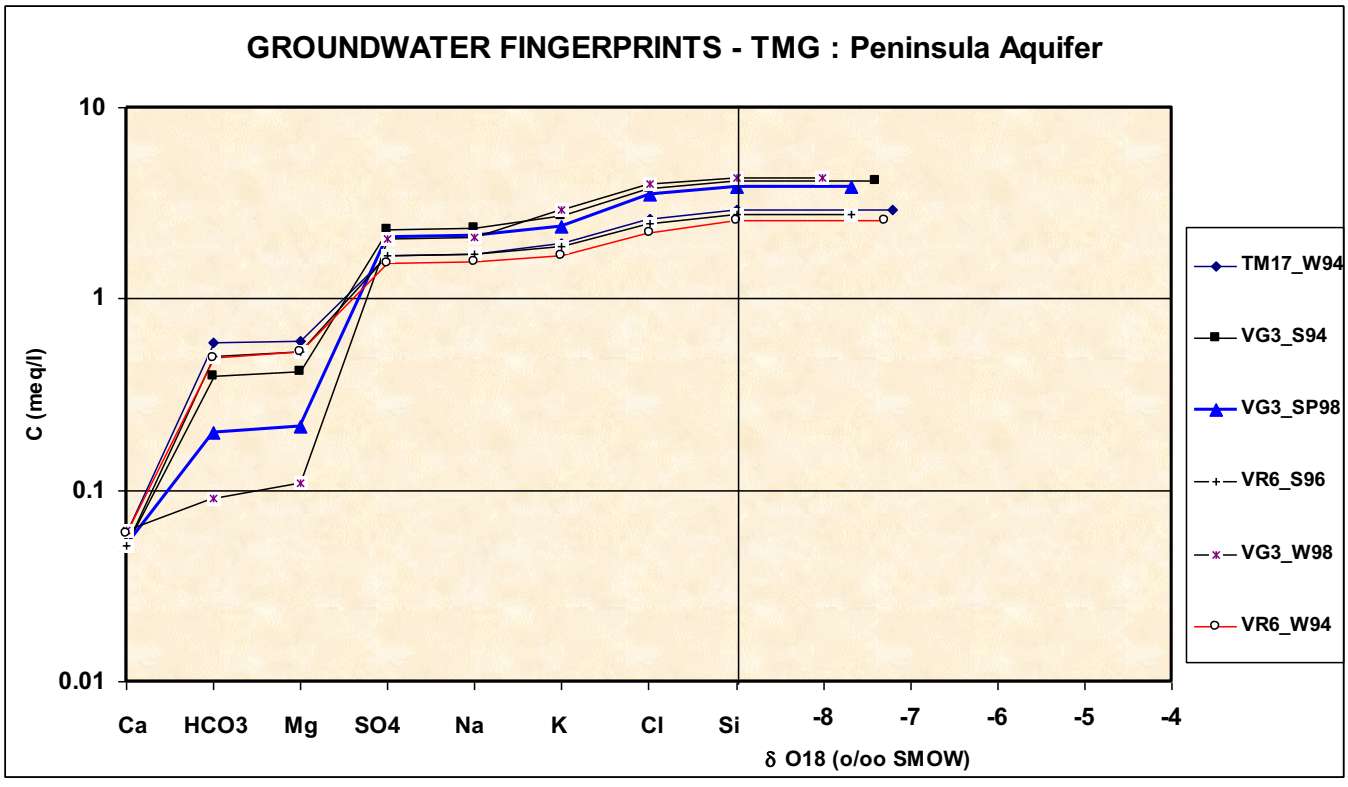

FIGURE H-11: COMPOSITE DIAGRAM – TMG : PENINSULA AQUIFER

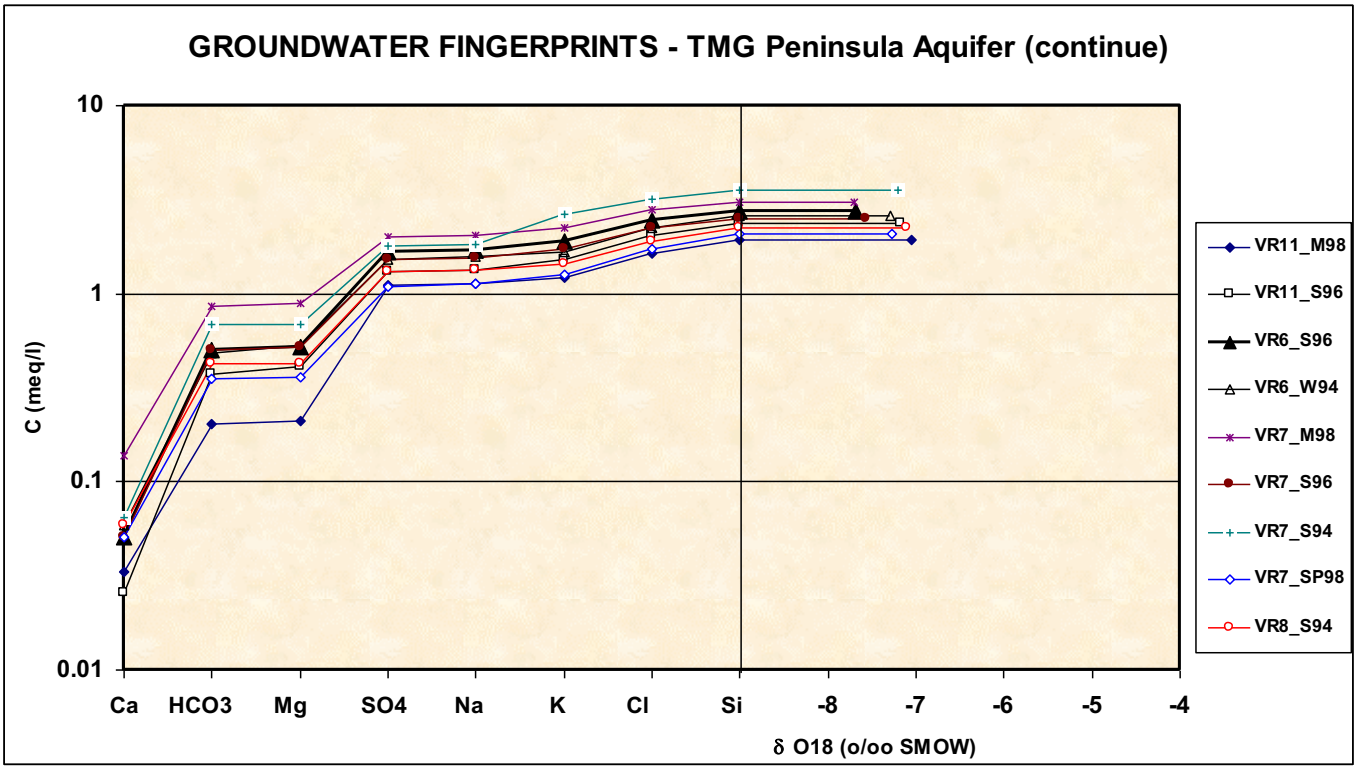

FIGURE H-12: COMPOSITE DIAGRAM – TMG NARDOUW WEST AQUIFER

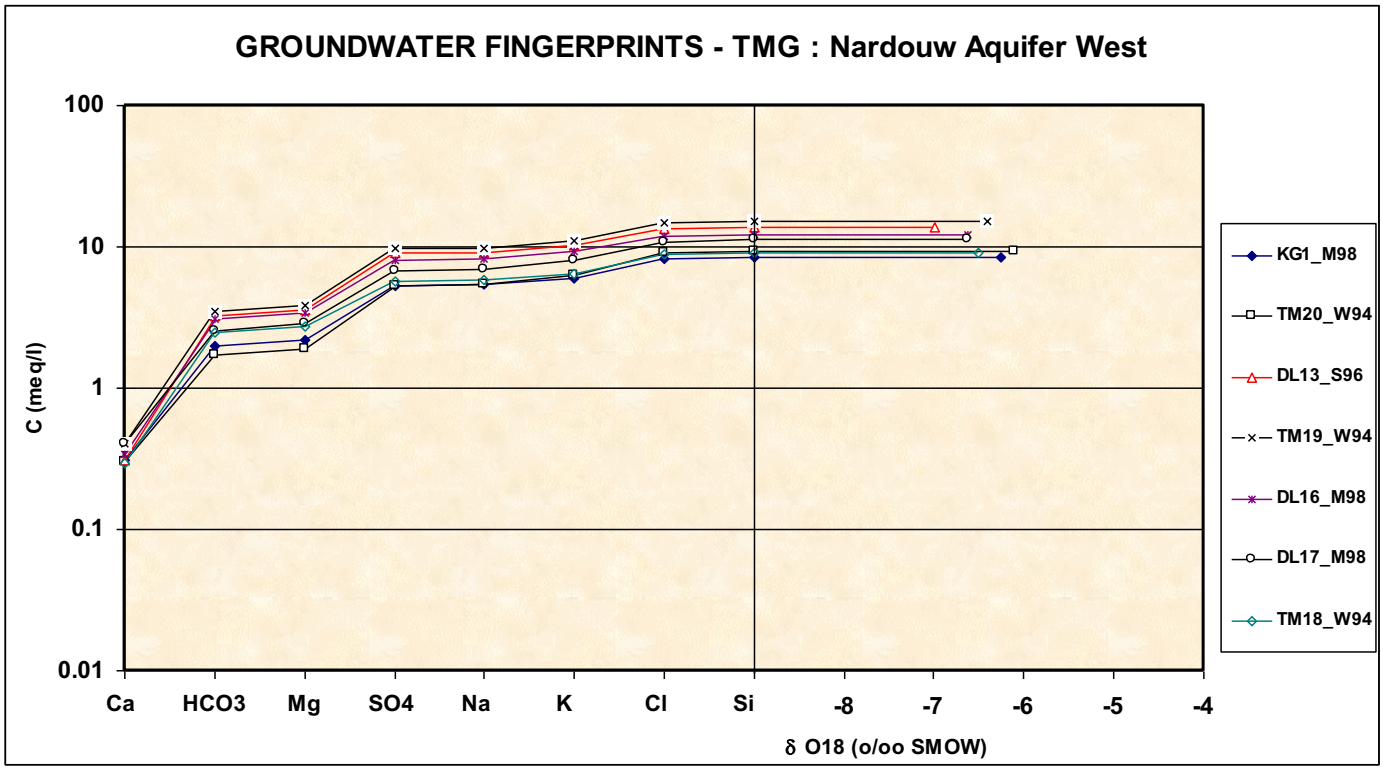

FIGURE H-13: COMPOSITE DIAGRAM – TMG ALLUVIAL AND NARDOUW EAST AQUIFERS

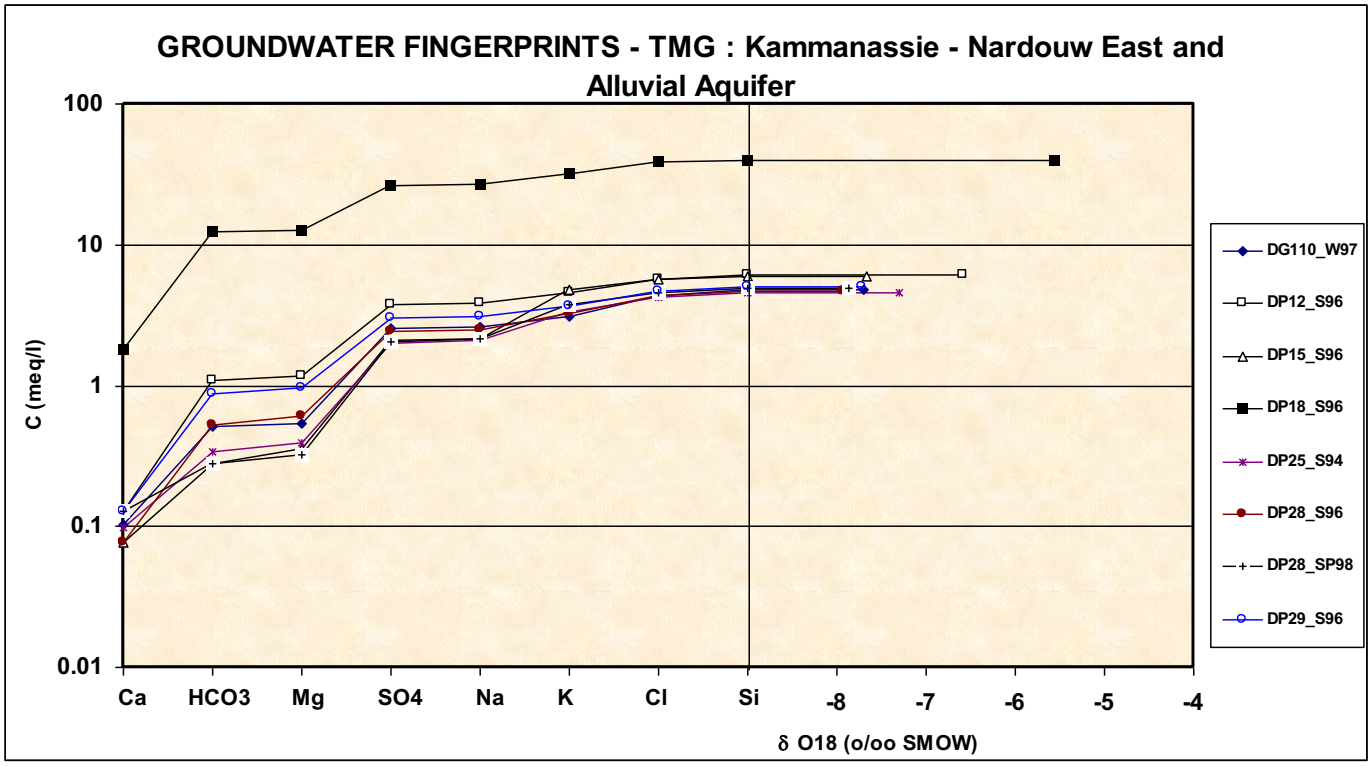

FIGURE H-14: COMPOSITE DIAGRAM – ADDITIONAL MONITORING BOREHOLES

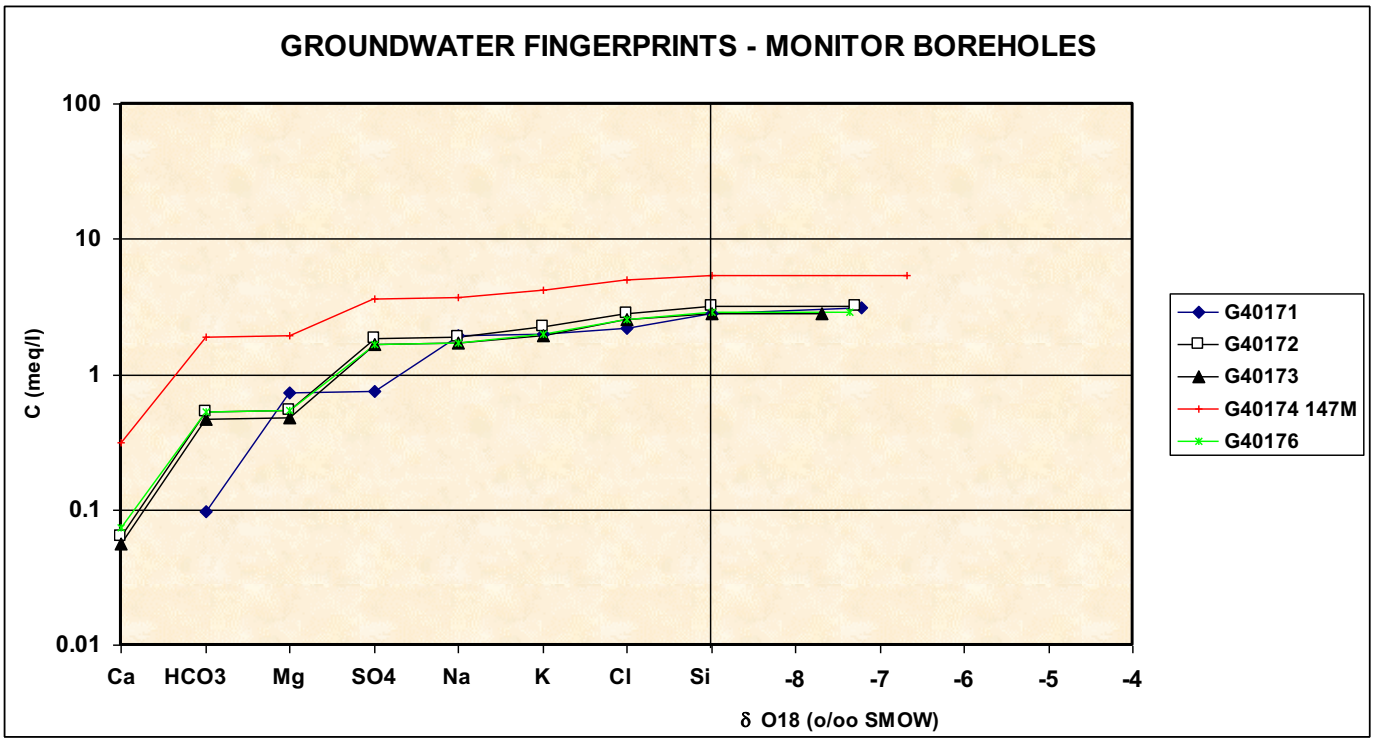

FIGURE H-15: COMPOSITE DIAGRAM – ADDITIONAL MONITORING BOREHOLES

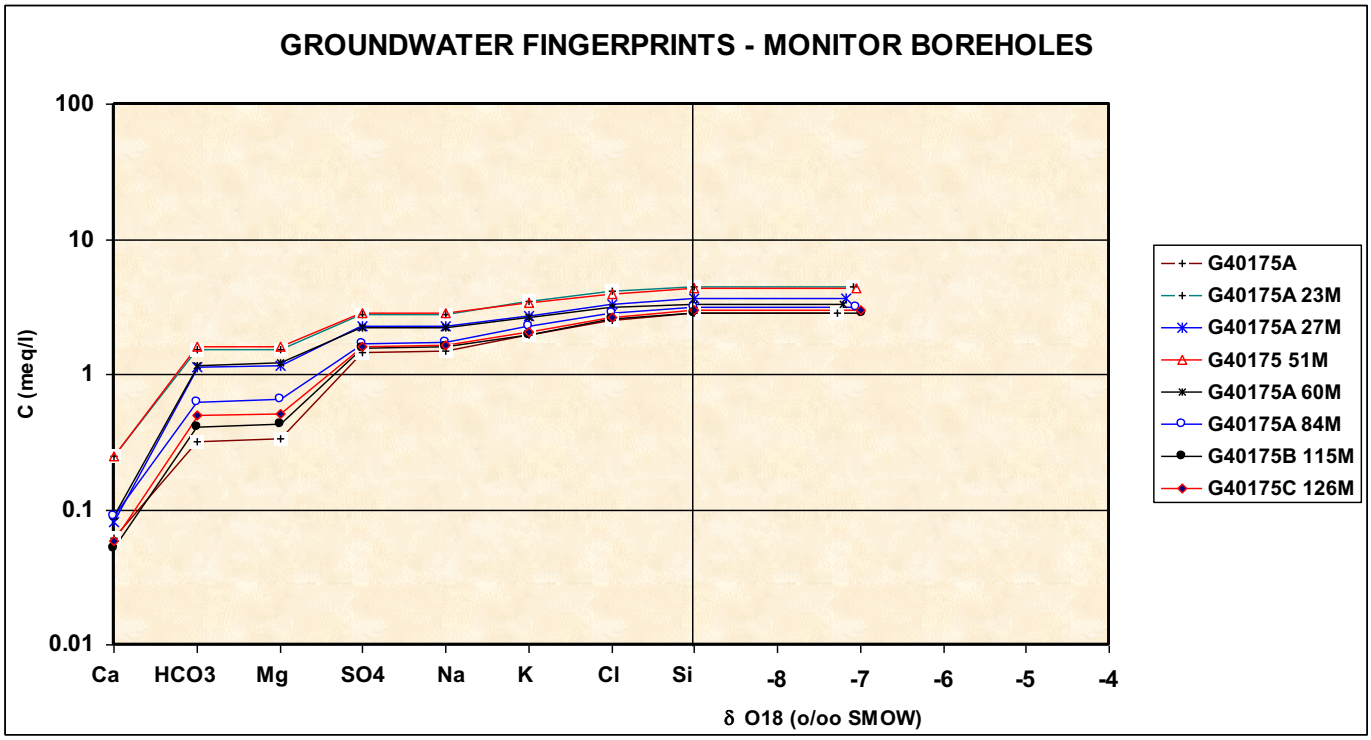

FIGURE H-16: COMPOSITE DIAGRAM – ADDITIONAL MONITORING BOREHOLES

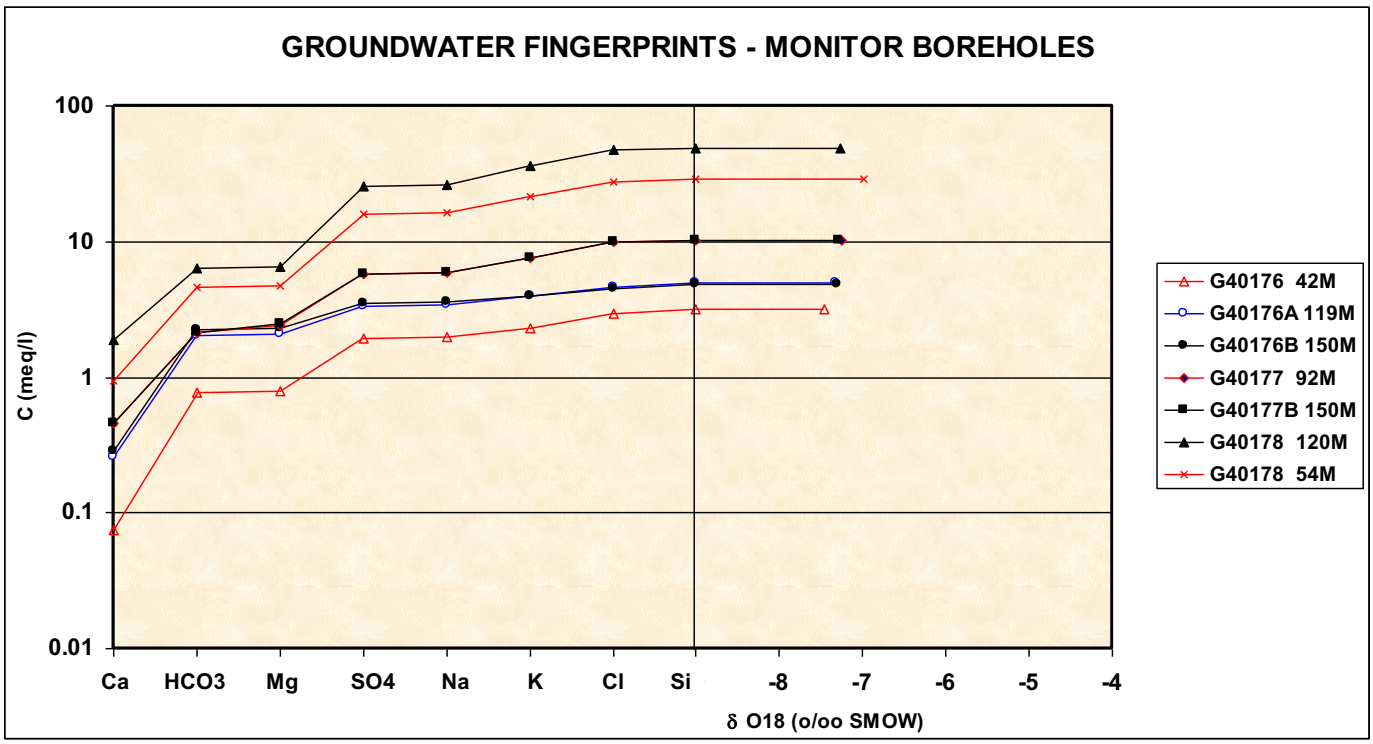

FIGURE H-17: COMPOSITE DIAGRAM – CANGO AND TMG AQUIFER – OUDTSHOORN AUGMENTATION STUDY

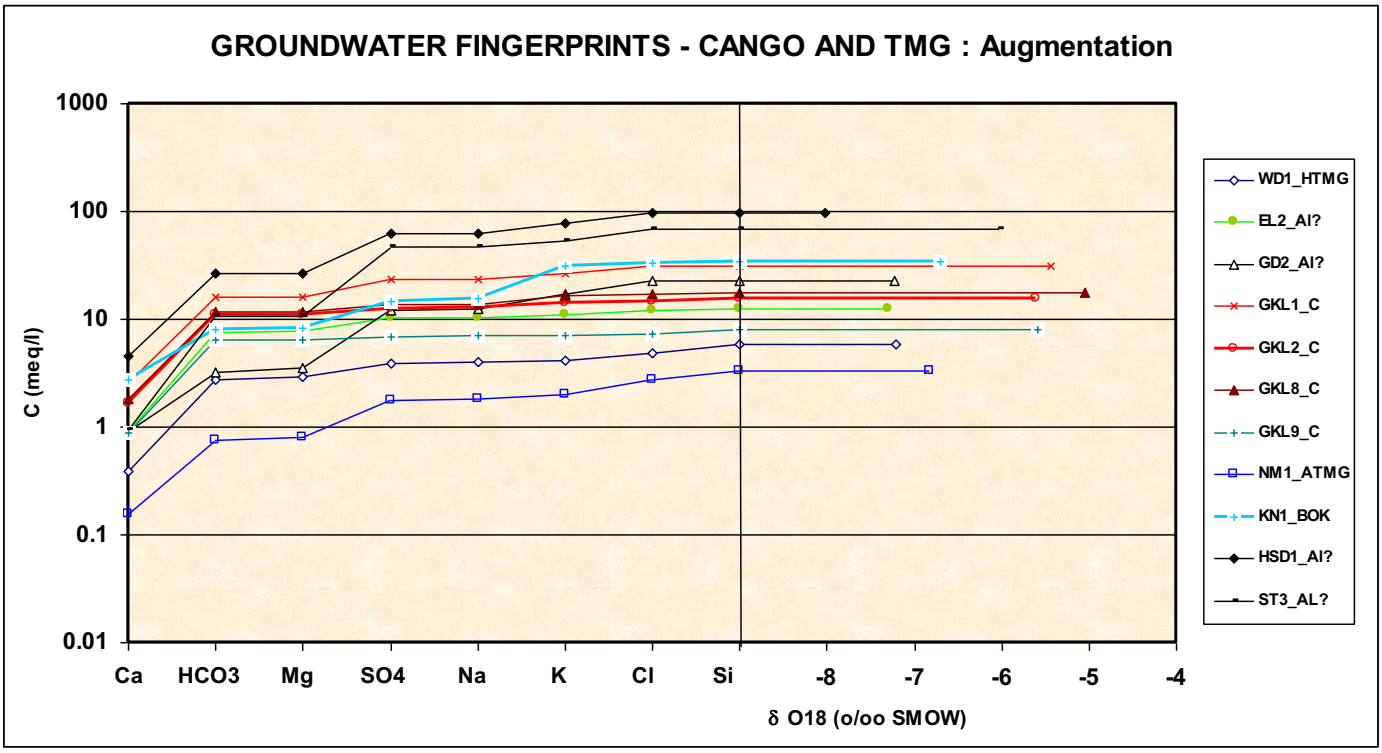

FIGURE H-18: COMPOSITE DIAGRAM – ALLUVIAL AND CRETACEOUS AQUIFERS – OUDTSHOORN AUGMENTATION STUDY

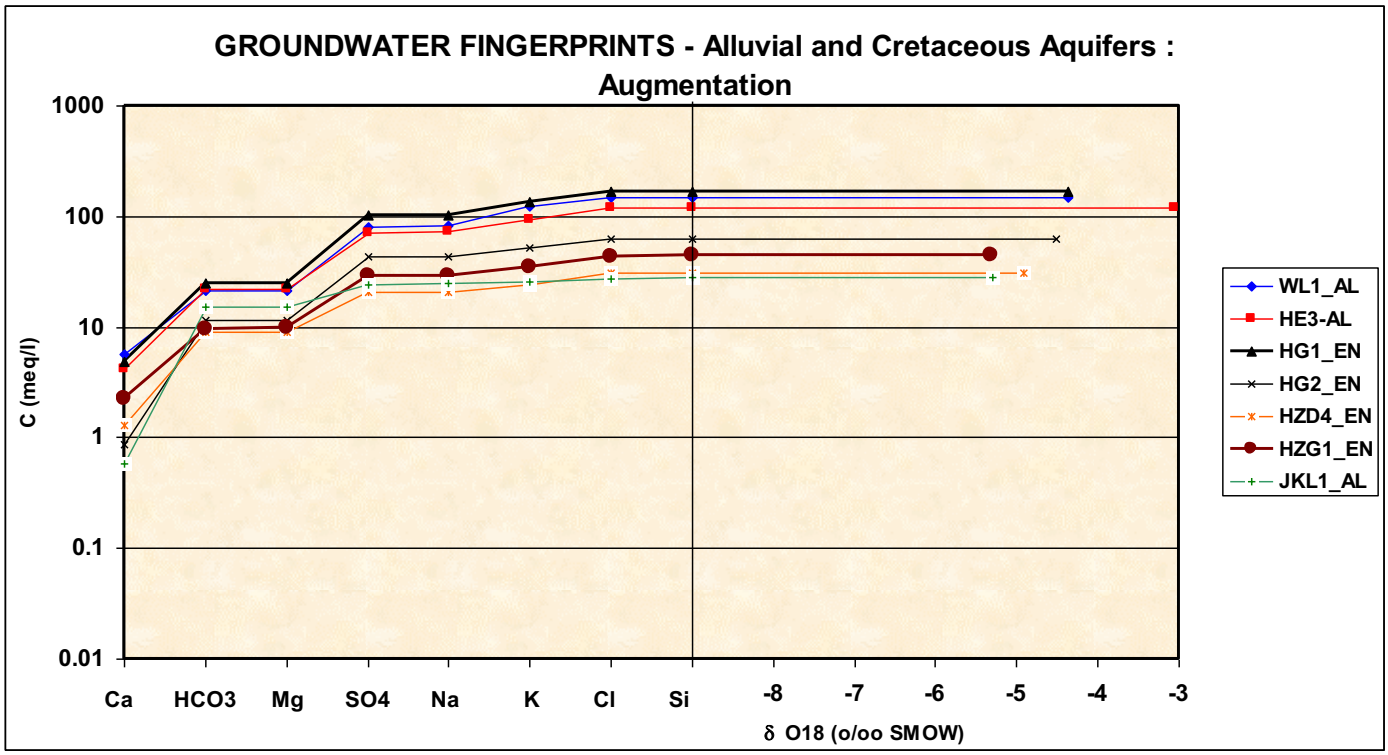

FIGURE H-19: COMPOSITE DIAGRAM – TMG HOT SPRINGS

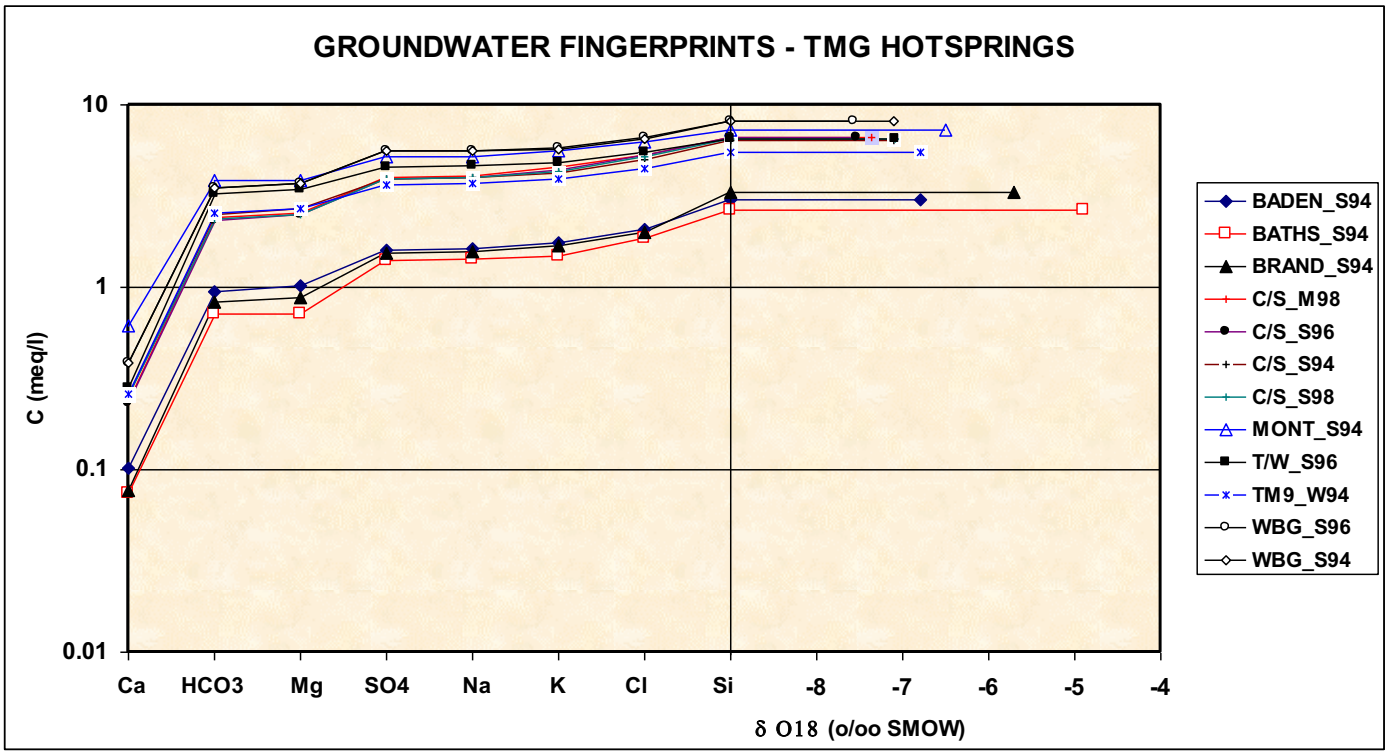

APPENDIX I: CLUSTER ANALYSIS

FIGURE I-1: CLUSTER ANALYSIS, USING ALL HYDROCHEMISTRY DATA FOR LITTLE KAROO STUDY AREA

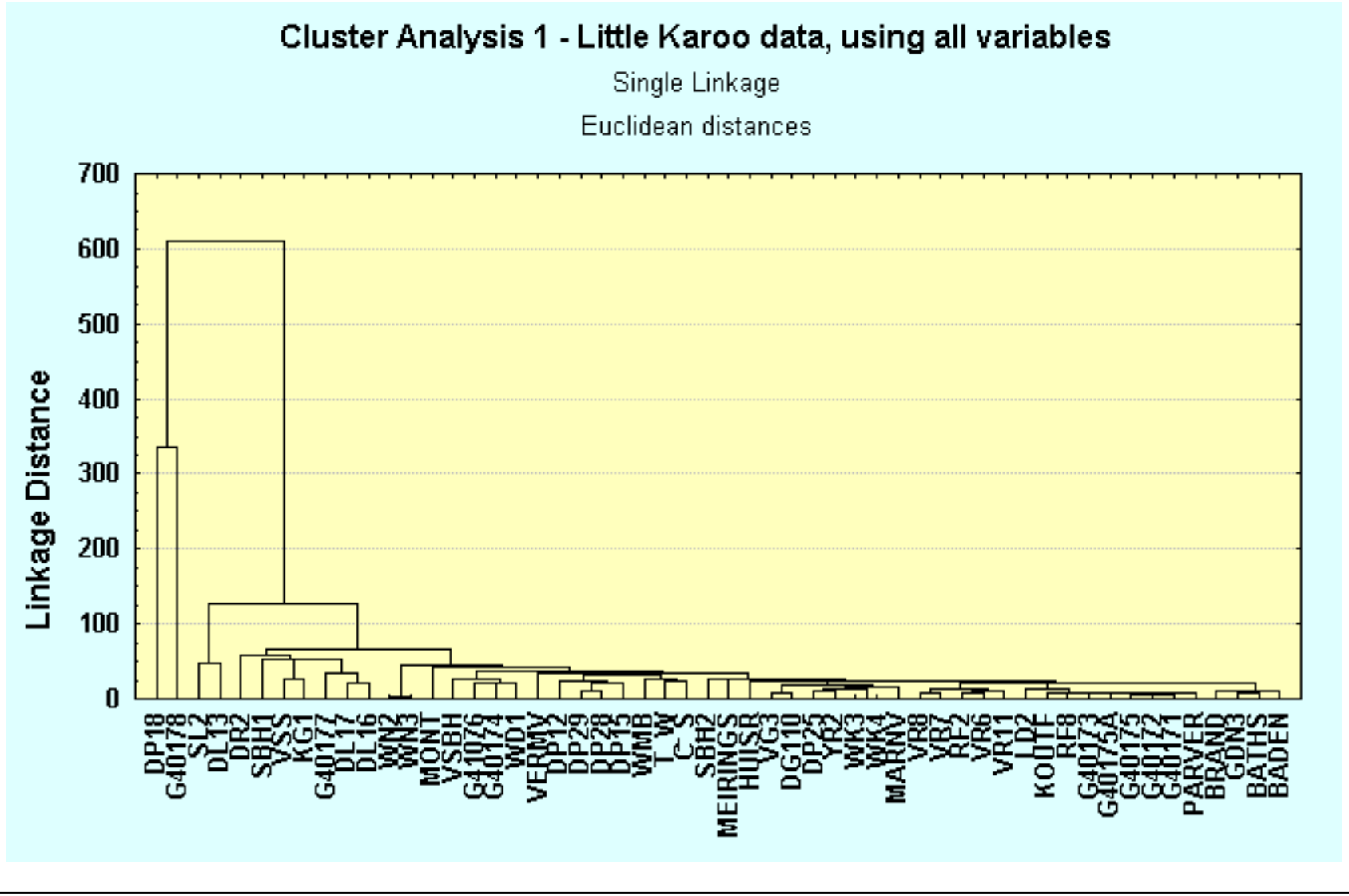

FIGURE I-2 : CLUSTER ANALYSIS, USING ALL HYDROCHEMISTRY DATA FOR LITTLE KAROO STUDY AREA

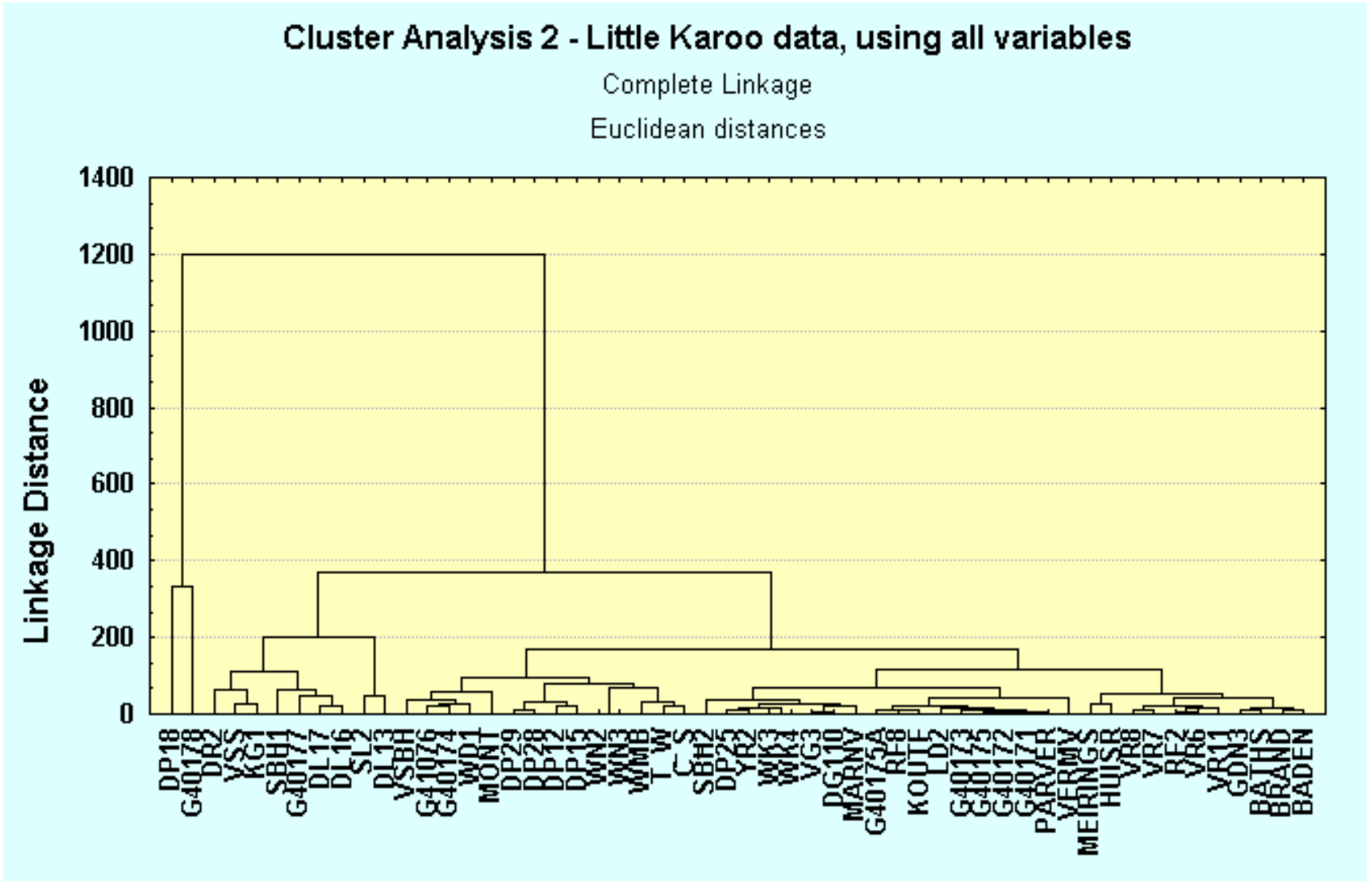

FIGURE I-3 : CLUSTER ANALYSIS, LITTLE KAROO HYDROCHEMISTRY DATA EXCLUDING DP18 AND G40178

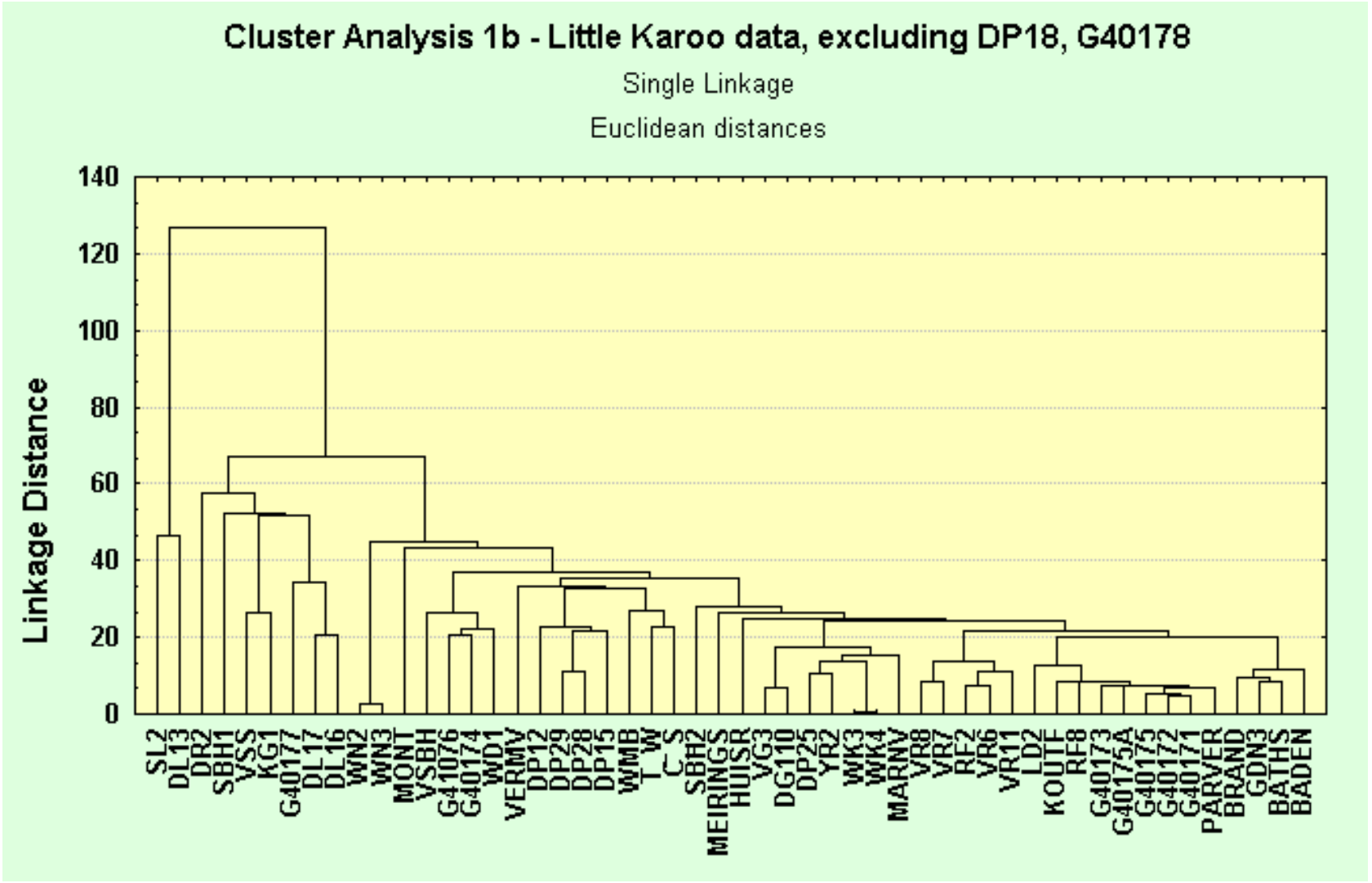

FIGURE I-4 : CLUSTER ANALYSIS, LITTLE KAROO HYDROCHEMISTRY DATA EXCLUDING CERTAIN HOT SPRINGS

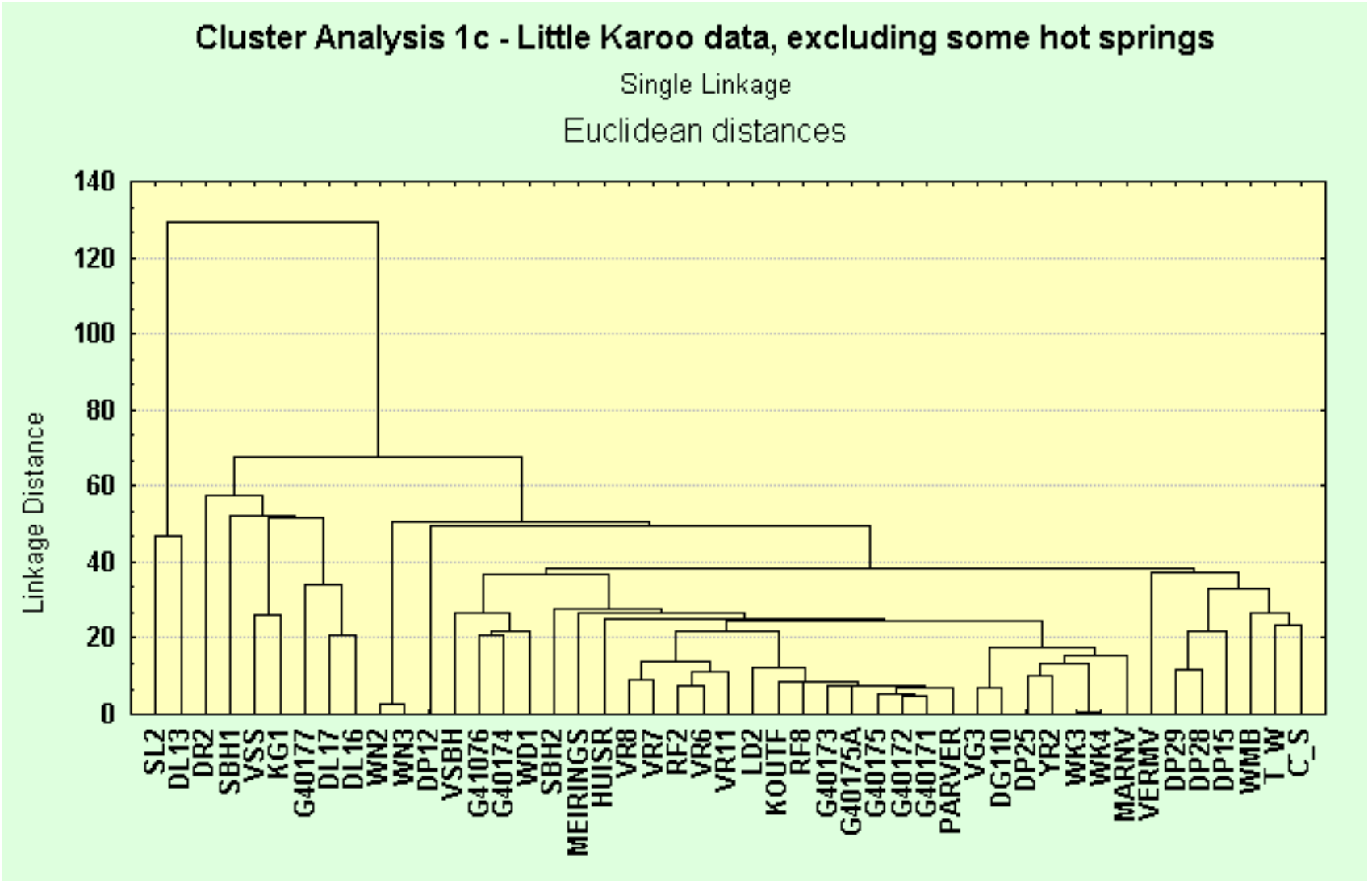

FIGURE I-5 : CLUSTER ANALYSIS, LITTLE KAROO HYDROCHEMISTRY DATA EXCLUDING NON LITTLE KAROO HOT SPRINGS

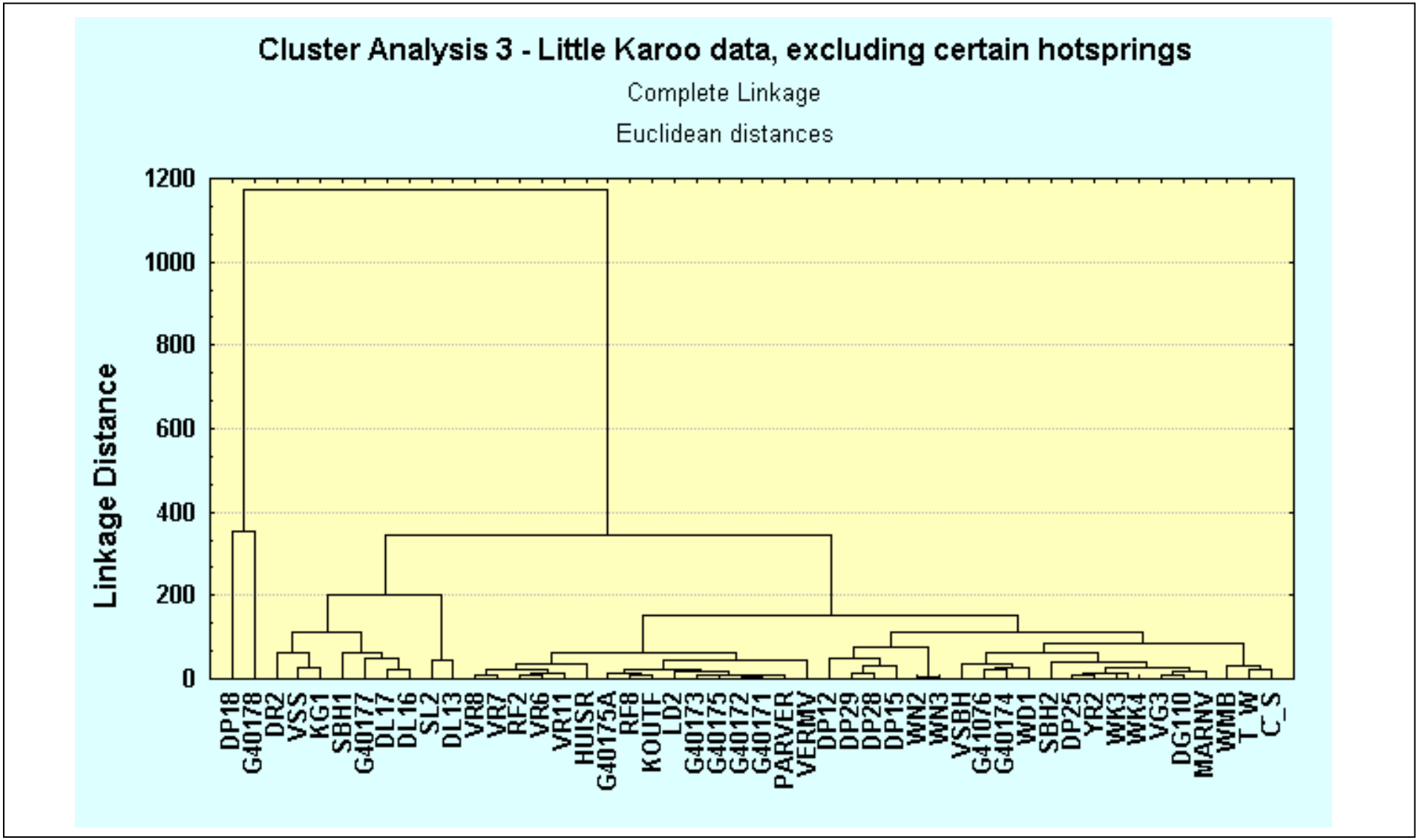

FIGURE I-6 : CLUSTER ANALYSIS, ONLY USING HYDROCHEMISTRY DATA OF TMG AQUIFERS

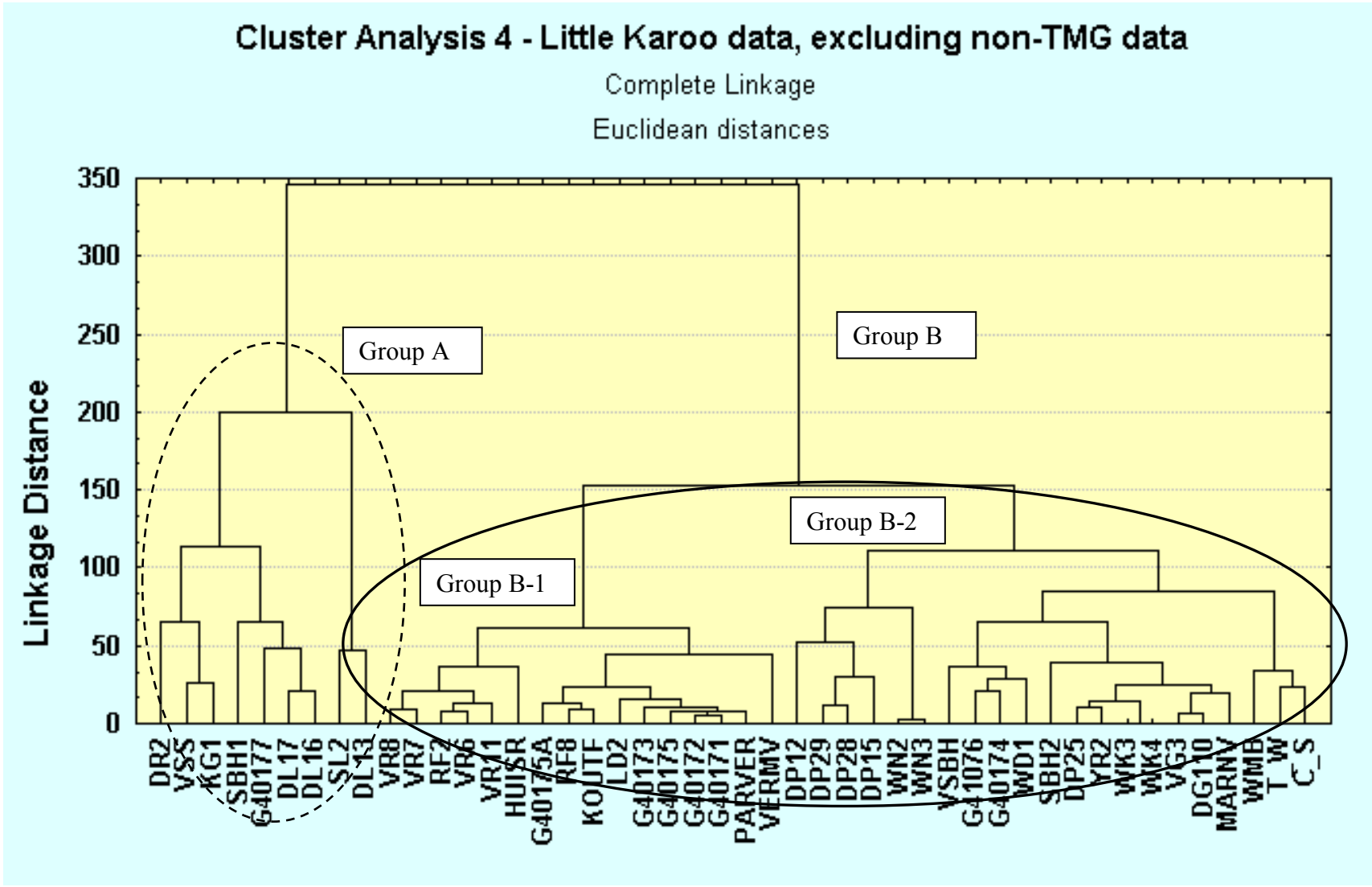

FIGURE I-7 : CLUSTER ANALYSIS, ONLY USING HYDROCHEMISTRY DATA FOR EASTERN SECTION

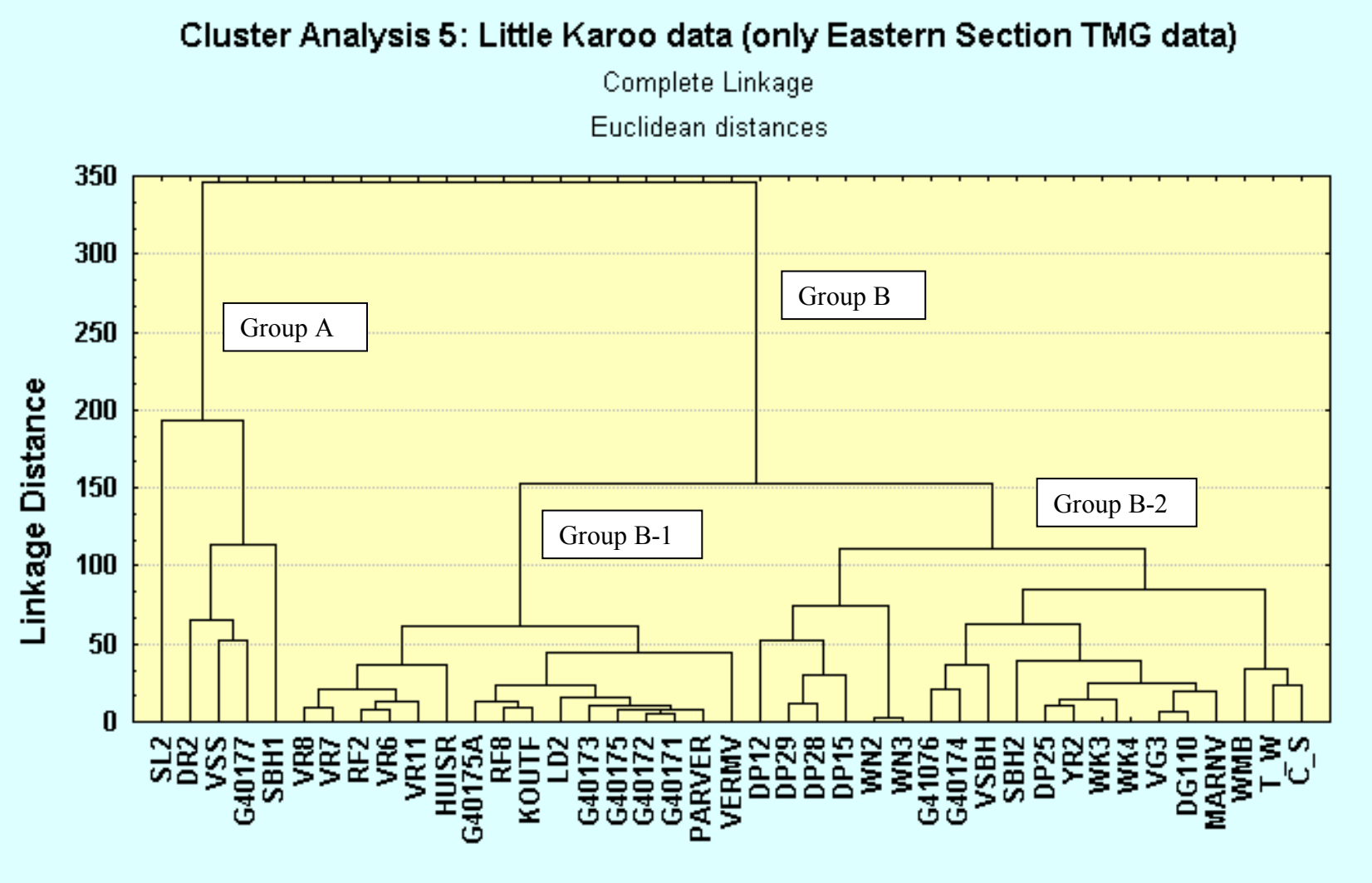

FIGURE I-8 : CLUSTER ANALYSIS, USING ONLY HYDROCHEMISTRY KAMMANASSIE MOUNTAIN

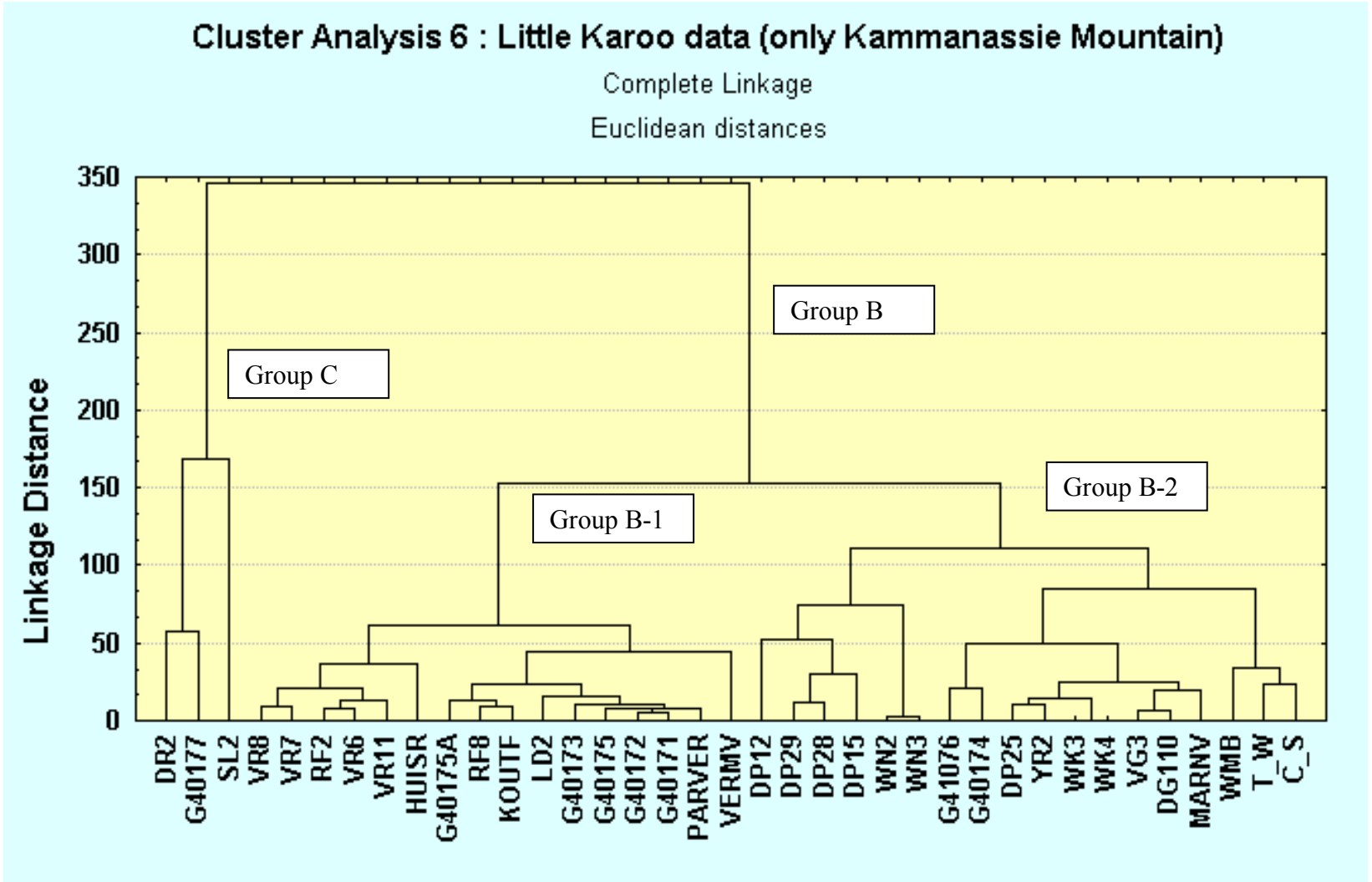

FIGURE I-9 : CLUSTER ANALYSIS, USING ONLY HYDROCHEMISTRY OF WESTERN NARDOUW AQUIFER

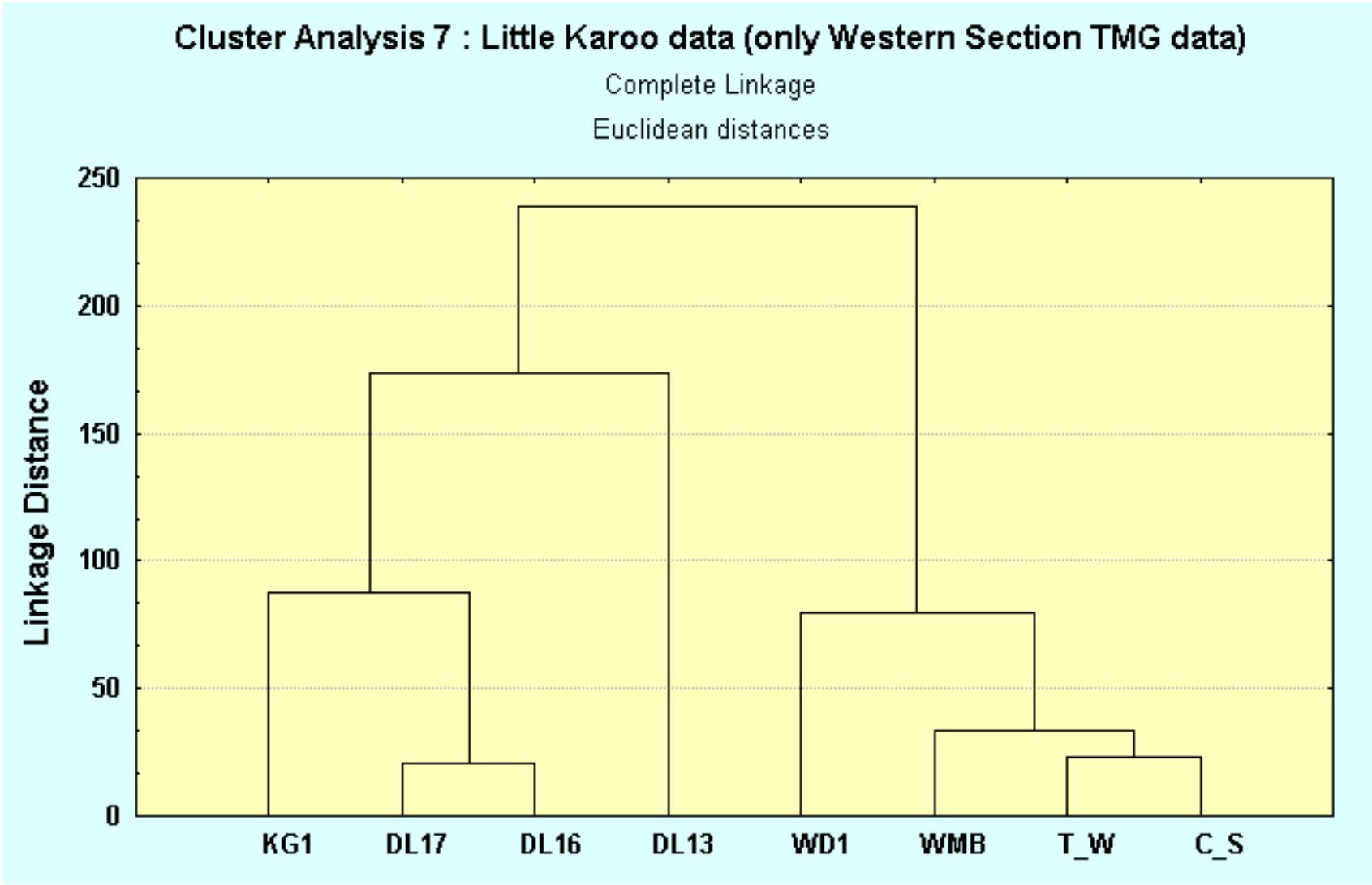

APPENDIX J: FC METHOD

FIGURE J-1: FC DATA SHEET – VR7

DATA sheet: Enter general info and data of constant rate pumping test and recovery (optional)			
Country:	RSA	Geology:	TMG - PENINSULA
Region:	KLEIN KARAOO	Depth of BH:	177
Owner:	DWAF	Water strikes:	78 and 129
X-coord:	3720760.90	Date of Test:	Sep-97
Y-coord:	41648.00	Contractor:	Callie Calitz

CONSTANT RATE TEST DATA : enter values in cells which are coloured light yellow

Borehole:		VR7									
Q (l/s)=	20					Recovery data					
t (min)	s (m)	avg s'	avg s''	avg T	avg S	Time t'	Res_s	t/t'	WI rise	s'	Rec_T
0.50	5					0.1	15.66	41401	0		
1.00	8.69					1.5	7.83	2761	7.83	7.10	
2.00	10.83	9.29	-2.00			2	6.03	2071	9.63	15.88	
2.50	11.27	5.12	-1.91	62.70	0.00E+00	2.5	4.29	1657	11.37	9.40	40.5
3.00	11.63	3.20	-2.05	106.45	0.00E+00	3.5	3.64	1184	12.02	3.18	95.8
4.00	11.92	1.99	-1.66	144.74	0.00E+00	5	3.33	829	12.33	1.20	214.9
5.00	12.04	1.34	-1.38	259.69	0.00E+00	7	3.28	592.4	12.38	0.83	329.2
7.00	12.21	0.93	-0.81	353.11	0.00E+00	9	3.11	461	12.55	0.88	612.6
9.00	12.26	0.83	-0.28	433.56	0.00E+00	12	3.07	346	12.59	0.19	#NUM!
12.00	12.33	0.83	0.02	360.37	0.00E+00	15	3.07	277	12.59	-0.19	#NUM!
120.00	13.273	0.92	0.13	353.30	0.00E+00	20	3.11	208	12.55	-0.10	#NUM!
150.00	13.305	0.96	0.18	322.31	0.00E+00	25	3.09	166.6	12.57	0.23	#NUM!
180.00	13.418	1.01	-0.10	310.34	0.00E+00	30	3.07	139	12.59	0.51	701.4
210.00	13.505	0.95	0.17	303.30	0.00E+00	35	3.015	119.3	12.65	0.80	507.0
225.00	13.5	1.01	0.77	303.30	0.00E+00	40	2.97	104.5	12.69	0.60	474.9
240.00	13.54	1.16	1.48	258.11	0.00E+00	45	2.95	93	12.71	0.61	476.0
300.00	13.625	1.59	1.16	201.23	0.00E+00	50	2.91	83.8	12.75	0.80	#DIV/0!
360.00	13.8	1.84	0.43	151.98	0.00E+00	60	2.85	70	12.81	#DIV/0!	#DIV/0!
600.00	14.372	1.88	-0.16	151.98	0.00E+00			#####	#####	#DIV/0!	#DIV/0!
1140.00	14.815	1.56	-0.45	151.98	0.00E+00			#####	#####	#DIV/0!	#DIV/0!
1380.00	14.862	1.38	0.39	151.98	0.00E+00			#####	#####	#DIV/0!	#DIV/0!
1620.00	14.958	1.50	0.56	151.98	0.00E+00			#####	#####	#DIV/0!	#DIV/0!
1740.00	14.988	1.63	0.43	147.24	0.00E+00			#####	#####	#DIV/0!	#DIV/0!

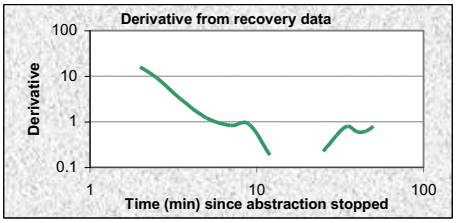

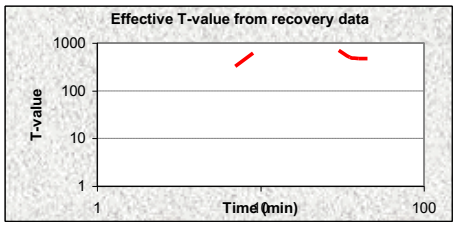

FIGURE J-2: DERIVATIVE PLOT VR7

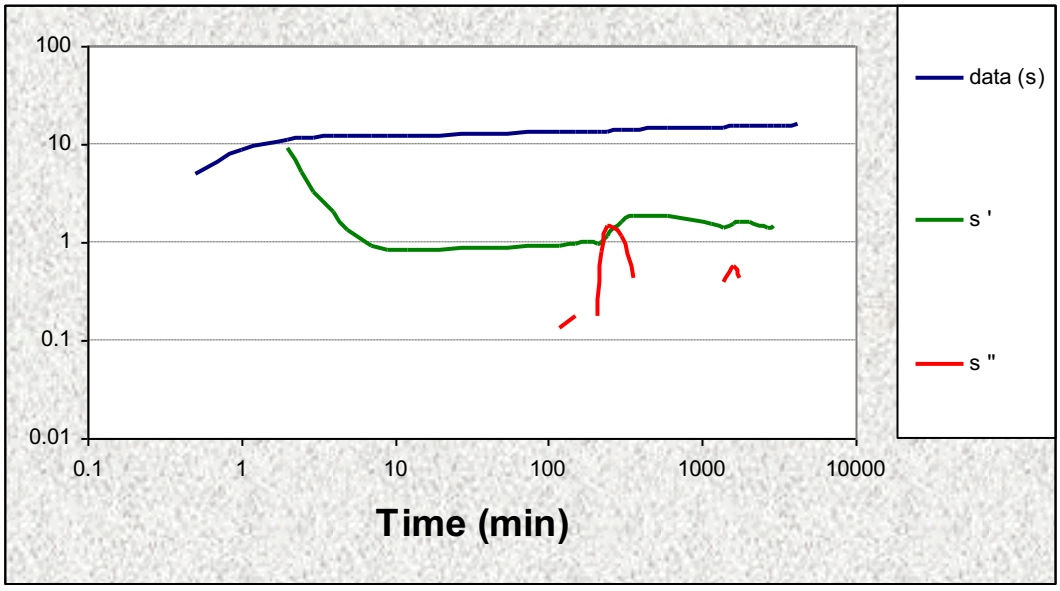

FIGURE J-3: TRANSMISSIVITY AND STORATIVITY WITH TIME – VR7

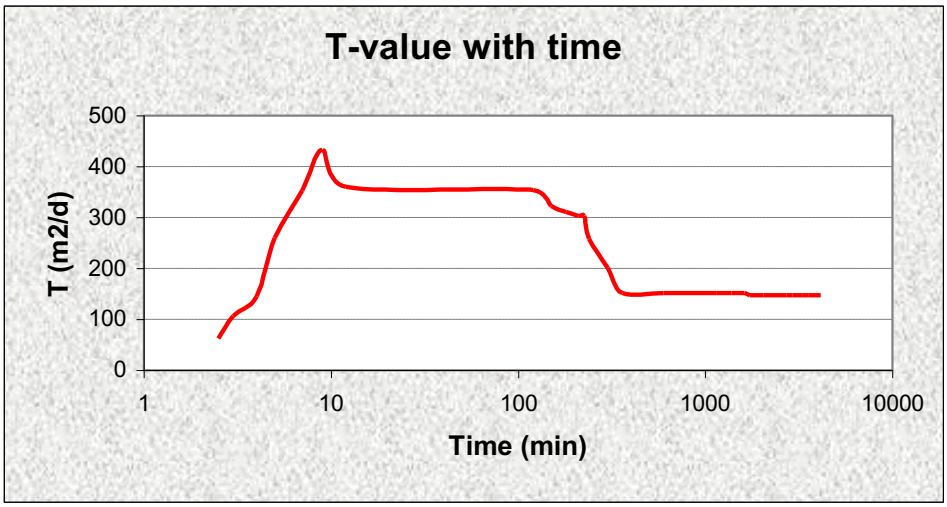

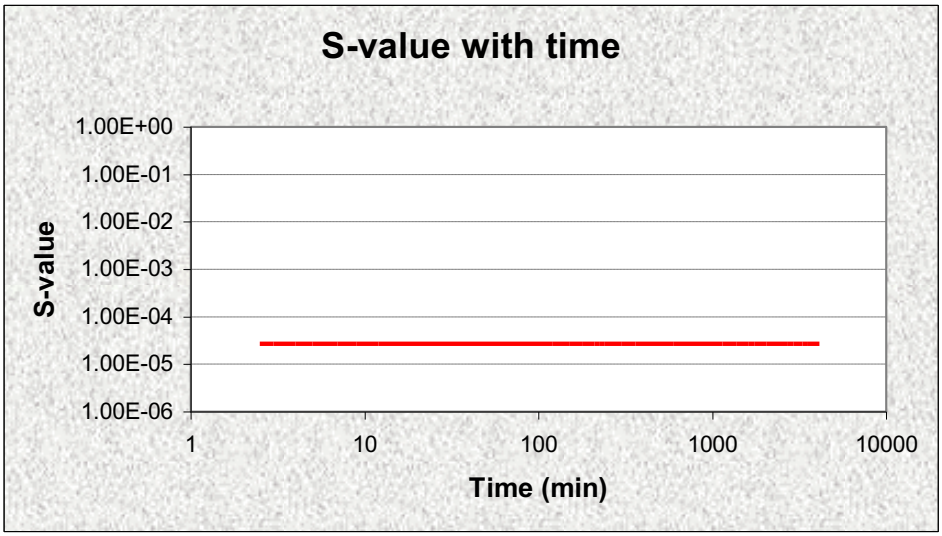

FIGURE J-4 : DIAGNOSTIC PLOTS – VR7

VR7

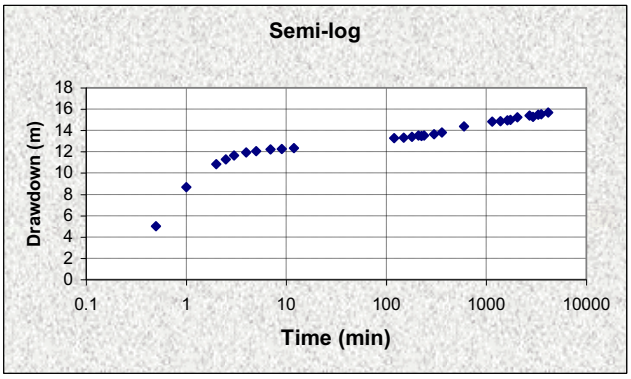

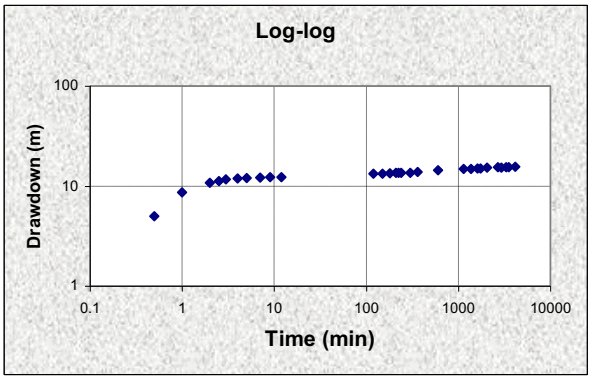

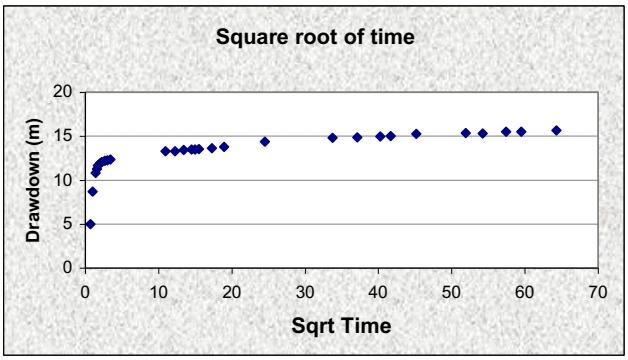

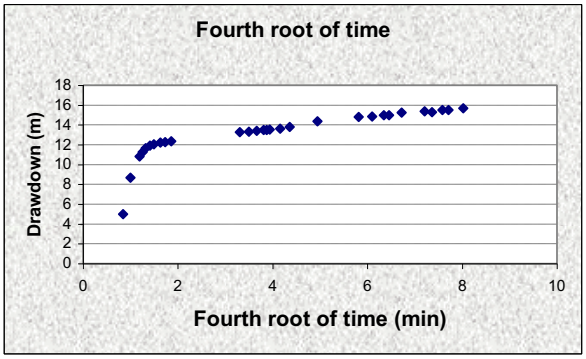

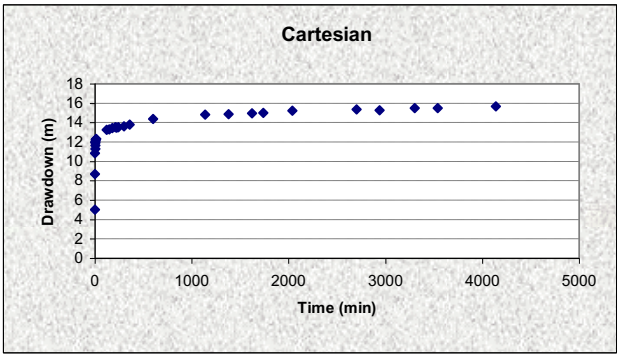

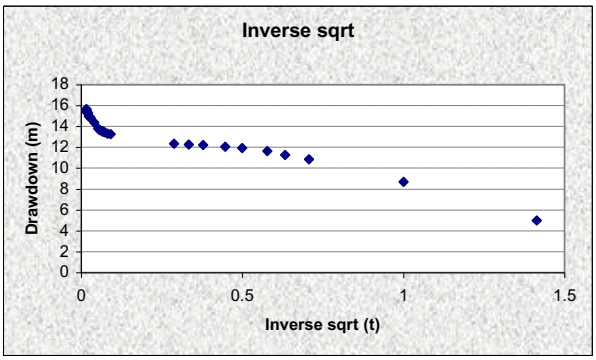

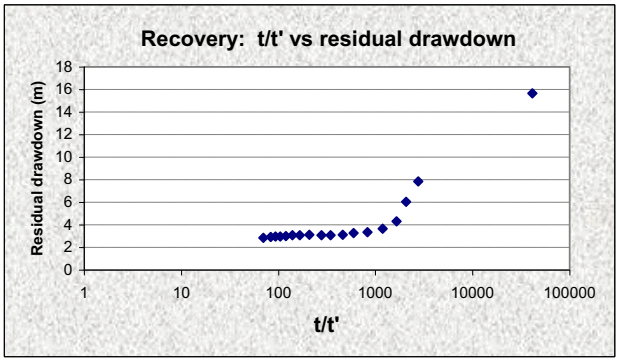

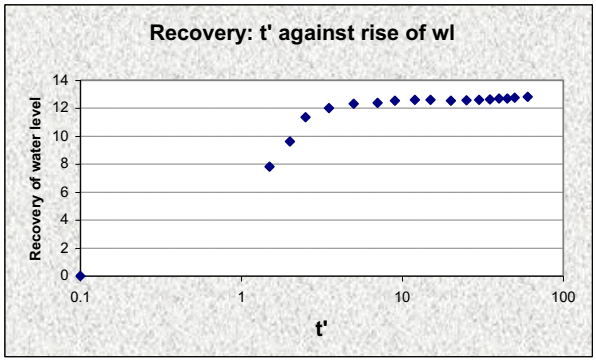

FIGURE J-5: SUSTAINABLE YIELD USING BASIC SOLUTION 68% SAFETY – VR7

FC-METHOD : Estimation of the sustainable yield of a borehole

VR7

Extrapolation time in years = (enter)	5	2628000	Extrapol.time in minutes
Effective borehole radius (r_e) = (enter)	7.16	7.16	← Est. r_e — From r(e) sheet
Q (l/s) from pumping test =	20	16.80	← Est. r_e — Qualified guess
s_a (available drawdown), sigma_s = (enter)	40		← Sigma_s from risk
Annual effective recharge (mm) =	0	40.00	s_available working drawdown(m)
t(end) and s(end) of pumping test =	4140	15.66	End time and drawdown of test
Average maximum derivative = (enter)	2.2	1.9	Estimate of average of max deriv
Average second derivative = (enter)	0.0	0.0	Estimate of average second deriv
Derivative at radial flow period = (enter)	1.88		Read from derivative graph
	T-early[m^2/d] =	168.20	Aqui. thick (m) = 20
T and S estimates from derivatives	T-late [m^2/d] =	143.74	Est. S-late = 1.10E-03
(To obtain correct S-value, use program RPTSOLV)	S-late =	1.10E-03	S-estimate could be wrong

BASIC SOLUTION

(Using derivatives + subjective information about boundaries)

(No values of T and S are necessary)

	No boundaries	Maximum influence of boundaries at long time: 1 no-flow	2 no-flow	Closed no-flow
sWell (Extrapol.time) =	21.83	27.99	34.16	52.65
Q_sust (l/s) =	36.65	28.58	23.42	15.19
	Best case	→		**Worst case**

Average Q_sust (l/s) = 24.71 with standard deviation= 9.01

WARNING!! Est. Q_sust > Q during pumping test

Suggestion:check available drawdown and rech

(If no information exists about boundaries skip advanced solution and go to final recommendation)

FIGURE J-6: SUSTAINABLE YIELD USING BASIC SOLUTION 95% SAFETY – VR7

FC-METHOD : Estimation of the sustainable yield of a borehole

VR7

Extrapolation time in years = (enter)	5	2628000	Extrapol.time in minutes
Effective borehole radius (r_e) = (enter)	7.16	7.16	← Est. r_e — From r(e) sheet
Q (l/s) from pumping test =	20	16.80	← Est. r_e — Qualified guess
s_a (available drawdown), sigma_s = (enter)	40	18	← Sigma_s from risk
Annual effective recharge (mm) =	0	22.00	s_available working drawdown(m)
t(end) and s(end) of pumping test =	4140	15.66	End time and drawdown of test
Average maximum derivative = (enter)	2.2	1.9	Estimate of average of max deriv
Average second derivative = (enter)	0.0	0.0	Estimate of average second deriv
Derivative at radial flow period = (enter)	1.88		Read from derivative graph
	T-early[m^2/d] =	168.20	Aqui. thick (m) = 20
T and S estimates from derivatives	T-late [m^2/d] =	143.74	Est. S-late = 1.10E-03
(To obtain correct S-value, use program RPTSOLV)	S-late =	1.10E-03	S-estimate could be wrong

BASIC SOLUTION

(Using derivatives + subjective information about boundaries)

(No values of T and S are necessary)

	No boundaries	Maximum influence of boundaries at long time: 1 no-flow	2 no-flow	Closed no-flow
sWell (Extrapol.time) =	21.83	27.99	34.16	52.65
Q_sust (l/s) =	20.16	15.72	12.88	8.36
	Best case	→		**Worst case**

Average Q_sust (l/s) = 13.59 with standard deviation= 4.96

(If no information exists about boundaries skip advanced solution and go to final recommendation)

FINAL RECOMMENDED ABSTRACTION RATE

Abstraction rate (l/s) for 24 hr/d = (enter)	20.00
Total amount of water allowed to be abstracted per month (m^3) =	51840

COMMENTS

Q_sust with 68% safety = 24.71

Q_sust with 95% safety = 13.6

FIGURE J-7: SUSTAINABLE YIELD USING ADVANCED SOLUTION 1 – SINGLE BARRIER (C/S) – VR7

ADVANCED SOLUTION

(Using derivatives+ knowledge on boundaries and other boreholes)

(Late T-and S-values a priori + distance to boundary)

T-late [m^2/d] = (enter) →	143.74				
S-late = (enter) →	1.00E-03				
1. BOUNDARY INFORMATION (choose a or b)	(Code =9999 = dummy value if not applicable)				
(a) Barrier (no-flow) boundaries →	Closed Square	Single Barrier	Intersect. 90°	2 Parallel Barriers	
Bound. distance a[meter] : (enter)	9999	2200	9999	9999	
Bound. distance b[meter] : (enter)			9999	9999	
s_Bound(t = Extrapol.time) [m] =	5.02	3.29	1.73	1.61	
(b) Fix head boundary + no-flow →	Closed Fix	Single Fix	90°Fix+no-flow	// Fix+no-flow	
Bound. distance to fix head a[meter] : (enter)	9999	9999	9999	9999	
Bound. distance to no-flow b[meter] : (enter)			9999	9999	
s_Bound(t = Extrapol.time) [m] =	-1.80	-0.70	-0.64	-0.19	
2. INFLUENCE OF OTHER BOREHOLES →	Q (l/s)	r (m)	u_r	W(u,r)	
BH1			0.00E+00	#NUM!	
BH2			0.00E+00	#NUM!	
s_(influence of BH1,BH2) =	0.00	0.00	4.89E-08	16.26	
SOLUTION INCLUDING BOUNDS AND BH's					
Fix head + No-flow : Q_sust (l/s) =	9999.00	9999.00	9999.00	9999.00	
No-flow : Q_sust (l/s) =	9999.00	31.86	9999.00	9999.00	
Enter selected Q for risk analysis = (enter) →	30.00	Sigma_s =	3.370		

(Go to Risk sheet and perform risk analysis from which sigma_s will be estimated : only for barrier boundaries)

RISK ANALYSIS – ADVANCED SOLUTION 1 – VR7

Single barrier boundary: Use = 2200

SENSITIVITY CALCULATION:

	T	S	a
Numerical Derivative Factor :	0.01	0.01	0.01
s_Theis(t = Extrapol.time) [m]	23.34	22.28	23.44	23.34
s_Bound(t = Extrapol.time) [m] =	4.93	4.76	5.03	4.90
s_Total = s_Theis+s_Boundary [m]	28.27	27.03	28.47	28.24

Sensitivities:

ds/dY (t = Extrapol.time):	-2.49E+01		
ds/dW (t = Extrapol.time):		-2.85E+00	
ds/da (t = Extrapol.time):			-1.27E-03

Uncertainties:	%	Value
% error of late T-value = (enter)	33	47.4336
sigma (Y)		0.103
% error of late S-value = (enter)	100	1.00E-03
sigma (W)		0.693
% error in bound. distance (a) = (enter)	33	726

Result:

sigma (s_Total, t= Extrapol.time) [m] =	3.37

ADVANCE SOLUTION 1: SINGLE BOUNDARY – VR7

FINAL RECOMMENDED ABSTRACTION RATE

Abstraction rate (l/s) for 24 hr/d = (enter)	25.00
Total amount of water allowed to be abstracted per month (m^3) =	64800

COMMENTS

Q_sust with 68% safety =	29.2
Q_sust with 95% safety =	26.5

FIGURE J-8: ADVANCED SOLUTION 2: TWO PARALLEL BOUNDARIES – VR7

ADVANCED SOLUTION

(Using derivatives+ knowledge on boundaries and other boreholes)

(Late T-and S-values a priori + distance to boundary)

T-late [m²/d] = (enter) →	143.74				
S-late = (enter) →	1.00E-03				
1. BOUNDARY INFORMATION (choose a or b)	(Code =9999 = dummy value if not applicable)				
(a) Barrier (no-flow) boundaries →	Closed Square	Single Barrier	Intersect. 90°	2 Parallel Barriers	
Bound. distance a[meter] : (enter)	9999	9999	9999	16000	
Bound. distance b[meter] : (enter)			9999	2200	
s_Bound(t = Extrapol.time) [m] =	5.02	0.70	1.73	3.87	
(b) Fix head boundary + no-flow →	Closed Fix	Single Fix	90°Fix+no-flow	// Fix+no-flow	
Bound. distance to fix head a[meter] : (enter)	9999	9999	9999	9999	
Bound. distance to no-flow b[meter] : (enter)			9999	9999	
s_Bound(t = Extrapol.time) [m] =	-1.80	-0.70	-0.64	-0.19	
2. INFLUENCE OF OTHER BOREHOLES →	Q (l/s)	r (m)	u_r	W(u,r)	
BH1			0.00E+00	#NUM!	
BH2			0.00E+00	#NUM!	
s_(influence of BH1,BH2) =	0.00	0.00	4.89E-08	16.26	
SOLUTION INCLUDING BOUNDS AND BH's					
Fix head + No-flow : Q_sust (l/s) =	9999.00	9999.00	9999.00	9999.00	
No-flow : Q_sust (l/s) =	9999.00	9999.00	9999.00	25.89	
Enter selected Q for risk analysis = (enter) →	26.00	Sigma_s =	4.026		

(Go to Risk sheet and perform risk analysis from which sigma_s will be estimated : only for barrier boundaries)

RISK ANALYSIS ADVANCED SOLUTION 2 – VR7

Two parallel barrier boundaries : Use = 16000 (T), 2200 (S)

SENSITIVITY CALCULATION:		T	S	a	b
Numerical Derivative Factor		0.01	0.01	0.01	0.01
s_Theis(t = Extrapol.time) [m]	20.23	19.31	20.31	20.23	20.23
s_Bound(t = Extrapol.time) [m] =	5.37	5.26	5.59	5.34	5.35
s_Total = s_Theis + s_Boundary [m]	25.60	24.57	25.91	25.57	25.58
Sensitivities:					
ds/dY (t = Extrapol.time):		-2.08E+01			
ds/dW (t = Extrapol.time):			-4.44E+00		
ds/da (t = Extrapol.time):				-2.27E-04	
ds/db (t = Extrapol.time):					-1.15E-03

Uncertainties:	**%**	**Value**
% error of late T-value = (enter)	**33**	47.4336
sigma (Y)		0.103
% error of late S-value = (enter)	**100**	1.00E-03
sigma (W)		0.693
% error in bound. distance (a) = (enter)	**33**	5280
% error in bound. distance (b) = (enter)	**33**	726
Result:		
sigma (s_Total, t= Extrapol.time) [m] =	4.03	

RECOMMENDED ABSTRACTION FROM ADVANCED SOLUTION 2 – VR7

FINAL RECOMMENDED ABSTRACTION RATE

Abstraction rate (l/s) for 24 hr/d = (enter)	26.00
Total amount of water allowed to be abstracted per month (m³) =	67392

COMMENTS

Q_sust with 68% safety = 28

Q_sust with 95% safety = 25

FIGURE J-9: ADVANCED SOLUTION 3 – VR7

ADVANCED SOLUTION

(Using derivatives+ knowledge on boundaries and other boreholes)

(Late T-and S-values a priori + distance to boundary)

T-late [m^2/d] = (enter) →	143.74				
S-late = (enter) →	1.00E-03				
1. BOUNDARY INFORMATION (choose a or b)	(Code =9999 = dummy value if not applicable)				
(a) Barrier (no-flow) boundaries →	Closed Square	Single Barrier	Intersect. 90°	2 Parallel Barriers	
Bound. distance a[meter] : (enter)	9999	9999	9999	16000	
Bound. distance b[meter] : (enter)			9999	2200	
s_Bound(t = Extrapol.time) [m] =	5.02	0.70	1.73	3.87	
(b) Fix head boundary + no-flow →	Closed Fix	Single Fix	90°Fix+no-flow	// Fix+no-flow	
Bound. distance to fix head a[meter] : (enter)	9999	9999	9999	9999	
Bound. distance to no-flow b[meter] : (enter)			9999	9999	
s_Bound(t = Extrapol.time) [m] =	-1.80	-0.70	-0.64	-0.19	
2. INFLUENCE OF OTHER BOREHOLES →	Q (l/s)	r (m)	u_r	W(u,r)	
BH1	6	400	1.52E-04	8.21	
BH2	7.4	400	1.52E-04	8.21	
s_(influence of BH1,BH2) =	2.36	2.91	4.89E-08	16.26	
SOLUTION INCLUDING BOUNDS AND BH's					
Fix head + No-flow : Q_sust (l/s) =	9999.00	9999.00	9999.00	9999.00	
No-flow : Q_sust (l/s) =	9999.00	9999.00	9999.00	25.84	
Enter selected Q for risk analysis = (enter) →	26.00	Sigma_s =	4.026		

(Go to Risk sheet and perform risk analysis from which sigma_s will be estimated : only for barrier boundaries)

RISK ANALYSIS ADVANCED SOLUTION 3 – VR7

Two parallel barrier boundaries : Use = 16000 (T) 2200 (S)

SENSITIVITY CALCULATION:

		T	S	a	b
Numerical Derivative Factor		0.01	0.01	0.01	0.01
s_Theis(t = Extrapol.time) [m]	20.23	19.31	20.31	20.23	20.23
s_Bound(t = Extrapol.time) [m] =	5.37	5.26	5.59	5.34	5.35
s_Total = s_Theis + s_Boundary [m]	25.60	24.57	25.91	25.57	25.58
Sensitivities:					
ds/dY (t = Extrapol.time):		-2.08E+01			
ds/dW (t = Extrapol.time):			-4.44E+00		
ds/da (t = Extrapol.time):				-2.27E-04	
ds/db (t = Extrapol.time):					-1.15E-03

	%	Value
Uncertainties:		
% error of late T-value = (enter)	33	47.4336
sigma (Y)		0.103
% error of late S-value = (enter)	100	1.00E-03
sigma (W)		0.693
% error in bound. distance (a) = (enter)	33	5280
% error in bound. distance (b) = (enter)	33	726
Result:		
sigma (s_Total, t= Extrapol.time) [m] =		4.03

RESULTS – ADVANCED SOLUTION 3 – VR7

FINAL RECOMMENDED ABSTRACTION RATE

Abstraction rate (l/s) for 24 hr/d = (enter)	20.00
Total amount of water allowed to be abstracted per month (m^3) =	51840

COMMENTS

Q_sust with 68% safety = 23

Q_sust with 95% safety = 20

FIGURE J-10: ADVANCED SOLUTION WORST CASE SCENARIO – VR7

ADVANCED SOLUTION

(Using derivatives+ knowledge on boundaries and other boreholes)

(Late T-and S-values a priori + distance to boundary)

T-late [m^2/d] = (enter) →	143.74			
S-late = (enter) →	1.00E-03			
1. BOUNDARY INFORMATION (choose a or b)	(Code =9999 = dummy value if not applicable)			
(a) Barrier (no-flow) boundaries →	Closed Square	Single Barrier	Intersect. 90°	2 Parallel Barriers
Bound. distance a[meter] : (enter)	4000	9999	9999	9999
Bound. distance b[meter] : (enter)			9999	9999
s_Bound(t = Extrapol.time) [m] =	44.65	0.70	1.73	1.61
(b) Fix head boundary + no-flow →	Closed Fix	Single Fix	90°Fix+no-flow	// Fix+no-flow
Bound. distance to fix head a[meter] : (enter)	9999	9999	9999	9999
Bound. distance to no-flow b[meter] : (enter)			9999	9999
s_Bound(t = Extrapol.time) [m] =	-1.80	-0.70	-0.64	-0.19
2. INFLUENCE OF OTHER BOREHOLES →	Q (l/s)	r (m)	u_r	W(u,r)
BH1	6	400	1.52E-04	8.21
BH2	7.4	400	1.52E-04	8.21
s_(influence of BH1,BH2) =	2.36	2.91	4.89E-08	16.26
SOLUTION INCLUDING BOUNDS AND BH's				
Fix head + No-flow : Q_sust (l/s) =	9999.00	9999.00	9999.00	9999.00
No-flow : Q_sust (l/s) =	11.15	9999.00	9999.00	9999.00
Enter selected Q for risk analysis = (enter) →	11.00	Sigma_s =	26.021	

(Go to Risk sheet and perform risk analysis from which sigma_s will be estimated : only for barrier boundaries)

RISK ANALYSIS – WORSE CASE SCENARIO – VR7

Closed square boundary: Use = 4000

SENSITIVITY CALCULATION:

	T	S	a
Numerical Derivative Factor	0.01	0.01	0.01
s_Theis(t = Extrapol.time) [m]	8.17	8.59	8.56
s_Bound(t = Extrapol.time) [m] =	24.66	26.46	24.04
s_total = s_Theis+s_Boundary [m]	32.83	35.06	32.59
Sensitivities:			
ds/dY (t = Extrapol.time):	-5.87E+00		
ds/dW (t = Extrapol.time):		-2.81E+01	
ds/da (t = Extrapol.time):			-1.31E-02

	%	Value
Uncertainties:		
% error of late T-value = (enter)	33	47.4336
sigma (Y)		0.103
% error of late S-value = (enter)	100	1.00E-03
sigma (W)		0.693
% error in bound. distance (a) = (enter)	33	1320
Result:		
sigma (s_total, t= Extrapol.time) [m] =	26.02	

RECOMMENDED YIELD – WORSE CASE SCENARIO – VR7

FINAL RECOMMENDED ABSTRACTION RATE

Abstraction rate (l/s) for 24 hr/d = (enter)	1.00
Total amount of water allowed to be abstracted per month (m^3) =	2592

COMMENTS

Q_sust with 68% safety =	3.9
Q_sust with 95% safety =	-3.36

FIGURE J-11: COOPER JACOB – VR7

Cooper-Jacob method

VR7

T(m^2/d) =	276.2	r_e (m)=	7.16
S =	1.58E-12	Q (l/s) =	20

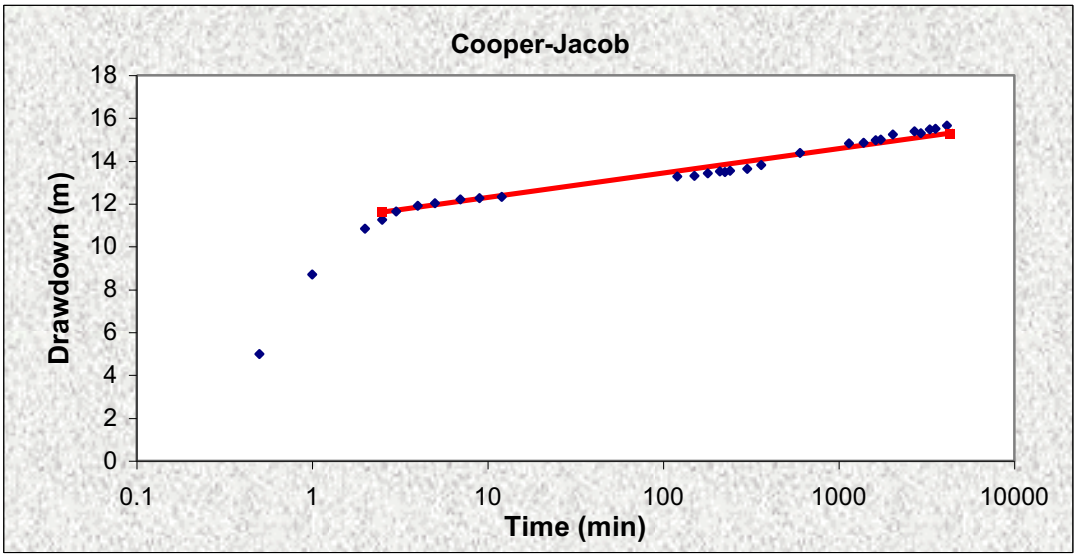

FIGURE J-12: STEP DRAWDOWN ANALYSIS

VR7

STEP DRAWDOWN AND MULTIRATE ANALYSIS

Enter field step test data at bottom of sheet

STEP DRAWDOWN	no	MULTI RATE	yes

	Q (l/s)	Q (m^3/d)	s_i (m)	Sigma s_i	Sigma s_i/Q_i
Step 1	2.8	241.92	1.26	1.26	0.00520833
Step 2	6.5	561.6	2.8	2.8	0.00498575
Step 3	9.8	846.72	4.86	4.86	0.0057398
Step 4	15.3	1321.92	7.72	7.72	0.00583999
Step 5	20.2	1745.28	10.26	10.26	0.00587871
Step 6	25.9	2237.76	14.21	14.21	0.0063501
Step 7	35	3024	20.25	20.25	0.00669643

B =	4.9E-03	d/m^2
C =	5.9E-07	d^2/m^5

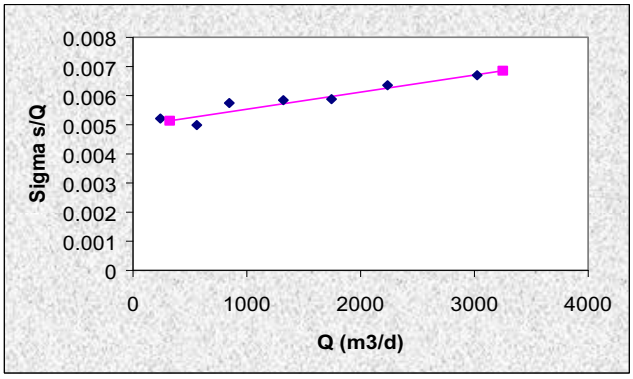

Q (l/s)	Well effiency(%)
2.8	97
6.5	94
9.8	91
15.3	86
20.2	83
25.9	79
35	74

FIGURE J-12 (CONTINUED): STEP DRAWDOWN TEST DATA – VR7

Step test data

	Step1	Step1	Step3	Step4	Step5	Step6	Step7
Q (l/s) =	2.8	6.5	9.8	15.8	20.2	25.9	35
t(min)	s (m)	s (m)	s (m)	s (m)	s (m)	s (m)	s (m)
0.1	0	1.26	2.8	4.86	7.72	10.26	14.21
0.5	1.35	1.93	3.54	6.24	8.7	11.61	16.37
1	1.42	2.72	3.97	6.7	9.13	12.44	17.6
1.5	1.34	2.62	4.29	6.93	9.44	12.8	18.08
2	1.23	2.58	4.32	7.11	9.62	13.06	18.44
2.5	1.09	2.58	4.39	7.2	9.78	13.22	18.7
3	1.01	2.59	4.41	7.23	9.86	13.35	18.87
3.5	1.01	2.59	4.42	7.27	9.96	13.41	19.08
4	1.02	2.6	4.43	7.32	10.03	13.46	19.11
4.5	1.03	2.6	4.44	7.32	10.07	13.54	19.13
5	1.03	2.61	4.44	7.34	10.11	13.57	19.23
7	1.06	2.65	4.45	7.41	10.13	13.64	19.26
9	1.09	2.66	4.49	7.45	10.15	13.72	19.44
12	1.14	2.69	4.59	7.51	10.16	13.82	19.7
15	1.16	2.7	4.6	7.53	10.17	13.91	19.74
20	1.19	2.71	4.65	7.57	10.19	13.98	19.77
25	1.19	2.73	4.78	7.6	10.22	14.02	19.83
30	1.23	2.75	4.78	7.62	10.23	14.05	20.05
35	1.25	2.76	4.78	7.65	10.25	14.11	20.05
40	1.25	2.77	4.79	7.66	10.25	14.13	20.05
45	1.25	2.78	4.82	7.68	10.25	14.16	20.07
50	1.25	2.76	4.85	7.68	10.25	14.18	20.19
60	1.26	2.8	4.86	7.72	10.26	14.21	20.25

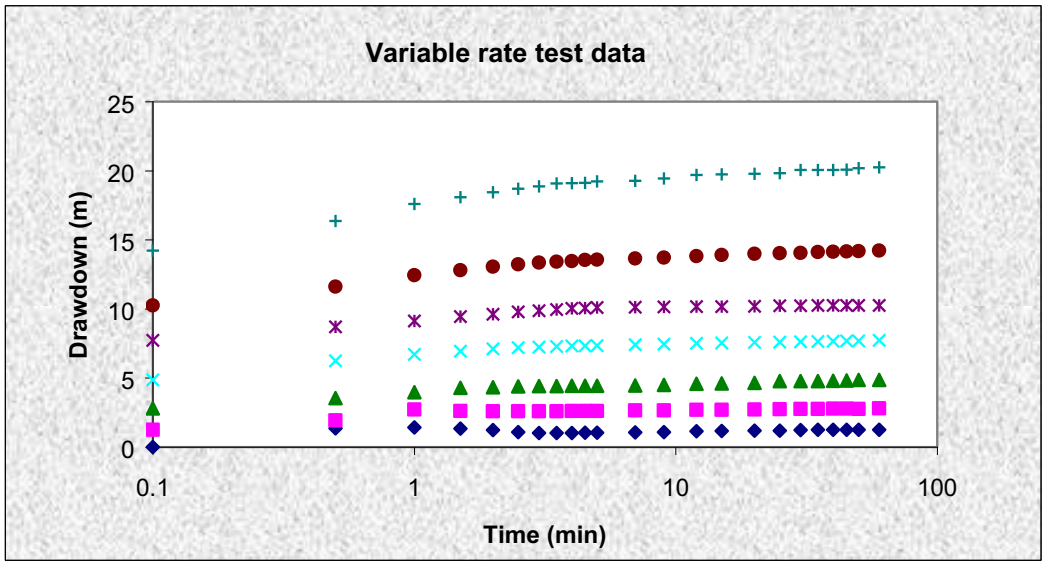

FIGURE J-13: FC DATA SHEET– VR6

DATA sheet: Enter general info and data of constant rate pumping test and recovery (optional)

Country:	SOUTH AFRICA	**Geology:**	TMG PENINSULA
Region:	LITTLE KAROO	**Depth of BH:**	250
Owner:	DWAF	**Water strikes:**	228
X-coord:	3720431.00	**Date of Test:**	Sep-97
Y-coord:	42082.90	**Contractor:**	CALLIE CALITZ

CONSTANT RATE TEST DATA : enter values in cells which are coloured light yellow

Borehole:		**VR6**									
Q (l/s)=	15.4					**Recovery data**					
t (min)	**s (m)**	avg s'	avg s"	avg T	avg S	**Time t'**	**Res_s**	t/t'	WI rise	s'	Rec_T
1.00	13.32					0.1	82.23	43201	1.22		
1.50	17.19					0.5	67.52	8641	15.93	26.31	
2.00	20.6	39.46	-1.17			1	54.8	4321	28.65	46.59	
2.50	23.79	27.17	-1.54	8.21	6.51E-06	1.5	45.04	2881	38.41	58.61	4.4
3.00	26.59	21.03	-2.10	10.59	6.51E-06	2	37.09	2161	46.36	61.16	4.2
3.50	26.97	13.91	-2.34	17.84	6.51E-06	2.5	31.5	1729	51.95	53.21	4.5
4.00	27.61	10.52	-0.14	28.36	6.51E-06	3	27.75	1441	55.7	48.02	5.8
4.50	27.94	12.47	1.82	24.50	6.51E-06	3.5	24.48	1235	58.97	29.48	10.2
5.00	28.46	19.95	2.48	10.72	6.51E-06	4	24.13	1081	59.32	9.56	13.7
7.00	30.39	32.07	1.08	6.92	8.88E-06	5	23.03	865	60.42	19.98	14.7
12.00	42.51	37.85	-0.01	5.90	1.35E-05	7	19.38	618.1	64.07	23.73	12.0
15.00	46.67	34.95	-0.68	6.52	1.35E-05	9	16.99	481	66.46	17.64	13.4
20.00	49.86	26.68	-1.56	8.80	1.35E-05	12	15.23	361	68.22	14.37	17.6
25.00	52.86	17.14	-2.77	13.26	1.35E-05	15	13.8	289	69.65	10.53	22.2
30.00	53.1	9.06	-1.99	24.59	1.35E-05	20	12.86	217	70.59	8.73	24.6
35.00	53.61	8.23	1.64	59.46	1.35E-05	25	11.85	173.8	71.6	10.56	24.3
40.00	53.62	12.35	5.09	17.72	1.35E-05	30	11	145	72.45	10.94	22.7
45.00	53.92	28.70	5.10	7.27	1.47E-05	35	10.25	124.4	73.2	10.66	22.9
50.00	57.27	43.22	1.75	4.74	3.53E-05	40	9.67	109	73.78	10.35	23.5
60.00	62.26	41.10	-1.49	4.74	3.53E-05	45	9.12	97	74.33	10.02	24.5
70.00	64.11	27.76	-2.88	4.74	3.53E-05	50	8.7	87.4	74.75	9.46	25.5
80.00	64.89	18.08	-2.81	4.74	3.53E-05	60	7.94	73	75.51	9.18	26.1
90.00	65.65	13.30	-1.83	4.74	3.53E-05	70	7.36	62.71	76.09	9.35	25.9
100.00	65.98	11.46	-1.02	4.74	3.53E-05	80	6.77	55	76.68	9.72	28.4
120.00	67.37	9.92	-0.77	4.74	3.53E-05	90	6.3	49	77.15	6.95	32.9
150.00	67.77	8.44	-0.47	4.74	3.53E-05	110	5.79	40.27	77.66	6.00	39.7
200.00	68.94	8.07	0.14	4.74	3.53E-05	140	5.15	31.86	78.3	5.54	40.7
250.00	69.63	8.80	0.50	4.74	3.53E-05	190	4.47	23.74	78.98	6.43	38.8
300.00	69.9	10.09	0.38	4.74	3.53E-05	240	3.63	19	79.82	6.92	45.2
400.00	72.44	10.29	0.10	4.74	3.53E-05	290	3.21	15.9	80.24	3.52	54.6
500.00	72.59	10.60	0.56	4.74	3.53E-05	390	2.87	12.08	80.58	3.64	65.1
600.00	73.27	12.33	0.79	4.74	3.53E-05	490	2.37	9.816	81.08	4.10	68.9
700.00	74.2	13.83	0.11	4.74	3.53E-05	590	2.14	8.322	81.31	2.96	76.2
800.00	76.01	13.35	-1.27	4.74	3.53E-05	690	1.93	7.261	81.52	2.69	92.9
900.00	76.16	10.28	-1.68	4.74	3.53E-05	790	1.8	6.468	81.65	2.26	108.7
1000.00	75.8	9.09	-1.02	4.74	3.53E-05	890	1.68	5.854	81.77	1.85	129.7
1100.00	77.58	8.34	-1.71	4.74	3.53E-05	990	1.62	5.364	81.83	1.59	135.1
1300.00	76.77	5.70	-2.97	4.74	3.53E-05	1090	1.54	4.963	81.91	2.00	127.7
1440.00	78.16	4.25	#NUM!	4.74	3.53E-05	1190	1.46	4.63	81.99	2.19	119.6
1560.00	77.65	#NUM!	#NUM!	4.74	3.53E-05	1290	1.38	4.349	82.07	1.93	128.2
1680.00	77.42	#NUM!	#NUM!	-28.84	3.53E-05	1390	1.33	4.108	82.12	1.62	111.8
1800.00	78.36	#NUM!	#NUM!	-28.84	3.53E-05	1530	1.26	3.824	82.19	3.30	91.8
1920.00	75.89	#NUM!	#NUM!	-28.84	3.53E-05	2010	0.82	3.149	82.63	3.49	86.1
2040.00	77.75	27.30	#NUM!	-28.84	3.53E-05	2148	0.76	3.011	82.69	1.97	90.0
2160.00	79.55	40.64	1.11	-28.84	3.53E-05	2340	0.69	2.846	82.76	2.89	108.4
2280.00	80.35	32.33	-5.47	-28.84	3.53E-05	2560	0.54	2.688	82.91	1.99	#NUM!
2400.00	81.17	22.99	-4.80	-28.84	3.53E-05	2920	0.49	2.479	82.96	-2.34	#DIV/0!
2520.00	80.72	19.64	-2.89	-28.84	3.53E-05	3500	0.84	2.234	82.61	#DIV/0!	#DIV/0!
2640.00	81.65	17.41	-8.02	-28.84	3.53E-05			#####	#####	#DIV/0!	#DIV/0!
2760.00	82.27	9.71	-16.36	-28.84	3.53E-05			#####	#####	#DIV/0!	#DIV/0!
2880.00	82.08	4.28	#NUM!	-28.84	3.53E-05			#####	#####	#DIV/0!	#DIV/0!
3000	81.8	#NUM!	#NUM!	-28.84	3.53E-05			#####	#####	#DIV/0!	#DIV/0!
3120	82.49	#NUM!	#NUM!	-33.31	3.53E-05			#####	#####	#DIV/0!	#DIV/0!
3240	82.03	#NUM!	#NUM!	-33.31	3.53E-05			#####	#####	#DIV/0!	#DIV/0!
3360	81.15	#NUM!	#NUM!	-163.79	3.53E-05			#####	#####	#DIV/0!	#DIV/0!
3480	82.09	#NUM!	#NUM!	-163.79	3.53E-05			#####	#####	#DIV/0!	#DIV/0!
3600	82.25	27.11	#NUM!	-163.79	3.53E-05			#####	#####	#DIV/0!	#DIV/0!
3720	82.78	20.48	#NUM!	-163.79	3.53E-05			#####	#####	#DIV/0!	#DIV/0!
3840	83.45	#NUM!	#NUM!	-163.79	3.53E-05			#####	#####	#DIV/0!	#DIV/0!
3960	83.25	#NUM!	#NUM!	-163.79	3.53E-05			#####	#####	#DIV/0!	#DIV/0!
4080	82.53	#NUM!	#NUM!	-163.79	3.53E-05			#####	#####	#DIV/0!	#DIV/0!
4200	82.38	#NUM!	#NUM!	-163.79	3.53E-05			#####	#####	#DIV/0!	#DIV/0!
4320	82.23	#NUM!	#NUM!	-163.79	3.53E-05			#####	#####	#DIV/0!	#DIV/0!

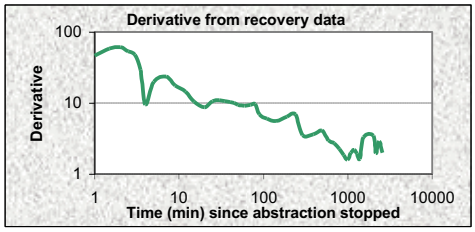

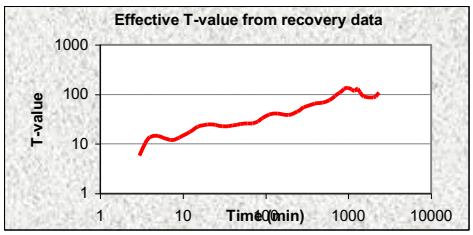

FIGURE J-14: DIAGNOSTIC PLOTS VR6

DIAGNOSTIC PLOTS

VR6

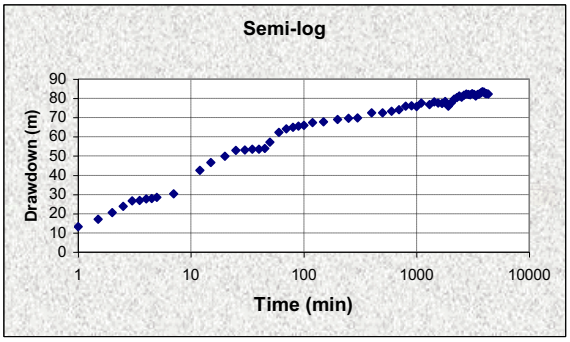

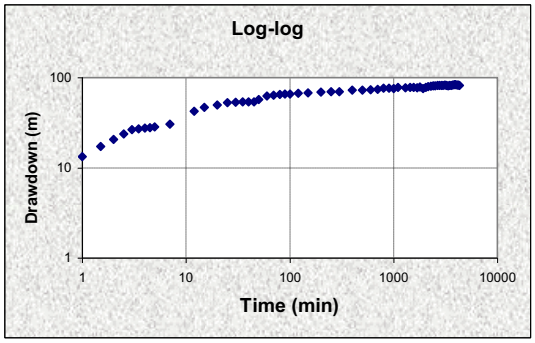

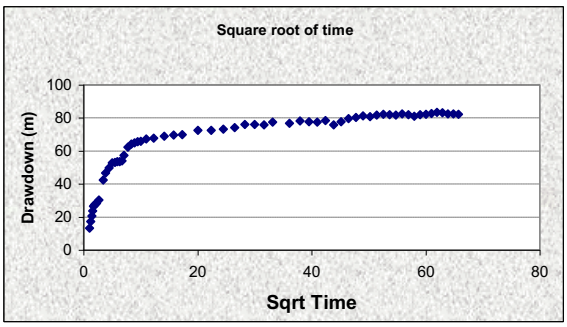

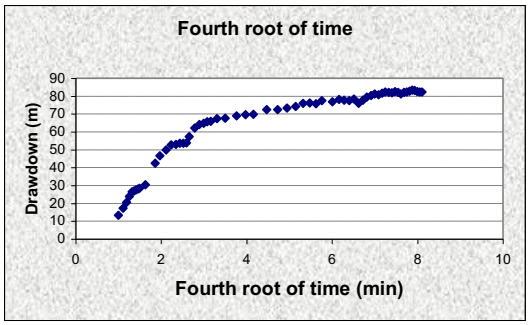

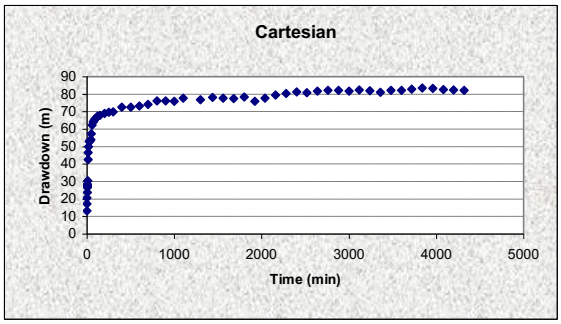

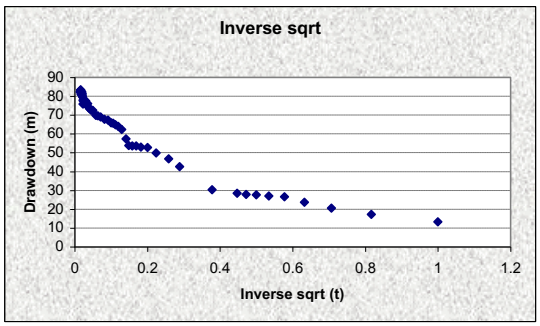

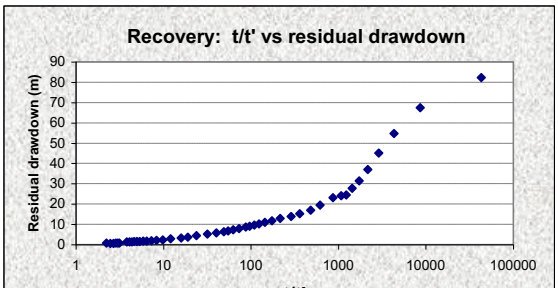

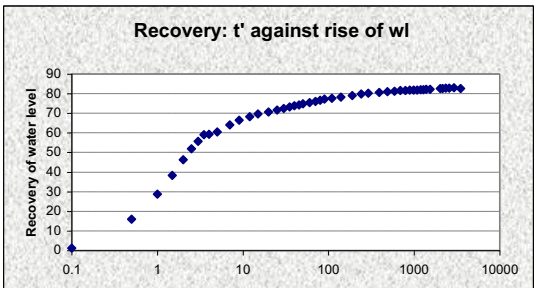

FIGURE J-15: STEP DRAWDOWN TEST – VR6

VR6

STEP DRAWDOWN AND MULTIRATE ANALYSIS

Enter field step test data at bottom of sheet

STEP DRAWDOWN	no	MULTI RATE	yes

	Q (l/s)	Q (m^3/d)	s_i (m)	Sigma s_i	Sigma s_i/Q_i
Step 1	2.4	207.36	4	4	0.01929012
Step 2	5	432	9.58	9.58	0.02217593
Step 3	6.7	578.88	16.22	16.22	0.02801962
Step 4	8.6	743.04	22.78	22.78	0.03065784
Step 5	14.3	1235.52	47.33	47.33	0.03830776
Step 6	20.8	1797.12	92.99	92.99	0.0517439
Step 7		0			0

B =	1.4E-02	d/m^2
C =	2.1E-05	d^2/m^5

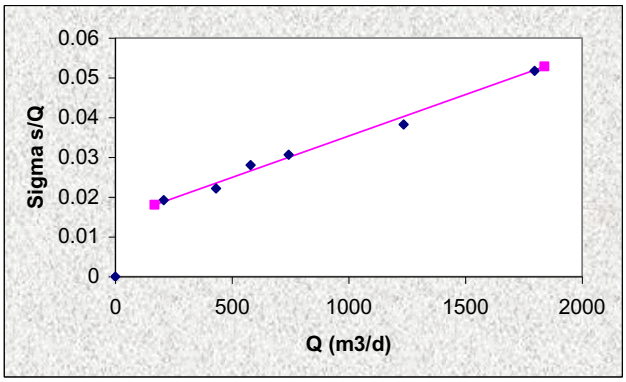

Q (l/s)	Well effiency(%)
2.4	77
5	62
6.7	55
8.6	48
14.3	36
20.8	28

FIGURE J-15 (CONTINUED): STEP DRAWDOWN TEST – VR6

Step test data

	Step1	Step1	Step3	Step4	Step5	Step6	Step7
Q (l/s) =	2.4	5	6.7	8.6	14.3	20.8	
t(min)	s (m)	s (m)	s (m)	s (m)	s (m)	s (m)	s (m)
0.1	0	4	9.58	16.22	22.78	47.33	
0.5	1.35	5.35		16.77	25.3	50.18	
1	1.95	5.97	12.21	17.69	26.42	54.6	
1.5	2.28	6.39	12.69	18.4	27.55	60.16	
2	2.43	6.73	13.04	18.93	28.07	62.07	
2.5	2.48	6.85	13.28	19.31	28.48	65.21	
3	2.51	7.2	13.49	19.73	28.93	67.4	
3.5	2.53	7.42	13.64	20	29.3	69.41	
4	2.56	7.52	13.81	20.21	30.44	71.2	
4.5	2.61	7.63	13.91	20.2	32.11	75.84	
5	2.68	7.7	14.02	20.38	33.36	76.56	
7	2.85	7.84	14.29	20.66	37.93	78.43	
9	2.99	8.01	14.49	20.97	39.1	81.2	
12	3.16	8.23	14.75	21.24	40.01	83.93	
15	3.27	8.4	14.94	21.41	42.17	85.78	
20	3.44	8.61	15.22	21.67	43.43	87.46	
25	3.58	8.83	15.42	21.84	44.6	88.59	
30	3.62	8.89	15.58	22.09	45.1	89.65	
35	3.74	9.12	15.75	22.24	45.64	90.89	
40	3.8	9.24	15.87	22.36	46.14	91.24	
45	3.89	9.35	15.98	22.49	46.47	91.82	
50	3.92	9.43	16.07	22.64	46.99	92.04	
60	4	9.58	16.22	22.78	47.33	92.99	

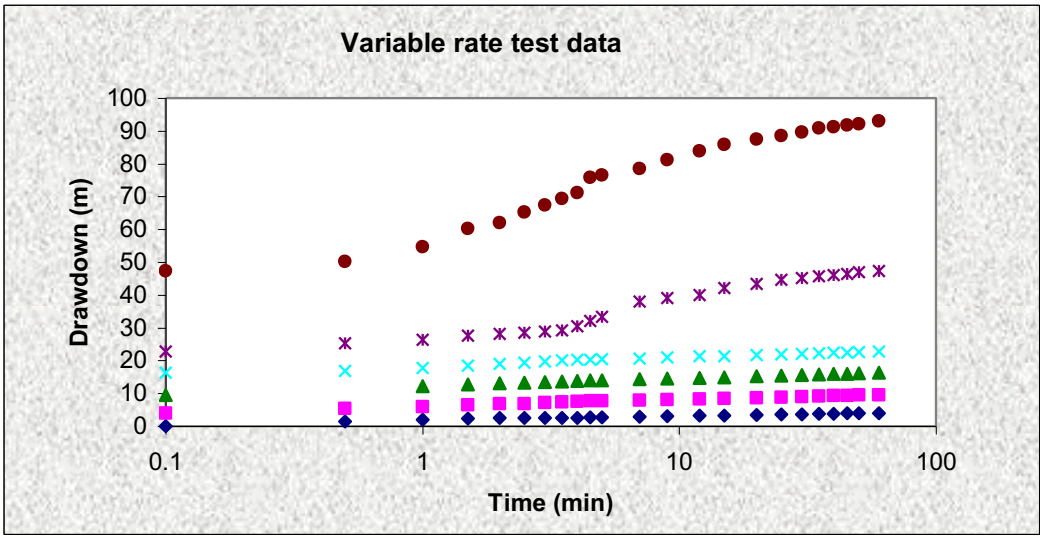

FIGURE J-16: DERIVATIVE PLOTS – VR6

DERIVATIVE PLOTS AND T-AND S-VALUES

VR6

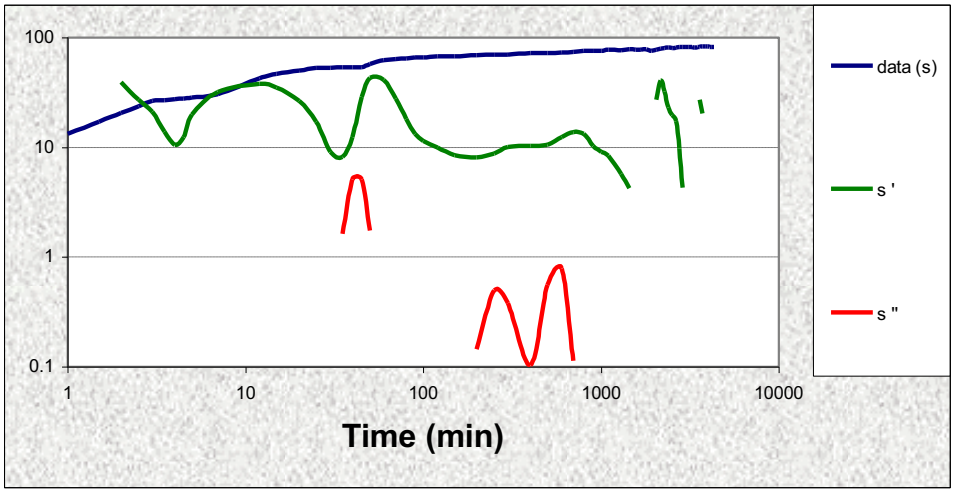

log derivative = 0.17 → good fracture network

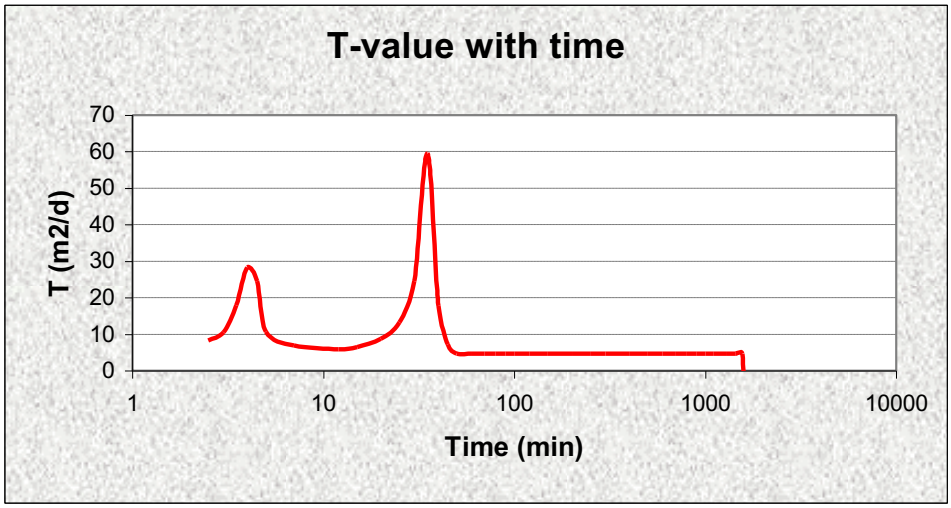

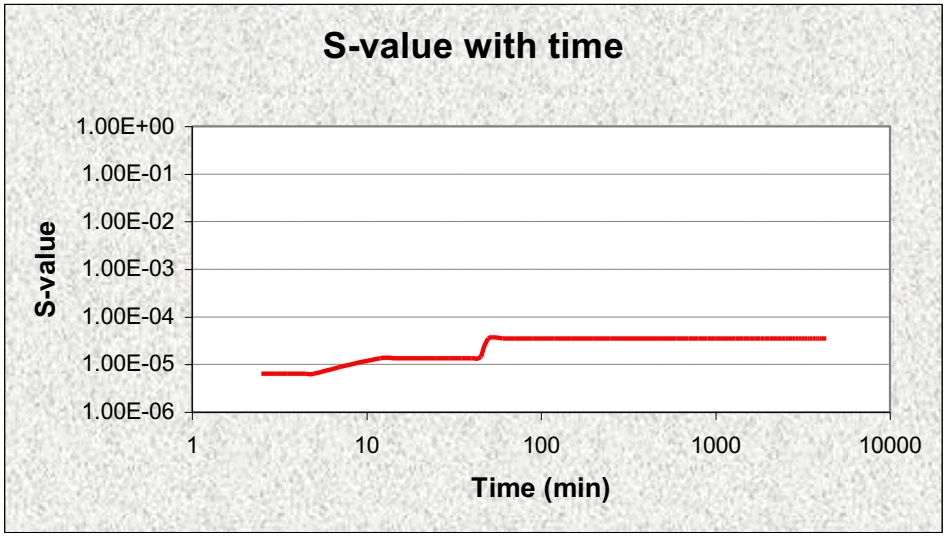

FIGURE J-17: TRANSMISSIVITY AND STORATIVITY OVER TIME

FIGURE J-18: SUSTAINABLE YIELD – BASIC SOLUTION 68 % SAFETY – VR6

FC-METHOD : Estimation of the sustainable yield of a borehole

VR6

Extrapolation time in years = (enter)	5	2628000	Extrapol.time in minutes	
Effective borehole radius (r_e) = (enter)	27.06	27.06	← Est. r_e	From r(e) sheet
Q (l/s) from pumping test =	15.4	4.86	← Est. r_e	Qualified guess
s_a (available drawdown), sigma_s = (enter)	170		← Sigma_s from risk	
Annual effective recharge (mm) =	0	170.00	s_available working drawdown(m)	
t(end) and s(end) of pumping test =	4320	83.45	End time and drawdown of test	
Average maximum derivative = (enter)	35.0	43.2	Estimate of average of max deriv	
Average second derivative = (enter)	0.0	-0.3	Estimate of average second deriv	
Derivative at radial flow period = (enter)	8.44		Read from derivative graph	
	T-early[m^2/d] =	28.85	Aqui. thick (m)	20
T and S estimates from derivatives	T-late [m^2/d] =	6.96	Est. S-late =	1.10E-03
(To obtain correct S-value, use program RPTSOLV)	S-late =	1.10E-03	S-estimate could be wrong	

BASIC SOLUTION

(Using derivatives + subjective information about boundaries)

(No values of T and S are necessary)

	No boundaries	Maximum influence of boundaries at long time: 1 no-flow	2 no-flow	Closed no-flow
sWell (Extrapol.time) =	180.89	278.34	375.78	668.12
Q_sust (l/s) =	14.47	9.41	6.97	3.92
	Best case	→		Worst case

Average Q_sust (l/s) = 7.81

with standard deviation= 4.46

(If no information exists about boundaries skip advanced solution and go to final recommendation)

RECOMMENDED YIELD BASIC SOLUTION – VR6

FINAL RECOMMENDED ABSTRACTION RATE

Abstraction rate (l/s) for 24 hr/d = (enter)	7.00
Total amount of water allowed to be abstracted per month (m^3) =	18144

COMMENTS

Q_sust with 68% safety =	7.81
Q_sust with 95% safety =	7.4

FIGURE J-19: COOPER JACOB ANALYSIS – VR6

Cooper-Jacob method

VR6

T(m^2/d) =	16.7	r_e (m)=	27.06
S =	2.78E-07	Q (l/s) =	15.4

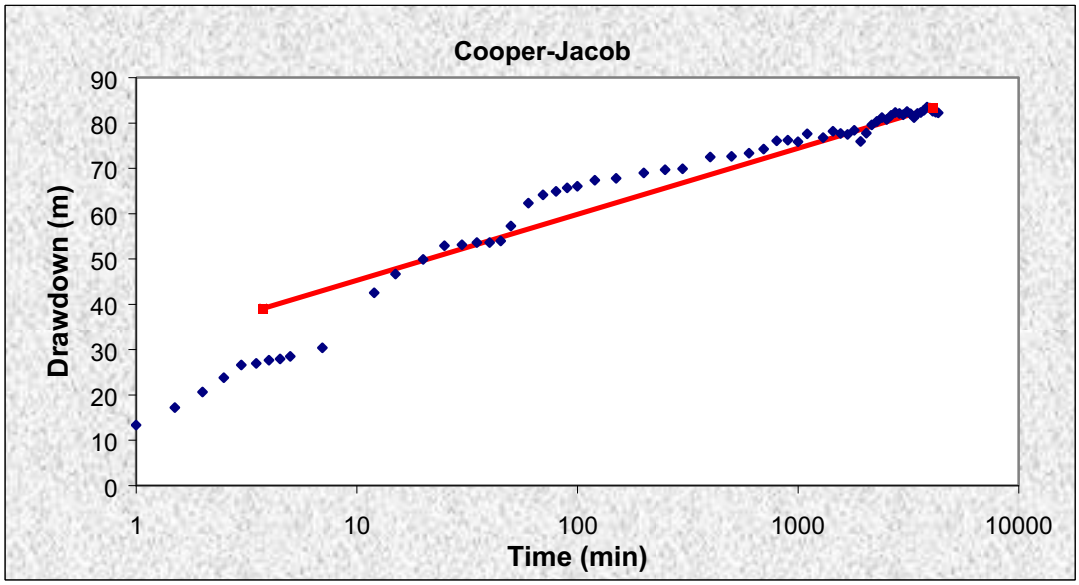

FIGURE J-20: STEP DRAWDOWN TEST – VR8

VR8

STEP DRAWDOWN AND MULTIRATE ANALYSIS

Enter field step test data at bottom of sheet

STEP DRAWDOWN	no	MULTI RATE	yes	

	Q (l/s)	Q (m^3/d)	s_i (m)	Sigma s_i	Sigma s_i/Q_i
Step 1	4.2	362.88	3.63	3.63	0.01000331
Step 2	9.5	820.8	10.91	10.91	0.01329191
Step 3	16	1382.4	28.45	28.45	0.02058015
Step 4	22	1900.8	48.09	48.09	0.02529987
Step 5		0			0
Step 6		0			0
Step 7		0			0

B =	6.5E-03	d/m^2
C =	9.3E-06	d^2/m^5

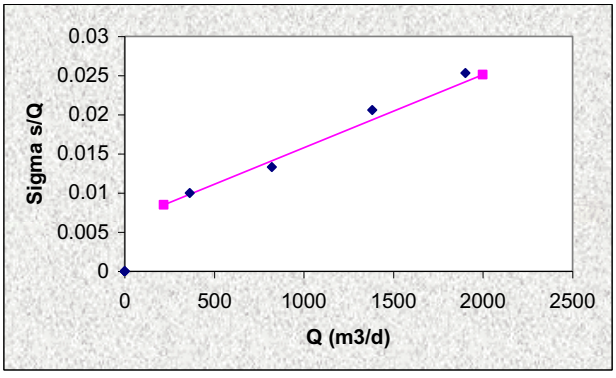

Q (l/s)	Well effiency(%)
4.2	66
9.5	46
16	33
22	27

FIGURE J-20 (CONTINUED) STEP DRAWDOWN TEST –VR8

Step test data							
	Step1	Step1	Step3	Step4	Step5	Step6	Step7
Q (l/s) =	4.2	9.5	16	22			
t(min)	s (m)	s (m)	s (m)	s (m)	s (m)	s (m)	s (m)
1	2.39	3.63	10.91	28.45			
2	2.91	6.49	11.29	28.79			
3	2.96	8.14	12.84	29.19			
4	2.63	8.84	18.03	31.09			
5	2.39	9.24	20.63	37.65			
6	2.29	9.53	22.53	41.17			
7	2.04	10.07	23.79	41.87			
8	1.79	10.7	24.67	43.59			
9	1.55	10.99	25.21	44.34			
10	1.56	11.22	25.59	45.48			
12	1.91	11.34	26.09	46.35			
15	2.31	11.64	26.15	46.72			
20	2.92	12	26.39	47.06			
25	3.14	12.03	26.92	47.51			
30	3.31	10.64	27.47	48.07			
35	3.39	10.51	27.52	48.09			
40	3.56	10.84	27.91				
50	3.29	10.86	27.99				
60	3.63	10.91	28.45				

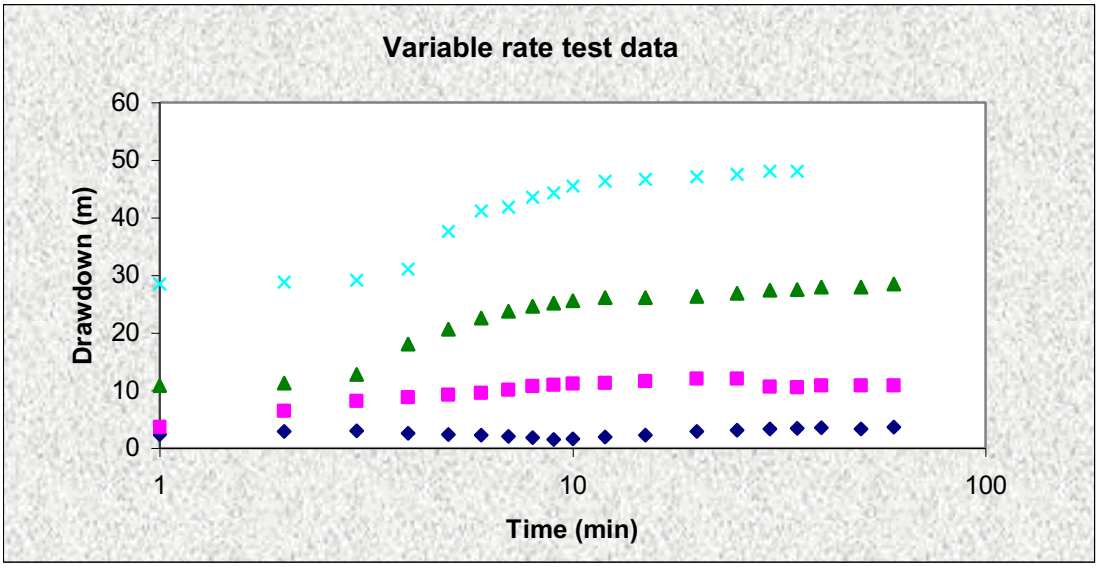

FIGURE J-21: FC DATA SHEET – VR11

DATA sheet: Enter general info and data of constant rate pumping test and recovery (optional)

Country:	SOUTH AFRICA	Geology:	TMG PENINSULA
Region:	LITTLE KAROO	Depth of BH:	224.5
Owner:	DWAF	Water strikes:	200
X-coord:	3721304.80	Date of Test:	Sep-97
Y-coord:	40941.70	Contractor:	CALLIE CALITZ

CONSTANT RATE TEST DATA : enter values in cells which are coloured light yellow

Borehole:		VR11									
Q (l/s)=	15.4					Recovery data					
t (min)	s (m)	avg s'	avg s''	avg T	avg S	Time t'	Res_s	t/t'	WI rise	s'	Rec_T
1.00	5.79					0.1	14.57	43201	0		
2.00	6.96					1	8.32	4321	6.25	6.81	
3.00	7.54	6.30	-0.98			2	5.47	2161	9.1	8.87	
4.00	8	4.01	-0.57	61.49	0.00E+00	3	4.12	1441	10.45	4.32	53.9
5.00	8.46	4.19	0.19	57.22	0.00E+00	4	4.24	1081	10.33	2.40	49.0
6.00	8.76	4.35	0.19	55.79	0.00E+00	5	3.55	865	11.02	11.80	34.0
7.00	9.08	4.48	#NUM!	54.92	0.00E+00	6	2.13	721	12.44	12.95	27.0
8.00	9.32	#NUM!	#NUM!	52.48	0.00E+00	7	1.68	618.1	12.89	4.77	36.7
9.00	9.58	#NUM!	#NUM!	52.48	0.00E+00	8	1.54	541	13.03	4.71	137.6
10.00	9.79	#NUM!	#NUM!	52.48	0.00E+00	9	1.16	481	13.41	0.25	98.7
11.00		#NUM!	#NUM!	52.48	0.00E+00	10	1.53	433	13.04	12.94	370.8
12.00	10.13	#NUM!	#NUM!	52.48	0.00E+00	11		393.7	14.57	0.09	#NUM!
15.00	10.5	#NUM!	#NUM!	52.48	0.00E+00	12	1.57	361	13	-7.75	#NUM!
20.00	10.97	#NUM!	#NUM!	68.79	0.00E+00	15	1.37	289	13.2	0.30	#NUM!
25.00	11.33	2.70	#NUM!	83.07	0.00E+00	20	1.49	217	13.08	-0.17	#NUM!
30.00	11.48	1.93	-1.68	128.67	0.00E+00	25	1.4	173.8	13.17	0.42	#NUM!
40.00	11.71	1.22	-2.22	187.60	0.00E+00	30	1.42	145	13.15	-0.14	#NUM!
50.00	11.78	0.70	-2.35	187.60	0.00E+00	40	1.43	109	13.14	0.21	#NUM!
60.00	11.79	0.46	-1.54	187.60	0.00E+00	50	1.37	87.4	13.2	0.41	1073.0
70.00	11.82	0.39	-0.30	187.60	0.00E+00	60	1.36	73	13.21	0.14	1177.1
80.00	11.83	0.42	0.83	187.60	0.00E+00	70	1.35	62.71	13.22	0.16	1502.7
100.00	11.91	0.57	1.36	187.60	0.00E+00	80	1.34	55	13.23	0.19	1157.4
150.00	11.93	0.99	1.61	187.60	0.00E+00	100	1.32	44.2	13.25	0.30	936.5
200.00	12.05	1.72	1.13	110.72	0.00E+00	150	1.26	29.8	13.31	0.30	809.6
300.00	12.68	2.19	0.07	98.99	0.00E+00	200	1.23	22.6	13.34	0.30	826.0
420.00	13.07	1.83	-0.94	98.99	0.00E+00	300	1.17	15.4	13.4	0.28	827.7
600.00	13.16	1.18	-1.67	98.99	0.00E+00	420	1.14	11.29	13.43	0.30	#DIV/0!
780.00	13.37	0.65	-1.82	98.99	0.00E+00	600	1.08	8.2	13.49	#DIV/0!	#DIV/0!
1080.00	13.39	0.39	-0.65	98.99	0.00E+00			#####	#####	#DIV/0!	#DIV/0!
1440.00	13.39	0.42	1.54	98.99	0.00E+00			#####	#####	#DIV/0!	#DIV/0!
1800.00	13.37	0.72	2.84	98.99	0.00E+00			#####	#####	#DIV/0!	#DIV/0!
2160.00	13.57	1.37	2.42	98.99	0.00E+00			#####	#####	#DIV/0!	#DIV/0!
2520.00	13.64	1.76	0.88	98.99	0.00E+00			#####	#####	#DIV/0!	#DIV/0!
2880.00	13.81	1.83	1.05	98.99	0.00E+00			#####	#####	#DIV/0!	#DIV/0!
3240.00	13.86	2.24	#NUM!	98.99	0.00E+00			#####	#####	#DIV/0!	#DIV/0!
3600.00	13.95	#NUM!	#NUM!	68.97	0.00E+00			#####	#####	#DIV/0!	#DIV/0!
3960.00	14.02	#NUM!	#NUM!	68.97	0.00E+00			#####	#####	#DIV/0!	#DIV/0!
4320.00	14.57	#NUM!	#NUM!	68.97	0.00E+00			#####	#####	#DIV/0!	#DIV/0!

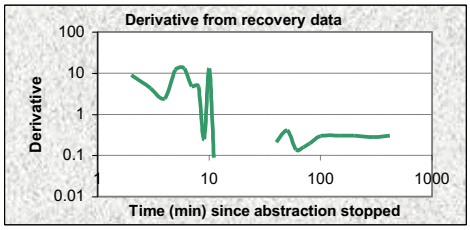

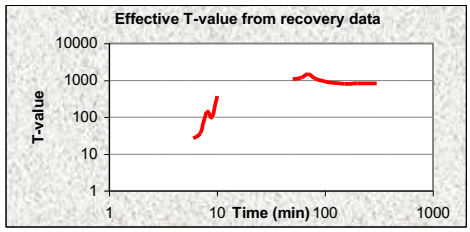

FIGURE J-22: DIAGNOSTIC PLOTS – VR11

DIAGNOSTIC PLOTS

Borehole:

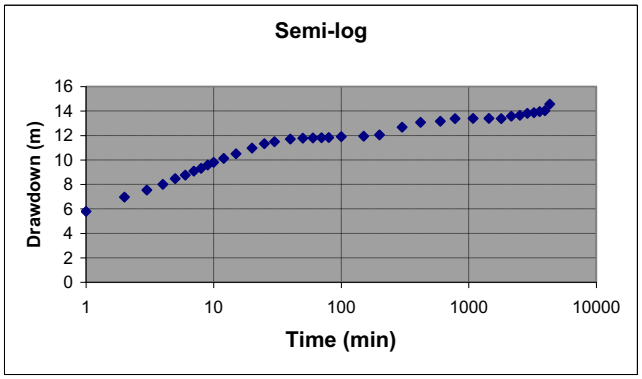

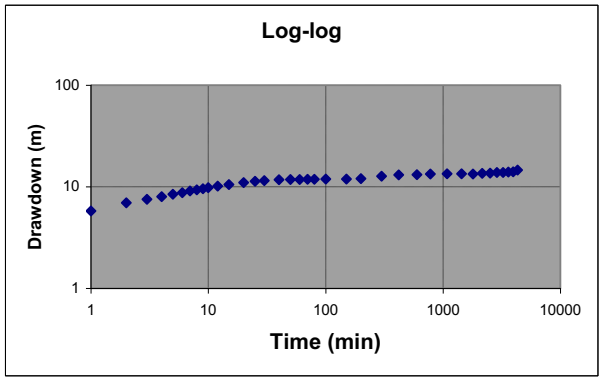

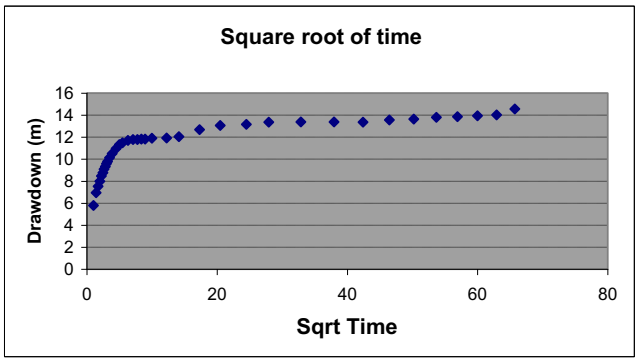

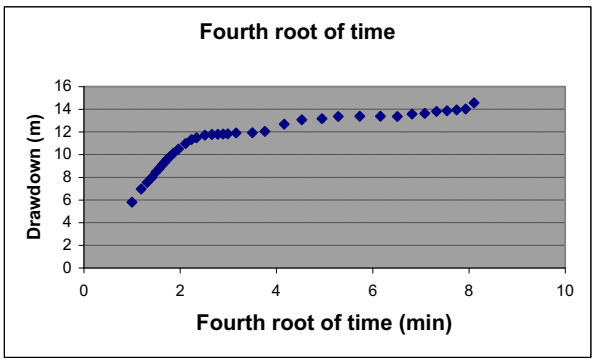

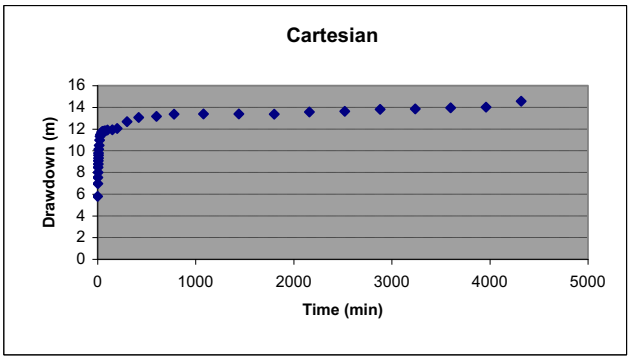

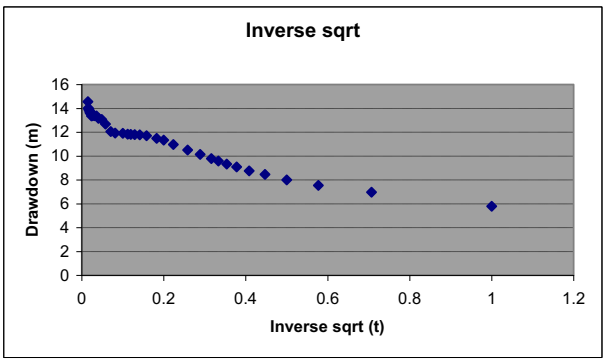

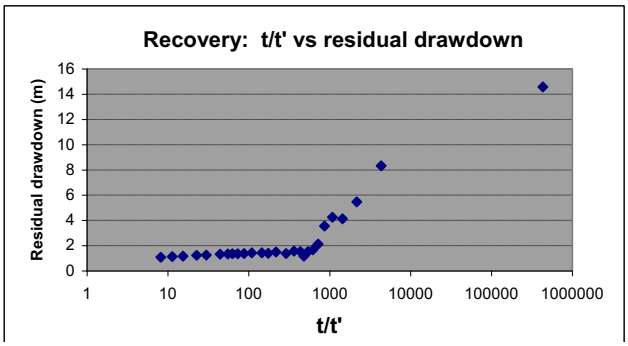

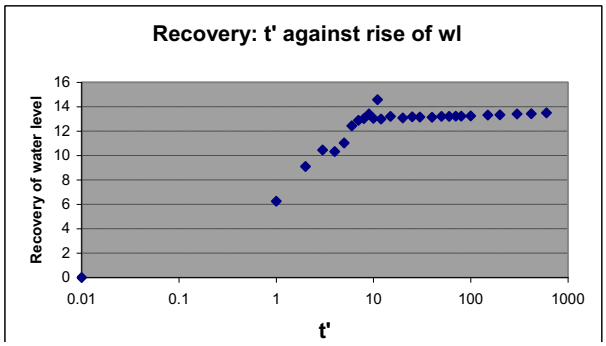

FIGURE J-23: TRANSMISSIVITY AND STORATIVITY WITH TIME – VR11

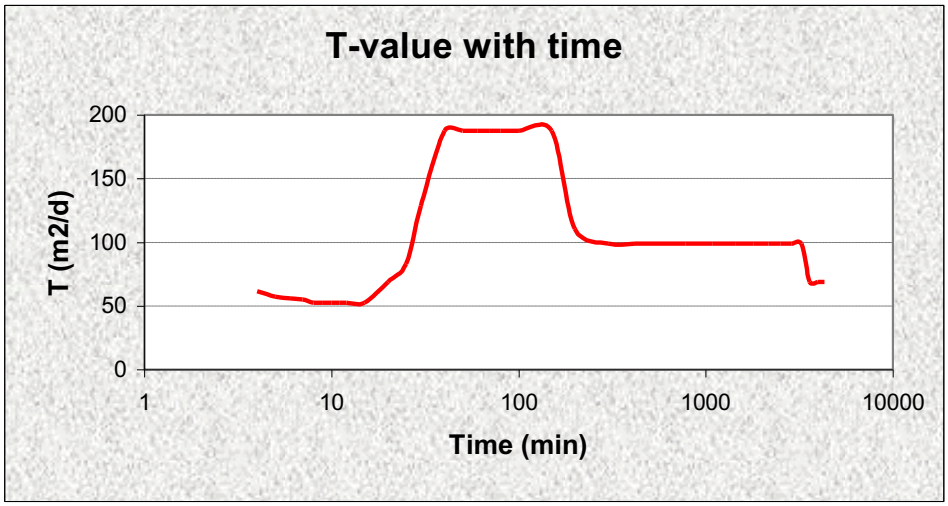

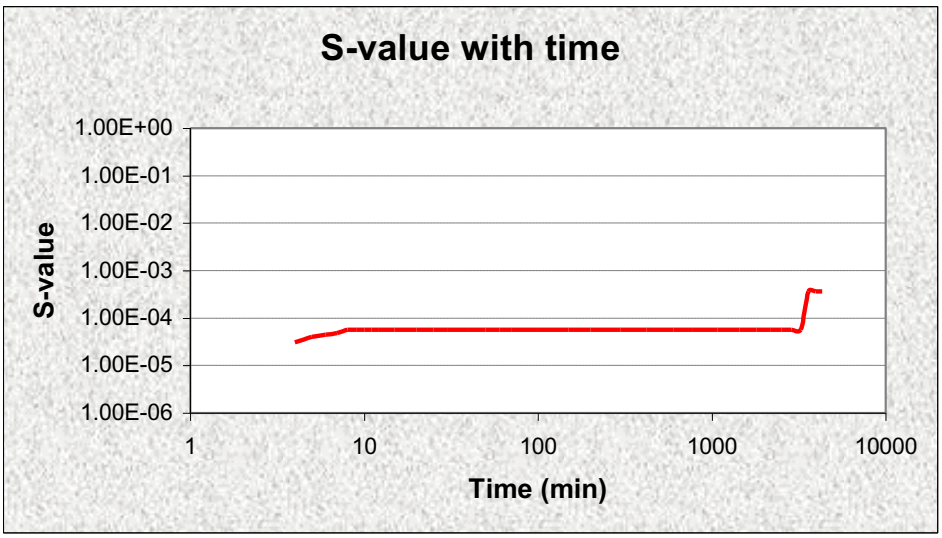

FIGURE J-24: DERIVATIVE PLOT – VR11

DERIVATIVE PLOTS AND T-AND S-VALUES

VR11

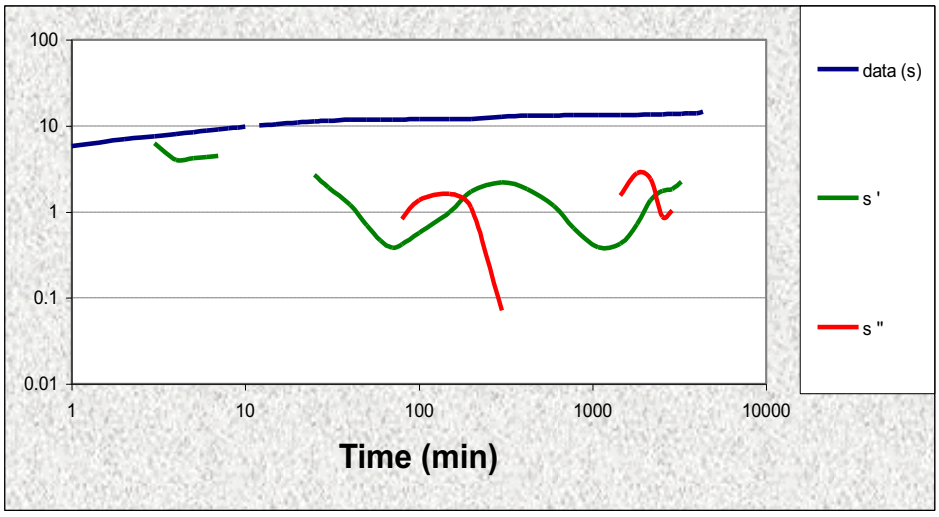

log derivative = 0.06 → very good fracture network

FIGURE J-25: STEP DRAWDOWN TEST – VR11

VR11

STEP DRAWDOWN AND MULTIRATE ANALYSIS

Enter field step test data at bottom of sheet

STEP DRAWDOWN	no	MULTI RATE	yes

	Q (l/s)	Q (m^3/d)	s_i (m)	Sigma s_i	Sigma s_i/Q_i
Step 1	4.1	354.24	4.58	4.58	0.01292909
Step 2	6.9	596.16	10.57	10.57	0.01773014
Step 3	10	864	19.11	19.11	0.02211806
Step 4	12.5	1080	32.5	32.5	0.03009259
Step 5		0			0
Step 6		0			0
Step 7		0			0

B =	6.9E-03	d/m^2
C =	1.8E-05	d^2/m^5

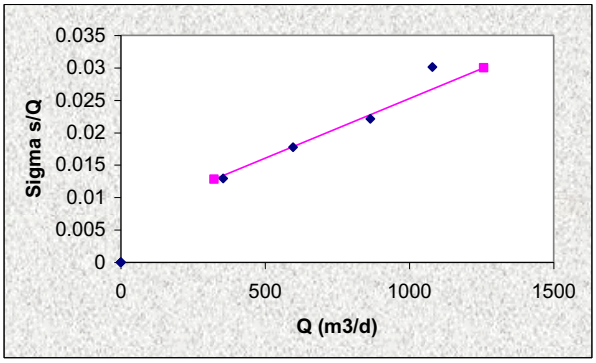

Q (l/s)	Well effiency(%)
4.1	51
6.9	38
10	30
12.5	26

FIGURE J-25 (CONTINUED) STEP DRAWDOWN DATA – VR11

Step test data							
	Step1	Step1	Step3	Step4	Step5	Step6	Step7
Q (l/s) =	4.1	6.9	10	12.5			
t(min)	s (m)	s (m)	s (m)	s (m)	s (m)	s (m)	s (m)
1	2.61	4.58	10.57	19.11			
2	4.05	6.09	10.62	19.34			
3	3.89	7.18	12.78	19.5			
4	3.61	7.82	13.78	20.29			
5	3.63	8.12	14.75	23.55			
6	3.69	8.39	15.33	24.73			
7	3.83	8.59	15.84	26.08			
8	3.56	8.82	16.19	27.19			
9	3.95	8.99	16.53	27.99			
10	4.04	9.08	16.79	28.83			
12	4.14	9.16	17.09	29.55			
15	4.28	9.35	17.17	29.99			
20	4.38	9.55	17.49	30.73			
25	4.5	9.75	17.88	31.49			
30	4.5	10.01	18.23	32.5			
35	4.53	10.12	18.55				
40	4.55	10.29	18.76				
50	4.57	10.39	18.85				
60	4.58	10.57	19.11				

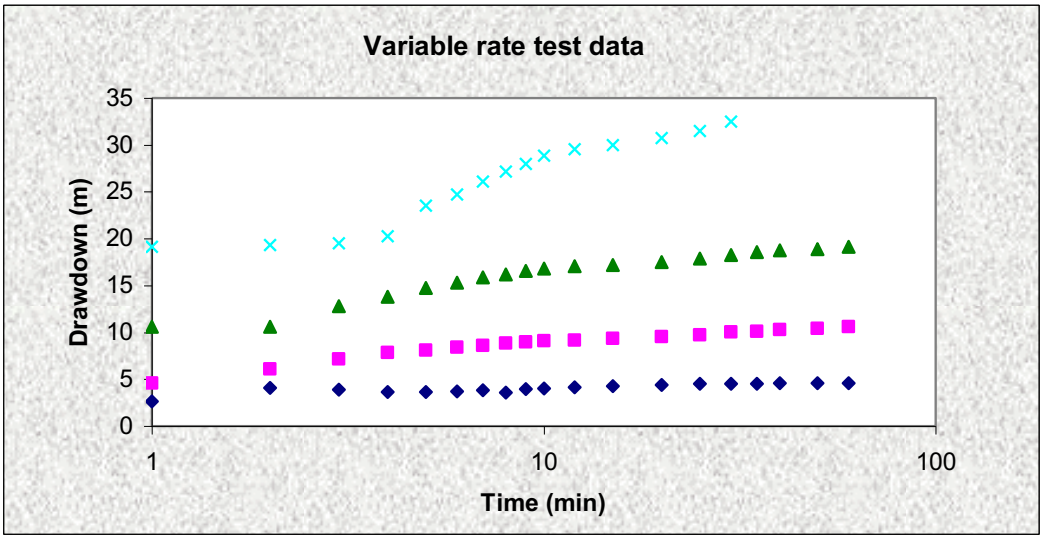

FIGURE J-26: COOPER JACOB ANALYSIS – VR11

Cooper-Jacob method

VR11

$T(m^2/d)$ =	160.9	r_e (m)=	10.28
S =	4.26E-09	Q (l/s) =	15.4

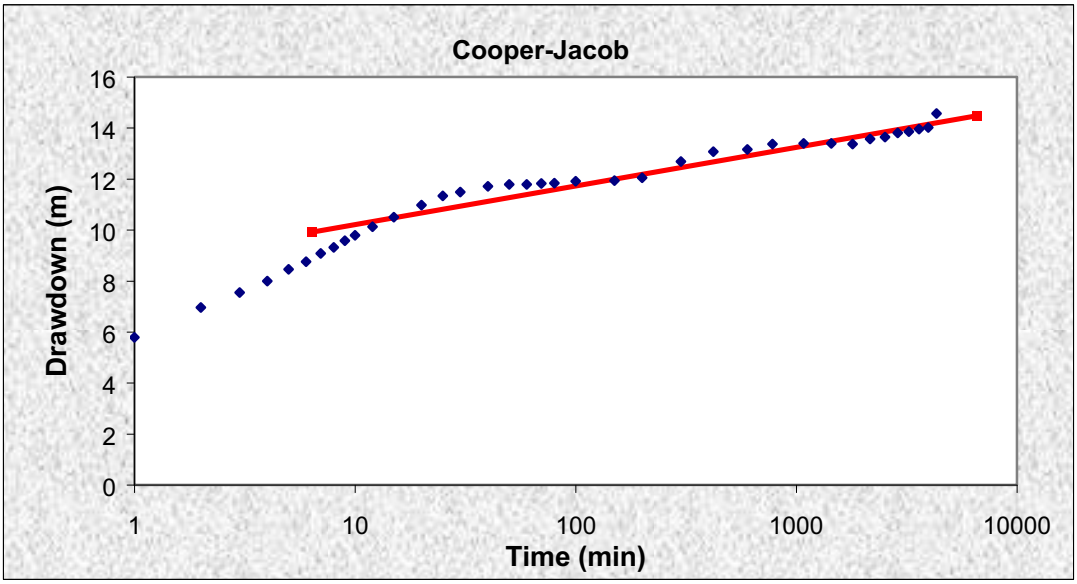

FIGURE J-27: SUSTAINABLE YIELD - BASIC SOLUTION VR11

FC-METHOD : Estimation of the sustainable yield of a borehole

VR11

Extrapolation time in years = (enter)	5	2628000	Extrapol.time in minutes	
Effective borehole radius (r_e) = (enter)	10.28	10.28	← Est. r_e	From r(e) sheet
Q (l/s) from pumping test =	15.4	11.17	← Est. r_e	Qualified guess
s_a (available drawdown), sigma_s = (enter)	49		← Sigma_s from risk	
Annual effective recharge (mm) =	0	49.00	s_available working drawdown(m)	
t(end) and s(end) of pumping test =	4320	14.57	End time and drawdown of test	
Average maximum derivative = (enter)	2.7	2.7	Estimate of average of max deriv	
Average second derivative = (enter)	0.0	0.0	Estimate of average second deriv	
Derivative at radial flow period = (enter)	2.19		Read from derivative graph	
	T-early[m^2/d] =	111.18	Aqui. thick (m)	20
T and S estimates from derivatives	T-late [m^2/d] =	90.26	Est. S-late =	1.10E-03
(To obtain correct S-value, use program RPTSOLV)	S-late =	1.10E-03	S-estimate could be wrong	

BASIC SOLUTION

(Using derivatives + subjective information about boundaries)

(No values of T and S are necessary)

	No boundaries	Maximum influence of boundaries at long time: 1 no-flow	2 no-flow	Closed no-flow
sWell (Extrapol.time) =	22.09	29.60	37.11	59.65
Q_sust (l/s) =	34.16	25.49	20.33	12.65
	Best case	→		Worst case
Average Q_sust (l/s) =	21.75	WARNING!! Est. Q_sust > Q during pumping test		
with standard deviation=	9.03	Suggestion:check available drawdown and rech		

(If no information exists about boundaries skip advanced solution and go to final recommendation)

FINAL RECOMMENDED ABSTRACTION RATE

Abstraction rate (l/s) for 24 hr/d = (enter)	12.00
Total amount of water allowed to be abstracted per month (m^3) =	31104

COMMENTS

Q_sust with 68% safety =	21.8
Q_sust with 95% safety =	13.8

FIGURE J-28: SUSTAINABLE YIELD - ADVANCED SOLUTION 1 – VR11

ADVANCED SOLUTION

(Using derivatives+ knowledge on boundaries and other boreholes)

(Late T-and S-values a priori + distance to boundary)

T-late [m^2/d] = (enter)	90.26				
S-late = (enter)	1.00E-03				
1. BOUNDARY INFORMATION (choose a or b)	(Code =9999 = dummy value if not applicable)				
(a) Barrier (no-flow) boundaries	Closed Square	Single Barrier	Intersect. 90°	2 Parallel Barriers	
Bound. distance a[meter] : (enter)	9999	9999	9999	16000	
Bound. distance b[meter] : (enter)			9999	2200	
s_Bound(t = Extrapol.time) [m] =	3.10	0.53	1.23	3.75	
(b) Fix head boundary + no-flow	Closed Fix	Single Fix	90°Fix+no-flow	// Fix+no-flow	
Bound. distance to fix head a[meter] : (enter)	9999	9999	9999	9999	
Bound. distance to no-flow b[meter] : (enter)			9999	9999	
s_Bound(t = Extrapol.time) [m] =	-1.52	-0.53	-0.36	-0.07	
2. INFLUENCE OF OTHER BOREHOLES	Q (l/s)	r (m)	u_r	W(u,r)	
BH1	7.4	450	3.07E-04	7.51	
BH2			0.00E+00	#NUM!	
s_(influence of BH1,BH2) =	4.24	0.00	1.61E-07	15.07	
SOLUTION INCLUDING BOUNDS AND BH's					
Fix head + No-flow : Q_sust (l/s) =	9999.00	9999.00	9999.00	9999.00	
No-flow : Q_sust (l/s) =	9999.00	9999.00	9999.00	20.94	
Enter selected Q for risk analysis = (enter)	20.00	Sigma_s =	4.046		

(Go to Risk sheet and perform risk analysis from which sigma_s will be estimated : only for barrier boundaries)

FINAL RECOMMENDED ABSTRACTION RATE

Abstraction rate (l/s) for 24 hr/d = (enter)	15.00
Total amount of water allowed to be abstracted per month (m^3) =	38880

COMMENTS

Q_sust with 68% safety =	23.02
Q_sust with 95% safety =	21

RISK ANALYSIS ADVANCED SOLUTION 1 – VR11

Two parallel barrier boundaries : Use = 16000 2200

SENSITIVITY CALCULATION:

		T	S	a	b
Numerical Derivative Factor		0.01	0.01	0.01	0.01
s_Theis(t = Extrapol.time) [m]	22.97	22.02	23.07	22.97	22.97
s_Bound(t = Extrapol.time) [m] =	5.07	4.97	5.26	5.05	5.04
s_Total = s_Theis + s_Boundary [m]	28.04	26.99	28.34	28.02	28.01
Sensitivities:					
ds/dY (t = Extrapol.time):		-2.33E+01			
ds/dW (t = Extrapol.time):			-4.32E+00		
ds/da (t = Extrapol.time):				-1.48E-04	
ds/db (t = Extrapol.time):					-1.37E-03

Uncertainties:	%	Value
% error of late T-value = (enter)	33	29.7847352
sigma (Y)		0.103
% error of late S-value = (enter)	100	1.00E-03
sigma (W)		0.693
% error in bound. distance (a) = (enter)	33	5280
% error in bound. distance (b) = (enter)	33	726
Result:		
sigma (s_Total, t= Extrapol.time) [m] =	4.05	

FIGURE J-29: SUSTAINABLE YIELD ADVANCED SOLUTION2 – VR11

ADVANCED SOLUTION

(Using derivatives+ knowledge on boundaries and other boreholes)

(Late T-and S-values a priori + distance to boundary)

T-late [m²/d] = (enter)	→	90.26			
S-late = (enter)	→	1.00E-03			
1. BOUNDARY INFORMATION (choose a or b)		(Code =9999 = dummy value if not applicable)			
(a) Barrier (no-flow) boundaries	→	Closed Square	Single Barrier	Intersect. 90°	2 Parallel Barriers
Bound. distance a[meter] : (enter)		9999	9999	2000	9999
Bound. distance b[meter] : (enter)				1800	9999
s_Bound(t = Extrapol.time) [m] =		3.10	0.53	10.71	1.12
(b) Fix head boundary + no-flow	→	Closed Fix	Single Fix	90°Fix+no-flow	// Fix+no-flow
Bound. distance to fix head a[meter] : (enter)		9999	9999	9999	9999
Bound. distance to no-flow b[meter] : (enter)				9999	9999
s_Bound(t = Extrapol.time) [m] =		-1.52	-0.53	-0.36	-0.07
2. INFLUENCE OF OTHER BOREHOLES	→	Q (l/s)	r (m)	u_r	W(u,r)
BH1		7.4	450	3.07E-04	7.51
BH2				0.00E+00	#NUM!
s_(influence of BH1,BH2) =		4.24	0.00	1.61E-07	15.07
SOLUTION INCLUDING BOUNDS AND BH's					
Fix head + No-flow : Q_sust (l/s) =		9999.00	9999.00	9999.00	9999.00
No-flow : Q_sust (l/s) =		9999.00	9999.00	16.55	9999.00
Enter selected Q for risk analysis = (enter)	→	16.70	Sigma_s =	4.667	

(Go to Risk sheet and perform risk analysis from which sigma_s will be estimated : only for barrier boundaries)

FINAL RECOMMENDED ABSTRACTION RATE

Abstraction rate (l/s) for 24 hr/d = (enter)	15.00
Total amount of water allowed to be abstracted per month (m³) =	38880

COMMENTS

Q_sust with 68% safety =	18.42
Q_sust with 95% safety =	16.55

RISK ANALYSIS ADVANCED SOLUTION 2 – VR11

Two barrier boundaries intersecting at 90⁰: Use = 2000 1800

SENSITIVITY CALCULATION:		T	S	a	b
Numerical Derivative Factor		0.01	0.01	0.01	0.01
s_Theis(t = Extrapol.time) [m]	19.18	18.39	19.27	19.18	19.18
s_Bound(t = Extrapol.time) [m] =	11.62	11.26	11.87	11.58	11.58
s_Total = s_Theis + s_Boundary [m]	30.79	29.65	31.14	30.76	30.76
Sensitivities:					
ds/dY (t = Extrapol.time):		-2.53E+01			
ds/dW (t = Extrapol.time):			-4.98E+00		
ds/da (t = Extrapol.time):				-1.91E-03	
ds/db (t = Extrapol.time):					-1.99E-03

Uncertainties:	%	Value
% error of late T-value = (enter)	33	29.7847352
sigma (Y)		0.103
% error of late S-value = (enter)	100	1.00E-03
sigma (W)		0.693
% error in bound. distance (a) = (enter)	33	660
% error in bound. distance (b) = (enter)	33	594
Result:		
sigma (s_Total, t= Extrapol.time) [m] =		4.67

FIGURE J-30: FC DATA SHEET – DP28

DATA sheet: Enter general info and data of constant rate pumping test and recovery (optional)

Country:	South Africa	Geology:	TMG- Nardouw
Region:	Little Karoo	Depth of BH:	246
Owner:	DWAF	Water strikes:	122, 151, 195, 210
X-coord:	3717072.80	Date of Test:	Nov-99
Y-coord:	50426.10	Contractor:	Callie Calitz

CONSTANT RATE TEST DATA : enter values in cells which are coloured light yellow

Borehole:		DP28									
Q (l/s)=	21.1					Recovery data					
t (min)	s (m)	avg s'	avg s"	avg T	avg S	Time t'	Res_s	t/t'	WI rise	s'	Rec_T
1.00	2.94					0.01	11.88	4E+05	0		
2.00	3.72					1	5.46	4321	6.42	3.07	
3.00	4.21	4.90	-0.60			2	5	2161	6.88	1.45	
4.00	4.75	3.60	-0.54	88.87	0.00E+00	3	4.77	1441	7.11	1.02	393.2
5.00	5.12	3.53	-0.38	90.30	0.00E+00	4	4.7	1081	7.18	0.41	641.0
6.00	5.38	3.17	-0.70	105.39	0.00E+00	5	4.68	865	7.2	0.34	758.9
7.00	5.57	2.79	#NUM!	123.03	0.00E+00	6	4.64	721	7.24	0.61	533.5
8.00	5.71	#NUM!	#NUM!	131.24	0.00E+00	7	4.59	618.1	7.29	1.19	332.9
9.00	5.82	#NUM!	#NUM!	131.24	0.00E+00	8	4.49	541	7.39	1.38	301.0
10.00	5.97	#NUM!	#NUM!	131.24	0.00E+00	9	4.44	481	7.44	0.83	86.5
11.00		#NUM!	#NUM!	131.24	0.00E+00	10	4.41	433	7.47	50.07	71.6
12.00	6.16	#NUM!	#NUM!	131.24	0.00E+00	11		393.7	11.88	2.43	#NUM!
15.00	6.41	#NUM!	#NUM!	131.24	0.00E+00	12	4.35	361	7.53	-25.67	#NUM!
20.00	6.7	#NUM!	#NUM!	157.45	0.00E+00	15	4.32	289	7.56	0.64	#NUM!
25.00	6.87	1.84	#NUM!	184.11	0.00E+00	20	4.21	217	7.67	1.03	372.6
30.00	7	1.67	-0.36	205.62	0.00E+00	25	4.09	173.8	7.79	1.08	329.0
40.00	7.19	1.57	-0.26	211.26	0.00E+00	30	4.02	145	7.86	0.93	355.2
50.00	7.36	1.48	-0.36	211.26	0.00E+00	40	3.9	109	7.98	0.82	395.0
60.00	7.46	1.37	-0.41	211.26	0.00E+00	50	3.84	87.4	8.04	0.79	400.9
70.00	7.55	1.28	-0.27	211.26	0.00E+00	60	3.76	73	8.12	0.89	362.0
80.00	7.61	1.26	-0.05	211.26	0.00E+00	70	3.71	62.71	8.17	1.11	298.1
100.00	7.74	1.28	0.17	211.26	0.00E+00	80	3.62	55	8.26	1.41	279.6
150.00	7.97	1.41	0.33	211.26	0.00E+00	100	3.49	44.2	8.39	1.08	276.4
200.00	8.12	1.62	0.44	202.34	0.00E+00	150	3.32	29.8	8.56	1.15	299.1
300.00	8.4	1.93	0.43	170.89	0.00E+00	200	3.14	22.6	8.74	1.11	241.0
420.00	8.8	2.20	0.26	149.13	0.00E+00	300	2.98	15.4	8.9	2.07	#DIV/0!
600.00	9.14	2.32	0.12	136.57	0.00E+00	420	2.46	11.29	9.42	#DIV/0!	#DIV/0!
780.00	9.37	2.38	0.09	136.57	0.00E+00			#####	#####	#DIV/0!	#DIV/0!
1080.00	9.86	2.45	0.29	136.57	0.00E+00			#####	#####	#DIV/0!	#DIV/0!
1440.00	9.9	2.78	0.58	124.92	0.00E+00			#####	#####	#DIV/0!	#DIV/0!
1800.00	10.38	3.23	0.62	99.60	0.00E+00			#####	#####	#DIV/0!	#DIV/0!
2160.00	10.59	3.63	0.59	88.90	0.00E+00			#####	#####	#DIV/0!	#DIV/0!
2520.00	10.97	3.98	0.58	87.87	0.00E+00			#####	#####	#DIV/0!	#DIV/0!
2880.00	10.98	4.26	0.51	75.66	0.00E+00			#####	#####	#DIV/0!	#DIV/0!
3240.00	11.44	4.55	#NUM!	72.03	0.00E+00			#####	#####	#DIV/0!	#DIV/0!
3600.00	11.56	#NUM!	#NUM!	72.03	0.00E+00			#####	#####	#DIV/0!	#DIV/0!
3960.00	11.75	#NUM!	#NUM!	72.03	0.00E+00			#####	#####	#DIV/0!	#DIV/0!
4320.00	11.88	#NUM!	#NUM!	72.03	0.00E+00			#####	#####	#DIV/0!	#DIV/0!

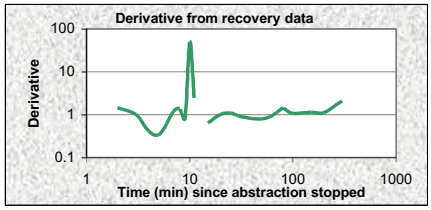

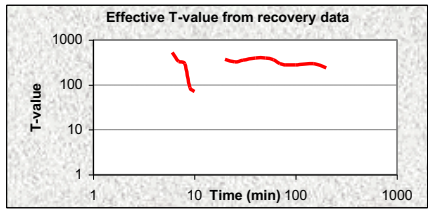

FIGURE J-31: DERIVATIVE PLOT – DP28

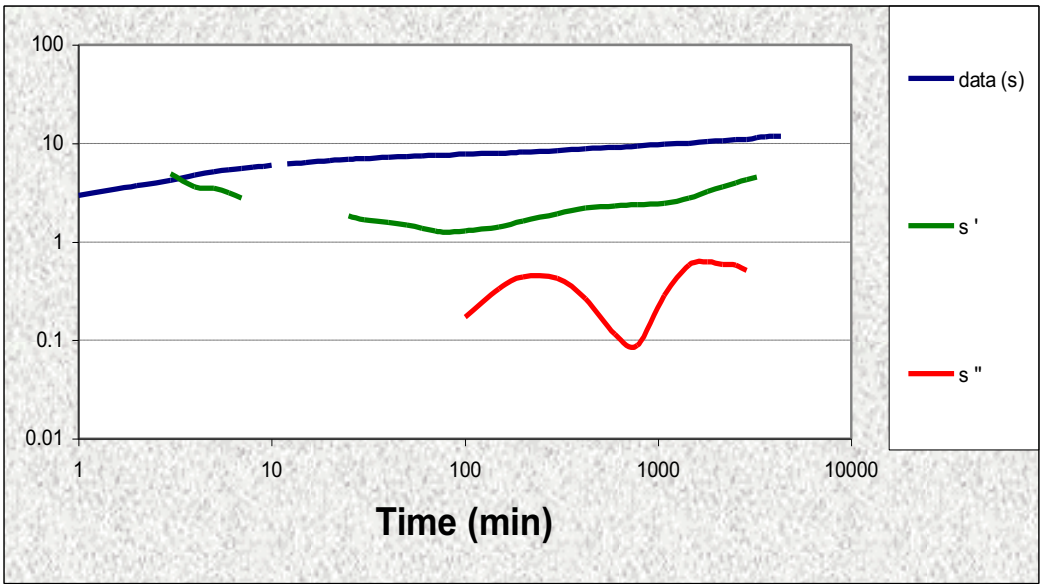

log derivative = 0.10 → very good fracture network

FIGURE J-32: TRANSMISSIVITY AND STORATIVITY WITH TIME – DP28

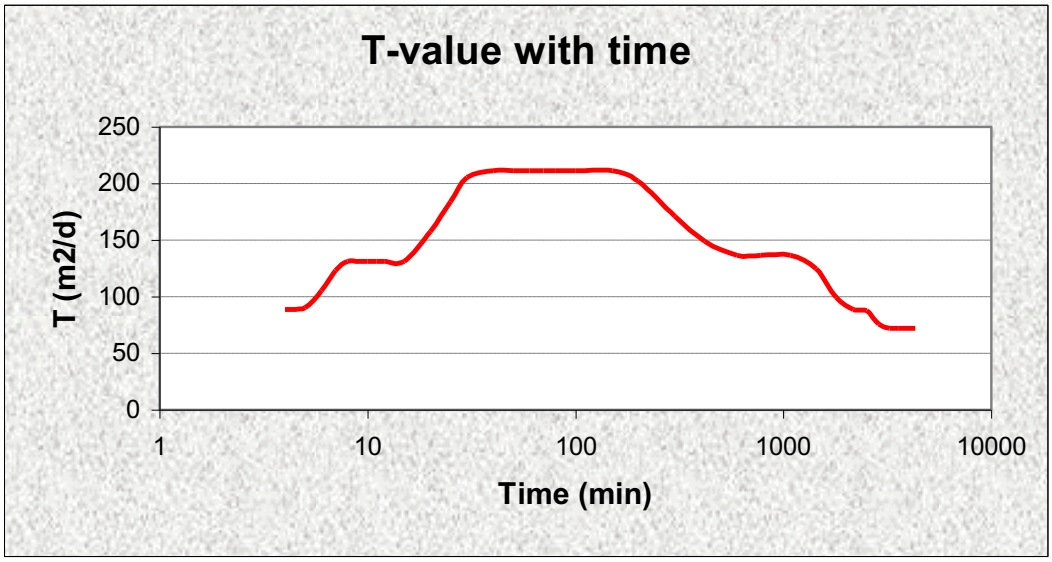

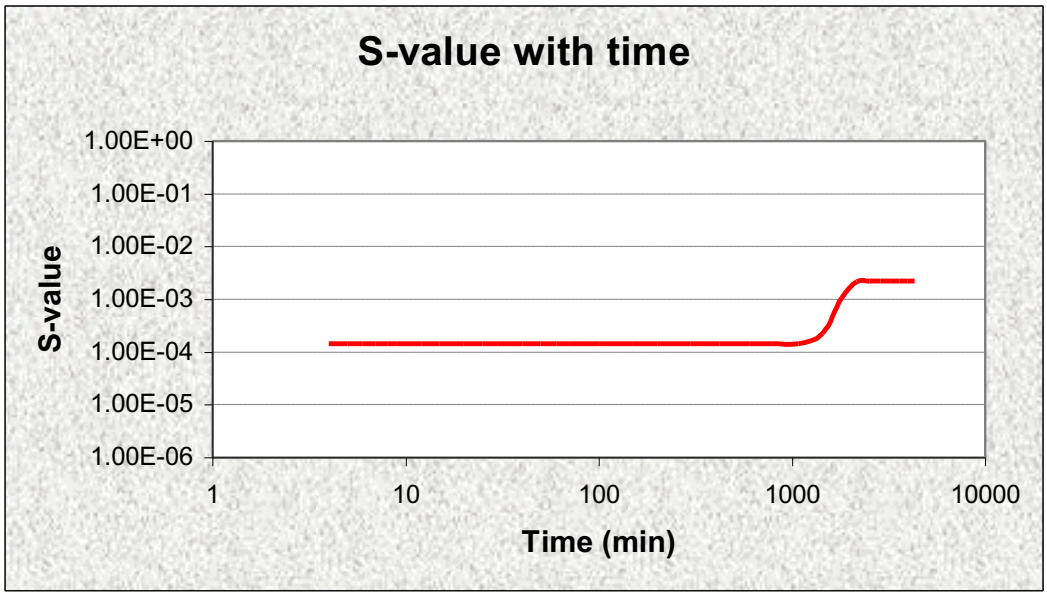

FIGURE J-33: DIAGNOSTIC PLOTS – DP28

DIAGNOSTIC PLOTS

DP28

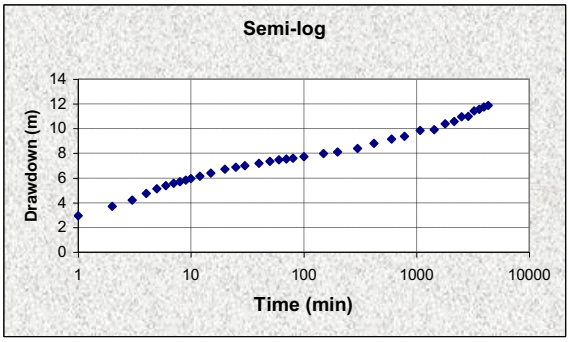

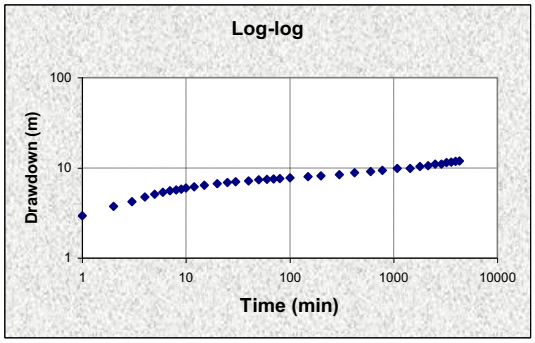

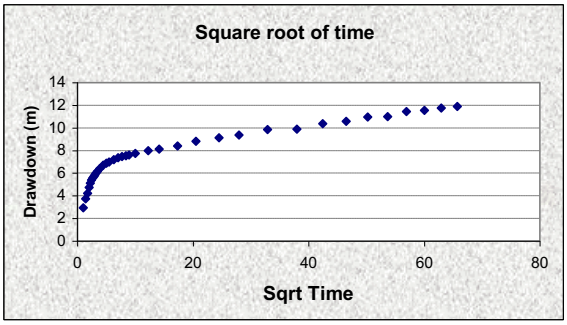

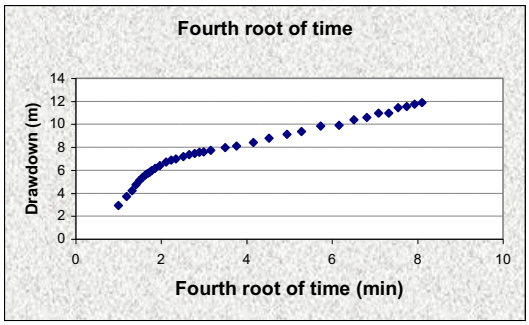

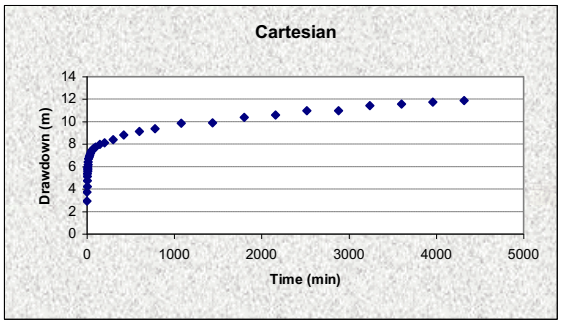

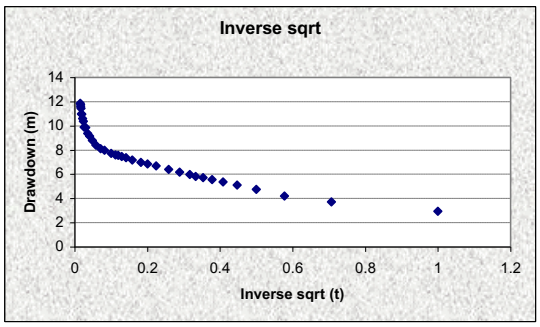

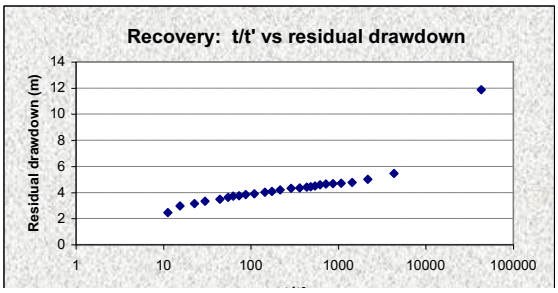

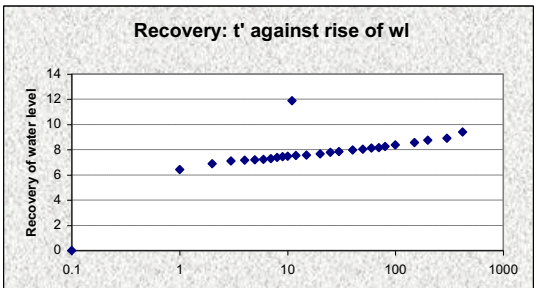

FIGURE J-33: STEP DRAWDOWN TEST – DP28

DP28

STEP DRAWDOWN AND MULTIRATE ANALYSIS

Enter field step test data at bottom of sheet

STEP DRAWDOWN	no	MULTI RATE	yes

	Q (l/s)	Q (m^3/d)	s_i (m)	Sigma s_i	Sigma s_i/Q_i
Step 1	4.4	380.16	1.1	1.1	0.00289352
Step 2	9.4	812.16	2.63	2.63	0.00323828
Step 3	16.8	1451.52	5.3	5.3	0.00365134
Step 4	24.9	2151.36	10.12	10.12	0.004704
Step 5	27.7	2393.28	12.72	12.72	0.00531488
Step 6		0			0
Step 7		0			0

B =	2.1E-03	d/m^2
C =	1.2E-06	d^2/m^5

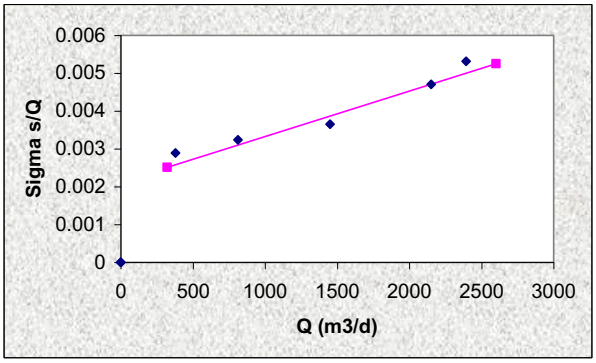

Q (l/s)	Well effiency(%)
4.4	82
9.4	68
16.8	55
24.9	45
27.7	42

FIGURE J-34 (CONTINUED): STEP DRAWDOWN TEST – DP28

Step test data

	Step1	Step1	Step3	Step4	Step5	Step6	Step7
Q (l/s) =	4.4	9.4	16.8	24.9	27.7		
t(min)	s (m)	s (m)	s (m)	s (m)	s (m)	s (m)	s (m)
1	0.84	1.79	3.28	7.62	11.41		
2	0.76	1.84	3.76	8.3	11.54		
3	0.63	2.03	3.96	8.45	11.64		
4	0.7	2.11	4.15	8.71	11.71		
5	0.73	2.15	4.27	8.86	11.78		
6	0.78	2.2	4.4	8.98	11.8		
7	0.785	2.24	4.48	9.08	11.88		
8	0.79	2.26	4.55	9.17	11.91		
9	0.82	2.28	4.72	9.23	11.96		
10	0.83	2.29	4.66	9.28	11.99		
12	0.86	2.34	4.72	9.38	12.03		
15	0.89	2.36	4.82	9.48	12.11		
20	0.94	2.41	4.9	9.61	12.2		
25	0.98	2.44	4.96	9.66	12.32		
30	0.98	2.45	5	9.72	12.39		
35	1.01	2.49	5.06	9.8	12.44		
40	1.03	2.5	5.09	9.83	12.445		
50	1.05	2.54	5.14	9.85	12.48		
60	1.06	2.56	5.19	9.93	12.53		
80	1.1	2.6	5.26	10.04	12.62		
100	1.1	2.63	5.3	10.12	12.72		

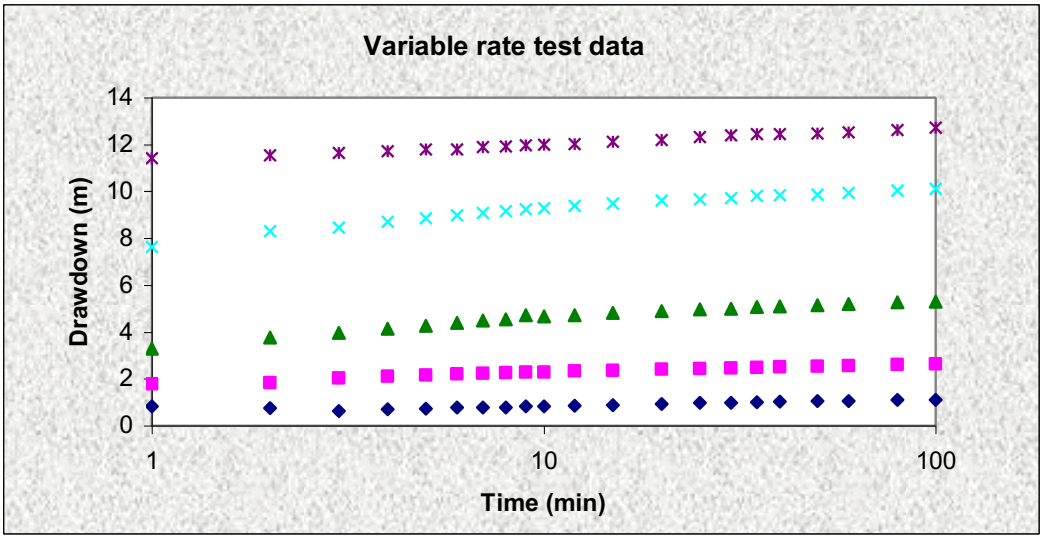

FIGURE J-35: SUSTAINABLE YIELD – BASIC SOLUTION: DP28

FC-METHOD : Estimation of the sustainable yield of a borehole

DP28

Extrapolation time in years = (enter)	5	2628000	Extrapol.time in minutes	
Effective borehole radius (r_e) = (enter)	13.81	13.81	← Est. r_e	From r(e) sheet
Q (l/s) from pumping test =	21.1	30.14	← Est. r_e	Qualified guess
s_a (available drawdown), sigma_s = (enter)	40		← Sigma_s from risk	
Annual effective recharge (mm) =	0	40.00	s_available working drawdown(m)	
t(end) and s(end) of pumping test =	4320	11.88	End time and drawdown of test	
Average maximum derivative = (enter)	3.2	4.5	Estimate of average of max deriv	
Average second derivative = (enter)	0.0	0.0	Estimate of average second deriv	
Derivative at radial flow period = (enter)	1.26		Read from derivative graph	
	T-early[m^2/d] =	264.77	Aqui. thick (m)	20
T and S estimates from derivatives	T-late [m^2/d] =	104.26	Est. S-late =	1.10E-03
(To obtain correct S-value, use program RPTSOLV)	S-late =	2.20E-03	S-estimate could be wrong	

BASIC SOLUTION

(Using derivatives + subjective information about boundaries)

(No values of T and S are necessary)

	No boundaries	Maximum influence of boundaries at long time: 1 no-flow	2 no-flow	Closed no-flow
sWell (Extrapol.time) =	20.79	29.70	38.61	65.34
Q_sust (l/s) =	40.60	28.42	21.86	12.92
	Best case	→		**Worst case**
Average Q_sust (l/s) =	**23.89**	WARNING!! Est. Q_sust > Q during pumping test		
with standard deviation=	11.65	Suggestion:check available drawdown and rech		

(If no information exists about boundaries skip advanced solution and go to final recommendation)

FINAL RECOMMENDED ABSTRACTION RATE

Abstraction rate (l/s) for 24 hr/d = (enter)	10.00
Total amount of water allowed to be abstracted per month (m^3) =	25920

COMMENTS

Q_sust with 68% safety =	16.93
Q_sust with 95% safety =	9.97

FIGURE J-36: COOPER-JACOB SOLUTION – DP28

Cooper-Jacob method

DP28

T(m^2/d) =	**215.9**	r_e (m)=	13.81 →
S =	**1.75E-06**	Q (l/s) =	21.1

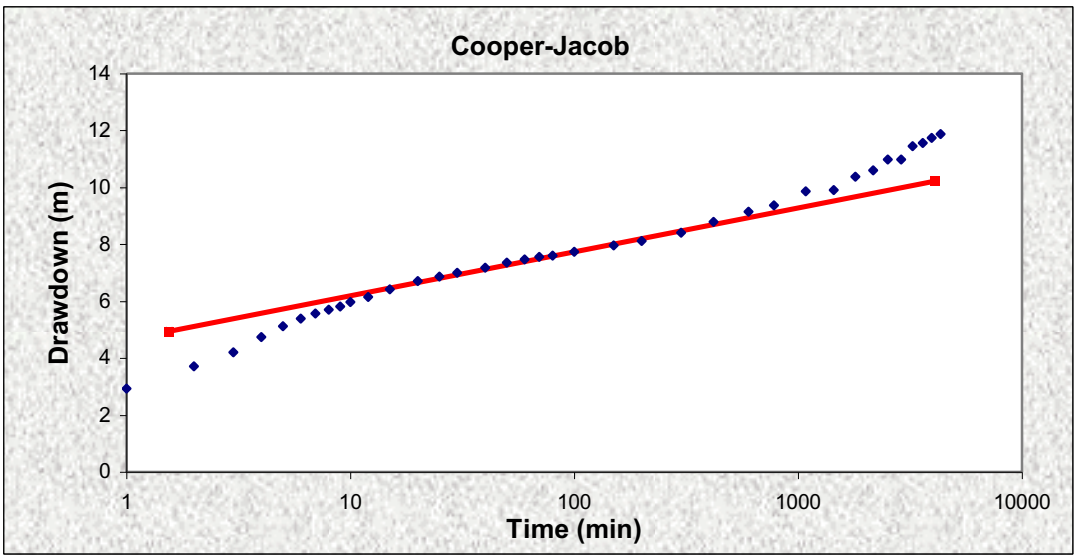

FIGURE J-37: ADVANCED SOLUTION 1 INCLUDING OTHER BOKKRAAL BOREHOLES – DP28

ADVANCED SOLUTION

(Using derivatives+ knowledge on boundaries and other boreholes)

(Late T-and S-values a priori + distance to boundary)

T-late [m^2/d] = (enter) →	104.26				
S-late = (enter) →	1.00E-03				
1. BOUNDARY INFORMATION (choose a or b)	(Code =9999 = dummy value if not applicable)				
(a) Barrier (no-flow) boundaries →	Closed Square	Single Barrier	Intersect. 90°	2 Parallel Barriers	
Bound. distance a[meter] : (enter)	9999	6000	9999	9999	
Bound. distance b[meter] : (enter)			9999	9999	
s_Bound(t = Extrapol.time) [m] =	4.60	1.77	1.76	1.60	
(b) Fix head boundary + no-flow →	Closed Fix	Single Fix	90°Fix+no-flow	// Fix+no-flow	
Bound. distance to fix head a[meter] : (enter)	9999	9999	9999	9999	
Bound. distance to no-flow b[meter] : (enter)			9999	9999	
s_Bound(t = Extrapol.time) [m] =	-2.05	-0.74	-0.56	-0.12	
2. INFLUENCE OF OTHER BOREHOLES →	Q (l/s)	r (m)	u_r	W(u,r)	
BH1	6	50	3.28E-06	12.05	
BH2	9	50	3.28E-06	12.05	
s_(influence of BH1,BH2) =	4.77	7.16	2.51E-07	14.62	
SOLUTION INCLUDING BOUNDS AND BH's					
Fix head + No-flow : Q_sust (l/s) =	9999.00	9999.00	9999.00	9999.00	
No-flow : Q_sust (l/s) =	9999.00	21.26	9999.00	9999.00	
Enter selected Q for risk analysis = (enter) →	20.00	Sigma_s =	2.618		

(Go to Risk sheet and perform risk analysis from which sigma_s will be estimated : only for barrier boundaries)

FINAL RECOMMENDED ABSTRACTION RATE

Abstraction rate (l/s) for 24 hr/d = (enter)	10.00
Total amount of water allowed to be abstracted per month (m^3) =	25920

COMMENTS

Q_sust with 68% safety =	22.87
Q_sust with 95% safety =	21.26

ADVANCED SOLUTION 1 INCLUDING OTHER BOKKRAAL BOREHOLES (DP28) – RISK ANALYSIS

Single barrier boundary: Use = 6000

SENSITIVITY CALCULATION:

		T	S	a
Numerical Derivative Factor :		0.01	0.01	0.01
s_Theis(t = Extrapol.time) [m]	19.30	18.48	19.39	19.30
s_Bound(t = Extrapol.time) [m] =	1.67	1.65	1.75	1.65
s_Total = s_Theis+s_Boundary [m]	20.97	20.13	21.14	20.95
Sensitivities:				
ds/dY (t = Extrapol.time):		-1.82E+01		
ds/dW (t = Extrapol.time):			-2.42E+00	
ds/da (t = Extrapol.time):				-3.62E-04

	%	Value
Uncertainties:		
% error of late T-value = (enter)	33	34.404183
sigma (Y)		0.103
% error of late S-value = (enter)	100	1.00E-03
sigma (W)		0.693
% error in bound. distance (a) = (enter)	33	1980
Result:		
sigma (s_Total, t= Extrapol.time) [m] =	2.62	

FIGURE J-38: ADVANCED SOLUTION 2 – DP28: INCLUDING OTHER BOKKRAAL BOREHOLES, SINGLE BOUNDARY 100 M AWAY

FC-METHOD : Estimation of the sustainable yield of a borehole

DP28

Extrapolation time in years = (enter)	5	2628000	Extrapol.time in minutes	
Effective borehole radius (r_e) = (enter)	13.81	13.81	Est. r_e	From r(e) sheet
Q (l/s) from pumping test =	21.1	30.14	Est. r_e	Qualified guess
s_a (available drawdown), sigma_s = (enter)	40	2.8	Sigma_s from risk	
Annual effective recharge (mm) =	0	37.20	s_available working drawdown(m)	
t(end) and s(end) of pumping test =	4320	11.88	End time and drawdown of test	
Average maximum derivative = (enter)	3.2	4.5	Estimate of average of max deriv	
Average second derivative = (enter)	0.0	0.0	Estimate of average second deriv	
Derivative at radial flow period = (enter)	1.26		Read from derivative graph	
	T-early[m^2/d] =	264.77	Aqui. thick (m)	20
T and S estimates from derivatives	T-late [m^2/d] =	104.26	~~Est. S-late =~~	1.10E-03
(To obtain correct S-value, use program RPTSOLV)	S-late =	2.20E-03	S-estimate could be wrong	

BASIC SOLUTION

(Using derivatives + subjective information about boundaries)

(No values of T and S are necessary)

	Maximum influence of boundaries at long time			
	No boundaries	1 no-flow	2 no-flow	Closed no-flow
sWell (Extrapol.time) =	32.71	41.62	50.53	77.26
Q_sust (l/s) =	23.99	18.86	15.53	10.16
	Best case →			**Worst case**

Average Q_sust (l/s) = 16.35

with standard deviation= 5.81

(If no information exists about boundaries skip advanced solution and go to final recommendation)

ADVANCED SOLUTION

(Using derivatives+ knowledge on boundaries and other boreholes)

(Late T-and S-values a priori + distance to boundary)

T-late [m^2/d] = (enter) → 104.26

S-late = (enter) → 1.00E-03

1. BOUNDARY INFORMATION (choose a or b) (Code =9999 = dummy value if not applicable)

(a) Barrier (no-flow) boundaries →	Closed Square	Single Barrier	Intersect. 90°	2 Parallel Barriers
Bound. distance a[meter] : (enter)	9999	100	9999	9999
Bound. distance b[meter] : (enter)			9999	9999
s_Bound(t = Extrapol.time) [m] =	4.60	12.91	1.76	1.60
(b) Fix head boundary + no-flow →	Closed Fix	Single Fix	90°Fix+no-flow	// Fix+no-flow
Bound. distance to fix head a[meter] : (enter)	9999	9999	9999	9999
Bound. distance to no-flow b[meter] : (enter)			9999	9999
s_Bound(t = Extrapol.time) [m] =	-2.05	-0.74	-0.56	-0.12
2. INFLUENCE OF OTHER BOREHOLES →	Q (l/s)	r (m)	u_r	W(u,r)
BH1	6	50	3.28E-06	12.05
BH2	9	50	3.28E-06	12.05
s_(influence of BH1,BH2) =	4.77	7.16	2.51E-07	14.62

SOLUTION INCLUDING BOUNDS AND BH's

Fix head + No-flow : Q_sust (l/s) =	9999.00	9999.00	9999.00	9999.00
No-flow : Q_sust (l/s) =	9999.00	17.20	9999.00	9999.00
Enter selected Q for risk analysis = (enter) →	16.00	Sigma_s =	2.846	

FINAL RECOMMENDED ABSTRACTION RATE

Abstraction rate (l/s) for 24 hr/d = (enter)	15.00
Total amount of water allowed to be abstracted per month (m^3) =	38880

COMMENTS

Q_sust with 68% safety = 17.2

Q_sust with 95% safety = 16

DP28 – ADVANCED SOLUTION 2 – RISK ANALYSIS

Single barrier boundary: Use = 100

SENSITIVITY CALCULATION:

	T	S	a
Numerical Derivative Factor :	0.01	0.01	0.01
s_Theis(t = Extrapol.time) [m]	14.78	15.51	15.44
s_Bound(t = Extrapol.time) [m] =	9.40	9.87	9.77
s_Total = s_Theis+s_Boundary [m]	24.18	25.38	25.21
Sensitivities:			
ds/dY (t = Extrapol.time):	-2.26E+01		
ds/dW (t = Extrapol.time):		-2.11E+00	
ds/da (t = Extrapol.time):			-2.10E-02

Uncertainties:	**%**	**Value**
% error of late T-value = (enter)	**33**	34.404183
sigma (Y)		0.103
% error of late S-value = (enter)	**100**	1.00E-03
sigma (W)		0.693
% error in bound. distance (a) = (enter)	**33**	33
Result:		
sigma (s_Total, t= Extrapol.time) [m] =	2.85	

FIGURE J-39: STEP DRAWDOWN TEST – DG110

DG110

STEP DRAWDOWN AND MULTIRATE ANALYSIS

Enter field step test data at bottom of sheet

STEP DRAWDOWN: no MULTI RATE: yes

	Q (l/s)	Q (m^3/d)	s_i (m)	Sigma s_i	Sigma s_i/Q_i
Step 1	1.9	164.16	2.33	2.33	0.01419347
Step 2	3.99	344.736	6.06	6.06	0.01757867
Step 3	5.96	514.944	9.66	9.66	0.01875932
Step 4	9.6	829.44	18.25	18.25	0.0220028
Step 5	14.69	1269.216	37.29	37.29	0.02938034
Step 6	17.7	1529.28	52.76	52.76	0.0344999
Step 7		0			0

B =	1.3E-02	d/m^2
C =	1.3E-05	d^2/m^5

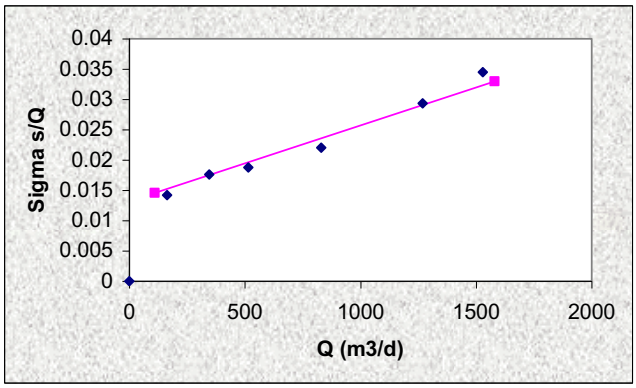

Q (l/s)	Well effiency(%)
1.9	87
3.99	75
5.96	67
9.6	56
14.69	45
17.7	41

FIGURE J-39 (CONTINUED) STEP DRAWDOWN TEST – DG110

Step test data

	Step1	Step1	Step3	Step4	Step5	Step6	Step7
Q (l/s) =	1.9	3.99	5.96	9.6	14.69	17.7	
t(min)	s (m)	s (m)	s (m)	s (m)	s (m)	s (m)	s (m)
0.5	0.83		6.74			38.52	
1	1.53	2.49	6.97	11.09	20.01	39.75	
1.5	1.78	2.95	7.23	11.92	21.09	41.1	
2	1.82	3.2	7.38	12.25	21.91	41.96	
2.5	1.74	3.59	7.52	12.7	22.68	42.55	
3	1.73	3.66	7.61	13.05	23.5	43.16	
3.5	1.74	3.79	7.71	13.29	24	43.57	
4	1.78	3.86	7.76	13.5	24.41	44.05	
4.5	1.78	3.96	7.83	13.73	24.83	44.43	
5	1.79	4.03	7.85	13.9	25.19	44.78	
7	1.83	4.23	8.08	14.42	26.61	45.75	
9	1.89	4.46	8.24	14.82	27.35	46.45	
12	1.95	4.65	8.39	15.32	28.93	48.03	
15	2.01	4.82	8.58	15.73	30.69	48.8	
20	2.06	5.07	8.82	16.37	32.34	50	
25	2.11	5.32	8.96	16.72	33.28	50.96	
30	2.17	5.38	9.08	17.06	34.17	51.73	
35	2.22	5.59	9.25	17.36	34.91	52.36	
40	2.25	5.72	9.37	17.6	35.61	52.54	
45	2.28	5.87	9.47	17.8	36.62	52.61	
50	2.28	5.91	9.51	18.01	36.88	52.72	
60	2.33	6.06	9.66	18.25	37.29	52.76	

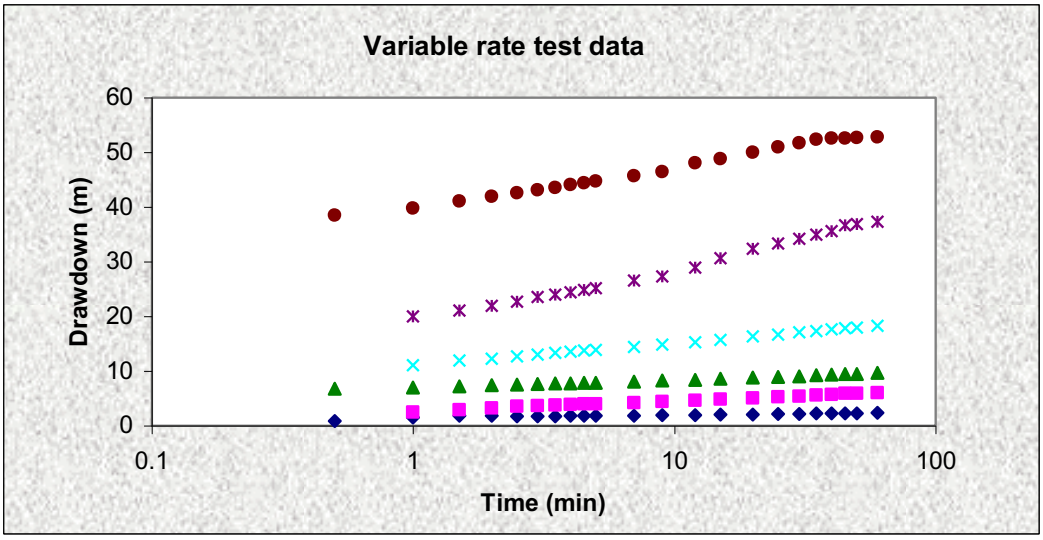

FIGURE J-40: FC DATA SET – DP15

DATA sheet: Enter general info and data of constant rate pumping test and recovery (optional)

Country:	South Africa	**Geology:**	TMG- Nardouw
Region:	Little Karoo	**Depth of BH:**	224.5
Owner:	DWAF	**Water strikes:**	139,183, 187
X-coord:	3717093.20	**Date of Test:**	Nov-97
Y-coord:	50468.50	**Contractor:**	Callie Calitz

CONSTANT RATE TEST DATA : enter values in cells which are coloured light yellow

Borehole:		DP15									
Q (l/s)=	5.7					Recovery data					
t (min)	s (m)	avg s'	avg s''	avg T	avg S	Time t'	Res_s	t/t'	WI rise	s'	Rec_T
1.00	2.07					0.01	6.1	4E+05	0.09		
2.00	3.28					1	1.08	4321	5.11	2.39	
3.00	3.2	#NUM!	#NUM!			2	0.74	2161	5.45	0.83	
4.00	3.21	#NUM!	#NUM!	0.00	0.00E+00	3	0.7	1441	5.49	-0.33	#NUM!
5.00	3.18	#NUM!	#NUM!	-1007.41	0.00E+00	4	0.85	1081	5.34	-1.09	#NUM!
6.00	3.18	#NUM!	#NUM!	-1437.52	0.00E+00	5	0.94	865	5.25	-1.62	#NUM!
7.00	3.18	#NUM!	#NUM!	1636.54	0.00E+00	6	1.14	721	5.05	-1.34	#NUM!
8.00	3.18	0.20	#NUM!	359.58	0.00E+00	7	1.13	618.1	5.06	0.24	#NUM!
9.00	3.2	0.48	5.14	152.69	0.00E+00	8	1.11	541	5.08	0.46	277.9
10.00	3.24	0.68	1.74	118.26	0.00E+00	9	1.08	481	5.11	0.31	282.8
11.00	3.29	0.71	0.16	127.77	0.00E+00	10	1.08	433	5.11	0.23	#NUM!
12.00	3.29	0.71	0.00	134.82	0.00E+00	11	1.06	393.7	5.13	-0.12	#NUM!
15.00	3.35	0.75	0.31	119.14	0.00E+00	12	1.09	361	5.1	0.30	#NUM!
20.00	3.48	0.81	0.13	107.42	0.00E+00	15	1.03	289	5.16	0.49	222.6
25.00	3.55	0.81	0.01	108.74	0.00E+00	20	0.98	217	5.21	0.45	165.7
30.00	3.61	0.81	0.04	118.49	0.00E+00	25	0.93	173.8	5.26	0.73	153.7
40.00	3.72	0.83	0.07	106.67	0.00E+00	30	0.85	145	5.34	0.62	134.9
50.00	3.77	0.84	-0.06	102.77	0.00E+00	40	0.8	109	5.39	0.66	118.5
60.00	3.9	0.82	-0.35	102.77	0.00E+00	50	0.7	87.4	5.49	1.08	97.8
70.00	3.9	0.75	-0.62	102.77	0.00E+00	60	0.61	73	5.58	1.10	86.4
80.00	3.95	0.66	-0.66	102.77	0.00E+00	70	0.54	62.71	5.65	0.96	87.3
100.00	4.07	0.57	-0.16	102.77	0.00E+00	80	0.49	55	5.7	1.04	94.6
150.00	4.08	0.68	0.75	102.77	0.00E+00	100	0.38	44.2	5.81	0.86	100.9
200.00	4.17	0.99	1.24	81.20	0.00E+00	150	0.25	29.8	5.94	0.79	108.9
300.00	4.31	1.67	1.04	51.05	0.00E+00	200	0.14	22.6	6.05	0.83	#DIV/0!
420.00	4.8	2.10	0.10	38.17	0.00E+00	300	0	15.4	6.19	#DIV/0!	#DIV/0!
600.00	5.19	1.84	-0.71	38.17	0.00E+00			#####	#####	#DIV/0!	#DIV/0!
780.00	5.38	1.36	-0.76	38.17	0.00E+00			#####	#####	#DIV/0!	#DIV/0!
1080.00	5.46	1.15	0.13	38.17	0.00E+00			#####	#####	#DIV/0!	#DIV/0!
1440.00	5.52	1.42	1.11	38.17	0.00E+00			#####	#####	#DIV/0!	#DIV/0!
1800.00	5.75	1.95	0.21	38.17	0.00E+00			#####	#####	#DIV/0!	#DIV/0!
2160.00	5.97	1.71	#NUM!	36.21	0.00E+00			#####	#####	#DIV/0!	#DIV/0!
2520.00	6.19	#NUM!	#NUM!	36.21	0.00E+00			#####	#####	#DIV/0!	#DIV/0!
2880.00	6.19	#NUM!	#NUM!	-115.78	0.00E+00			#####	#####	#DIV/0!	#DIV/0!
3240.00	5.91	#NUM!	#NUM!	-115.78	0.00E+00			#####	#####	#DIV/0!	#DIV/0!
3600.00	6.02	#NUM!	#NUM!	-115.78	0.00E+00			#####	#####	#DIV/0!	#DIV/0!
3960.00	6.03	#NUM!	#NUM!	-115.78	0.00E+00			#####	#####	#DIV/0!	#DIV/0!
4320.00	6.1	#NUM!	#NUM!	-115.78	0.00E+00			#####	#####	#DIV/0!	#DIV/0!
		#NUM!	#NUM!	-115.78	0.00E+00			#####	#####	#DIV/0!	#DIV/0!

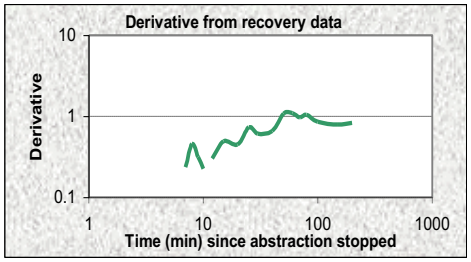

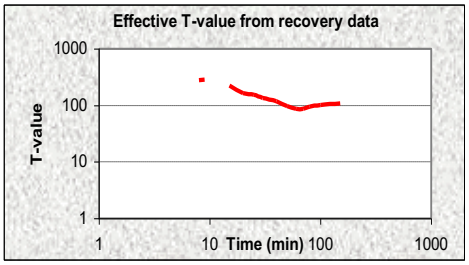

FIGURE J-41: DERIVATIVE PLOTS – DP15

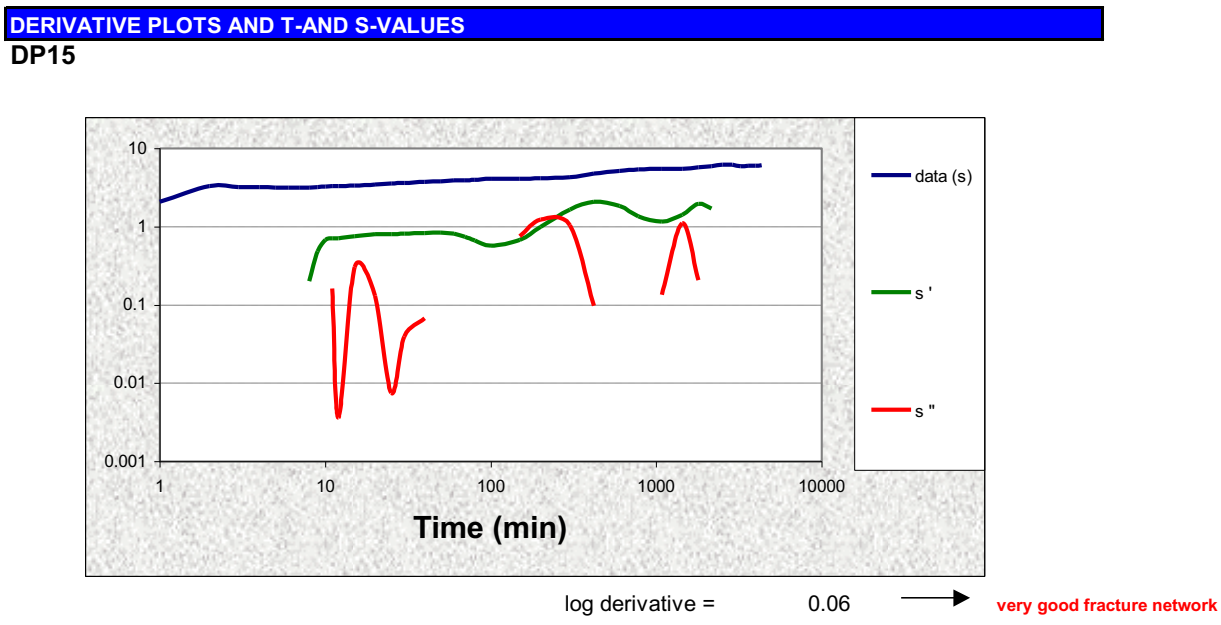

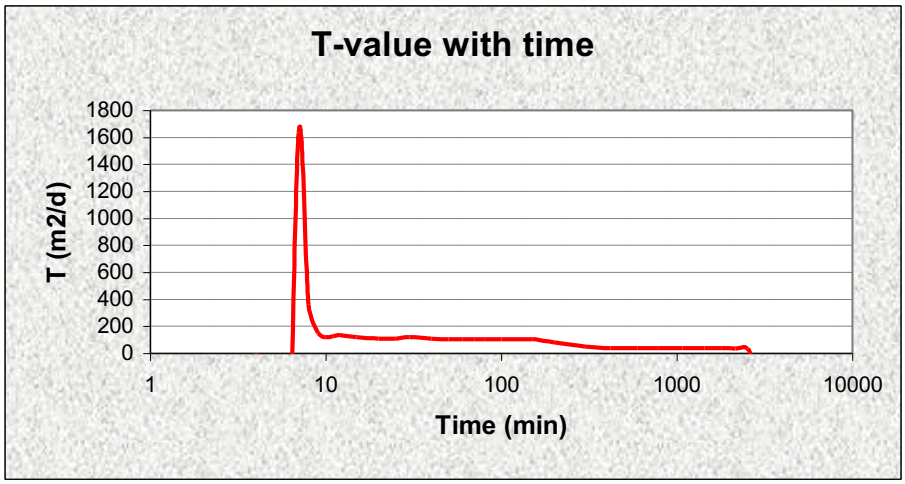

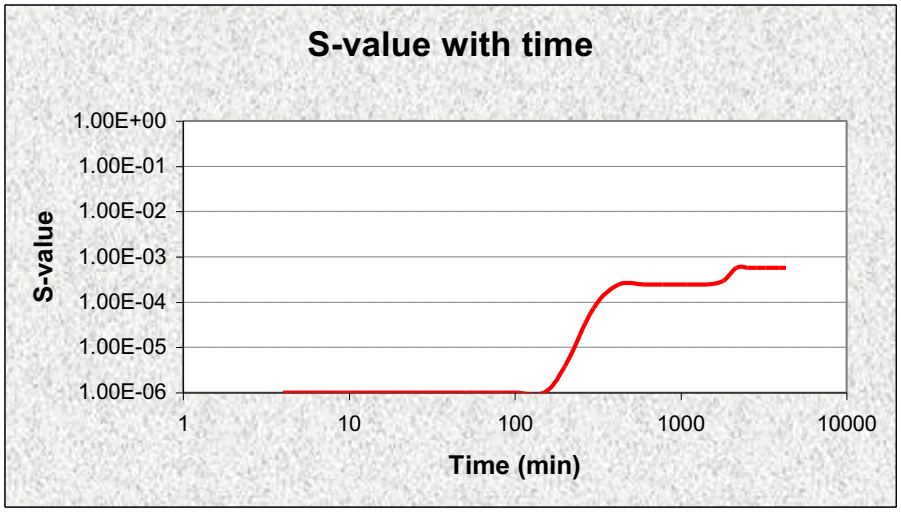

FIGURE J-42: TRANSMISSIVITY AND STORATIVITY WITH TIME – DP15

FIGURE J-43: DIAGNOSTIC PLOTS – DP15

DIAGNOSTIC PLOTS

DP15

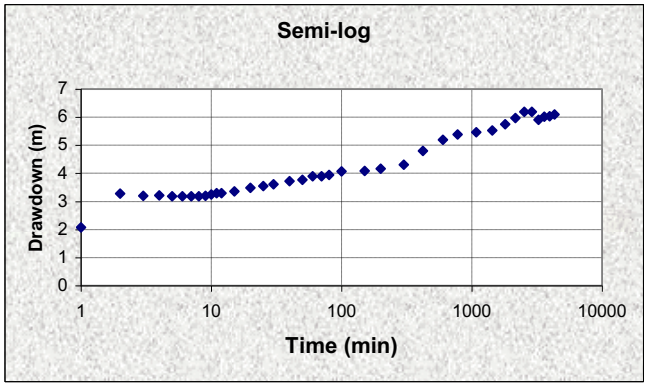

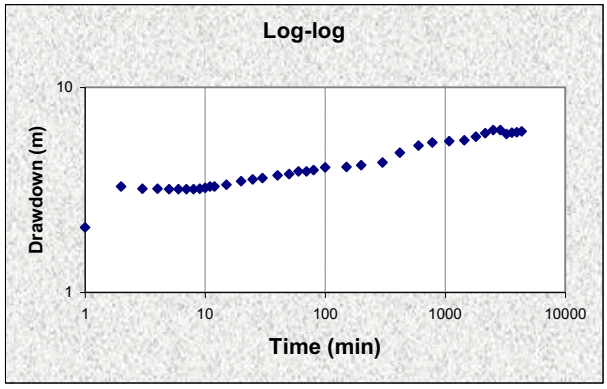

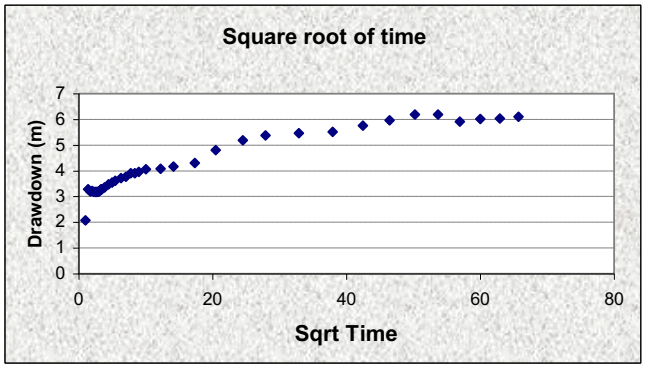

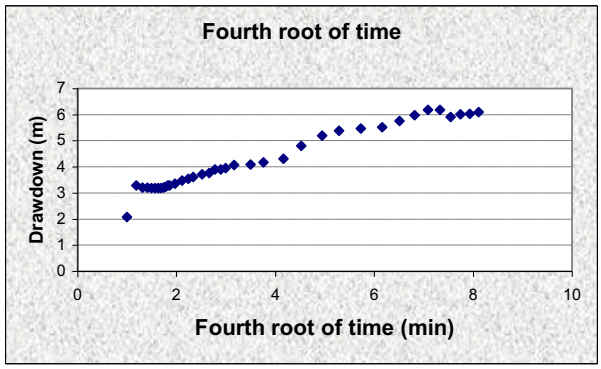

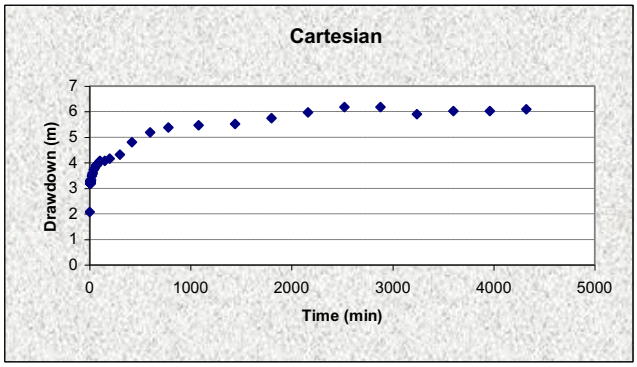

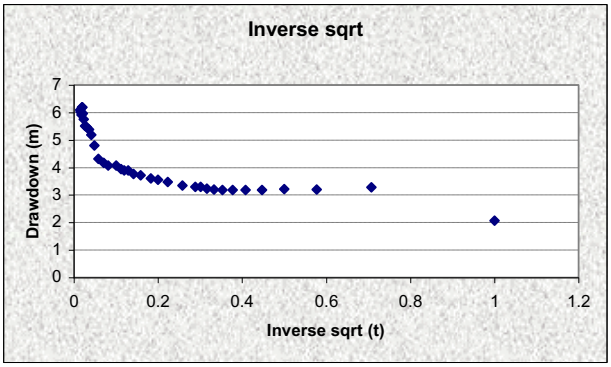

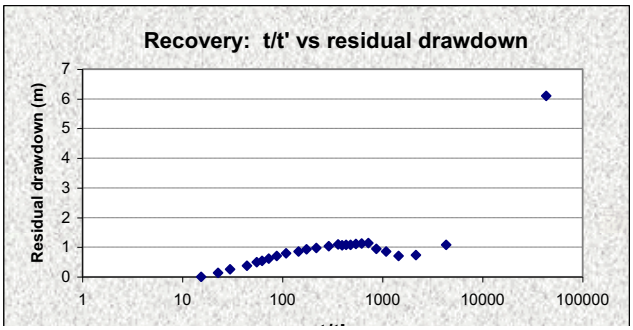

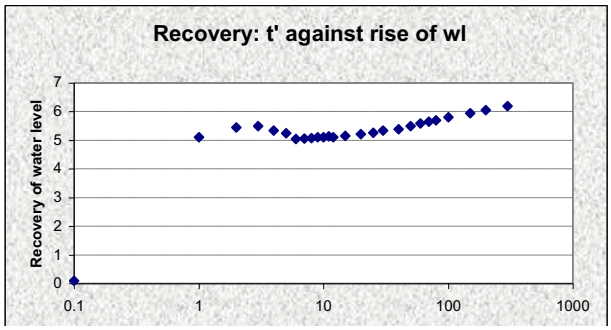

FIGURE J-44: STEP DRAWDOWN TEST – DP15

DP15

STEP DRAWDOWN AND MULTIRATE ANALYSIS

Enter field step test data at bottom of sheet

STEP DRAWDOWN	no	MULTI RATE	yes

	Q (l/s)	Q (m^3/d)	s_i (m)	Sigma s_i	Sigma s_i/Q_i
Step 1	1.7	146.88	0.58	0.58	0.0039488
Step 2	3.6	311.04	2.17	2.17	0.00697659
Step 3	6.9	596.16	6.72	6.72	0.01127214
Step 4	9.4	812.16	15.63	15.63	0.01924498
Step 5		0			0
Step 6		0			0
Step 7		0			0

B =	1.6E-03	d/m^2
C =	2.0E-05	d^2/m^5

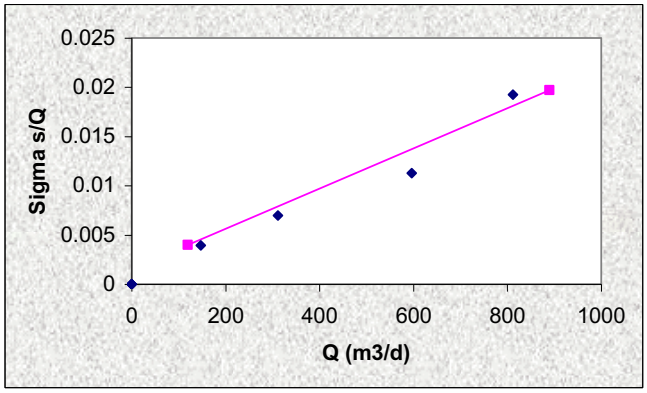

Q (l/s)	Well effiency(%)
1.7	34
3.6	20
6.9	11
9.4	9

FIGURE J-44 (CONTINUED): STEP DRAWDOWN TEST – DP15

Step test data

	Step1	Step1	Step3	Step4	Step5	Step6	Step7
Q (l/s) =	1.7	3.6	6.9	9.4			
t(min)	s (m)	s (m)	s (m)	s (m)	s (m)	s (m)	s (m)
1	0.47	0.58	2.17	6.72			
2	0.47	1.37	5.24	14.12			
3	0.47	1.66	6.44	15.65			
4	0.39	1.82	6.88	15.64			
5	0.39	1.84	6.88	15.64			
6	0.39	1.86	6.35	15.63			
7	0.47	1.86	6.32	15.63			
8	0.49	1.87	6.25	15.63			
9	0.5	1.91					
10	0.51	1.94	6.2				
12	0.51	1.94	6.2				
15	0.53	1.94	6.2				
20	0.53	1.95	6.24				
25	0.55	2.02	6.36				
30	0.55	2.05	6.39				
35	0.55	2.07	6.45				
40	0.58	2.1	6.54				
50	0.58	2.13	6.6				
60	0.58	2.14	6.7				

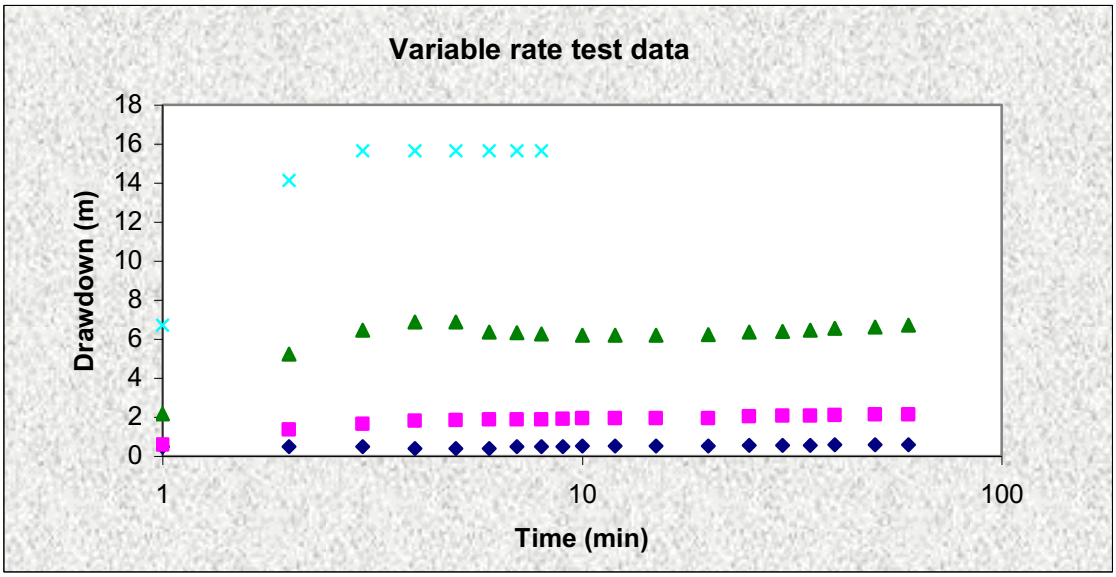

FIGURE J-45: COOPER-JACOB METHOD – DP15

Cooper-Jacob method

DP15

$T(m^2/d)$ =	85.5	r_e (m)=	28.35
S =	1.68E-06	Q (l/s) =	5.7

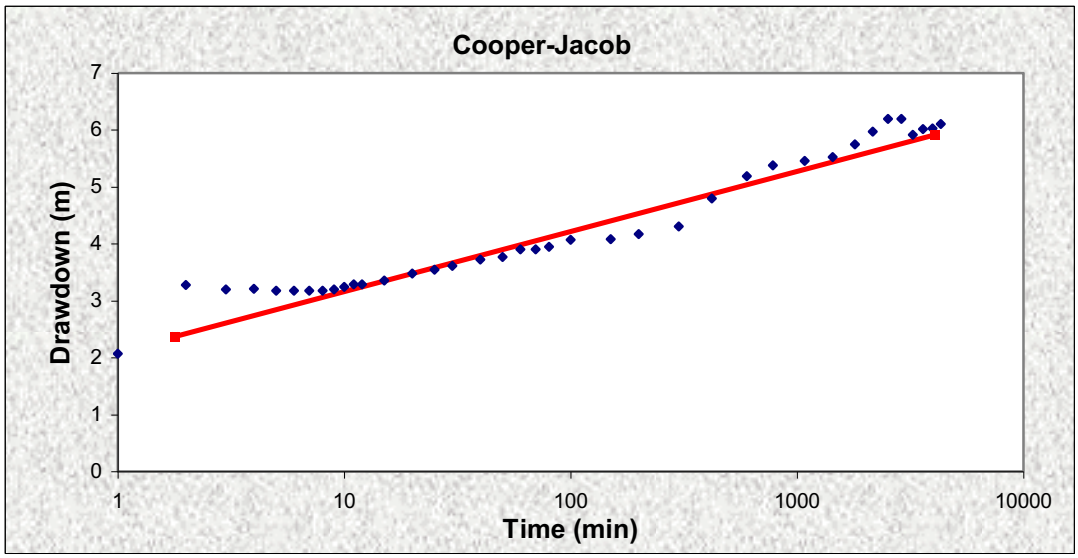

FIGURE J-46: SUSTAINABLE YIELD – BASIC SOLUTION – DP15

FC-METHOD : Estimation of the sustainable yield of a borehole

DP15

Extrapolation time in years = (enter)	5	2628000	Extrapol.time in minutes	
Effective borehole radius (r_e) = (enter)	14.98	14.98	← Est. r_e	From r(e) sheet
Q (l/s) from pumping test =	5.7	11.57	← Est. r_e	Qualified guess
s_a (available drawdown), sigma_s = (enter)	100		← Sigma_s from risk	
Annual effective recharge (mm) =	0	100.00	s_available working drawdown(m)	
t(end) and s(end) of pumping test =	4320	6.19	End time and drawdown of test	
Average maximum derivative = (enter)	2.1	2.1	Estimate of average of max deriv	
Average second derivative = (enter)	0.0	0.0	Estimate of average second deriv	
Derivative at radial flow period = (enter)	1.36		Read from derivative graph	
	T-early[m^2/d] =	66.27	Aqui. thick (m)	20
T and S estimates from derivatives	T-late [m^2/d] =	42.92	Est. S-late =	1.10E-03
(To obtain correct S-value, use program RPTSOLV)	S-late =	2.05E-03	S-estimate could be wrong	

BASIC SOLUTION

(Using derivatives + subjective information about boundaries)

(No values of T and S are necessary)

	No boundaries	Maximum influence of boundaries at long time: 1 no-flow	2 no-flow	Closed no-flow
sWell (Extrapol.time) =	12.08	17.92	23.77	41.31
Q_sust (l/s) =	47.20	31.80	23.98	13.80
	Best case	→		**Worst case**

Average Q_sust (l/s) = 26.55 — WARNING!! Est. Q_sust > Q during pumping test

with standard deviation= 14.09 — Suggestion:check available drawdown and rech

(If no information exists about boundaries skip advanced solution and go to final recommendation)

FINAL RECOMMENDED ABSTRACTION RATE

Abstraction rate (l/s) for 24 hr/d = (enter)	15.00
Total amount of water allowed to be abstracted per month (m^3) =	38880

COMMENTS

Q_sust with 68% safety = 22.81

Q_sust with 95% safety = 19.06

FIGURE J-47: SUSTAINABLE YIELD ADVANCED SOLUTION – DP15

ADVANCED SOLUTION

(Using derivatives+ knowledge on boundaries and other boreholes)

(Late T-and S-values a priori + distance to boundary)

T-late [m²/d] = (enter)	42.92				
S-late = (enter)	1.00E-03				
1. BOUNDARY INFORMATION (choose a or b)	(Code =9999 = dummy value if not applicable)				
(a) Barrier (no-flow) boundaries	Closed Square	Single Barrier	Intersect. 90°	2 Parallel Barriers	
Bound. distance a[meter] : (enter)	9999	6000	9999	9999	
Bound. distance b[meter] : (enter)			9999	9999	
s_Bound(t = Extrapol.time) [m] =	0.61	0.56	0.28	0.26	
(b) Fix head boundary + no-flow	Closed Fix	Single Fix	90°Fix+no-flow	// Fix+no-flow	
Bound. distance to fix head a[meter] : (enter)	9999	9999	9999	9999	
Bound. distance to no-flow b[meter] : (enter)			9999	9999	
s_Bound(t = Extrapol.time) [m] =	-0.45	-0.13	-0.04	0.00	
2. INFLUENCE OF OTHER BOREHOLES	Q (l/s)	r (m)	u_r	W(u,r)	
BH1	12	50	7.98E-06	11.16	
BH2	9	50	7.98E-06	11.16	
s_(influence of BH1,BH2) =	21.47	16.10	7.17E-07	13.57	
SOLUTION INCLUDING BOUNDS AND BH's					
Fix head + No-flow : Q_sust (l/s) =	9999.00	9999.00	9999.00	9999.00	
No-flow : Q_sust (l/s) =	9999.00	10.84	9999.00	9999.00	
Enter selected Q for risk analysis = (enter)	8.00	Sigma_s =	2.255		

(Go to Risk sheet and perform risk analysis from which sigma_s will be estimated : only for barrier boundaries)

FINAL RECOMMENDED ABSTRACTION RATE

Abstraction rate (l/s) for 24 hr/d = (enter)	10.00
Total amount of water allowed to be abstracted per month (m³) =	25920

COMMENTS

Q_sust with 68% safety = 11.1

Q_sust with 95% safety = 10.84

RISK ANALYSIS ADVANCED SOLUTION – DP15

Single barrier boundary: Use = 6000

SENSITIVITY CALCULATION:

		T	S	a
Numerical Derivative Factor :		0.01	0.01	0.01
s_Theis(t = Extrapol.time) [m]	17.40	16.81	17.49	17.40
s_Bound(t = Extrapol.time) [m] =	0.78	0.79	0.84	0.77
s_Total = s_Theis+s_Boundary [m]	18.19	17.59	18.33	18.17
Sensitivities:				
ds/dY (t = Extrapol.time):		-1.58E+01		
ds/dW (t = Extrapol.time):			-2.10E+00	
ds/da (t = Extrapol.time):				-2.67E-04

	%	Value
Uncertainties:		
% error of late T-value = (enter)	33	14.1623177
sigma (Y)		0.103
% error of late S-value = (enter)	100	1.00E-03
sigma (W)		0.693
% error in bound. distance (a) = (enter)	33	1980
Result:		
sigma (s_Total, t= Extrapol.time) [m] =	2.26	

FIGURE J-48: STEP DRAWDOWN TEST – DP12

DP12

STEP DRAWDOWN AND MULTIRATE ANALYSIS

Enter field step test data at bottom of sheet

STEP DRAWDOWN	no	MULTI RATE	yes

	Q (l/s)	Q (m^3/d)	s_i (m)	Sigma s_i	Sigma s_i/Q_i
Step 1	2.4	207.36	2.2	2.2	0.01060957
Step 2	5.4	466.56	5.88	5.88	0.01260288
Step 3	9.2	794.88	11.2	11.2	0.01409018
Step 4	15.5	1339.2	23.27	23.27	0.01737605
Step 5	20.8	1797.12	41.69	41.69	0.02319823
Step 6	27.1	2341.44	61.87	61.87	0.02642391
Step 7		0			0

B =	8.3E-03	d/m^2
C =	7.9E-06	d^2/m^5

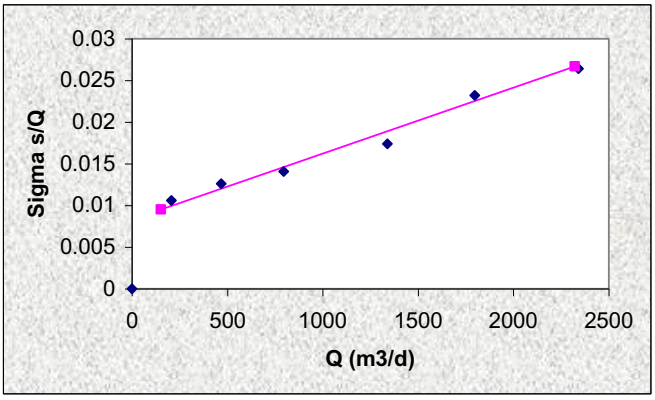

Q (l/s)	Well effiency(%)
2.4	83
5.4	69
9.2	57
15.5	44
20.8	37
27.1	31

FIGURE J-48 (CONTINUED) STEP DRAWDOWN TEST – DP12

Step test data

	Step1	Step1	Step3	Step4	Step5	Step6	Step7
Q (l/s) =	2.4	5.4	9.2	15.5	20.8	27.1	
t(min)	s (m)	s (m)	s (m)	s (m)	s (m)	s (m)	s (m)
0.5	1.55	2.2	5.83	11.11	22.84	39.09	
1	2.18	2.8	5.88	11.15	22.97	39.81	
1.5	2.34	3.46	6.78	11.2	23.1	40.38	
2	2.4	3.89	7.61	13.2	23.27	40.96	
2.5	2.33	4.21	8.22	14.53	26.15	41.69	
3	2.19	4.37	8.68	15.65	27.18	42.68	
3.5	2.04	4.54	8.95	16.42	28.07	45.27	
4	1.88	4.64	9.19	17.04	28.82	48	
4.5	1.72	4.73	9.39	17.58	29.44	50.3	
5	1.68	4.86	9.54	18.12	30.03	51.87	
7	1.65	4.92	9.68	18.42	30.46	53.32	
9	1.72	5.12	9.78	18.77	30.94	54.3	
12	1.81	5.25	9.98	19.06	31.35	55.44	
15	1.88	5.34	10.19	19.93	32.65	56.39	
20	2	5.41	10.34	20.51	33.13	58	
25	2.06	5.53	10.49	21.13	33.73	59.57	
30	2.11	5.61	10.67	21.5	34.86	61.87	
35	2.12	5.66	10.78	21.94	35.77		
40	2.13	5.71	10.87	22.26	36.85		
45	2.16	5.74	10.98	22.48	37.62		
50	2.17	5.77	11.07	22.65	38.25		
60	2.2	5.83	11.11	22.84	39.09		

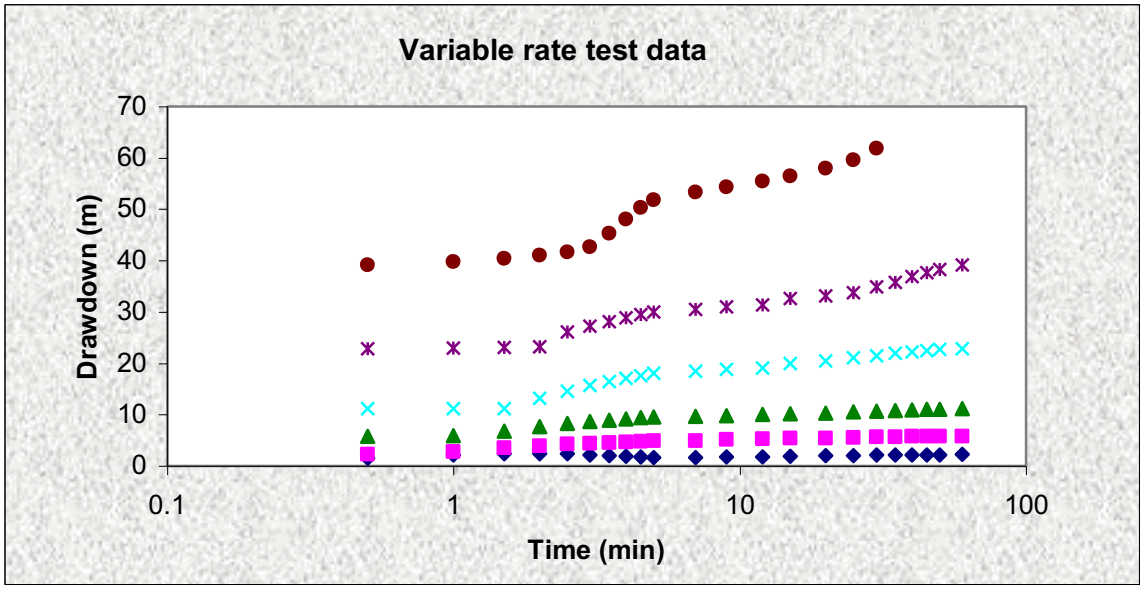

FIGURE J-49: STEP DRAWDOWN TEST – DP25

DP25

STEP DRAWDOWN AND MULTIRATE ANALYSIS

Enter field step test data at bottom of sheet

STEP DRAWDOWN	no	MULTI RATE	yes

	Q (l/s)	Q (m^3/d)	s_i (m)	Sigma s_i	Sigma s_i/Q_i
Step 1	6.97	602.208	4.85	4.85	0.0080537
Step 2	11.33	978.912	7.77	7.77	0.00793738
Step 3	19	1641.6	16.11	16.11	0.0098136
Step 4	26	2246.4	28.25	28.25	0.01257568
Step 5		0			0
Step 6		0			0
Step 7		0			0

B =	5.5E-03	d/m^2
C =	3.1E-06	d^2/m^5

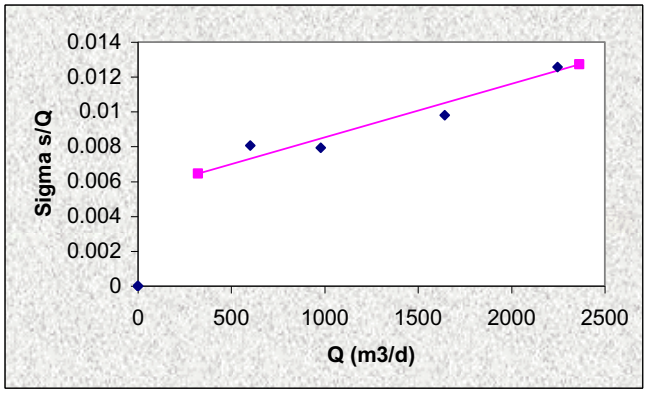

Q (l/s)	Well effiency(%)
6.97	75
11.33	65
19	52
26	44

FIGURE J-49 (CONTINUED): STEP DRAWDOWN TEST – DP25

Step test data							
	Step1	Step1	Step3	Step4	Step5	Step6	Step7
Q (l/s) =	7.97	11.33	19	26			
t(min)	s (m)	s (m)	s (m)	s (m)	s (m)	s (m)	s (m)
1	3.12	6.47	9.13	17.13			
2	3.2	6.87	11.12	18.71			
3	3.39	7.16	12.31	21.36			
4	3.46	7.35	13.17	22.69			
5	3.61	7.36	13.87	23.67			
6	4.42	7.39	14.27	24.36			
7	4.58	7.4	14.61	24.83			
8	4.39	7.42	14.87	25.26			
9	4.42	7.45	15.01	25.67			
10	4.46	7.45	15.07	25.95			
12	4.49	7.48	15.25	26.36			
15	4.54	7.49	15.37	26.76			
20	4.62	7.5	15.65	26.96			
25	4.64	7.54	15.71	27.25			
30	4.7	7.59	15.74	27.45			
35	4.7	7.61	15.76	27.59			
40	4.7	7.61	15.83	27.74			
50	4.73	7.63	15.91	27.79			
60	4.75	7.67	15.91	27.88			
80	4.77	7.77	16	28.12			
100	4.85	7.77	16.11	28.25			

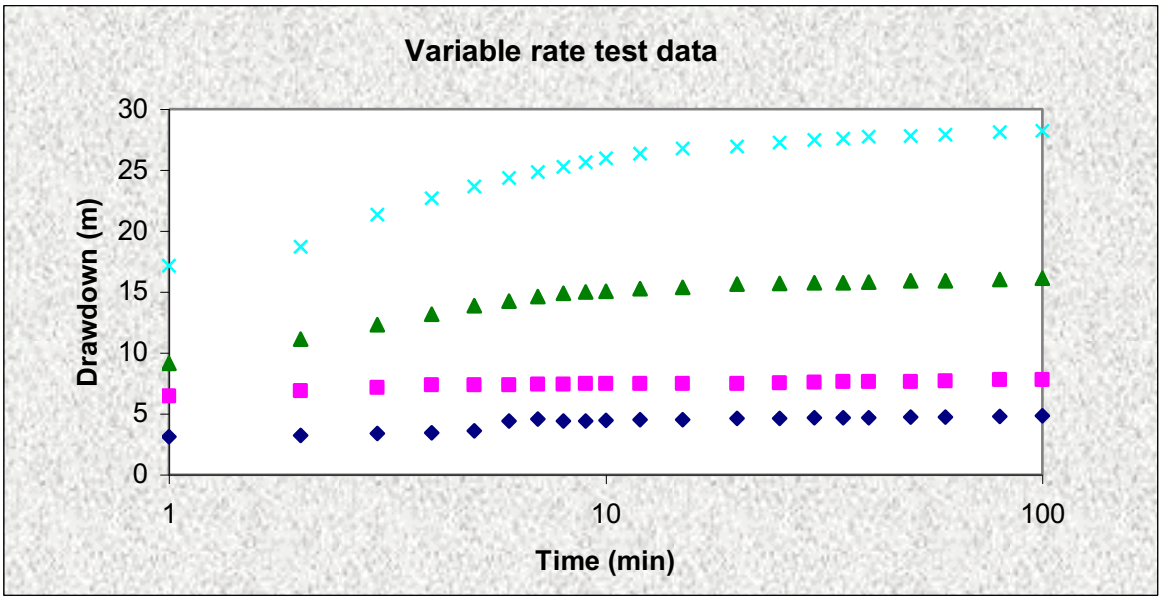

FIGURE J-50: STEP DRAWDOWN TEST – DP29

DP29

STEP DRAWDOWN AND MULTIRATE ANALYSIS

Enter field step test data at bottom of sheet

STEP DRAWDOWN	no	MULTI RATE	yes

	Q (l/s)	Q (m^3/d)	s_i (m)	Sigma s_i	Sigma s_i/Q_i
Step 1	6.1	527.04	11.63	11.63	0.02206664
Step 2	8.3	717.12	21.82	21.82	0.03042726
Step 3	11.1	959.04	38	38	0.03962296
Step 4		0			0
Step 5		0			0
Step 6		0			0
Step 7		0			0

B =	5.3E-03	d/m^2
C =	3.4E-05	d^2/m^5

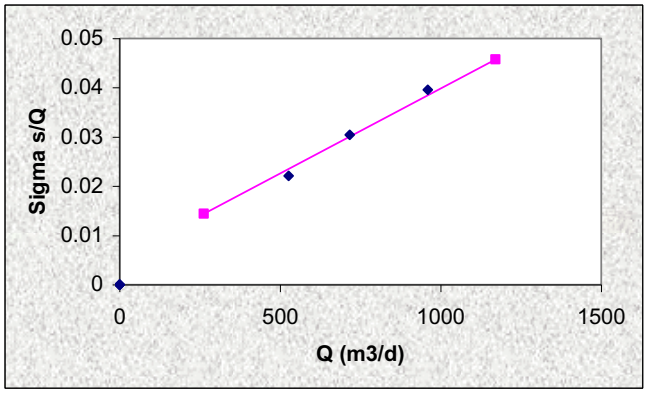

Q (l/s)	Well effiency(%)
6.1	23
8.3	18
11.1	14

FIGURE J-50 (CONTINUED) STEP DRAWDOWN TEST – DP29

Step test data							
	Step1	Step1	Step3	Step4	Step5	Step6	Step7
Q (l/s) =	6.1	8.3	11.1				
t(min)	s (m)	s (m)	s (m)	s (m)	s (m)	s (m)	s (m)
1	5.93	13.71	23.84				
2	7.11	15.06	25.08				
3	7.64	16.24	25.97				
4	8.08	16.94	26.8				
5	8.53	17.66	27.42				
6	8.78	18.12	28.01				
7	9.09	18.52	28.49				
8	9.3	18.84	28.89				
9	9.44	19.1	29.33				
10	9.6	19.39	29.6				
12	9.83	19.81	30.36				
15	10.13	20.33	31.38				
20	10.44	20.82	32.35				
25	10.74	21.12	33.52				
30	10.97	21.3	33.44				
35	11.18	21.44	34.45				
40	11.28	21.59	36				
50	11.43	21.97	38				
60	11.46	21.89					
80	11.58	21.82					
100	11.63	21.82					

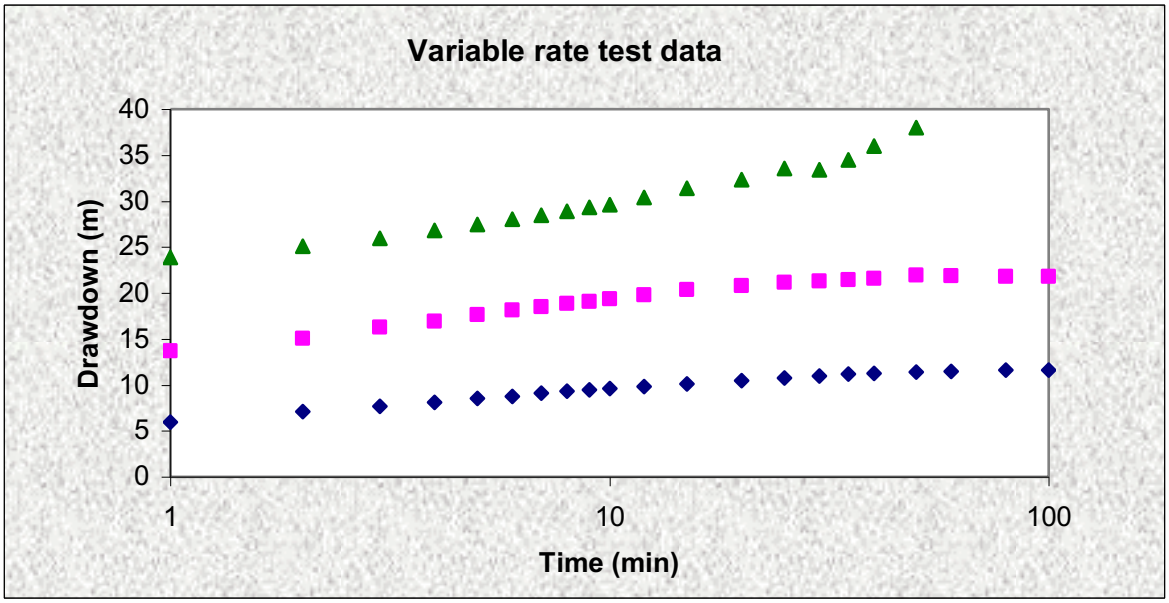

FIGURE J-51: FC DATA SHEET – DP18

DATA sheet: Enter general info and data of constant rate pumping test and recovery (optional)

Country:	South Africa	**Geology:**	Alluvium
Region:	Little Karoo	**Depth of BH:**	17
Owner:	DWAF	**Water strikes:**	9
X-coord:	3715403.70	**Date of Test:**	Nov-97
Y-coord:	49135.50	**Contractor:**	Callie Calitz

CONSTANT RATE TEST DATA : enter values in cells which are coloured light yellow

Borehole:		**DP18**									
Q (l/s)=	13.2					**Recovery data**					
t (min)	**s (m)**	avg s'	avg s"	avg T	avg S	**Time t'**	**Res_s**	t/t'	WI rise	s'	Rec_T
1.00	2.42					0.1	6.63	28801	0		
2.00	2.72					1	1.4	2881	5.23	4.38	
3.00	2.72	#NUM!	#NUM!			2	1.3	1441	5.33	0.28	
4.00	2.02	#NUM!	#NUM!	0.00	0.00E+00	3	1.27	961	5.36	0.26	732.6
5.00	2.22	#NUM!	#NUM!	-265.84	0.00E+00	4	1.22	721	5.41	0.32	861.1
6.00	2.02	#NUM!	#NUM!	439.92	0.00E+00	5	1.2	577	5.43	0.17	790.4
7.00	2.22	0.61	#NUM!	350.33	0.00E+00	6	1.19	481	5.44	0.34	688.6
8.00	2.21	0.48	-2.07	265.32	0.00E+00	7	1.15	412.4	5.48	0.48	669.4
9.00	2.25	0.38	-3.68	889.98	0.00E+00	8	1.13	361	5.5	0.19	998.4
10.00	2.25	0.21	#NUM!	687.31	0.00E+00	9	1.13	321	5.5	0.10	1603.9
11.00	2.25	#NUM!	#NUM!	1687.58	0.00E+00	10	1.12	289	5.51	0.12	1458.3
12.00	2.29	#NUM!	#NUM!	-1548.21	0.00E+00	11	1.12	262.8	5.51	0.25	956.1
15.00	2.22	#NUM!	#NUM!	-1162.55	0.00E+00	12	1.1	241	5.53	0.36	629.1
20.00	2.22	#NUM!	#NUM!	-1982.37	0.00E+00	15	1.07	193	5.56	0.41	552.8
25.00	2.22	#NUM!	#NUM!	514.09	0.00E+00	20	1.01	145	5.62	0.37	644.7
30.00	2.23	0.73	#NUM!	209.89	0.00E+00	25	0.99	116.2	5.64	0.23	765.4
40.00	2.51	0.78	-1.76	213.51	0.00E+00	30	0.97	97	5.66	0.24	1054.2
50.00	2.51	0.36	-2.78	213.51	0.00E+00	40	0.94	73	5.69	0.14	931.5
60.00	2.51	0.25	0.06	213.51	0.00E+00	50	0.94	58.6	5.69	0.33	640.3
70.00	2.51	0.29	2.80	213.51	0.00E+00	60	0.88	49	5.75	0.75	438.3
80.00	2.55	0.61	3.49	213.51	0.00E+00	70	0.83	42.14	5.8	0.44	606.8
100.00	2.63	0.92	1.40	213.51	0.00E+00	90	0.8	33	5.83	0.12	765.0
150.00	2.815	1.23	0.78	180.25	0.00E+00	140	0.79	21.57	5.84	0.38	721.4
200.00	2.91	1.58	0.57	117.80	0.00E+00	190	0.67	16.16	5.96	0.52	455.4
300.00	3.37	1.84	0.14	108.46	0.00E+00	290	0.62	10.93	6.01	0.49	393.6
420.00	3.68	1.76	-0.16	108.46	0.00E+00	410	0.503	8.024	6.127	0.58	424.5
600.00	3.81	1.66	0.21	108.46	0.00E+00	590	0.44	5.881	6.19	0.42	420.8
780.00	4.1	1.96	0.96	108.46	0.00E+00	770	0.389	4.74	6.241	0.50	437.5
1080.00	4.21	2.96	1.62	69.11	0.00E+00	1070	0.31	3.692	6.32	0.52	476.7
1440.00	4.55	4.89	1.43	39.55	0.00E+00	1430	0.25	3.014	6.38	0.32	522.0
1800.00	5.68	6.39	#NUM!	28.36	0.00E+00	1790	0.24	2.609	6.39	0.38	533.5
2160.00	6.15	#NUM!	#NUM!	28.36	0.00E+00	2150	0.18	2.34	6.45	0.49	842.6
2520.00	6.53	#NUM!	#NUM!	28.36	0.00E+00	2510	0.17	2.147	6.46	0.08	789.5
2880.00	6.63	#NUM!	#NUM!	28.36	0.00E+00	2870	0.17	2.003	6.46	0.47	662.7
		#NUM!	#NUM!	28.36	0.00E+00	3410	0.11	1.845	6.52	0.82	336.5
		#NUM!	#NUM!	28.36	0.00E+00	3830	0.067	1.752	6.563	0.62	277.3
		#NUM!	#NUM!	28.36	0.00E+00	4130	0.06	1.697	6.57	0.84	#DIV/0!
		#NUM!	#NUM!	28.36	0.00E+00	4490	0.01	1.641	6.62	#DIV/0!	#DIV/0!

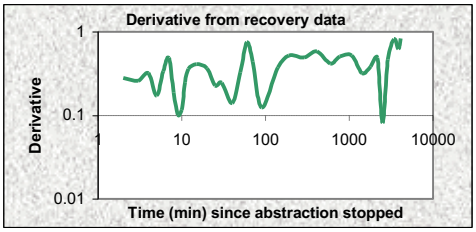

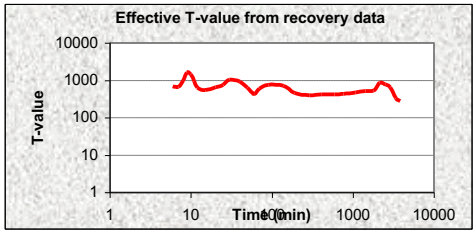

FIGURE J-52: DERIVATIVE PLOTS – DP18

DERIVATIVE PLOTS AND T-AND S-VALUES

DP18

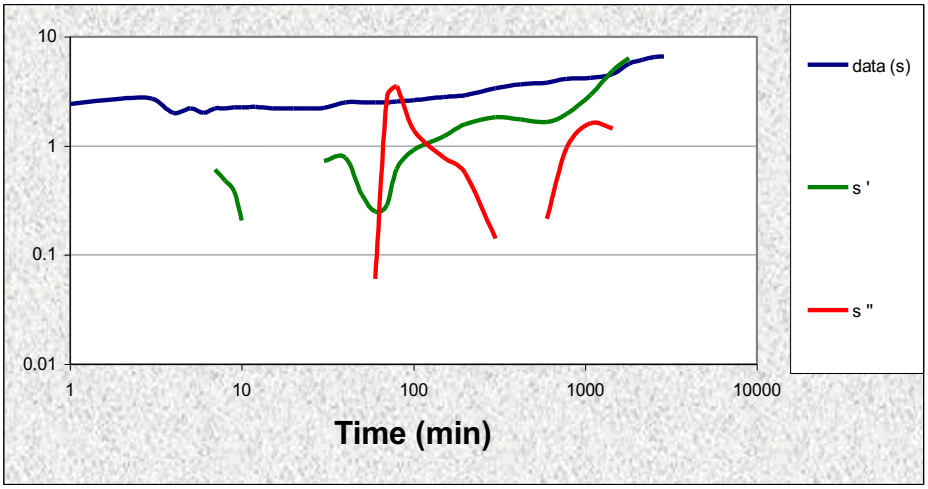

log derivative = 0.08 → very good fracture network

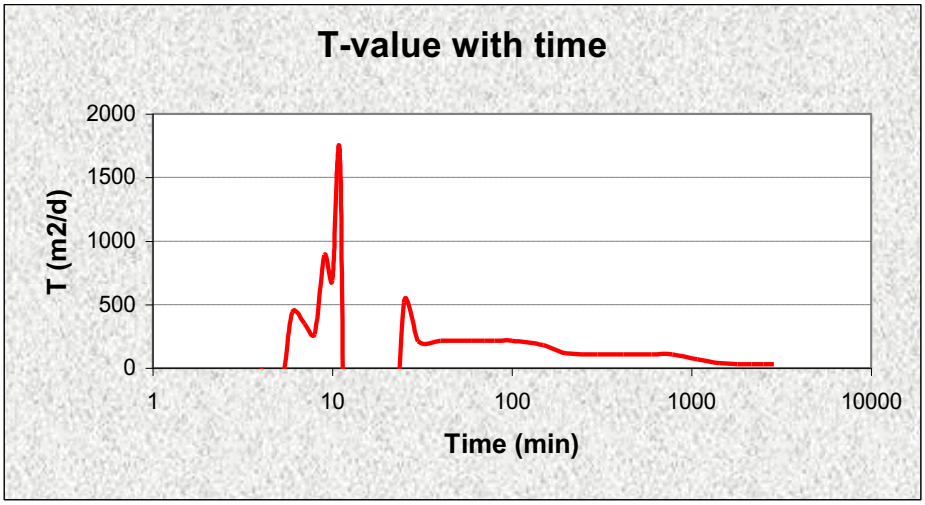

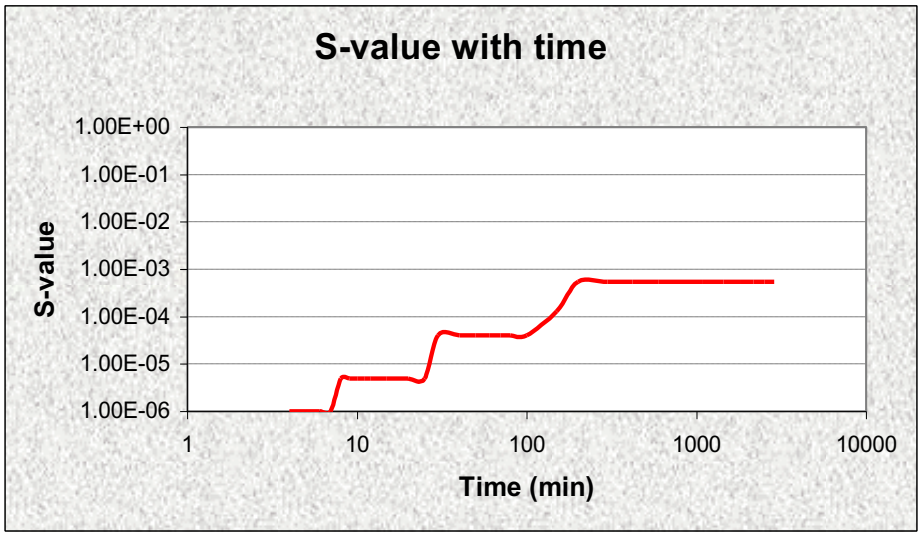

FIGURE J-53: TRANSMISSIVITY AND STORATIVITY WITH TIME – DP18

FIGURE J-54: DIAGNOSTIC PLOTS – DP18

DIAGNOSTIC PLOTS

DP18

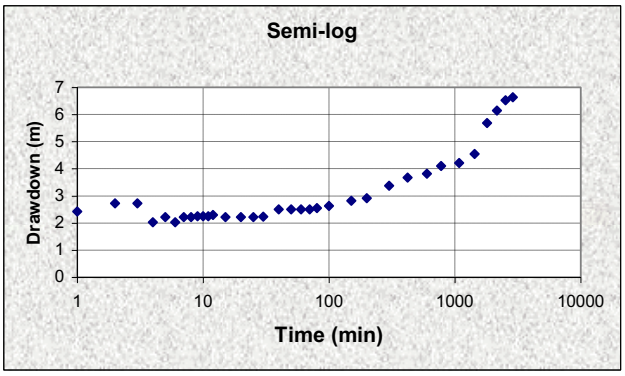

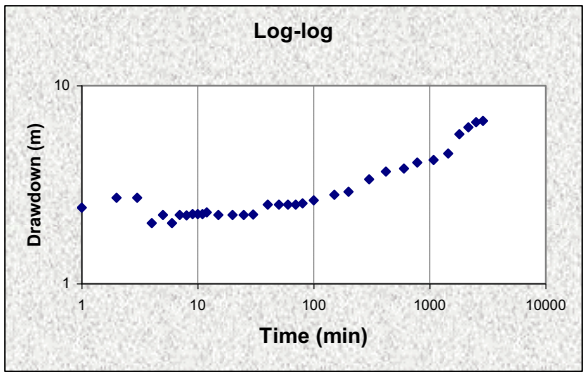

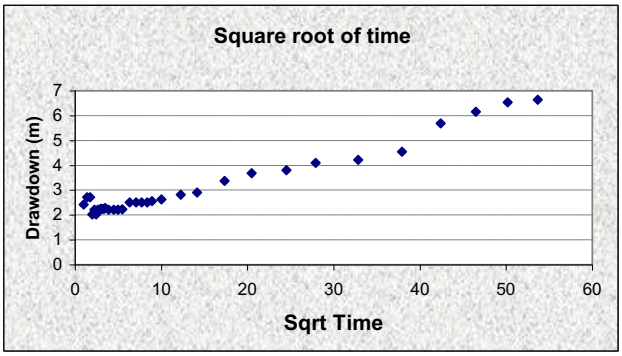

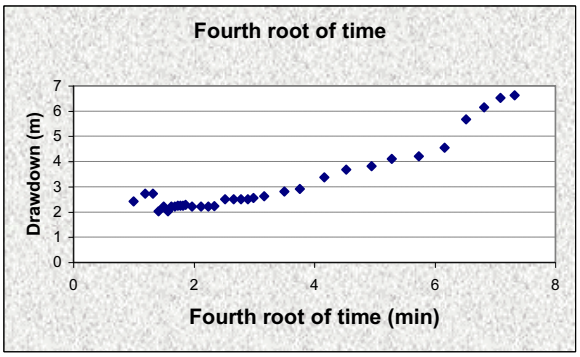

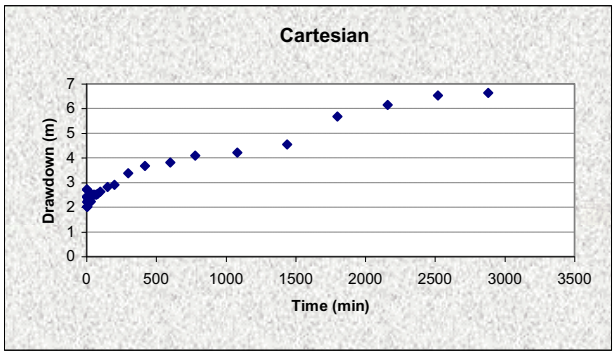

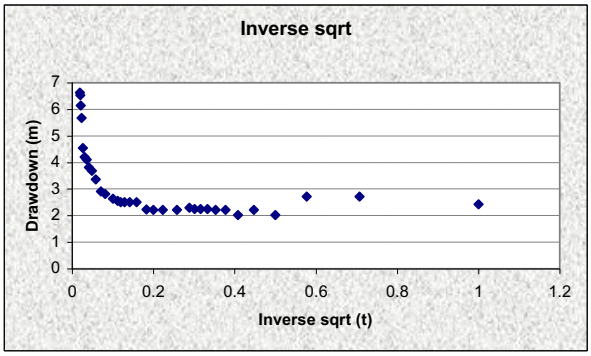

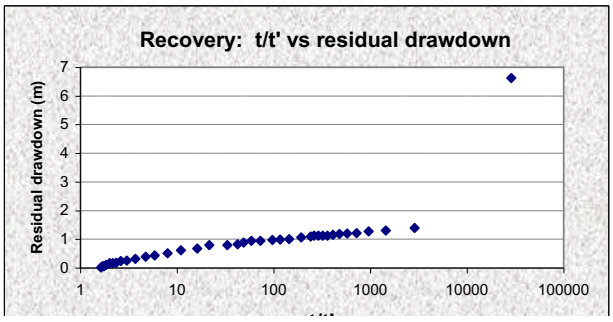

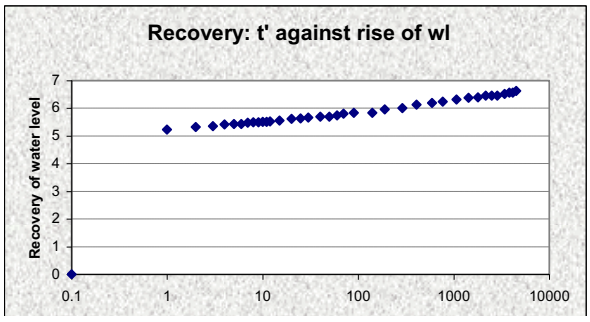

FIGURE J-55: STEP DRAWDOWN TEST – DP18

DP18

STEP DRAWDOWN AND MULTIRATE ANALYSIS

Enter field step test data at bottom of sheet

STEP DRAWDOWN	no	MULTI RATE	yes

	Q (l/s)	Q (m^3/d)	s_i (m)	Sigma s_i	Sigma s_i/Q_i
Step 1	5.7	492.48	0.74	0.74	0.0015026
Step 2	11.1	959.04	1.74	1.74	0.00181431
Step 3	16.7	1442.88	4.67	4.67	0.00323658
Step 4	20	1728	6.66	6.66	0.00385417
Step 5		0			0
Step 6		0			0
Step 7		0			0

B =	5.1E-04	d/m^2
C =	1.8E-06	d^2/m^5

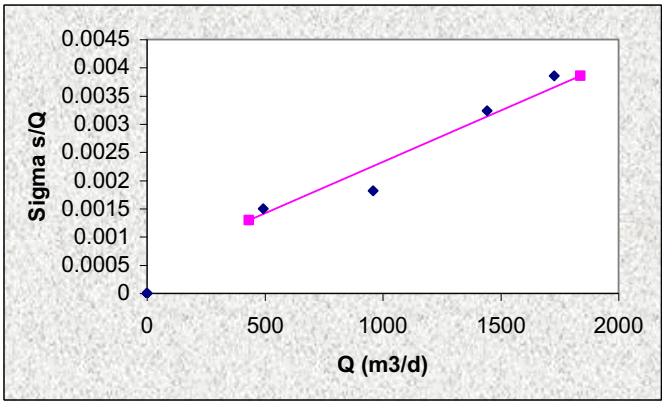

Q (l/s)	Well effiency(%)
5.7	36
11.1	23
16.7	16
20	14

FIGURE J-55 (CONTINUED) STEP DRAWDOWN TEST – DP18

Step test data							
	Step1	Step1	Step3	Step4	Step5	Step6	Step7
Q (l/s) =	5.7	11.1	16.7	20			
t(min)	s (m)	s (m)	s (m)	s (m)	s (m)	s (m)	s (m)
1	1.01	1.35	2.83	5.87			
2	0.76	1.44	3.29	5.92			
3	0.76	1.48	3.51	6.42			
4	0.64	1.5	3.64	6.63			
5	0.64	1.54	3.65	6.65			
6	0.67	1.56	3.69	6.652			
7	0.69	1.56	3.74	6.652			
8	0.69	1.57	3.77	6.652			
9	0.69	1.57	3.782	6.652			
10	0.69	1.56	3.82	6.652			
12	0.68	1.57	3.91	6.653			
15	0.67	1.57	3.995				
20	0.67	1.58	4.03				
25	0.68	1.59	4.04				
30	0.69	1.635	4.04				
35	0.699	1.64	4.15				
40	0.73	1.652	4.22				
50	0.73	1.66	4.31				
60	0.73	1.71	4.44				
80	0.74	1.74	4.67				

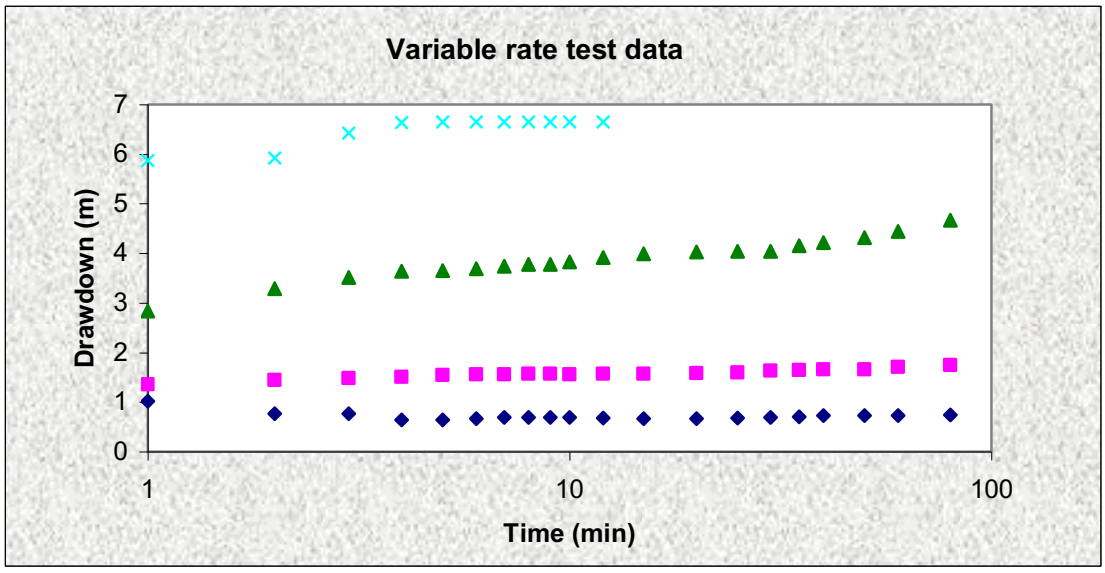

FIGURE J-56: COOPER-JACOB – DP18

Cooper-Jacob method

DP18

T(m^2/d) =	341.6	r_e (m)=	31.91
S =	9.28E-07	Q (l/s) =	13.2

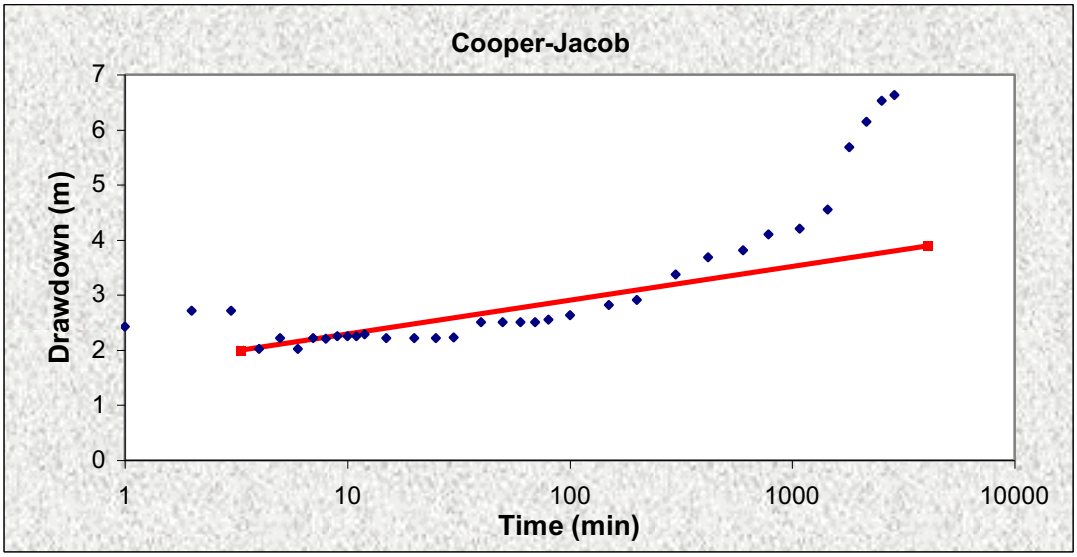

FIGURE J-57: SUSTAINABLE YIELD - BASIC SOLUTION – DP18

FC-METHOD : Estimation of the sustainable yield of a borehole

DP18

Extrapolation time in years = (enter)	5	2628000	Extrapol.time in minutes
Effective borehole radius (r_e) = (enter)	31.91	31.91	← Est. r_e — From r(e) sheet
Q (l/s) from pumping test =	13.2	22.91	← Est. r_e — Qualified guess
s_a (available drawdown), sigma_s = (enter)	5	2.64	← Sigma_s from risk
Annual effective recharge (mm) =	0	2.36	s_available working drawdown(m)
t(end) and s(end) of pumping test =	2880	6.63	End time and drawdown of test
Average maximum derivative = (enter)	3.0	6.4	Estimate of average of max deriv
Average second derivative = (enter)	0.0	0.0	Estimate of average second deriv
Derivative at radial flow period = (enter)	1.76		Read from derivative graph
	T-early[m^2/d] =	118.58	Aqui. thick (m) — 5
T and S estimates from derivatives	T-late [m^2/d] =	70.51	Est. S-late = — 2.75E-04
(To obtain correct S-value, use program RPTSOLV)	S-late =	5.50E-04	S-estimate could be wrong

BASIC SOLUTION

(Using derivatives + subjective information about boundaries)

(No values of T and S are necessary)

	No boundaries	Maximum influence of boundaries at long time: 1 no-flow	2 no-flow	Closed no-flow
sWell (Extrapol.time) =	15.60	24.36	33.13	59.41
Q_sust (l/s) =	2.00	1.28	0.94	0.52
	Best case			Worst case

Average Q_sust (l/s) = 1.06

with standard deviation= 0.62

(If no information exists about boundaries skip advanced solution and go to final recommendation)

FINAL RECOMMENDED ABSTRACTION RATE

Abstraction rate (l/s) for 24 hr/d = (enter)	1.00
Total amount of water allowed to be abstracted per month (m^3) =	2592

COMMENTS

Q_sust with 68% safety = 1.32

Q_sust with 95% safety = 1.06

FIGURE J-58: SUSTAINABLE YIELD – DP18 ADVANCED SOLUTION

ADVANCED SOLUTION

(Using derivatives+ knowledge on boundaries and other boreholes)

(Late T-and S-values a priori + distance to boundary)

T-late [m^2/d] = (enter) →	70.51				
S-late = (enter) →	1.00E-03				
1. BOUNDARY INFORMATION (choose a or b)	(Code =9999 = dummy value if not applicable)				
(a) Barrier (no-flow) boundaries →	Closed Square	Single Barrier	Intersect. 90°	2 Parallel Barriers	
Bound. distance a[meter] : (enter)	9999	9999	9999	9999	
Bound. distance b[meter] : (enter)			9999	9999	
s_Bound(t = Extrapol.time) [m] =	2.26	0.42	0.95	0.86	
(b) Fix head boundary + no-flow →	Closed Fix	Single Fix	90°Fix+no-flow	// Fix+no-flow	
Bound. distance to fix head a[meter] : (enter)	9999	50	9999	9999	
Bound. distance to no-flow b[meter] : (enter)			9999	9999	
s_Bound(t = Extrapol.time) [m] =	-1.29	-13.23	-0.24	-0.03	
2. INFLUENCE OF OTHER BOREHOLES →	Q (l/s)	r (m)	u_r	W(u,r)	
BH1			0.00E+00	#NUM!	
BH2			0.00E+00	#NUM!	
s_(influence of BH1,BH2) =	0.00	0.00	1.98E-06	12.56	
SOLUTION INCLUDING BOUNDS AND BH's					
Fix head + No-flow : Q_sust (l/s) =	9999.00	10.59	9999.00	9999.00	
No-flow : Q_sust (l/s) =	9999.00	9999.00	9999.00	9999.00	
Enter selected Q for risk analysis = (enter) →	10.00	Sigma_s =	0.000		

(Go to Risk sheet and perform risk analysis from which sigma_s will be estimated : only for barrier boundaries)

FINAL RECOMMENDED ABSTRACTION RATE

Abstraction rate (l/s) for 24 hr/d = (enter)	10.00
Total amount of water allowed to be abstracted per month (m^3) =	25920

COMMENTS

Q_sust with 68% safety =

Q_sust with 95% safety =

FIGURE J-59: FC DATA SHEET – VG3

DATA sheet: Enter data of constant rate pumping test and recovery (optional)

CONSTANT RATE TEST DATA : enter values in cells which are coloured light yellow

Borehole: VG3

Q (l/s)=	8.8					Recovery data					
t (min)	s (m)	avg s'	avg s''	avg T	avg S	Time t'	Res_s	t/t'	WI rise	s'	Rec_T
1.00	13					0.1	48.88	43001	0		
2.00	16					1	35.35	4301	13.53	16.88	
3.00	17.66	15.65	-0.90			2	25.45	2151	23.43	33.37	
4.00	18.75	10.33	-0.91	13.76	1.00E-06	3	19.4	1434	29.48	36.34	3.9
5.00	19.81	9.12	-0.63	12.54	1.23E-06	4	14.47	1076	34.41	38.88	4.1
6.00	20.8	8.29	0.45	20.60	1.23E-06	5	10.78	861	38.1	28.70	5.0
7.00	21.58	9.85	2.67	18.33	1.23E-06	6	9.48	717.7	39.4	19.61	6.2
8.00	20.1	16.51	3.98	7.45	5.03E-06	7	7.9	615.3	40.98	19.95	7.8
9.00	23.56	27.30	1.89	4.38	9.14E-06	8	7	538.5	41.88	14.41	9.2
10.00	24.88	26.89	-2.19	4.05	9.99E-06	9	6.33	478.8	42.55	12.19	12.0
11.00	26	18.56	-3.37	7.80	9.99E-06	10	5.82	431	43.06	8.76	15.9
12.00	26.54	13.23	-2.15	13.32	9.99E-06	11	5.57	391.9	43.31	6.31	19.6
15.00	26.22	12.81	0.25	11.19	9.99E-06	12	5.32	359.3	43.56	6.45	22.3
20.00	29.43	15.19	0.41	8.60	9.99E-06	15	4.7	287.7	44.18	5.93	22.8
25.00	30.89	15.90	-0.12	7.98	9.99E-06	20	4	216	44.88	5.98	24.3
30.00	32.02	14.47	-0.57	9.76	9.99E-06	25	3.37	173	45.51	5.33	27.8
40.00	33.96	12.04	-0.65	11.41	9.99E-06	30	3.07	144.3	45.81	3.93	32.0
50.00	35.01	10.66	-0.36	11.41	9.99E-06	40	2.57	108.5	46.31	3.93	36.5
60.00	35.1	10.15	-0.34	11.41	9.99E-06	50	2.2	87	46.68	3.59	39.3
70.00	36.4	9.48	-0.68	11.41	9.99E-06	60	1.94	72.67	46.94	3.15	42.1
80.00	36.9	8.04	-0.86	11.41	9.99E-06	70	1.74	62.43	47.14	3.20	45.0
100.00	37.56	6.69	-0.67	11.41	9.99E-06	80	1.54	54.75	47.34	2.94	49.8
150.00	38.38	5.95	-0.22	11.41	9.99E-06	100	1.28	44	47.6	2.32	59.4
200.00	39.31	5.72	-0.23	11.41	9.99E-06	150	0.9	29.67	47.98	1.88	81.3
300.00	40.61	5.03	-0.50	11.41	9.99E-06	200	0.72	22.5	48.16	1.15	110.2
420.00	40.71	4.00	-0.67	11.41	9.99E-06	300	0.55	15.33	48.33	0.93	148.8
600.00	41.8	3.19	-0.38	11.41	9.99E-06	420	0.42	11.24	48.46	0.76	178.3
780.00	41.8	3.07	0.33	11.41	9.99E-06	600	0.32	8.167	48.56	0.67	219.0
1080.00	41.8	3.88	0.89	11.41	9.99E-06	780	0.24	6.513	48.64	0.50	269.0
1440.00	42.91	5.07	0.37	11.41	9.99E-06	1080	0.19	4.981	48.69	0.41	275.2
1800.00	43.44	5.04	0.49	11.41	9.99E-06	1440	0.13	3.986	48.75	0.62	241.8
2160.00	44.04	6.20	2.36	11.41	9.99E-06	1800	0.05	3.389	48.83	0.74	#DIV/0!
2520.00	44.01	9.82	4.11	11.41	9.99E-06	2160	0	2.991	48.88	######	#DIV/0!
2880.00	44.01	19.94	3.46	5.75	2.76E-04			#####	#####	######	#DIV/0!
3240.00	47.56	25.28	#NUM!	4.63	5.26E-04			#####	#####	######	#DIV/0!
3600.00	48.31	#####	#NUM!	4.63	5.26E-04			#####	#####	######	#DIV/0!
3960.00	48.54	#####	#NUM!	4.63	5.26E-04			#####	#####	######	#DIV/0!
4300.00	48.88	#####	#NUM!	4.63	5.26E-04			#####	#####	######	#DIV/0!
		#####	#NUM!	4.63	5.26E-04			#####	#####	######	#DIV/0!

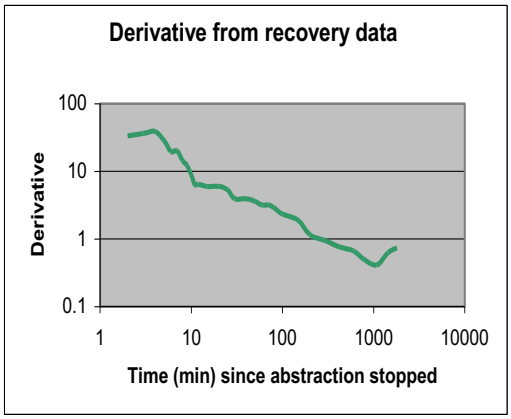

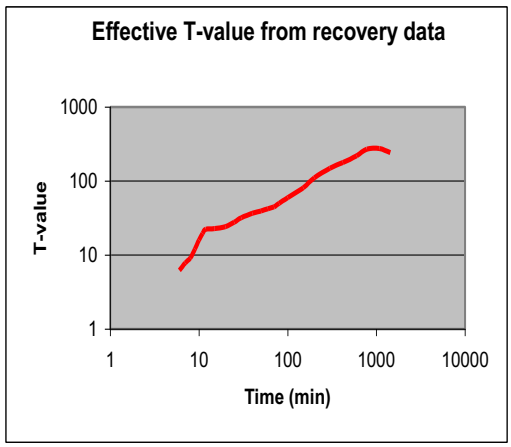

FIGURE J-60: DERIVATIVE PLOT VG3

DERIVATIVE PLOTS AND T-AND S-VALUES

VG3

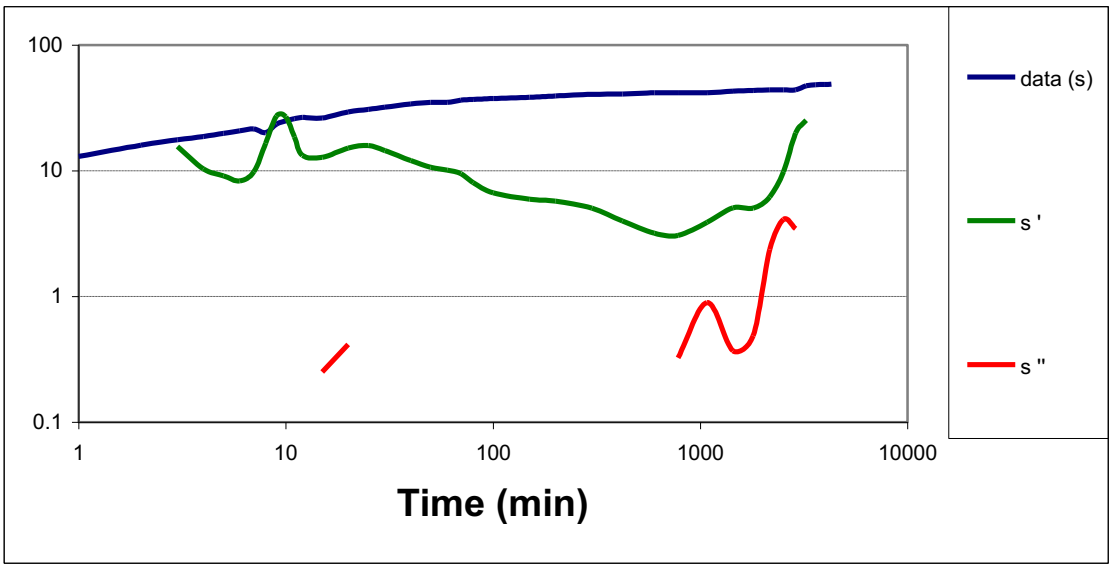

log derivative = 0.14 → **good fracture network**

FIGURE J-61: COOPER-JACOB ANALYSIS –VG3

Cooper-Jacob method

VG3

T(m^2/d) =	**20.6**	r_e (m)=	2.46 →
S =	**2.79E-06**	Q (l/s) =	8.8

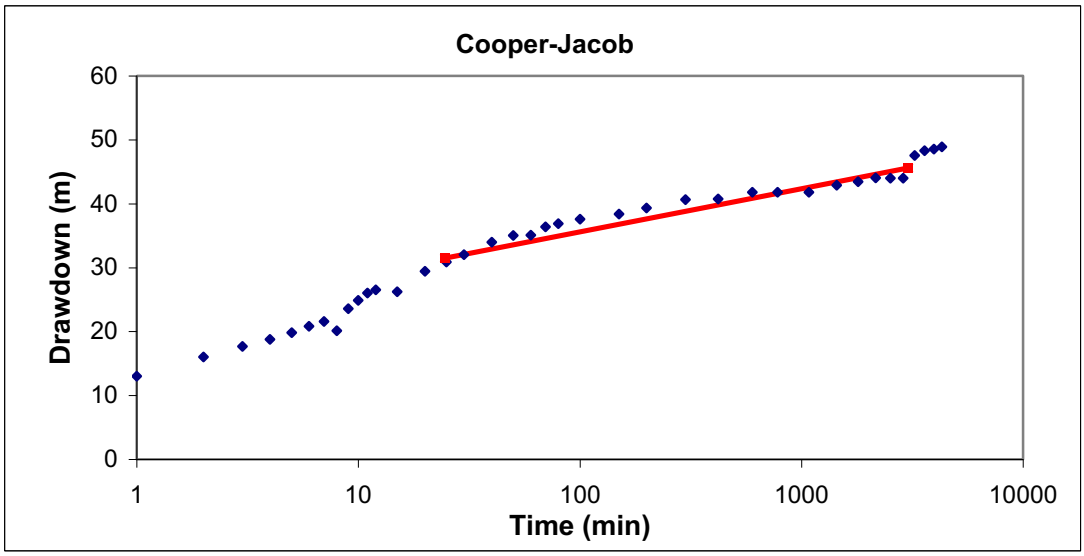

FIGURE J-62: VARIATION OF TRANSMISSIVITY AND STORAGE

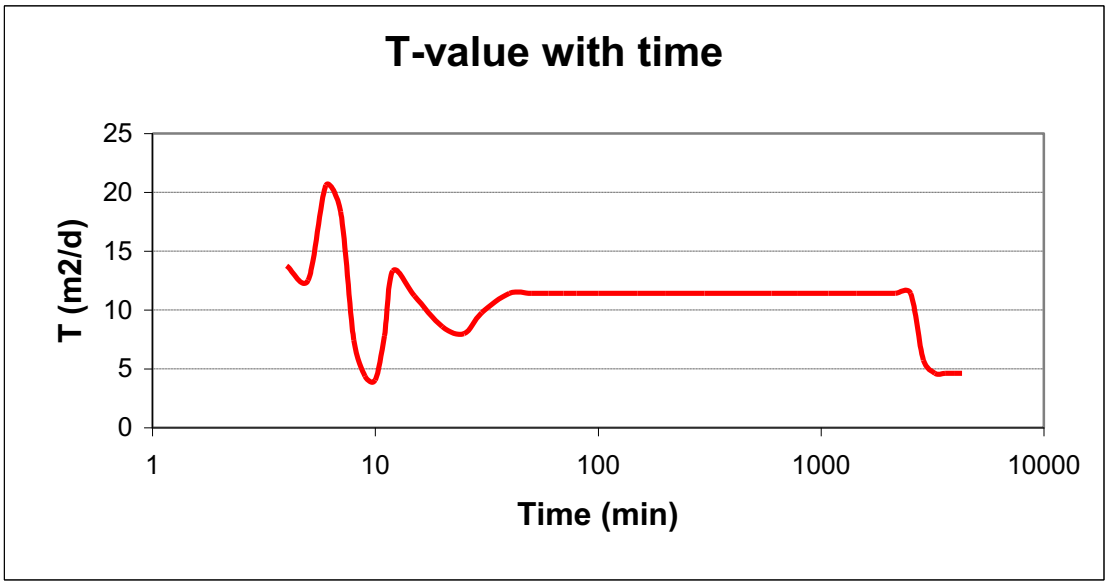

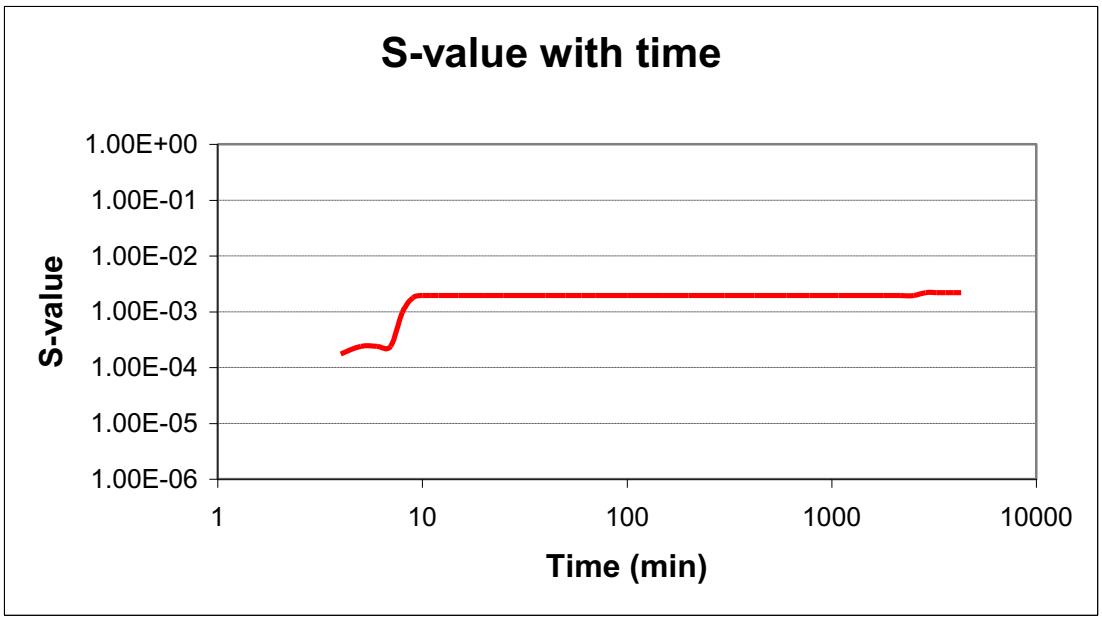

FIGURE J-63: DIAGNOSTIC PLOTS VG3

DIAGNOSTIC PLOTS Main Data

VG3

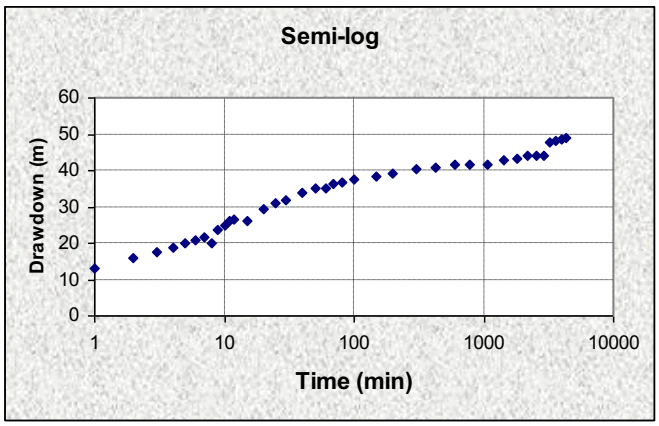

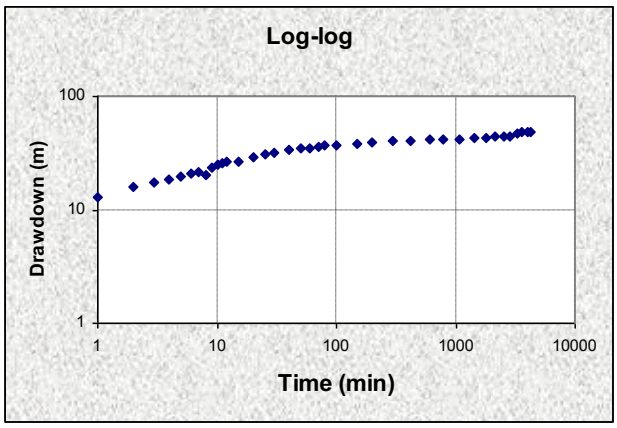

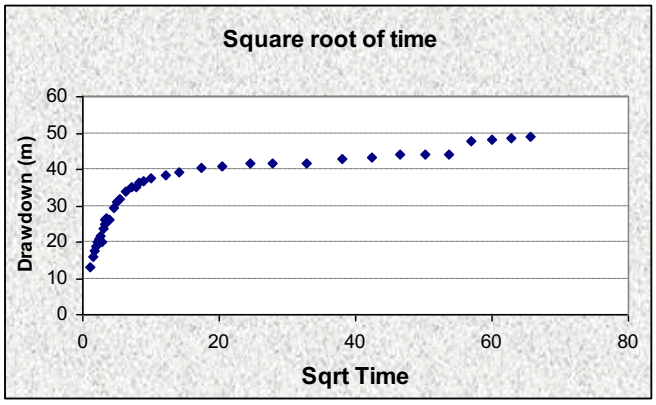

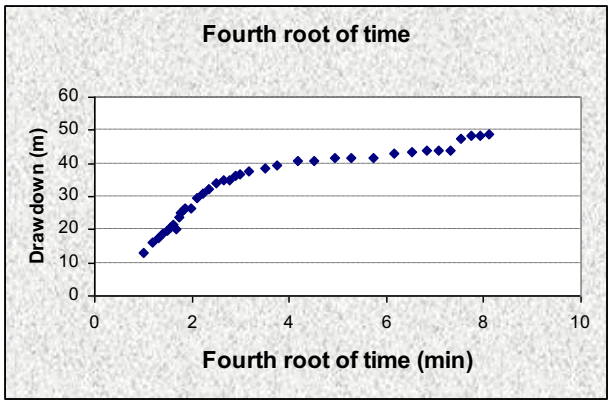

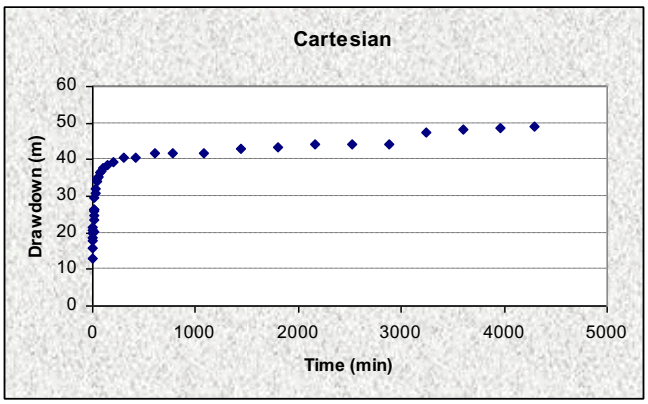

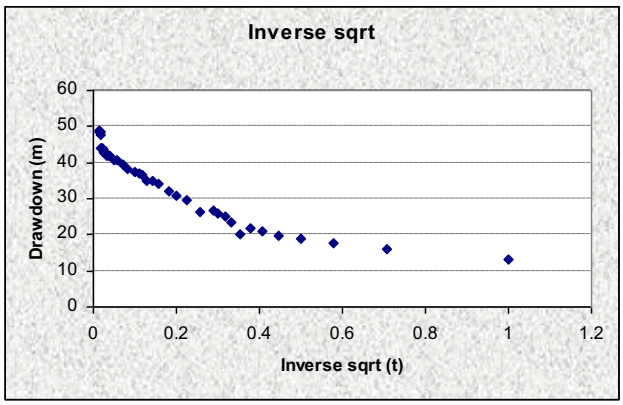

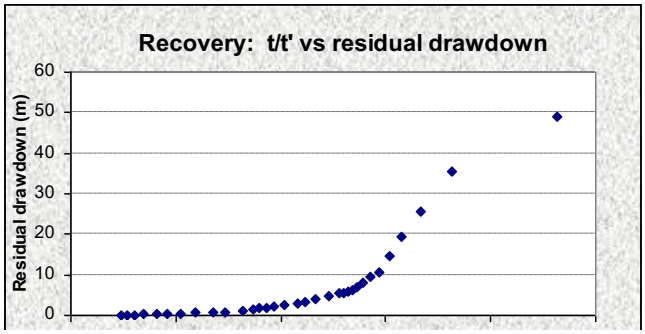

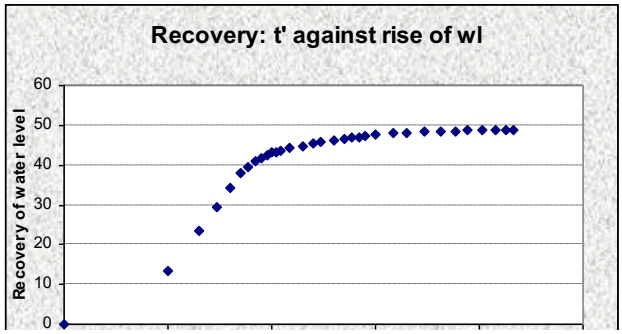

FIGURE J-64: STEP DRAWDOWN TEST RESULTS – VG3

Borehole: VG3 - FIRST TEST MULDER

STEP DRAWDOWN AND MULTIRATE ANALYSIS

Enter field step test data at bottom of sheet

STEP DRAWDOWN	yes	MULTI RATE	no

Mulder test

	Q (l/s)	Q (m^3/d)	s_i (m)	Sigma s_i	Sigma s_i/Q_i
Step 1	4.7	406.08	9.31	9.31	0.02292652
Step 2	7.1	613.44	19.08	28.39	0.04627999
Step 3	10.6	915.84	61.74	90.13	0.09841239
Step 4	13	1123.2	105.55	195.68	0.17421652
Step 5					
Step 6					
Step 7					

B =	**-5.8E-02**	d/m^2
C =	**1.8E-04**	d^2/m^5

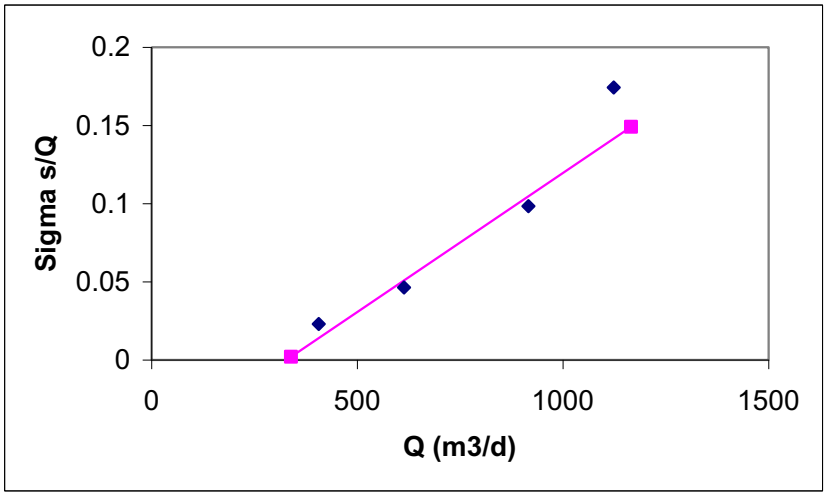

purple dot Help parameters to fit l

x_0	324.864 →	339
x_1	1347.84 →	1166
y_0	0.018341 →	0.002
y_1	0.20906 →	0.149

Q (l/s)	Well effiency(%)
4.7	-418
7.1	-115
10.6	-56
13	-41

FIGURE J-64: STEPDRAWDOWN TEST (CONTINUED)

Step test data

	Step1	Step1	Step3	Step4	Step5	Step6	Step7
Q (l/s) =	4.7	7.1	10.6	13			
t(min)	s (m)	s (m)	s (m)	s (m)	s (m)	s (m)	s (m)
1	10.91	9.31	19.05	59.5			
2	14.74	11.5	19.08	60.94			
3	14.21	13.31	24.11	61.69			
4	14.08	14.31	28.22	67.74			
5	11.3	15.21	30.31	72.34			
6	9.99	15.68	32.12	76.2			
7	9.3	16.2	33.08	80.17			
8	8.88	16.45	35.32	85.13			
9	8.65	16.75	37.65	89.3			
10	8.57	16.95	40.25	92.38			
12	8.54	17.17	42.14	97.45			
15	8.59	17.39	43.65				
20	8.63	17.71	45.76				
25	8.73	18.05	48.14				
30	8.82	18.29	51.45				
35	8.9	18.45	53.01				
40	8.95	18.67	56.62				
50	9.04	18.95	58.1				
60	9.31	19.05	59.5				

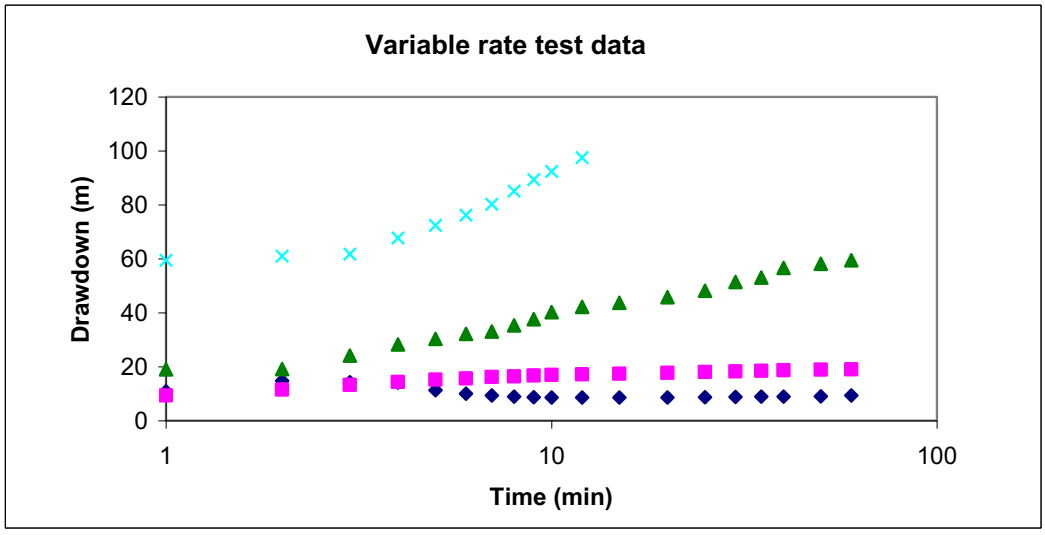

FIGURE J-65: SUSTAINABLE YIELD BASIC SOLUTION – VG3

FC-METHOD : Estimation of the sustainable yield of a borehole

VG3

Extrapolation time in years = (enter)	5	2628000	Extrapol.time in minutes	
Effective borehole radius (r_e) = (enter)	2.46	2.46	← Est. r_e	From r(e) sheet
Q (l/s) from pumping test =	8.8	2.84	← Est. r_e	Qualified guess
s_a (available drawdown), sigma_s = (enter)	100		← Sigma_s from risk	
Annual effective recharge (mm) =	0	100.00	s_available working drawdown(m)	
t(end) and s(end) of pumping test =	4300	48.88	End time and drawdown of test	
Average maximum derivative = (enter)	10.5	25.3	Estimate of average of max deriv	
Average second derivative = (enter)	0.0	0.0	Estimate of average second deriv	
Derivative at radial flow period = (enter)	3.19		Read from derivative graph	
	T-early[m^2/d] =	43.62	Aqui. thick (m)	20
T and S estimates from derivatives	T-late [m^2/d] =	13.25	Est. S-late =	1.10E-03
(To obtain correct S-value, use program RPTSOLV)	S-late =	2.20E-03	S-estimate could be wrong	

BASIC SOLUTION

(Using derivatives + subjective information about boundaries)

(No values of T and S are necessary)

		Maximum influence of boundaries at long time		
	No boundaries	1 no-flow	2 no-flow	Closed no-flow
sWell (Extrapol.time) =	78.27	107.52	136.78	224.54
Q_sust (l/s) =	11.24	8.18	6.43	3.92
	Best case	→		**Worst case**

Average Q_sust (l/s) = 6.94

with standard deviation= 3.08

(If no information exists about boundaries skip advanced solution and go to final recommendation)

FIGURE J-66: SUSTAINABLE YIELD ADVANCE SOLUTION VG3

ADVANCED SOLUTION

(Using derivatives+ knowledge on boundaries and other boreholes)

(Late T-and S-values a priori + distance to boundary)

T-late [m^2/d] = (enter) →	13.25				
S-late = (enter) →	1.00E-03				
1. BOUNDARY INFORMATION (choose a or b)		(Code =9999 = dummy value if not applicable)			
(a) Barrier (no-flow) boundaries →		Closed Square	Single Barrier	Intersect. 90°	2 Parallel Barriers
Bound. distance a[meter] : (enter)		9999	9999	9999	9999
Bound. distance b[meter] : (enter)				9999	9999
s_Bound(t = Extrapol.time) [m] =		0.06	0.01	0.03	0.03
(b) Fix head boundary + no-flow →		Closed Fix	Single Fix	90°Fix+no-flow	// Fix+no-flow
Bound. distance to fix head a[meter] : (enter)		9999	9999	9999	9999
Bound. distance to no-flow b[meter] : (enter)				9999	9999
s_Bound(t = Extrapol.time) [m] =		-0.06	-0.01	0.00	0.00
2. INFLUENCE OF OTHER BOREHOLES →		Q (l/s)	r (m)	u_r	W(u,r)
BH1				0.00E+00	#NUM!
BH2				0.00E+00	#NUM!
s_(influence of BH1,BH2) =		0.00	0.00	6.27E-08	16.01
SOLUTION INCLUDING BOUNDS AND BH's					
Fix head + No-flow : Q_sust (l/s) =		9999.00	9999.00	9999.00	9999.00
No-flow : Q_sust (l/s) =		9999.00	9999.00	9999.00	9999.00
Enter selected Q for risk analysis = (enter) →		5.00	Sigma_s =	0.000	

FINAL RECOMMENDED ABSTRACTION RATE

Abstraction rate (l/s) for 24 hr/d = (enter)	5.00
Total amount of water allowed to be abstracted per month (m^3) =	12960

COMMENTS

Q_sust with 68% safety =

Q_sust with 95% safety =

APPENDIX K: WELLMAN

APPENDIX K-1

WELLMAN DESIGN

FIGURE K-1A: WELLMAN – TITLE PAGE

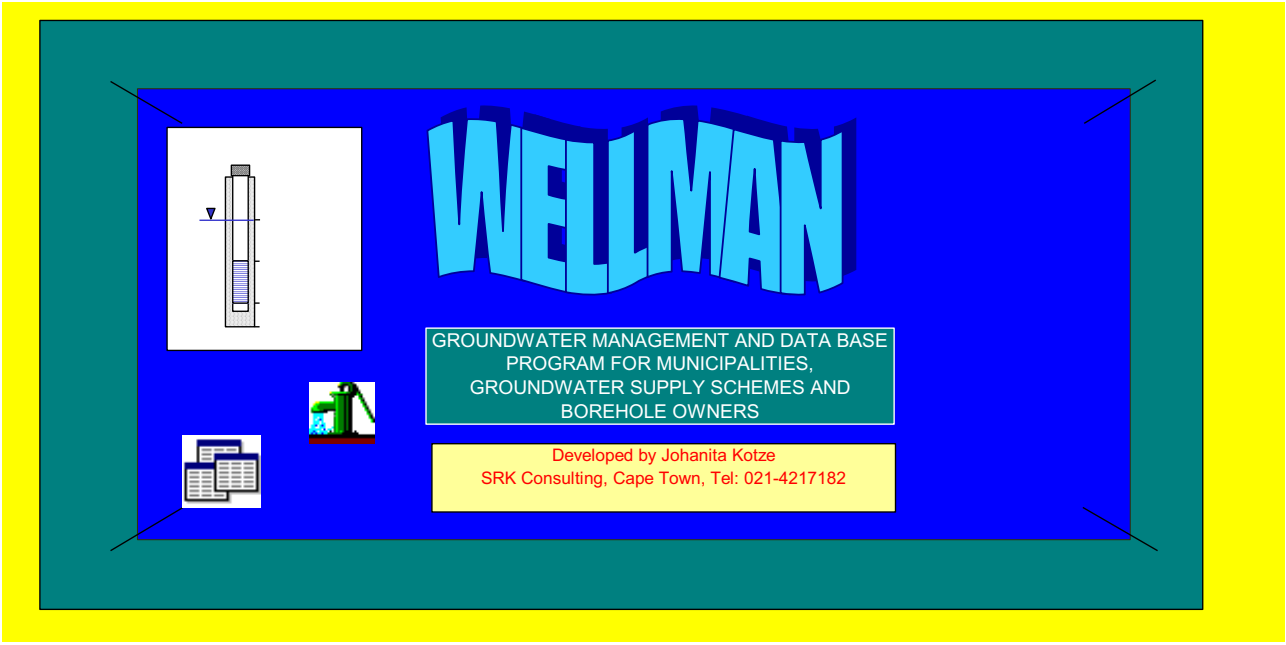

FIGURE K-1B: MAIN MENU SHEET

Main Menu sheet

Region	Little Karoo		OBS_wl	MAP	Rainfall	Title page	Annual Abstraction	Springflow	Isotopes
District	Oudtshoorn								
Water Board	Overberg			Tel. Number	044 2724634				
	Enter BH Number								
Example	Example			This is an example					
Borehole 1	VG3	Go to BH 1		Production Borehole - Voorzorg, Vermaaks Wellfield					
Borehole 2	VR6	Go to BH 2		Production Borehole - Upper Vermaaks River Valley - Vermaaks Wellfield					
Borehole 3	VR7	Go to BH 3		Highest Yielding Production Borehole - Vermaaks Wellfield					
Borehole 4	VR8	Go to BH 4		Production Borehole - Upper Vermaaks River Valley - Vermaaks Wellfield					
Borehole 5	VR11	Go to BH 5		Production Borehole - Upper Vermaaks River Valley - Vermaaks Wellfield					
Borehole 6	DP10	Go to BH 6		Production Borehole - Varkieskloof					
Borehole 7	DP12	Go to BH 7		Production Borehole - Varkieskloof					
Borehole 8	DP29	Go to BH 8		Production Borehole - Varkieskloof					
Borehole 9	DP15	Go to BH 9		Production Borehole - Bokkraal					
Borehole 10	DP25	Go to BH 10		Production Borehole - Bokkraal					
Borehole 11	DP28	Go to BH 11		Production Borehole - Bokkraal					
Borehole 12	DG110	Go to BH 12		Production Borehole - Droëkloof					
Borehole 13	DP18	Go to BH 13		Production Borehole - Olifants River "Brug"					
	Enter Wellfield Name								
Wellfield 1	VERMAAKS	Go to Wellfield 1		Production Boreholes VG3, VR6, VR7, VR8 and VR11					
Wellfield 2	VARKIESKLOOF	Go to Wellfield 2		Production Boreholes DP10, DP12 and DP29					
Wellfield 3	BOKKRAAL	Go to Wellfield 3		Production Boreholes DP15, DP25 and DP28					
Wellfield 3	DROEKLOOF&OLIFANTS	Go to Wellfield 4		Production Boreholes DP18 and DG110					

FIGURE K-1C: WELLMAN – GO TO EXAMPLE

BH number	VG3	Wellman Groundwater Management and Data base program							
Wellfield	Vermaaks								
Municipality	Overberg	Y	42820.8	Main water strike (m) =	190	Recommended Q (l/s) =	2.5	216	m3/d
Owner	DWAF	X	3715464.4	BH depth (m) =	206.7	Q (FC-Method)			
Geological formation	TMG - NAR	Altitude	497.3	Use of water	Domestic	Q (Theis-Method)	3	259.2	m3/d
Topo map sheet #		Drilled	15/4/89	Depth of pump instal	148	Q (Guess)			
Screen Type	PVC	IWL (m)	6.02	Blow Yield (l/s) =	12	Q (Equal Volume)	2.3	201	m3/d
Screen Depth	96.5 - 150	Diameter	208	Other water strikes (m)=	110, 174	KW of pump			
Screen Depth	150 - 206.7	Diameter	168	Pump	submersible	Max. Q of pump (l/s)	4	346	m3/d

Other comments:
Borehole is situated in a closed boundary (Average distance = 1 km)

DATA | CHEM | EN_ISO | Geology | Pump test | Manage | Main

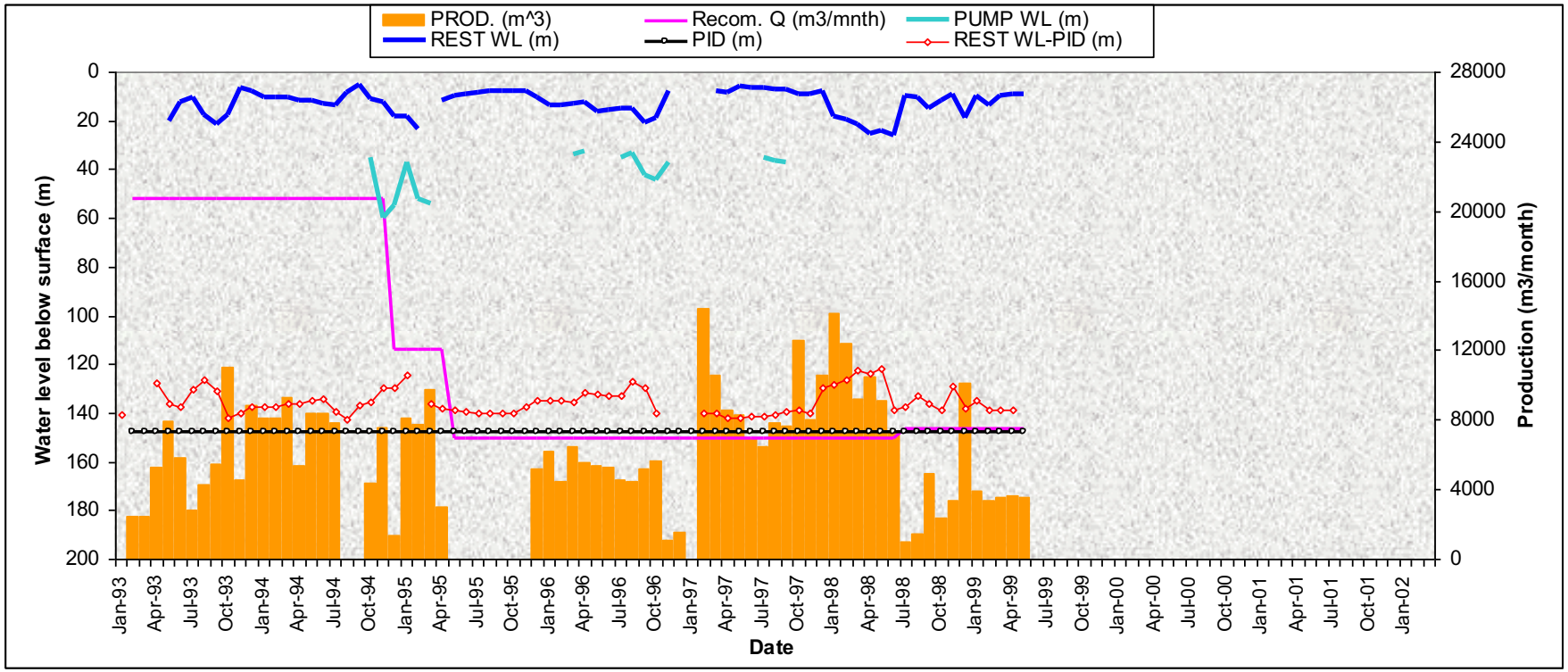

FIGURE K-1D: WELLMAN – BOREHOLE EXAMPLE PRODUCTION DATA

TOP

VG3

DATE	PUMP WL (m)	REST WL (m)	PID (m)	PROD. (m^3)	Recom. Q (m3/mnth)	HOURS (h)	YIELD (m^3/h)	D-DOWN (m)	PWL-PID (m)	Water strike (m)	Month Index	REST WL-PID (m)	Remarks
Jan-93		7.1	148	2455	20700					190	1	140.9	
Feb-93			148	2455	20700					190	2		
Mar-93			148	5248	20700					190	3		
Apr-93		20.4	148	7938.86	20700					190	4	127.6	
May-93		12.1	148	5849.58	20700					190	5	135.9	
Jun-93		10.33	148	2836.34	20700					190	6	137.67	
Jul-93		17.7	148	4285.26	20700					190	7	130.3	
Aug-93		21.6	148	5500.63	20700					190	8	126.4	
Sep-93		17.38	148	11041.94	20700					190	9	130.62	
Oct-93		6.2	148	4560	20700					190	10	141.8	
Nov-93		8	148	8856	20700					190	11	140	
Dec-93		10.3	148	8086	20700					190	12	137.7	
Jan-94		10.49	148	8150	20700					190	13	137.51	
Feb-94		10.5	148	9312	20700					190	14	137.5	
Mar-94		11.9	148	5349	20700					190	15	136.1	
Apr-94		11.92	148	8370	20700					190	16	136.08	
May-94		13.1	148	8366	20700					190	17	134.9	
Jun-94		13.56	148	7853	20700					190	18	134.44	
Jul-94		8.3	148	0	20700					190	19	139.7	PUMP REMOVED
Aug-94		5.33	148	0	20700					190	20	142.67	PUMP REMOVED
Sep-94	35.08	11	148	4388	20700		20.304	24.08	112.92	190	21	137	INACCURATED TRANSD
Oct-94	59.9	12.22	148	7563	20700		20.844	47.68	88.1	190	22	135.78	INACCURATED TRANSD
Nov-94	54.8	18.14	148	1362	12000		20.7	36.66	93.2	190	23	129.86	INACCURATED TRANSD
Dec-94	37.28	18.55	148	8131	12000		17.712	18.73	110.72	190	24	129.45	INACCURATED TRANSD
Jan-95	52.2	23.41	148	7732	12000		15.084	28.79	95.8	190	25	124.59	INACCURATED TRANSD
Feb-95	54.35		148	9774	12000		14.688		93.65	190	26		INACCURATED TRANSD
Mar-95		11.62	148	3038	12000					190	27	136.38	BOREHOLE NOT IN USI
Apr-95		9.72	148	0	6900					190	28	138.28	BOREHOLE NOT IN USI
May-95		8.97	148	0	6900					190	29	139.03	BOREHOLE NOT IN USI

FIGURE K-1E: WELLMAN – BOREHOLE CHEMISTRY DATA SET

Chemistry TOP Go to Environmental Isotopes Go to CHEM PLOTS

Class II	150-370	1000-2450	4-5 or 9.5-10	200-400	70-100		1.5-3.5	200-600	10-20		400-600			
Class III	>370	>2450	>4 or >10	>400	>100		>3.5	>600	>20		>600			
Date	**EC**	**TDS**	**pH**	**Sodium**	**Magnesium**	**Calcium**	**Flouride**	**Chloride**	**Nitrate**		**Sulphate**	**TAL**	**Phosphate**	**Silicon**
	mg/L	mg/L		mg/L	mg/L	mg/L	mg/L	mg/L	mg/L		mg/L	mg/L	mg/L	mg/L
Oct-92	20.9	89	5.6	25	4	2	<0.1	43	0.9		6	<0.005	<4	4.7
Nov-92														
Dec-92														
Jan-93	18.3	88	6.3	23	3	2	0.2	37	1.06		8	0.007	7	5.4
Feb-93														
Mar-93	16.2	90	5.5	26.2	3.5	2.4	0.12	41.3	0.993		4.6	0.008	3.9	3.55
Apr-93														
May-93														
Jun-93														
Jul-93														
Aug-93														
Sep-93														
Oct-93														
Nov-93														
Dec-93														
Jan-94														
Feb-94														
Mar-94														
Apr-94														
May-94														
Jun-94														
Jul-94														
Aug-94														
Sep-94	18													

FIGURE K-1F: WELLMAN – CHEM PLOTS (EXAMPLE)

TOP

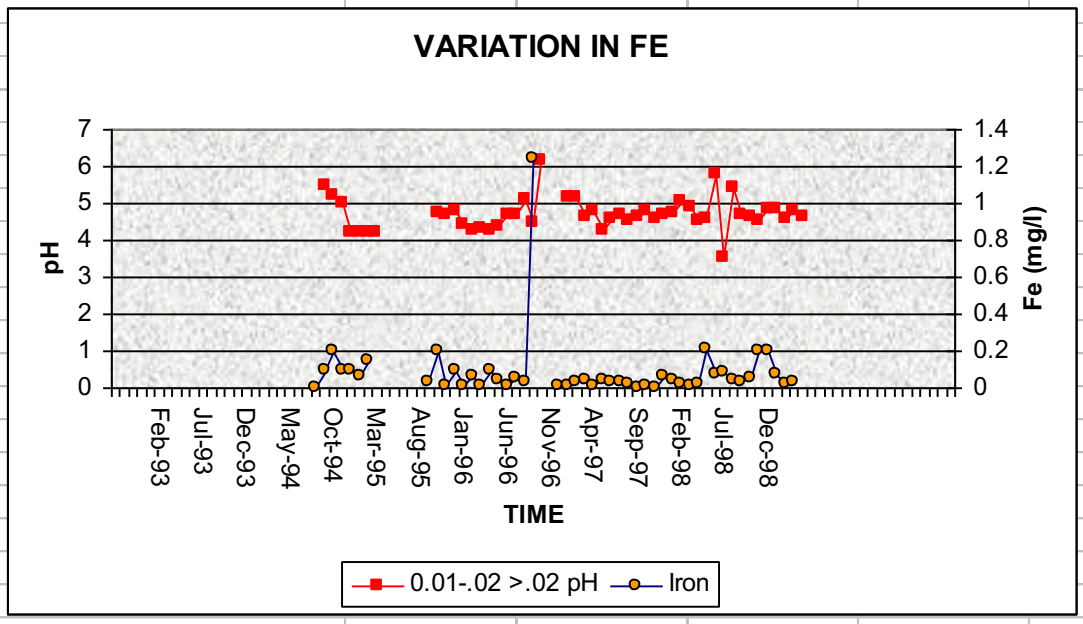

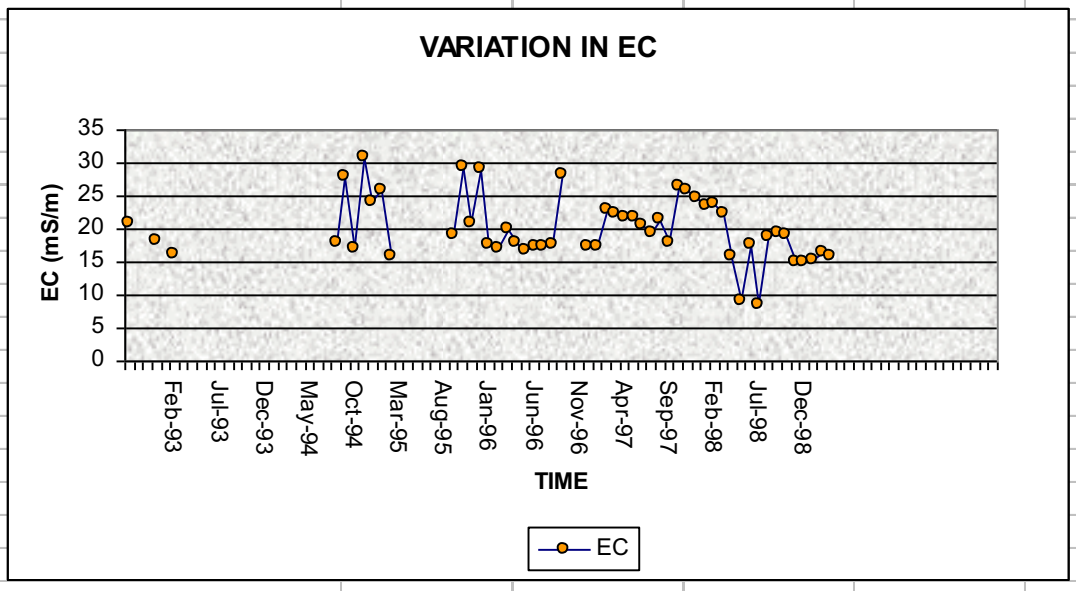

FIGURE K-1G: WELLMAN - RAINFALL SUB MENU

Monthly Rainfall (mm)

Date	Rain (mm)
Dec-90	32
Jan-91	9
Feb-91	19
Mar-91	119
Apr-91	20
May-91	30
Jun-91	47
Jul-91	0
Aug-91	29
Sep-91	108
Oct-91	5
Nov-91	21
Dec-91	10
Jan-92	59
Feb-92	35
Mar-92	27
Apr-92	35
May-92	42
Jun-92	105
Jul-92	63
Aug-92	27
Sep-92	167
Oct-92	4
Nov-92	0
Dec-92	46
Jan-93	35
Feb-93	12
Mar-93	114
Apr-93	41
May-93	42
Jun-93	44
Jul-93	28
Aug-93	105
Sep-93	2

set start date

Main

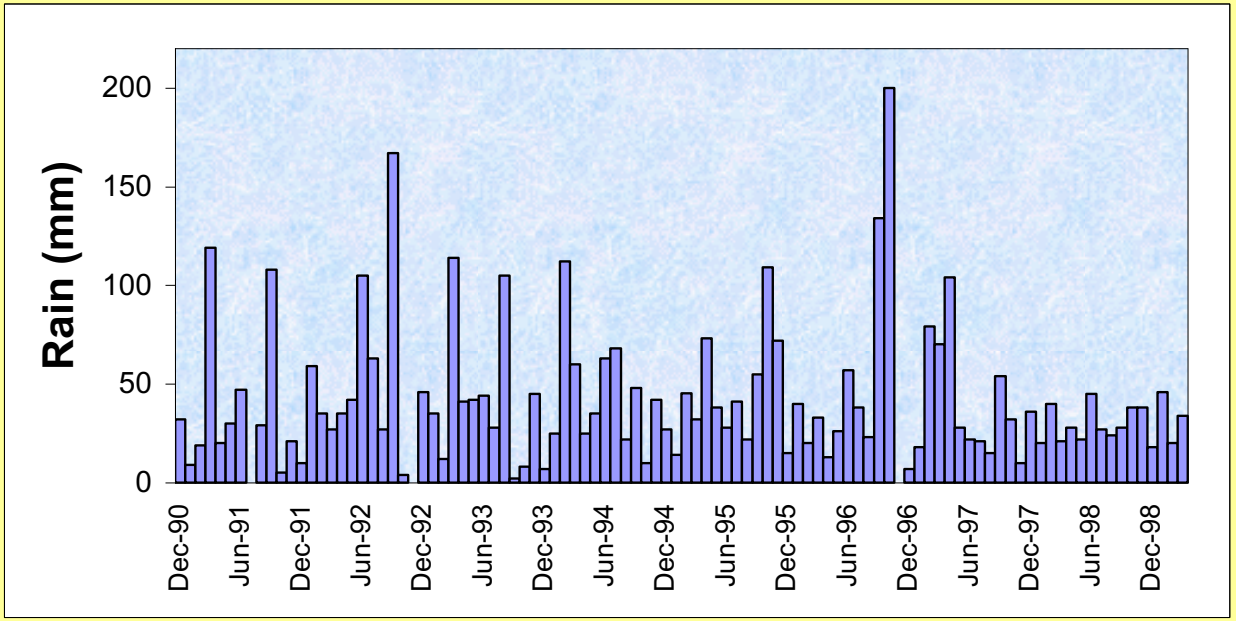

RAINFALL STATISTICS

	ANNUAL_TOT					
1991	439					
1992	574		AVERAGE	41.94141414		
1993	522		MAX	200		
1994	517		MIN	0		
1995	556.2		VARIANCE	1257.498982		
1996	599		STDDEV	35.46123209		
1997	460		MEDIAN	32		
1998	367		NORMAL	0.010036784		

FIGURE K-1H: WELLMAN – BOREHOLE EXAMPLE – ENVIRONMENTAL ISOTOPE DATA

Environmental Isotopes TOP

	Location	Tritium	Carbon 14	Oxygen 18	Deuterium	Radon
		(TU)	(pMC)	(o/oo)	(o/oo)	
Jul-94	VG3			-7.4	-49	
Jul-97	VG 3	1.3±0.2	78.1	-7.68	-43.3	4
Jun-98	VG3		78.72	-8.02		

FIGURE K-1I: WELLMAN – BOREHOLE EXAMPLE GEOLOGICAL INFORMATION

GEOLOGICAL LOG TOP

Depth (m)	Description
0 - 13	Alluvial deposits: Boulders and cobbles in a clay matrix
13 - 110	Dark sandstone layer, very little shale lenses (Baviaanskloof Formation - Nardouw Subgroup)
110 - 206.7	White, coarse-grained quartzite (Skurweberg Formation - Nardouw Subgroup)
	Fractures at 48, 186, 165-169, 186 m
	Solid from 196 m

FIGURE K-1J: WELLMAN – BOREHOLE EXAMPLE – PUMPTEST DATA

TOP

Pumping test data			
Date of test	22-27/05/90		
Abstr. Rate Q (l/s)	8.8		
Time (min)	Drawdown (m)	t'	res. s (m)
1	13	0.001	48.88
2	16	1	35.35
3	17.66	2	25.45
4	18.75	3	19.4
5	19.81	4	14.47
6	20.8	5	10.78
7	21.58	6	9.48
8	20.1	7	7.9
9	23.56	8	7
10	24.88	9	6.33
11	26	10	5.82
12	26.54	11	5.57
15	26.22	12	5.32
20	29.43	15	4.7
25	30.89	20	4
30	32.02	25	3.37
40	33.96	30	3.07
50	35.01	40	2.57
60	35.1	50	2.2
70	36.4	60	1.94
80	36.9	70	1.74
100	37.56	80	1.54
150	38.38	100	1.28
200	39.31	150	0.9
300	40.61	200	0.72
420	40.71	300	0.55
600	41.8	420	0.42
780	41.8	600	0.32
1080	41.8	780	0.24
1440	42.91	1080	0.19
1800	43.44	1440	0.13
2160	44.04	1800	0.05
2520	44.01	2160	0

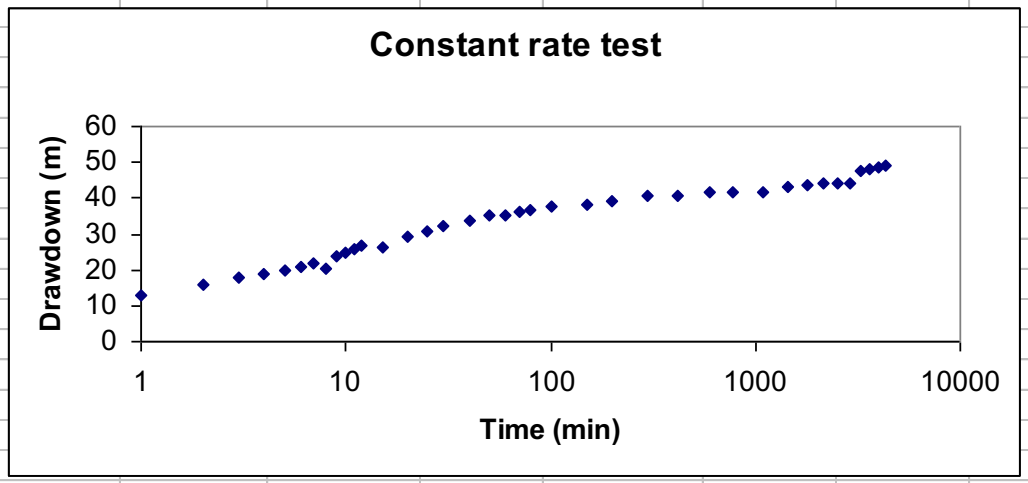

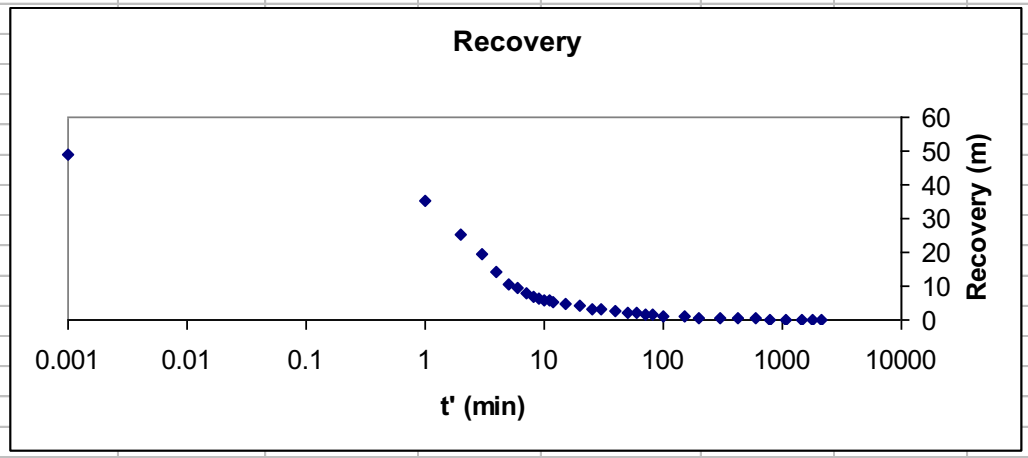

FIGURE K-1J(CONTINUED): WELLMAN – EXAMPLE – PUMPTEST DATA

Step test data							
Nov-97	Step1	Step2	Step3	Step4	Step5	Step6	Step7
Q (l/s) =	4	5.8	10.6	15.5			
t(min)	s (m)	s (m)	s (m)	s (m)	s (m)	s (m)	s (m)
	4	5.8	10.6	15.5	0	0	0
0.1	0.001	6.05	10.4	33.5			
0.5	0.91	7.19	15.13	37.68			
1	3.63	7.73	15.94	38.98			
1.5	3.93	8.14	16.89	41.4			
2	4.24	8.41	17.56	45.7			
2.5	4.53	8.63	18.32	47.38			
3	4.61	8.81	18.78	50.56			
3.5	4.72	8.86	19.37	53.87			
4	4.88	8.95	19.86	56.6			
4.5	4.96	8.99	20.25	58.78			
5	5.05	9.08	20.96				
7	5.33	9.26	23.68				
9	5.44	9.36	24.71				
12	5.6	9.56	26.64				
15	5.67	9.68	27.39				
20	5.74	9.85	28.13				
25	5.8	9.94	28.24				
30	5.86	10.05	28.93				
35	5.89	10.13	30.04				
40	5.92	10.21	30.61				
45	5.96	10.27	30.8				
50	5.99	10.31	31.15				
60	6.05	10.4	33.5				

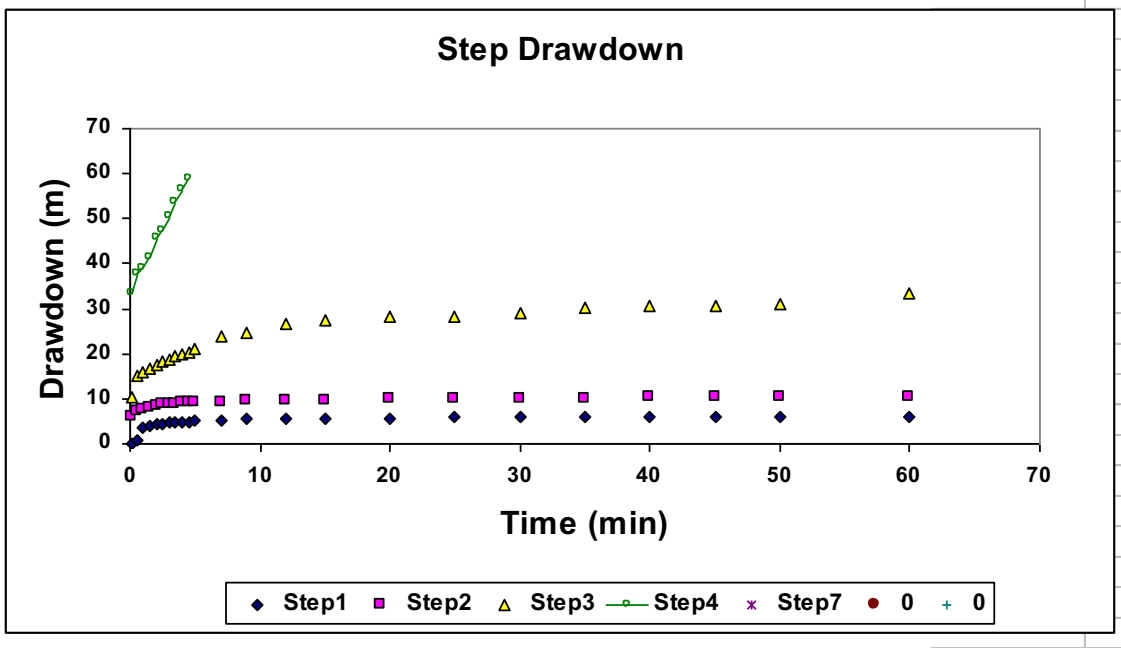

FIGURE K-1K: WELLMAN – BOREHOLE EXAMPLE – EQUAL VOLUME METHOD – MANAGE

Management TOP

Q_s (m^3/d) =	201
Q_s (l/s) =	2.3

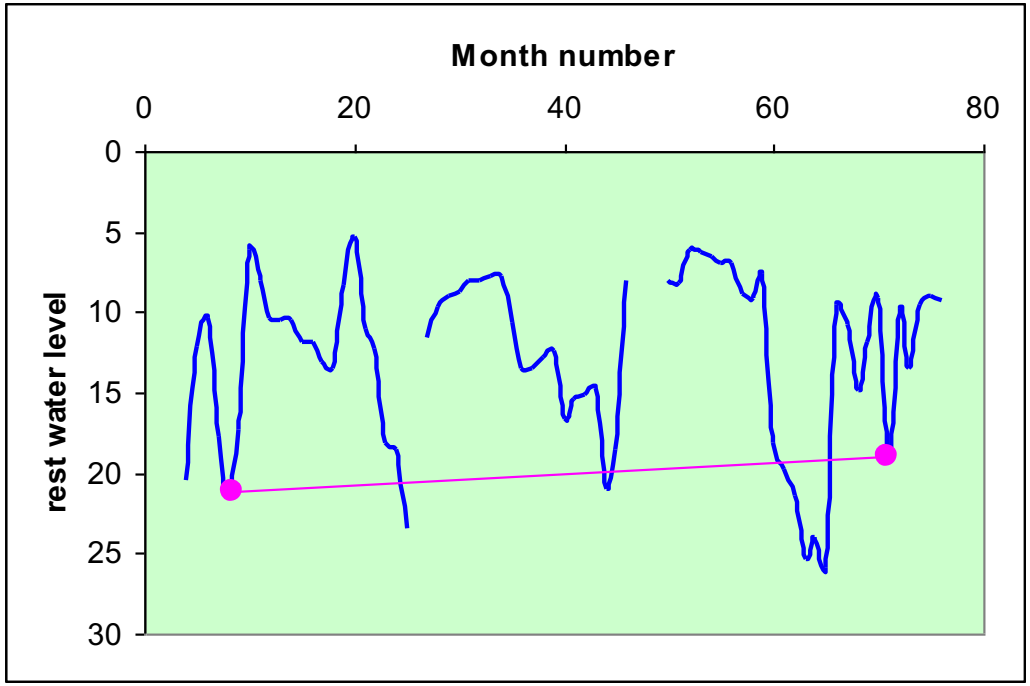

x_0	0 →	8.4
x_1	20 →	70.8
y_0	58 →	21.1
y_1	183 →	19

8.4

8	start of equal volume	70.8
71	end of equal volume	

FIGURE K-1L: WELLMAN – GO TO WELLFIELD 1 (EXAMPLE)

Annual Abstraction from Vermaaks wellfield

Main

Go to Varkieskloof Wellfield

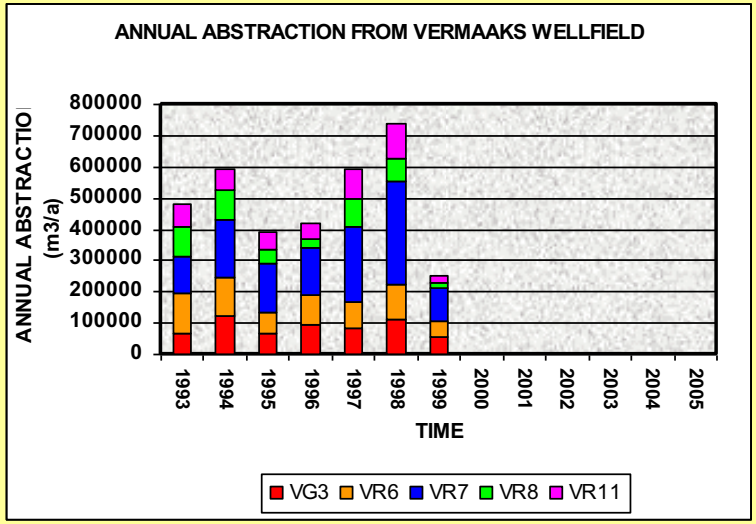

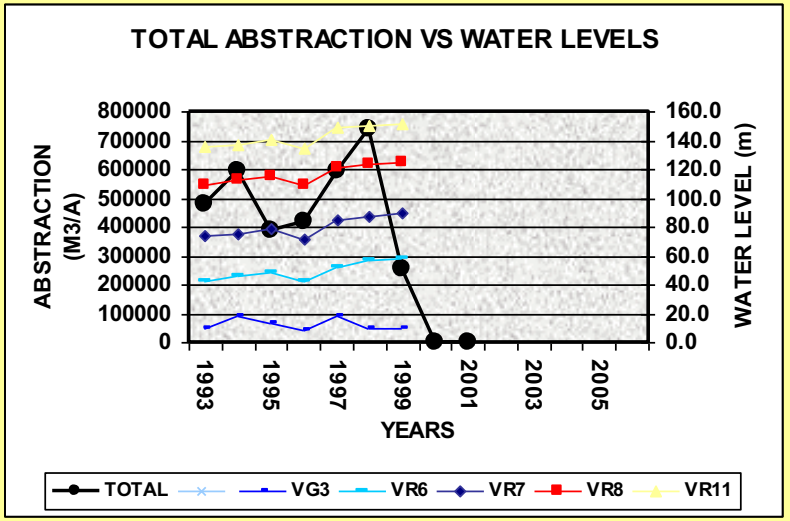

	1993	1994	1995	1996	1997	1998	1999	2000	2001	2002	2003	2004	2005	2006
VG3	69113	122688	65816	95475	84958	111903	53880	0	0					
VR6	127794	122688	65816	95475	84958	111903	53880	0	0					
VR7	116539	187577	161723	152159	237528	328435	105032	0	0					
VR8	94066	90351	39894	23515	90673	75459	17811	0	0					
VR11	71485	71851	55610	54251	97133	108883	22864	0	0					
TOTAL	478998	595155	388859	420875	595250	736583	253467	0	0					
WATER LEVEL														
VG3	10.3	18.6	13.4	8.0	18.1	9.9	9.3							
VR6	43.0	46.4	48.7	42.4	52.5	56.8	58.6							
VR7	74.2	74.6	78.5	71.7	84.6	87.7	89.7							
VR8	108.7	112.4	115.6	109.6	120.9	123.9	125.4							
VR11	135.5	136.9	141.0	134.9	149.0	149.8	151.0							

FIGURE K-1M: WELLMAN - OBSERVATION WELL SUB-MENU

Main

WATER LEVEL ELEVATIONS OVER TIME -

	VARKIESKLOOF			GRAPH	BOKKRAAL			GRAPH				OLIFANTS RIVER				GRAPH
BH	DP10	DP12	DP29	DP27	DP15	DP25	DP28	DP13	DP14	DP20	RN1	DP18	DP16	DP17	DP24	DP19
HH	456.50	468.50	463.10	458.30	451.10	449.10	459.10	458.90	451.40	448.80	468.60	351.10	351.20	349.10	350.70	350.80
Jul-85	396.50															
Apr-86	381.90															
Sep-87	366.20															
May-89																
Jun-89																
Jul-89																
Aug-89								356.35								
Sep-89								355.65								
Oct-89								355.74								
Nov-89											362.40					347.04
Dec-89								368.20					346.93			347.00
Jan-90										351.30	362.28		347.20	347.04		347.27
Feb-90	306.50				345.60					350.50	361.78		347.10	346.96		
Mar-90	306.50				346.10					349.51	361.08		346.82	346.89		
Apr-90					343.08					346.56	359.49		346.77	346.70		
May-90									347.40	349.05	362.21		347.78	347.68		
Jun-90									346.01	347.96	361.99		347.90			
Jul-90									344.95	347.74	361.75		348.09	347.99		
Aug-90	342.40	341.20			347.30	341.30	341.70	346.91	345.23	347.80	356.35	347.50	348.26	348.15		
Sep-90								345.81	344.20	346.76	355.41		347.02	347.02		
Oct-90					346.10			345.43	343.88	346.52	354.80		346.36	346.68		
Nov-90								345.04	344.17	346.30	354.15					
Dec-90								344.89	344.55	346.00	354.00		345.94	346.25		
Jan-91		339.25				344.23		344.92	344.66	345.95	353.10		345.59	345.95	345.99	
Feb-91				336.40	330.64	343.57		344.20	343.67	345.74	352.64			345.77	345.77	
Mar-91		332.83		339.10	345.00	335.20	341.10	341.70	342.30	344.62	352.58			346.15	346.10	346.23
Apr-91		342.13	341.45	341.38	340.31	338.60	341.45	341.83	342.14	344.73	352.65			345.90	345.85	345.98
May-91			341.50	339.52	340.00		341.35	341.66	341.90	344.49	351.70			346.04	346.13	346.08
Jun-91		343.90	342.69	342.72	339.61		340.96	341.26	341.45	344.13	351.13			346.33	346.37	346.40
Jul-91		344.32	343.30	343.10	340.00		341.20	341.43	341.57	344.26	350.65			345.83	345.84	345.86
Aug-91		344.42	344.15		339.68		340.97	341.27	341.36	344.00				345.50	345.49	345.53
Sep-91		331.47	340.55		339.08		340.58	340.80	341.25	343.79	349.70		334.25	339.25		

FIGURE K-1N: WELLMAN - OBSERVATION WELL WATER LEVEL CHANGES OVER TIME FOR EACH WELLFIELD

BACK

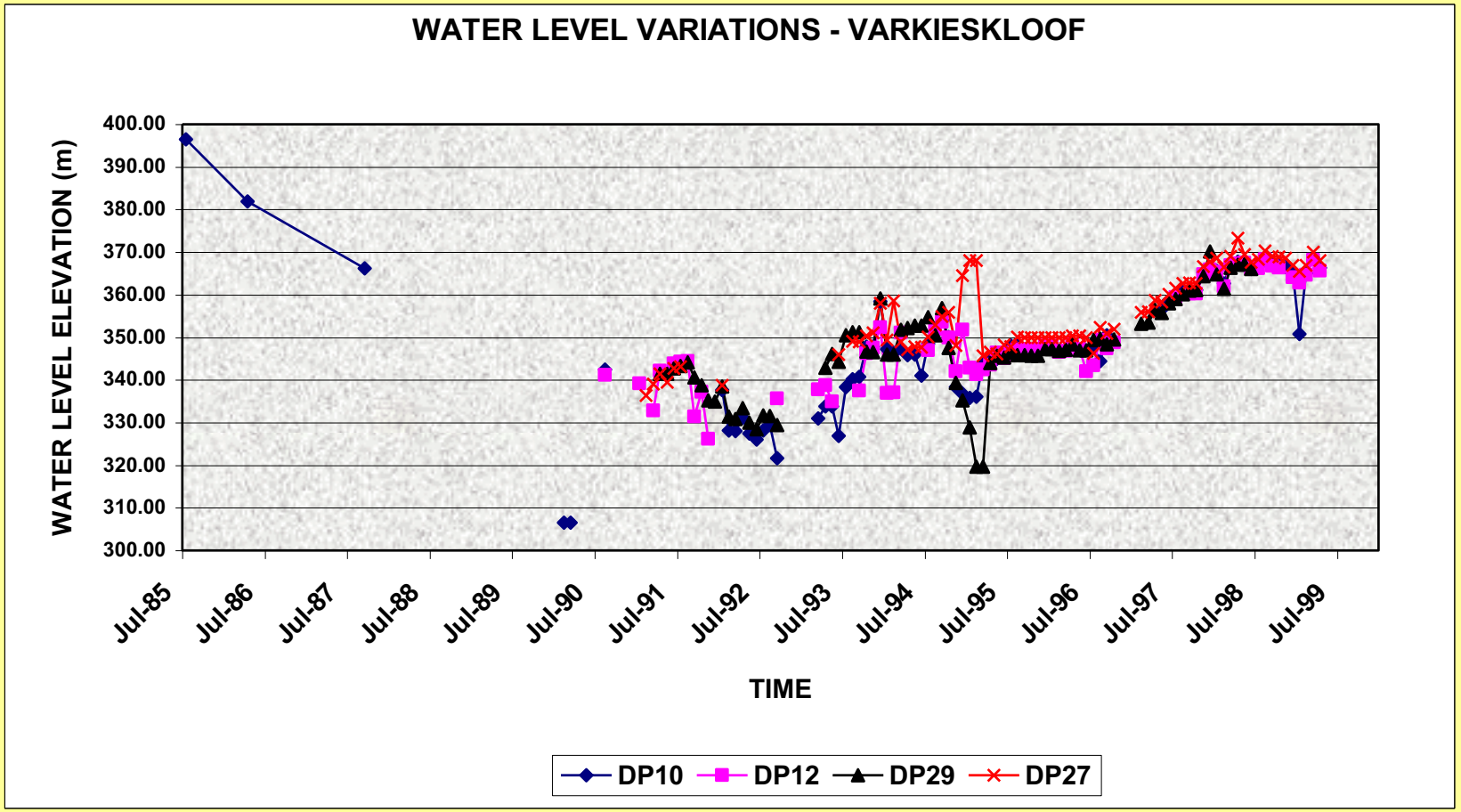

FIGURE K-1O: WELLMAN - MAP SUB ROUTINE

Locality map showing production and important monitoring borehole positions

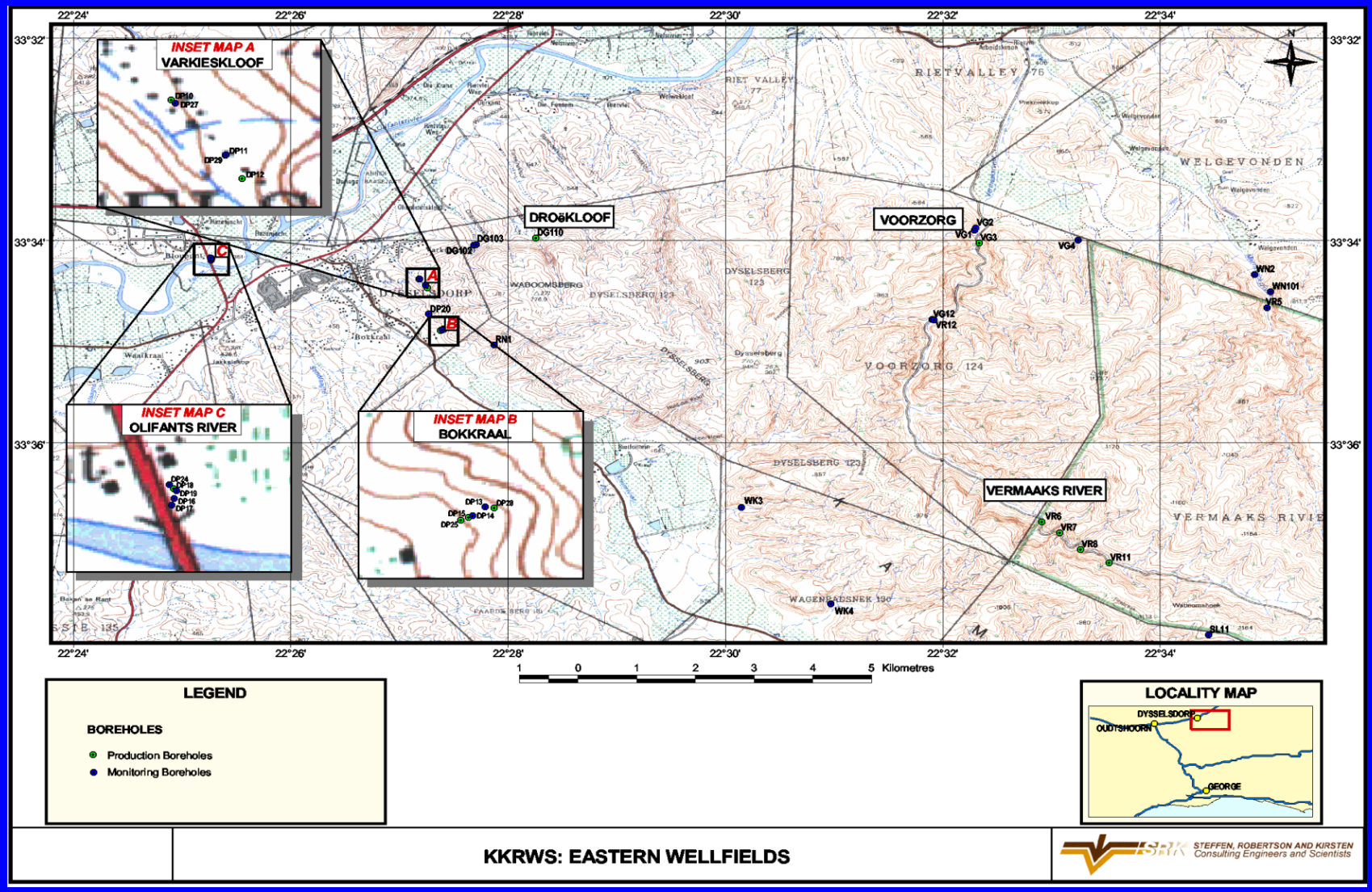

FIGURE K-1P: WELLMAN - ANNUAL ABSTRACTION SUBMENU

Main | Go to data An_AB

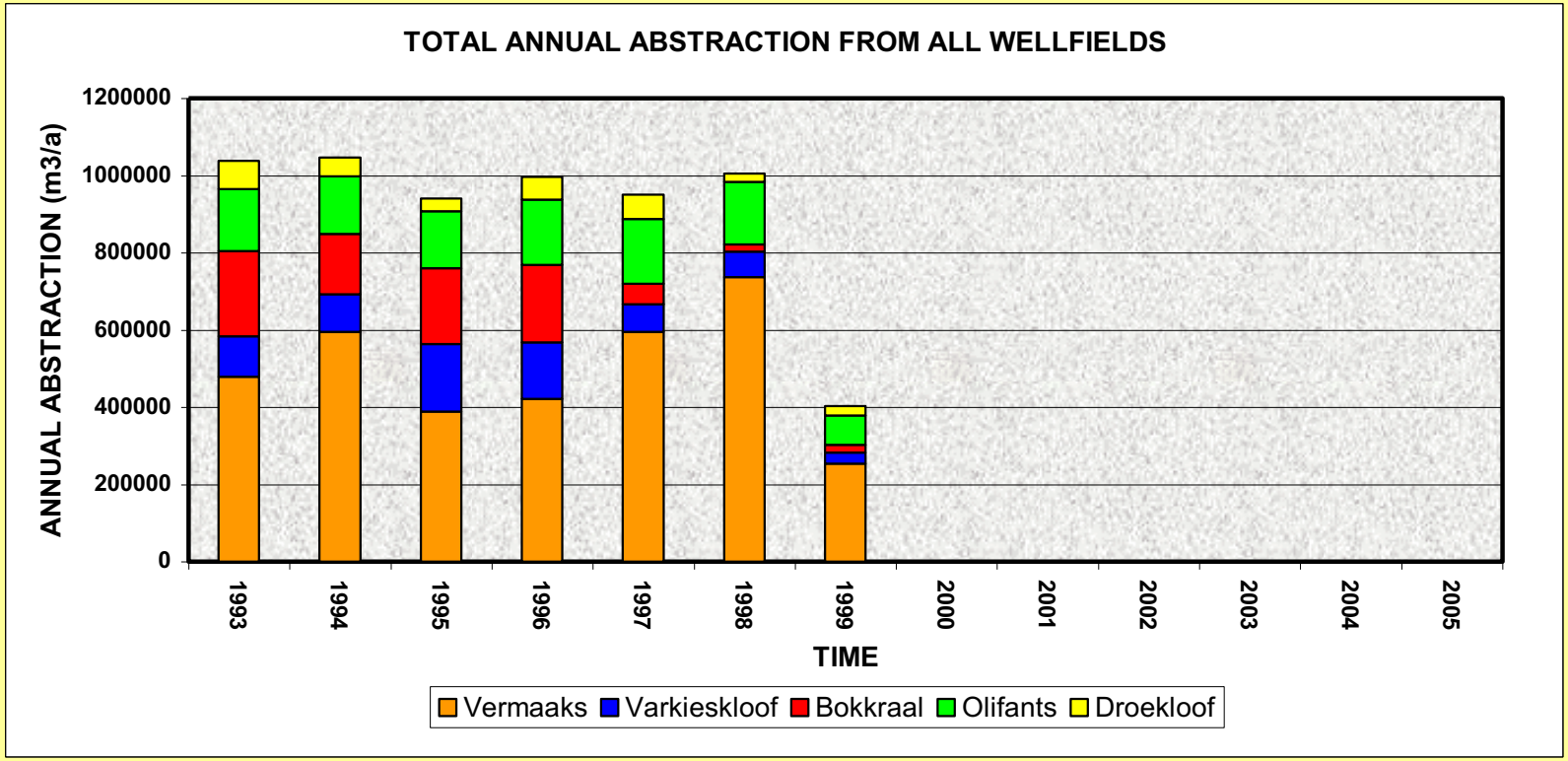

Main | Graph

	1993	1994	1995	1996	1997	1998	1999
Vermaaks	478998	595155	388859	420875	595250	736583	253467
Varkieskloof	104557	96811	175185	147113	71679	66895	28375
Bokkraal	220429	157261	195671	200940	52631	18082	21355
Olifants	160658	148416	147955	168040	167241	162120	75266
Droekloof	73645	49071	32293	59087	64042	21233	24480
TOTAL	1038286	1046714	939963	996055	950843	1004913	402943

FIGURE K-1Q: WELLMAN - SPRINGFLOW SUBMENU

Main

DATA

SPRINGFLOW VARIATION OVER TIME

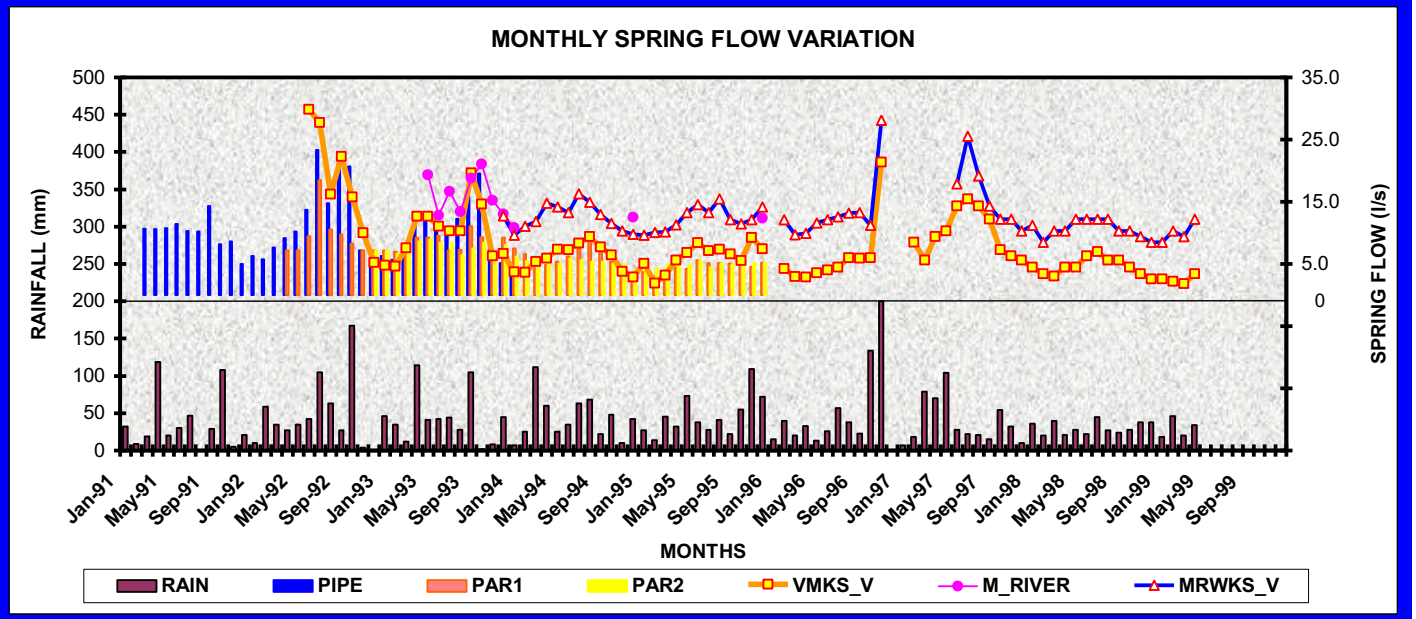

TOP

SPRINGFLOW DATA

MONTH	RAIN	PIPE	PAR1	PAR2	VMKS_V	M_RIVER	MRWKS_V	COMMENT
Jan-91	32							
Feb-91	9							
Mar-91	19	10.7						
Apr-91	119	10.6						
May-91	20	10.8						
Jun-91	30	11.5						
Jul-91	47	10.3						
Aug-91	0	10.2						
Sep-91	29	14.3						
Oct-91	108	8.2						
Nov-91	5	8.7						
Dec-91	21	5.0						
Jan-92	10	6.3						
Feb-92	59	5.8						

FIGURE K-1R: WELLMAN - ISOTOPES SUBMENU

Main DATA

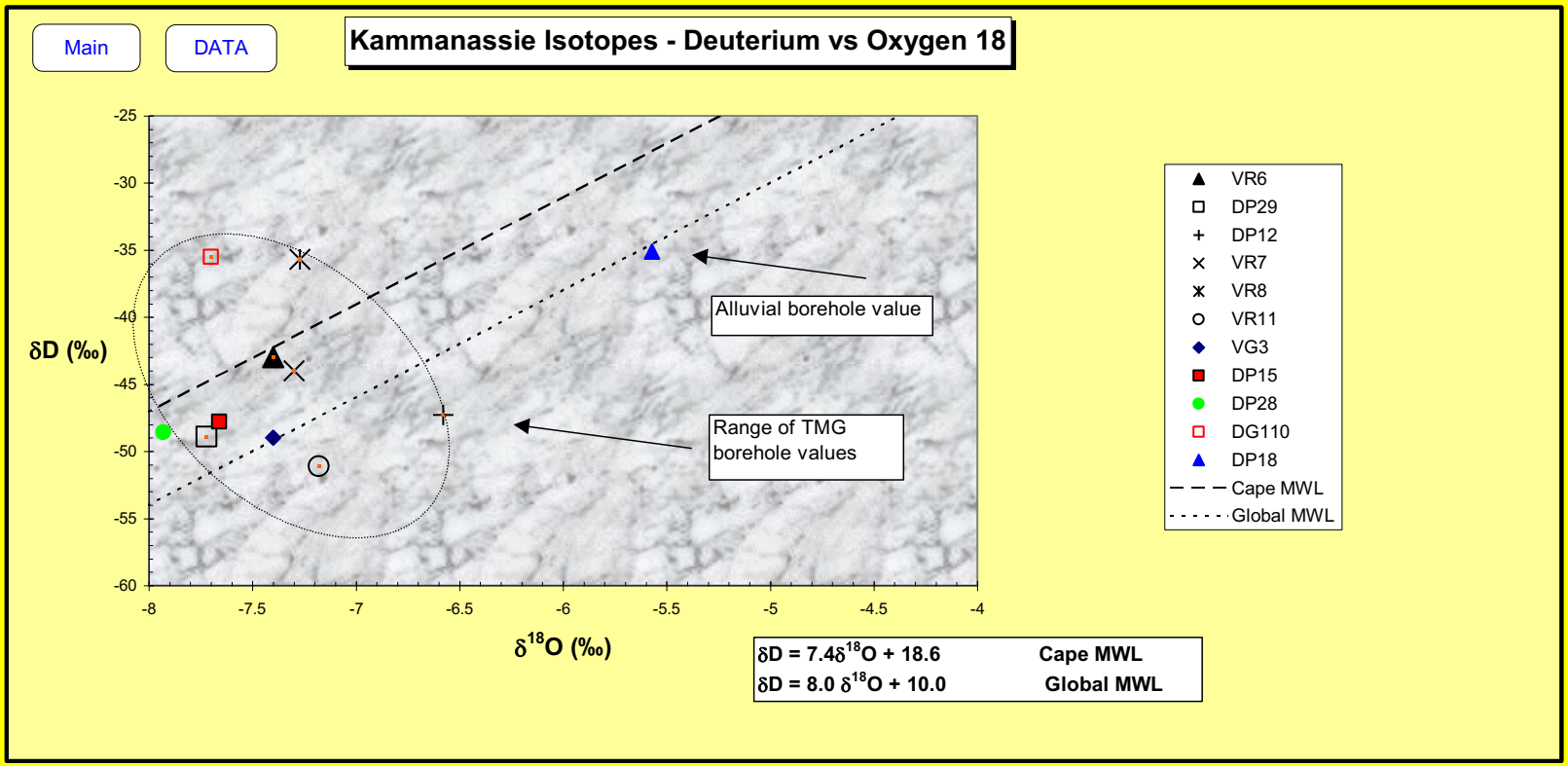

Main TOP

	VG3	VR6	VR7	VR8	VR11	DP12	DP29	DP15	DP28	DG110	DP18	Cape MWL	Global MWL	Global MWL
δD (‰)	-49	-43	-44	-35.7	-51.1	-47.3	-48.9	-47.8	-48.6	-35.5	-35.1	-9.44	-12.4	-19.6
$\delta^{18}O$ (‰)	-7.4	-7.4	-7.3	-7.27	-7.18	-6.58	-7.72	-7.66	-7.93	-7.7	-5.57	-3.8	-2.8	-3.7

APPENDIX K-2

Go to Borehole submenu - WELLMAN

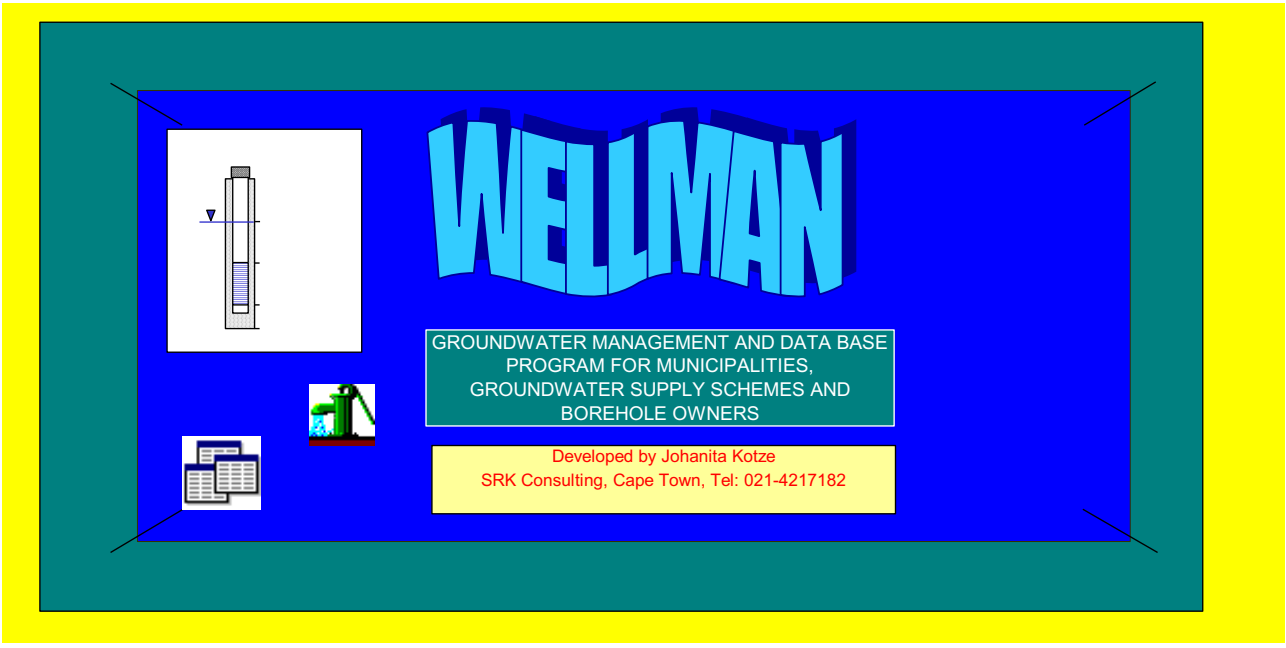

FIGURE K-2A: GO TO BH1 – SUMMARY OF ALL BOREHOLE 1'S HYDROGEOLOGICAL INFORMATION

BH number	VG3	Wellman Groundwater Management and Data base program							
Wellfield	Vermaaks								
Municipality	Overberg	Y	42820.8	Main water strike (m) =	190	Recommended Q (l/s) =	2.5	216	m3/d
Owner	DWAF	X	3715464.4	BH depth (m) =	206.7	Q (FC-Method)			
Geological formation	TMG - NAR	Altitude	497.3	Use of water	Domestic	Q (Theis-Method)	3	259	m3/d
Topo map sheet #		Drilled	15/4/89	Depth of pump instal	148	Q (Guess)			
Screen Type	PVC	IWL (m)	6.02	Blow Yield (l/s) =	12	Q (Equal Volume)	2.3	201	m3/d
Screen Depth	96.5 - 150	Diameter	208	Other water strikes (m)=	110, 174	KW of pump			
Screen Depth	150 - 206.7	Diameter	168	Pump	submersible	Max. Q of pump (l/s)	4	346	m3/d

Other comments:
Borehole is situated in a closed boundary (Average distance = 1 km)

DATA | CHEM | EN_ISO | Geology | Pump test | Manage | Main

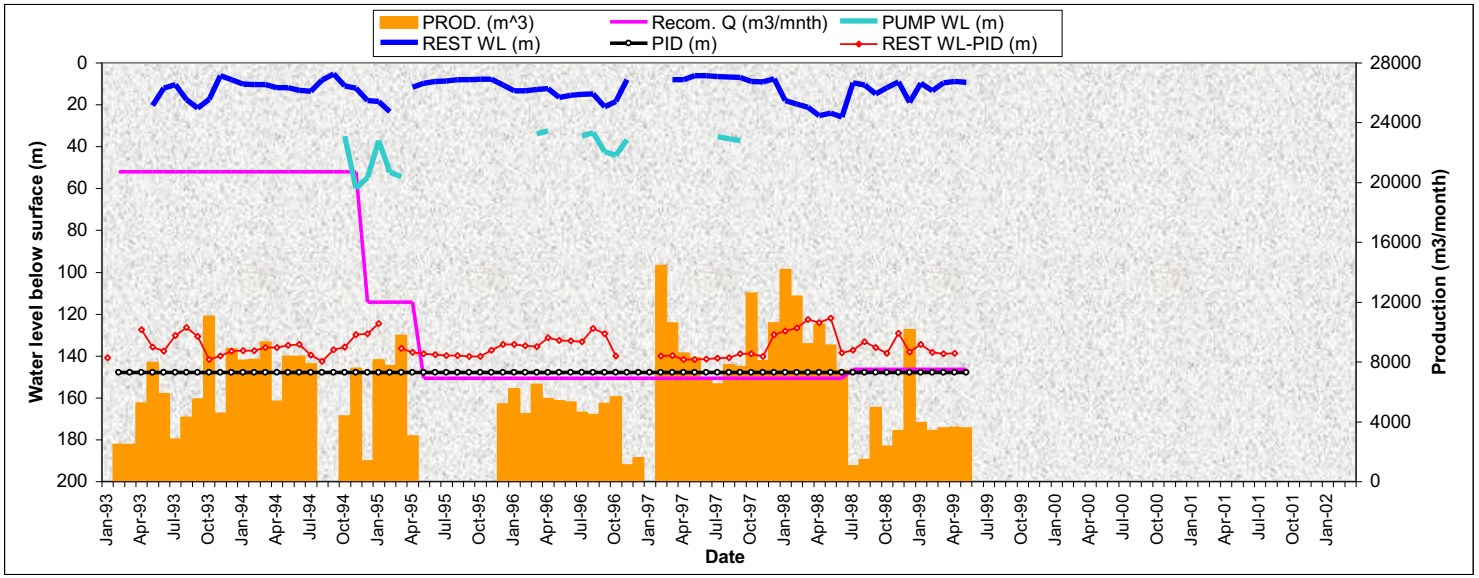

TOP

VG3

DATE	PUMP WL (m)	REST WL (m)	PID (m)	PROD. (m^3)	Recom. Q (m3/mnth)	HOURS (h)	YIELD (m^3/h)	D-DOWN (m)	PWL-PID (m)	Water strike (m)	Month Index	REST WL-PID (m)
Jan-93		7.1	148	2455	20700					190	1	140.9
Feb-93			148	2455	20700					190	2	
Mar-93			148	5248	20700					190	3	
Apr-93		20.4	148	7938.86	20700					190	4	127.6

FIGURE K-2B: GO TO BH 1 – SUB ROUTINE CHEM

Chemistry TOP Go to Environmental Isotopes Go to CHEM PLOTS

Class II	150-370	1000-2450	4-5 or 9.5-10	200-400	70-100		1.5-3.5	200-600	10-20		400-600		
Class III	>370	>2450	>4 or >10	>400	>100		>3.5	>600	>20		>600		
Date	EC	TDS	pH	Sodium	Magnesium	Calcium	Flouride	Chloride	Nitrate		Sulphate	TAL	Phosphate
	mg/L	mg/L		mg/L	mg/L	mg/L	mg/L	mg/L	mg/L		mg/L	mg/L	mg/L
Oct-92	20.9	89	5.6	25	4	2	<0.1	43	0.9		6	<0.005	<4
Nov-92													
Dec-92													
Jan-93	18.3	88	6.3	23	3	2	0.2	37	1.06		8	0.007	7
Feb-93													
Mar-93	16.2	90	5.5	26.2	3.5	2.4	0.12	41.3	0.993		4.6	0.008	3.9
Apr-93													
May-93													
Jun-93													
Jul-93													
Aug-93													
Sep-93													

FIGURE K-2C: GO TO BH 1 – SUB ROUTINE ENV_ISO

Environmental Isotopes TOP

	Location	Tritium	Carbon 14	Oxygen 18	Deuterium	Radon
		(TU)	(pMC)	(o/oo)	(o/oo)	
Jul-94	VG3			-7.4	-49	
Jul-97	VG 3	1.3±0.2	78.1	-7.68	-43.3	4
Jun-98	VG3		78.72	-8.02		

FIGURE K-2D: GO TO BH 1 SUB ROUTINE GEOLOGY

GEOLOGICAL LOG TOP

Depth (m)	Description
0 - 13	Alluvial deposits: Boulders and cobbles in a clay matrix
13 - 110	Dark sandstone layer, very little shale lenses (Baviaanskloof Formation - Nardouw Subgroup)
110 - 206.7	White, coarse-grained quartzite (Skurweberg Formation - Nardouw Subgroup)
	Fractures at 48, 186, 165-169, 186 m
	Solid from 196 m

FIGURE K-2E: WELLMAN – CHEM PLOTS (EXAMPLE)

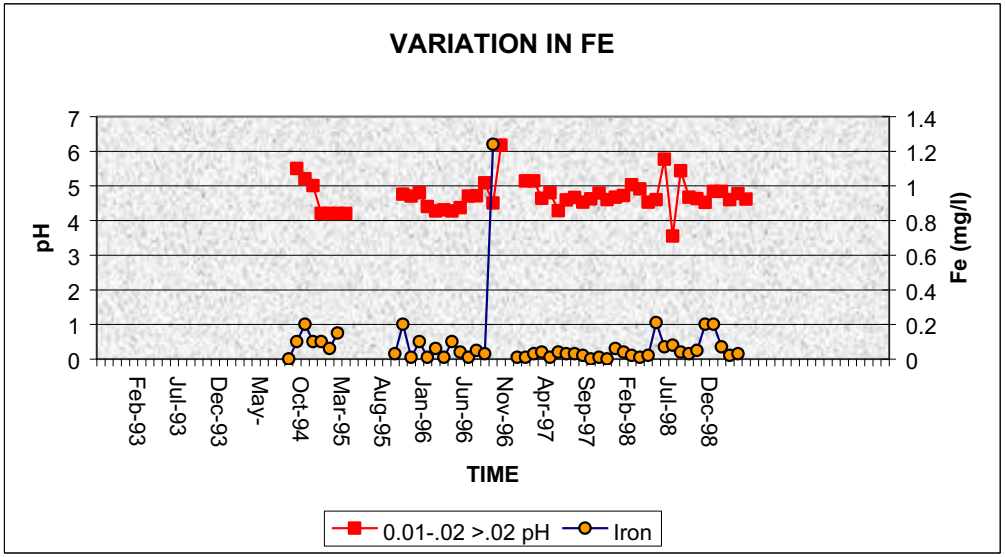

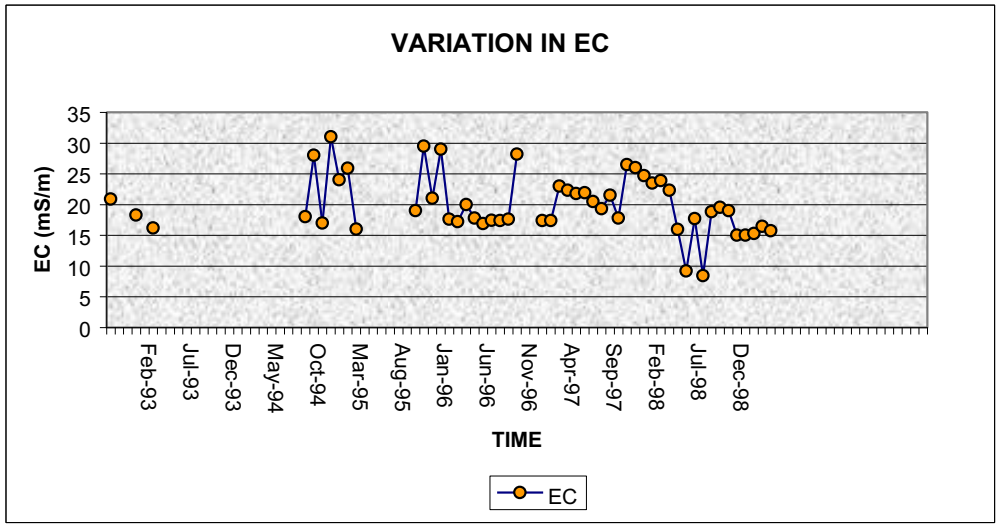

FIGURE K-2F: GO TO BH 1 – SUBROUTINE PUMPTEST

TOP

Pumping test data			
Date of test	22-27/05/90		
Abstr. Rate Q (l/s)	8.8		
Time (min)	Drawdown (m)	t'	res. s (m)
1	13	0.001	48.88
2	16	1	35.35
3	17.66	2	25.45
4	18.75	3	19.4
5	19.81	4	14.47
6	20.8	5	10.78
7	21.58	6	9.48
8	20.1	7	7.9
9	23.56	8	7
10	24.88	9	6.33
11	26	10	5.82
12	26.54	11	5.57
15	26.22	12	5.32
20	29.43	15	4.7
25	30.89	20	4
30	32.02	25	3.37
40	33.96	30	3.07
50	35.01	40	2.57
60	35.1	50	2.2
70	36.4	60	1.94
80	36.9	70	1.74
100	37.56	80	1.54
150	38.38	100	1.28
200	39.31	150	0.9
300	40.61	200	0.72
420	40.71	300	0.55
600	41.8	420	0.42
780	41.8	600	0.32
1080	41.8	780	0.24
1440	42.91	1080	0.19
1800	43.44	1440	0.13
2160	44.04	1800	0.05
2520	44.01	2160	0
2880	44.01		
3240	47.56		
3600	48.31		
3960	48.54		
4300	48.88		

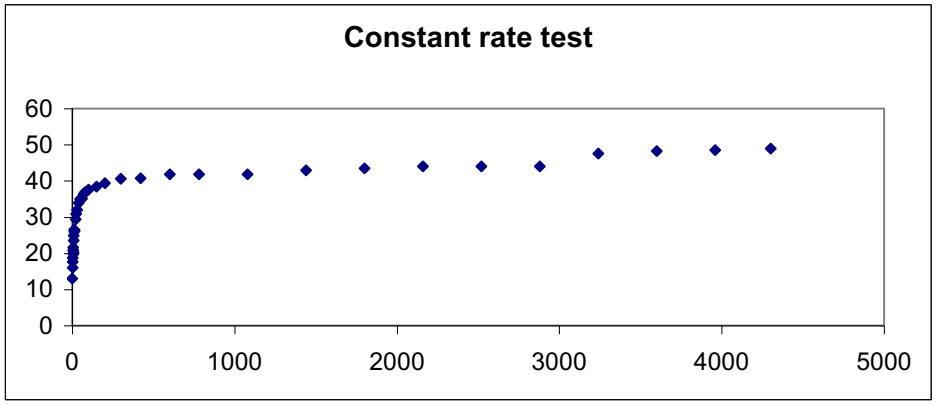

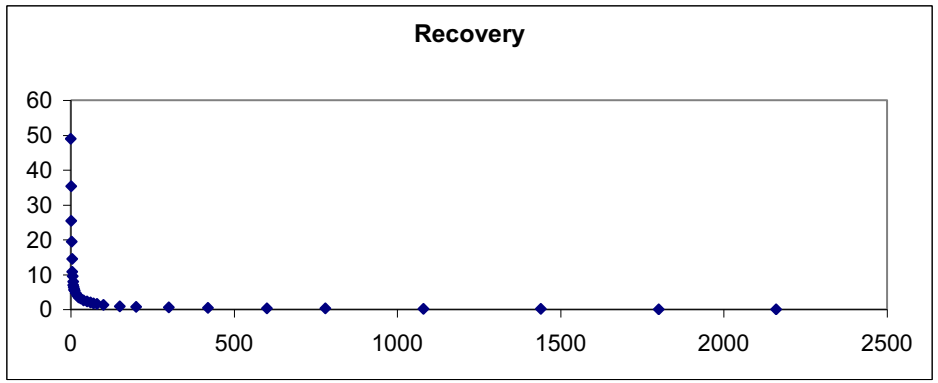

FIGURE K-2G: GO TO BH 1 – SUBROUTINE PUMPTEST (CONTINUE)

Step test data							
Nov-97	Step1	Step2	Step3	Step4	Step5	Step6	Step7
Q (l/s) =	4	5.8	10.6	15.5			
t(min)	s (m)	s (m)	s (m)	s (m)	s (m)	s (m)	s (m)
	4	5.8	10.6	15.5	0	0	0
0.1	0.001	6.05	10.4	33.5			
0.5	0.91	7.19	15.13	37.68			
1	3.63	7.73	15.94	38.98			
1.5	3.93	8.14	16.89	41.4			
2	4.24	8.41	17.56	45.7			
2.5	4.53	8.63	18.32	47.38			
3	4.61	8.81	18.78	50.56			
3.5	4.72	8.86	19.37	53.87			
4	4.88	8.95	19.86	56.6			
4.5	4.96	8.99	20.25	58.78			
5	5.05	9.08	20.96				
7	5.33	9.26	23.68				
9	5.44	9.36	24.71				
12	5.6	9.56	26.64				
15	5.67	9.68	27.39				
20	5.74	9.85	28.13				
25	5.8	9.94	28.24				
30	5.86	10.05	28.93				
35	5.89	10.13	30.04				
40	5.92	10.21	30.61				
45	5.96	10.27	30.8				
50	5.99	10.31	31.15				
60	6.05	10.4	33.5				

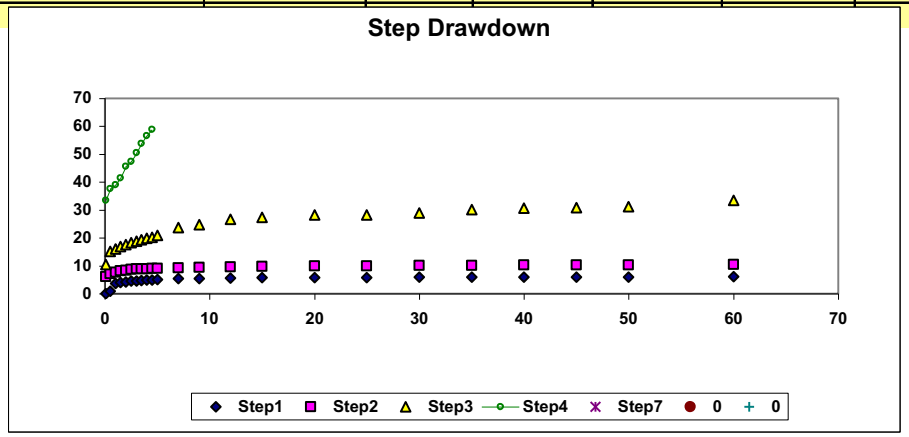

FIGURE K-2H: GO TO BH 1 SUB ROUTINE MANAGE

Management

TOP

Q_s (m^3/d) =	173
Q_s (l/s) =	2.0

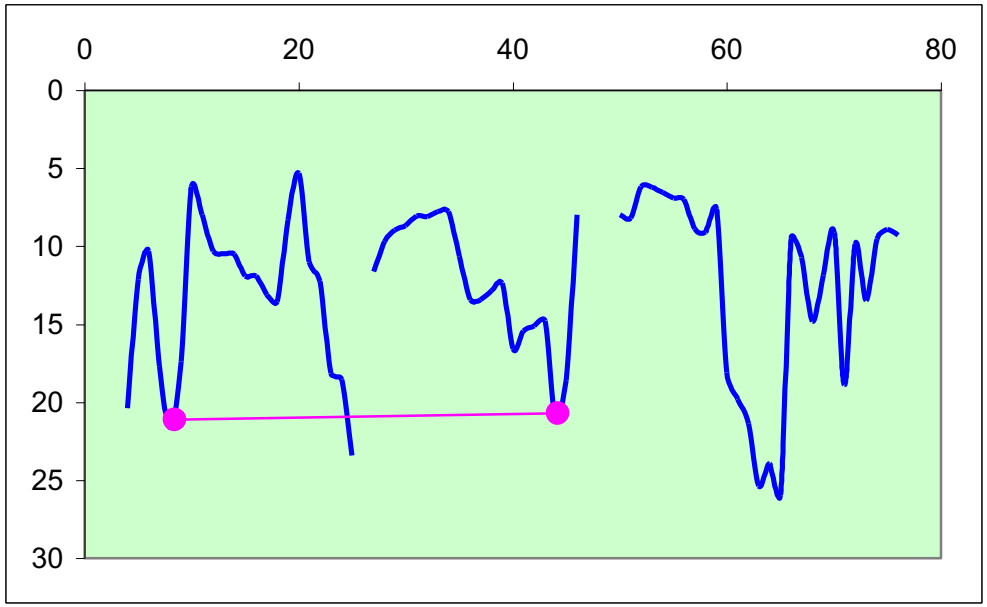

x_0	0	8.4
x_1	20	44.2
y_0	58	21.1
y_1	183	20.7

8	start of equal volume
44	end of equal volume

APPENDIX K: WELLMAN (continue)

APPENDIX K-3

Go to Wellfield submenu - WELLMAN

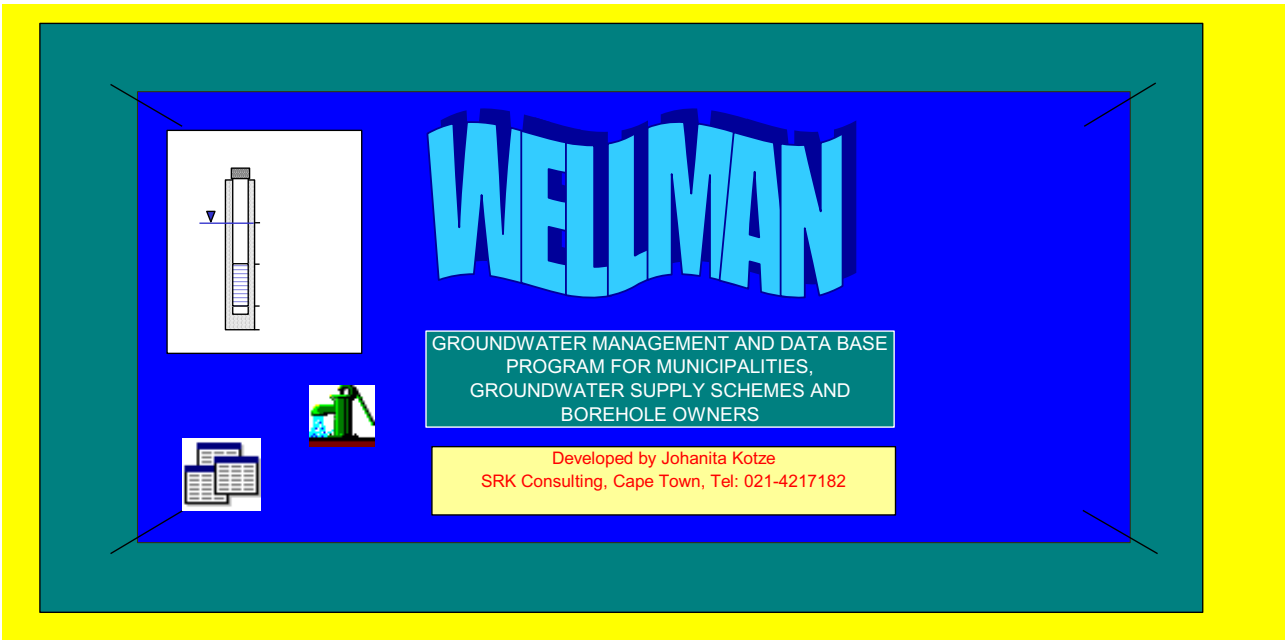

FIGURE K-3A: GO TO WELLFIELD1 – SUMMARY OF ANNUAL ABSTRACTION FROM VERMAAKS WELLFIELD

Annual Abstraction from Vermaaks wellfield

Main

Go to Varkieskloof Wellfield

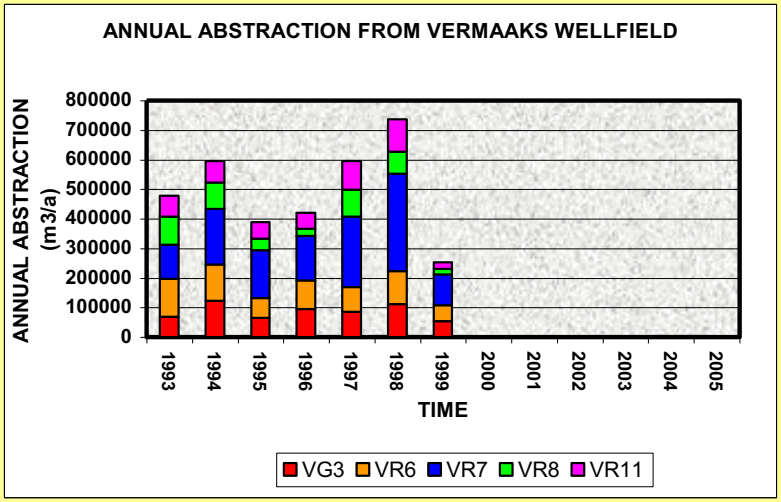

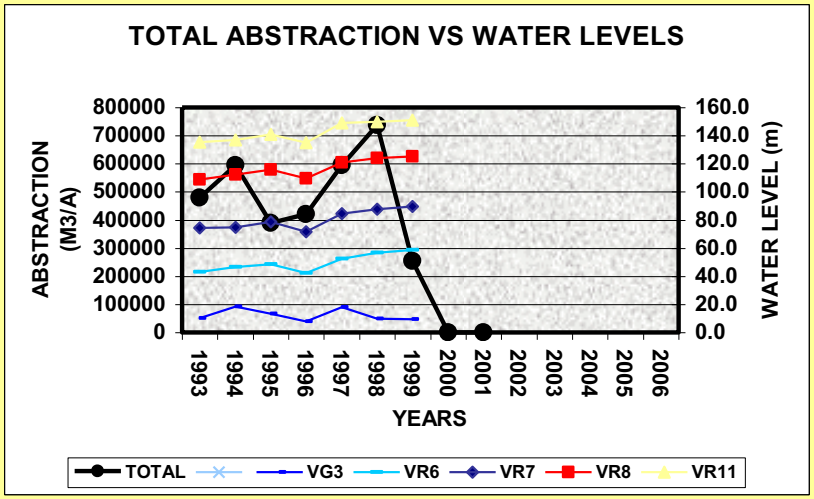

	1993	1994	1995	1996	1997	1998	1999	2000	2001	2002	2003	2004	2005
VG3	69113	122688	65816	95475	84958	111903	53880	0	0				
VR6	127794	122688	65816	95475	84958	111903	53880	0	0				
VR7	116539	187577	161723	152159	237528	328435	105032	0	0				
VR8	94066	90351	39894	23515	90673	75459	17811	0	0				
VR11	71485	71851	55610	54251	97133	108883	22864	0	0				
TOTAL	478998	595155	388859	420875	595250	736583	253467	0	0				
WATER LEVEL													
VG3	10.3	18.6	13.4	8.0	18.1	9.9	9.3						
VR6	43.0	46.4	48.7	42.4	52.5	56.8	58.6						
VR7	74.2	74.6	78.5	71.7	84.6	87.7	89.7						
VR8	108.7	112.4	115.6	109.6	120.9	123.9	125.4						
VR11	135.5	136.9	141.0	134.9	149.0	149.8	151.0						

FIGURE K-3B: GO TO WELLFIELD2 – SUMMARY OF ANNUAL ABSTRACTION FROM VARKIESKLOOF WELLFIELD

Annual Abstraction from Varkieskloof wellfield

Main

Go to Bokkraal Wellfield

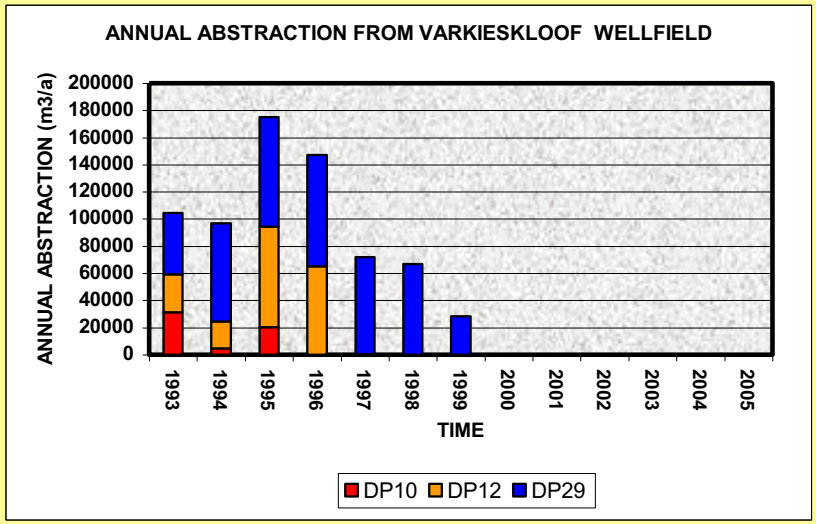

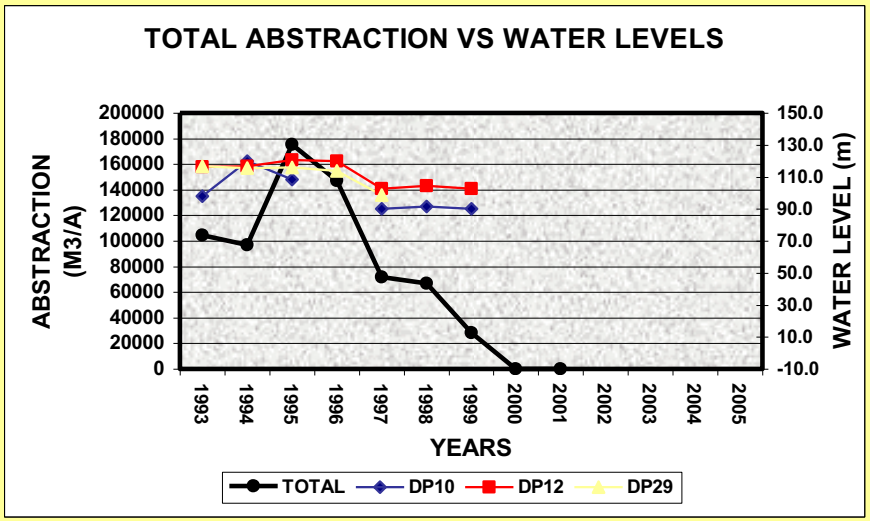

	1993	1994	1995	1996	1997	1998	1999	2000	2001	2002	2003	2004	2005
DP10	31436	4797	20304	0	0	0	0	0	0				
DP12	27624	19784	73960	64942	294	0	0	0	0				
DP29	45497	72230	80921	82171	71385	66895	28375	0	0				
TOTAL	104557	96811	175185	147113	71679	66895	28375	0	0				
WATER LEVEL													
DP10	98.1	119.7	108.3		90.1	91.4	90.2						
DP12	116.2	116.7	120.6	119.7	102.6	104.4	102.8						
DP29	116.6	115.6	115.8	113.6	98.7								

FIGURE K-4C: GO TO WELLFIELD3 – SUMMARY OF ANNUAL ABSTRACTION FROM BOKKRAAL WELLFIELD

Annual Abstraction from Bokkraal wellfield

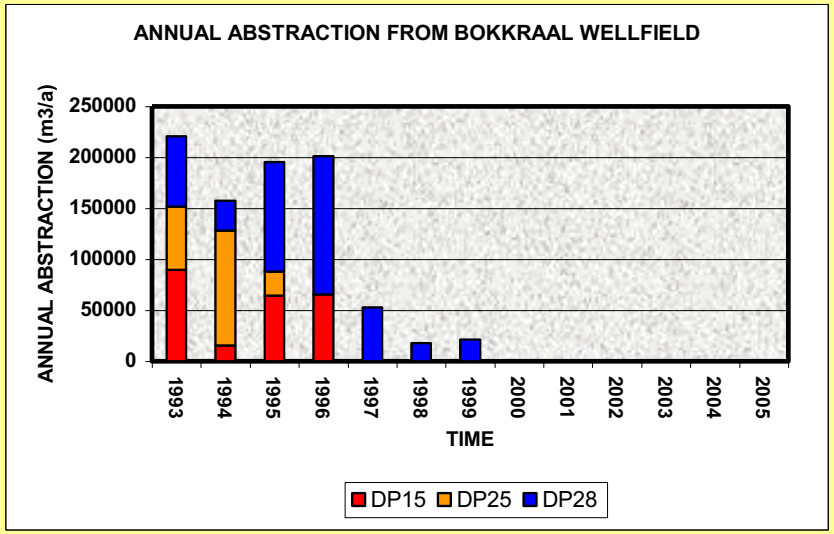

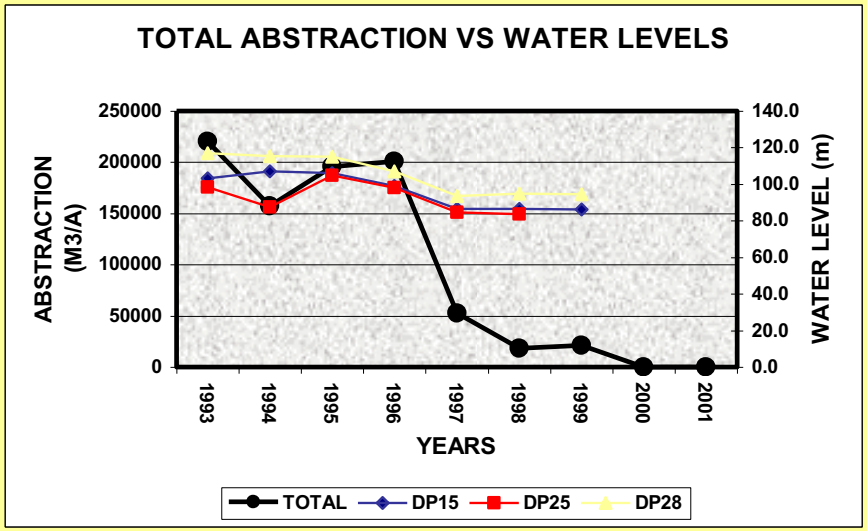

	1993	1994	1995	1996	1997	1998	1999	2000	2001	2002	2003	2004	2005	2006
DP15	89547	15496	64305	65468	0	0	0	0	0					
DP25	62108	112811	23809	0	0	0	0	0	0					
DP28	68775	28954	107557	135472	52631	18082	21355	0	0					
TOTAL	220429	157261	195671	200940	52631	18082	21355	0	0					
WATER LEVEL														
DP15	103.0	107.2	105.9	99.0	86.6	86.6	86.0							
DP25	98.2	87.5	104.9	98.1	84.5	83.5								
DP28	116.9	115.4	115.0	107.1	93.7	94.8	94.4							

FIGURE K-3D: GO TO WELLFIELD3 – SUMMARY OF ANNUAL ABSTRACTION FROM DROËKLOOF AND OLIFANTS RIVER WELLFIELD

Annual Abstraction from Droekloof and Olifants River

Main

Go to TOTAL ANNUAL ABSTRACTION -ALL WELLFIELDS

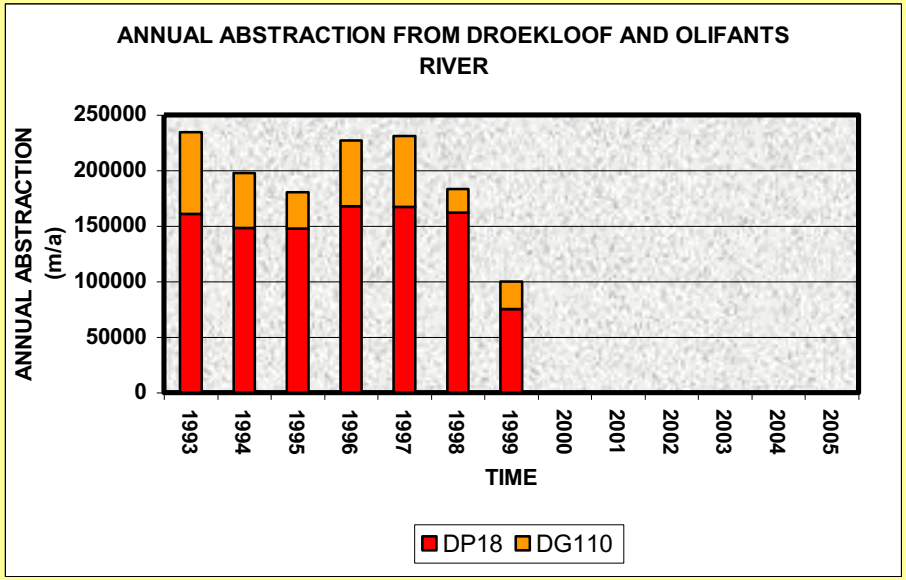

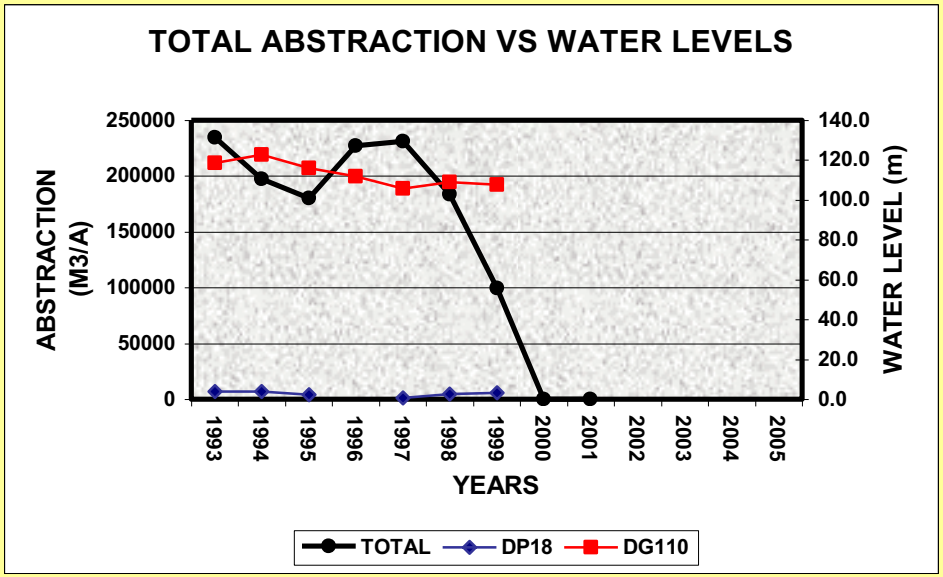

	1993	1994	1995	1996	1997	1998	1999	2000	2001	2002	2003	2004	2005
DP18	160658	148416	147955	168040	167241	162120	75266	0	0				
DG110	73645	49071	32293	59087	64042	21233	24480	0	0				
TOTAL	234303	197487	180248	227127	231283	183353	99746	0	0				
WATER LEVEL													
DP18	3.9	3.8	2.4		0.7	2.5	3.2						
DG110	118.5	122.8	115.9	111.9	105.6	109.0	107.6						

FIGURE K-3E: GO TO ABSTRACTION – SUMMARY OF ANNUAL ABSTRACTION FROM ALL WELLFIELDS

Total Annual Abstraction from ALL WELLFIELDS - Eastern Section

Main | Go to data An_AB

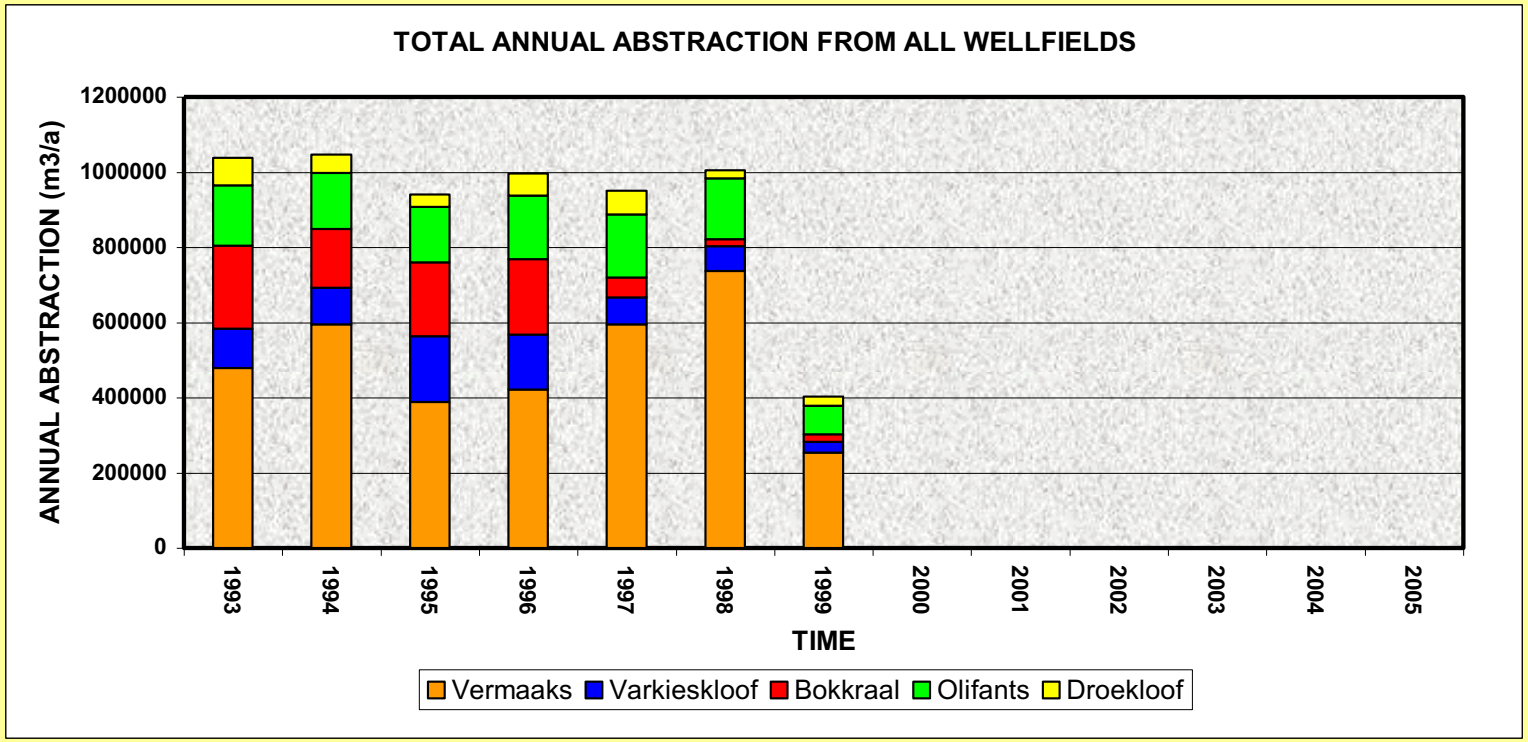

Main | Graph

	1993	1994	1995	1996	1997	1998	1999	2000	2001	2002	2003	2004	2005
Vermaaks	478998	595155	388859	420875	595250	736583	253467	0	0				
Varkieskloof	104557	96811	175185	147113	71679	66895	28375	0	0				
Bokkraal	220429	157261	195671	200940	52631	18082	21355	0	0				
Olifants	160658	148416	147955	168040	167241	162120	75266	0	0				
Droekloof	73645	49071	32293	59087	64042	21233	24480	0	0				
TOTAL	1038286	1046714	939963	996055	950843	1004913	402943	0	0				

APPENDIX K: WELLMAN (continue)

APPENDIX K-4

OBSERVATION WELL DATA - WELLMAN

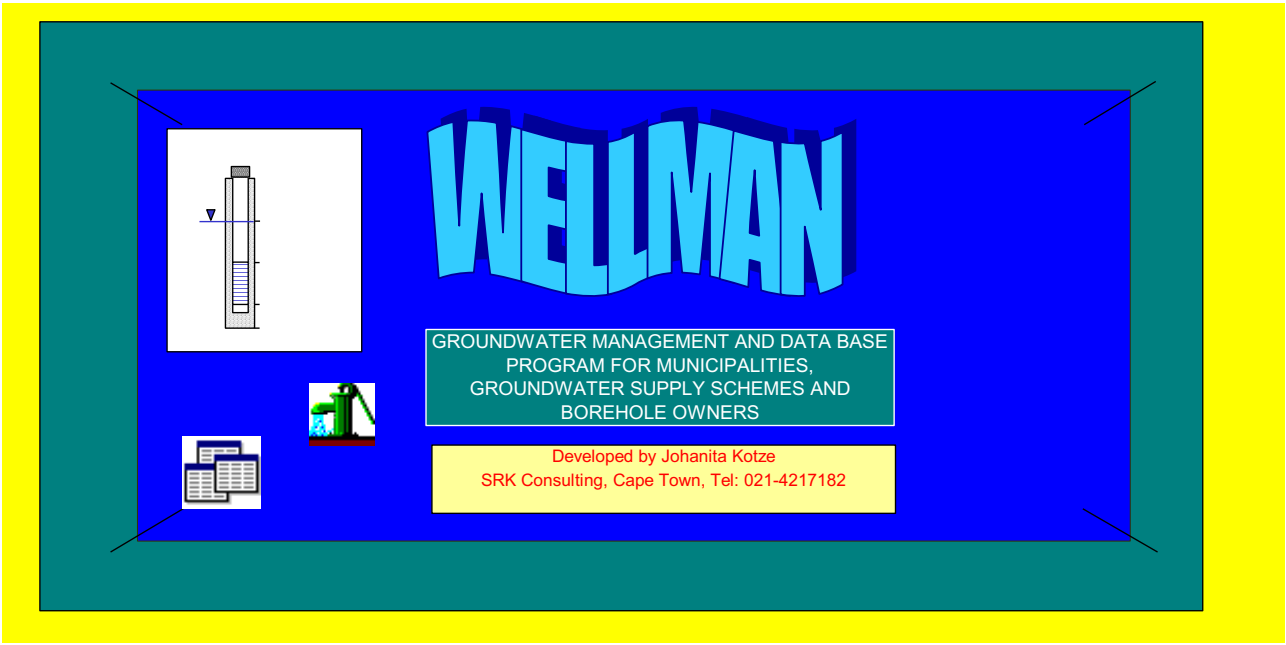

FIGURE K-4A: OBSERVATION WELL WATER LEVEL CHANGES OVER TIME FOR VARKIESKLOOF WELLFIELD

BACK

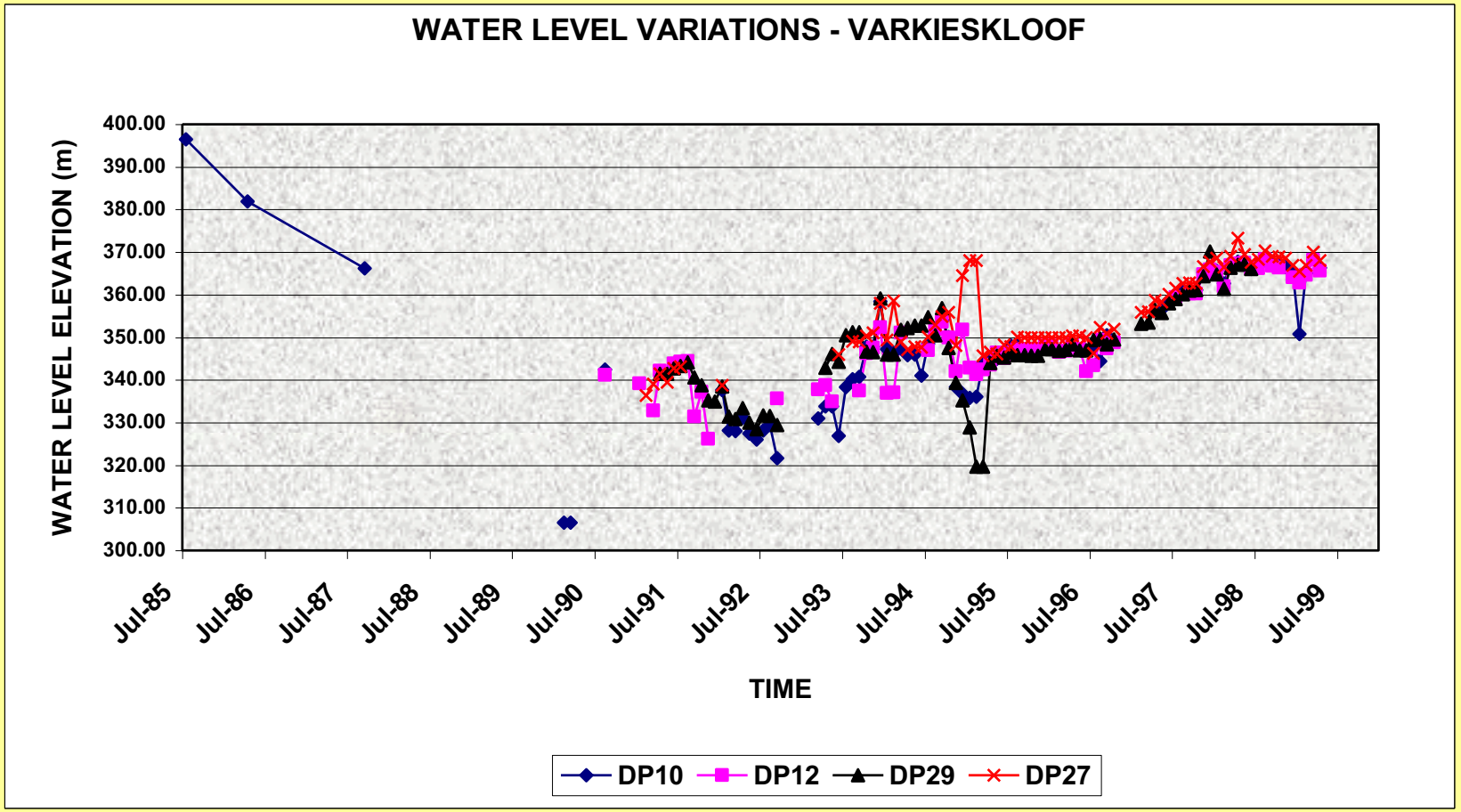

FIGURE K-4B: OBSERVATION WELL WATER LEVEL CHANGES OVER TIME FOR BOKKRAAL WELLFIELD

BACK

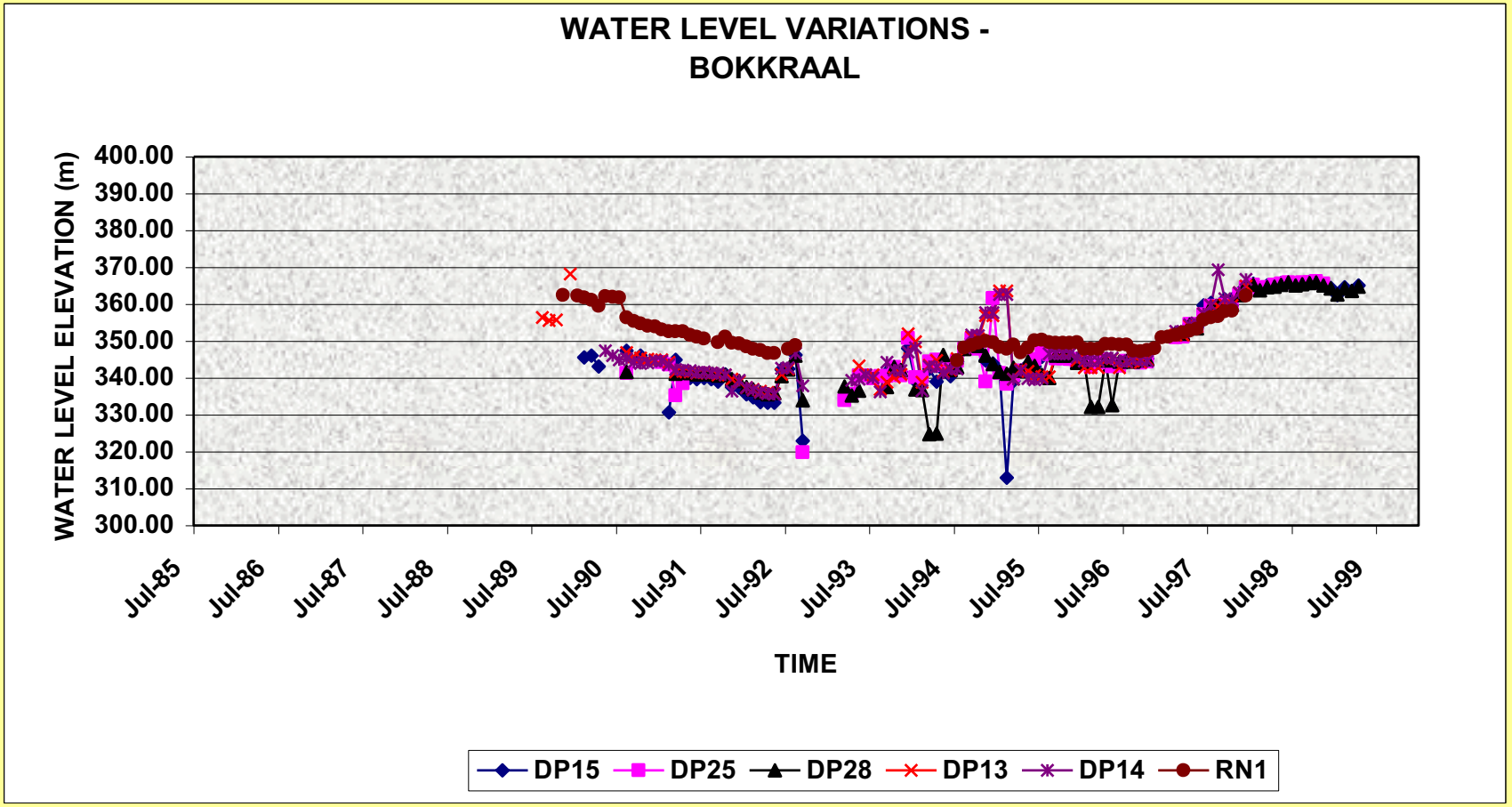

FIGURE K4-C: OBSERVATION WELL WATER LEVEL CHANGES OVER TIME FOR OLIFANTS RIVER WELLFIELD

BACK

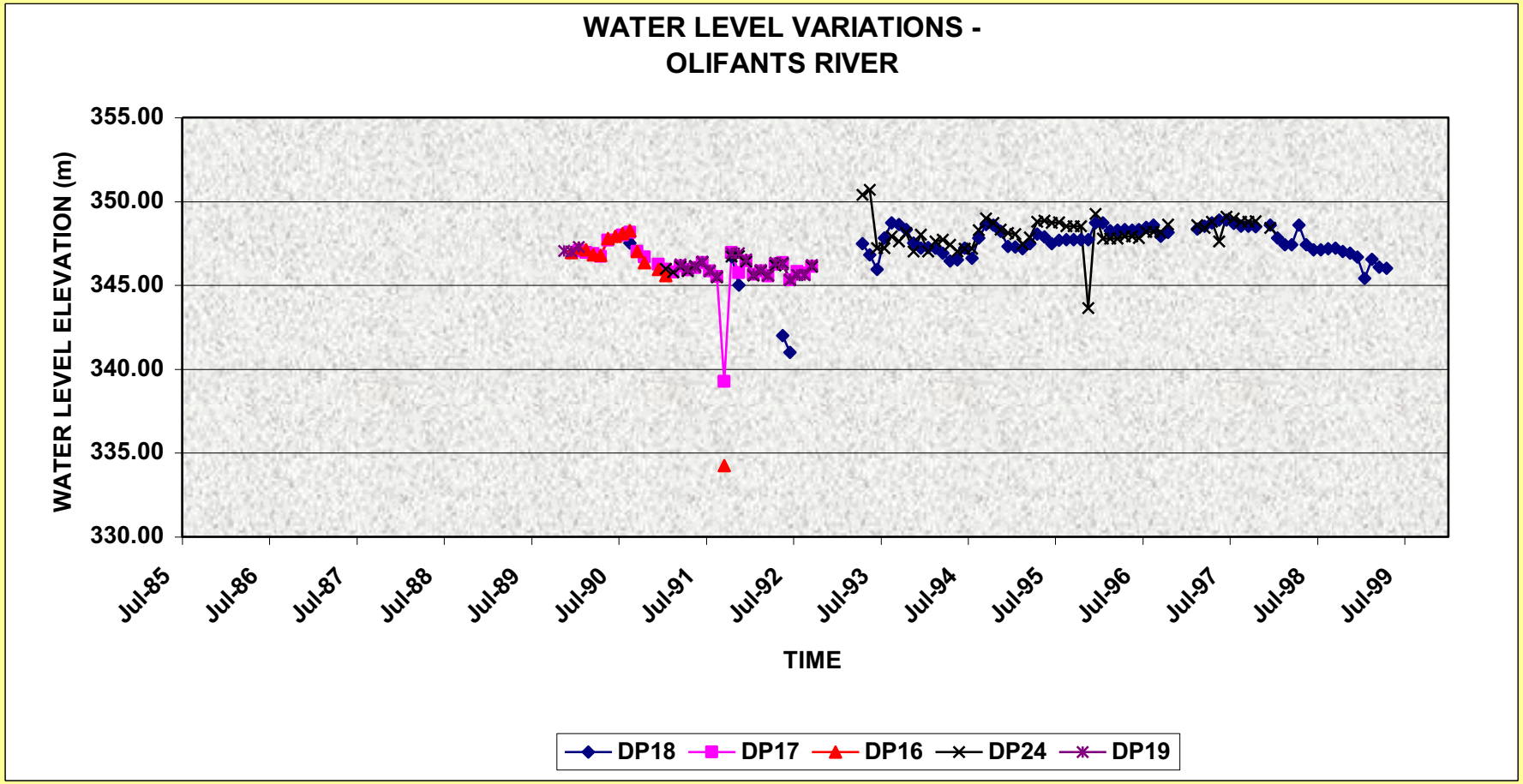

FIGURE K-4D: OBSERVATION WELL WATER LEVEL CHANGES OVER TIME FOR VOORZORG

BACK

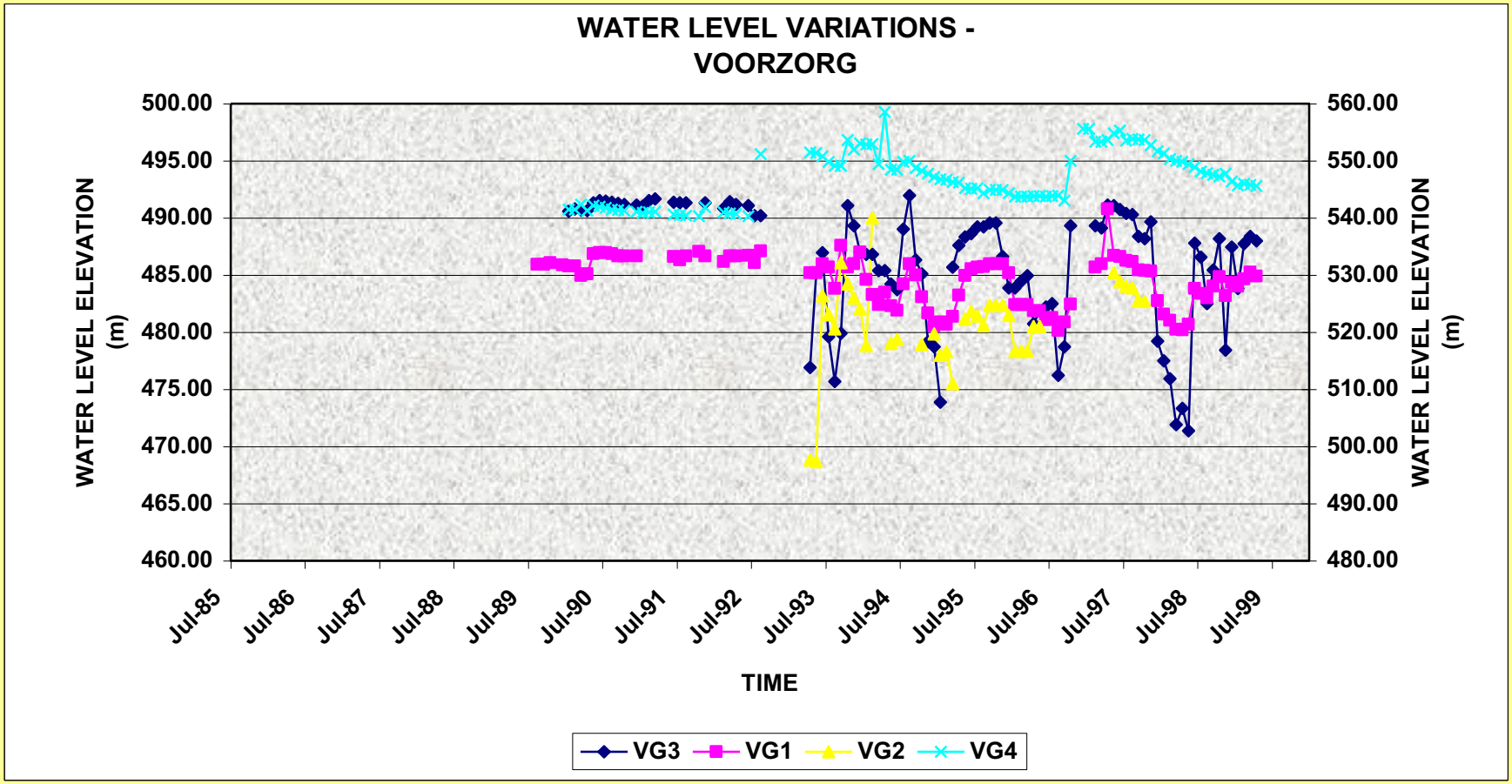

FIGURE K-4E: OBSERVATION WELL WATER LEVEL CHANGES OVER TIME FOR VERMAAKS RIVER WELLFIELD

BACK

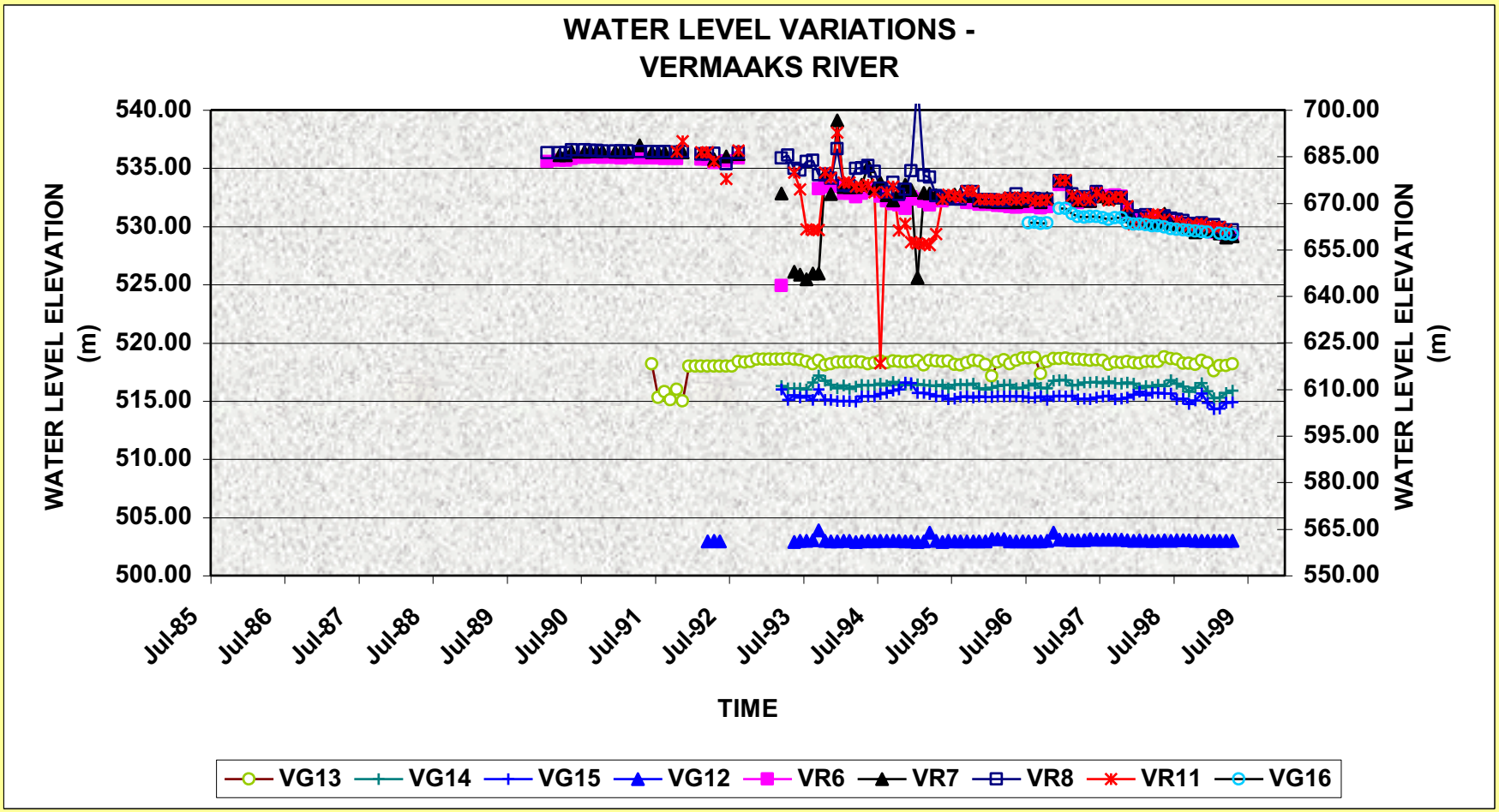

FIGURE K-4F: OBSERVATION WELL WATER LEVEL CHANGES OVER TIME FOR DROËKLOOF WELLFIELD

BACK

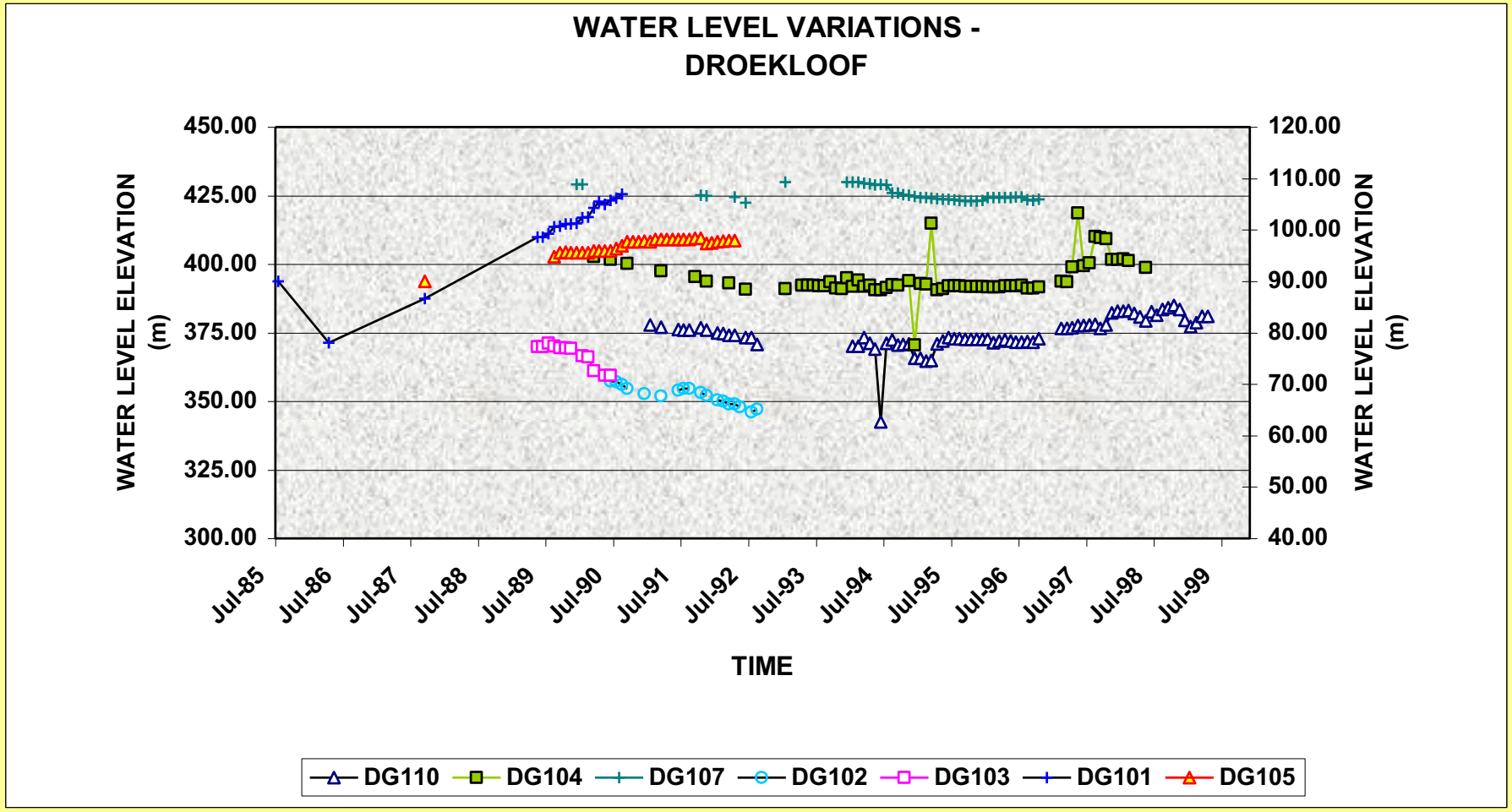

FIGURE K-4G: OBSERVATION WELL WATER LEVEL CHANGES OVER TIME FOR DROËKLOOF WELLFIELD

BACK

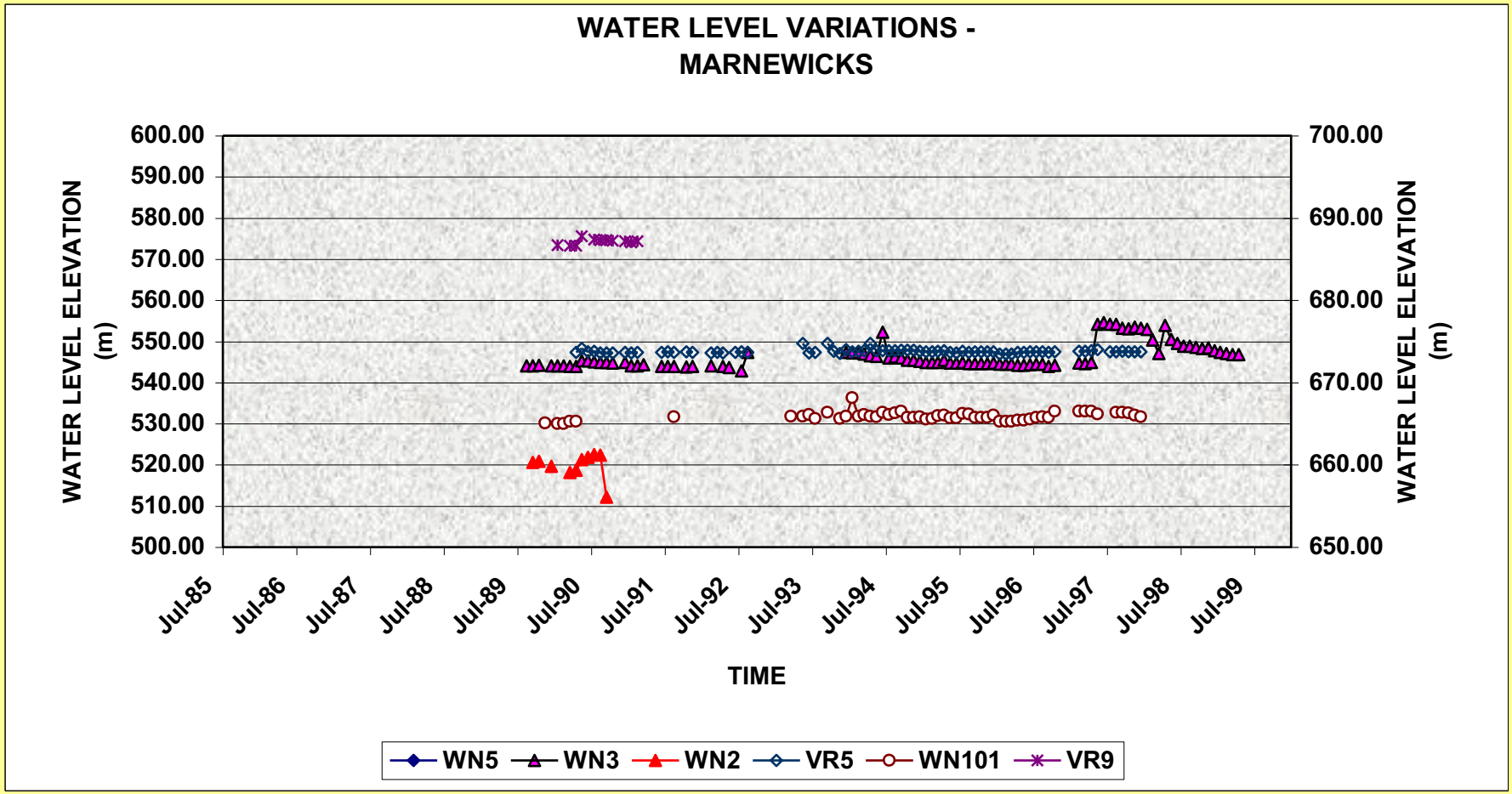

FIGURE K-4H: OBSERVATION WELL WATER LEVEL CHANGES OVER TIME FOR SOUTHERN KAMMANASSIE MOUNTAINS

BACK

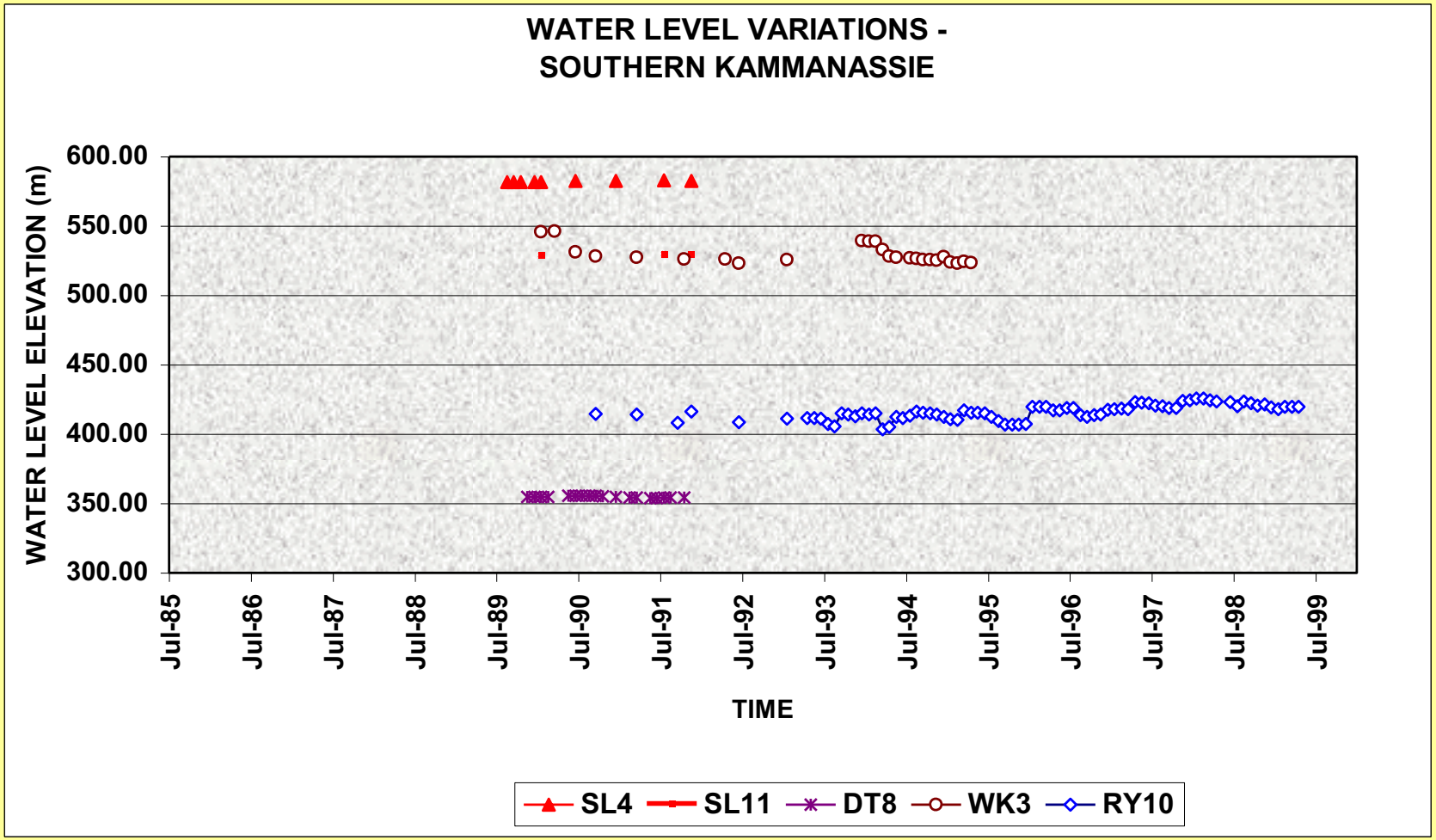

APPENDIX K: WELLMAN (continue)

APPENDIX K-5

MANAGEMENT – EQUAL VOLUME METHOD

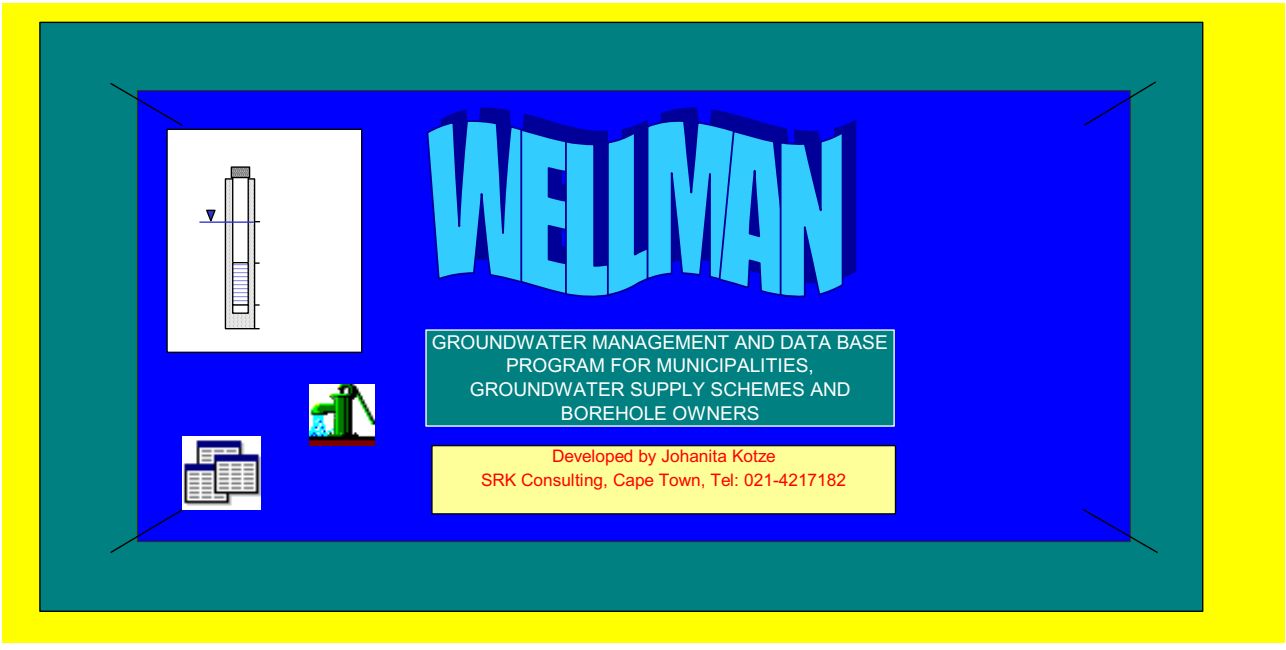

FIGURE K-5A: WELLMAN – MANAGEMENT – VG3

BOREHOLE MANAGEMENT VG3

Q_s (m^3/d) =	197
Q_s (l/s) =	2.3

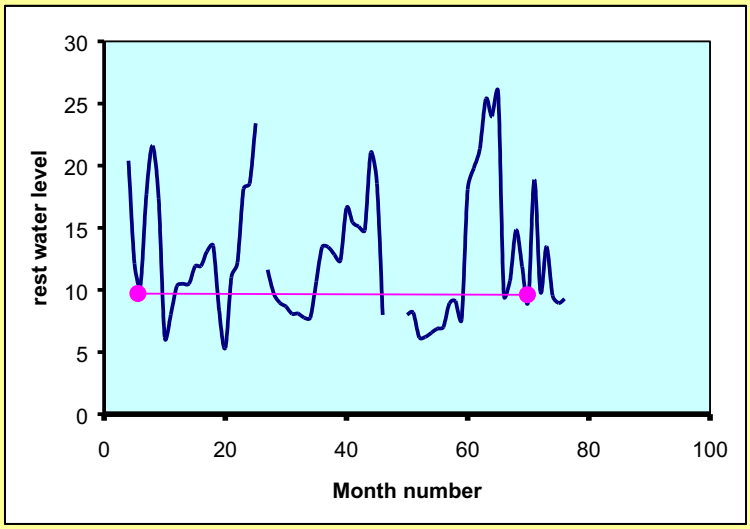

x_0	0	5.6
x_1	20	69.9
y_0	58	9.7
y_1	183	9.6

6	start of equal volume	5.6
70	end of equal volume	69.9

FIGURE K-5B: WELLMAN – MANAGEMENT – VR6

BOREHOLE MANAGEMENT VR6

Q_s (m^3/d) =	281
Q_s (l/s) =	3.3

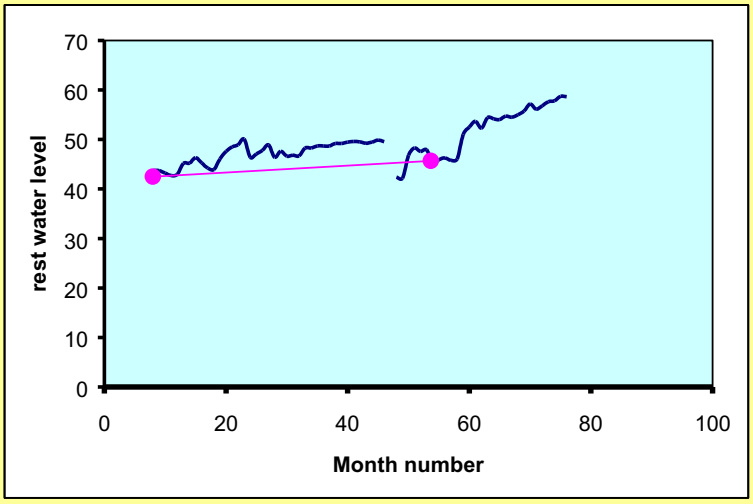

x_0	0	8
x_1	20	53.7
y_0	44	42.5
y_1	53	45.7

8	start of equal volume
54	end of equal volume

FIGURE K-5C: WELLMAN – MANAGEMENT – VR7

BOREHOLE MANAGEMENT VR7

Q_s (m^3/d) =	492
Q_s (l/s) =	5.7

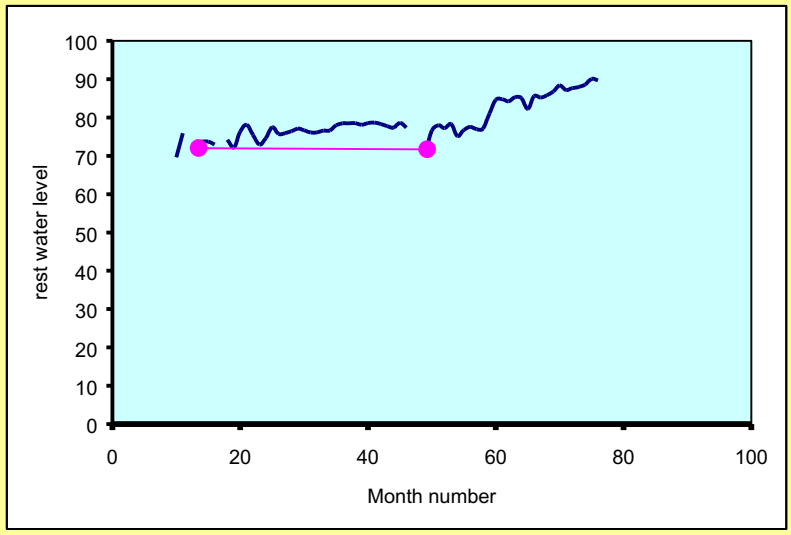

x_0	0	13.5
x_1	20	49.3
y_0	43	72
y_1	99	71.7

14	start of equal volume
49	end of equal volume

FIGURE K-5D: WELLMAN – MANAGEMENT – VR8

BOREHOLE MANAGEMENT VR8

Q_s (m^3/d) =	174
Q_s (l/s) =	2.0

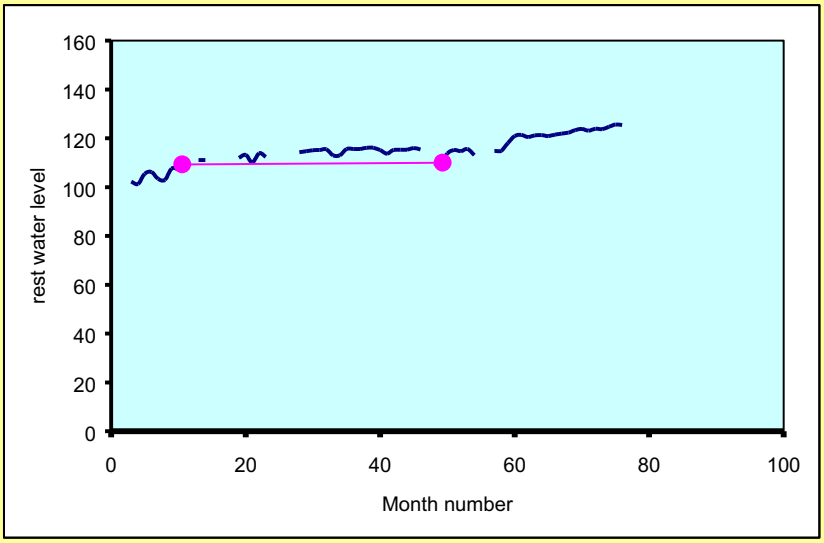

x_0	0	10.6
x_1	20	49.3
y_0	43	109.3
y_1	58	110

11	start of equal volume
49	end of equal volume

FIGURE K-5E: WELLMAN – MANAGEMENT – VR11

BOREHOLE MANAGEMENT VR11

Q_s (m^3/d) =	174
Q_s (l/s) =	2.0

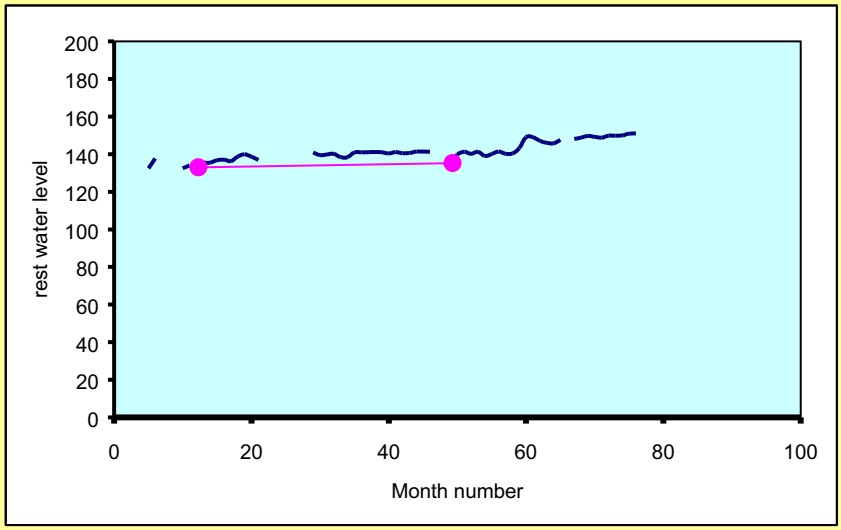

x_0	0	12.3
x_1	20	49.3
y_0	35	133
y_1	44	135.2

12	start of equal volume
49	end of equal volume

FIGURE K-5F: WELLMAN – MANAGEMENT – DP10

BOREHOLE MANAGEMENT DP10

Q_s (m^3/d) =	18
Q_s (l/s) =	0.2

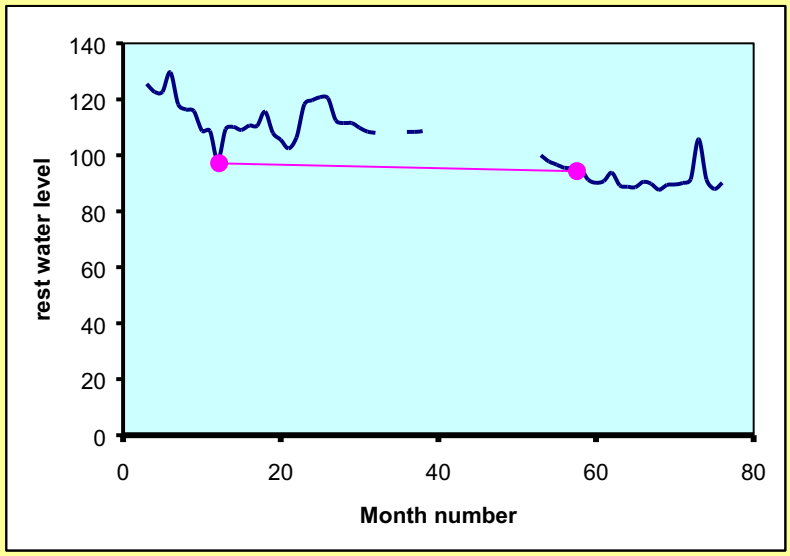

x_0	0	12.2
x_1	20	57.6
y_0	97	97.1
y_1	97	94.3

12	start of equal volume
58	end of equal volume

FIGURE K-5G: WELLMAN – MANAGEMENT – DP12

BOREHOLE MANAGEMENT DP12

Q_s (m^3/d) =	117
Q_s (l/s) =	1.4

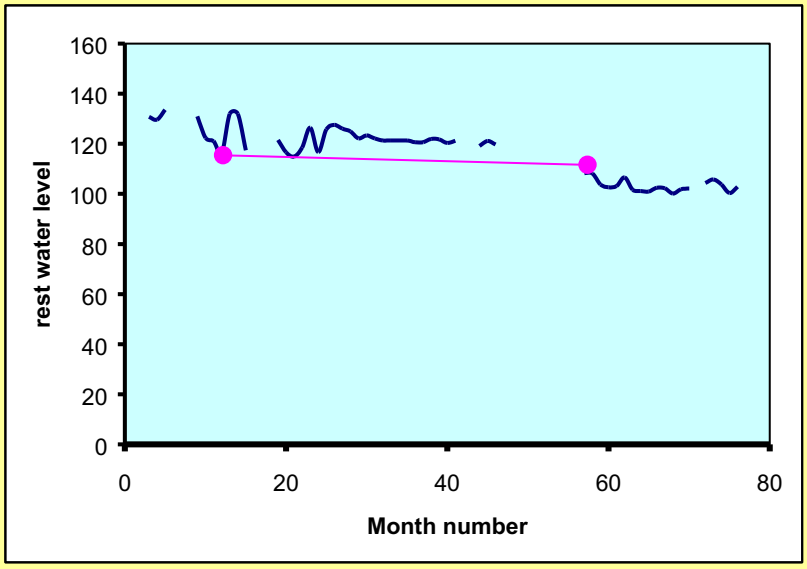

x_0	0	12.2
x_1	20	57.4
y_0	126	115.4
y_1	126	111.6

12	start of equal volume
57	end of equal volume

FIGURE K-5H: WELLMAN – MANAGEMENT – DP29

BOREHOLE MANAGEMENT DP29

Q_s (m^3/d) =	218
Q_s (l/s) =	2.5

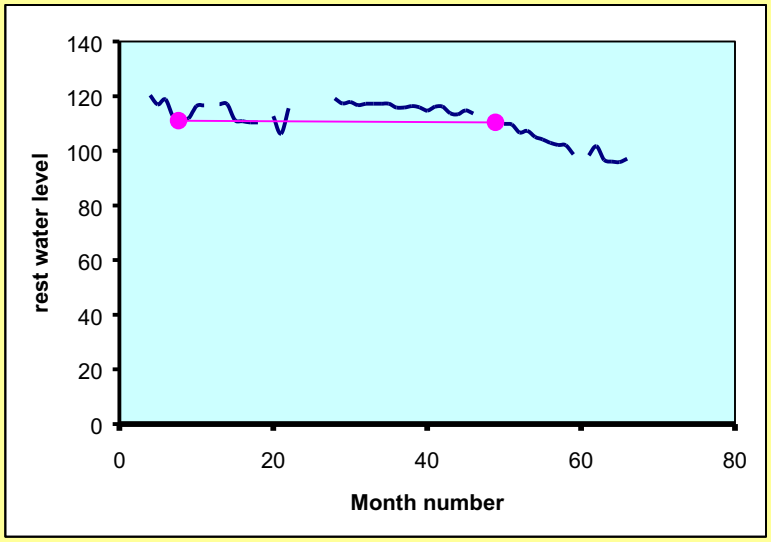

x_0	0	7.7
x_1	20	48.9
y_0	95	111
y_1	107	110.4

8	start of equal volume
49	end of equal volume

FIGURE K-5I: WELLMAN – MANAGEMENT – DP15

BOREHOLE MANAGEMENT DP15

Q_s (m^3/d) =	153
Q_s (l/s) =	1.8

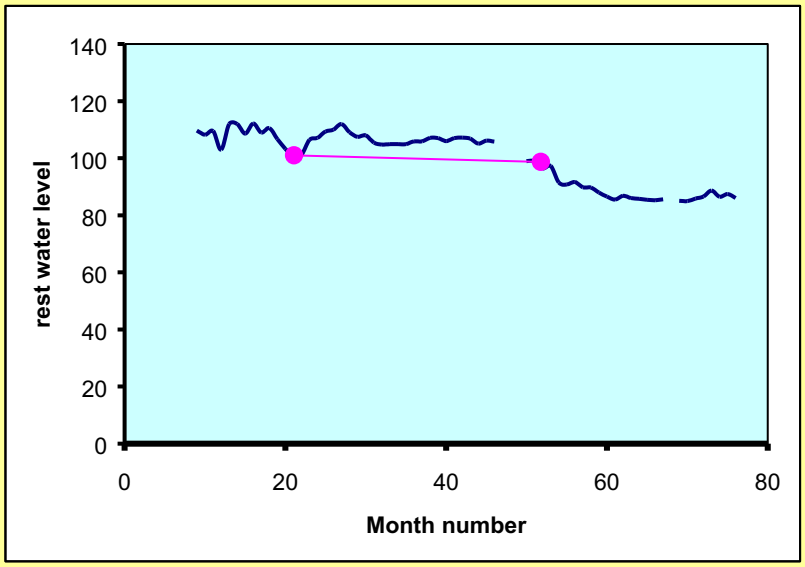

x_0	0	21.1
x_1	20	51.8
y_0	82	101
y_1	124	98.7

21	start of equal volume
52	end of equal volume

FIGURE K-5J: WELLMAN – MANAGEMENT – DP25

BOREHOLE MANAGEMENT DP25

Q_s (m^3/d) =	129
Q_s (l/s) =	1.5

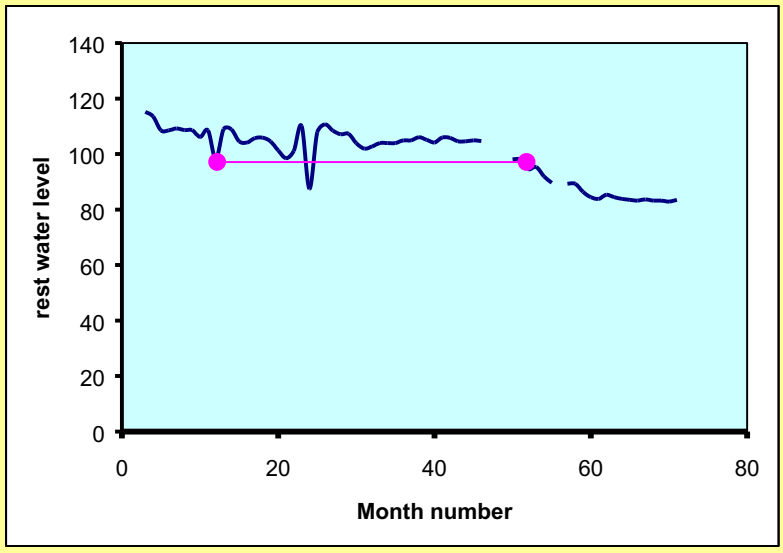

x_0	0	12.2
x_1	20	51.8
y_0	86	97.1
y_1	97	97.1

12	start of equal volume
52	end of equal volume

FIGURE K-5K: WELLMAN – MANAGEMENT – DP28

BOREHOLE MANAGEMENT **DP28**

Q_s (m^3/d) =	325
Q_s (l/s) =	3.8

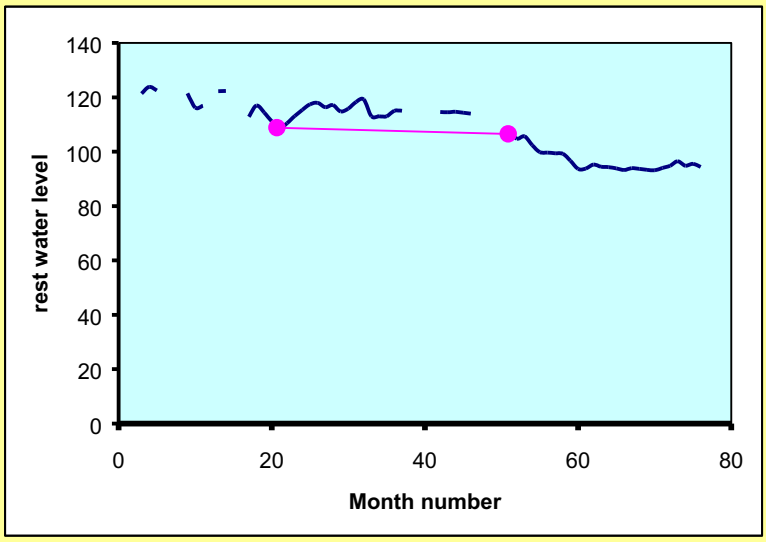

x_0	0	20.7
x_1	20	50.9
y_0	82	108.8
y_1	100	106.5

21	start of equal volume
51	end of equal volume

FIGURE K-5L: WELLMAN – MANAGEMENT – DG110

BOREHOLE MANAGEMENT **DG110**

Q_s (m^3/d) =	152
Q_s (l/s) =	1.8

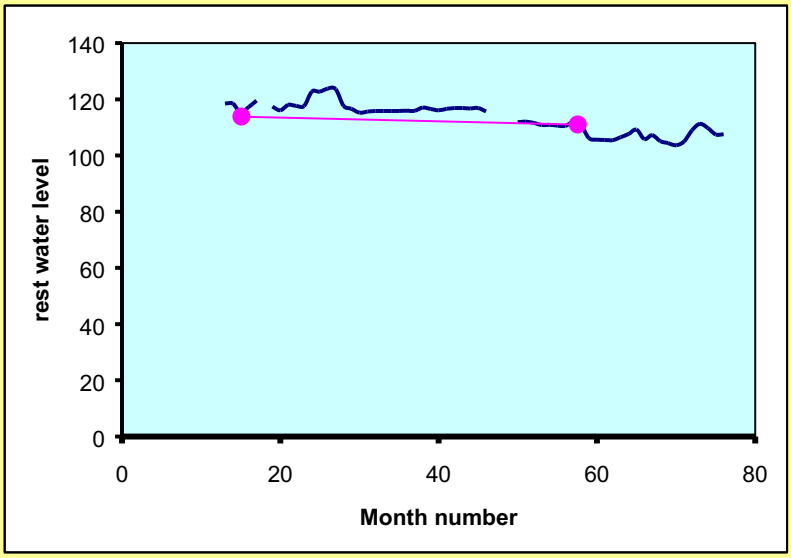

x_0	0	15.1
x_1	20	57.6
y_0	81	113.8
y_1	91	111

15	start of equal volume
58	end of equal volume

FIGURE K-5M: WELLMAN – MANAGEMENT – DP18

BOREHOLE MANAGEMENT **DP18**

Q_s (m^3/d) =	452
Q_s (l/s) =	5.2

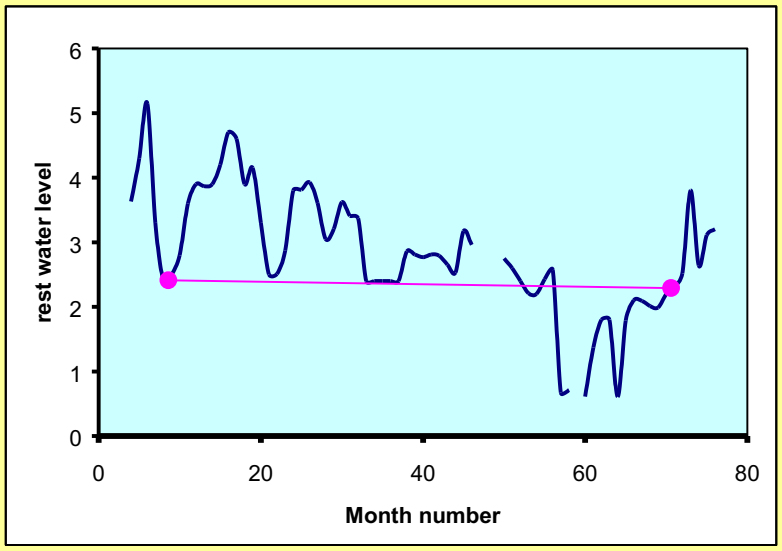

x_0	0	8.6
x_1	20	70.6
y_0	899	2.41
y_1	899	2.29

9	start of equal volume
71	end of equal volume

APPENDIX K: WELLMAN (continue)

APPENDIX K-6
PUMP TEST DATA SUMMARY

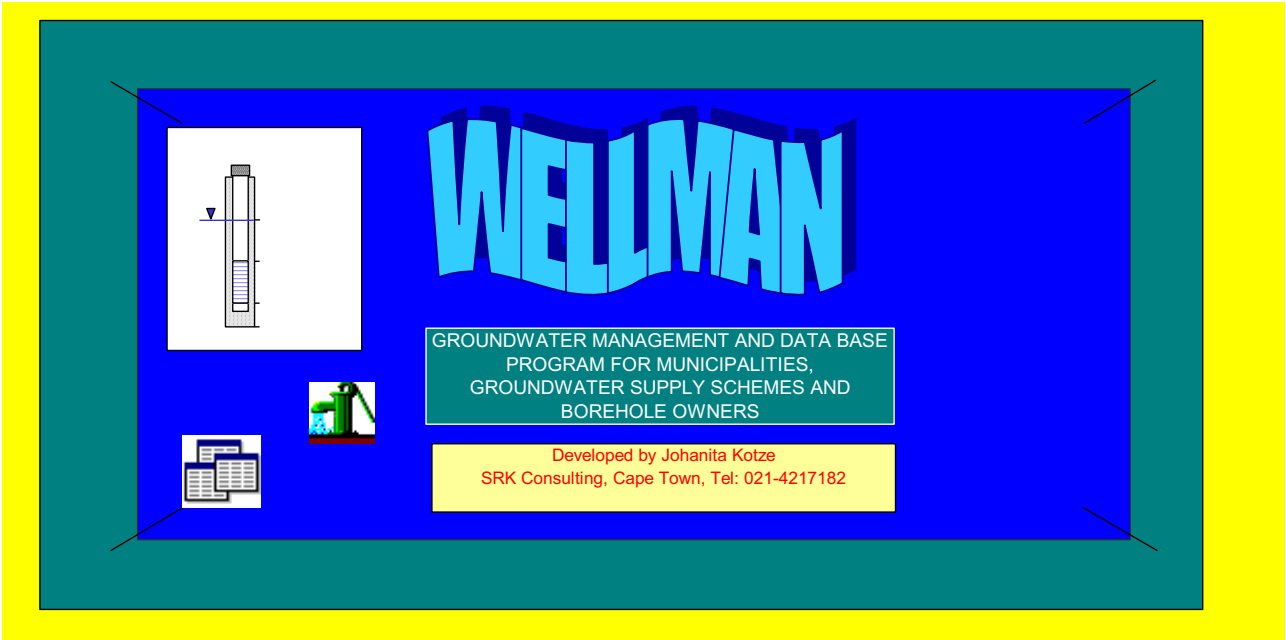

FIGURE K-6A: PUMP TEST DATA VG3

Date of test	22-27/05/90		
Abstr. Rate Q (l/s)	8.8		
Time (min)	Drawdown (m)	t'	res. s (m)
1	13	0.001	48.88
2	16	1	35.35
3	17.66	2	25.45
4	18.75	3	19.4
5	19.81	4	14.47
6	20.8	5	10.78
7	21.58	6	9.48
8	20.1	7	7.9
9	23.56	8	7
10	24.88	9	6.33
11	26	10	5.82
12	26.54	11	5.57
15	26.22	12	5.32
20	29.43	15	4.7
25	30.89	20	4
30	32.02	25	3.37
40	33.96	30	3.07
50	35.01	40	2.57
60	35.1	50	2.2
70	36.4	60	1.94
80	36.9	70	1.74
100	37.56	80	1.54
150	38.38	100	1.28
200	39.31	150	0.9
300	40.61	200	0.72
420	40.71	300	0.55
600	41.8	420	0.42
780	41.8	600	0.32
1080	41.8	780	0.24
1440	42.91	1080	0.19
1800	43.44	1440	0.13
2160	44.04	1800	0.05
2520	44.01	2160	0
2880	44.01		
3240	47.56		
3600	48.31		
3960	48.54		
4300	48.88		

FIGURE K-6A: PUMP TEST DATA VG3 (CONTINUED)

Step test data				
Nov-97	Step1	Step2	Step3	Step4
Q (l/s) =	4	5.8	10.6	15.5
t(min)	s (m)	s (m)	s (m)	s (m)
	4	5.8	10.6	15.5
0.1	0.001	6.05	10.4	33.5
0.5	0.91	7.19	15.13	37.68
1	3.63	7.73	15.94	38.98
1.5	3.93	8.14	16.89	41.4
2	4.24	8.41	17.56	45.7
2.5	4.53	8.63	18.32	47.38
3	4.61	8.81	18.78	50.56
3.5	4.72	8.86	19.37	53.87
4	4.88	8.95	19.86	56.6
4.5	4.96	8.99	20.25	58.78
5	5.05	9.08	20.96	
7	5.33	9.26	23.68	
9	5.44	9.36	24.71	
12	5.6	9.56	26.64	
15	5.67	9.68	27.39	
20	5.74	9.85	28.13	
25	5.8	9.94	28.24	
30	5.86	10.05	28.93	
35	5.89	10.13	30.04	
40	5.92	10.21	30.61	
45	5.96	10.27	30.8	
50	5.99	10.31	31.15	
60	6.05	10.4	33.5	

FIGURE K-6B: PUMP TEST DATA VR6

Time (min)	Drawdown (m)	t'	res. s (m)
0.1	5	0.01	82.23
1	13.32	0.5	67.52
1.5	17.19	1	54.8
2	20.6	1.5	45.04
2.5	23.79	2	37.09
3	26.59	2.5	31.5
3.5	26.97	3	27.75
4	27.61	3.5	24.48
4.5	27.94	4	24.13
5	28.46	5	23.03
7	30.39	7	19.38
12	42.51	9	16.99
15	46.67	12	15.23
20	49.86	15	13.8
25	52.86	20	12.86
30	53.1	25	11.85
35	53.61	30	11
40	53.62	35	10.25
45	53.92	40	9.67
50	57.27	45	9.12
60	62.26	50	8.7
70	64.11	60	7.94
80	64.89	70	7.36
90	65.65	80	6.77
100	65.98	90	6.3
120	67.37	110	5.79
150	67.77	140	5.15
200	68.94	190	4.47
250	69.63	240	3.63
300	69.9	290	3.21
400	72.44	390	2.87
500	72.59	490	2.37
600	73.27	590	2.14
700	74.2	690	1.93
800	76.01	790	1.8
900	76.16	890	1.68
1000	75.8	990	1.62
1100	77.58	1090	1.54
1300	76.77	1190	1.46
1440	78.16	1290	1.38
1560	77.65	1390	1.33
1680	77.42	1530	1.26
1800	78.36	2010	0.82
1920	75.89	2148	0.76
2040	77.75	2340	0.69
2160	79.55	2560	0.54
2280	80.35	2920	0.49
2400	81.17	3500	0.84
2520	80.72		
2640	81.65		
2760	82.27		
2880	82.08		
3000	81.8		
3120	82.49		
3240	82.03		
3360	81.15		
3480	82.09		
3600	82.25		
3720	82.78		
3840	83.45		
3960	83.25		
4080	82.53		
4200	82.38		
4320	82.23		

FIGURE K-6B: PUMP TEST DATA VR6 (CONTINUED)

Step test data						
Dec-97	Step1	Step2	Step3	Step4	Step5	Step6
Q (l/s) =	2.4	5	6.7	8.6	14.3	20.8
t(min)	s (m)	s (m)	s (m)	s (m)	s (m)	s (m)
	2.4	5	6.7	8.6	14.3	20.8
0.01	0	4	9.58	16.22	22.78	47.33
0.5	1.35	5.35		16.77	25.3	50.18
1	1.95	5.97	12.21	17.69	26.42	54.6
1.5	2.28	6.39	12.69	18.4	27.55	60.16
2	2.43	6.73	13.04	18.93	28.07	62.07
2.5	2.48	6.85	13.28	19.31	28.48	65.21
3	2.51	7.2	13.49	19.73	28.93	67.4
3.5	2.53	7.42	13.64	20	29.3	69.41
4	2.56	7.52	13.81	20.21	30.44	71.2
4.5	2.61	7.63	13.91	20.2	32.11	75.84
5	2.68	7.7	14.02	20.38	33.36	76.56
7	2.85	7.84	14.29	20.66	37.93	78.43
9	2.99	8.01	14.49	20.97	39.1	81.2
12	3.16	8.23	14.75	21.24	40.01	83.93
15	3.27	8.4	14.94	21.41	42.17	85.78
20	3.44	8.61	15.22	21.67	43.43	87.46
25	3.58	8.83	15.42	21.84	44.6	88.59
30	3.62	8.89	15.58	22.09	45.1	89.65
35	3.74	9.12	15.75	22.24	45.64	90.89
40	3.8	9.24	15.87	22.36	46.14	91.24
45	3.89	9.35	15.98	22.49	46.47	91.82
50	3.92	9.43	16.07	22.64	46.99	92.04
60	4	9.58	16.22	22.78	47.33	92.99

FIGURE K-6C: PUMP TEST DATA VR7

Pumping test data			
Date of test	14-01-97		
Abstr. Rate Q (l/s)	15.4		
Time (min)	Drawdown (m)	t'	res. s (m)
0.5	5	0	15.66
1	8.69	1.5	7.83
2	10.83	2	6.03
2.5	11.27	2.5	4.29
3	11.63	3.5	3.64
4	11.92	5	3.33
5	12.04	7	3.28
7	12.21	9	3.11
9	12.26	12	3.07
12	12.33	15	3.07
120	13.273	20	3.11
150	13.305	25	3.09
180	13.418	30	3.07
210	13.505	35	3.015
225	13.5	40	2.97
240	13.54	45	2.95
300	13.625	50	2.91
360	13.8	60	2.85
600	14.372		
1140	14.815		
1380	14.862		
1620	14.958		
1740	14.988		
2040	15.243		
2700	15.38		
2940	15.29		
3300	15.485		
3540	15.502		
4140	15.66		

FIGURE K-6C: PUMP TEST DATA VR7 (CONTINUED)

Step test data							
Dec-97	Step1	Step2	Step3	Step4	Step5	Step6	Step7
Q (l/s) =	2.8	6.5	9.8	15.8	20.2	25.9	35
t(min)	s (m)	s (m)	s (m)	s (m)	s (m)	s (m)	s (m)
	2.8	6.5	9.8	15.8	20.2	25.9	35
0.01	0	1.26	2.8	4.86	7.72	10.26	14.21
0.5	1.35	1.93	3.54	6.24	8.7	11.61	16.37
1	1.42	2.72	3.97	6.7	9.13	12.44	17.6
1.5	1.34	2.62	4.29	6.93	9.44	12.8	18.08
2	1.23	2.58	4.32	7.11	9.62	13.06	18.44
2.5	1.09	2.58	4.39	7.2	9.78	13.22	18.7
3	1.01	2.59	4.41	7.23	9.86	13.35	18.87
3.5	1.01	2.59	4.42	7.27	9.96	13.41	19.08
4	1.02	2.6	4.43	7.32	10.03	13.46	19.11
4.5	1.03	2.6	4.44	7.32	10.07	13.54	19.13
5	1.03	2.61	4.44	7.34	10.11	13.57	19.23
7	1.06	2.65	4.45	7.41	10.13	13.64	19.26
9	1.09	2.66	4.49	7.45	10.15	13.72	19.44
12	1.14	2.69	4.59	7.51	10.16	13.82	19.7
15	1.16	2.7	4.6	7.53	10.17	13.91	19.74
20	1.19	2.71	4.65	7.57	10.19	13.98	19.77
25	1.19	2.73	4.78	7.6	10.22	14.02	19.83
30	1.23	2.75	4.78	7.62	10.23	14.05	20.05
35	1.25	2.76	4.78	7.65	10.25	14.11	20.05
40	1.25	2.77	4.79	7.66	10.25	14.13	20.05
45	1.25	2.78	4.82	7.68	10.25	14.16	20.07
50	1.25	2.76	4.85	7.68	10.25	14.18	20.19
60	1.26	2.8	4.86	7.72	10.26	14.21	20.25

FIGURE K-6D: PUMP TEST DATA VR8

Step test data				
Jun-92	Step1	Step2	Step3	Step4
Q (l/s) =	4.2	9.5	16	22
t(min)	s (m)	s (m)	s (m)	s (m)
	4.2	9.5	16	22
1	2.39	3.63	10.91	28.45
2	2.91	6.49	11.29	28.79
3	2.96	8.14	12.84	29.19
4	2.63	8.84	18.03	31.09
5	2.39	9.24	20.63	37.65
6	2.29	9.53	22.53	41.17
7	2.04	10.07	23.79	41.87
8	1.79	10.7	24.67	43.59
9	1.55	10.99	25.21	44.34
10	1.56	11.22	25.59	45.48
12	1.91	11.34	26.09	46.35
15	2.31	11.64	26.15	46.72
20	2.92	12	26.39	47.06
25	3.14	12.03	26.92	47.51
30	3.31	10.64	27.47	48.07
35	3.39	10.51	27.52	48.09
40	3.56	10.84	27.91	
50	3.29	10.86	27.99	
60	3.63	10.91	28.45	

FIGURE K-6E: PUMP TEST DATA VR11

Pumping test data			
Date of test	14-01-97		
Abstr. Rate Q (l/s)	15.4		
Time (min)	Drawdown (m)	t'	res. s (m)
1	5.79	0.01	14.57
2	6.96	1	8.32
3	7.54	2	5.47
4	8	3	4.12
5	8.46	4	4.24
6	8.76	5	3.55
7	9.08	6	2.13
8	9.32	7	1.68
9	9.58	8	1.54
10	9.79	9	1.16
11		10	1.53
12	10.13	11	
15	10.5	12	1.57
20	10.97	15	1.37
25	11.33	20	1.49
30	11.48	25	1.4
40	11.71	30	1.42
50	11.78	40	1.43
60	11.79	50	1.37
70	11.82	60	1.36
80	11.83	70	1.35
100	11.91	80	1.34
150	11.93	100	1.32
200	12.05	150	1.26
300	12.68	200	1.23
420	13.07	300	1.17
600	13.16	420	1.14
780	13.37	600	1.08
1080	13.39		
1440	13.39		
1800	13.37		
2160	13.57		
2520	13.64		
2880	13.81		
3240	13.86		
3600	13.95		
3960	14.02		
4320	14.57		

FIGURE K-6E: PUMP TEST DATA VR11 (CONTINUED)

Step test data				
Oct-91	Step1	Step2	Step3	Step4
Q (l/s) =	4.1	6.9	10	12.5
t(min)	s (m)	s (m)	s (m)	s (m)
	4.1	6.9	10	12.5
1	2.61	4.58	10.57	19.11
2	4.05	6.09	10.62	19.34
3	3.89	7.18	12.78	19.5
4	3.61	7.82	13.78	20.29
5	3.63	8.12	14.75	23.55
6	3.69	8.39	15.33	24.73
7	3.83	8.59	15.84	26.08
8	3.56	8.82	16.19	27.19
9	3.95	8.99	16.53	27.99
10	4.04	9.08	16.79	28.83
12	4.14	9.16	17.09	29.55
15	4.28	9.35	17.17	29.99
20	4.38	9.55	17.49	30.73
25	4.5	9.75	17.88	31.49
30	4.5	10.01	18.23	32.5
35	4.53	10.12	18.55	
40	4.55	10.29	18.76	
50	4.57	10.39	18.85	
60	4.58	10.57	19.11	

FIGURE K-6F: PUMP TEST DATA DP18

Pumping test data			
Date of test	mulder-92		
Abstr. Rate Q (l/s)	13.2		
Time (min)	Drawdown (m)	t'	res. s (m)
1	2.42	0.1	6.63
2	2.72	1	1.4
3	2.72	2	1.3
4	2.02	3	1.27
5	2.22	4	1.22
6	2.02	5	1.2
7	2.22	6	1.19
8	2.21	7	1.15
9	2.25	8	1.13
10	2.25	9	1.13
11	2.25	10	1.12
12	2.29	11	1.12
15	2.22	12	1.1
20	2.22	15	1.07
25	2.22	20	1.01
30	2.23	25	0.99
40	2.51	30	0.97
50	2.51	40	0.94
60	2.51	50	0.94
70	2.51	60	0.88
80	2.55	70	0.83
100	2.63	90	0.8
150	2.815	140	0.79
200	2.91	190	0.67
300	3.37	290	0.62
420	3.68	410	0.503
600	3.81	590	0.44
780	4.1	770	0.389
1080	4.21	1070	0.31
1440	4.55	1430	0.25
1800	5.68	1790	0.24
2160	6.15	2150	0.18
2520	6.53	2510	0.17
2880	6.63	2870	0.17
		3410	0.11
		3830	0.067
		4130	0.06
		4490	0.01

FIGURE K-6G: PUMP TEST DATA DP18 (CONTINUED)

Step test data				
Mulder-92	Step1	Step2	Step3	Step4
Q (l/s) =	5.7	11.1	16.7	20
t(min)	s (m)	s (m)	s (m)	s (m)
	5.7	11.1	16.7	20
1	1.01	1.35	2.83	5.87
2	0.76	1.44	3.29	5.92
3	0.76	1.48	3.51	6.42
4	0.64	1.5	3.64	6.63
5	0.64	1.54	3.65	6.65
6	0.67	1.56	3.69	6.652
7	0.69	1.56	3.74	6.652
8	0.69	1.57	3.77	6.652
9	0.69	1.57	3.782	6.652
10	0.69	1.56	3.82	6.652
12	0.68	1.57	3.91	6.653
15	0.67	1.57	3.995	
20	0.67	1.58	4.03	
25	0.68	1.59	4.04	
30	0.69	1.635	4.04	
35	0.699	1.64	4.15	
40	0.73	1.652	4.22	
50	0.73	1.66	4.31	
60	0.73	1.71	4.44	
80	0.74	1.74	4.67	

FIGURE K-6H: PUMP TEST DATA DG110

Step test data			
MULDER-92	Step1	Step2	Step3
Q (l/s) =	4.3	9.4	19.1
t(min)	s (m)	s (m)	s (m)
	4.3	9.4	19.1
1	2.04	6.15	14.88
2	2.06	6.76	16.91
3	1.94	6.87	18.05
4	2.09	6.94	18.84
5	2.2	7.11	19.47
6	2.31	7.26	20.01
7	2.44	7.38	20.48
8	2.46	7.5	20.95
9	2.57	7.62	21.52
10	2.62	7.71	21.75
12	2.76	7.82	22.02
15	2.93	8.03	22.62
20	2.93	8.29	23.68
25	3.41	8.67	24.6
30	3.56	8.99	25.4
35	3.73	9.26	26.13
40	3.86	9.51	26.86
50	4.07	9.76	28.02
60	4.3	10.59	29.16
80	4.6	11.22	31.06
100	4.81	11.72	32.92

FIGURE K-6I: PUMP TEST DATA DP28

Pumping test data			
Date of test	Mulder-92		
Abstr. Rate Q (l/s)	21.1		
Time (min)	Drawdown (m)	t'	res. s (m)
1	2.94	0.01	11.88
2	3.72	1	5.46
3	4.21	2	5
4	4.75	3	4.77
5	5.12	4	4.7
6	5.38	5	4.68
7	5.57	6	4.64
8	5.71	7	4.59
9	5.82	8	4.49
10	5.97	9	4.44
11		10	4.41
12	6.16	11	
15	6.41	12	4.35
20	6.7	15	4.32
25	6.87	20	4.21
30	7	25	4.09
40	7.19	30	4.02
50	7.36	40	3.9
60	7.46	50	3.84
70	7.55	60	3.76
80	7.61	70	3.71
100	7.74	80	3.62
150	7.97	100	3.49
200	8.12	150	3.32
300	8.4	200	3.14
420	8.8	300	2.98
600	9.14	420	2.46
780	9.37		
1080	9.86		
1440	9.9		
1800	10.38		
2160	10.59		
2520	10.97		
2880	10.98		
3240	11.44		
3600	11.56		
3960	11.75		
4320	11.88		

FIGURE K-6J: PUMP TEST DATA DP28 (CONTINUED)

Step test data					
Mulder-92	Step1	Step2	Step3	Step4	Step5
Q (l/s) =	4.4	9.4	16.8	24.9	27.7
t(min)	s (m)	s (m)	s (m)	s (m)	s (m)
	4.4	9.4	16.8	24.9	27.7
1	0.84	1.79	3.28	7.62	11.41
2	0.76	1.84	3.76	8.3	11.54
3	0.63	2.03	3.96	8.45	11.64
4	0.7	2.11	4.15	8.71	11.71
5	0.73	2.15	4.27	8.86	11.78
6	0.78	2.2	4.4	8.98	11.8
7	0.785	2.24	4.48	9.08	11.88
8	0.79	2.26	4.55	9.17	11.91
9	0.82	2.28	4.72	9.23	11.96
10	0.83	2.29	4.66	9.28	11.99
12	0.86	2.34	4.72	9.38	12.03
15	0.89	2.36	4.82	9.48	12.11
20	0.94	2.41	4.9	9.61	12.2
25	0.98	2.44	4.96	9.66	12.32
30	0.98	2.45	5	9.72	12.39
35	1.01	2.49	5.06	9.8	12.44
40	1.03	2.5	5.09	9.83	12.445
50	1.05	2.54	5.14	9.85	12.48
60	1.06	2.56	5.19	9.93	12.53
80	1.1	2.6	5.26	10.04	12.62
100	1.1	2.63	5.3	10.12	12.72

FIGURE K-6K: PUMP TEST DATA DP15

Pumping test data			
Date of test	Mulder-92		
Abstr. Rate Q (l/s)	5.7		
Time (min)	Drawdown (m)	t'	res. s (m)
1	2.07	0.01	6.1
2	3.28	1	1.08
3	3.2	2	0.74
4	3.21	3	0.7
5	3.18	4	0.85
6	3.18	5	0.94
7	3.18	6	1.14
8	3.18	7	1.13
9	3.2	8	1.11
10	3.24	9	1.08
11	3.29	10	1.08
12	3.29	11	1.06
15	3.35	12	1.09
20	3.48	15	1.03
25	3.55	20	0.98
30	3.61	25	0.93
40	3.72	30	0.85
50	3.77	40	0.8
60	3.9	50	0.7
70	3.9	60	0.61
80	3.95	70	0.54
100	4.07	80	0.49
150	4.08	100	0.38
200	4.17	150	0.25
300	4.31	200	0.14
420	4.8	300	0
600	5.19		
780	5.38		
1080	5.46		
1440	5.52		
1800	5.75		
2160	5.97		
2520	6.19		
2880	6.19		
3240	5.91		
3600	6.02		
3960	6.03		
4320	6.1		

FIGURE K-6K: PUMP TEST DATA DP15 (CONTINUED)

Step test data				
Mulder-92	Step1	Step2	Step3	Step4
Q (l/s) =	1.7	3.6	6.9	9.4
t(min)	s (m)	s (m)	s (m)	s (m)
	1.7	3.6	6.9	9.4
1	0.47	0.58	2.17	6.72
2	0.47	1.37	5.24	14.12
3	0.47	1.66	6.44	15.65
4	0.39	1.82	6.88	15.64
5	0.39	1.84	6.88	15.64
6	0.39	1.86	6.35	15.63
7	0.47	1.86	6.32	15.63
8	0.49	1.87	6.25	15.63
9	0.5	1.91		
10	0.51	1.94	6.2	
12	0.51	1.94	6.2	
15	0.53	1.94	6.2	
20	0.53	1.95	6.24	
25	0.55	2.02	6.36	
30	0.55	2.05	6.39	
35	0.55	2.07	6.45	
40	0.58	2.1	6.54	
50	0.58	2.13	6.6	
60	0.58	2.14	6.7	

FIGURE K-6L: PUMP TEST DATA DP29

Step test data			
Mulder-92	Step1	Step2	Step3
Q (l/s) =	6.1	8.3	11.1
t(min)	s (m)	s (m)	s (m)
	6.1	8.3	11.1
1	5.93	13.71	23.84
2	7.11	15.06	25.08
3	7.64	16.24	25.97
4	8.08	16.94	26.8
5	8.53	17.66	27.42
6	8.78	18.12	28.01
7	9.09	18.52	28.49
8	9.3	18.84	28.89
9	9.44	19.1	29.33
10	9.6	19.39	29.6
12	9.83	19.81	30.36
15	10.13	20.33	31.38
20	10.44	20.82	32.35
25	10.74	21.12	33.52
30	10.97	21.3	33.44
35	11.18	21.44	34.45
40	11.28	21.59	36
50	11.43	21.97	38
60	11.46	21.89	
80	11.58	21.82	
100	11.63	21.82	

FIGURE K-6M: PUMP TEST DATA DP12

Step test data						
JEFF	Step1	Step2	Step3	Step4	Step5	Step6
Q (l/s) =	2.4	5.4	9.2	15.5	20.8	27.1
t(min)	s (m)	s (m)	s (m)	s (m)	s (m)	s (m)
	2.4	5.4	9.2	15.5	20.8	27.1
0.5	1.55	2.2	5.83	11.11	22.84	39.09
1	2.18	2.8	5.88	11.15	22.97	39.81
1.5	2.34	3.46	6.78	11.2	23.1	40.38
2	2.4	3.89	7.61	13.2	23.27	40.96
2.5	2.33	4.21	8.22	14.53	26.15	41.69
3	2.19	4.37	8.68	15.65	27.18	42.68
3.5	2.04	4.54	8.95	16.42	28.07	45.27
4	1.88	4.64	9.19	17.04	28.82	48
4.5	1.72	4.73	9.39	17.58	29.44	50.3
5	1.68	4.86	9.54	18.12	30.03	51.87
7	1.65	4.92	9.68	18.42	30.46	53.32
9	1.72	5.12	9.78	18.77	30.94	54.3
12	1.81	5.25	9.98	19.06	31.35	55.44
15	1.88	5.34	10.19	19.93	32.65	56.39
20	2	5.41	10.34	20.51	33.13	58
25	2.06	5.53	10.49	21.13	33.73	59.57
30	2.11	5.61	10.67	21.5	34.86	61.87
35	2.12	5.66	10.78	21.94	35.77	
40	2.13	5.71	10.87	22.26	36.85	
45	2.16	5.74	10.98	22.48	37.62	
50	2.17	5.77	11.07	22.65	38.25	
60	2.2	5.83	11.11	22.84	39.09	

APPENDIX K: WELLMAN (continue)

APPENDIX K-7
Go to Borehole 1 - 13 - WELLMAN

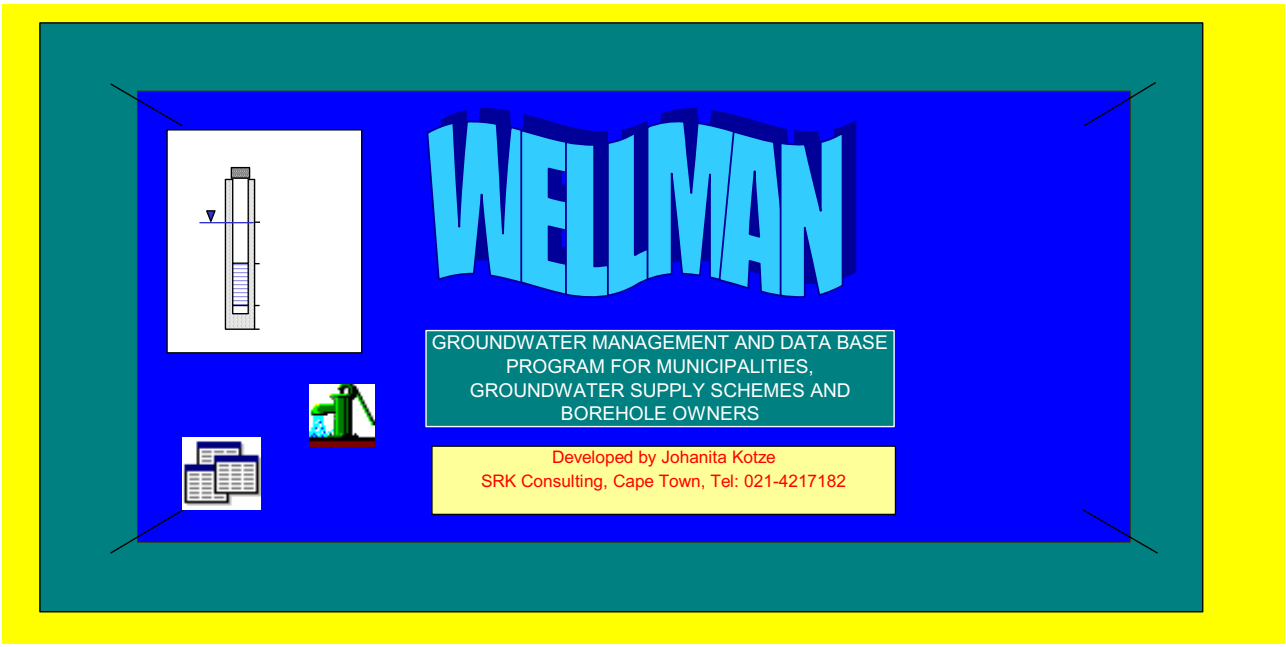

GO TO BH1 – SUMMARY OF ALL RELEVANT HYDROGEOLOGICAL INFORMATION – VG3

BH number	**VG3**	**Wellman Groundwater Management and Data base program**							
Wellfield	**Vermaaks**								
Municipality	**Overberg**	**Y**	**42820.8**	**Main water strike (m) =**	**190**	**Recommended Q (l/s) =**	**2.5**	**216**	m3/d
Owner	**DWAF**	**X**	**3715464.4**	**BH depth (m) =**	**206.7**	**Q (FC-Method)**	**4.5**	**389**	
Geological formation	**TMG - NAR**	**Altitude**	**497.3**	**Use of water**	**Domestic**	**Q (Theis-Method)**	**5.5**	**475**	m3/d
Topo map sheet #		**Drilled**	**15/4/89**	**Depth of pump instal**	**148**	**Q (Guess)**			
Screen Type	**PVC**	**IWL (m)**	**6.02**	**Blow Yield (l/s) =**	**12**	**Q (Equal Volume)**	**2.0**	**173**	m3/d
Screen Depth	**96.5 - 150**	**Diameter**	**208**	**Other water strikes (m)=**	**110, 174**	**KW of pump**			
Screen Depth	**150 - 206.7**	**Diameter**	**168**	**Pump**	**submersible**	**Max. Q of pump (l/s)**	**4.0**	**346**	m3/d

Other comments:
Borehole is situated in a closed boundary (Average distance = 1 km)

DATA | CHEM | EN_ISO | Geology | Pump test | Manage | Main

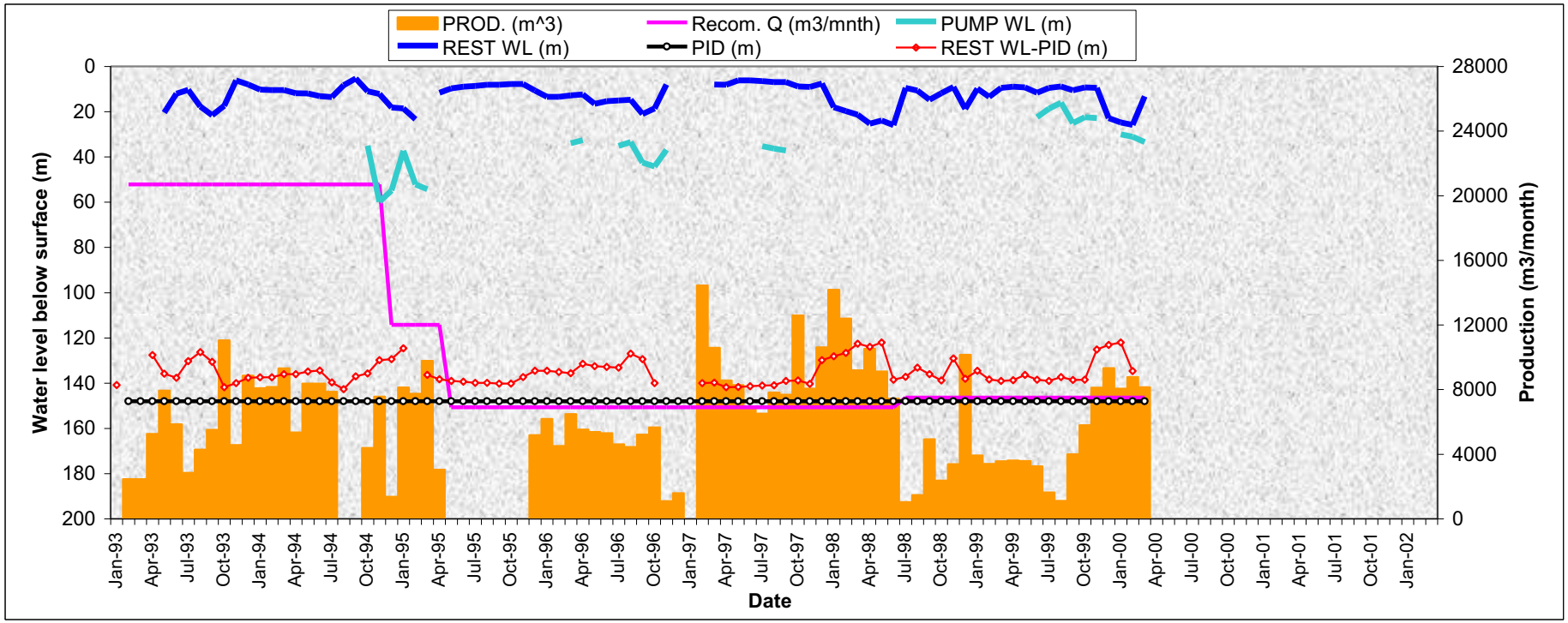

GO TO BH2 – SUMMARY OF ALL RELEVANT HYDROGEOLOGICAL INFORMATION – VR6

BH number	VR6	Wellman Groundwater Management and Data base program							
Wellfield	Vermaaks								
Municipality	Overberg	Y	42082.9	Main water strike (m) =	228	Recommended Q (l/s) =	2.5	216	m3/d
Owner	DWAF	X	3720431.7	BH depth (m) =	250	Q (FC-Method)	7.4	639	m3/d
Geological formation	TMG - PEN	Altitude	718.3	Use of water	Domestic	Q (Theis-Method)	7.6	657	m3/d
Topo map sheet #		Drilled	29/08/89	Depth of pump instal	165	Q (Guess)			
Screen Type	PVC	IWL (m)	34.64	Blow Yield (l/s) =	15	Q (Equal Volume)	2.7	230	m3/d
Screen Depth	108.7 - 230	Diameter	208	Other water strikes (m)=	none	KW of pump			
Screen Depth	230 - 250	Diameter	open	Pump	submersible	Max. Q of pump (l/s)	3.5	302	m3/d

Other comments:
Borehole is situated in a closed boundary (Average distance = 1 km)

DATA | CHEM | EN_ISO | Geology | Pump test | Manage | Main

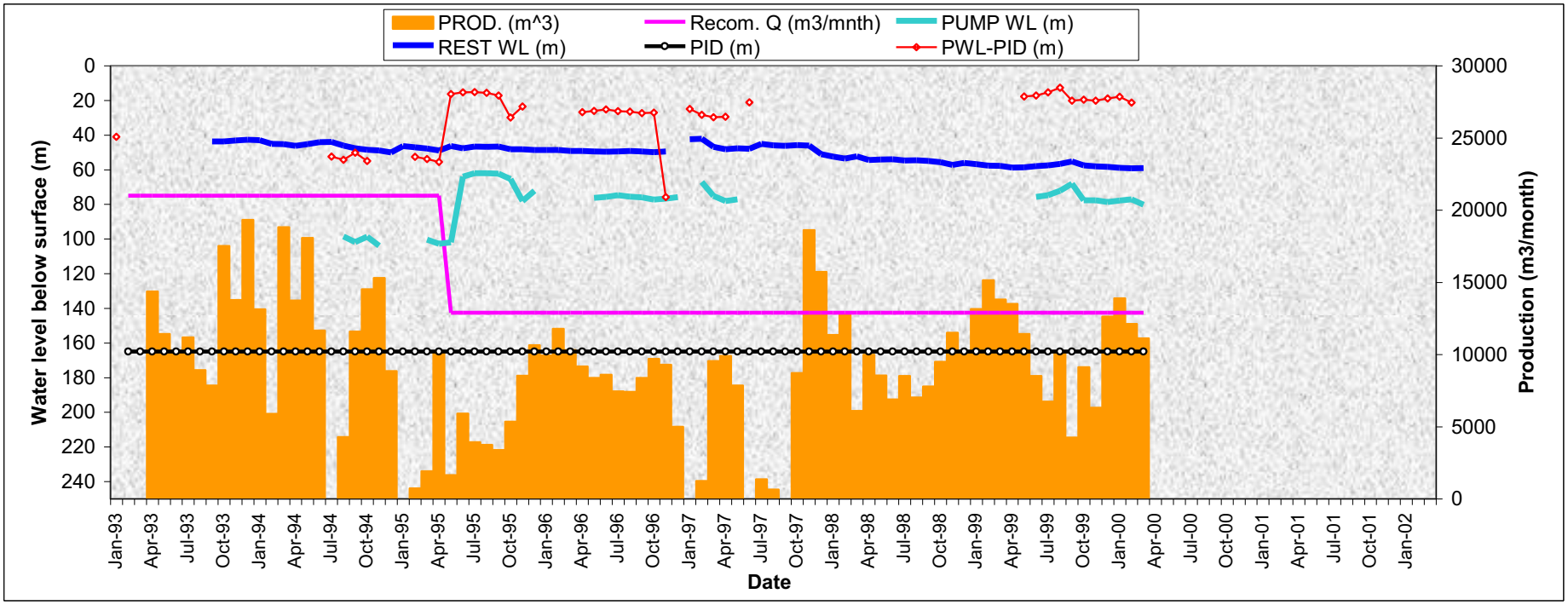

GO TO BH3 – SUMMARY OF ALL RELEVANT HYDROGEOLOGICAL INFORMATION – VR7

BH number	VR7	Wellman Groundwater Management and Data base program							
Wellfield	Vermaaks								
Municipality	Overberg	Y	41 648.0	Main water strike (m) =	129	Recommended Q (l/s) =	10.0	864	m3/d
Owner	DWAF	X	3720 760.9	BH depth (m) =	177	Q (FC-Method)	12.9	1115	
Geological formation	TMG - PEN	Altitude	748.9	Use of water	Domestic	Q (Theis-Method)	13.0	1123	m3/d
Topo map sheet #		Drilled	89/10/09	Depth of pump instal	150	Q (Guess)			
Screen Type	PVC	IWL (m)	63.3	Blow Yield (l/s) =	15	Q (Equal Volume)	6.3	546	m3/d
Screen Depth	53 - 152	Diameter	208	Other water strikes (m)=	78	KW of pump			
Screen Depth	152 - 177	Diameter	168	Pump	submersible	Max. Q of pump (l/s)	15.0	1296	m3/d

Other comments:
Borehole is situated in a closed boundary (Average distance = 1 km)

DATA | CHEM | EN_ISO | Geology | Pump test | Manage | Main

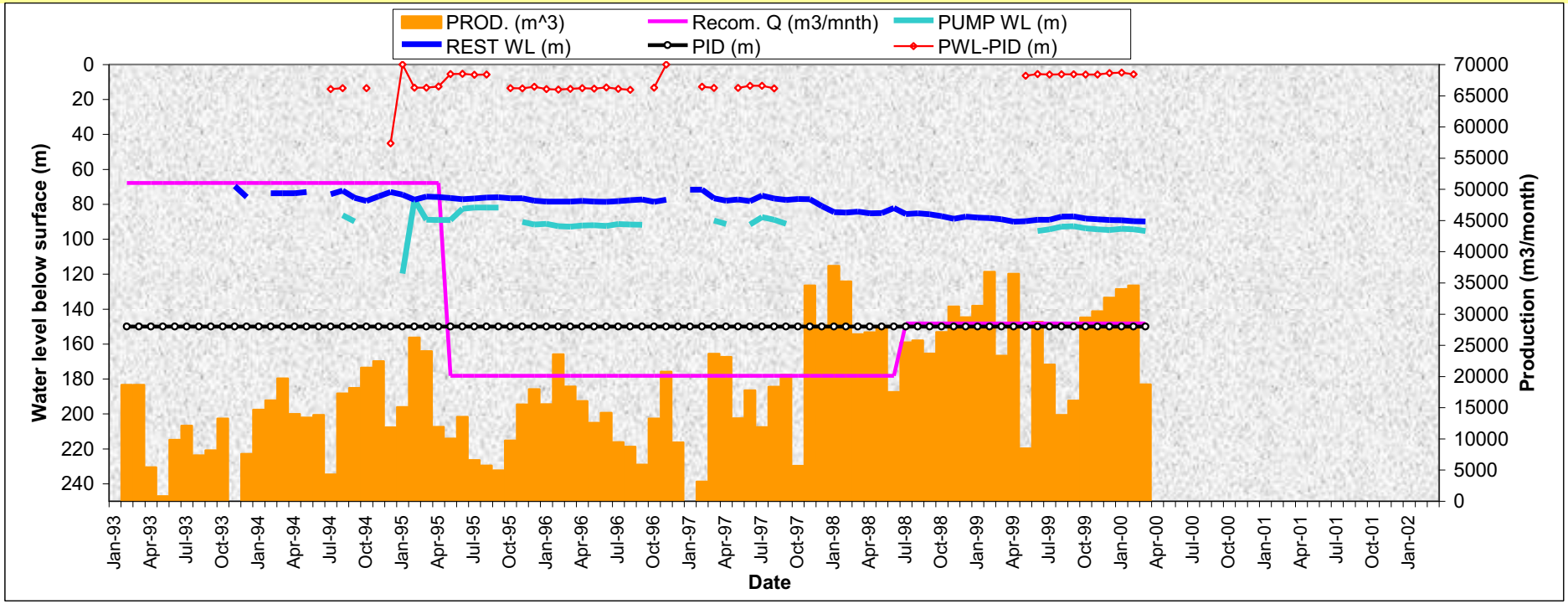

GO TO BH4 – SUMMARY OF ALL RELEVANT HYDROGEOLOGICAL INFORMATION – VR8

BH number	VR8	Wellman Groundwater Management and Data base program							
Wellfield	Vermaaks								
Municipality	Overberg	Y	41 351.5	Main water strike (m) =	234	Recommended Q (l/s) =	3.0	259	m3/d
Owner	DWAF	X	3721 065.7	BH depth (m) =	251.3	Q (FC-Method)			
Geological formation	TMG - PEN	Altitude	786.7	Use of water	Domestic	Q (Theis-Method)			
Topo map sheet #		Drilled	31/07/1989	Depth of pump instal	163	Q (Guess)			
Screen Type	PVC	IWL (m)	100.5	Blow Yield (l/s) =	13	Q (Equal Volume)	2.0	175	m3/d
Screen Depth	89.9 - 164.6	Diameter	208	Other water strikes (m)=	113, 156, 170	KW of pump			
Screen Depth	164.6 - 251.3	Diameter	165	Pump	submersible	Max. Q of pump (l/s)	5.0	432	m3/d

Other comments:
Borehole is situated in a closed boundary (Average distance = 1 km)

DATA | CHEM | EN_ISO | Geology | Pump test | Manage | Main

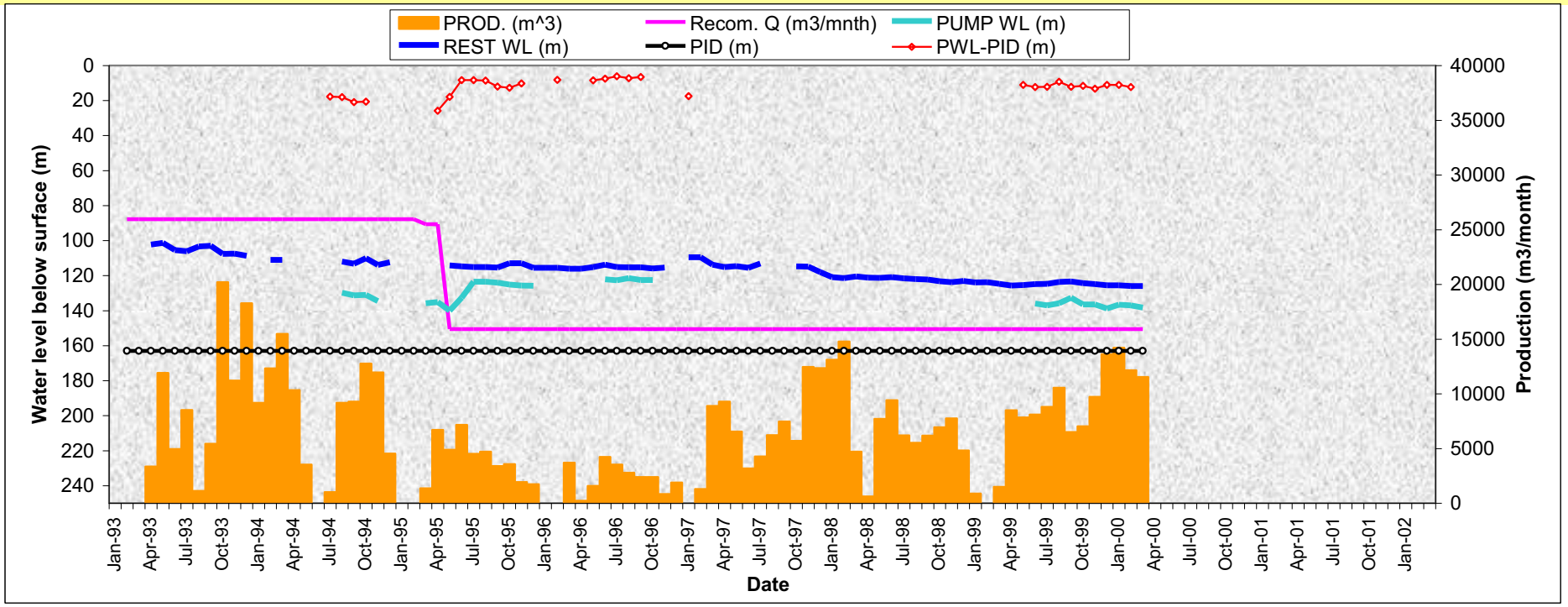

GO TO BH5 – SUMMARY OF ALL RELEVANT HYDROGEOLOGICAL INFORMATION – VR11

BH number	VR11	Wellman Groundwater Management and Data base program							
Wellfield	Vermaaks								
Municipality	Overberg	Y	40 941.7	Main water strike (m) =	200	Recommended Q (l/s) =	3.0	259	m3/d
Owner	DWAF	X	3 721 304.8	BH depth (m) =	224.5	Q (FC-Method)	9.9	855	m3/d
Geological formation	TMG - PEN	Altitude	812.2	Use of water	Domestic	Q (Theis-Method)	12.5	1080	m3/d
Topo map sheet #		Drilled	15/10/1991	Depth of pump instal	180	Q (Guess)			
Screen Type	PVC	IWL (m)	125.5	Blow Yield (l/s) =	20	Q (Equal Volume)	2.3	202	m3/d
Screen Depth	185 - 224.5	Diameter	208	Other water strikes (m)=	139, 183	KW of pump			
Screen Depth		Diameter		Pump	submersible	Max. Q of pump (l/s)	4.0	346	m3/d

Other comments:
Borehole is situated in a closed boundary (Average distance = 1 km)

DATA | CHEM | EN_ISO | Geology | Pump test | Manage | Main

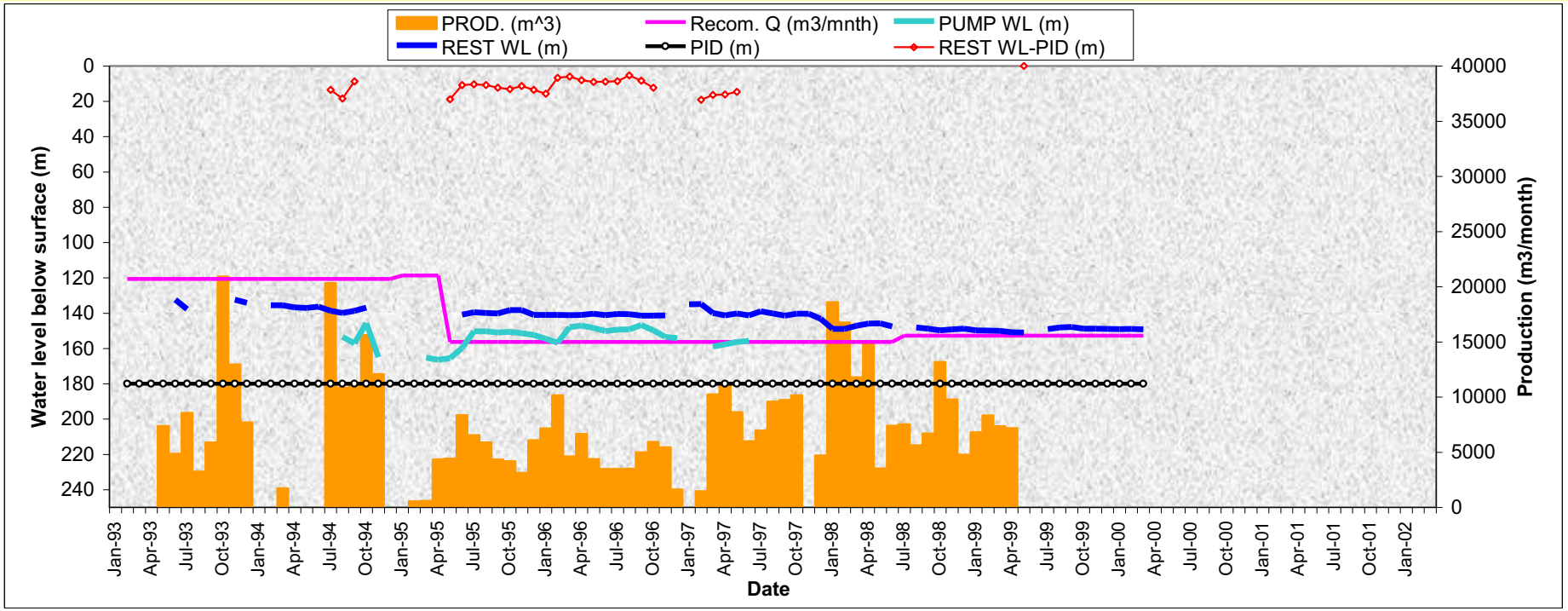

GO TO BH6 – SUMMARY OF ALL RELEVANT HYDROGEOLOGICAL INFORMATION – DP10

BH number	DP10	Wellman Groundwater Management and Data base program							
Wellfield	Varkieskloof								
Municipality	Overberg	Y	50 790.8	Main water strike (m) =	183	Recommended Q (l/s) =	2	172.8	m3/d
Owner	DWAF	X	3716158.5	BH depth (m) =	210	Q (FC-Method)			
Geological formation	TMG - Nardouw	Altitude	456.5	Use of water	Domestic	Q (Theis-Method)			
Topo map sheet #		Drilled	24/02/1992	Depth of pump instal	180	Q (Guess)			
Screen Type	PVC	IWL (m)	114.07	Blow Yield (l/s) =	7.5	Q (Equal Volume)	0.4	34	m3/d
Screen Depth	73 - 210	Diameter	208	Other water strikes (m)=		KW of pump			
Screen Depth		Diameter		Pump	submersible	Max. Q of pump (l/s)	2.5	216	m3/d

Other comments:
Borehole is situated in a closed boundary (Average distance = 1 km)

DATA | CHEM | EN_ISO | Geology | Pump test | Manage | Main

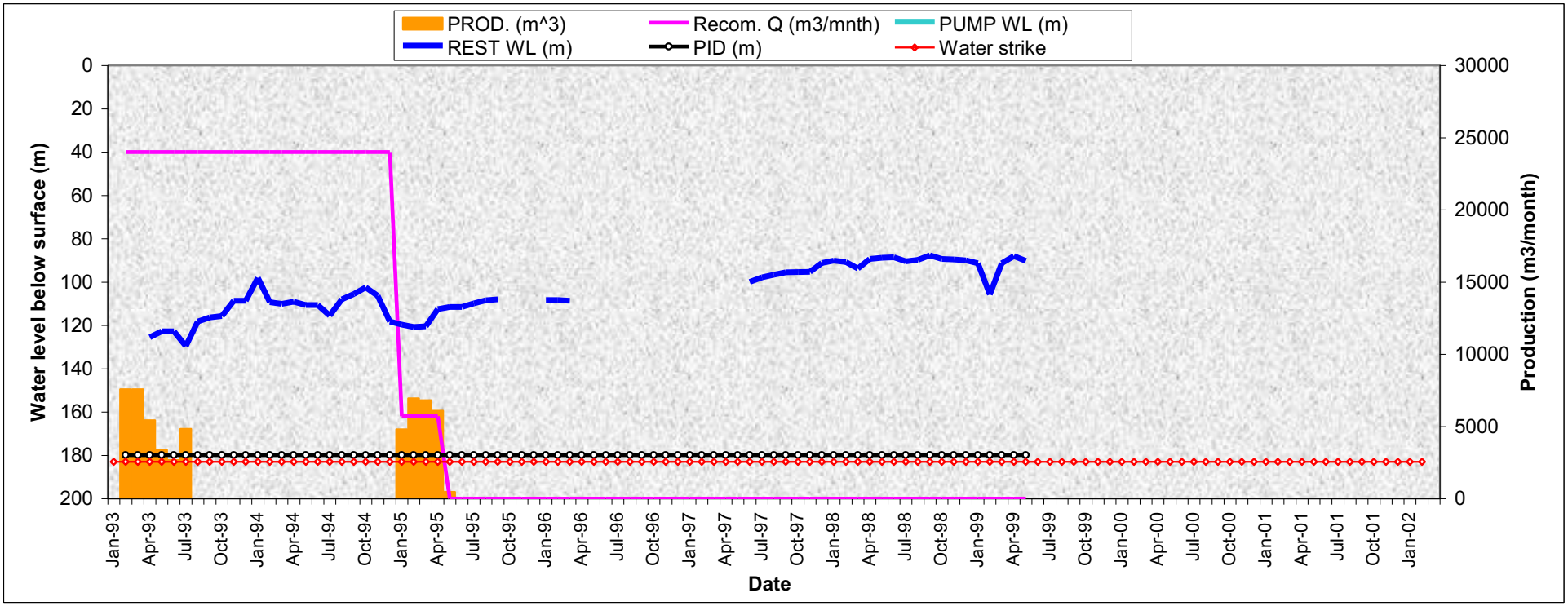

GO TO BH7 – SUMMARY OF ALL RELEVANT HYDROGEOLOGICAL INFORMATION – DP12

BH number	DP12	Wellman Groundwater Management and Data base program							
Wellfield	Varkieskloof								
Municipality	Overberg	Y	50 673.2	Main water strike (m) =	186	Recommended Q (l/s) =	3	259.2	m3/d
Owner	DWAF	X	3716324.5	BH depth (m) =	192	Q (FC-Method)			
Geological formation	TMG - Nardouw	Altitude	468.5	Use of water	Domestic	Q (Theis-Method)			
Topo map sheet #		Drilled	23/04/91	Depth of pump instal	180	Q (Guess)			
Screen Type	PVC	IWL (m)	126.4	Blow Yield (l/s) =	20	Q (Equal Volume)	1.9	163	m3/d
Screen Depth	66 - 192	Diameter	208	Other water strikes (m)=		KW of pump			
Screen Depth		Diameter		Pump	submersible	Max. Q of pump (l/s)	4	346	m3/d

Other comments:
Borehole is situated in a closed boundary (Average distance = 1 km)

DATA | CHEM | EN_ISO | Geology | Pump test | Manage | Main

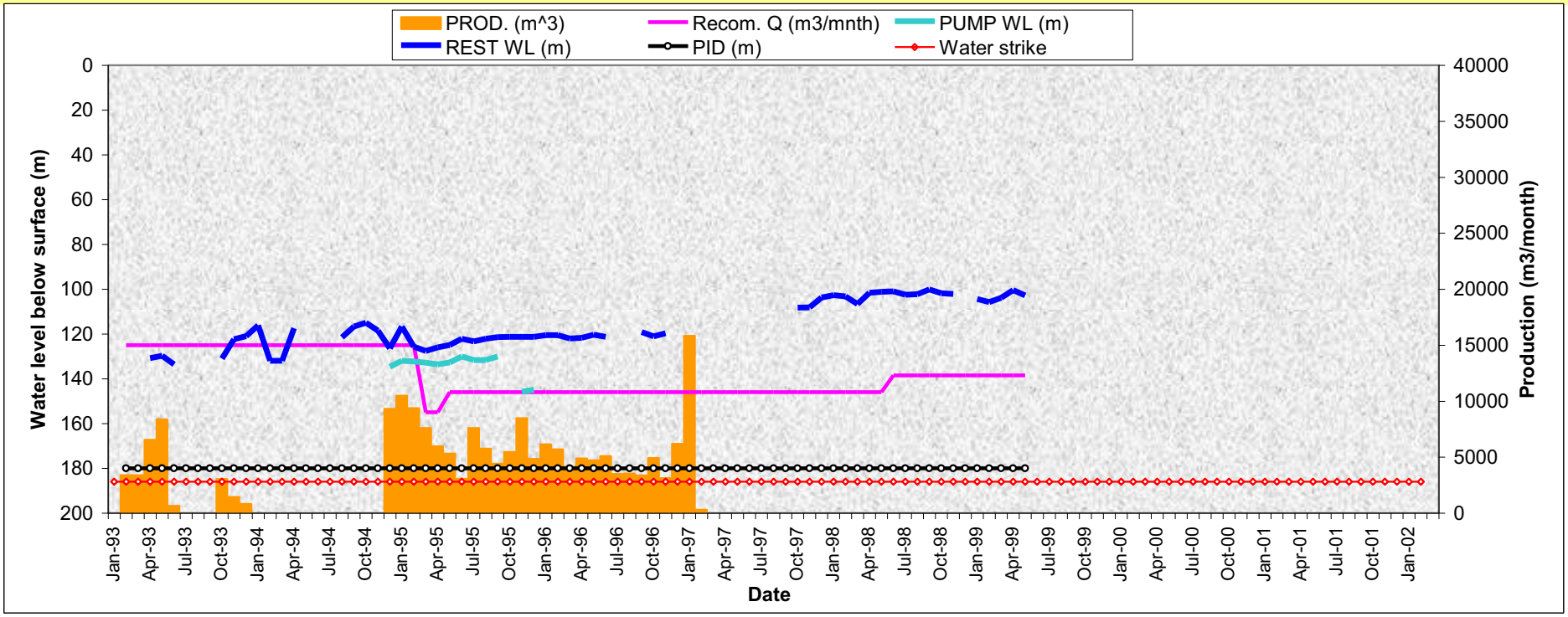

GO TO BH8 – SUMMARY OF ALL RELEVANT HYDROGEOLOGICAL INFORMATION – DP29

BH number	DP29	Wellman Groundwater Management and Data base program							
Wellfield	Varkieskloof								
Municipality	Overberg	Y	50701.4	Main water strike (m) =	185	Recommended Q (l/s) =	3	259.2	m3/d
Owner	DWAF	X	3716277.4	BH depth (m) =	240	Q (FC-Method)			
Geological formation	TMG - Nardouw	Altitude	463.1	Use of water	Domestic	Q (Theis-Method)			
Topo map sheet #		Drilled	91/03/06	Depth of pump instal	180	Q (Guess)			
Screen Type	PVC	IWL (m)	120.6	Blow Yield (l/s) =	4	Q (Equal Volume)	2.6	222	m3/d
Screen Depth	unknown	Diameter	208	Other water strikes (m)=	160	KW of pump			
Screen Depth		Diameter		Pump	submersible	Max. Q of pump (l/s)	6	518	m3/d

Other comments:
Borehole is situated in a closed boundary (Average distance = 1 km)

DATA | CHEM | EN_ISO | Geology | Pump test | Manage | Main

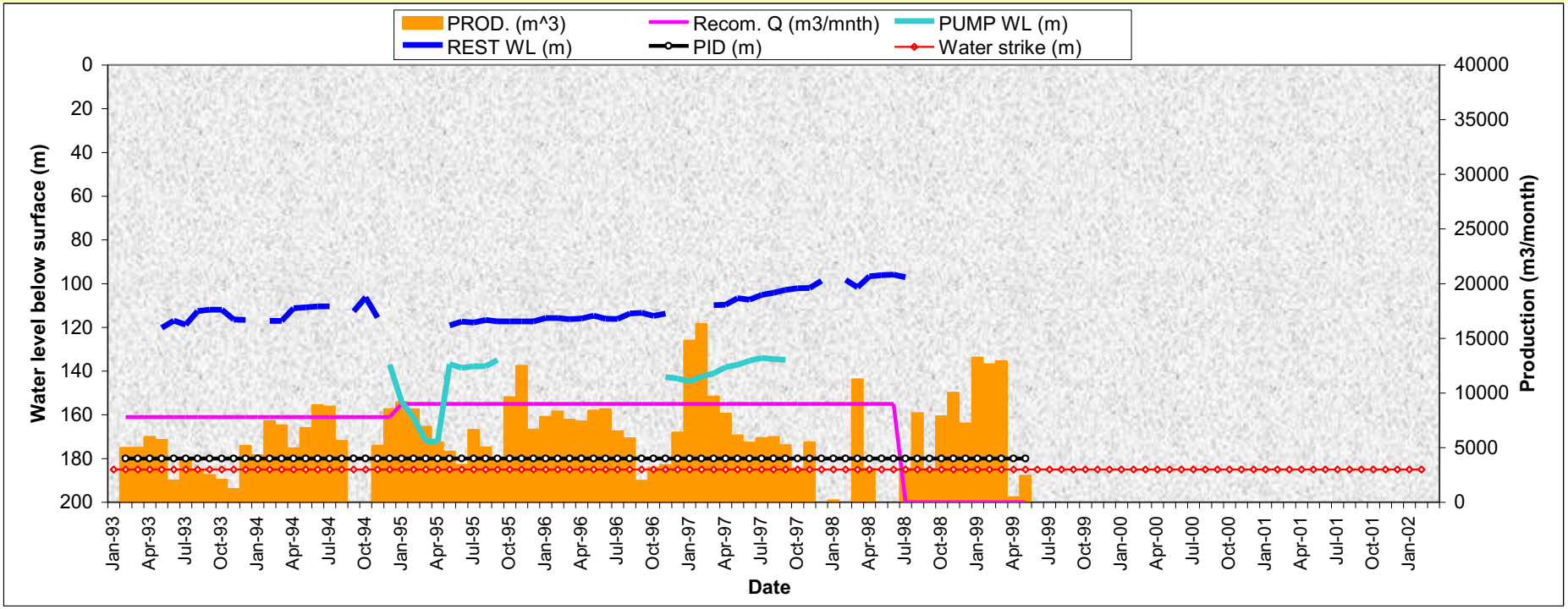

GO TO BH9 – SUMMARY OF ALL RELEVANT HYDROGEOLOGICAL INFORMATION – DP15

BH number	DP15	Wellman Groundwater Management and Data base program							
Wellfield	Bokkraal								
Municipality	Overberg	Y	50468.5	Main water strike (m) =	187	Recommended Q (l/s) =	5.0	432	m3/d
Owner	DWAF	X	3717093.2	BH depth (m) =	224.5	Q (FC-Method)	6.7	579	m3/d
Geological formation	TMG - Nardouw	Altitude	451.1	Use of water	Domestic	Q (Theis-Method)	6.7	579	m3/d
Topo map sheet #		Drilled	18/04/91	Depth of pump instal	180	Q (Guess)			
Screen Type	PVC	IWL (m)	103.8	Blow Yield (l/s) =	20	Q (Equal Volume)	1.9	165	m3/d
Screen Depth	50 - 207	Diameter	208	Other water strikes (m)=	139, 183	KW of pump			
Screen Depth		Diameter		Pump	submersible	Max. Q of pump (l/s)	6.0	518	m3/d

Other comments:
Borehole is situated in a closed boundary (Average distance = 1 km)

DATA | CHEM | EN_ISO | Geology | Pump test | Manage | Main

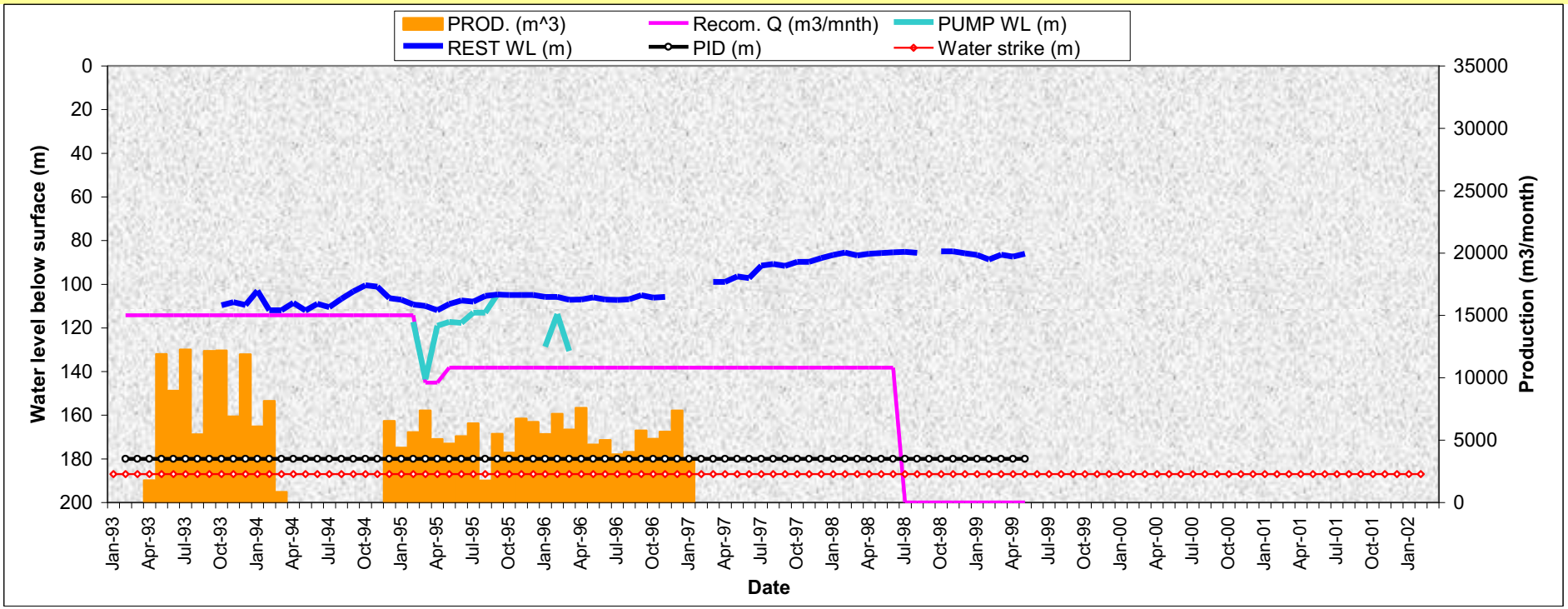

GO TO BH10 – SUMMARY OF ALL RELEVANT HYDROGEOLOGICAL INFORMATION – DP25

BH number	DP25	Wellman Groundwater Management and Data base program							
Wellfield	BOKKRAAL								
Municipality	Overberg	Y	50480.9	Main water strike (m) =	200	Recommended Q (l/s) =	3	259.2	m3/d
Owner	DWAF	X	3717098.7	BH depth (m) =	203	Q (FC-Method)			
Geological formation	TMG - NAR	Altitude	449.1	Use of water	Domestic	Q (Theis-Method)			
Topo map sheet #		Drilled	90/01/11	Depth of pump instal	170	Q (Guess)			
Screen Type	PVC	IWL (m)	104.9	Blow Yield (l/s) =	20	Q (Equal Volume)	1.7	147	m3/d
Screen Depth	9 - 203	Diameter	208	Other water strikes (m)=	109, 166	KW of pump			
Screen Depth		Diameter		Pump	submersible	Max. Q of pump (l/s)	6	518	m3/d

Other comments:
Borehole is situated in a closed boundary (Average distance = 1 km)

DATA | CHEM | EN_ISO | Geology | Pump test | Manage | Main

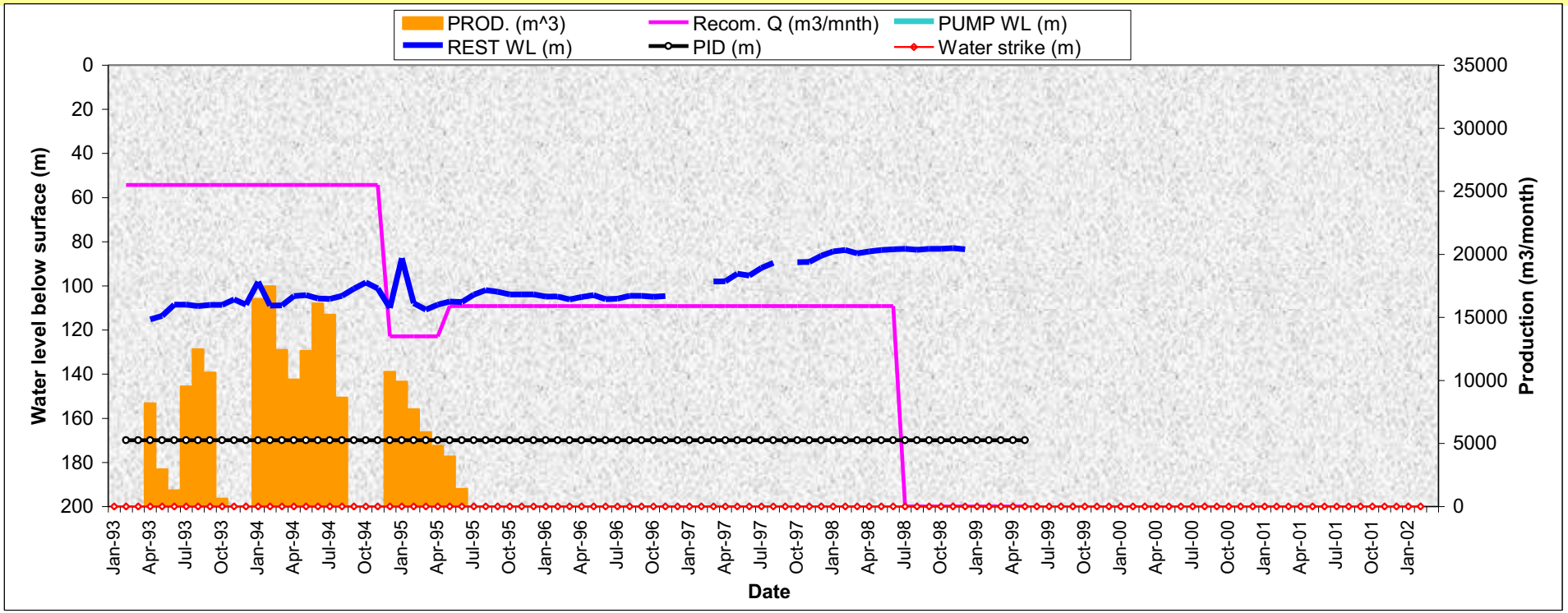

GO TO BH11 – SUMMARY OF ALL RELEVANT HYDROGEOLOGICAL INFORMATION – DP28

BH number	DP28	Wellman Groundwater Management and Data base program							
Wellfield	Bokkraal								
Municipality	Overberg	Y	50426.1	Main water strike (m) =	195	Recommended Q (l/s) =	5.0	432	m3/d
Owner	DWAF	X	3717072.8	BH depth (m) =	246	Q (FC-Method)	16.7	1443	m3/d
Geological formation	TMG - Nardouw	Altitude	459.1	Use of water	Domestic	Q (Theis-Method)	21.0	1814	m3/d
Topo map sheet #		Drilled	91/08/03	Depth of pump instal	170	Q (Guess)			
Screen Type	PVC	IWL (m)	117.8	Blow Yield (l/s) =	21	Q (Equal Volume)	3.8	326	m3/d
Screen Depth	121 - 170	Diameter	208	Other water strikes (m)=	122, 151, 210	KW of pump			
Screen Depth	170 - 246	Diameter	open	Pump	submersible	Max. Q of pump (l/s)	9.0	778	m3/d

Other comments:
Borehole is situated in a closed boundary (Average distance = 1 km)

DATA | CHEM | EN_ISO | Geology | Pump test | Manage | Main

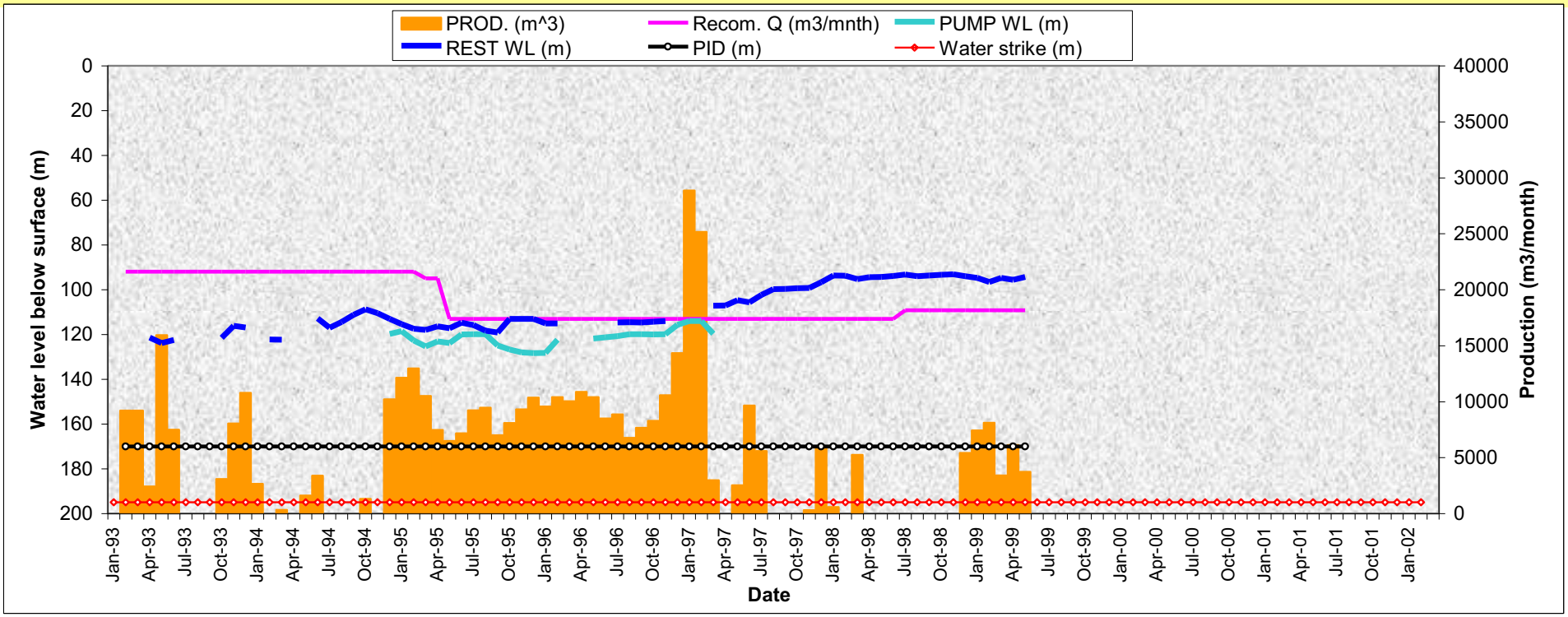

GO TO BH12 – SUMMARY OF ALL RELEVANT HYDROGEOLOGICAL INFORMATION – DG110

BH number	**DG110**	**Wellman Groundwater Management and Data base program**							
Wellfield	**Droëkloof**								
Municipality	**Overberg**	**Y**	**49 135.5**	**Main water strike (m) =**	**200**	**Recommended Q (l/s) =**	**2**	**172.8**	m3/d
Owner	**DWAF**	**X**	**3715403.7**	**BH depth (m) =**	**212**	**Q (FC-Method)**			
Geological formation	**TMG - Nardouw**	**Altitude**	**488.5**	**Use of water**	**Domestic**	**Q (Theis-Method)**			
Topo map sheet #		**Drilled**	**90/02/11**	**Depth of pump instal**	**200**	**Q (Guess)**			
Screen Type	**PVC**	**IWL (m)**	**110.6**	**Blow Yield (l/s) =**	**10**	**Q (Equal Volume)**	**1.6**	**134**	m3/d
Screen Depth	**92 - 212**	**Diameter**	**208**	**Other water strikes (m)=**	**114, 137**	**KW of pump**			
Screen Depth		**Diameter**		**Pump**	**submersible**	**Max. Q of pump (l/s)**	**2.5**	**216**	m3/d

Other comments:
Borehole is situated in a closed boundary (Average distance = 1 km)

DATA | CHEM | EN_ISO | Geology | Pump test | Manage | Main

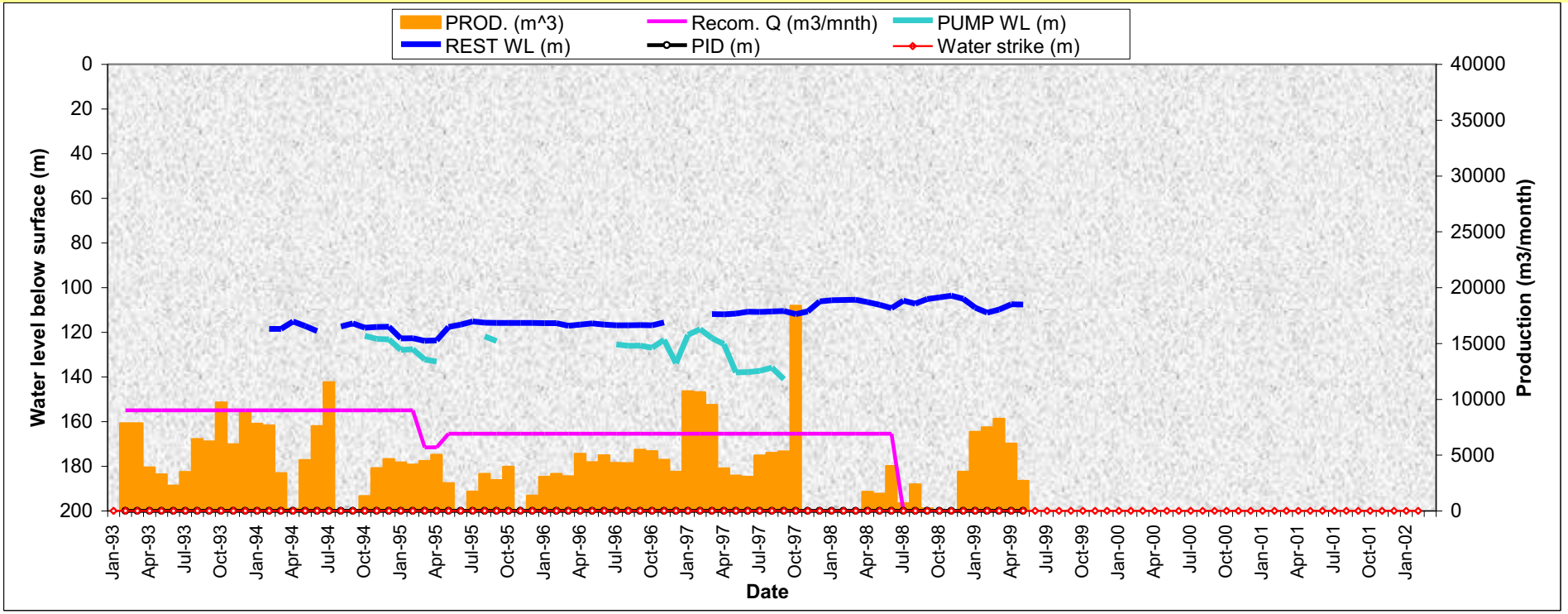

GO TO BH13 – SUMMARY OF ALL RELEVANT HYDROGEOLOGICAL INFORMATION – DP18

BH number	**DP18**	**Wellman Groundwater Management and Data base program**							
Wellfield	**Olifants**								
Municipality	**Overberg**	**Y**	**49 135.5**	**Main water strike (m) =**	**9**	**Recommended Q (l/s) =**	**6.0**	**518**	m3/d
Owner	**DWAF**	**X**	**3715403.7**	**BH depth (m) =**	**17**	**Q (FC-Method)**	**10.0**	**864**	
Geological formation	**Alluvium**	**Altitude**	**488.5**	**Use of water**	**Domestic**	**Q (Theis-Method)**	**10.6**	**916**	m3/d
Topo map sheet #		**Drilled**	**90/02/11**	**Depth of pump instal**	**14**	**Q (Guess)**			
Screen Type	**PVC**	**IWL (m)**	**3.6**	**Blow Yield (l/s) =**	**15**	**Q (Equal Volume)**	**5.4**	**463**	m3/d
Screen Depth	**2 - 9.4**	**Diameter**	**208**	**Other water strikes (m)=**		**KW of pump**			
Screen Depth		**Diameter**		**Pump**	**submersible**	**Max. Q of pump (l/s)**	**12.0**	**1037**	m3/d

Other comments:
Borehole is situated in a closed boundary (Average distance = 1 km)

DATA | CHEM | EN_ISO | Geology | Pump test | Manage | Main

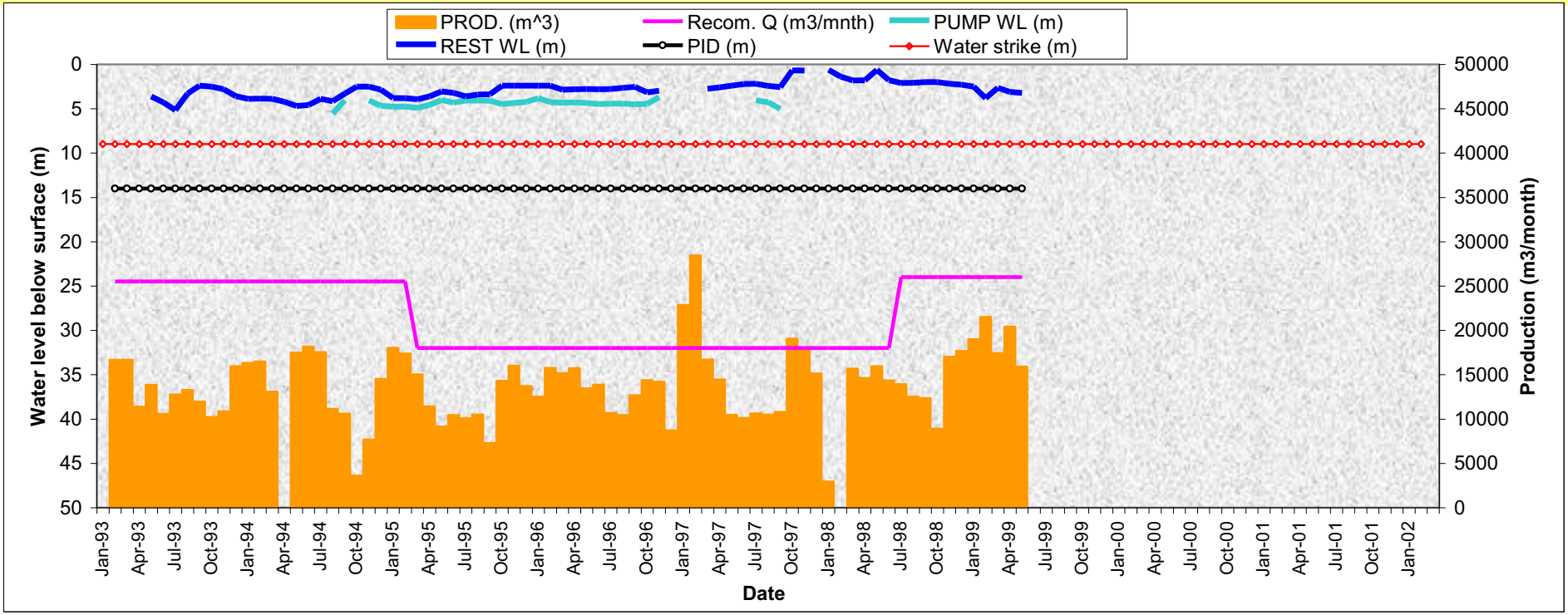

APPENDIX L: RECOMMENDATIONS

The main recommendations following from this research are:

In order to manage or develop any part of the TMG Super Aquifer a holistic view of all components of the conceptual hydrogeological model and their interaction needs to be understood. The following aspects need to be considered in order to improve management of TMG Aquifers:

1. The TMG Super Aquifer needs to be divided into hydrogeological compartments, in terms of the following:

   - Remote sensing and satellite lineament analysis, together with geological interpretation, is required to define the aquifer geometry and to define permeable aquizones, linking different lithological units.
   - The lithology of the host aquifer, i.e. Nardouw versus Peninsula Aquifer.
   - Definition of the conceptual hydrogeological model for each section of the TMG Super Aquifer.
   - Based on the conceptual hydrogeological model for each section of the Super Aquifer, a preliminary water balance calculation needs to be carried out. This requires that recharge and outflows (abstraction and springflow) for each section of the TMG Super Aquifer be determined.

2. The impact of abstraction on baseflow in streams and on vegetation needs to be addressed. Abstraction will eventually impact spring flow and the minimum spring flow requirement that will limit impact on the environment needs to be defined.

3. It must be anticipated that with the growth in water demand, groundwater abstraction from the TMG Aquifers in the Western Cape will become increasingly important. A monitoring borehole network should be put in place in each of the sections of the TMG Super Aquifer to collect information to improve our understanding of the dynamics of the system. It is proposed that such monitoring networks include the following:

   - Network of monitoring boreholes sited on permeable structures and outside of these zones as well, identified by remote sensing and lineament mapping across the aquifer under consideration, to clarify all aspects of the conceptual model.
   - Monthly water level measurements at monitoring boreholes.
   - Environmental isotope and hydrochemical sampling to be carried out on at least an annual basis.

- Adequate distribution of rainfall gauges.
- Sampling of rainwater for Cl and $\delta^{18}O$.
- Determine recharge from relationship of Cl in groundwater and rainwater and spring water and $^{14}C/^{3}C$ mean residence times.
- Carry out a spring survey and characterise the springs in the study area.
- Capture all the information in a database such as Wellman.
- Conduct pumping tests and determine the aquifer parameters.

4. During development of a wellfield the following needs to be considered:

- Use remote sensing and satellite lineament mapping to site boreholes.
- Nardouw Aquifers at lower altitudes in the absence of permeable connections to the recharge zones in the mountains can pose all sorts of management problems, such as iron-bacteriological clogging of borehole screens and should be avoided.
- Identify potential highly permeable aquizones, connected to the Nardouw Aquifer at lower altitudes with the recharge areas.
- Characterise fracture styles, geometry and density, providing pathways for recharged groundwater in the mountains to flow in folded bedding planes to lower elevations in aquizones.
- Determine from first principles the radius of influence for boreholes.
- Avoid siting of boreholes upstream of the C/S Aquitard and rather target permeable aquizones at lower altitudes.
- Establish a good spring flow record, before abstraction commences.
- Carry out pump testing and apply comprehensive aquifer testing analysis techniques in conjunction with a water balance to determine the sustainable yield of boreholes and wellfields.
- Use hydrochemistry and environmental isotopes in conjunction with satellite lineament mapping to characterise groundwater flow paths.
- Characterise environmental concerns in the study area and try to minimise negative impacts by selecting better pumping targets, based on the conceptual hydrogeological model.

5. Sophisticated methods of analysis must be applied to the interpretation of field data and long-term monitoring data to establish the long-term yield of the aquifer, rather than the capacity of the borehole.

6. An exploration drilling program addressing the following aspects should be developed:

- Thickness of Cretaceous sediments.
- Water levels in the Swartberg and Outeniqua Mountains.
- Monitoring boreholes in the Peninsula Aquifers of the Kammanassie, Swartberg, Rooiberg and Outeniqua Mountains, to establish flow inter-relationships between the local catchments.

7. Permeability testing of boreholes. A core drilled borehole is planned to a depth of approximately 500 m in the project area. Due to the high cost of such a borehole it is recommended that as much quality hydrogeological information as possible is gathered from this borehole.

- Determination of the vertical hydraulic conductivity profile using packers and constant head testing is an excellent method. In a diamond drill hole it is often convenient and quick to use wireline packers, which enable testing without withdrawing the drill string. The alternative is to complete the borehole and conduct double packer testing at selected intervals.
- In the latter case downhole geophysical logging using a caliper probe, natural gamma, gamma-gamma and temperature normally precede packer testing to enable structural and flow zones to be identified and evaluate packer seating conditions. Where wireline packers are used, geophysical logging normally takes place once the drilling and packer testing is completed.

8. Detailed and careful sampling for full range of isotopes.

9. Borehole logging

The following should be carried out:

- Caliper – for borehole profile, fractures (not always with core drilling), washouts and poor seating positions.
- Natural Gamma – for clay content or radioactive minerals and lithological changes.
- Gamma-gamma – for bulk rock density, fracture zones, lithological changes.
- Temperature – for determination of flow zones and geothermal gradient.

9. Remote sensing

- In recent work by Umvoto Africa in the CAGE project area near Citrusdal more advanced filtering tools were used to delineate recharge zones. The methodology

involved comparison of winter and summer Landsat TM images, whereby changes in vegetation over the seasons reflect potential seepage zones. Further, statistical tools were applied to filter out fractures of a certain orientation, whereafter the number of fractures in a particular fracture set were counted and the fracture spatial densities calculated in order to determine the scaling effects on hydraulic conductivity. This approach seems to be very useful and should be considered in future research extensions in the Klein Karoo area.

- Further remote sensing work should include statistical modelling of the fracture system, e.g. polygonisation and discretisation, using different filtering techniques. Numerical flow simulation is also required in order to identify different fracture clusters, density of fracture clusters and inter-connecting fracture clusters in order to determine scaling effects on hydraulic conductivity.

10. Trace elements

- It is recommended that further trace element sampling be carried out. In particular, the dissolution of feldspars and associated trace elements, e.g. Ba, Sr and Al needs to be investigated further. The low EC and TDS values of groundwater in the TMG Aquifers makes trace elements an important tool in understanding the dissolution chemistry and flow paths of groundwater in the TMG Aquifers.

11. Iron bacteria problem

- The management of iron-bacteriological clogging of borehole screens and fractures in boreholes requires expensive borehole construction and borehole rehabilitation programs. These conditions should be avoided wherever possible. Warning signs for potential iron-bacteriological clogging in the Klein Karoo are the following:
- Presence of the following trace elements in groundwater: Ni, Cu, Zn and Co, mostly due to dissolution of minerals containing these trace elements in shales and quartz veins, containing pyrite, resulting in the reducing conditions.

    - Reducing conditions in groundwater.
    - Close to the Bokkeveld contact.
    - No hydraulic connection with the recharge area.

12. Management of Eastern Sector of KKRWSS

In terms of management of the Eastern Sector of the KKRWSS, the following needs to be carried out:

- Installation of further monitoring boreholes in the Keystone Block Aquizone.
- Monitoring of groundwater abstraction and water levels in the Aquizone, other than the KKRWSS.
- Determine the storage of the Keystone Block Aquizone more accurately.
- Adjust the borehole yields of the production boreholes as recommended herein.
- Complete satellite lineament analysis and explore for more production boreholes near the Kammanassie Mountains, according to the conceptual hydrogeological model.
- Monitor spring flow and rainfall variations across the Kammanassie Mountains.
- Rainfall sampling for chloride.
- Extend the monitoring network in the Peninsula Aquifer towards the Outeniqua and Swartberg Mountains.
- Ongoing isotope monitoring of output and more detailed isotope data on rainfall and springflows.

13. Database

Establish a GIS Arcview and Access database containing all the borehole, structural, geological, hydrochemical and environmental isotope as well as hydrogeological information for each section of the TMG Super Aquifer.